

UNIVERSITY OF ZAGREB FACULTY OF AGRICULTURE
 AGRICULTURAL ENGINEERING DEPARTMENT
 FACULTY OF AGRICULTURE UNIVERSITY OF OSIJEK
 FACULTY OF AGRICULTURE AND LIFE SCIENCES UNIVERSITY OF MARIBOR
 AGRICULTURAL INSTITUTE OF SLOVENIA
 INSTITUTE OF AGRICULTURAL ENGINEERING, BOKU, VIENNA
 NATIONAL INSTITUTE FOR AGRICULTURAL MACHINERY - INMA BUCHAREST
 CROATIAN AGRICULTURAL ENGINEERING SOCIETY



PROCEEDINGS OF THE
 46th INTERNATIONAL SYMPOSIUM

Actual Tasks on Agricultural Engineering

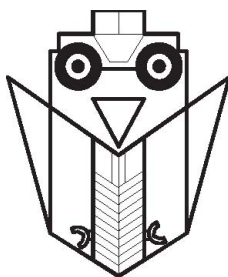
OPATIJA, CROATIA, 27th FEBRUARY - 1st MARCH 2018



SVEUČILIŠTE U ZAGREBU AGRONOMSKI FAKULTET
ZAVOD ZA MEHANIZACIJU POLJOPRIVREDE
POLJOPRIVREDNI FAKULTET SVEUČILIŠTA U OSIJEKU
UNIVERZA V MARIBORU FAKULTETA ZA KMETIJSTVO IN
BIOSISTEMSKE VEDE
KMETIJSKI INŠTITUT SLOVENIJE
INSTITUT ZA POLJOPRIVREDNU TEHNIKU, BOKU, BEČ
NACIONALNI INSTITUT ZA POLJOPRIVREDNU MEHANIZACIJU -
INMA BUKUREŠT
HRVATSKA UDRUGA ZA POLJOPRIVREDNU TEHNIKU



AKTUALNI ZADACI MEHANIZACIJE POLJOPRIVREDE



ZBORNİK RADOVA

46. MEĐUNARODNOG SIMPOZIJA

Opatija, 27. veljače – 1. ožujka 2018.

Published by	University of Zagreb, Faculty of Agriculture, Department of Agricultural Engineering Svetošimunska 25, 10000 Zagreb, Croatia
Izdavač	Sveučilište u Zagrebu, Agronomski fakultet, Zavod za mehanizaciju poljoprivrede, Svetošimunska 25, 10000 Zagreb, Hrvatska
Editor-in-Chief / Glavni i odgovorni urednik	Nikola Bilandžija (e-mail: nbilandzija@agr.hr)
Technical editor / Tehnički urednik	Dragan Tupajić
Organising committee / Organizacijski odbor	
Đuro Banaj Nikola Bilandžija Krešimir Čopec Goran Fabijanić Mateja Grubor	Dubravko Filipović Zlatko Koronc Igor Kovačev Stjepan Sito
Scientific committee / Znanstveni odbor	
Prof. dr. Đuro Banaj, HR Ing. Jaroslav Čepl, CSc., CZ Prof. dr. Aleksandra Dimitrijević, RS Assist. prof. dr. Đorđe Đatkov, RS Prof. dr. Ettore Gasparetto, IT Prof. dr. Ivo Grgić, HR Prof. dr. Andreas Gronauer, AT Dr. Viktor Jejić, SI Prof. dr. Silvio Košutić, Chairman, HR Prof. dr. Miran Lakota, SI Prof. dr. Milan Martinov, RS Prof. dr. Dumitru Mnerie, RO	Prof. dr. Joachim Mueller, DE Prof. dr. Pietro Picuno, IT Prof. dr. Stjepan Pliestić, HR Prof. dr. Egidijus Sarauskis, LT Prof. dr. John Schueller, USA Prof. dr. Peter Schulze-Lammers, DE Prof. dr. Denis Stajanko, SI Prof. dr. Dumitru Tucu, RO Assist. prof. dr. Peter Vindiš, SI Dr. Valentin Vladut, RO Prof. dr. Daniele De Wrachien, IT

ISSN 1848-4425

<http://atae.agr.hr>

Cover painting / Slika s naslovnice: Dušan Jejić

Cover design / Oblikovanje naslovnice: Kreativna Točka by Marko Košutić

All papers in the Proceedings are peer reviewed

Svi radovi u Zborniku su recenzirani

Papers from the Proceedings have been indexed since 1997 into databases: /

Radovi u Zborniku su indeksirani u bazama podataka od 1997.:

Clarivate Analytics: Web of Science Core Collection: Conference Proceedings Citation Index
CAB International - Agricultural Engineering Abstracts

SPONZORI – SPONSORS

MINISTARSTVO ZNANOSTI I OBRAZOVANJA
REPUBLIKE HRVATSKE /
MINISTRY OF SCIENCE AND EDUCATION OF
THE REPUBLIC OF CROATIA

ZAKLADA HRVATSKE AKADEMIJE ZNANOSTI I
UMJETNOSTI /
THE FOUNDATION OF THE CROATIAN ACADEMY
OF SCIENCES AND ARTS

INA MAZIVA d.o.o. – ZAGREB

PRIČA O TRAKTORU S NASLOVNICE

Lanz Bulldog HL

Priča o masovnoj proizvodnji traktora s užarenom glavom počinje nakon Prvog svjetskog rata, kada Lanz, Mannheim, Njemačka (najveći europski proizvođač mehanizacije početkom 20. stoljeća i kasnije), 1921. godine započinje proizvodnju jednostavnog stabilnog motora s užarenom glavom hlađenog otparivanjem vode. Motor je potom ugrađen na podvozje s kotačima koje je vukla konjska zaprega. Ta je izvedba kasnije nadopunjena – dograđen je sklop koji je povezivao motor sa stražnjim kotačima. Time je Lanzov stacionarni motor postao samohodni stroj – traktor. Takva jednostavna izvedba traktora bila je namijenjena za pogon stacionarnih strojeva u poljoprivredi – vršalica, pumpi za navodnjavanje, kružnih pila za drvo, slamoreznica. U industriji je služio za pogon drobilica kamena, električnih generatora i transport (na tvrdog podlozi mogao je povući prikolicu najveće mase 7 tona). Traktor je nazvan Bulldog zbog karakterističnog oblika motora, koji je sprijeda nalikovao glavi buldoga (užarena glava motora). Pored osnovne poljoprivredne izvedbe, u ponudi je bila i verzija s pogonom na sva četiri kotača za rad u voćnjacima i vinogradima, izvedba za rad na močvarnim tlima (s proširenim čeličnim kotačima), tricikl izvedba po uzoru na američke traktore za kultivaciju kukuruza. Konceptija Bulldoga je bila tako uspješna da su se na njega ugledali i drugi europski proizvođači traktora: Landini, Orsi, HSCS, Bubba, Ursus, S.F.Vierzon, Bolinder, Marshal. „Otac“ ovog legendarnog traktora bio je dr. Fritz Huber, koji je zagovarao koncepciju jednostavnog, robusnog i jeftinog traktora prikladnog za poljoprivredu. Velika je prednost motora s užarenom glavom činjenica da kao pogonsko gorivo može koristiti različite frakcije nafte, biljno ulje, životinjske masnoće, otpadna motorna ulja, zemni plin, ugljenu prašinu. Korištenje jeftinijih goriva (u odnosu na benzin ili mineralni dizel) omogućilo je i siromašnijim poljoprivrednicima da mehaniziraju teške radne operacije. Uz to, motori s užarenom glavom bili su zahvaljujući niskom broju okretaja ($400 - 700 \text{ min}^{-1}$) i izrazito dugovječni. Postoje slučajevi u kojima su ovi motori na traktorima radili do 40.000 radnih sati (nakon izmjene dijelova podložnih trošenju, npr. klipnih prstenova, motor je bez problema dalje radio). Snaga motora na Lanzovom Bulldogu HL iznosila je 8,8 kW (12 KS), zapremina oko 6000 cm^3 , a masa traktora ovisno o izvedbi od 1850 kg do 2360 kg. Traktor nije imao mjenjač, a brzina kretanja regulirala se brzinom vrtnje motora. Za kretanje unazad trebalo je zaustaviti motor te ga pomoću zamašnjaka pokrenuti u suprotnom smjeru. Najveća brzina kretanja iznosila je $4,2 \text{ km h}^{-1}$. Postojala je i izvedba Bulldoga koji je imao mjenjač s dva stupnja prijenosa. U prvom stupnju traktor je postizao 6 km h^{-1} , a u drugom 12 km h^{-1} , što je posebno naglašavano u promotivnom materijalima. Proizvodnja HL modela trajala je od 1921. do 1927. godine, kada je zamijenjen sofisticiranijim modelom. U stručnoj literaturi iz područja traktorske tehnike neko je vrijeme smatrano da je Lanz bio prvi proizvođač traktora s užarenom glavom u svijetu, no danas ga se smatra najmasovnijim proizvođačem (spominje se da su prvi traktori s užarenom glavom uvedeni u Švedskoj između 1913. i 1919. godine). Lanz je do kraja 1950-ih proizveo više od 220.000 traktora s užarenom glavom.

Dr. sc. Viktor Jejčić

STORY ABOUT TRACTOR FROM COVER PAGE

Lanz Bulldog HL

The story of a hot bulb fired semi-diesel engine tractor large-scale production started after the First World War, when the Lanz company, of Manheim, Germany (the biggest producer of agricultural mechanization at the beginning of the 20th century), began in the year 1921 the production of a simple stationary hot-bulb fired semi-diesel engine with evaporative cooling. The engine was just mounted to a chassis with wheels that was drawn by horses. This version was later updated with a system that connected the engine with the rear wheels. This simple version of the tractor was intended to power stationary agricultural machines, such as thresher, pump for irrigation, circular jigsaw, straw cutter and so on. In industry this tractor was used to power stone crusher, electric generator and transport (the tractor was able to pull on a hard surface trailer up to maximum 7 tones load). The tractor was named Bulldog due to the specific shape of its engine, whose front part resembled the English dog species. Besides the basic agricultural version, the manufacturer offered following versions: an all-wheel drive intended for work in orchards and vine yards, a version for working on swampy soils (due to wider steel wheels), a tricycle version for corn cultivation like American row-crop tractors. The Bulldog tractor concept was so successful that other European tractor producers – Landini, Orsi, HSCS, Bubba, Ursus, S.F. Vierzon, Bolinder, Marshal – followed it. The designer of this legendary tractor was dr. Fritz Huber, who supported concept of a simple, robust and cheap tractor suitable for agriculture. The great advantage of this engine was its ability to be fueled by crude oil, plant oil, waste sump oil, animal fat, powdered coal and natural gas. The hot-bulb fired semi-diesel engines were – due to operating at low speed ($400-700 \text{ min}^{-1}$) – very durable. Some records proved cases where these tractor engines completed up to 40,000 working hours (after general repair these engines continued to work perfectly). The Lanz's Bulldog HL was powered by an engine of 8.8 kW (12 HP), the displacement of the engine was 6,224 cm³, the weight of the tractor depended on a model and varied from 1,850 to 2,360 kg. The Bulldog HL had no gearbox, only engine speed controls. In order to move in reverse, the engine had to be stopped and then restarted in the opposite direction by a flywheel. The maximal traveling speed of the Bulldog HL tractor was 4.2 km h⁻¹. There was a Bulldog version equipped with a two-speed gearbox (first gear max. speed $v = 6,0 \text{ km h}^{-1}$, second gear max. speed $v = 12.0 \text{ km h}^{-1}$). The Lanz's Bulldog HL tractor was in production from 1921 to 1927, when it was replaced with a more sophisticated model. The earlier expert literature on the history of tractors took Lanz as the World's No. 1 producer of tractors with the hot-bulb fired semi-diesel engine, but today Lanz is taken only as the World's No. 1 large-scale tractor producer. Some sources mention that the first tractors with hot-bulb fired semi-diesel engines were introduced in Sweden between 1913 and 1919. Until the end of the 1950s, Lanz produced over 220,000 tractors with hot-bulb fired semi-diesel engines.

Viktor Jejič, Ph.D

PREDGOVOR

Poštovane kolegice i kolege,
Poštovani čitatelji,

Sa zadovoljstvom Vam predstavljam Zbornik radova sa 46. međunarodnog Simpozija „Aktualni zadaci mehanizacije poljoprivrede“, koji se kao i prethodnih godina održao u Opatiji, Republika Hrvatska od 27. veljače do 1. ožujka 2018. godine. Simpozij je pružio mogućnost sudionicima iz 10 različitih zemalja da prezentiraju i raspravljaju o svojim znanstvenim dostignućima u području poljoprivredne tehnike i biosustava.

Ovogodišnji Zbornik radova sadrži ukupno 65 radova, od toga iz Austrije 1, Češke 2, Kanade 1, Filipina 1, Hrvatske 8, Italije 4, Njemačke 2, Rumunjske 37, Slovenije 6 i Srbije 3. Svaki rad tiskan u Zborniku je prošao postupak recenzije te je poslan dopisnom autoru na autorizaciju teksta. Pristup elektroničkoj verziji Zbornika radova je besplatan na adresi <http://atae.agr.hr/proceedings.htm>. Od 1997. godine, radovi objavljeni u Zborniku uvršteni su u baze podataka Clarivate Analytics: Web of Science Core Collection - Conference Proceedings Citation Indeks i CAB International - Agricultural Engineering Abstracts.

Suorganizatori ovogodišnjeg Simpozija od strane međunarodnih strukovnih udruga su *Commission of Agricultural and Biosystems Engineering (CIGR)*, *European Network for Advanced Engineering in Agriculture and Environment (EurAgEng)* i *Asian Association for Agricultural Engineering (AAAE)*.

Zahvaljujem svim autorima, recenzentima te kolegama iz organizacijskog i znanstvenog odbora, koji su svojim radom i svesrdnom pomoći omogućili održavanje ovogodišnjeg Simpozija. Također, zahvaljujem se i sponzorima odnosno Ministarstvu znanosti i obrazovanja Republike Hrvatske, Zakladi Hrvatske akademije znanosti i umjetnosti te tvrtki INA MAZIVA d.o.o.

Zagreb, ožujak 2018.

Doc. dr. sc. Nikola Bilandžija
Glavni urednik

PREFACE

Dear Colleagues,

Dear readers,

I am very pleased to introduce the Proceedings of the 46th International Symposium "Actual Tasks on Agricultural Engineering" that like in the previous years took place in Opatija, Republic of Croatia from February 27th to March 1st, 2018.

The Symposium provided an opportunity to participants coming from 10 different countries to present and discuss on their respective research findings in Agricultural and Biosystems Engineering area. This year's Proceedings includes 65 articles from Austria 1, Canada 1, Croatia 8, Czech Republic 2, Germany 2, Italy 4, Philippines 1, Romania 37, Serbia 3 and Slovenia 6. Each published paper in the Proceedings has been under peer-review process and the papers were sent to the corresponding author on text authorization. Access to the web edition of the Proceedings is free of charge at the website <http://atae.agr.hr/proceedings.htm>. Since 1997, papers published in the Symposium Proceedings are included in the Clarivate Analytics: Web of Science Core Collection – Conference Proceedings Citation Index and CAB International - Agricultural Engineering Abstracts.

International professional associations as co-organizers of this year's Symposium are International Commission of Agricultural and Biosystems Engineering (CIGR), European Network for Advanced Engineering in Agriculture and Environment (EurAgEng) and Asian Association for Agricultural Engineering (AAAE).

I would like to express my gratitude to our members of the Organising and Scientific Committee for their tremendous efforts. Without their support, the conference could not have been the success that it was. I also acknowledge the authors themselves, without whose expert input there would not have been conference. I would also like to thank all reviewers for their time and effort in reviewing the papers. Without their commitment it would not be possible to have the important 'referee' status assigned to papers in the proceedings.

It is my pleasant duty to acknowledge the continuous financial support from the Ministry of Science and Education of the Republic of Croatia, The Foundation of the Croatian Academy of Sciences and Arts and the INA MAZIVA company.

Zagreb, March 2018.

Assist. Prof. Nikola Bilandžija, PhD
Editor-in-Chief

SADRŽAJ – CONTENTS

Milan MARTINOV, Andreas GRONAUER, Silvio KOŠUTIĆ	19
Highlights of 27 th club of Bologna meeting Sažetak 27. Susreta kluba Bologna	
Rares HALBAC-COTOARA-ZAMFIR, Cristina HALBAC-COTOARA-ZAMFIR ...	29
Adapting to climate changes – a challenge for Romanian agriculture Prilagodba klimatskim promjenama – izazov za poljoprivredu Rumunjske	
Rares HALBAC-COTOARA-ZAMFIR	37
Brief introduction on water harvesting and its potential in western Romania Kratak uvod o prikupljanju vode i njezin potencijal u zapadnoj Rumunjskoj	
Carmen Otilia RUSĂNESCU, Marin RUSĂNESCU, Mihaela BEGEA, Gigel PARASCHIV, Sorin Ștefan BIRIȘ, Gheorghe VOICU, Ileana Nicoleta POPESCU	45
Assessing the risk of aridity: a case study Bucharest – Romania Procjena štetnosti suše: primjer Bukurešt - Rumunjska	
Dan-Teodor BALANESCU, Vlad-Mario HOMUTESCU	57
Agricultural machinery hybrid propulsion system based on combined cycle gas and steam turbines Sustav hibridnog pogona poljoprivrednih strojeva kombinacijom plinske i parne turbine	
Baldwin G. JALLORINA, Victorino T. TAYLAN, Ireneo C. AGULTO, Helen F. GAVINO, Vitaliana U. MALAMUG, Emmanuel V. SICAT	67
Harnessing the irrigation water flows for micro-hydro power generation Iskorištavanje vodenih tokova od navodnjavanja za pogon mikro hidro-elektana	
Anamarija BANAJ, Đuro BANAJ, Vjekoslav TADIĆ, Davor PETROVIĆ, Dario KNEŽEVIĆ	79
Comparison of standard and twin row seeding on sunflower yield Usporedba standardne i "twin row" sjetve suncokreta s obzirom na prinos	
Gheorghe BOLINTINEANU, Dan ÇUJBESCU, Cătălin PERSU, Iuliana GĂGEANU, Laurentiu VLĂDUȚOIU, Mihaela NIȚU, Augustina PRUTEANU, Nicoleta UNGUREANU	89
Researches of the bulb planting process in field and laboratory conditions Istraživanje procesa sadnje lukovica u poljskim i laboratorijskim uvjetima	

Gabriel-Alexandru CONSTANTIN, George IPATE, Gheorghe VOICU, Gabriel MUȘUROI, Mariana-Gabriela MUNTEANU, Maria DRAGOMIR	99
Evaluation of hand-arm vibration transmitted during soil tillage based on Arduino and MPU9250 motion sensor Ocjena vibracija prenesenih na sustav šaka-ruka prilikom obrade tla korištenjem Arduina i senzora pokreta MPU9250	
Gabriel GHEORGHE, Cătălin PERSU, Dan CUJBESCU, Marinela MATEESCU	107
Influence of attack angle to draft force variation of a furrow opener at mulch foil planter Utjecaj napadnog kuta na vučni otpor otvarača brazde u sjetvi pod malč foliju	
Zlatko KORONC, Dubravko FILIPOVIĆ, Goran FABIJANIĆ	117
Tractor DI diesel engine performances using different types of diesel fuel Karakteristike traktorskog dizel motora s direktnim ubrizgavanjem pri korištenju različitih vrsta dizelskog goriva	
Alina OVANISOF, Ovidiu VASILE, Maria DRAGOMIR	129
Analysis of human whole-body vibration exposure on a U650 tractor Analiza izloženosti vibracijama na tijelo rukovatelja korištenjem traktora U650	
Gheorghe VOICU, Magdalena - Laura TOMA, Elena - Madalina STEFAN, Paula TUDOR, Mihaela - Florentina DUTU	139
Grain pile stratification process on sieves of harvester cleaning system Uslojavanje zrna na sitima za čišćenje u kombajnu	
Dorel STOICA, Iulian-Claudiu DUȚU, Gheorghe VOICU, Mihaela-Florentina DUȚU.....	149
Influence of the oscillation frequency on the separation process at the conical sieves Utjecaj frekvencije oscilacija koničnih sita na postupak separacije	
Ioan ȚENU, Oana-Raluca COORDUNEANU, Petru CÂRLESCU, Radu ROȘCA.....	157
Design and construction of a fertilizer spreader for glass houses and greenhouses Projektiranje i konstrukcija raspodjeljivača gnojiva u plastenicima i staklenicima	
Dan VIDREAN, Florinel Cosmin BOJA, Alin TEUȘDEA, Cristina Ioana DRAGOMIR, Nicușor Flavius BOJA.....	169
Assesment of soil impact after using a vibro-combinator Utjecaj primjene kultivatora s elastičnim motičicama u obradi na svojstva tla	

Nelus-Evelin GHEORGHİȚĂ, Sorin-Stefan BIRIȘ, Nicoleta UNGUREANU, Sorin IORDACHE, Maria PRUNĂU	181
Study on adapting the parameters of vibratory tillage to the resonance frequency of the agricultural soil Prilagodba parametara vibrirajućih elemenata oruđa za obradu tla rezonantnoj frekvenciji tla	
Nicoleta UNGUREANU, Valentin VLĂDUȚ, Cătălin PERSU, Dan CUJBESCU, Marius Remus OPRESCU, Iulian VOICEA	189
Study on the compaction under front and rear wheel of a 40 kW tractor on plowed soil Zbijanje pooranog tla kotačima traktora snage 40 kW	
Nicoleta UNGUREANU, Valentin VLĂDUȚ, Sorin-Ștefan BIRIȘ, Gigel PARASCHIV, Mirela DINCĂ, Bianca Ștefania ZĂBAVĂ, Vasilica ȘTEFAN, Neluș EVELIN	201
FEM modelling of machinery induced compaction for the sustainable use of agricultural sandy soils FEM modeliranje zbijanja tla mehanizacijom u svrhu održivog korištenja pjeskovitih poljoprivrednih tala	
Davor PETROVIĆ, Đuro BANAJ, Vjekoslav TADIĆ, Dario KNEŽEVIĆ, Anamarija BANAJ	213
Impact of technical spraying factors on ground and air drift in cherry orchard Utjecaj tehničkih čimbenika raspršivanja na zemljišno i zračno zanošenje tekućine u nasadu višnje	
Gabriel GHEORGHE, Cătălin PERSU, Marian MIHAI, Dan CUJBESCU, Sorin BIRIȘ, Edmond MAICAN	223
Theoretical simulation for protective structure of operator cabin against falling object Teorijska simulacija kabine za zaštitu rukovatelja od padajućih predmeta	
Edmond MAICAN, Sorin-Ștefan BIRIȘ, Cătălin PERȘU, Mihaela DUȚU, Mihai Gabriel MATACHE, Sorin IORDACHE, Călin ALFIANU	231
Nonlinear impact resistance simulation of a newly designed roof from an agricultural tractor cabin Nelinearna simulacija otpornosti na udarce nove konstrukcije krova traktorske kabine	
Adriana MUSCALU, Mariana BIRSAN, Ladislau DAVID, Ion GRIGORE, Ana Cristina FATU, Catalina TUDORA.....	239
Harvesting and processing of french marigold to obtain products with new uses Žetva i dorada kadifce za dobivanje proizvoda novih namjena	

Heinz BERNHARDT, Michael MEDERLE, Maximilian TREIBER, Sascha WÖR	245
Aspects of digitization in agricultural logistics in Germany Mogućnosti digitalizacije u logistici poljoprivrede Njemačke	
Nikola VAJDA, Damijan KELC, Peter VINDIŠ, Peter BERK, Jurij RAKUN, Denis STAJNKO, Miran LAKOTA	253
Increase of soil tillage efficiency with using of RTK – navigation Povećanje učinkovitosti obrade tla korištenjem RTK - navigacije	
Vergil MURARU, Petru CARDEI, Sebastian MURARU, Cornelia MURARU-IONEL, Paula CONDRUZ	263
Convergence of different models for the same structure in computer aided engineering Konvergencija različitih modela računalnog projektiranja iste strukture	
Martin HÖHENDINGER, Sascha WÖRZ, Hans-Jürgen KRIEG, Reinhard DIETRICH, Lorenz FRECH, Jörn STUMPENHAUSEN, Heinz BERNHARDT	273
Integration of weather influences into an on-farm-energy management system Integracija utjecaja vremenskih prilika u sustavu upravljanja energijom na farmama	
Fabrizio MAZZETTO, Raimondo GALLO	283
Solutions to automate operational monitoring activities of agro-forestry tasks Mogućnosti automatizacije nadzornih aktivnosti u poljoprivredi i šumarstvu	
Dan CUJBESCU, Gheorghe BOLINTINEANU, Cătălin PERSU, Iuliana GĂGEANU, Mihaela NIȚU, Augstina PRUTEANU, Gheorghe VOICU, Nicoleta UNGUREANU	293
Assessing the quality and energy indices of precision planters Procjena kvalitete i energetske značajke preciznih sijačica	
Javier LIZASOAIN, Jonas LEBER, Susanne FRÜHAUF, Kwankao KARNPAKDEE, Bernhard WLCEK, Andreas GRONAUER, Alexander BAUER	305
Demand driven biogas production by discontinuous feeding strategies Proizvodnja bioplina prema potražnji uz diskontinuiranu strategiju dobave	
Bernard GOYETTE, Rajinikanth RAJAGOPAL, Jean-François HINCE, Md. Saifur RAHAMAN	315
A scale-up procedure for processing high-solid content food waste and dairy manure in a low temperature anaerobic digester Analiza postupka obrade visokog udjela krutog otpada hrane i gnoja iz mljekarske proizvodnje u anaerobnom fermentoru s niskom temperaturom	

Mateja GRUBOR, Ana MATIN, Nikola BILANDŽIJA, Vanja JURIŠIĆ, Ivan KOPILOVIĆ, Tajana KRIČKA	323
Comparison of energy properties of wheat variety „Kraljica“ with unregistered varieties „Brkulja“	
Usporedba energetske značajke sorte pšenice „Kraljica“ s neregistriranim sortom „Brkulja“	
Denis STAJNKO, Miran LAKOTA, Damijan KELC, Rajko BERNIK.....	331
Possibilities for introduction of wood gas generator on a family farm – Slovenia case study	
Mogućnosti uvođenja generatora plina na drvenu masu na obiteljska gospodarstva – primjer Slovenije	
Mariana FERDEȘ, Mirela DINCĂ, Bianca ZĂBAVĂ, Gigel PARASCHIV, Mariana MUNTEANU, Mariana IONESCU	341
Laccase enzyme production and biomass growth in liquid cultures of wood-degrading fungal strains	
Proizvodnja enzima lakaze i rasta biomase u tekućim kulturama drveta - degradirajući gljivični sojevi	
Mirela DINCĂ, Mariana FERDEȘ, Bianca ZĂBAVĂ, Gigel PARASCHIV, Nicoleta UNGUREANU, Valentin VLĂDUȚ, Georgiana MOICEANU	349
Lignocellulosic biomass pretreatment by hydrolytic fungal strains	
Predtretman lignocelulozne biomase hidrolitičkim gljivičnim sojevima	
Simina MARIS, Lavinia Maria CERNESCU, Stefan-Alfred MARIS, Doina DARVASI, Titus SLAVICI.....	359
Determining efficient mixtures of biomass for pellet production	
Određivanje učinkovitosti umješavanja biomase za proizvodnju peleta	
Georgiana MOICEANU, Mihai CHIȚOIU, Gheorghe VOICU, Gigel PARASCHIV, Valentin VLĂDUȚ, Iulia GĂGEANU, Mirela DINCĂ	369
Comparison between miscanthus and willow energy consumption during grinding	
Usporedba potrošnje energije tijekom usitnjavanja trave miscanthus i vrbe	
Cristian SORICĂ, Mariana FERDES, Ion PIRNĂ, Valentin VLĂDUȚ, Elena SORICĂ, Ion GRIGORE	379
Effects of UV-C irradiation upon the reference strains of some food-associated microorganisms	
Učinci UV-C ozračenja na referentne sojeve mikroorganizama s hrane	

Tajana KRIČKA, Mateja GRUBOR, Ivana TADIĆ, Vanja JURIŠIĆ, Ana MATIN	389
Changes in physical and chemical characteristics of coffee beans after thermal processing by roasting	
Promjene u fizikalnim i kemijskim karakteristikama zrna kave nakon termičkog procesa tostiranja	
Ranko KOPRIVICA, Jan TURAN, Biljana VELJKOVIĆ, Dušan RADIVOJEVIĆ, Nikola BOKAN, Dragan ĐUROVIĆ, Dragoslav ĐOKIĆ, Igor BALALIĆ	397
Physical properties of oil rapeseed kernels at different moisture content and varieties	
Utjecaj sorte i raznolikosti vlage na fizikalna svojstva sjemena uljane repice	
Petru Marian CÂRLESCU, Ioan ȚENU, Radu ROȘCA, Adriana Teodora MUSCALU, Nicolae Valentin VLĂDUT	407
CFD simulation of an innovative vertical dryer for agricultural seeds drying	
CFD simulacija inovativne vertikalne sušare za zrno	
Petru Marian CÂRLESCU, Vlad Nicolae ARSENOAIA, Ioan ȚENU, Adriana Teodora MUSCALU, Mariana Silvia BÂRSAN	419
Researches of mass and heat transfer of an innovative vertical dryer	
Istraživanje prijenosa mase i topline inovativne vertikalne sušare	
Cristian SORICĂ, Marian VINTILĂ, Valentin VLĂDUȚ, Mihai MATACHE, Elena SORICĂ, Ion GRIGORE	429
Energy indices of an equipment during fast freezing of berries	
Energetski indeksi opreme tijekom brzog smrzavanja bobica	
Lucian V. FECHETE TUTUNARU, Nicolae FILIP, Elena Mihaela NAGY, Mihai MATACHE	439
Influence of input flow over grain mill efficiency utilisation	
Utjecaj ulaznog protoka na efikasnost iskorištenja mlina za zrno	
Mariana-Gabriela MUNTEANU, Gheorghe VOICU, George IPATE, Nelus Evelin GHEORGHITĂ, Gabriel-Alexandru CONSTANTIN, Iulian-Claudiu DUTU, Irina-Aura ISTRATE	447
Aspects regarding the flow of the mixture flour-water at different temperatures, through small diameter channels	
Utjecaj temperature na protok smjese brašna i vode kroz otvore malih promjera	
Alina MĂRGEAN, Vasile PĂDUREANU, Mirabela Ioana LUPU	457
Application of ultrasound in winemaking process	
Primjena ultrazvuka u procesu proizvodnje vina	

Mihai Gabriel MATAACHE, Corina MOGA, Cristina COVALIU, Iulian VOICEA, Catalin PERSU	465
Flotation system for agricultural wastewater treatment Flotacijski sustavi za uporabu otpadnih voda iz poljoprivrede	
Augustina PRUTEANU, Valentin VLĂDUȚ, Mihai MATAACHE, Mihaela NIȚU.....	473
Experimental researches on the quality of sorting process of medicinal plants Eksperimentalno istraživanje kvalitete procesa sortiranja ljekovitog bilja	
Roxana Mihaela BABANATIS MERCE, Theoharis BABANATSAS, Stefan MARIS, Dumitru TUCU, Oana Corina GHERGAN	485
Study of an automatic olives sorting system Istraživanje sustava automatskog sortiranja maslina	
Viktor JEJČIČ, Fouad AL-MANSOUR, Tomaž POJE	491
Carbon footprint of final wheat products from family farms Otisak ugljika završnih proizvoda pšenice na obiteljskim gospodarstvima	
Jaroslav ČEPL, Pavel KASAL, Milan ČÍŽEK, Andrea SVOBODOVA, Václav MAYER, Daniel VEJCHAR.....	499
The effect of drip irrigation on potato yield and quality Utjecaj navodnjavanja kap po kap na prinos i kvalitetu krumpira	
Aleksandra DIMITRIJEVIĆ, Brankica ŠUNDEK, Nikola MATOVIĆ, Zoran MILEUSNIĆ, Rajko MIODRAGOVIĆ	509
Spinach production conditions in the different types of greenhouse constructions Uvjeti proizvodnje špinata u različitim konstrukcijskim tipovima staklenika	
George IPATE, Gabriel-Alexandru CONSTANTIN, Gheorghe VOICU, Gabriel MUSUROI, Mariana-Gabriela MUNTEANU, Elena-Madalina STEFAN.....	517
Real-time measurement of solar ultraviolet exposure in a plastic greenhouse Mjerenje ultraljubičastog zračenja u plastenicima	
Dragoș MANEA, Costin MIRCEA, Eugen MARIN, Petru CÂRDEI, Gabriel GHEORGHE, Florin POP	525
The effect of roots area cooling on tomatoes yield in solar Utjecaj hlađenja korijenovog prostora na prinos rajčice u plasteniku	

Petre-Florinel NENU, Luisa-Izabel DUNGAN, Lavinia CERNESCU, Titus SLAVICI	531
Energetic and economic considerations on thermal regime effectiveness in a greenhouse Energetska i ekonomska razmatranja učinkovitosti toplinskog režima u staklenicima	
Tomáš LOŠÁK, Jaroslav HLUŠEK, Ivana LAMPARTOVÁ, Lubica POSPÍŠILOVÁ, Pavel ČERMÁK, Gabriela MÜHLBACHOVÁ, Ladislav VARGA, Július ÁRVAY, Boris LAZAREVIĆ	543
Phosphorus fertilization as a component of growing technology of barley Gnojidba fosforom kao sastavnica tehnologije uzgoja ječma	
Damijan KELC, Peter VINDIŠ, Peter BERK, Jurij RAKUN, Denis STAJNKO, Miran LAKOTA.....	551
Testing lettuce, cultivar 'Ljubljanska ledenka', for 'baby leaf' production Istraživanje zelene salate, kultivara 'Ljubljanska ledenka', za 'baby leaf' proizvodnju	
Alberto BARBARESI, Daniele TORREGGIANI, Viviana MAIOLI, Patrizia TASSINARI.....	561
Assessment of building solution effectiveness on a winery thermal behaviour Vrednovanje učinkovitosti građevinskih rješenja na toplinski režim vinarije	
Josip TOMIĆ, Krešimir ČOPEC, Dubravko FILIPOVIĆ, Stjepan PLIESTIĆ, Neven VOĆA	573
Collection and disposal of waste lubricant oils in the Republic of Croatia with a view to state in agriculture Sakupljanje i zbrinjavanje otpadnih mazivih ulja u Republici Hrvatskoj s osvrtom na stanje u poljoprivredi	
Pietro PICUNO, Dina STATUTO	583
New curricula and teaching programmes on sustainable agriculture: the "Sagri" project Novi kurikulumi i nastavni programi za održivu poljoprivredu: "Sagri" projekt	
Dina STATUTO, Martina BOCHICCHIO, Carmela SICA, Pietro PICUNO	595
Experimental development of clay bricks reinforced with agricultural by-products Eksperimentalni razvoj glinenih opeka ojačanih s nusproizvodima iz poljoprivrede	

Ivo GRGIĆ, Jernej PRIŠENK, Vladimir LEVAK, Tea KOVAČ, Magdalena ZRAKIĆ	605
Production prices of selected agricultural products in the Republic of Croatia and reference prices of European Union Odnos proizvođačkih cijena odabranih poljoprivrednih proizvoda u Republici Hrvatskoj i referentnih cijena u Europskoj uniji	
Ivo GRGIĆ, Lari HADELAN, Josip GUGIĆ, Paula JURJEVIĆ, Magdalena ZRAKIĆ	615
Foreign trade of the Republic of Croatia with economic groups in selected agricultural and food products from 2010 to 2017 Vanjskotrgovinska razmjena Republike Hrvatske s ekonomskim grupacijama za odabrane poljoprivredno-prehrambene proizvode u vremenu 2010. - 2017. godine	
Tomaz POJE	627
Analyse of registered tractors in Slovenia in the year 2016 Analiza registriranih traktora u Sloveniji u 2016. godini	
Tomaz POJE	635
Analysis of traffic accidents with tractors in Slovenia Analiza prometnih nesreća s traktorima u Sloveniji	
—	



HIGHLIGHTS OF 27TH CLUB OF BOLOGNA MEETING

Milan MARTINOV¹, Andreas GRONAUER², Silvio KOSUTIC^{3*}

¹ Faculty of Technical Sciences, University of Novi Sad, Serbia

² Institute of Agricultural Engineering, Department of Sustainable Agricultural Systems, University of Natural Resources and Life Sciences, Vienna, Austria

³ Agricultural Engineering Department, Faculty of Agriculture, University of Zagreb, Croatia

*E-mail of corresponding author: skosutic@agr.hr

SUMMARY

Club of Bologna, world task force on strategies for development of agricultural mechanisation, at 27th annual meeting in Hannover, presented importance of 4.0 Industry, and applicability in agricultural machinery. It were demonstrated three examples, and new term Agriculture 4.0 was promoted. Further were presented newest achievements related to application of ISO BUS and forestry mechanization. Finally, are considered the problems and possible solutions for sustainable mechanization in developing countries, case Africa.

Keywords: Club of Bologna, 4.0 Industry, ISO BUS, forest mechanization, agricultural mechanization for developing countries

INTRODUCTION

Club of Bologna (CoB), a world task-force on the strategies for the development of agricultural mechanisation belongs, for sure, to the, Worldwide, most important organizations in the field of agricultural and biosystems engineering. It was founded 1989 as a free and nonprofit organization, supported by Italian agricultural and earth moving machinery manufacturers association *FederUnacoma*. CoB gathers members from 31 countries and has 93 full members. Common, and most significant, CoB's activity is annual members' meetings, held alternatively in Bologna, during exhibition EIMA, and Hannover, during *Agritechnica*.

4.0 INDUSTRY AND AGRICULTURAL MECHANISATION

In his introductory presentation *Axel Munack* defined new term 4.0 Industry, as a forth, and the newest, step of its evolution. Industry 4.0, was the first time presented in Hannover 2012. creating what has been called a "*smart factory*". The very essential definition is: "Within

the modular structured *smart factories*, cyber-physical systems monitor physical processes, create a virtual copy of the physical world and make decentralized decisions. Over the IoT (Internet of Things), cyber-physical systems communicate and cooperate with each other and with humans in real time, and via the *Internet of Services*, both internal and cross-organizational services are offered and used by participants of the value chain." The motivation of CoB was to tackle implementation of 4.0 principles and practice in industry of agricultural mechanization. At the first moment this new term and approach induces some doubts and resistant to futuristic vision. We may not forget our skepticism regarding Internet or cell phones, and these are now common and almost unavoidable part of our life.

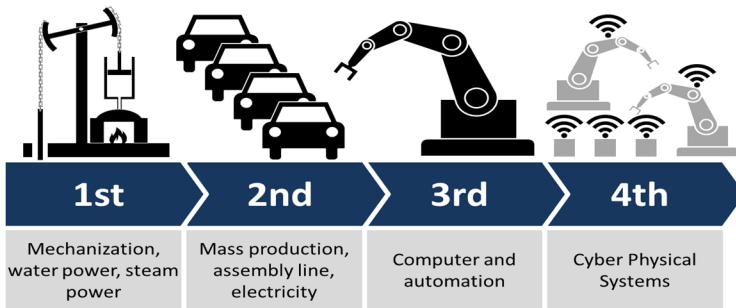


Figure 1. Industry 4.0 what does it mean
(Roser at AllAboutLean.com; Munack, 2017)

The the first presentation **Industry 4.0: Impact on Both Development and Product** of *Massimo Ribaldone*, from SDF Group, gave a historic overview on the development of machine design and examples of application by machinery manufacturer. Their intention, as very practical example, is to develop predictive maintenance for tractors and other machinery. By using contemporary sensors and IoT would be imminent failure detected.

This will be followed by timely supply of needed spare parts and will reduce maintenance/repairatory time. The same information, including operation conditions, can be used for design planning and corrections.

Second presenter was *Franco Oliaro*, coming from company ROJ, Italy, producer of hard and software for industry. In his presentation **Smart Logistic for Effective Process** he

described activity of the company of more than 240 employees, related to 4.0 industry and potentials for agriculture and agricultural mechanization.

As example of in own production applied utilization of digital information to trace the different materials and automate their handling, are listed following objectives:

- to reduce the material handling;
- to reduce the inventory failures;
- to implement flexibility with discipline;
- to find one place for everything and everything in its place;
- to set a FIFO (First In First Out) rule;
- to implement the material traceability.

This, smart logistic system, integrated with the ERP (Enterprise Resource Planning), enables application of 4.0 industry approach.

Their intention is to enable same application to agricultural machinery, e.g. for logging the seeding and fertilizing process (lot, operator, date, quantity) and remote diagnostic by using IoT ready systems.

Ulrich Adam, Secretary General of European Agricultural Machinery (CEMA), presentation was: **Agriculture 4.0 – the Challenges Ahead and What To Do About Them**. He introduced the term Agriculture 4.0., which should be logical upgrading of Smart and Digital Farming. In *Global Opportunity Report 2016*, developed by DNV GL, UNGC and Monday Morning Global Institute, Smart Farming take, in category Opportunities ranked by potential positive impact on society, first place, among fifteen listed issues.

Author set the question: How will Agriculture 4.0 impact the supply chain? Better use of IT will:

- Optimize the inputs (Precision Farming).
- Manage mechanization more efficiently & use of energy resources.
- Enhance crop storage techniques & reduce crop losses.
- Provide better information about market demand & seasonal fluctuation.
- Improve transport & logistics services.
- Optimize retailer stocking & storage (less waste).

Now, in Agriculture 4.0, are expected many new players. It was illustrated using potato cultivation and potato processing as examples.

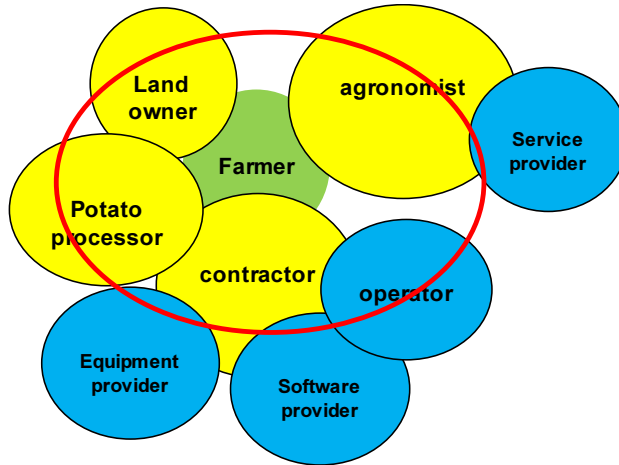


Figure 2. Complex data exchange system and contractual data sovereignty using potato production as an example (Adam, 2017)

A farmer is renting land to grow contracted potatoes. A contractor does the work on the field. The farmer is using an external agronomist for data-related activities. It is needed contracts related to data exchange: for the operation of the data systems, for the usage of the data for machinery related purposes, for sharing data with external parties (dealer, sub-contractors), etc.

Connected with this appears the problem of data security and potential misuse. EU started with development of *EU Code of Conduct on Agricultural Data Sharing – Core Objectives* (last update 27th of October 2017), that can help overcoming of this.

Another vast hindrance for performing Agriculture 4.0 is slow renewal of mechanization. Even in developed Germany, with 1.2 million tractors, their average age is 27.5 years. Annual fleet renewal is by only about 33,000 new tractors.

Final message of the presentation was: Agriculture 4.0 – a Unique Opportunity: Working Together to Master the Challenges/Disruption to Reap the Benefits!

NEW DEVELOPMENTS IN ISO BUS, THE INDUSTRY PERSPECTIVE

Marcello Mongiardo from CNH presented today's status and future development of ISO BUS as an unavoidable control system of modern agricultural machinery and implements that is now after the 15 years in the market at point to improve its capabilities beyond today's level. *Peter van der Vlugt* from Kverneland Group presented AEF-ISOBUS: State of the Art and Future Directions showing whole development and standardization from the Agriculture Industry Electronics Foundation (AEF) point of view.

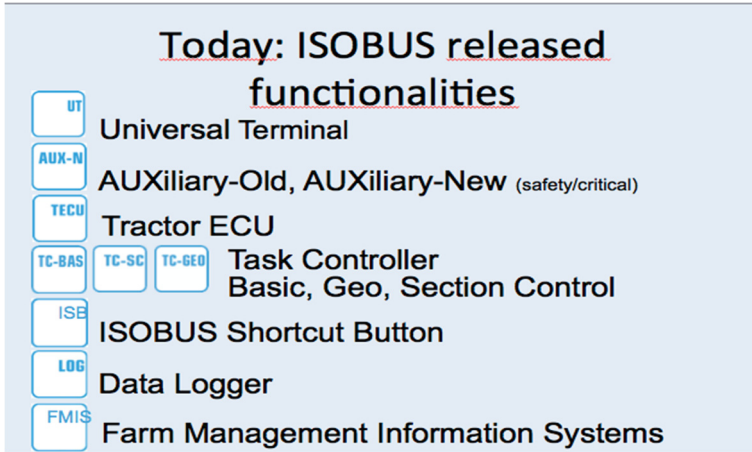


Figure 3. Today ISOBUS released functionalities (Mongiardo, 2017)

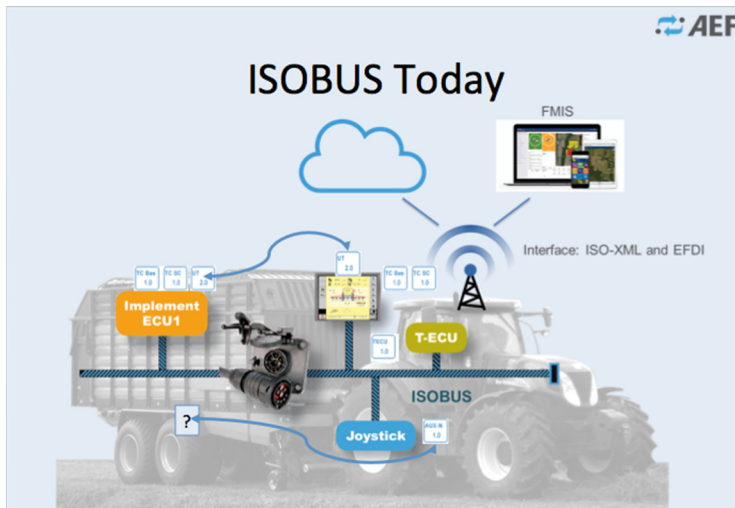


Figure 4. ISOBUS Today (Van der Vlugt, 2017)

Tractor Implement Management is one of the next steps in the near future. Within AEF manufactures are creating a robust way of opening automation to “trusted equipments” defining rules to clarify liability and guarantee a “plug and play” approach to the customers.

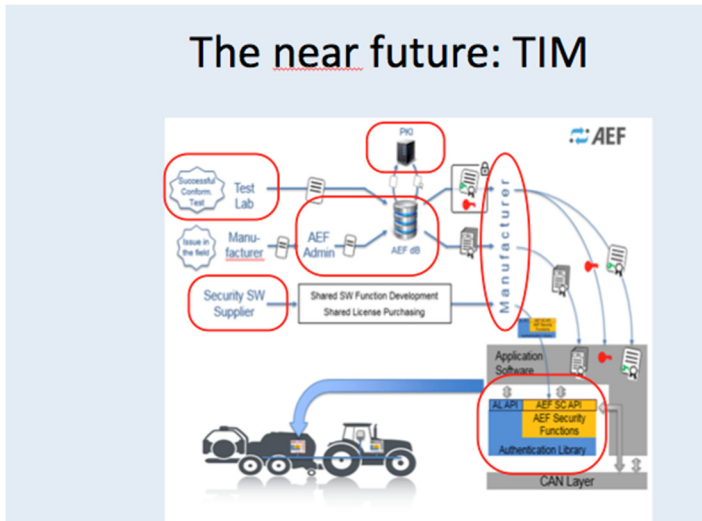


Figure 4. The near future: TIM - Tractor Implement Management (Mongiardo 2017)

Future challenges in ISOBUS development are focused at three points:

1. COPL (Cost Optimized Physical Layer):

Cost optimization allowing a higher diffusion of the ISOBUS technology (also more suitable for smaller machines). The goal is to reach lower volumes and smaller application.

2. WIC (Wireless Infield Communication):

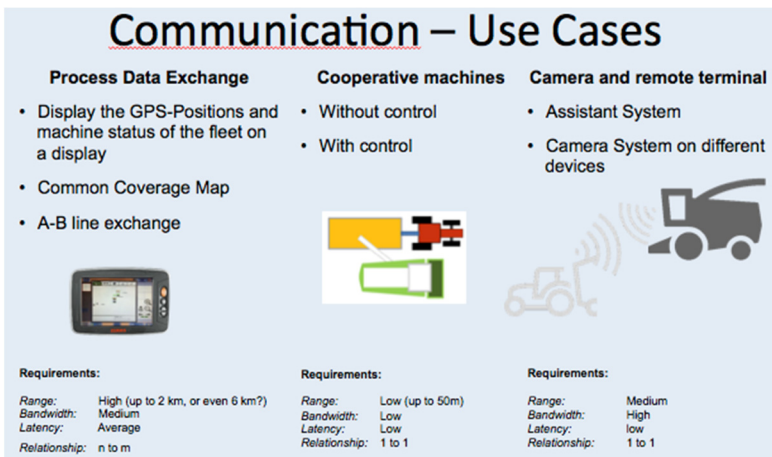



Figure 5. Wireless Infield Communication- Use Cases (Mongiardo, 2017)



Wireless Infield Communication

- Investigating technologies to meet the industry future needs
 - Existing technologies 802.11-based Wifi standards
 - Car-to-car standard 802.11p
 - System architecture has to allow upcoming communication standards like 5G
- Definition of protocols and methods to exchange data
- Use Cases include:
 - Process Data Exchange
 - Co-operative machines
 - Camera and Remote Terminal




Figure 6. Wireless Infield Communication (Van der Vlugt, 2017)

3. HIS (High Speed ISOBUS):

- Distributed high resolution position/correction signals.
- Digital Video Systems.
- Improved Service and Diagnosis (flash ECUs, Log-files, raw data streams for debugging).
- Mobile Internet on ISOBUS for dedicated server/client requests.
- High Voltage data Connection.

As technology evolves, manufacturers must take advantage of new opportunities with the end goal of providing farmers with a higher productive, higher quality and more efficient farming cycle.

FORESTRY MECHANIZATION

Ute Seeling head of the German Centre for Forest Work and Technology presented a broad overview on “**Challenges and Drivers for Forest Technologies and Techniques in Forestry**”. She introduced a historical overview of the development of mechanisation in forest management and a classification of the processes and machinery available today according to its suitability for use in sloping terrain (fig. 7).

Developments in management with permanent tramlines resp. logging trails and aspects of working conditions (safety, physical and psychological workload), economic efficiency and environmental aspects were presented with a specific focus on German situation. In Germany the Forrester workers decreased approx. to the half within the last 20 years and fully mechanised processing reached 90 % of harvesting. Future developments focuses on safety and soil protection (also related to increase of machine weight (fig. 8) and regarding to digitization (caused by related developments in sensors, positioning, telecommunications and big data management) on automatization, robotics.

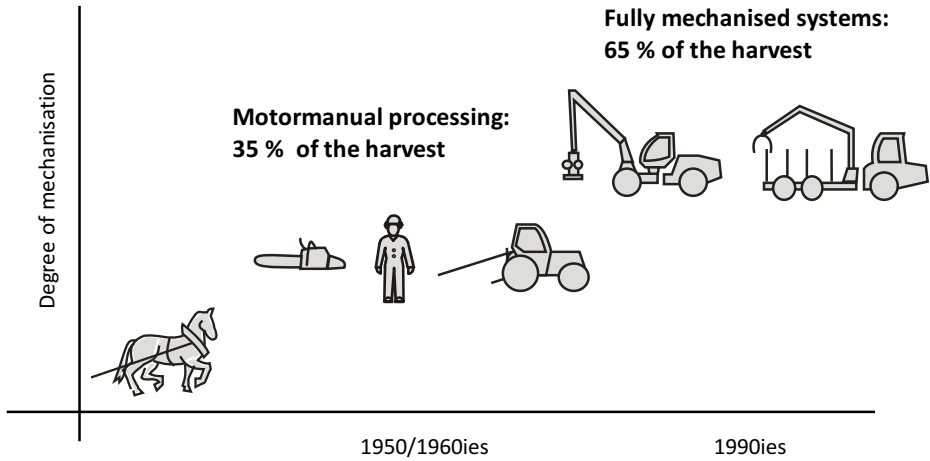


Figure 7. Development of forest mechanisation a historical view (Seeling, 2017)

Profound changes are expected in regard to:

- increased productivity;
- improved security;
- increased soil protection;
- improved environmental protection;
- reliable certification.

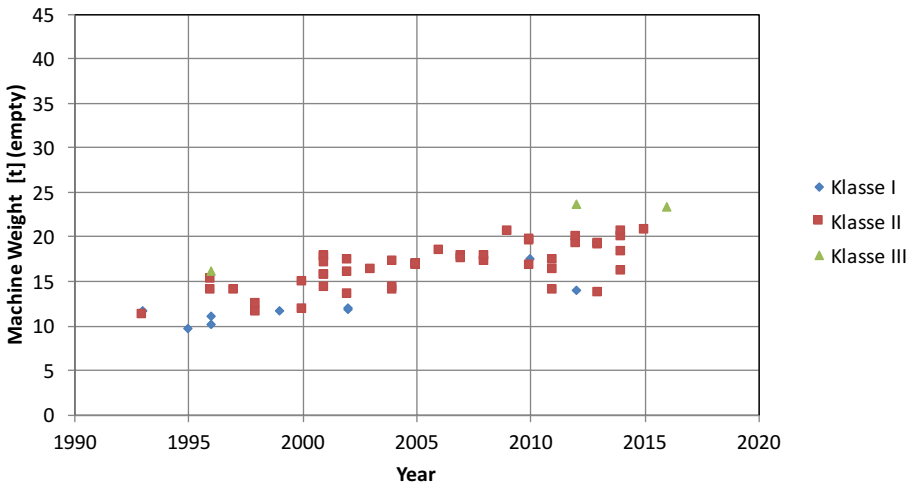


Figure 8. Development of machine weights within 20 years (example forwarder) (Seeling, 2017)

The next steps in the development of the forestry on the one hand will implement digitalization (work preparation via GIS/GPS, optimized bucking, logistics via GIS/GPS and internet, documentation via GIS/GPS, Data-communication via E-Mail/Cloud computing) and on the other hand transparently trace the interconnection of data flows in a "forestry 4.0" system, which integrates the whole chain from forest cultivation to wood processing industry right up to the end customer.

The presentation by *Raffaele Cavalli* from Department of land, environment, agriculture and forestry University Padua shed light on the topic "**Ground Yarding Operations in Mountainous Terrain**" and its importance taking into account that mountain forests represent a remarkable 23% of the Earth's forest cover and the necessity that forest operations have to be subordinated to the multifunction of mountain forests (ecosystem services). Beside traditional tree harvesting techniques (see fig. 9) new steep-slope harvesting machines with specialized undercarriages and carriers have been shown to safely access and operate on terrain up to 70% slope, like winch-assist systems (different man driven machines up to robots).

Its benefits can be seen in aspects of safety, productivity and additivity to local conditions and design of logistics. New developments focus on remote control and tele-operation. Last development, the tele-operation method interrupts the physical connection between the forest worker and the working area, which means that the forest worker is directly connected to the working machine using cameras, sensors, microphones and additional positioning software in a protected environment (virtual reality). Increase of safety, comfort and productivity of the operator can be expected. Conclusion summarized "The implementation of tele-operated, semi-autonomous and fully autonomous forestry equipment, in conjunction with constantly improving winch-assist technology, will provide a platform for safely extending the range of ground-based equipment to previously infeasible terrain conditions."

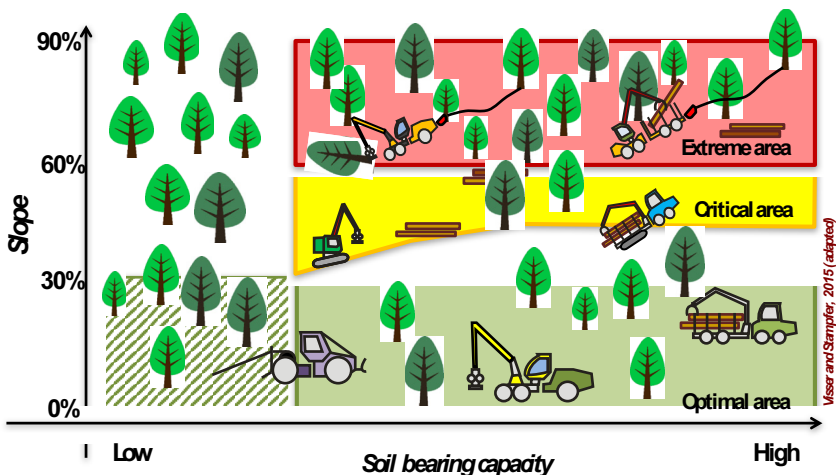


Figure 9. Steep-slope ground based harvesting operations in mountain forests (Cavalli, 2017)

NAIROBI CONFERENCE REPORT

Social and ethic aspects are highly respected by CoB. This is demonstrated by introduction of agricultural mechanization problems in underdeveloped and developing countries in annual meetings. By this meeting was reported about situation in Africa, related to Nairobi Conference **Sustainable Agricultural Mechanization**, and reported by *Josef Kienzle*, FAO-Group leader of Mechanization group. Based on discussed problems it was proposed to consider possible aids of developed countries to find appropriate solutions for sustainable mechanization in developing countries. One of tasks can be development of adequate and affordable tractor.

NOTE: Literature references can be requested from the authors. All presentations and written papers are available at: <http://www.clubofbologna.org/en/meetings-proceedings.php>.



ADAPTING TO CLIMATE CHANGES – A CHALLENGE FOR ROMANIAN AGRICULTURE

Rares HALBAC-COTOARA-ZAMFIR*, Cristina HALBAC-COTOARA-ZAMFIR

Department of Hydrotechnics, Politehnica University of Timisoara,
1A G. Enescu Street, Timisoara, 300022, Timisoara, Romania
E-mail of corresponding author: raresh_81@yahoo.com

SUMMARY

The process of adapting to climate changes is and will continue to be a challenging process considering the uncertainties related to climate evolution within the next decades. However, climate change is only one driver among many that will shape agriculture and rural areas in future decades. Adaptation means anticipating the adverse effects of climate change and taking appropriate action to prevent or minimise the damage they can cause, or taking advantage of opportunities that may arise.

In Romania, 62% of the land area is used for agriculture, followed by forests and other land with forest vegetation. Climate projections resulted from running a series of regional climate models seems to indicate that agricultural areas in Romania will be negatively affected by a number of changes with different levels of intensities.

Adapting to climate changes is thus a very challenging issue for Romanian agriculture requiring a special attention and an inter- and multi-disciplinary approach.

Keywords: climate changes, adapting, agriculture

INTRODUCTION

Mitigating the effects of climate change in agriculture is a priority objective in the EU's strategic development actions. The interdisciplinary nature of the actions involves a global approach by identifying and correlating the activities of development and implementation of intra- and inter-sectorial measures and responses to the effects of climate change.

Climate variability influences all sectors of the economy, but farming remains the most vulnerable, and its impact is more acute at present, as climate change and variability is becoming more and more pronounced.

At Central and Eastern Europe, scenarios show a clear decrease in precipitation, especially in the summer season, so a pluviometric deficiency will affect all areas of activity, mainly agriculture, population and ecosystems. Studies on temperatures and precipitations from Romania indicate that this country has experienced a warming of about 0.5°C in annual mean temperature since 1901 (even higher in southern areas) but without being detected any change of uniform long-term precipitation pattern (Busuioac et al., 2007; Cazacioc, 2007).

The complex impacts of climate change on agriculture underpin the need for risk-based decision-making in order to maintain adequate harvest standards and promote sustainable agriculture. Thus, variability and climate change must be addressed through day-to-day agricultural activities, through mitigation strategies and adaptation measures.

CLIMATE CHANGES – HOW TO APPROACH THEM

The process of adapting to climate changes is a process of adjustment to actual or expected climate and its effects, in order to moderate harm or exploit beneficial opportunities (IPCC SREX, 2012). Society's ability to cope with the impacts of climate change and avoid unacceptable levels of social and environmental costs decreases inversely proportional with an increase of climate changes severity.

Central to the concept of adaptation is the idea to reduce the vulnerability of natural and human systems to climate change through a modification of these systems (transformation). However, there are a significant number of researchers which focused on the competition between "resilience" and "adaptation" as key responses to meeting the challenge of climate change (Adger et al., 2005; Nelson et al., 2007; Dietz et al., 2009; Brown, 2013; McEvoy et al., 2013).

The levels of climate changes will also draw the border between the adaptation approach and transformation approach (severe climate change levels) when adaptation measures can be much more disruptive and costly (NRC, 2010). A transformation process will mean the altering of fundamental attributes of a system (IPCC SREX, 2012). It may have several aims as responses to correspondent triggers (table 1)

Table 1. Transformation approach

		Transformation's triggers	
		Reaction	Action
Transformation's aim	Conservation	Responding actions after a major natural hazard event	Preparing actions for a potential major natural hazard event
	Changing	A new state	A new position

Agriculture is the sector where climate change requires a complex of measures in the frame of a holistic approach, from different angles and different perspectives. Moreover, considering that agricultural activities are by nature prone to risks and uncertainties of various nature, the processes of adaptation and/ or transformation should take in consideration that many of these risks have a climatic component and most of them will be affected by climate change, either in intensity, scope or frequency.

Climate change adaptation measures for agriculture were studied worldwide, in different contexts:

- increasing the efficiency of land drainage and irrigation systems (Bos and Nugteren, 1990; Smedema et al, 1996; Vincent et al, 2002; Ali, 2011),
- support systems for irrigation systems based on satellite data (Kustas and Anderson, 2009; D'Urso et al, 2010; Rembold et al, 2013),
- deficit irrigation (Kang et al, 2000; Fereres and Soriano, 2007; Richard and Ole Sander, 2014),
- water harvesting (Critchley and Siegert, 1991; Oweis et al, 2012),
- adapting building codes to future climate conditions and extreme weather events (Travis, 2014; Schneider, 2015),
- strategies for flood defences (Wilby and Keenan, 2012; Muis et al, 2015; Alfieri et al, 2016),
- nature-based solutions for hydro-meteorological risks.

Policies will also play an important role in enhancing the ability of agriculture to adapt to climate change, while also contributing to other environmental goals. All these aforementioned measures, as well as many others, can be organized in 3 main categories of adaptation (Wreford et al., 2010):

- Reducing the sensitivity of the affected agricultural system,
- Altering the exposure of an agricultural system,
- Increasing the resilience of the agricultural system.

However, adaptation measures in agriculture need to be sustainable, effective and efficient. The robustness to uncertainty and flexibility, the ability to change in response to altered circumstances and the avoidance of under- and over-investment in adaptation technologies are imperatives in implementing an adaptation strategy in agriculture (Wreford et al., 2010).

ADAPTING ROMANIAN AGRICULTURE TO CLIMATE CHANGES

Romania has a transitional temperate-continental climate and characterized by oceanic influences from the West, Mediterranean modulations from the South-West and excessive continental effects from the North-East. The climate data recorded over the last decades have shown a progressive warming of the atmosphere simultaneously with an increased frequency of extreme events, rapid alternations of severe heat/drought and heavy precipitation being more and more present.

From a wide perspective, the climate in Romania knew a temperature increase while the precipitations volumes remained in the same range but with several peaks, values recorded mainly in spring and autumn (figures 1 and 2).

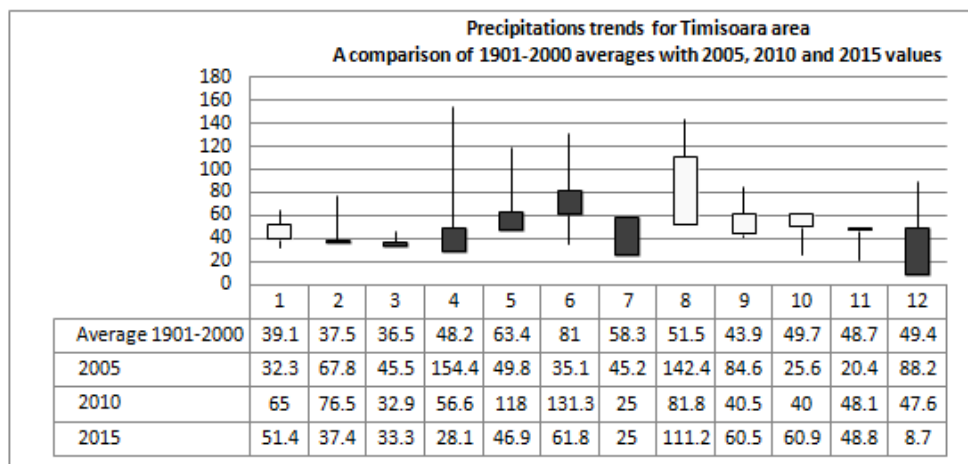


Figure 1. Precipitations trends for western Romania (Timisoara area)

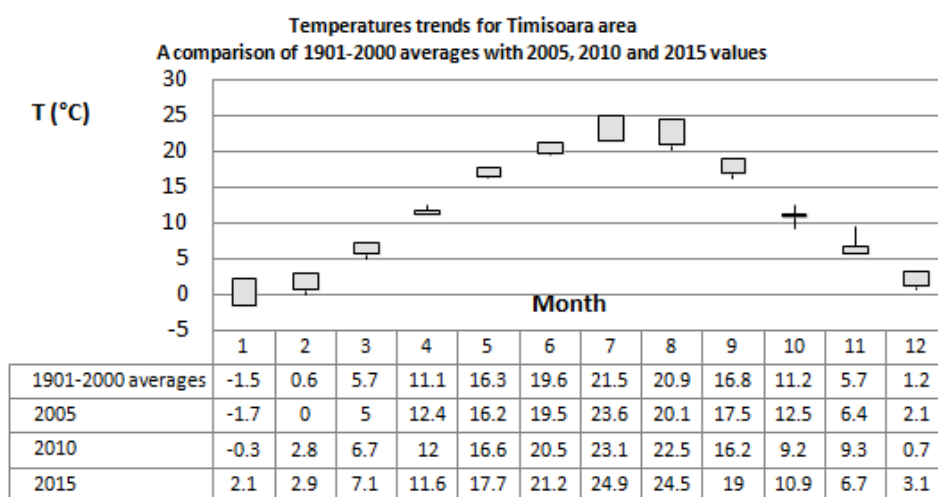


Figure 2. Temperatures trends for western Romania (Timisoara area)

The major impact of climate changes in Romania can be identified mainly in agricultural sector but also in spatial planning field. Socio-economic factors that are influencing the capacity of farmers to adapt to the effects of climate change are the following:

- characteristics of the agricultural holding;
- diversification of crops and animal husbandry as well as the availability of other sources of income;
- the access to information and knowledge on climate change and solutions to adapt to the effects of climate change
- the socio-economic context as a whole

- the access to technology and infrastructure
- the access to active intervention services in the atmosphere, preventive services acting in the sense of elimination / reduction of damages caused by dangerous meteorological phenomena

Having a significant rural population dependent on agricultural activities and one of the largest agricultural sectors in Eastern Europe, Romania made strong efforts in achieving an intensive and productive agriculture mainly during Communist period. This has been achieved by implementing land reclamation and improvement systems consisting in land drainage systems – to counter humidity excess from western Romania – respectively in large irrigation system to face drought conditions from Southern Romania. Unfortunately, many of these works were joined by severely deforestations.

For designing land drainage system can be used two major theories: the steady-state flow theory and the non-steady-state flow theory. The steady-state equations are based on the assumption that the drain discharge equals the recharge to the groundwater, and consequently that the water-table remains in the same position. In reality, water-table recharge is function of time and, as a consequence, the underground flow to drains is not constant. However, Romanian land drainage systems were designed using a methodology based on Ernst equation improved by adding a factor which introduces the effects of head losses at water entrance in drains. The solution failed to respond to current climate challenges considering that this intensive land drainage conducted to a dramatic decrease of groundwater level leading to land degradation and the need to apply irrigation measures.

The fall of the communist regime in Romania at the end of the 1989 and the beginning of a period of transition from a central planned to the market economy lead to an excessive fragmentation of land and the emergence of a large number of subsistence farms without the capacity of implementing sustainable land management measures. At the same time, after 1990s all the irrigation and land drainage works kept degrading, negatively affecting soil quality and land productivity.

In Southern Romania, what was considered to be 30 years ago a sustainable measure of land reclamation and improvement – the implementation of large irrigation systems – to the detriment of environment conservation (forests), finally proved to be a wrong measure from several environmental and economic reasons. All these large irrigation systems were high energy consumers requiring high costs for operation.

A progress in reviving the irrigation systems can be identified in western Romania, where private owners realized the importance of applying these works as measure to counteract climate changes effects. A positive example is Fantanele-Sagu irrigation system which was designed in 1966, the completing and expansion phase being finalized in 1974 for an area of 9418 ha. Major repairs were made in 2002 and since then have been executed other repairs only for maintenance and operation. Long term disposal is exceeded, from economically point of view being not viable to repair these units, the proposed solution being to replace them with modern and reliable aggregate pumping the same flow.

Considering the over 40 years of operation it was necessary to change the pumps (due to lower yields of operation), the engines and other components of these stations which don't answer to actual requirements. The rehabilitation solutions based on replacing several components with modern ones will help to improve performance of irrigation system so that it will be able to provide:

- decreasing of operating and maintenance costs by increasing efficiency and providing modern technology;
- reducing power consumption by increase efficiency in water delivery and distribution.

Other similar measures are in an incipient phase for irrigation systems located in Southern Romania but, due to lack of funds and Governmental interest, it is difficult to estimate when these measures will be completely implemented and with which effects.

Unfortunately, Romania doesn't have a tradition in using alternative resources of fresh water like water from fog and dew for additional use in irrigating small farms. There are only few studies on these aspects and without a relevant impact.

Water scarcity and water logging resulting from an increase variability of temperatures and precipitation distributions patterns presents a negative impact on agricultural productions, impact which can be reduced by implementing engineering measures. As adaptation measures aimed to mitigate these aforementioned negative effects, Romania has mainly based on applied (quantitative orientated) hydrotechnical techniques like irrigation and drainage and very less on water management in rainfed agriculture, recycled water reuse, water and land conservation and watershed management.

In 2005, severe flooding affected almost the whole Romanian territory. The pumping stations from land drainage systems were flooded or their capacity to remove the water excess was overrun. Following these events, the pumping stations located in areas prone to floods were modernized by changing the classical pumps with submersible pumps. However, these changes are not sufficient enough for mitigating the climate change effects in terms of water excess management. Large land drainage systems still suffer due to lack of maintenance, reduced capacity of water evacuation, an inadequate monitoring of these works operation in correlation with the complexity of climate change effects.

It should be mentioned the efforts in adopting and implementing specialized programs for irrigation and land drainage systems design, in modelling their hydrological effects and in understanding how they should respond to different climate change challenges. Computer engineering is an important academic field which brought a significant contribution in developing reliable tools for adapting to climate changes in different economic sectors.

Adapting building codes to future climate conditions and extreme weather events is another approach of agricultural engineering adaptation to climate changes. Currently, Eurocodes for constructions are applied in Romania, along with national standards but none of these norms and standards is directly linked to climate change being also partially outdated in terms of climate projections. Specialists in the field recommended the update and periodic revision of the parameters on which technical standards are based (temperature, humidity etc.) thus ensuring that Romania buildings are able to respond to climate variability challenges.

CONCLUSIONS

The agricultural sector is prone to substantially changes due to alterations of climate components. Adapting agriculture to climate change does not require reinventing agricultural practices. Instead, it requires adapting good agricultural practices to meet changing and often more difficult environmental conditions. Long-term planning and policy intervention as well as public policies will be necessary for sustaining the farmers in their efforts to know a smooth transition to a more resilient agricultural system. Moreover, more research is needed to assess the climate change consequences (of all kinds) at regional and local level for a better understanding of adaptation strategies and measures importance.

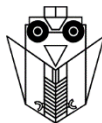
The climate change adaptation component of the National Climate Change Strategy 2013-2020 is intended to represent a general and practical approach to adaptation to the effects of climate change in Romania, providing the direction and guidance of different sectors to

establish specific action plans that will be periodically updated, taking into account the latest scientific conclusions on climate scenarios as well as sectorial needs. The exchange of information, methodologies and tools among scientists working in the field of disaster risk management and climate change management could improve the sustainability of the development process. A proactive research and education policy is needed to promote a better understanding of the impacts of climate change and the development of skills, methods and technologies to cope with the consequences of climate change. In addition, issues linking policies - including at local level - to long-term agricultural planning, adaptation of production to climate change and a strategic analysis of agro-industrial resource management are crucial for a country like Romania.

REFERENCES

- Adger, W.N., Hughes, T.P., Folke, C., Carpenter, S.R., Rockström, J. (2005). Social-ecological resilience to coastal disasters. *Science* 309(5737):1036–1039.
- Alfieri, L., Feyen, L., Di Baldassarre, G. (2016). Increasing flood risk under climate change: a pan-European assessment of the benefits of four adaptation strategies. *Climatic Change* 136:507–521.
- Ali M.H. (2011). *Practices of Irrigation and On-Farm Water Management*. Vol. 2. Springer, New York.
- Bos, M.G., Nugteren J. (1990). *On irrigation efficiencies* 4th edition. ILRI 19. Wageningen, Netherlands.
- Brown, K. (2013). Global environmental change. A social turn for resilience? *Prog. Hum. Geogr.* 38(1):107-111.
- Critchley W., Siebert K. (1991). *Water harvesting. A Manual for the Design and Construction of Water harvesting Schemes for Plant Production*. FAO, Rome.
- Dietz, T., Gardner, G.T., Gilligan, J., Stern, P.C., Vandenberg, M.P. (2009). Household actions can provide a behavioural wedge to rapidly reduce US carbon emissions. *Proc. Natl. Acad. Sci.* 106(44):18452–18456.
- D’Urso, G., Richter, K., Calera, A., Osann, M.A., Escadafal, R., Garatuza-Pajan, J., Vuolo, F. (2010). Earth observation products for operation irrigation management in the context of PLEIADeS project. *Agric. Water. Manag.* 98(2):271-282.
- Fereres, E., Soriano, M.A. (2007). Deficit irrigation for reducing agricultural water use. *Journal of Experimental Botany* 58(2):147–159.
- IPCC (2012). *Managing the Risks of Extreme Events and Disasters to Advance Climate Change Adaptation*. A Special Report of Working Groups I and II of the Intergovernmental Panel on Climate Change. Cambridge University Press, Cambridge, UK and New York, NY, USA.
- Kang, S.Z., Shi, P., Pan, Y.H., Liang, Z.S., Hu, X.T., Zhang, J. (2000). Soil water distribution, uniformity and water-use efficiency under alternate furrow irrigation in arid areas. *Irrigation Science* 19:181-190.
- Kustas, W.P., Anderson, M. (2009). Advances in thermal infrared remote sensing for land surface modelling. *Agric. Forest Meteorol.* 149:2071-2081.
- McEvoy, D., Fünfgeld, H., Bosomworth, K. (2013). Resilience and climate change adaptation: the importance of framing. *Plan. Practice Res.* 28(3):1–14.
- Muis, S., Ward, P.J., Güneralp, B., Aerts, J.C.J.H., Jongman, B. (2015). Flood risk and adaptation strategies under climate change and urban expansion: A probabilistic analysis using global data. *Science of the Total Environment* 445–457.
- National Research Council (2010). *America's Climate Choices: Panel on Adapting to the Impacts of Climate Change*. National Academic Press, Washington D.C., USA (online available at: <http://www.nap.edu/catalog/12783.html>).

- Nelson, D.R., Adger, W.N., Brown, K. (2007). Adaptation to environmental change: contributions of a resilience framework. *Annu. Rev. Environ. Resources* 32(1):395.
- Oweis, T.Y., Prinz, D., Hachum, A.Y. (2012). *Water Harvesting for Agriculture in the DA*. ICARDA, CRC Press/ Balkema, Leiden, the Netherlands.
- Rembold, F., Atzberger, C., Rojas, O., Savin, I. (2013). Using low resolution satellite imagery for yield prediction and yield anomaly detection. *Remote Sens.* 5(4):1704-1733.
- Richards, M., Ole Sander, B. (2014). Alternate wetting and drying in irrigated rice. Implementation guidance for policymakers and investors. Practice Brief. Climate Smart Agriculture. CGIAR. CCAFS. IRRI.
- Schneider, R.O. (2016). *Managing the climate crisis: assessing our risks, options and prospects*. ABC-CLIO, USA.
- Smedema, L.K., Abdel, Dayem S.M., Vlotman, W.F., Abdel Aziz, A., Van Leeuwen, H. (1996). Key note address for performance assessment of land drainage systems. Workshop on the Evaluation of Performance of Subsurface Drainage Systems. Cairo, Egypt.
- Travis, W.R. (2014). Weather and climate extremes: Pacemakers of adaptation? *Weather and Climate Extremes* 5-6 (2014):29-39.
- Vincent, B., Vlotman, W.F., Zimmer D. (2002). Performance assessment and potential indicators for drainage systems. Draft publication ICID working group on drainage (Source: <http://www.icid.org>).
- Wilby, R.L., Keenan, R. (2012). Adapting to flood risk under climate change, *Progress in Physical Geography* 36(3):348 – 378.
- Wreford, A., Moran, D., Adger, N. (2010). *Climate Change and Agriculture. Impacts, Adaptation and Mitigation*. OECD Publishing, Paris.



BRIEF INTRODUCTION ON WATER HARVESTING AND ITS POTENTIAL IN WESTERN ROMANIA

Rares HALBAC-COTOARA-ZAMFIR

Department of Hydrotechnics, Politehnica University of Timisoara,
1A G. Enescu Street, Timisoara, 300022, Timisoara, Romania
E-mail of corresponding author: rashesh_81@yahoo.com

SUMMARY

Climate change are and will continue to generate severe challenges on water resources from agricultural sector affecting aspects related to food, energy, fiber, water security etc. The existing risks will be emphasized especially in the regions where water scarcity is already a concern. A current major issue is to identify alternative solutions for covering water needs in areas where water scarcity become a current reality. One potential way of providing supplementary water is through water harvesting. Unfortunately, water harvesting is still not seen as a reliable water source in western Romania. Few studies had focused on this alternative water source. This paper will make a brief review of some water harvesting introductive aspects and will take a short look at this measure from a Romanian perspective.

Keywords: water harvesting, potential, western Romania

INTRODUCTION

In the current context of climate changes and the need of identifying sustainable solutions for climate change adaptations in all economical sectors, agricultural water engineering is the science on which we need to rely and which can be defined as being the science which deals with the design of necessary technical tools necessary to manage water in agriculture: irrigation and land drainage, water table management, water harvesting, water re-use, control of water erosion etc. Currently there is a strong need in tailoring water management strategies to meet changing local/ regional needs ensuring that water resources are developed and managed in an equitable manner. In 2013, of the 1.5 billion hectares of cropland worldwide, more than 80 percent depend on rainfall alone, contributing to at least two-thirds of global food production (Rockström et al., 2007; FAOSTAT, 2012)

A current major issue is to identify alternative solutions for covering water needs in areas where water scarcity become a current reality. One potential way of providing supplementary water is through the collection (harvesting) of precipitation, dew and fog. A special attention must be granted to rainfall pattern which is likely to know changes in the future as a consequence of climate change, situation that may affect the performance of a rainwater harvesting system.

Water Harvesting. Definition, technologies and applicability - a brief introduction

Water harvesting (WH) has been defined and classified in a number of ways by various authors over the years. In summary, we can define water harvesting as the collection and management of flood water or surface irrigation to increase the amount of water available for domestic and agricultural use, and for ecosystem maintenance. The aim of water harvesting is to collect runoff or groundwater from areas of surplus or where it is not used, store it and make it available, where and when there is water shortage. This results in an increase in water availability by either:

- impeding and trapping surface runoff;
- maximising water runoff storage;
- trapping and harvesting sub-surface water (Mekdaschi and Liniger, 2013).

The basic principle of water harvesting is to capture precipitation falling in one area and transfer it to another, thereby increasing the amount of water available in the latter. The basic components of a water harvesting system are a catchment or collection area, the runoff conveyance system, a storage component and an application area (figure 1).

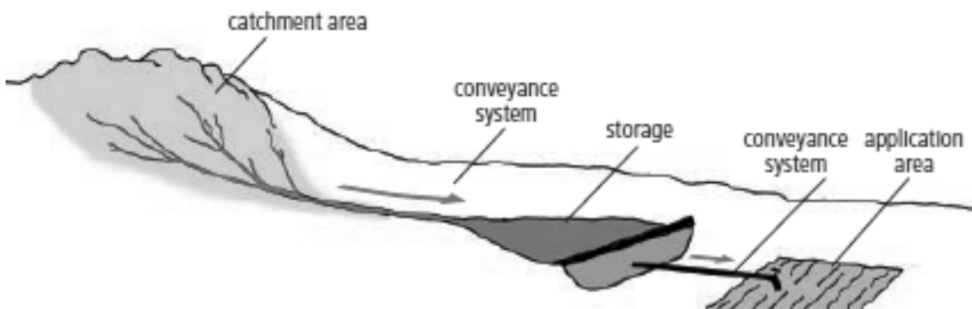


Figure 1. Basic components of a Water Harvesting systems (catchment area, storage and application area are clearly separated and connected by conveyance systems) (Mekdaschi and Liniger, 2013)

Water harvesting – together with *in situ* water conservation: can also be conceptualised within the “3R” approach (Van Steenberg and Tuinhof, 2009) where the 3Rs are “Retention, Recharge and Reuse” of water resources. In brief, this approach is based around “water buffering” where the focus is on strengthening natural processes of storing excess water, above and below ground, for later productive use and for environmental benefits.

Water harvesting is also an important part of integrated water resource management.

The applicability and impact of water harvesting technologies depend on local conditions. There are specific “pros” and “cons” associated with water harvesting. On the “pro” side, improving the efficiency with which rainfall is used reduces pressure on traditional water resources and hence on water itself (Oweis et al., 2012). Water harvesting offers a cheaper alternative to expensive water schemes in areas with low-input agriculture, particularly if the technology implemented builds on traditional practices. However, there are also hidden indirect benefits which are less obvious and more difficult to quantify. Unfortunately, water harvesting technologies also come with uncertainties and risks, first of them being their dependence on variable rainfall.

Three things are required in maximizing dew collection: maximizing surface area, finding the most effective materials that could attract and effective methods of delivering and collecting this water (Mekdaschi and Liniger, 2013).

The collection of fog water is a simple technology which is based on a mesh exposed to the atmosphere through which fog is pushed by the wind. A fraction of the fog droplets is deposited on the mesh material by impaction and, when more and more fog droplets are deposited, they combine to form larger droplets which run down the mesh material into a collector. A typical fog collector is made of fine-mesh net. The mesh is often suspended 1.5 m above the ground between two vertical posts. The size of the collector depends on topography and the intended use of the water. Differences between various fog collector designs exist regarding their size and shape, as well as the mesh material used. A FCS has a $1 \times 1 \text{ m}^2$ surface, with a base 2 m above ground and is installed perpendicularly to the wind direction that is associated with the occurrence of fog. It has now been used to measure fog fluxes in about 40 countries.

Fog and dew collecting structures were extensively studied in countries affected by water scarcity or where the pressure on surface water resources is very high. A “Fog water collector”, was implemented for the first time in the mid-eighties by the Meteorological Service of Canada (MSC) on Mount Sutton – Quebec, with the aim of studying the constituents of the collected fog. However, the most successful and documented project regarding drinking water collection, took place since 1990 in El Tofo Mountain for use in the community of Chugungo in northern Chile (Dale, 2013), initiative of the National Forest Corporation and the Catholic University of Chile, with funding of the International Development Research Centre (IDRC) and the collaboration of the MSC from Canada. Soon after, non profit organizations set up facilities in Yemen, Chile, Guatemala, Haiti and Nepal. The easy, inexpensive fabrication of those devices make possible that villagers from 25 countries worldwide use them. Furey (1998), besides a review of current status, also describes detailed technical design in a pilot study. A number of other summaries of fog collection experiments have been made (e.g., Kerfoot, 1968; Stadtmuller, 1987; Schemenauer and Cereceda, 1991; Vong et al., 1991). Some of them clearly show the importance of fog as a wet deposition pathway (Schemenauer and Cereceda, 1994).

Dr. Benz Kotzen (Kotzen, 2015) made a valuable long study focusing on maximizing dew collection using new and novel forms and materials commenced with a literature review and then the testing of nearly two hundred materials and forms using a dew simulation chamber. The research asserts that whereas present and past dew collection studies have focused on passive slippery, hydrophobic, inclined planar forms, that there are other forms that show potential for collecting dew. His research presents a number of potential new paths for maximizing dew collection which should be taken further and tested in the field. Unfortunately, Romania doesn't have a tradition in using alternative resources of fresh water like water from fog and dew for additional use in irrigating small farms.

WATER HARVESTING AND SOME CONSIDERATION OF ITS POTENTIAL IN WESTERN ROMANIA

For an efficient use of water harvesting techniques, these should be approached as parts of integrated water resources management. Hudson (1987) proposes four different water management strategies:

- Management of excess water from rainfall or seasonal flooding through controlled drainage and water storage for future use - most suitable in humid and sub-humid conditions as well as semi-arid and arid conditions (floodwater harvesting)
- Increasing rainwater capture and availability, making use of surface runoff; suitable for dry sub-humid to arid conditions (rainwater harvesting)
- Reducing *in situ* water loss: improving direct water infiltration and reducing evaporation; soil water conservation practices that prevent surface runoff and keep rainwater in place (e.g. conservation agriculture, level bench terraces, mulching, dew harvesting); suitable for sub-humid to semi-arid conditions (*in situ* water conservation).
- Increasing water use efficiency (e.g. good agronomic practice, including use of best-suited planting material and fertility management).

Western Romania is also frequently affected by water excess, this periods alternating with drought events of different intensities. The climate of the studied territory is characterized by great complexity and diversity of atmospheric phenomena that often give rise to periods of long lasting high rainfall. Rainfall has a predominant role in the formation and maintenance of excess moisture. The relief is a factor that determines, together with rainfall, flooding and water excess due to its diversity and distribution of natural units according to their average altitude. The phenomena of floods and the excess water occur mainly in low fields and meadows where, because of the plan relief and strong decrease of water flow, they accumulate in large quantities on the surface, flows and stagnate at soil surface. The management of water excess in this area is based on land drainage arrangements which were implemented since the second half of XX century.

Unfortunately, all the water drained by these systems is evacuated in surface water bodies affecting their quality. However, the current state-of-art will be highly affected by climate changes in the next decades, part of the impacts being already visible. An EEA study from 2012 indicates that Romania will know a decrease in summer precipitations even at annual level, precipitations volumes will know an ascendant trend (figure 2).

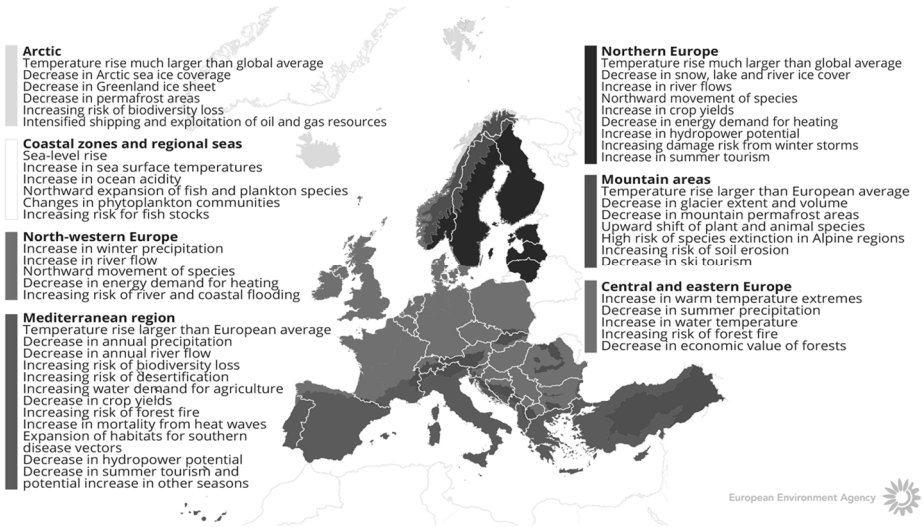


Figure 2. Key observed and projected impacts from climate change for the main regions in Europe (EEA, 2012)

An analysis of the values provided by regional climatological centre indicated that in comparison with the precipitation average for 1901-2000, the annual precipitations for 2005 – 2015 seem to know a decreasing trend. Overall, the differences are not highly visible and their influence on rainwater harvesting is reduced (figures 3 and 4).

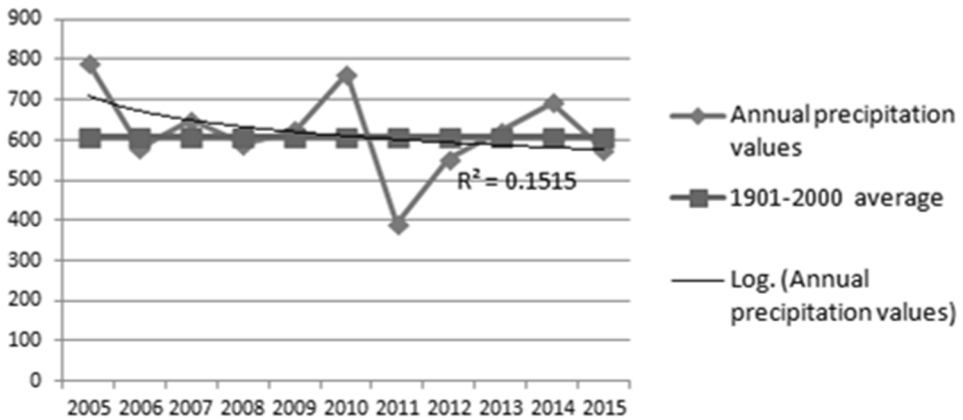


Figure 3. Trend of annual precipitations between 2005 and 2015 in comparison with 1901-2000 period average

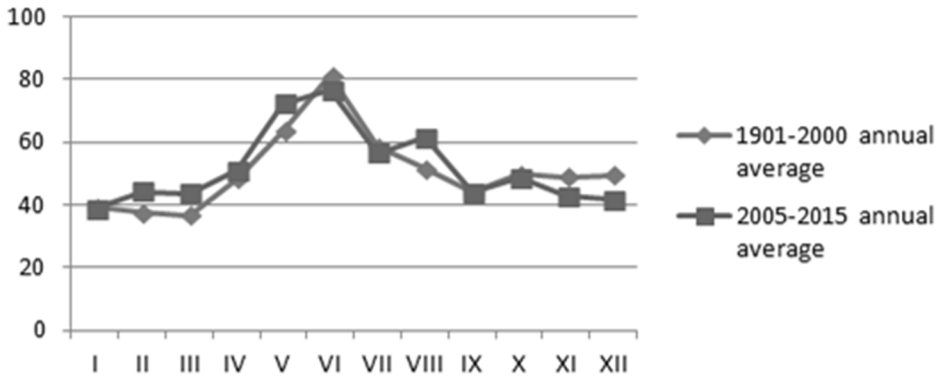


Figure 4. Comparison of 1901-2000 multi-annual monthly averages and 2005-2015 multi-annual monthly averages

From previous figures we can observe that during critical period for agricultural crops (autumn, spring), the precipitations volumes are quite low, sometimes even last century average. Moreover, the lack of solid precipitations in winter may lead to freezing crops mainly in January and February when western Romania is usually affected by frosts (sometimes for up to 2 weeks long and with values around -15°C - -20°C).

The peak of annual precipitations in western Romania can be identified in May and June with a second high levels period in August. Unfortunately, this distribution can't contribute in a significant manner in emphasizing agricultural productions. Moreover, rainwater harvesting using collectors (barrels, pipes etc.) in western Romania is almost inexistent. Some farmers use to collect rainwater in big barrels for different purposes but the process is not known as a best-practice for agricultural purposes.

As a best-practice in collecting rain water for agricultural purposes, we can identify vineyard digging. Vineyard digging is a very old land management practice having several purposes mainly related to quantitative and qualitative aspects of grapes production. Basically, this practice is referring to covering and digging up the lower part of the trunks in autumn and spring seasons and adding manure for increasing soil fertility. This work has as main aim to protect the plant against winter cold. Following the discussions with several local owners of vineyard, we discovered that there are no ecological or environmental sustainable issues considered in this practice. By digging up the lower part of trunks in spring there are created some low dikes which have an important role in harvesting the rain water, mitigating surface runoff, increase water infiltration and offer protection against soil erosion. As mentioned before, these potential benefits don't constitute the main reasons for farmers in practicing vineyard digging.

Being located in an area where summers can be very dry, these dikes can provide support in water harvesting for vineyard, this being important source water considering the lack of other resources in the near areas. Vineyard digging also can aim at optimizing wine production by reducing competition for water and nutrients between grapevines and weeds and by preventing the outbreak of pests and diseases.



Figure 5. Vineyard having small dikes parallel with the slope

The Standard Fog Collector (SFC) is mainly used in exploratory studies to evaluate the amount of fog water that can be collected at given sites. The construction and use of this flat mesh panel is described in detail in Schemenauer and Cereceda (1994). The SFC has a $1 \times 1 \text{ m}^2$ surface, with a base 2 m above ground and is installed perpendicularly to the wind direction that is associated with the occurrence of fog. It has now been used to measure fog fluxes in about 40 countries. The collection rate of a fog collector is determined by the fog liquid water content (LWC), the size distribution of fog droplets, the size and arrangement of the mesh material, and the wind speed.

Girja Sharan (2011) made a review of peak dew collections in one night from artificial surfaces at various locations and mentioned for Romania a value of 0.17 mm/night. However, it is not presented the source of this information, the structures which were used and/or the area from which it was collected.

Unfortunately, given the lack of information on the number of days with fog (this number can be estimated, based on an analysis of surrounding areas, at 30 days/ year) and considering that the water quantities resulted from dew collection is very low, we can conclude that, at this for the moment, water harvesting from fog and dew is not a reliable resource for agricultural purposes in western Romania.

CONCLUSIONS

Current challenges like climate change, increasing population, growing shortages of safe drinking water emphasize the importance of implementing a sustainable water management. Water harvesting can represent a long-term solution for these problems but initiatives are still too scattered, and experiences related to “best” WH practices are poorly shared. Moreover, Policies, legal regulation and governmental budgets dedicated to water

harvesting are almost inexistent and very often fail to include this practice in integrated water resource management.

Even water harvesting is being increasingly promoted as a coping strategy, socio-economic, institutional and human/ cultural aspects as well as appropriate approaches are crucial for successful implementation. In addition, the use of subsidies and incentives and the capacity building are key aspects behind adoption and upscaling water harvesting best practices.

In Romania, water harvesting from precipitations is still at a very incipient phase, mostly used for small scale purposes. Regarding the water harvesting from fog and dew, they are not considered reliable resources for agricultural purposes in western Romania

REFERENCES

- Dale, S. (2013). Collecting fog on El Tofo. International Development Research Centre. IDRC publications, Ottawa.
- EEA (2012). Climate change, impacts and vulnerability in Europe 2012. An indicator-based report. EEA Report No 12/2012. European Environment Agency. Copenhagen, Denmark
- FAOSTAT (2012). Database. Food and Agriculture Organization (FAO), Rome (accessed October 2016).
- Furey, S.G. (1998). Fogwater harvesting for community water supply. MSc Thesis. Cranfield University, UK.
- Hudson, N.W. (1987). Soil and water conservation in semi-arid areas. Food and Agriculture Organization of the United Nations (FAO). Rome, Italy.
- Kerfoot, O. (1968). Precipitation on vegetation. *Forest Abstract* 29:8-20.
- Kotzen, B. (2015). Innovation and evolution of forms and materials for maximising dew collection. *Ecocycles* 1(1):39-50.
- Mekdaschi, S.R. and Liniger, H. (2013). Water harvesting: guidelines to good practice. Centre for Development and Environment (CDE). Bern. Rainwater Harvesting Implementation Network (RAIN). Amsterdam. MetaMeta. Wageningen. The International Fund for Agricultural Development (IFAD), Rome.
- Oweis, T.Y., Prinz, D., Hachum, A.Y. (2012). Water Harvesting for Agriculture in the DA. ICARDA. CRC Press/ Balkema, Leiden, the Netherlands.
- Rockstrom, J., Karlberg, L., Wani, S. P., Barron, J., Hatibu, N., Oweis, T., Bruggeman, A., Farahani, J., Qiang, Z. (2010). *Agricultural Water Management* 97:543–550.
- Schemenauer, R.S. and Cereceda, P. (1991). Fog water collection in arid coastal locations. *Ambio* 20:303-308.
- Schemenauer, R.S. and Cereceda, P. (1994). A proposed standard fog collector for use in high-elevation regions. *J. Applied Meteorology* 33(11):1313-1322.
- Sharan, G. (2011). Harvesting dew with radiation cooled condensers to supplement drinking water supply in semi-arid coastal Northwest India. *International Journal for Service Learning in Engineering* 6(1):130-150.
- Stadtmuller T. (1987). Cloud forests in the humid tropics. The United Nations University, USA.
- Van Steenbergen, F., A. Tuinhof. (2009). Managing the Water Buffer for Development and Climate Change Adaptation: Groundwater Recharge, Retention, Reuse and Rainwater Storage. UNESCO International Hydrological Programme. Paris, France.
- Vong, R.J., Sigmon, J.T., Mueller, S.F. (1991). Cloud water deposition to Appalachian Forests. *Environ. Sci. Technol.* 25:1014-1021.



ASSESSING THE RISK OF ARIDITY - A CASE STUDY BUCHAREST ROMANIA

Carmen Otilia RUSĂNESCU^{1*}, Marin RUSĂNESCU², Mihaela BEGEA¹,
Gigel PARASCHIV¹, Sorin Ștefan BIRIȘ¹, Gheorghe VOICU¹,
Ileana Nicoleta POPESCU³

¹ Faculty of Biotechnical Systems Engineering, Polytechnic University of Bucharest,
Splaiul Independenței no 313, București 060042, Romania

² Valplast Industrie Bucharest, Precise, no. 9, Bucharest, Romania

³ Faculty of Materials Engineering and Mechanics, Valahia University of Targoviste,
Aleea Sinaia nr.13, 130004, Târgoviște, Romania

*E-mail of corresponding author: rusanescuotilia@gmail.com

ABSTRACT

In this paper, aridity from Bucharest Romania, was analyzed on the basis of de Martonne aridity index. The de Martonne aridity index characterize aridity and allows delineation arid climates or humid and semi-humid or semi-arid. The topics of research are environmental and agricultural topics and the results of research can be used in environmental engineering and agriculture.

We calculated the annual Lang rain factor. Lang rain factor highlights succession of rainy and dry months, taking into account the report of precipitation / temperature as an expression of incoming and outgoing water from the system. Lang rain factor values indicate a semiarid climate in years: 2009, 2010, 2011, 2012, 2013, 2015 and humid year in 2014.

We studied the Emberger's pluviothermic index in order to characterize the aridity of the climate, according to the average maximum temperatures of the warmest month and averages minimum temperatures of the coldest month as well as annual average (precipitation), surprising influence of relative humidity on climate. Based on Emberger's pluviothermic index, the obtained values indicate a semi-humid climate in years 2011, 2012 and humid climate in the years 2009, 2010, 2013, 2014, 2015.

It was observed that in the analyzed period, according to all calculated indices Bucharest is characterised by a semi-humid and humid climate with exception of some months in the period where semiarid climate was determined.

Key words: Aridity; Martonne Index; Lang rain factor; Emberger's pluviothermic index, vegetation

INTRODUCTION

Bucharest is located in the S-SE Romania, having the geographic coordinates between 25°49'50 and "26°27'15" eastern longitude (this coordinated marks ground zero for Romania in terms of land; it is marked by monument in front of the church of St. George) and between 44°44'30 and "44°14'05" north latitude, consisting of two administrative units: Bucharest (the capital) and Ilfov who in 2012 comprised 8 cities, 32 communes and 91 villages. The Bucharest area is 1821 km², representing 0.76% of the total area of Romania. Bucharest region is bounded by the counties of Prahova (N), Ialomita (E-NE), Calarasi (E-SE), Giurgiu (S-SW) and Dambovita (V-NV) (Ioja, 2009).

Bucharest is a city of plain flora and fauna of the temperate continental steppe grass. Flora consists mainly of trees ranging from hardwoods (oak, beech, chestnut, linden, willow floodplain rivers), fruit trees (plum, apricot, apple, pear, cherry, etc.) and shrubs (wild plums, wild rose, blackthorn, rosehip dwarf), colorful flowers and rich (chamomile, poppies, roses, cornflowers, daisies). The climate and topography in the surroundings of Bucharest are suitable for agriculture: cultivation of crops, vegetables and fruit trees. In addition, wild plants and damaging crops (which man tries to destroy-weeds) are growing. In forests, a wide variety of fungi, ferns and moss are growing (Rusănescu, 2014).

Bucharest falls into the category of large conurbations located in southeastern Europe, characterized by an anthropic environment generated by its own spatial development in historical time.

Precipitation is an important meteorological parameter in assessing air quality by cleaning air in the lower layer, where industrial activities take place (Ioja, 2009). To prevent and combat the negative effects in theory and application by providing usable reserves of soil moisture as a source of food rivers it is very important to know annual and multiannual precipitation scheme, its variability over time, frequency form and intensity (Stoica and Rusanescu, 2013a). The energy that contain precipitation is divided into two, the kinetic energy of precipitation (force their flick direct role in the destruction of aggregates from soil) and their energy potential, energy runoff on slopes and whites, with a role in detachment and transport parts of broken rock in its path (Stoica and Stanciu, 2013).

In Romania, the drought is determined by the prolonged activity of the high barrier centers, i.e. the anti-cyclones which bring air masses with high thermodynamic stability and with a very low content of water vapour (about 5 mg / m³). These qualities of thermal and hygrometric enhances evapotranspiration leading to decreased soil water reserves and the emergence imbalance between increased water needs of the plants and diminished soil resources.

Dry periods that affected Romania were determined by persistent anticyclonic ridges type or type Azores High North African and even due to Scandinavian anticyclonic cores, supported by a free troposphere forever constant and tropical strong current from the southwest, warm and dry (Rusanescu et al, 2010).

The average duration of meteorological droughts in Romania, is between 16 days and 19 days in the western regions while in the eastern peak times it exceeds 60 days (Ioja, 2009).

In agriculture, it is very important to know the phenomena of dryness and drought (Stoica and Rusanescu, 2013b). Considering the increase in global warming (Rusanescu and Stoica, 2013), it is important to know the dryness and drought phenomena in order to cultivate appropriate crops in agriculture (Rusanescu and Stoica, 2013). It is important to correlate soil conditions and hybrids: a hybrid of corn with a long growing season (sown in April and harvested in November) should have a big yield (Rusanescu and Rusanescu, 2016). But it

takes the extreme temperature range during the flowering period when it needs water. The measure is to be replaced by a semi-hybrid, which yields stable crops (Rusanescu et al, 2016).

The climate particularities of a territory determine the spatial distribution of living creature communities, therefore materialize on a regional scale in bioclimatic conditions. Ecological potential and suitability of climatic conditions for the development of plant groups is reflected in the values of the main indices climatic ecometrics (Pătroescu, 1987).

In arid zone, water that exits from the system exceeds constant inputs. Currently more than a third of Earth's land is affected by aridity (Păltineanu et al, 2007).

Climatic aridity concept is characterized by low precipitation (arid period, arid year). The main factors that influence aridity are: precipitation, temperature, continental, albedo, etc. In terms of biogeography, insufficient water in the soil increase plant species production deficit and create gaps in vegetation cover. The influence of precipitation on plants plays an important role especially if their values are correlated with temperature values, resulting in indication of ecoclimatic indices to the degree of favourable climate for the cultivation and spontaneous species growth (Kuti et al., 2006, Szabados, 2006, Rusănescu et al., 2016).

In the present paper, to analyze the aridity phenomenon in Bucharest, the following indices were used: Aridity index of de Martonne, Lang rain factor, Emberger's pluviothermic index. It is recommended that technological measures for land preservation, follow-up of ecoclimatic indicators to develop a complex database in order to prevent and mitigate risk situations in agriculture (Stoica and Rusanescu, 2013b). By applying measures which reduce water losses from the soil, the soil water supply is maintained or enhanced (Stoica et al, 2015).

Among the anthropic factors that cause desertification, the most important are: severe reduction of areas occupied with forest vegetation, overburden, soil erosion, soil degradation in organic matter, salinisation, and chemical pollution (Rusanescu, 2014).

MATERIALS AND METHODS

In this paper, precipitation and temperature data recorded by weather station situated at the Faculty of Biotechnical Systems Engineering from Polytechnic University of Bucharest, (44.438°N Latitude, 26.047°E Longitude and 76.6 m elevation) were used.

AWS weather station model / EV, produced by Elettronica Veneta in 2007 has a range wireless transmission up to 300 m and integrated set of sensors, stanchion 1.77 m and related tripod. It is equipped with sensors for acquisition of meteorological parameters: temperature, pressure, relative humidity, wind direction and speed, precipitation, solar radiation intensity. Data is transmitted every hour throughout the day at the site. The system enables instant viewing of measurements of mentioned meteorological parameters. The measured values are transmitted from hour to hour throughout the day at the work point. The system allows instantaneous viewing of the meteorological parameter measurements (Technical Weather Station, 2009).

The maximum measurable intensity of precipitation is 0-300 mm / h.

Aridity index of de Martonne

Aridity index of de Martonne characterize aridity and allows delineation arid climates or humid and semi-humid or semi-arid. The classification is presented in table 1.

Table 1. Numerical index correlation with appropriate climate according to Aridity index of de Martonne (Gaceu, 2002; Dumitrașcu, 2006; Ioja, 2009; Satmari, 2010)

I _a	Climate
0-5	Hyper arid (absolute deserts, extremely arid)
5-15	Arid (desert regions)
15-20	Semi-arid
20-30	Semi-humid
30-60	Humid
>60	Very humid

Numerical values of index in correlation to vegetation areas and floors according to de Martonne are reported in table 2.

Table 2. Interpretation of aridity index according to de Martonne (Ioja, 2009)

I _a	Vegetation areas and floors
> 50	Alpine floor
45-50	Floor subalpine
40-45	Coniferous forests
35-40	Mixed forests
30-35	Beech forests
25-30	Oak Forest
20-25	Steppe
15-20	Tall grass steppe
10-15	Steppe grasses low
5-10	Arid zone
0-5	Extreme arid zone

Aridity index of de Martonne is calculated using equations 1 and 2.

$$I_{annual}dM = \frac{P}{T + 10} \quad (1)$$

where: P - annual precipitation (mm), T - the average annual temperature of the denominator additional intervening 10 °C, to obtain positive results in the regions with negative annual thermal environments, such as deserts or alpine mountain regions at mid-latitudes.

$$I_{lunar}dM = \frac{12P_i}{T_i + 10} \quad (2)$$

where: P - Monthly precipitation (mm), T -The average monthly air temperature (°C)

Lang rain factor

Lang rain factor is calculated for annual intervals for the months included in the growing season (Gaceu, 2002; Păltineanu et al., 2007). Lang rain factor highlights succession rainy and dry months, taking into account the report of precipitation / temperature as an expression of incoming and outgoing water from the system.

G. Manea noted that the limit of tree vegetation and steppe vegetation corresponds to areas where the index falls below 10 units, while the transition from steppe to desert vegetation is marked by values fall below 5 units (Manea, 2011).

According to the formula 3 humidity of a territory varies directly proportional with total annual precipitation and inversely proportional with the average annual temperature.

This is an example of an equation:

$$L = \frac{P}{T} \tag{3}$$

where: P – Total annual amount of precipitation; T - average annual temperature

Table 3 Presents numerical correlation between Lang rain factor and climate index characteristic of the area.

Table 3. Numerical correlation of Lang rain factor and climate characteristic (Barbu, 2001; Mărunțelu et al., 2013)

L	Climate characteristic
70<L<1000	Humid
40 <L<70	Semiarid
20<L<40	Mediterranean
L<20<0	Arid

Emberger’s pluviothermic index

Emberger’s pluviothermic index characterizes the degree of aridity of the climate, and is influenced by the annual amount of precipitation and the maximum and minimum annual air temperature (Runcanu et al., 2014).

This is an example of an equation:

$$Q = \frac{100 \cdot P}{M_i^2 - m_i^2} \tag{4}$$

where P - annual amount of precipitation, M_i^2 - maximum annual air temperature, m_i^2 – minimum annual air temperature

The types of climate according Emberger’s pluviothermic index are presented in table 4.

Table 4. Types of climate according Emberger’s pluviothermic index (Ioja, 2009)

Q	Climate
>90	Humid
50-90	Semi-humid
30-50	Semiarid
0-30	Arid

RESULTS AND DISCUSSION

Aridity index of de Martonne

Aridity was analyzed on the basis of de Martonne aridity index.

Aridity index of de Martonne expresses the restrictive nature of climate conditions for certain plant formations, it is calculated at annual and monthly bases and, was introduced in 1926 (De Martonne, 1926; Pătroescu, 1987; Quan et al., 2013; Some'e et al., 2013).

Based on precipitation and temperature values recorded by the weather station during the years 2009-2016 in Bucharest, de Martonne aridity index was calculated and semi-humid to humid climate was determined (figure 1).

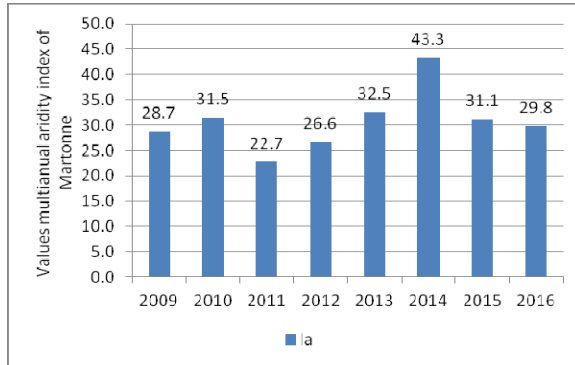


Figure 1. The multi-annual de Martonne aridity index calculated for Bucharest during the period 2009-2016

The multiannual values of de Martonne aridity index for Bucharest during the period 2009-2016 were classified as follows: in 2009 value 29.4 was determined which corresponds to the semi-humid climate, this climate is appropriate for vegetation of oak forests; for 2010, 31.5 humid climate, this climate is appropriate for vegetation of beech forests; for 2011, the value obtained was 22.7, semi-humid climate, steppe vegetation; 2012 26.3, semi-humid climate, forests of oak; 2013 and 2016 (26.4 and 29.8), semi-humid climate, beech forests; 2014 value of 40.9, corresponding to humid climate, vegetation coniferous forests; 2015 value of 31.6 humid climate, vegetation corresponding beech forests (Figure 1).

The distribution of de Martonne aridity index values in Romania was the subject of research of several researchers: Dumitrașcu, (2006); Păltineanu et al., (2007); Khalili et al., (2011); Croitoru and Piticar, (2013) also in other countries such as Deniz et al. (2011) and Rahimi et al. (2013).

Table 5. Average monthly de Martonne index of aridity calculated for Bucharest

IIdM	I	II	III	IV	V	VI	VII	VIII	IX	X	XI	XII
2009	53.7	38.2	27.2	8.6	24.2	35.4	48.5	24.0	26.7	32.7	15.6	5.9
2010	37.5	93.4	37.1	26.9	48.0	40.3	24.0	8.5	13.7	40.3	10.9	69.6
2011	25.9	16.7	4.2	19.6	59.5	29.5	25.5	18.9	0.0	21.1	2.3	41.4
2012	81.6	42.9	9.1	25.6	81.7	12.9	9.0	13.1	17.1	12.1	8.9	94.0
2013	77.4	45.2	51.0	16.0	35.3	48.6	11.3	21.2	36.8	42.9	27.1	0.4
2014	96.4	0.4	31.8	61.6	57.8	61.4	23.6	20.6	19.9	35.7	30.0	163.8
2015	38.7	37.5	71.8	25.9	20.3	22.8	20.3	29.8	32.5	34.1	63.2	1.6
2016	23.1	12.8	47.0	34.3	37.8	39.4	5.3	38.0	7.7	70.6	30.7	6.7
2009	humid	humid	semi-humid	arid	semi-humid	humid	humid	semi-humid	semi-humid	humid	semiarid	arid
2010	humid	humid	humid	semi-humid	humid	humid	semi-humid	arid	arid	humid	arid	very humid
2011	semi-humid	semiarid	hyper arid	semiarid	humid	semi-humid	semi-humid	semiarid	hyper arid	semi-humid	hyper arid	humid
2012	very humid	humid	arid	semi-humid	very humid	arid	arid	arid	semiarid	arid	arid	very humid
2013	very humid	humid	humid	semiarid	humid	humid	arid	semi-humid	humid	humid	semi-humid	hyper arid
2014	very humid	hyper arid	humid	very humid	humid	humid	semi-humid	semi-humid	semiarid	humid	semi-humid	very humid
2015	humid	humid	very humid	semi-humid	semi-humid	semi-humid	semi-humid	semi-humid	humid	humid	very humid	hyper arid
2016	semi-humid	arid	humid	humid	humid	humid	arid	humid	arid	very humid	humid	arid

I, II, III, IV, V, VI, VII, VIII, IX, X, XI, XII - months of the year

Analyzing the average monthly aridity index of de Martonne (Table 5) we observed that 2009 was characterized by a distribution range of values index of aridity of Martonne with high humid climate in February (38.2), June (35.4), July (48.5), September (32.7); semi-humid climate in the months: March (27.2), May (24.2), August (24) September (26.7); arid climate in the months: April (8.6), December (5.9).

For 2010, the mean index of de Martonne ranged from 8.5 in August (arid climates) to 69.6 in December very humid climate, February 93.4 very humid climate, humid climate in the months: January, March, May, June, October; semi-humid climate in the months: April, July; arid climate in the months: August, September, November.

Hiperarid climate in September 2011, March and November; semiarid climate in the months: February, April, August; in semi-humid climate: January, June, July, October; humid climate in May and December.

Year 2012 is presented below, according to the aridity index values of de Martonne arid climate in the months: March, June, August, October, November; semiarid climate in September due to high temperatures and the reduced amounts of precipitation for the period. Semi-humid climate in April; humid climate in February; very humid climate in the months: January, May and December.

2013 hiperarid climate in December, in arid climates: April and July; semi-humid climate in August and November; humid climate in the months: February, March, May, June, September, October; very humid climate in January.

2014 is characterized by climate hiperarid in February; semi-humid climate in September; humid climate in the months: March, May, October, November; very humid April, January, June, and December. The climate is hiperarid in December 2015 due to lack of precipitation, semi-humid in May; June July August; humid climate in January, February, September, October; very humid climate in March and November.

Average monthly analysed data indicate a slight aridity of the climate due to the urban environment, drawing attention to assessing the correct ratio between oxygenated surface and built surface in Bucharest.

De Martonne aridity index during the period July-September in Bucharest indicate monthly values between 8.5 and 20.5, which explains the phenomena of drying trees occurring in July (Pătroescu, 1987; Dragotă, 2003; Rusănescu and Rusănescu, 2016; Rusănescu et al., 2016).

Monthly de Martonne index values are representative values below 5 and 5-10, which indicate desert and semi-desert climate characteristics, involving a careful approach on the adaptation of species of crops and green spaces, irrigation systems design, management degradation sources air quality, energy consumption (especially in summer when use of air conditioners is a must). Determined monthly values are also important, i.e. above 90 in December and January 2014 indicates the existence of low temperatures and high precipitation amounts and highlights the importance and the emergence of the planning for town and country (impact assessment precipitation, energy consumption, the impact on crops).

In August, downward trend of the monthly averages of de Martonne aridity index is observed. Aridity index values of de Martonne draw attention to the Bucharest vulnerability to drought with implications for agricultural production, what leads to rising cost of living.

Lang rain factor

According to the numerical correlation of the Lang rain factor and climate characteristic (Table 3) and the results obtained in Figure 2 show that can be seen that Lang rain factor values are between 41.2 and 75.7, indicating a semiarid climate in years: 2009, 2010, 2011, 2012, 2013, 2015, 2016 and humid in 2014. Percentage analysis of determined annual values of Lang rain factor in the period 2009 - 2016 in Bucharest shows that 85.71% of the values are in the range between 40-70 (semiarid climate properly), and 14.29% of the values are greater than 70 (corresponding to humid climate).

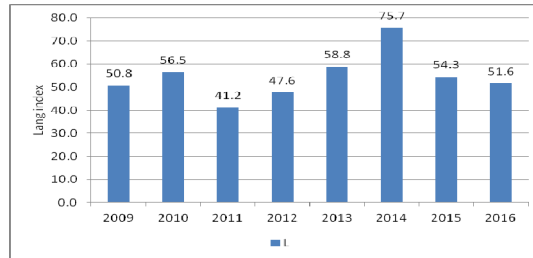


Figure 2. Lang rain factor for Bucharest during period, 2009-2016

Emberger's pluviothermic index

According to the Emberger's pluviothermic index are presented in Table 4, the results obtained and presented in Figure 3 show that, 2011 and 2012 years have semi-humid climate and the years 2009, 2010, 2013, 2014, 2015, 2016 humid climate.

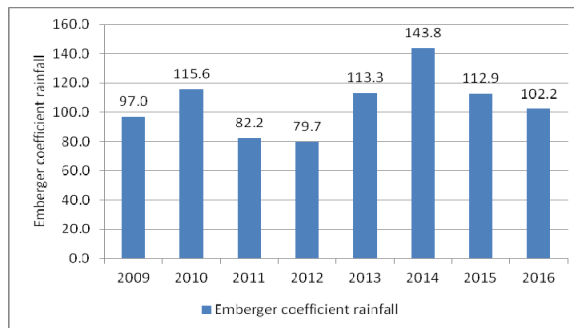


Figure 3. Values obtained values for Emberger's pluviothermic index in Bucharest (2009-2016)

CONCLUSIONS

The influence of the urban environment can cause changes in precipitation production. The effect of "heat island" can cause greater amounts of precipitation in cities. According to Lang rain factor, during the period 2009 – 2016, Bucharest is characterised by semiarid and humid climate.

Values of de Martonne aridity index during the years 2009-2016 indicated semi-humid and humid climate, vegetation appropriate for forests of oak, beech and steppe vegetation. Analysis of the monthly averages of de Martonne aridity index shows a reduced tendency to aridity due to urban environment climate, drawing attention to assessing the correct ratio oxygenated surface / surface built in Bucharest, explaining drying trees and vegetation since July.

Based on Emberger's precipitation coefficient values, the years 2011 and 2012 were characterised by semi-humid climate and the years 2009, 2010, 2013, 2014, 2015, 2016 by humid climate. All calculated indices have revealed in Bucharest a semi humid, humid and semiarid climate.

To avoid aridization of Bucharest the following is recommended: planning with alternating water bodies and lakes, forests, arable fields; minimal tillage of the soil (plowing is not recommended, because it would eliminate existing water); water conservation. Mentioned measures would include collection of precipitation in the tanks during winter time, by keeping plant debris on the ground (for example, winter corn stalks left on the field, and the snow would help to build water coming in spring).

Suitable culture should be chosen based on correlation of hybrids with soil and climate conditions. Floods are a natural phenomenon worsened by deforestation, hydrological planning and spatial planning as well as climate change have altered the way in which they occur.

Measures to limit and counter the effects of drought as climatic phenomenon with major risk to agriculture is the use of biological material resistant to water stress and heat and the use of agro-technical measures favorable for accumulation, conservation and the efficient use of water from precipitation, using a system of conservation agriculture based on soil protection and avoid desertification. Irrigation must be done during dry periods, especially when it overlaps periods with temperatures above 32 °C from June to August.

ACKNOWLEDGEMENT

This work was supported by Romanian national project PN-III-P2-2.1-BG-2016-0238 / Contract 22BG - Utilization in agriculture of by-products resulted from the manufacture of baker's yeast.

REFERENCES

- AWWS / EV, (2009). Weather Station Technical Paper from Elettronica Veneta.
- Barbu, I. (2001). Monitoring risk of droughts in the forests of Romania, Bucovina forestry, IX, 1-2, 37-51.
- Croitoru, A.E., Piticar, A. (2013). Changes in daily extreme temperatures in the extra-Carpathians regions of Romania. *International Journal of Climatology*, 33, 1987-2001.
- Deniz, A., Toros H., Incecik, S. (2011). Spatial variations of climate indices in Turkey, *International Journal of Climatology*, 31, 3, 394-403.

- De Martonne, E. (1926). Une nouvelle fonction climatologique: L'indice d'aridité, *La Meteorologie*, 449-458.
- Dragotă, C. (2003). Angot monthly precipitation index, indices and quantitative methods used in climatology, University of Oradea, 11-12.
- Dumitrașcu, M. (2006). Changes in Oltenia Plain Landscape, Romanian Academy Publishing House, Bucharest.
- Gaceu, O., (2002). Elements of practice climatology, University of Oradea.
- Iojă, I., (2009). Methods and techniques for assessing the environmental quality of the area metropolitană Bucharest.
- Khalili, D., Farnoud, T., Jamshidi, H., Kamgar-Haghighi, A.A., Zand-Parsa, S. (2011). Comparability Analyses of the SPI and RDI Meteorological Drought Indices in Different Climatic Zones, *Water Resources Management*, 6, 25, 1737-1757.
- Kuti, L., Kerek, B., Vatai, J. (2006). Problem and prognosis of excess water inundation based on agrogeological factors, *Carpatian Journal of Earth and Environmental Sciences*, 1, 1.
- Manea, G. (2011). Biogeography Elements. Bucharest: University Publishing House
- Mărușel, N., Istode, L., Coman, A. (2013). Ecometrici clues, modern tools used to monitor the evolution of ecosystems, biodiversity conservation and optimizing the design of ecological house, Bucharest.
- Păltineanu, C., Tănăsescu, N., Chițu, E., Mihăilescu, I. F. (2007). Relationships between the De Martonne aridity index and water requirements of some representative crops: A case study from Romania. *Int. Agrophysics*, 1, 21, 81-93.
- Pătroescu, M. (1987). Ecometric climatic indices and their relationship to space Subcarpathians biotic layer of Ramnicu Sarat and Buzau. *Annals of Univ. Bucharest. Geography Series*, 80-82.
- Prăvălie, R. (2013). Climate issues on aridity trends of Southern Oltenia in the last five decades. *Geographica Technica*, 1, 70-79.
- Quan, C., Han, S., Utescher, T., Zhang, C., Liu, Y.S. (2013). Validation of temperature-precipitation based aridity index: Paleoclimatic implications *Palaeogeography, Palaeoclimatology, Palaeoecology*, 386, 86-95.
- Rahimi, J., Ebrahimpour, M., Khalili, A. (2013). Spatial changes of Extended De Martonne climatic zones affected by climate change in Iran, *Theoretical and Applied Climatology*, 112, 3-4, 409-418.
- Runcanu, T., Bacinschi, D., Pescaru, I., Makkai, G., Tanczer, T. (2014). *Dictionary Meteorological Bucharest*, 112, 3, 409-418.
- Rusănescu, C.O. (2014). Precipitation indices in the city of Bucharest, *Hidraulica*, 3, pp.31-35.
- Rusanescu, C.O., Popescu I. N., David L. (2010). Relative humidity monitoring, *Advances in Environmental and Geological Science and Engineering*, 3 rd International Conference on Environmental and geological science and Engineering (EG' 10), 175-180.
- Rusănescu, M., Rusănescu, C. O. (2016). Temperature analysis in Bucharest (2009-2015), *Hidraulica*, no 3, 60-68.
- Rusănescu, C.O., Paraschiv, G., Biriș, S. Șt, Voicu Gh., Rusănescu, M. (2016). Characterization of Precipitation Regime in Bucharest (2009-2015), *Hidraulica*, 3, 34-41.
- Rusănescu, C. O., Stoica, D. (2013). Mathematical model for calculating carbon dioxide catalyst and without catalyst engine, *Metalurgia International*, 3, 81-84.
- Satmari, A., (2010). Practical works of biogeography, Publisher. Eurobit, Timisoara.
- Some'e, B.S, Ezani, A., Tabari, H. (2013). Spatiotemporal trends of aridity index in arid and semi-arid regions of Iran; *Theoretical and Applied Climatology*, 111, 149-160.
- Stoica, D., Rusanescu, C.O. (2013a). Research On The Influence Of Vibration Frequency on A Conical Sieve Suspended, *Metalurgia International*, XVIII 3, 84-86.
- Stoica, D., Stanciu, G. (2013). Influence the degree of sorting the separation process a conical sieve - *Digest Journal of Nanomaterials and Biostructures*, 8, 2, 513 - 518.

- Stoica, D., Rusanescu, C. O. (2013b). Research on variation of displacements, velocities and accelerations at a site selector blocks (fanner) grain, *Hidraulica*, 3, 38-42.
- Stoica, D., Voicu, Gh., Moise, V., Constantin, G. A., Carp-Ciocardia, C. (2015). Kinematic-structural analysis of actuating mechanism of a conical sieve with oscillating movement. Proceedings of the 43rd International Symposium on Agricultural Engineering, Actual Tasks on Agricultural Engineering, Opatija, Croatia, 525-535.
- Szabados, I. (2006). The effect of the precipitation on the tree ring width, *Carpatian Journal of Earth and Environmental Science*, 1, 2.
- Tufescu, V. (1966). Modeling natural relief and accelerated erosion, Publisher Socialist Republic of Romania, Bucharest.



AGRICULTURAL MACHINERY HYBRID PROPULSION SYSTEM BASED ON COMBINED CYCLE GAS AND STEAM TURBINES

Dan-Teodor BALANESCU*, Vlad-Mario HOMUTESCU

Department of Mechanical Engineering and Road Automotive Engineering, "Gheorghe Asachi"
Technical University of Iasi, Blvd Dimitrie Mangeron no.43, Iasi, 700050, Romania

*E-mail of corresponding author: balanescud@yahoo.com

SUMMARY

Hybrid electric systems represent a very attractive propulsion solution due to a significant fuel economy. Rating in relative terms, this technology is quite advanced in case of passenger cars but other categories, including agricultural machinery, are far behind. Typical configuration of a hybrid electric system includes a reciprocating (diesel or gasoline) engine. On the other hand, gas-steam turbine combined cycle units currently represent the most efficient and less pollutant technology for power generation in the range of high and medium powers. By combining the two advanced concepts – hybrid electric systems and combined cycle units – the current paper proposes a hybrid electric system concept including a low power combined cycle unit instead of the typical reciprocating engine. The unit operates with natural gas (CNG technology), which is more environmentally friendly than both diesel fuel and gasoline. The study indicated that proposed unit, providing 200 kW as output power, is a viable solution to be integrated in the hybrid electric propulsion system of a vehicle such as a tractor since it is much more performant than diesel engines with equivalent output power currently used for propulsion of vehicles. Besides, size and mass of the unit comply with space and mass restrictions imposed on tractors. An arrangement solution for the combined cycle unit components in the case of a tractor is also presented in the paper.

Key words: Hybrid electric system, combined cycle, tractor, performance, size

INTRODUCTION

Due to both zero local emissions and possibility of electricity generation from clean (renewable) sources, electric traction is currently assumed as a very attractive solution for vehicles propulsion. There are two types of pure electric vehicles (Chandran and Joshi, 2016): grid connected and battery based vehicles. Grid connected vehicles require an adequate

infrastructure, like underground or overhead cables – the case of electric trains, trams or trolley buses. Battery based vehicles are equipped with rechargeable batteries, which require power outlets to be charged. In spite of the great benefits of electric traction, mentioned above, battery based pure electric vehicles are still not widely used because of their high price, lack of charging facilities and short driving range (Ching, 2011). At present, there are examined law and policy strategies to overcome these drawbacks and to accelerate the spread of these vehicles (Barton and Schütte, 2017).

Beside pure electric vehicles, the battery based technology also includes the hybrid electric (HE) vehicles, which doesn't require regular charging from power outlets.

Compared with a conventional vehicle, a HE vehicle, consisting of one or several electric motors and a reciprocating (diesel or gasoline) engine, achieves significant fuel economy by applying a proper adaptive power management strategy (Guan and Chen, 2017), which implies optimum strategy for gear shifting as well as torque split between electric motor and internal combustion engines (ICE) (Heppeler et al., 2017). Besides, according to Abe (2010) and Correa et al. (2017), HE vehicles offer the best energy and environmental performances for short and medium terms if compare with conventional, hydrogen and pure electric vehicles. But, even under these considerations, replacement of a conventional vehicle with a HE vehicle does not bring economic benefits to the owner by default (these benefits are not only decided by fuel consumption but also by vehicle price, fuel price and travel mileage) and should be stimulated by subsidies (He and Fan, 2017). However, development and implementation of HE vehicles in transport field is quite advanced in the case of passenger cars while other categories (small transporters, trucks) are far behind (Doppstadt et al., 2017).

In what concerns agricultural machinery, reciprocating (diesel) engines currently represents the most used solution for propulsion. Obviously, grid connected pure electric traction is not a feasible solution for agricultural machinery since proper infrastructure cannot be ensured. Despite the all-electric tractor concept (called SESAM) recently developed by John Deere and based on two 150 kW electric motors, a pure electric battery tractor is also considered infeasible because diesel has an energy density (energy stored per unit volume, in $J\ m^{-3}$) considerably higher (50...100 times) than rechargeable batteries that should be used to store the energy for working process (Karner et al., 2014); besides, charging facilities could not be typically ensured while energy recovery by regenerative braking is limited in the case of agricultural machinery.

Unlike the pure electric propulsion, HE propulsion is assumed as a potential solution for agricultural machinery. Compared with the other automotive sectors, several drives of this machinery (e.g. chain feed drive, spreader drums, spreader discs) could benefit by hybridization beside traction drive-train (Karner et al., 2013). Two projects of HE tractors could be mentioned, namely ATC eDrive and John Deere e-Premium – a standard tractor having added a 20 kW electric generator (Karner et al., 2014), both including diesel engines, which is the typical ICE type (beside gasoline engine) of the HE propulsion systems.

By facing the main key challenge in the propulsion field, including agricultural machinery – maximum efficiency and minimum pollution – the present paper proposes a new approach in HE systems by integrating a gas-steam turbine combined cycle unit operating with natural gas (CNG unit) instead of the typical reciprocating ICE. This idea is based on the fact that combined cycle power plants currently represent the most advanced technology in high and medium power generation field, being able to offer up to 60% thermal efficiency in stand-alone operation (Robb, 2010). Thus, by combining two advanced technologies (HE propulsion systems and combined cycles), currently associated with two adjacent areas, the proposed concept aims to extend the use of combined cycles in the field of agricultural machinery where diesel engine is the leader since powers the majority of equipment. Besides,

operation with natural gas (more economical and environmental friendly than petroleum products) brings additional benefits. Thus, the profits are 20-25% comparing to gasoline and 10-15% compared to diesel while pollutant emissions are strongly reduced: 70 to 95% of CO, 20 to 30% of CO₂ and 50 to 87% of NO_x (Amrouche et al., 2012).

Two conditions are mandatory for the proposed concept to be assumed as viable: higher performance than diesels with equal power and framing in the assigned space inside the vehicle. Therefore, both performance and dimensional analysis were performed in the paper.

Presentation of the gas-steam turbine combined cycle unit

The proposed gas-steam turbine combined cycle unit, operating with natural gas, is presented in Fig. 1. Flue gas exhausted from gas power turbine (GT) enters in heat recovery steam generator (HRSG) – the link between gas turbine engine and steam turbine engine – and then is released into the atmosphere. HRSG generates steam (one pressure level), which drives the steam turbine (ST). GT and ST are connected to the transmission of HE propulsion system.

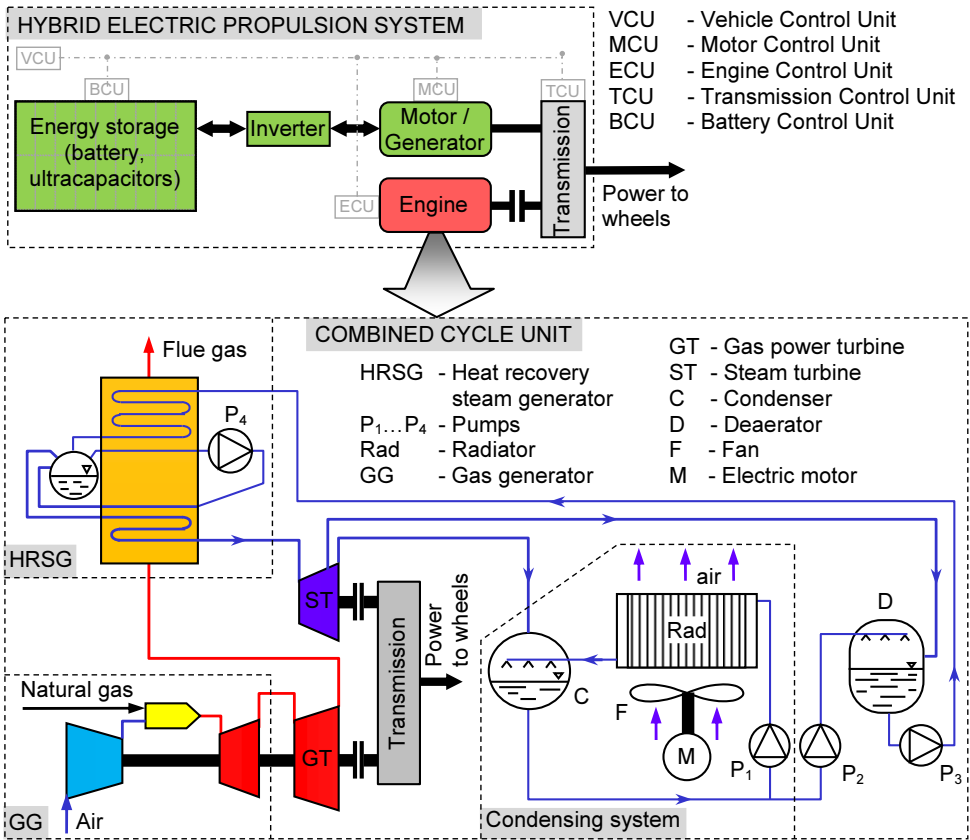


Figure 1. Schematic of the combined cycle unit integrated in the HE propulsion system

As can be seen in Fig. 1, the condensing system of the steam turbine engine is based on a forced convection air cooled radiator. This solution was adopted instead of the classic condensing system with cooling tower (typical for the stationary combined cycle units) because the cooling tower induces water loss, which is unacceptable in the case of a vehicle. Besides, the cooling tower would be very difficult integrated on a vehicle.

In the proposed condensing system, a fraction of the condensate flow leaving the condenser is subcooled in radiator and, further, is sprayed in the ST exhaust steam flow (in condenser). Thus, steam condensation occurs as result of a heat and mass transfer process.

MATERIALS AND METHODS

As for any power generation unit, the most relevant indicators of the combined cycle unit performance are output power, specific fuel consumption and efficiency, which were consequently calculated as described below, according to Kehlhofer et al. (2009). In what concerns dimensions and mass of the combined cycle unit, these are overwhelming decided by the heat exchangers (of HRSG and Rad – see Fig. 1). That is why volume and mass of heat exchangers were also calculated.

Output power of the combined cycle unit is expressed as

$$P = P_{GTE} + P_{STE} = \eta_m \cdot \dot{m}_a \cdot w_{PT} \left[1 + (AER \cdot AFR_s)^{-1} \right] \cdot (1 - \theta) + \eta_m \cdot \left[\dot{m}_s \cdot (h_s - h_{co}) - \dot{m}_{ES} \cdot (h_{ES} - h_{co}) \right] \quad [kW] \quad (1)$$

where:

P_{GTE} , P_{STE} - output power of the gas turbine engine / steam turbine engine, in kW;

η_m - mechanical efficiency of turbines;

\dot{m}_a - compressor inlet air mass flow, in $kg\ s^{-1}$;

w_{PT} - specific work of GT, in $kJ\ kg^{-1}$;

AER - air excess ratio;

AFR_s - stoichiometric air-fuel ratio, in $kg\ air\ kg\ fuel^{-1}$;

θ - fraction, from \dot{m}_a , of cooling air mass flow;

\dot{m}_s , \dot{m}_{ES} - steam mass flow at ST inlet / mass flow of extraction steam, in $kg\ s^{-1}$;

h_s , h_{ES} - specific enthalpy of steam at ST inlet / of extraction steam, in $kJ\ kg^{-1}$;

h_{co} - specific enthalpy of ST exhausted steam (condenser inlet).

Mass flows \dot{m}_s and \dot{m}_{ES} result from the thermal balance of HRSG and deaerator, respectively.

Specific fuel consumption is calculated with formula

$$SFC = FC \cdot P^{-1} = 3600 \cdot \dot{m}_a \cdot (1 - \theta) \cdot (AER \cdot AFR_s \cdot \rho_f \cdot P)^{-1} \quad [Nm^3\ kWh^{-1}], \quad (2)$$

where FC is fuel consumption of combined cycle unit, in $Nm^3\ h^{-1}$, while ρ_f is the absolute density of the fuel (natural gas), in $kg\ m^{-3}$. Based on SFC, CO₂ emission rate is expressed as

$$E_{CO_2} = 1000 \cdot \rho_f \cdot SFC \cdot g_c \cdot M_{CO_2} \cdot M_C^{-1} \quad [g\ kWh^{-1}], \quad (3)$$

where g_c is the carbon content of the fuel while M_{CO_2} and M_C are the molar masses of carbon dioxide and carbon, respectively.

Efficiency of the unit is given by

$$\eta_{cc} = 3600 \cdot P \cdot (FC \cdot LHV)^{-1}, \quad (4)$$

where LHV is lower heating value of fuel, in $kJ\ Nm^{-3}$.

Efficiencies of gas and steam turbine engines are calculated as

$$\eta_{GTE} = 3600 \cdot P_{GTE} \cdot (FC \cdot LHV)^{-1}, \quad (5)$$

$$\eta_{STE} = P_{STE} \cdot [\dot{m}_g \cdot (h_{IG} - h_{FG})]^{-1}, \quad (6)$$

where:

h_{IG} , h_{FG} - specific enthalpy of HRSG inlet / outlet flue gas, in kJ kg^{-1} ;

\dot{m}_g - flue gas mass flow, in kg s^{-1} .

Flue gas exhausted from GT enters in HRSG. Hence, HRSG inlet flue gas parameters (temperature, specific enthalpy) result from calculation of the expansion process in GT.

Volume and mass of HRSG heat exchangers and condensing system radiator are given by

$$V_{HRSG} = S_{HRSG} \cdot sv_{HRSG}^{-1}; \quad V_{rad} = S_{rad} \cdot sv_{rad}^{-1} \quad [m^3], \quad (7)$$

$$m_{HRSG} = ma_{HRSG} \cdot S_{HRSG}; \quad m_{rad} = ma_{rad} \cdot S_{rad} \quad [kg], \quad (8)$$

where:

S_{HRSG} , S_{rad} - heat-transfer surface area of heat exchangers of HRSG / condensing system radiator, in m^2 ;

sv_{HRSG} , sv_{rad} - surface to volume ratio of heat exchangers of HRSG / condensing system radiator ($\text{m}^2 \text{m}^{-3}$);

ma_{HRSG} , ma_{rad} - mass to surface area ratio of heat exchangers of HRSG / condensing system radiator (kg m^{-2}).

Heat exchangers of both HRSG and radiator are tubular type (water / steam is passing inside the tubes) in accordance with configurations presented in (Keys and London, 1984), with internal diameter of tubes of 9.53 mm, relative pitches (longitudinal and transverse) of 1.5 and wall thickness of 1 mm (HRSG) or 0.5 mm (radiator). In these conditions, $sv_{HRSG} = sv_{rad} = 222.14 \text{ m}^2 \text{m}^{-3}$, $ma_{HRSG} = 7.8 \text{ kg m}^{-2}$ and $ma_{rad} = 3.9 \text{ kg m}^{-2}$.

Heat exchange surfaces were calculated with the classic procedure, based on formula

$$S_{he} = \dot{Q} \cdot k^{-1} \cdot LMTD^{-1} \quad [m^2], \quad (9)$$

where:

\dot{Q} - rate of heat flow, in W;

k - overall heat transfer coefficient, in $\text{W m}^{-2} \text{K}^{-1}$;

LMTD - logarithmic mean temperature difference, in K.

Rate of flow is calculated with the known formula

$$\dot{Q} = 1000 \cdot \dot{m} \cdot (h_2 - h_1) \quad [W], \quad (10)$$

where:

\dot{m} - mass flow of the cold fluid, in kg s^{-1} ;

h_1 , h_2 - specific enthalpies of the cold fluid at the inlet and outlet of the heat exchanger, in kJ kg^{-1} .

Overall heat transfer coefficient was expressed as Ishigai (2010) and Lee (2010)

$$k = \psi (h_{cc}^{-1} + h_{ch}^{-1})^{-1} \quad [W m^{-2} K^{-1}], \quad (11)$$

where ψ is effectiveness factor of the heat exchanger while h_{cc} , h_{ch} are the convective heat transfer coefficients of the cold fluid and hot fluid, respectively. They are calculated as

$$h_{c(h)} = A \cdot \lambda_{c(h)} \cdot d^{-1} \cdot \text{Re}_{c(h)}^m \cdot \text{Pr}_{c(h)}^n \cdot C \quad [W m^{-2} K^{-1}], \quad (12)$$

where:

A - coefficient function by flow type (inside or over the tubes);

$\lambda_{c(h)}$ - thermal conductivity of cold / hot fluid, in $W m^{-1} K^{-1}$;

d - diameter of tubes – external, when fluid is flowing over the tubes, or internal, when fluid is flowing inside tubes, in m;

$Re_{c(h)}$ - Reynolds number for cold / hot fluid;

$Pr_{c(h)}$ - Prandtl number for cold / hot fluid;

C - correction factor function by flow type and geometry of heat exchanger.

RESULTS AND DISCUSSION

Calculations were made assuming a compressor inlet air mass flow $\dot{m}_a = 0.358 \text{ kg s}^{-1}$, a fraction of cooling air mass flow $\theta = 0.03$ and mechanical efficiency $\eta_m = 0.99$. It was considered that natural gas with LHV = $34240.6 \text{ kJ Nm}^{-3}$, $AFR_s = 16.72 \text{ kg air kg fuel}^{-1}$, $q_f = 0.711 \text{ kg Nm}^{-3}$ and $g_c = 0.75 \text{ kg C kg fuel}^{-1}$ is used as fuel.

The values of GG compression ratio and GG turbine inlet temperature were assumed 10 and 1500 K, respectively; it is noted that most advanced gas turbines currently operate with turbine inlet temperatures much higher, up to $1600 \text{ }^\circ\text{C} / 1873 \text{ K}$ (Singh, 2014).

A pressure loss of 3 % it was admitted in GG combustion chamber while isentropic efficiencies of compressor and turbines (gas and steam) were all assumed 0.86. Pressure and temperature of superheated steam delivered by HRSG were set to 160 bar and $560 \text{ }^\circ\text{C}$, respectively, while flue gas temperature at stack was fixed to $100 \text{ }^\circ\text{C}$.

By assuming an ambient air temperature of $15 \text{ }^\circ\text{C}$ and a temperature difference of 20 K between the ambient air and subcooled condensate as well as between condensate and air after radiator, it resulted an absolute condensing pressure of 0.4 bar for steam, which corresponds to a condensing temperature of $75.9 \text{ }^\circ\text{C}$.

Table 1. Performance and dimensional indicators of the combined cycle unit

Parameter	Unit	Notation	Value
Output power of the gas turbine engine	kW	P_{GTE}	119.4
Output power of the steam turbine engine	kW	P_{STE}	80.6
Output power of the combined cycle unit	kW	P	200
Steam mass flow	kg s^{-1}	\dot{m}_s	0.0757
Temperature of HRSG inlet gas	$^\circ\text{C}$	t_{IG}	691
Fuel consumption	$\text{Nm}^3 \text{ h}^{-1}$	FC	42
Specific Fuel Consumption	$\text{Nm}^3 \text{ kWh}^{-1}$	SFC	0.21
CO ₂ emission rate	g kWh^{-1}	E_{CO_2}	419
Efficiency of the gas turbine engine	-	η_{GTE}	0.299
Efficiency of the steam turbine engine	-	η_{STE}	0.341
Efficiency of the combined cycle unit	-	η_{CC}	0.501
Heat-transfer surface area of heat exchangers of HRSG	m^2	S_{HRSG}	35.6
Heat-transfer surface area of condensing system radiator	m^2	S_{rad}	116.7
Volume of heat exchangers of HRSG	m^3	V_{HRSG}	0.160
Volume of condensing system radiator	m^3	V_{rad}	0.525
Mass of heat exchangers of HRSG	kg	m_{HRSG}	278
Mass of condensing system radiator	kg	m_{rad}	455

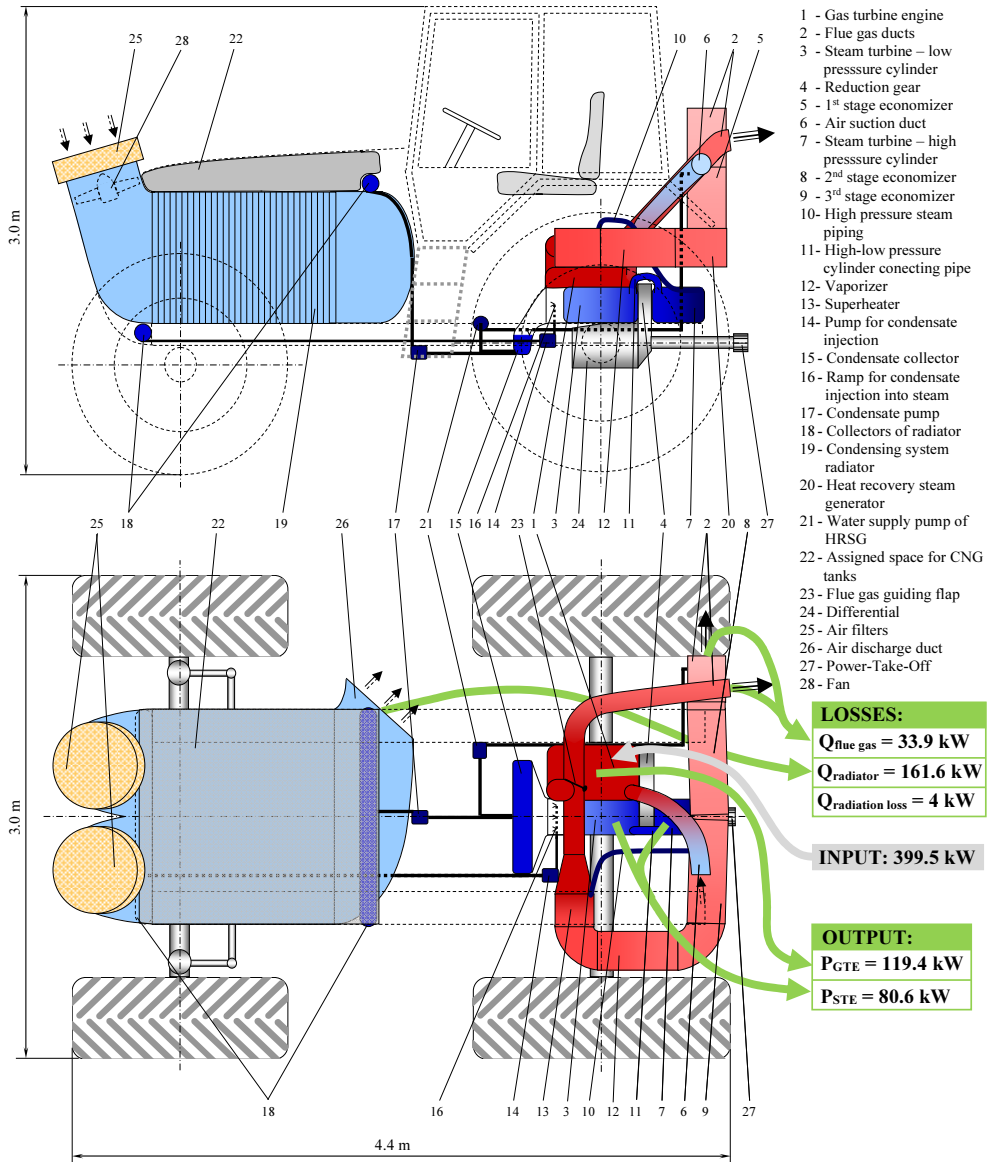


Figure 2. Arrangement of the combined cycle unit components

The calculated performance and dimensional indicators of the combined cycle unit are presented in Table 1. It can be observed that ST provides 80.6 kW of the entire 200 kW output power of the unit. Currently, there are commercially available steam turbines of even 15 kW (“Green steam turbine”) but operating with low inlet steam parameters (Amirante et al., 2017). Therefore, studies on small-scale steam turbines with high inlet parameters should be of first priority in further research on HE propulsion systems based on combined cycle units.

It should be pointed out the value of η_{cc} , namely 0.501, which indicates that efficiency of the analyzed unit is much higher than efficiency of the most advanced diesel engine (not only the challenger in what concerns integration in HE system but also the typical stand-alone engine type used for propulsion of tractors and other agricultural machinery) with similar output power, which is less than 0.42 (Takaishi et al., 2008). Besides, recent studies (Quiros et al., 2017) show that most advanced conventional diesel engines used for tractors propulsion are currently described by CO₂ emission rates of minimum 460 g bhp-h⁻¹ (617 g kWh⁻¹); the use of natural gas (CNG or LNG) instead of diesel fuel could offer a CO₂ emissions reduction of 10 - 20 % (Graham et al., 2008). CO₂ emission rate of the analyzed CNG combined cycle unit is 32 % lower, namely 419 g kWh⁻¹, which indicate it much less pollutant than diesel or natural gas engines.

Both volume and mass of HRSG heat exchangers (0.160 m³, 278 kg) and condensing system radiator (0.525 m³, 455 kg) can be easily accepted in the case of a tractor. Obviously, they would be proportionally reduced at lower output powers, so the proposed solution for propulsion should be viable even for lighter vehicles. Besides, size and mass could be drastically reduced (if they become unacceptable) by increasing the steam condensing pressure; a consequent reduction of performance should be assumed in this case. Extrapolating, assumption of operating parameters of the combined cycle unit it is a matter of optimization, depending by specific features of the vehicle type. It involves the most convenient compromise between performance and size & mass. Viability of the proposed concept remains valid as long as offers significantly higher performance than diesels.

A solution for the arrangement of the combined cycle unit components inside a tractor having length 4.4 m, height 3.0 m and width 3.0 m (the reference is John Deere 7710 model but 0.3 m wider) is presented in Fig. 2. It should be noted that the other component of HE system (motor/generator, inverter, batteries) are not represented. The assigned space for these components is placed in the rear side of the tractor.

CONCLUSIONS

The proposed propulsion concept associates two advanced technologies related to power generation in two adjacent areas: HE systems (used for propulsion) and combined cycles (used for electric power generation at high and medium level of power).

Operation of combined cycle unit with natural gas brings benefits in what concerns pollutant emissions because this fuel is more environmentally friendly than diesel fuel or gasoline.

The output power of the analyzed combined cycle unit is about 200 kW, which corresponds to the propulsion system of a tractor.

Efficiency of the analyzed combined cycle unit is considerably higher than efficiency of the most advanced diesel engines with similar power (0.501 versus 0.42) while CO₂ emission rate is significantly lower (419 g kWh⁻¹ versus 617 g kWh⁻¹). Besides, size and mass of the HRSG heat exchangers and condensing system radiator could be easily framed inside of the assigned propulsion system space of a tractor. As consequence, the proposed propulsion concept is a viable solution for tractors.

Size and mass of the combined cycle unit would be drastically reduced by increasing steam condensing pressure. Thus, proposed concept could be viable even in case of lighter vehicles. The mandatory condition subsidiary to the compromise achieved between performance and size & mass is to keep significantly higher performance than diesels.

Further research on HE propulsion systems based on combined cycle units should have development of small-scale steam turbines operating with high parameters as first priority.

ACKNOWLEDGEMENTS

This work was partly supported by the project POSCCE-A2-O2.2.1-2009-4-ENERED, ID nr. 911, co-financed by the European Social Fund within the Sectoral Operational Program "Increase of Economic Competitiveness".

REFERENCES

- Abe, H. (2010). Development of Toyota Plug-in Hybrid Vehicle. *Journal of Asian Electric Vehicles* 8 (2): 1399-1404.
- Amirante, R., De Palma, P., Distaso, E., Pantaleo, A.M., Tamburrano, P. (2017). Thermodynamic analysis of a small scale combined cycle for energy generation from carbon neutral biomass. *Energy Procedia* 129: 891-898.
- Amrouche, F., Benzaouib A., Harouadic, F., Mahmaha, B., Belhamela, M. (2012). Compressed Natural Gas: The new alternative fuel for the Algerian transportation sector. *Procedia Engineering* 33: 102-110.
- Barton, B. and Schütte, P. (2017). Electric vehicle law and policy: a comparative analysis. *Journal of Energy & Natural Resources Law* 35 (2): 147-170.
- Chandran, D. and Joshi M. (2016). Electric vehicles and driving range extension–A Literature review. *Journal of Advances in Vehicle Engineering* 2 (4): 219-227.
- Ching, T.V. (2011). Design of Electric Vehicle Charging Station in Macau. *Journal of Asian Electric Vehicles* 9 (1): 1453-1458.
- Correa, G., Munoz, P., falaguerra, T., Rodriguez, C.R. (2017). Performance comparison of conventional, hybrid, hydrogen and electric urban buses using well to wheel analysis. *Energy*, In Press.
- Doppstadt, C., Koberstein, A., Vigo, D. (2016). The Hybrid Electric Vehicle – Traveling Salesman Problem. *European Journal of Operational Research* 253 (3): 825-842.
- Graham, L.A., Rideout, G., Rosenblatt, D., Hendren, J. (2008). Greenhouse gas emissions from heavy-duty vehicles. *Atmospheric Environment* 42 (19): 4665-4681.
- Guan, J.C. and Chen, B.C. (2017). Adaptive Power Management Strategy for a Four-Mode Hybrid Electric Vehicle. *Energy Procedia* 105: 2403-2408.
- He, H. and Fan, J. (2017). When to switch to a hybrid electric vehicle: A replacement optimisation decision. *Journal of Cleaner Production* 148 (1): 295-303.
- Heppeler, G., Sonntag, M., Wohlhaupter, U., Sawodny, O. (2017). Predictive planning of optimal velocity and state of charge trajectories for hybrid electric vehicles. *Control Engineering Practice* 61: 229-243.
- Ishigai, S. (2010). *Steam Power Engineering: Thermal and Hydraulic Design Principles*, Cambridge University Press, Cambridge.
- Karner, J., Baldinger, M., Reichl, B. (2014). Prospects of Hybrid Systems on Agricultural Machinery. *Journal on Agricultural Engineering* 1 (1): 33-37.
- Karner, J., Baldinger, M., Schober, P., Reichl, B., Prankl, H. (2013). *Landtechnik* 68 (1): 22-25.
- Kays, W.M. and London, A.L. (1984). *Compact Heat Exchangers*, 3rd ed. McGraw-Hill, New York.
- Kehlhofer, R., Hannemann, F., Stirnimann, F., Rukes, B. (2009). *Combined-Cycle Gas&Steam Turbine Power Plants*, 3rd ed. PennWell, New York.
- Lee, H.S. (2010). *Thermal Design*. John Wiley & Sons, New Jersey.

- Quiros, D.C., Smith, J., Thiruvengadam, A., Huai, T., Hu, S. (2017). Greenhouse gas emissions from heavy-duty natural gas, hybrid, and conventional diesel on-road trucks during freight transport. *Atmospheric Environment* 168: 36-45.
- Robb, D. (2010). CCGT: Breaking the 60 per cent efficiency barrier. *Power Engineering International* 18 (3): 28-32.
- Singh, K. (2014). Advanced Materials for Land Based Gas Turbines. *Transactions of the Indian Institute of Metals* 67 (5): 601-615.
- Takaishi, T., Numata, A., Nakano, R., Sakaguchi, K. (2008). Approach to High Efficiency Diesel and Gas Engines. *Mitsubishi Heavy Industries, Ltd. Technical Review* 45 (1): 21-24.



HARNESSING THE IRRIGATION WATER FLOWS FOR MICRO-HYDRO POWER GENERATION

Baldwin G. JALLORINA^{1*}, Victorino T. TAYLAN², Ireneo C. AGULTO², Helen F. GAVINO², Vitaliana U. MALAMUG², Emmanuel V. SICAT²

¹ Philippine Center for Postharvest Development and Mechanization (PHilMech), CLSU Compound, Science City of Muñoz, 3120 Nueva Ecija, Philippines

² College of Engineering, Central Luzon State University (CLSU), Science City of Muñoz, 3120 Nueva Ecija, Philippines

*Email of corresponding author: bjallorina@yahoo.com

SUMMARY

This study was conducted to develop a low-head micro hydro power (MHP) generation system suitable for existing irrigation water flows. Specifically, this study aimed to design, fabricate, install an on-site MHP generation system, test and evaluate the technical performance and conduct economic analysis of the MHP generation system set-up.

The developed MHP generation system for irrigation water flows have five major components, namely: crossflow turbine, structural frame, water intake and conveyance channel, generator, and transmission assembly and wirings. It was installed and tested at the inclined drop of CASECNAN Irrigation System. It operates on the concept of low head and high flow volume water flows. Technical performance was established through a series of experiments using three different water flow rates (Q) and three different water exit notches (O) combinations. The power cost generated was determined through an economic analysis using the test and evaluation data.

Results of the experiment showed that the developed MHP generation system effectively harnessed irrigation water flow for power generation. It could generate 5kW electricity, using 7.5 kW, 220 V, 13.6 Amp, 60 Hz, 1,800 RPM, single-phase generator to transform the rotational energy into electricity. The generated power could be used for local lighting and other household use.

Key words: irrigation water flows; T12 crossflow turbine; low-head micro hydro

INTRODUCTION

Electrical energy is one basic component of a country's progress and development (OECD/IEA, 2007). In the Philippines, the demand for electricity is substantially increasing in line with the population growth, economic development and industrialization. However, the country is still experiencing continuous shortage of electrical power despite the increasing energy development (DOE, 2012). The supply of electricity in the rural areas remains one of the major problems in our present time. People living in these areas still do not have access to electricity (DOE, 2009).

This condition requires the need of technological alternatives to support the needed electrical demand. One of the technological alternatives is to generate electricity by harnessing other renewable energy sources such as irrigation water flows through MHP. The MHP is environment friendly and relatively cheap. It is very rationale to build such MHP generation projects to supplement ever increasing demand of electricity especially in the rural areas where construction of power lines is not possible.

Unfortunately, to date the current MHP design for low head and high flow volume water sources like irrigation systems require damming of canal which affects water flow and require huge investment. This calls for an affordable design of MHP generation system for low head and high flow volume sites that will be fitted of existing irrigation structures without the interference of the irrigation water flow, can be afforded by individual or small group of people in the community, fabricated, repaired and maintained locally.

MATERIALS AND METHODS

This section presents the methodologies and testing procedures used in the study.

Design and Fabrication of the MHP Generation System

Machine design

The consideration for the design of MHP generation system includes: existing irrigation structures, available head and water flow rates of the irrigation system, site accessibility and ease of installation. Figures 1 and 2 shows the operating range of varying turbines for a given head and flow in the selection of suitable turbine. A cross flow turbine was used in this research project since the available head of the potential sites were less than 3 meters and it can be fabricated locally. Computer Aided Design (CAD) was employed in the production of working drawings.

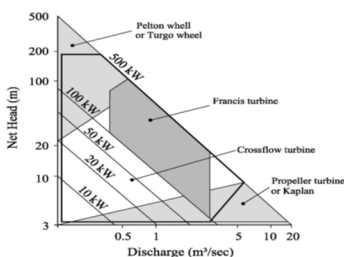


Figure 1. Head-flow ranges of small hydro turbines (Paish O., 2002).

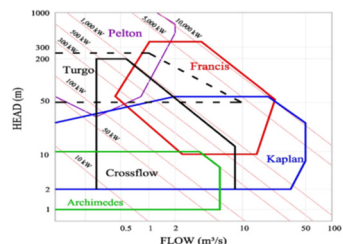


Figure 2. The various turbines in terms of head and flow rate (Fraenkel et al., 1999).

The calculation of the turbine performance values in the design were (Nakarmi et al., 1993):

Inlet width, b_0

$$b_0 = 1 / (q_{11} * D) * Q / \sqrt{H_{net}} \quad (1)$$

where:

b_0 – inlet width, m; H_{net} – net heat, m; Q – discharge (flow), m^3/sec ; q_{11} - unit discharge (flow) = 0.67 for T12; D – rotor diameter = 30 cm for T12

Therefore: $b_0 = 3.623 * Q / \sqrt{H_{net}} \quad (2)$

Shaft power output, P

$$P = 0.98 * Q * H_{net} * \eta \quad (3)$$

where:

P - power, kW; H_{net} – net heat, m; Q – discharge (flow), m^3/sec ; η – turbine efficiency: 0.65 for T12

Turbine speed, rpm

$$n = n_{11} / D * \sqrt{H_{net}} \quad (4)$$

where:

n – rotational speed, rpm; n_{11} – unit speed = 39 rpm for T12; D – runner diameter = 0.30 m

Runway speed

$$r_s = 1.8 * n_t \quad (5)$$

where: r_s – runway speed; n_t – rotational speed, rpm

Runner width

The turbine runner width (T_1) was computed by the formula:

$$T_1 = W_c - S_{si} \quad (6)$$

where:

T_1 – turbine runner width, m; W_c – width of the inclined drop, m; S_{si} – width for transmission assembly and working space, m

Diameter of shaft

It should not be too large that water strikes the shaft after passing through the first set of blades at the inlet using the following equation (Chattha et al. 2010).

$$d = 0.22D \quad (7)$$

where:

d – shaft diameter, m; D – runner diameter, m

Fabrication

Each designed parts were fabricated and assembled into a set of MHP generation system for irrigation water flows. Fabrication was conducted based on the approved design in AUTOCAD software. Fabrication activities were conducted at PHilMech fabrication shop except standard parts such as bearings, bolts and nuts and other elements which were purchased from the market.

Performance Testing of the MHP Generation System

Testing of Crossflow Turbine

The crossflow turbine had to undertake a series of tests to determine the optimum operations in terms of torque and rotational speed. The tests were conducted in three different water flow rates ($Q_1 = 0.242 \text{ m}^3/\text{sec}$, $Q_2 = 0.298 \text{ m}^3/\text{sec}$, and $Q_3 = 0.354 \text{ m}^3/\text{sec}$) and three different water exit notches of sluice gate ($O_1 = 2 \text{ cm}$, $O_2 = 5.81 \text{ cm}$, and $O_3 = 9.62 \text{ cm}$) combinations. These combinations were determined during the preliminary testing of the turbine. Flow rates and exit notches were controlled into the desired combination by adjusting the water intake and sluice gate, respectively.

The variables (water flow rates, Q and water exit notches, O) were considered as treatments in a Complete Randomized Design (CRD). The treatments are replicated three times. Analysis of variance (ANOVA) was used to determine the significant differences of the two different treatments. The comparison among treatment means was done using Duncan Multiple Range Test (DMRT), at 5 percent level of significance for the mean difference.

The turbine brake power (TBP) and turbine efficiency (E_{TUR}) were computed as:

$$TBP = (T \times N) / 974 \quad (8)$$

where:

TBP - Turbine Brake Power, kW T - shaft torque, kg meter; N - shaft speed, rpm

$$E_{TUR} = (\text{Turbine Brake Power} / \text{Theoretical Water Power}) \times 100 \quad (9)$$

where: Theoretical water power (P_{TW}) was computed by:

$$P_{TW} = \eta \rho g Q H \quad (10)$$

where:

P_{TW} - power generated in the turbine shaft, watt; η - turbine efficiency, normally 80-90%; ρ - water density, 1000 kg/m^3 ; g - gravitational acceleration, 9.81 m/sec^2 ; Q - flow rate, m^3/s and; H - net head, m

Performance Testing of MHP Generation System

The combination setting (water flow rates, Q and water exit notches) that produced highest torque was used in the performance testing of the MHP generation system coupled with a 7.5 kW, 220 V, 13.6 A, 60 Hz, 1,800 RPM, single-phase electric generator. Voltage and current produced were measured using multi-meter and clamp meter, respectively. Generator output power (P_{gen}) was computed as:

$$P_{gen} = V \times I \quad (11)$$

where: P_{gen} - generator output power, watt; V - voltage produced by the generator without load, volts, and I - current withdrawn from the generator by the load, amperes.

The conversion efficiency (E_{con}) was computed by:

$$E_{con} = (P_o / P_L) \times 100 \quad (12)$$

$$P_o = V \times I \quad (13)$$

where:

E_{con} - conversion efficiency, %; V - initial voltage of the generator w/o load, volt; I - current drawn by the load, ampere; P_o - output power of the generator, watt; P_L - applied load to the generator, watt

Economic Analysis

The economic analysis was computed based on fixed cost and variable cost. Assumptions were based on the 2017 prices in the area. The operation was assumed to be continuous for 24 hours a day in 228 days (two cropping seasons) in a year with economic life of 10 years.

RESULTS AND DISCUSSION

This section presents the results of the study and tackles its values.

The MHP Generation System

The flow and available heads of the existing irrigation structures of CASECNANN Irrigation System ranged from 3.28 to 14 m³/sec and from 1.5 to 3 m, respectively. This condition met the requirements in terms of flow and head for the design of a low-head MHP generation system.

Figure 3 show the developed MHP generation system for irrigation water flow built across the inclined drop of CASECNAN Irrigation System. It consists of five major components, namely: *Crossflow turbine, Structural frame, Water intake and conveyance channel, Generator, and Transmission assembly and wirings*. The turbine shaft was coupled to the generator shaft through a transmission assembly. The technical specification is presented in Table 1.



Parameters	Specifications
Dimension	
Length	244 cm
Width	141 cm
Depth	163 cm
Weight	
600 kgs	
Turbine Type	
Crossflow	
Rotor diameter	30 cm
Runner length	123.5 cm
Shaft diameter	5.08 cm
No. of blades	30 blades
Generator	
Single phase, 7.5 KW, 220 V, 13.6 Amp, 60 Hz, 1,800 rpm, Synchronous	
Methods of power transmission	Gear box and Belt and pulley system
Capacity	5 kW

Figure 3. The developed MHP generation system

Table 1. The Specification of the MHP

1. *Crossflow turbine*. Designed to transform the energy of flowing water into rotational energy. A t12 crossflow turbine model was selected in this research project was due to it can be fabricated locally and suitable for low head application. The t12 model is public

domain of Indonesian design crossflow turbine. It is a drum-shaped rotor composed of 30 blades, two side disks supported by four intermediate disks and shaft. The blades were made of 7.62 cm diameter pipe equally divided in three pieces. The side disks and intermediate disks of a rotor are round metal plates with radius cut slots throughout its outer periphery where the end of the blades are inserted and welded.

2. **Structural frame.** Designed to support the whole MHP generation system, hold the machine components together as well as bear and carry the weight of the unit. It was made of four columns G.I pipe built across the inclined drop at 2.5 m width and 5 m length. The beams were made of 15.24 cm channel steel bars where the MHP generation system was anchored.
3. **Water intake and Conveyance channel.** Designed to take and deliver the water into the turbine. It was made of steel plate flooring and G.I sheets sidings supported with angular bar. The water intake was connected in front of the water conveyance channel. Rollers made of engineering plastic were installed underneath the structure to support the movement of the water intake.
4. **Generator.** Single phase, 7.5 KW, 220 V, 13.6 Amp, 60 Hz, 1,800 RPM, synchronous generator was used to transform the rotational energy into electricity. Synchronous generators are used in most MHP projects because they have the ability to establish its own operating voltage and maintain frequency while it is operating (Harper, 2011).
5. **Transmission assembly and Wirings.** It comprised of gear boxes, V-belt drive systems and electrical wirings. Shafts are secured to the main frame structure through pillow blocks. Two pieces V-belt type was used for the pulley and belt system.

Performance of the Cross-flow Turbine

The performance of the developed crossflow turbine was measured in terms of turbine shaft rotational speed and torque. Three water flow rates (0.242 m³/sec, 0.298 m³/sec and 0.354 m³/sec) as affected by three different water exit notches (2 cm, 5.81 cm, and 9.62 cm) of sluice gates were used in the experiment with three replications.

Turbine Rotational Speed

Figure 4 shows the turbine rotational speed of three water flow rates at three different water exit notches combinations. The rotational speed produced ranged from 228.33 to 295 rpm. The highest was registered at 0.298 m³/sec water flow rate and 9.62 cm exit notch combination. The lowest was registered at 0.242 m³/sec flow rate and 2 cm exit notch combination. The difference was attributed to the increase in velocity of water which created rotation when water passes through the turbine until it reached the maximum discharge capacity of the turbine.

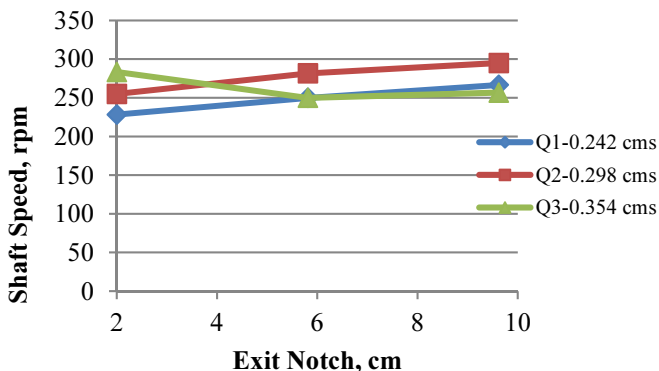


Figure 4. Turbine shaft rotational speed

Analysis of variance showed that the three water flow rates and the three exit notches were highly significant and significantly different respectively in terms of rotational speed. The treatments combinations were also highly significant different as shown in Table 2. These combination settings had an effect in terms of turbine rotational speed.

Table 2. The turbine rotational speed as affected by water discharge and exit notch

Water discharge, m ³ /sec	Exit notch (cm)			Average
	2.0	5.81	9.62	
0.242	228.33i	250.00h	266.67gh	248.33c
0.298	255.00h	281.67fg	295.00f	277.22a
0.354	283.33fg	250.00h	256.67h	263.33b
Average	255.56d	260.56d	272.78e	262.96

Means not sharing letter in common differ significantly by Duncan Multiple Range Test (DMRT).

Turbine Torque

Figure 5 shows the torque in three water flow rates at three different water exit notches combinations. The torque produced ranged from 124.25 Newton-meter (N m) to 281.16 N m. The highest torque of 281.16 N m produced at 0.354 m³/sec water flow rate with 5.81 cm exit notch combination while the 0.242 m³/sec water flow rate with 2.0 cm exit notch combination yielded the lowest torque of 124.25 N m. The increase of turbine torque was due to the increase in the amount of water that created centrifugal force when it passed through the turbine until it reached the maximum turbine water discharge capacity.

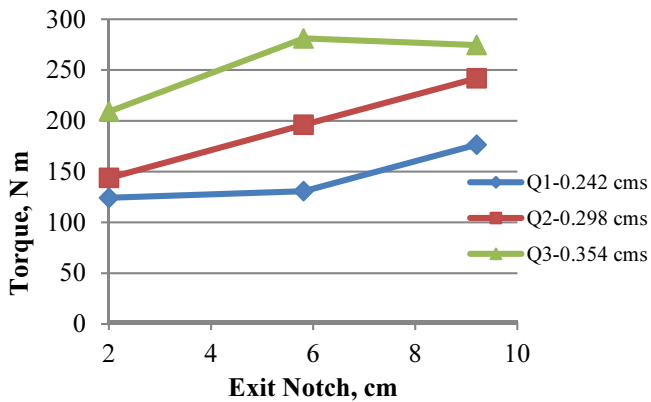


Figure 5. Turbine torque

Analysis of variance showed that the three water flow rates and exit notches were highly significant different in terms of turbine torque. It also showed that the water flow rates and exit notches combinations were significantly different (Table 3). This means that these combination settings had an effect in terms of turbine torque.

The computed turbine brake power (TBP) was 7.36 kW with water theoretical power of 13.05 kW. The computed turbine efficiency was 56.4%.

The optimum combination that produced the highest torque 0.354 m³/sec flow rates with 5.81 cm exit notch was used in the performance testing of the MHP generation system. Based on the computed turbine brake power (TBP), a 7.5 kW, 220 V, 13.6 A, 60 Hz, 1,800 RPM, single-phase generator was used to transform the rotational energy into electricity.

Table 3. The turbine torque as affected by water discharge and exit notch

Water discharge, m ³ /sec	Exit notch (cm)			Average
	2.0	5.81	9.62	
0.242	124.25l	130.72l	176.52jk	143.86c
0.298	143.86kl	196.13j	241.93hi	193.98b
0.354	209.18ij	281.16g	274.59gh	254.97a
Average	159.06f	202.70e	231.04d	197.60

Means not sharing letter in common differ significantly by Duncan Multiple Range Test (DMRT).

Performance of the MHP Generation System

Figure 6 shows the effect of applying varied loads (P_L) in voltage (V) developed by 7.5 kW synchronous electric generator. Regression equation is $P_L = -23.209V + 5034$ with $R^2 = 0.8317$. The voltage dropped from 250 to 52 volts upon applying increasing loads from 500 to 5,000 watts. The voltage drop was due to the increase of resistance on different loads.

Lamps and chargers have different rated voltages. For example, compact fluorescent light has rated voltage of 180 to 240 volts. LED lights, laptop and cell phone chargers have a rated voltage of 100 to 240 volts. Incandescent lamps will work even in very low voltage but

illumination will decrease depending on the decrease in voltage. The graph shows that the MHP generation system operating load was 2,000 watts having a voltage of not less than 100 volts based on the rated voltage of chargers and other electronic gadgets.

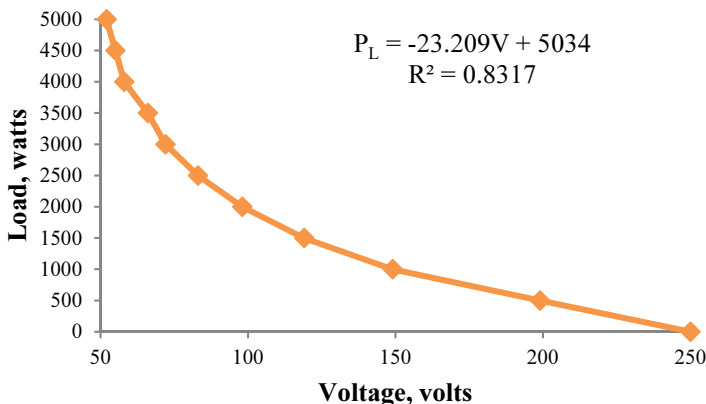


Figure 6. Effect of various applied loads in voltage of the 7.5 kW generator

The amount of current (I) withdrawn by each applied load in the generator is shown in Figure 7. Regression equation is $P_L = 601.52(I) - 671.66$ with $R^2 = 0.8903$. Current drawn from the generator increased from 1.8 to 7.9 amperes upon applying increasing load from 500 to 5,000 watts. The graph shows that the MHP could draw 5.4 amperes in 2,000 watts load operation.

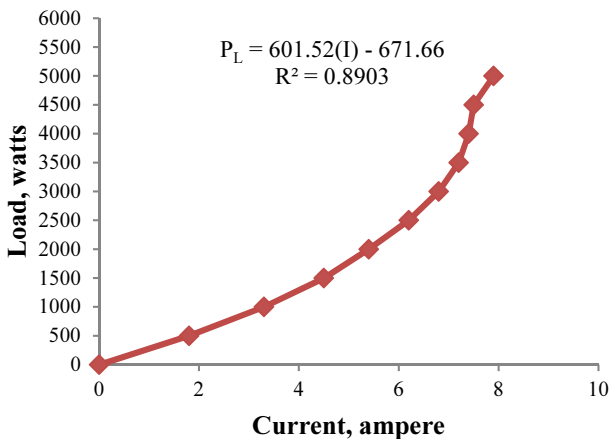


Figure 7. Effect of various applied loads in current of the 7.5 kW generator

Figure 8 shows the conversion efficiency (E_{con}) of the 7.5 kW synchronous electric generator. Regression equation is $P_L = -81.379 E_{con} + 7771.2$ with $R^2 = 0.9846$. Conversion efficiency dropped from 90 to 39.5% upon applying increasing load from 500 to 5,000 watts.

The decrease in conversion efficiency was due to the decrease in voltage of generator when applied increase load that induced resistance to current flow to the system.

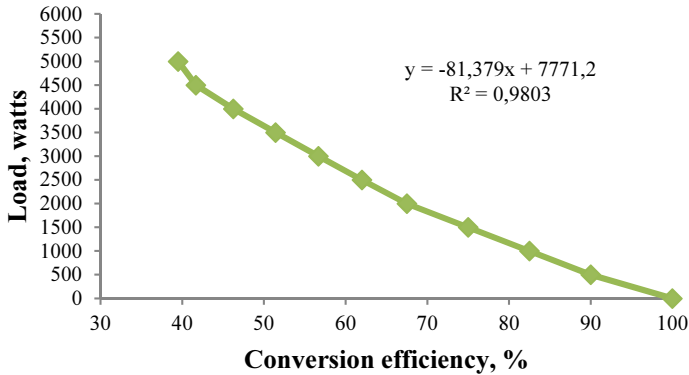


Figure 8. Effect of various applied loads in conversion efficiency of the generator.

Cost Analysis

The following economic performances of the MHP generation system excluding the power transmission systems were achieved: cost of power generated was Philippine Peso (PhP) 2.41 per kilowatt, the net income was projected at PhP 207,736 with investment cost of PhP 200,000, return on investment (ROI), internal rate of return (IRR), and payback period (PBP) were 106.98%, 111.44%, and 0.91 year, respectively.

CONCLUSIONS

Based on the results of the experiment, the following conclusions were drawn:

1. Each potential site is distinctive as it derives the power potential of the location which is based on the head and flow rate of the irrigation water. A t12 crossflow turbine was selected in this research project was due to it can be fabricated locally and suitable for low head application.
2. The developed MHP generation system using T12 crossflow turbine was installed and evaluated on-site in terms of technical performance. It had a dimension of 2.44 m length, 1.41 m width, and 1.63 m depth.
3. The computed turbine brake power (TBP), water theoretical power and turbine efficiency were 7.36 kW, 13.05 kW and 56.4%, respectively.
4. The developed MHP generation effectively harnessed irrigation water flow for power generation. It system could generate 5kW electricity in different water flow rates and different water exit notch combination settings in 1.72 m head.
5. The cost of generated electricity was Philippine Peso (PhP) 2.41/kW. This could be used for local lighting and other household use.

REFERENCES

- Chattha, J.A., Khan, M.S., Wasif, S.T., Ghani, O.A., and Zia M.O. (2010). Design of a cross-flow turbine for micro-hydro power application. In: Proceeding of ASME 2010 Power Conference. Chicago, Illinois, USA, July, 2010.
- Department Of Energy (2009). Energy Utilization Management Bureau. Manuals for Micro-hydropower Development in Rural Electrification. June 2009. Retrieved on March 22, 2014 at <https://www.researchgate.net/file.Post.html?idKey>.
- Department Of Energy (2012). Hydropower. Retrieved on March 22, 2014 at <https://www.doe.gov.ph/renewable-energy-res/hydropowr>.
- Fraenkel, P., Paish, O., Bokalders, V., Harvey, A., Brown, A., Edwards, R. (1999). Micro-hydro power:a guide for development workers. London: IT Publications.
- Harper, G. D. (2011). Planning and Installing Micro Hydro Systems: A Guide for Installers, Architects and Engineers. Earthscan Publications Ltd.
- Nakarmi, K., Arter, A., Widmer, R., and Eisenring, M. (1993). MHPG SERIES. Harnessing Water Power on a Small Scale. Volume 3. Crossflow Turbine Design and Equipment Engineering. Retrieved on June 24, 2016 at https://books.google.com/Cross_Flow_Turbpdf.
- OECD/IEA (2007). World Energy Outlook 2006, ed. R. Priddle. Paris: International Energy Agency.
- Paish, O. (2002). Small Hydro Power: Technology and Current Status. *Renewable and Sustainable Energy Reviews* 6 (6): 537-556.



USPOREDBA STANDARDNE I TWIN ROW SJETVE SUNCOKRETA S OBZIROM NA PRINOS

Anamarija BANAJ*, Đuro BANAJ, Vjekoslav TADIĆ, Davor PETROVIĆ,
Dario KNEŽEVIĆ

Poljoprivredni fakultet Sveučilišta J. J. Strossmayera u Osijeku, Zavod za mehanizaciju,
Vladimira Preloga 1, 31000 Osijek, Hrvatska

*E-mail dopisnog autora: abanaj@pfos.hr

SAŽETAK

U radu je prikazana usporedba rezultata primjene standardne i *twin row* sjetve suncokreta u Republici Hrvatskoj uporabom podtlačne sijačice PSK4-OLT Osijek i podtlačne sijačice tvrtke MaterMacc *Twin row-2*. Istraživanja su provedena na lokalitetu u Gorjanima, OPG Pero Zeko (45° 24' 21,77" N - 18° 23' 6,52" E) pri čemu je korišteno sjeme suncokreta siemenske kuće Syngenta – NK Neoma iz grupe srednje ranih hibrida s dužinom vegetacije od 110 do 130 dana. Hibrid Neoma zasijan je u standardnoj sjetvi s razmakom redova od 70 cm i u *twin row* sjetvi s razmakom udvojenih redova od 22 cm. Sjetva je obavljena 10. travnja 2017. godine. Standardna sjetva suncokreta obavljena je na predviđeni sklop od 71356 biljaka po hektaru ili 5 biljaka po metru dužine. Procijenjeni sklop u vrijeme nicanja iznosio je 59285 biljaka po hektaru. Prinos zrna u žetvi 31. kolovoza 2017. godine iznosio je 3608 kg ha⁻¹ sa standardnom devijacijom od 230,978 i koeficijentom varijacije od 6,40%. Prinos zrna u sjetvi *twin row*, s ostvarenim sklopom poniklih biljaka od 62480 biljaka, iznosio je 4048 kg ha⁻¹ ili 12,197% više u odnosu na standardnu sjetvu. Povećanjem sklopa u *twin row* sjetvi na 89460 poniklih biljaka dobiven je prinos od 4624 kg ha⁻¹ zrna s prosječnom vlagom od 6,46% što predstavlja povećanje od 1016 kg ha⁻¹ u odnosu na standardnu sjetvu.

Ključne riječi: suncokret, sjetva, *twin row* sijačica, prinos

UVOD

U Republici Hrvatskoj, u vegetacijskoj 2017. godini, suncokret je uzgajan na više od 42.000 hektara od čega je, desetak tisuća samo u Osječko-baranjskoj županiji s ukupnom proizvodnjom od 120 do 125 tisuća tona zrna. Europska unija, prema navodima Mijić, A (2017) ima značajan udio površina pod suncokretom i to približno 18%, a Hrvatska pripada u red zemalja s najvećim prosječnim prinosima. Tako naši poljoprivrednici zaslužuju visoku ocjenu kada je u pitanju suncokret. Radi toga svrstavamo se među tri "najbolje zemlje" s

ostvarenim prinosima. Hrvatska ima prosječan prinos od 2,68, Njemačka 2,38, a Austrija 2,27 t ha⁻¹. Najveći proizvođači suncokreta su Ruska Federacija (23,9%), Ukrajina (17,1%), Argentina (10,3%) te Indija s oko 8,2% od ukupnih svjetskih površina. Pozderović i sur. (2011) navode da Hrvatska svojim iznimnim geografskim položajem, a posebno istočni dio, ima povoljne klimatske uvjete, kvalitetno tlo za poljoprivrednu proizvodnju uz mogućnost navodnjavanja obradivih površina.

Prema navodima Markulj i sur. (2014) u razdoblju od 2004. do 2013. godine, suncokret se u Hrvatskoj uzgajao na prosječno 33.086 hektara godišnje, pri čemu je ostvaren prosječni urod zrna od 2,61 t ha⁻¹. Variranja u uzgojnim površinama i urodima zrna po godinama su velika. Najmanje požnjevenih površina je bilo 2007. godine (20 615 ha), dok je najviše bilo 2005. godine (49 769 ha). Isti autor navodi da je te iste godine ostvaren i najmanji prosječan urod zrna (1,60 t ha⁻¹ kao posljedica nepovoljnih klimatskih uvjeta za uzgoj suncokreta, za razliku od 2013. godine kada je prosječan urod zrna bio rekordnih 3,2 t ha⁻¹).

Kako navodi Pospišil, M. (2008) broj biljaka po hektaru i način sjetve ovise o hibridu i uvjetima uzgoja. Ekološki uvjeti mogu značajno modificirati komponente prinosa i fiziološke osobine suncokreta. Primjerice, u vlažnoj godini isti hibrid će dati značajno veći prinos sjemena s manjim brojem biljaka po hektaru, nego u suhoj godini. Za hibride dulje vegetacije preporučuju se sklopovi 45.000-50.000 biljaka po hektaru, a ranozrele 55.000-60.000 biljaka po hektaru u žetvi. Ako se kasniji hibridi siju u pregustom sklopu, prema navodima istog autora, glavice će biti manje kao i veličina i broj sjemenki u glavici, a biljke nešto više što stvara veću mogućnost za razvoj bolesti i polijeganje. U Hrvatskoj, kako navodi isti autor, sjetva suncokreta obavlja se na razmak redova od 70 i 75 cm.

Ovisno o proizvođačima sijačica udvojeni redovi siju se na međusobni razmak od 20, 22 ili 25 cm, a središnji razmak susjednih udvojenih redova iznosi 70 ili 75 cm tako da se berba može obaviti sa standardnim beračima za suncokret. *Twin row* sjetva omogućava bolje iskorištenje tla, sunčeve svjetlosti i u većini pokusa doprinosi ostvarenju jednakog ili većeg prinosa po hektaru. Razmak biljaka u sjetvi kod udvojenih redova značajno je veći jer se ovom tehnikom zasijava 284 reda po hektaru. Na tržištu poljoprivredne tehnike danas se mogu pronaći sijačice većeg broja proizvođača od kojih prednjače tvrtke *Great Plains*, *John Deere*, *Monosem*, *MaterMacc*, *CrustBuster*, *Speed King Inc*, *Kinze Manufacturing* i *Gaspardo*. Razlike između ponuđenih modela navedenih tvrtki zasigurno su u sjetvenom sustavu kao i razmaku između udvojenih redova koji iznosi 20, 22 ili 25 cm. Zarea i sur. (2005) su istraživali utjecaj različitih tehnika sjetve i međurednog razmaka odnosno sklopa na prinos suncokreta. Istraživanje je provedeno na poljima "Seed and Plant Institute, Karaj" u Iranu. Suncokret je sijan u širokim redovima (75 cm), u standardnim redovima (50 cm), u *twin row* kvadratnoj sjetvi i u *twin row* cik-cak sjetvi. Sjetva je u istraživanjima obavljena s 6, 8 i 10 biljaka ha⁻¹. Autori su utvrdili da se smanjenjem razmaka unutar redova povećava prinos. Također, rezultati su pokazali da su najveće prinose imali suncokreti posijani standardnom sjetvom i *twin row* sjetvom u cik-cak obliku pri sklopu od 8 biljaka ha⁻¹.

Cilj istraživanja bio je utvrditi, standardnim metodama, opravdanost primjene *twin row* tehnike sjetve suncokreta. Cilj ovoga rada je utvrditi eksploatacijsku pouzdanost sijačica u poljskim uvjetima rada u odnosu na ostvarenje indeksa kvalitete (*MISS - miss indeks*, *MULT - multiple indeks* i *QFI - quality of feed indeks*). Također prema rezultatima prinosa doći će se do drugog cilja, a to je opravdanost ili neprihvatljivost *twin row* sjetve suncokreta na ispitivanom lokalitetu. U radu su, također, utvrđene klimatske prilike i izvršena agrokemijska analiza tla u vegetacijskoj godini.

MATERIJALI I METODE

U ispitivanju je korištena sijačica tvrtke *MaterMacc*, koja je u proizvodnom programu tržištu poljoprivredne mehanizacije ponudila sijačicu za sjetvu s udvojenim redovima s razmakom redova od 22 cm. Sijačica se na tržištu pojavljuje pod komercijalnim nazivom *MaterMacc Twin Row-2*. Za standardnu sjetvu (razmak redova 70 cm) korištena je pneumatska sijačica *PSK 4-OLT Osijek* kao usporedba na ostvarenje prinosa (kg ha^{-1}).



MaterMacc Twin Row-2



PSK 4-OLT

Slika 1. Sijačica *MaterMacc Twin Row-2* i sijačica *PSK 4-OLT Osijek* s pripadajućim sjetvenim pločama

Figure 1. *MaterMacc Twin Row-2* planter and *PSK 4-OLT Osijek* planter with corresponding seed plates

Pokus je posijan 10. travnja 2017. godine na lokalitetu Gorjani, OPG Pero Zeko ($45^{\circ} 24' 21,77'' \text{ N} - 18^{\circ} 23' 6,52'' \text{ E}$) pri čemu je korišten hibrid suncokreta *NK Neoma* sjemenske kuće *Syngenta*. Sjetva suncokreta primjenom *twin row* tehnologije obavljena je na predviđene sklopove od 66.355 i 94.039 biljaka ha^{-1} , dok je sklop pri standardnoj sjetvi iznosio 71.356 biljaka ha^{-1} . Hibrid *NK Neoma* uvrštava se u grupu srednje ranih hibrida s dužinom od 110 do 130 vegetacijskih dana. Prednost ovoga hibrida je otpornost na djelovanje herbicida *Pulsar® 40* (IMI tehnologija). *NK Neoma* u razvoju ostvaruje stabljiku srednje visine, otpornu na lomljenje kao i na polijeganje tijekom vegetacije. Navedeni hibrid ima "glavu" s velikim brojem zrna srednje mase. U proizvodnji je relativno tolerantan na sušne uvjete uzgoja. Hibrid *NK Neoma* posjeduje visoku tolerantnost prema crnoj pjegavosti (*Phomopsis*), bijeloj truleži glave (*Sclerotinia*) i suhoj truleži (*Macrophomina*) te umjerenu tolerantnost na crnu pjegavost stabljike i bijelu trulež korijena. Prednosti ovoga hibrida u uzgoju su pozitivna reakcija na plodna tla, ali i dobra podnošljivost tla nešto lošije

kvalitete. Isto tako *NK Neoma* posjeduje visok potencijal za prinose i sadržaj ulja, te proizvođač preporuča sjetvu na sklop od 60.000 biljaka ha⁻¹. Prinos zrna je utvrđen kombajniranjem četiri reda suncokreta na duljini od 100 m u četiri ponavljanja. Mjerenje mase ovršenog zrna obavljeno je pomoću vage Weigh-Tronix, model 715. Dobivena masa zrna suncokreta s uzorkovane površine preračunata je u kg/ha.



Slika 2. Suncokret *NK Neoma* u sjetvi u udvojene redove razmaka 22 cm
Figure 2. Sunflower *NK Neoma* in seeding in twin rows spacing 22 cm

REZULTATI I RASPRAVA

Podešenost sijačica na ispitnom stolu i ostvarenje koeficijenta kvalitete rada

Utvrđivanje položaja skidača viška sjemena obavljeno je na ispitnom stolu Zavoda za mehanizaciju Poljoprivrednog fakulteta u Osijeku. Podešavanje položaja skidača obavljeno je simulacijom pri brzini rada sijačice od 5 km h⁻¹. Dobiveni rezultati ukazuju na problematiku ostvarenja najboljeg položaja skidača prema središnjem dijelu otvora ploče s obzirom na specifični oblik sjemenki suncokreta. Podešavanje sijačice *PSK-OLT* obavljeno je kod prijenosnog odnosa (*i*) 0,5777 sa sjetvenom pločom od 18 otvora \varnothing 3,5 mm i pri položaju skidača viška sjemena na br. 13. Uz dinamički promjer pogonskog kotača od 62,10 cm teorijski razmak zrna iznosio je 18,75 cm odnosno 10,4 biljaka po dužnom metru. Testiranje sijačice *MaterMacc Twin Row-2* obavljeno je pri korištenju sjetvene ploče s 12 otvora \varnothing 3,5 mm i pri prijenosnim odnosima (*i*) 0,3558 i 0,4308. Pogonski kotač je dinamičkog promjera 48 cm, pri čemu su ostvareni razmaci zrna u sjetvi od 35,35 i 29,20 cm.

Tablica 1. Statistički pokazatelji kvalitete rada sijačica u laboratorijskim uvjetima
Table 1. Statistical quality of the work of the planters in Laboratory Conditions

Sijačica/ Planter	\bar{x}	σ	Median	Mod	Očekivana \bar{x} (pouzdanost 95 %)/ Expected arithmetic mean value (reliability 95%)
PSK-OLT	19,123	4,640	18,72	19,11	18,945
	31,920	12,242	32,01	31,35	30,959
MaterMacc	39,198	17,411	38,94	39,60	37,669
					40,726

Za ocjenu ostvarenog razmaka zrna u sjetvi, primijenjen je ISO standard 7256/1 i 7256/2 odnosno kvaliteta rada sijačica analizirana je primijenom kvalitativnih indeksa. *MISS* (*miss indeks* - postotni udio razmaka koji su > 1,5 od predviđenog razmaka), *MULT* (*multiple indeks* - postotni udio razmaka koji su ≤ od 0,5 od predviđenog razmaka), *QFI* (*quality of feed indeks* - postotni udio razmaka 0,5 - 1,5 predviđenog razmaka).

Tablica 2. Ostvarene vrijednosti kvalitativnih indeksa
Table 2. Qualitative Indices Realized Values

Sijačica/ Planter	Tablični razmaci zrna/ Tabular grain spacing, cm	Duljina mjerenja/ Length of measurement, m	Postotni udio razmaka/ Percentage spacing ≤ 0,5 \bar{x}	Postotni udio razmaka/ Percentage spacing (0,5 - 1,5) \bar{x}	Postotni udio razmaka/ Percentage spacing > 1,5 \bar{x}
<i>PSK-OLT</i>	18,75	500	2,10	94,11	3,79
<i>MaterMacc</i>	29,20	200	7,83	84,98	7,19
	35,35	200	8,58	82,44	8,98

Klimatske prilike u vegetacijskoj 2017. godini

Srednja temperatura zraka u travnju, u mjesecu sjetve, iznosila je 11,8 °C s ukupno izmjerenih 71,7 mm oborina. U vrijeme berbe, u kolovozu srednja temperatura zraka iznosila je maksimalnih 24,2 °C s 27,1 mm oborina. Srednja temperatura zraka u lipnju iznosila je 22,9 °C da bi u srpnju dosegla maksimum od 24,2 °C kao i u kolovozu (tablica 3).

Tablica 3. Srednje mjesečne temperature zraka (°C) i godišnje količine oborina (mm) izmjerene na klimatološkoj postaji na području Đakova

Table 3. Average monthly air temperatures (°C) and annual rainfall (mm) measured at the climatological station in Đakovo

Srednje mjesečne vrijednosti izmjerene na klimatološkoj postaji Đakovo za razdoblje 1981.-2016. godine/Average monthly values measured at the Đakovo Climatological Station for the period 1981- 2016 years							
Mjesec/Month	IV	V	VI	VII	VIII	Σ	
Srednja temperatura zraka/Mean air temperature, °C	12,0	17,0	20,2	22,1	21,6	-	
Količina oborina/Total precipitation, mm	54,0	69,3	84,7	57,6	68,5	334,1	
Srednje mjesečne vrijednosti izmjerene na klimatološkoj postaji Đakovo u 2017. godini/ Average monthly values measured at the Đakovo Climatological Station in 2017							
Srednja temperatura zraka/Average air temperature, °C	11,8	17,9	22,9	24,2	24,2	-	
Količina oborina/Total precipitation, mm	71,7	65,8	71,9	33,3	27,1	269,8	

Rezultati utvrđivanja vrijednosti tla na pokušalistu (OPG Pero Zeko, Gorjani)

Značajnija svojstva tla na pokušalistu (45° 24' 21,77" N - 18° 23' 6,52" E) prikazana su u tablici 4.

Tablica 4. Agrokemijska analiza tla
Table 4. Agrochemical soil analysis

pH _{KCL}	pH _{HOH}	Humus, %	AL-P ₂ O ₅
6,04	6,42	2,55	19,72 mg/100g
AL-K ₂ O	CaCO ₃	HK	
16,48 mg/100g	1,26 cmol(+) kg^{-1}	2,63 cmol(+) kg^{-1}	

Rezultati vrijednosti eksploatacijskih pokazatelja kvalitete rada sijačica u vrijeme sjetve suncokreta

Ostvarene radne brzine te radne dubine u vrijeme sjetve na pokušalištu 004 – “Gorjani” OPG Pero Zeko prikazane su u tablici 5.

Tablica 5. Neke statističke vrijednosti eksploatacijskih pokazatelja kvalitete rada sijačica
Table 5 Some statistical values of exploitation performance indicators of the quality of planters

Sijačica/Planter	Brzina rada/Speed of work, km h ⁻¹				
	\bar{x}	σ	C. V., %	Minimalna vrijednost/ Minimum value	Maximalna vrijednost/ Maximum value
PSK-4 OLT Osijek	4,74	0,559	11,80	3,8	5,2
MaterMacc Twin Row - 2	4,52	0,526	11,64	3,7	5,1
Dubina rada/Depth of work, cm					
PSK-4 OLT Osijek	5,0	0,714	14,28	4,1	5,9
MaterMacc Twin Row - 2	5,38	0,327	6,08	4,9	5,8



Slika 3. Twin row sjetva suncokreta s razmakom udvojenih redova od 22 cm
Figure 3. Twin row seeding of sunflower with a spacing of twin rows of 22 cm

Rezultati postignutih sklopova posijanih hibrida nakon nicanja

Utvrđen broj i razmak biljaka unutar reda nakon nicanja suncokreta *NK Neoma* prikazani su u tablici 6.

Tablica 6. Utvrđen broj i razmak biljaka unutar reda nakon nicanja suncokreta *NK Neoma*
Table 6. Determined number and spacings of plants within a row after the sunflower *NK Neoma* emerges

Hibrid/ Hybrid	Sjetva-razmak redova/ Seeding-row spacing 70 i 22 * 48 cm	Sklop biljaka po ha u vrijeme nicanja/ Population per ha after emergence				
		\bar{x}	σ	C. V., %	Najmanja vrijednost/ Minimum value	Najveća vrijednost/ Maximum value
	Standard I - 71356	59285	2425,112	4,09	56800	62480
	Twin Row I -66355	62480	5185,107	8,30	56800	68160
	Twin Row II- 94039	89460	3666,424	4,10	85200	93720
		Razmak biljaka unutar reda nakon nicanja, cm				
<i>NK Neoma</i>	Način sjetve/ Seeding technique	\bar{x}	σ	C. V., %	Najmanja vrijednost/ Minimum value	Najveća vrijednost/ Maximum value
	Standard I -71356	23,97	6,009	25,07	10	42
	Twin Row I -66355	45,23	5,296	11,71	29	52
	Twin Row II- 94039	31,57	5,859	18,56	22	54

Prinosi zrna u žrtvi suncokreta (vlažnosti do 10%) kod standardne i *twin row* sjetve hibrida *NK Neoma* prikazani su u tablici 7.

Tablica 7. Prinosi zrna u žetvi suncokreta (vlažnosti do 10%) kod standardne i twin row sjetve hibrida NK Neoma (31. kolovoza 2017. godine)

Table 7. Grain yields in harvest (humidity up to 10%) for standard and twin-row seeding of NK Neoma (August 31, 2017)

Hibrid/ Hybrid	Razmak redova/Row spacing 70 i 22 * 53 cm	Utvrđena vrijednost vlažnosti u žetvi/Determined moisture value in harvest, %				
		\bar{x}	σ	C. V., %	Najmanja vrijednost/ Minimum value	Najveća vrijednost/ Maximum value
	Standard I - 59285	8,88	0,148	1,67	8,70	9,10
	Twin Row I -62480	6,50	0,255	3,92	6,20	6,80
	Twin Row II- 89460	6,46	0,134	2,08	6,30	6,60
		Prinos/Yield, kg ha ⁻¹				
NK Neoma	Način sjetve/ Seeding technique	\bar{x}	σ	C. V., %	Najmanja vrijednost/ Minimum value	Najveća vrijednost/ Maximum value
	Standard I - 59285	3608	230,978	6,40	3378	3895
	Twin Row I -62480	4048	115,719	2,86	3945	4212
	Twin Row II- 89460	4624	127,464	2,76	4489	4786

ZAKLJUČCI

Temeljem provedenih istraživanja mogu se donijeti sljedeći zaključci:

- Temeljem meteoroloških podataka, prvenstveno promatrajući srednje mjesečne temperature zraka i mjesečne količine oborina, možemo zaključiti da je vegetacijska godina 2017. bila pogodna za proizvodnju suncokreta na lokalitetu *Gorjani*, OPG Pero Zeko.
- U standardnoj sjetvi s pneumatskom sijačicom *PSK4-OLT Osijek*, hibrid sjemenske kuće *Syngenta – NK Neoma* u sklopu od 59285 biljaka ha⁻¹ nakon nicanja ostvario je prinos od 3608 kg ha⁻¹ suhog zrna s prosječnom vlažnošću od 8,88%,
- *Twin row* sjetva sa ostvarenim sklopom od 62480 biljaka ha⁻¹ kod istog hibrida polučila je prinos od 4048 kg ha⁻¹ zrna s prosječnom vlažnošću od 6,50% što čini povećanje u odnosu na standardnu sjetvu od 12,19%.
- *Twin row* sjetva suncokreta *NK-Neoma* sa sijačicom *MaterMacc Twin Row-2* s ostvarenim sklopom od 89460 biljka ha⁻¹ dobiven je prinos od 4624 biljka ha⁻¹ zrna s prosječnom vlagom od 6,46% što predstavlja povećanje od 1016 kg ha⁻¹ prinosa u odnosu na standardnu sjetvu.

LITERATURA

- Banaj, A., Kurkutović, L., Banaj Đ., Menđušić, I. (2017): Application of MATERMACC twin row - 2 seeder in corn sowing, 10. međunarodni znanstveno-stručni skup "Poljoprivreda u zaštiti prirode i okoliša", Vukovar, 5.- 7. lipnja 2017, 180-186.
- Banaj, A., Šumanovac, L., Heffer, G., Tadić, V., Banaj Đ., (2017): Yield of corn grain by sowing in twin rows with MATERMACC - 2 planter, International Scientific Symposium: Actual Tasks on Agricultural Engineering, Agronomy faculty in Zagreb; Opatija, Croatia, 141 – 152.
- Čuljat M. (1989): Primjena tehnike za proizvodnju soje s naglaskom na tehniku sjetve i zaštite, Zbornik radova VIII savjetovanja "Biološki, tehnički i organizacijski aspekti unapređenja i proširenja proizvodnje soje u Slavoniji i Baranji", 154 – 158, Osijek, 1989.
- Jurković, D., Kajić, N., Banaj, A., Tadić, V., Banaj, Đ., Jović, J., (2017): Twin Row technology maize sowing, Agriculture Symposium "Agrosym 2017, Jahorina, October 5-8, 2017.
- Markulj, A., Liović, I., Mijić, A., Sudarić, A., Josipović, . Matoša Kočar, M. (2014): Zašto proizvoditi suncokret, Agronomski glasnik 3/2014, 163-176.
- Pospišil M. (2008): Sjetva suncokreta, Glasnik zaštite bilja 4/2008, 95-100.
- Pozderović, A., Pichler, A., Paragović, K. (2011): Proizvodnja, uvoz, izvoz i potrošnja hrane u Republici Hrvatskoj od 1997. do 2010. Zbornik sažetaka – Okolišno prihvatljiva proizvodnja kvalitetne i sigurne hrane, 13-14.
- Zarea, M. J., Ghalavand, A., Daneshian, J. (2005): Effect of planting patterns of sunflower on yield and extinction coefficient, Agron. Sustain. Dev. 25 (2005) 513–518.
- ***https://www.agroklub.com/ratarstvo/hrvatska-druga-u-eu-po-prinosima_suncokreta/35836/ (zadnji pristup: 20. 10. 2017.)

COMPARISON OF STANDARD AND TWIN ROW SEEDING ON SUNFLOWER YIELD

SUMMARY

The paper presents comparison of results of single row and twin row planting in Croatia by using pneumatic PSK4-OLT planter and pneumatic MaterMacc Twin Row-2 planters. The researches were conducted on locality Gorjani, OPG Pero Zeko (45° 24' 21,77" N - 18° 23' 6,52" E) whereby was used sunflower hybrid NK Neoma, Syngenta which is mid-early hybrid with length of vegetation from 110 to 130 days. Hybrid NK Neoma was planted in standard 70 cm single rows and twin rows with 22 cm apart. The experiment was planted at the tenth of April 2017. The seeding rate of the single row planting was 71356 plants ha⁻¹ or 5 plants per square meter. The estimated population after emergence was 59285 plants ha⁻¹. The experiment was harvested in August, 31. 2017. And the yield was 3608 kg with $\sigma=230,878$ and C. V.=6,40%. The estimated population in twin row planting was 62480 plants/ha, and the yield was 4048 kg ha⁻¹ or 12,97% more than yield of single row planting. By increasing the population (89460 plants ha⁻¹ after emergence) the yield was 4624 kg ha⁻¹ which represents an increase of 1016 kg ha⁻¹ more than the yield of single row planting.

Key words: sunflower, seeding, twin row seeder, yield



RESEARCHES OF THE BULB PLANTING PROCESS IN FIELD AND LABORATORY CONDITIONS

Gheorghe BOLINTINEANU^{1*}, Dan CUJBESCU¹, Cătălin PERSU¹,
Iuliana GĂGEANU¹, Laurentiu VLĂDUȚOIU¹, Mihaela NIȚU¹, Augstina
PRUTEANU¹, Nicoleta UNGUREANU²

¹ Testing Department, INMA, Ion Ionescu de la Brad Blv. No. 6, Sector 1, Bucharest, Romania

² Department of Biotechnical Systems, University POLITEHNICA of Bucharest,
Splaiul Independentei nr. 313, Sector 6, Bucharest, Romania

*E-mail of corresponding author: bolintineanu_gh@yahoo.com

SUMMARY

In the paper we performed an analysis of the qualitative working indices and the energy indices of a bulb planter with eight planting sections. Experiments were performed with bulbs ranging in size from 7 to 20 mm. Under laboratory conditions, the average irregularity was determined on the working width (between 5 and 9.8%), instability of the norm to be planted as well as the degree of damage (1.8%). In the experiments in the field were determined the productive indices of the planting machine.

Keywords: planting bulbs machine, planting depth, bulbs, uniformity.

INTRODUCTION

Bulb planters are designed to replace the manual planting of the bulbs, which is a rather strenuous operation because it is performed in a squatting position. These machines ensure an even depth of incorporation of the bulbs into the soil. Research on the field of bulb planters focused on the possibility of plant bulb placement at the bottom of ditches (Kawaguchi et al., 2015) or on the working time, work position of the workers and the subsequent plant growth (Kawaguchi et al., 2015). A six-row onion bulb planter has been evaluated in terms of missing index, multiple index and quality of feed index (Grewal et al., 2015).

Research was also conducted on the development of an inclined plate metering device for planting onion bulb for the seed purpose and this metering device is applicable to small onion bulb usually less than 35 mm (Bairwa, 2016). There are also concerns about the possibility of using the GPS system to monitor the functional and economic indicators of the

planting operation (Păunescu et al., 2010). Ongoing concerns were also in the development and optimization of the distributors of bulb planters (Cârdei et al., 2011).

The bulb planter must meet the following requirements (Uceanu et al., 2008):

- to require a small number of workers;
- to have increased mobility during operation and to have high safety in operation;
- to maintain during operation the made adjustments;
- to have multiple, rigorous adjustment possibilities and to be able to achieve the usual minimum and maximum norm provided in the agro-technical requirements.

MATERIALS AND METHODS

The experiment was carried out in 2016 at Moara Domnescă farm. The machine used in the experimental research operates with cup dispensers, placing the garlic, chives or other planting material in the furrow opened by the coulter. Covering of the furrows is ensured by the compaction wheels and the levelling blades placed behind the coulter, that produce a proper compaction of the germination bed and a good quality of planting. The bulbs of garlic or chives are placed in the machine's feeding hopper, whereupon the chain-operated cups will take up the planting material, that reaches in the soil, in the furrows opened by the coulter, that can be adjusted to a depth of 3 - 12 cm, to the desired density.

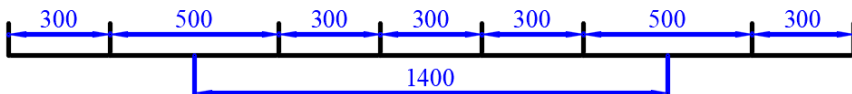


Figure 1. The experiment scheme

The machine consists of the following main parts: a frame constructed in the form of a square sectional frame, two support wheels, eight sections, two transmission mechanisms (one for each half of the workstations), each trained from one support wheel, two tracer markers and trailer attachment carrier.

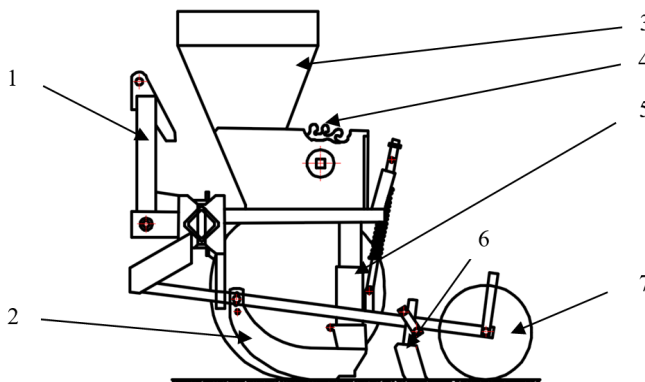


Figure 2. Scheme of a section of the bulb planter

- 1 – frame; 2 – coulter; 3 – bulb hopper; 4 – distributor; 5 – driving tube for bulbs;
6 – levelling blades; 7 – compaction wheel

The characteristics of the materials used in the experimental research are given in Table 1.

Table 1. Characteristics of the materials used in the experimental research

No.	Specification	M. U.	Chive	Garlic
1.	Bulb diameter	mm	7-20	-
	Percentage of healthy bulbs	%	94.7	94.2
2.	germinated	%	3.8	3.1
	hollow	%	1.5	-
	rotten	%	-	2.7
3.	Average diameter	mm	12.6	10.1
4.	Average length	mm	19.8	23.4
5.	Average weight	g	2.67	0.9

In laboratory, experiments were determined the following indices:

- the amount of chive and garlic bulbs that can be distributed per hectare at machine settings for the minimum, maximum and usual norm according to the agrotechnical requirements.

The amount of bulbs that can be distributed by the machine was determined as follows:

The transmission mechanism and the distribution devices of the planting machine were adjusted to ensure the distribution of minimal, maximum and usual amounts of bulbs. The machine was equipped with eight planting sections and was driven by the tractor on a distance corresponding to an area of 100 m², and the bulbs were collected from each section. The operation average speeds during testing were 5.5 km h⁻¹ and 6.7 km h⁻¹. The weighings were made with an accuracy of 1 g, and the tests were made in 3 repetitions.

- the average unevenness of bulbs distribution on the working width.

This index was determined using the data obtained while determining the amounts of chive and garlic bulbs that can be distributed by the machine at the adjustment for one of the usual norms.

This index was calculated with the relationship:

$$e = \frac{\sum_{i=1}^n (Q_m - Q_i)}{Q_m \cdot n} \cdot 100 \quad (1)$$

where:

- e is the irregularity of distribution on the working width (%);
- Q_m is the average amount of bulbs distributed through a coulter (g);
- Q_i is the amount of bulbs distributed through each coulter (g);
- n is the number of dispersers in operation.
- instability of the planting norm.

Instability of the planting norm was determined for one of the usual norms and it was computed using the relation:

$$i = \frac{\sum_{1}^n (N_m - N_i)}{N_m \cdot n} \cdot 100 \quad (2)$$

where:

- i is the instability of the planting norm (%);
- N_m is the average norm at 3 repetitions (kg h^{-1});
- N_i is the norm per hectare for each repetition (kg h^{-1});
- n is the number of repetitions.
- the degree of bulbs damage.

To determine the degree of bulb damage, their analysis was performed after they were distributed by the machine. Tests were made with an amount of 5 kg of chive and 5 kg of garlic that were previously tested beforehand to not contain damaged bulbs. The degree of bulbs damage was calculated with the relationship:

$$V = \frac{G_v}{G_i} \cdot 100 \quad (3)$$

where:

- V is the degree of bulbs damage (%);
- G_v is the initial mass of bulbs introduced in the machine (kg);
- G_i is the mass of bulbs damaged by the machine (kg).

Tests in field – laboratory conditions were made in plots whose characteristics are presented in Table 2.

Table 2. Characteristics of the plot on which experimental research was conducted

No.	Index name	Characteristics
1.	Type of soil	forest brown red
2.	Microrelief	without bumps
3.	Previously performed works	autumn tillage, disked and processed by the combiner
4.	Moisture in the horizon 0-10 cm	17-18.5 %
5.	The degree of soil crushing	without clods larger than 5 cm
6.	Covering by plant debris	no plant debris

The bulb planter is equipped with eight sections. Transmission adjustment: 15x32 (0.47), 15x22 (0.68) and 27x32 (0.84) for chives, respectively for garlic it was used the adjustment 15x32 corresponding to the distance between bulbs on a row of 7.0 cm. The adjusted working depth was 4.0 cm and the travel average speeds were 5.5 km h^{-1} and 6.7 km h^{-1} .

The following indices were determined in the field-laboratory tests:

- the average number of bulbs planted per hectare, the distance between bulbs and plants per row and the uniformity of distribution of bulbs and plants per row. Measurements were made immediately after planting by uncovering the bulbs distributed in the soil as well as after plant emergence. Garlic measurements were made only after unpacking. For each planted row were made 100 measurements in 3 repetitions. With the obtained data were calculated the average distance between bulbs and plants per row as well as the average number of bulbs, respectively plants per hectare.

- average working depth and uniformity of depth.
The average working depth achieved at planting and the uniformity of depth was determined after plant emergence by measuring the distance from the bulb to the soil surface to a precision of 1 mm. There were made 20 measurements per each row in 3 different areas. After the measurements, were computed the average depth, the degree of unevenness of the planting depth and the deviation from the average depth.
- the distance between rows and the average distance between rows.
The distance between rows and the average deviation from the adjusted distance was determined by performing 20 measurements on each row in 3 repetitions.
The determined energy indices were:
 - the force and tractive power, medium and maximum, required by the machine determined with the QuantumX MX 1615 data acquisition system;
 - speed of movement in operation determined with data acquisition system Datron DAS 3 (measuring range: ± 10 V) and speed sensor S 400 (measuring range: 0,5 - 250 km h⁻¹);
 - fuel consumption determined with fuel consumption measuring system Flowtronic 215 (measuring range: up to 60 l h⁻¹);
 - wheel slip.
 Measurements were made using a laboratory tractor (30 kW) equipped with a force transducer and a consumer appliance.

RESULTS AND DISCUSSION

The average results obtained from the measurements and calculations for the amount of bulbs per hectare, for chives ($\phi_{\text{bulb}}=7\text{-}20\text{mm}$ and $m_{1 \text{ bulb}}=2.67\text{g}$), are presented in Table 3.

Table 3. Amount of chive bulbs that can be distributed per hectare

No.	Transmission ratio	Average working speed (km h ⁻¹)	Average distance between rows (cm)	35	39	45	48
1.	0.47	5.5	Bulb amount (kg ha ⁻¹)	1075	965.2	835.1	785
			No. of bulbs per hectare	403,000	361,500	312,780	29,4000
		6.7	Bulb amount (kg ha ⁻¹)	1150	1031.8	895.7	835
			No. of bulbs per hectare	430,700	386,500	335,500	313,000
2.	0.68	5.5	Bulb amount (kg ha ⁻¹)	1985	1780	1545	1445
			No. of bulbs per hectare	743,500	667,000	579,000	542,000
		6.7	Bulb amount (kg ha ⁻¹)	2210	1980	1715	1610
			No. of bulbs per hectare	828,000	742,000	643,000	604,000
3.	0.84	5.5	Bulb amount (kg ha ⁻¹)	2469	2225	1910	1795
			No. of bulbs per hectare	925,000	834,000	715,000	672,000
		6.7	Bulb amount (kg ha ⁻¹)	3105	2783	2550	2525
			No. of bulbs per hectare	1163000	1042000	955000	946000

Figure 3 shows the variation of the amount of garlic bulbs, depending on the working speed and the transmission ratio of the transmission of the bulb distributor.

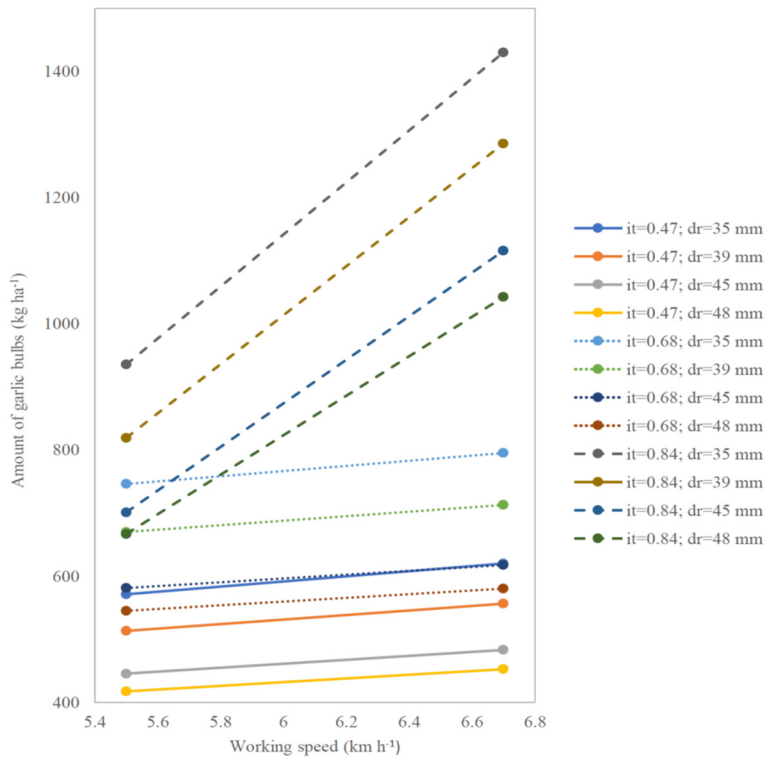


Figure 3. Variation of the amount of garlic bulbs, depending on the working speed and the transmission ratio of the transmission of the bulb distributor

Table 4. Average unevenness, average instability of the planting norm and the average degree of damage to the bulbs for an adjusted distance between rows of 39 cm

Material used	Average amount of bulbs distributed by the machine (kg ha ⁻¹)	Average working speed (km h ⁻¹)	Average unevenness of distribution per working width (%)	Average instability of planting norm (%)	Average degree of damage (%)
Chive	845.0	5.5	5.8	1.85	1.8
	903.5	6.7	9.8	1.4	
Garlic	513.2	5.5	7.4	3.2	1.5
	556.3	6.7	9.5	0.5	

Table 4 shows the indices obtained in the experiments under laboratory conditions, for 39 cm distance between rows: the unevenness of distribution on the working width, the instability of the planting norm and the degree of damage to the bulbs.

In Table 5 are presented: the average distance between bulbs per row, the number of bulbs, the uniformity of distribution and the indices obtained for chive bulbs in field experiments.

Table 5. Average distance between bulbs per row, number of bulbs and the uniformity of distribution, indices obtained for chive bulbs (field experiments)

Transmission ratio	Average distance between bulbs per row (cm)	Number of bulbs per hectare	Uniformity of distribution (%)
0.47	8.55	305,000	82.1
0.68	5.48	465,000	78.3

Figure 4 presents the graphical variation for the uniformity of distribution of garlic bulbs per row.

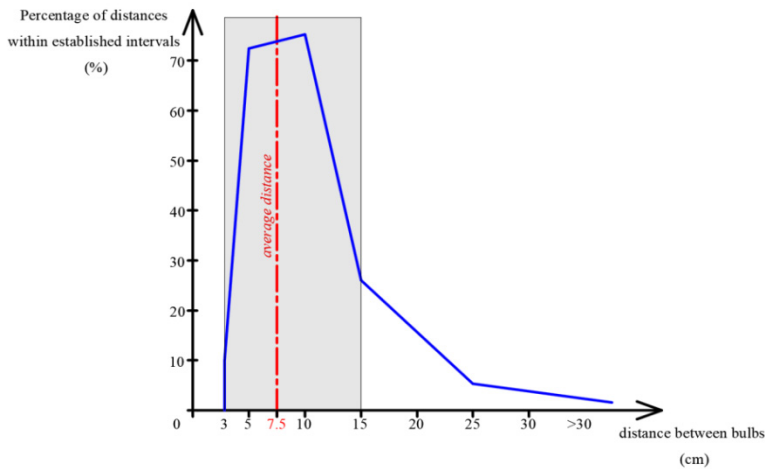


Figure 4. Variation of uniformity of distribution for garlic bulbs per row

In Table 6 are presented the indices of variation in the depth of bulb burying.

Table 6. Indices of variation in the depth of bulb burying

No.	Specification	Values
1.	Average depth (cm)	4.53
2.	Deviation from the average depth (cm)	0.67
3.	The degree of unevenness of the depth (%)	15.2
4.	Percentage of depths in the optimum range (%)	82
5.	Smaller depths (%)	7
6.	Larger depths (%)	11

In Table 7 are presented the indices: the average distance between rows, the average deviation from the adjusted distance and the average deviation from the achieved distance, determined by performing 20 measurements per each row in 3 repetitions.

Table 7. Average distance between rows, average deviation from the adjusted distance and the average deviation from the achieved distance

No.	Specification	Interval between sections								Average working speed (km h ⁻¹)
		1-2	2-3	3-4	4-5	5-6	6-7	7-8	8-1	
1.	Average distance between rows (cm)	29.6	65.3	30.4	32.4	30.6	65.2	29.3	33.8	5.5
		30.1	65.2	30.5	31.4	31.1	64.4	30.5	34.5	6.7
2.	Average deviation from the adjusted distance	0.4	0.7	0.4	2.4	0.6	0.8	0.7	4.5	5.5
		0.1	0.8	0.5	1.4	1.1	1.6	0.5	3.8	6.7
3.	Average deviation from the achieved distance	1.5	1.5	2.1	2.3	2.3	1.3	1.6	2.5	5.5
		1.4	1.9	1.8	1.7	2.7	1.5	1.8	2.5	6.7

The values of energy indices determined for a working depth of 4-5 cm using 8 coulters are presented in Table 8.

Table 8. Determined energy indices

No.	Specification	M.U.	Achieved values
1.	Working speed	km h ⁻¹	6.0
2.	Traction force	daN	311
3.	Traction power	kW	5.12
4.	Wheel slip	%	2.88

Analyzing the obtained results (Tables 3, 4 and Figure 2), the following were found:

- from the amount of bulbs distributed per hectare by the machine, in case of the chives (fraction 7 - 20), it resulted that the machine achieves densities ranging between 294,000 - 743,500 bulbs hectare⁻¹, for an average bulb weight of 2.67 g;
- for garlic, the machine can achieve densities ranging between 464,000 – 689,000 bulbs hectare⁻¹, for the variety used in experiments having the average weight of a bulb of 0.9 g;
- the machine provides the densities required by agrotechnical norms, namely 300,000 – 500,000 bulbs hectare⁻¹ for chives and 400,000 – 600,000 bulbs hectare⁻¹ for garlic.

In terms of the qualitative working indices of the distribution devices, it resulted that these are in line with the imposed agrotechnical requirements, namely:

- average unevenness of distribution on the working width: 5.8 - 9.8% versus 10% admitted;
- instability of the planting norm: 0.5 - 1.85% versus 5% maximum admitted, and the degree of damage ranges between 1.5% and 1.8% versus 5% maximum admitted.

Analyzing the results of the determinations in Tables 5, 6, 7, 8 and Figure 3, the following are observed:

- the average number of bulbs and plants per hectare and also the average distance between bulbs respectively between plants per row (Table 5) shows that the machine has achieved the densities required by the adjustments made;

- the uniformity of distribution of the bulbs respectively of the plants per row, in the case of the chives, 78.3% to 82.1% of the distances measured between the bulbs were recorded within the set interval, i.e. between 3-15 cm;
- for garlic 72.4% to 76.5% of the distances measured between the bulbs were within the set interval, i.e. between 3 - 15 cm (Figure 3);
- with regard to the planting depth (Table 6), the machine performed the planting of the bulbs at an average depth of 4.53 cm (compared to 4 cm adjusted depth) with a deviation of 0.67 cm from the average depth and a degree of unevenness of the depth of 15.2%, which highlights the good quality of the planting work in terms of the depth of bulbs burial;
- regarding the maintenance of the distance between the rows, the data in Table 7 highlighted that the machine performed the planting of the bulbs corresponding to the adjusted distances between the rows;
- with regard to the energy indices (Table 8), it resulted that the machine required, in operation, an average traction force of 311 daN and a traction power of 5.12 kW, with the skidding of tractor wheels of 2.88%.

Bakhtiari and Loghavi (2009) worked on innovatively designed tractor-mounted, ground-wheel driven, triple unit, row crop precision planter capable of planting three rows of garlic (*Allium sativum* L.) clove on each raised bed. The results showed that the new machine is capable of planting 220,000 plants/ha at the seeding depth and spacing of 12.3 and 22.7 cm, respectively. Brajesh et al. (2014) designed, fabricated and tested a self-propelled precision garlic planter. It was observed that the placement of garlic cloves were at uniform depth under a range 4.2 cm to 5.2 cm. The actual field capacity was found to be 0.065 ha h⁻¹ with field efficiency of 79.84 %. Benjaphragairat et al. (2010) focused on increasing the planter capacity by reducing the draft of the planter, increasing the field efficiency by increasing the optimum number of rows and increasing the uniformity of the seed. The percentage of germination was 74.57 %.

CONCLUSIONS

High values of quality working indices determined in laboratory conditions lead to their increase in field conditions and will enhance the performances of planting machines.

The planting machine ensures the densities demanded by agrotechnical norms, respectively 300,000-500,000 bulbs hectare⁻¹ for chives and 400,000-600,000 bulbs hectare⁻¹ for garlic.

As for quality working indices of distribution devices, it results that they fitted in the agrotechnical requirements imposed, the average distribution unevenness on the working width being 5.8-9.8% compared to the maximum 10% permitted, the instability of the planting norm was 0.5-1.85% compared to the maximum 5% permitted, and the degree of harming is situated between 1.5% and 1.8% compared to the maximum 5% admitted.

The average planting depth of the bulbs was 4.53 compared to the 4 cm pre-set and had a degree of depth unevenness of 15.2%.

Energy indices determined show that the machine required, during operation, an average traction force of 311 daN and a traction power of 5.12kN, the tractor's wheel slip being 2.88%.

REFERENCES

- Bairwa, J. (2016). Development of Inclined Plate Metering Device for Manually Operated Onion Bulb Planter, Master of Technology theses, Department of Farm Machinery and Power Engineering College of Agricultural Engineering, India
- Bakhtiari, M. R. and Loghavi M. (2014). Development and Evaluation of an Innovative Garlic Clove Precision Planter, *Journal of Agricultural Science and Technology*, Vol. 11, pp 125-136
- Cârdei, P., Manea, D., Popescu, S., Lazăr, S. (2011). Mathematical model of the distribution device working on the mechanical-pneumatic sowing machine SDC, *INMATEH - Agricultural Engineering*, Vol. 34 (2), pp. 5-12
- Benjaphragairat, J., Sakurai H., Ito, N. (2010). Design and control of metering system and furrow openers for garlic planter, *International Agricultural Engineering Journal* 19(2): 39 - 46
- Grewal, R. S., Khurana, R., Manes, G. S., Dixit, A., Verma, A. (2015). Development and evaluation of tractor operated inclined plate metering device for onion seed planting, *Agricultural Engineering International: CIGR Journal*, Vol. 17, Issue 2, pp: 31-38
- Kawaguchi, T., Minamida, H., Kawamoto, Y., Satou, A., Ozaki, Y. (2015). Development of the Planting Machine for Allium×wakegi Araki Bulbs and Evaluation of the Accuracy of Machine Planting, *Japanese Journal of Farm Work Research* 50(2), pp: 25-35
- Kawaguchi, T., Minamida, H., Kawamoto, Y., Satou, A., Ozaki, Y. (2015). Improvement of Workability of Machine Planting with a Simplified Planting Machine for Allium × wakegi Araki Bulbs, *Japanese Journal of Farm Work Research* 50(4), pp: 91-101
- Păunescu, D., Brătucu, Gh., Păunescu, S., Atanasov, At. (2010). Research regarding the use of the GPS in monitoring agricultural sowing. *INMATEH - Agricultural Engineering*, vol. 31 (2), pp. 79-86
- Uceanu, E., Bolintineanu, Gh., Vlăduț, V. (2008). Researches regarding the identification of qualitative characteristics at the soil work, *SCIENTIFIC RESEARCHES (INMATEH)*, ISSN: 1583 – 1019, vol.1, pp: 67-79



EVALUATION OF HAND-ARM VIBRATION TRANSMITTED DURING SOIL TILLAGE BASED ON ARDUINO AND MPU9250 MOTION SENSOR

Gabriel-Alexandru CONSTANTIN*, George IPATE, Gheorghe VOICU,
Gabriel MUȘUROI, Mariana-Gabriela MUNTEANU, Maria DRAGOMIR

Politehnica University of Bucharest, Faculty of Biotechnical Systems Engineering
313 Splaiul Independentei, sector 6, Bucuresti, Romania

*E-mail of corresponding author: gabriel_alex99@yahoo.com

SUMMARY

Irrespective of the industrial activity it comes from, vibrations act on the human body causing discomfort to the operator, can change its activity or even may have more or less serious effects on its health. In paper is presented the estimating of vibration exposure to agricultural workers during soil processing operations with a pedestrian-controlled tractor BCS 740 in a greenhouse. It should be noted that pedestrian-controlled tractor was equipped with a rotary cultivator which performs a rotary tillage from top to down. The vibration measurement system has been achieved with the development platform "open source" Arduino and of an electronic device IMU type MPU9250 Ivensense. Processing and analysis of measurement data was performed with a program developed in MATLAB. The experimental results obtained show that exposures of workers are below the exposure action value and the risks from hand-arm vibration is reduced to a minimum. The system used in experiments is less expensive compared to other vibration measurement systems.

Key words: vibration exposure, Arduino, operator, greenhouse, IMU sensor

INTRODUCTION

The human body is characterized by a fragility that is also manifested in the case of exposure to vibrational phenomena. This has led to in-depth research into the area of determining and combating the negative effects of vibrations on the human body. At the same time, the limits of human exposure to vibrations were imposed by legislative means depending on the working conditions, (European Directive 2002/44/EC).

Work Safety and Health Guide on Mechanical Vibrations defines two vibration transmission systems in the human body: vibrations transmitted to the hand-arm system and

vibrations transmitted to the whole body. In the case of vibrations transmitted to the hand-arm system, the handle of a machine or the surface of a piece to be worked, in contact with the hand, vibrates quickly, and this movement is transmitted to the hand and arm. Workers whose hands are regularly exposed to hand-arm vibrations, may suffer destruction of the tissues of the hands and arms, which causes the symptoms collectively known as hand-arm vibration syndrome. This may result in long-term blood flow disorders in the fingers and disorders of the neurological and locomotor functions of the hand and arm. Vascular, neurological and bone and joint malformations caused by hand-arm vibrations are recognized as occupational diseases in a number of Member States of the European Union.

People from a biological point of view (and not only) are distinct entities and respond differently to environmental aggressions, in relation to their native resistance, with their degree of health, their personality and temperament, etc. On the other hand, we cannot always make experimental determinations *in vivo*. All these findings, highlights the opportunity of biomechanical modelling of the human body subjected to vibration, modelling used in the literature frequently.

Biomechanical models used in the literature are based on models of rheological behaviour. Thus, the first biomechanical model of the human body, used to determine the impedance and frequency response in the vertical direction, was made by Dieckmann in 1957, based on a Kelvin-Voigt model (figure 1), (Truța and Arghir, 2010).

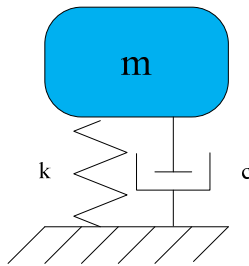


Figure 1. Dieckman biomechanical model (Truța and Arghir, 2010)

Numerous research has been conducted to study the vibrations transmitted to human operators during agricultural works. The vast majority of them investigate the exposure of tractor drivers to vibrations transmitted to the whole body (Boshuizen et. all, 1990, Gomez et. all, 2013, Bovenzi and Betta, 1994). It has been pointed out that long-term exposure to vibrations ranging from 2 to 20 Hz can cause severe diseases such as spinal column degenerative pathologies. Also, has been observed that with changing soil profile and tractor speed, the accelerations resulting from ground input present similar spectral trends (Cuttini et al., 2017). Manetto et. all, 2013 study vibration risk in hand-held harvesters for olives. They found a high level of hand-arm vibrations, in range of 8-20 $m s^{-2}$, due to hand contact with the handle. Hassan (2013) has conducted a study to determine an optimum operator's daily exposure limit in field conditions from the handles of a single-axle tractor. The results of his study show that the magnitude of vibrations during the various activities varies in the range 4.5 - 10.5 $m s^{-2}$ and increases with the increase of the forward speed.

This paper has as main objective to evaluate the influence of vibrations on the hand and arms through the palm and fingers in the soil processing activities based on the smart and low cost instrumental systems. Results show that proposed solution can collect and present data in a mobile environment.

MATERIALS AND METHODS

The experimental work has deployed in the greenhouse with polyethylene film roof, available in UPB campus, Department of Biotechnical Systems. To classify the vibrations according to their degree of discomfort and the risk of injury they produce to workers, measurements were made for hand-arm vibrations in the soil-processing activity with a pedestrian-controlled tractor BCS 740. Pedestrian-controlled tractor was equipped with a rotary cultivator which performs a rotary tillage from top to down. The inertial motion sensor was mounted whit a handle adaptor on pedestrian-controlled tractor handlebars. In figure 2, is presented the assembly used for the experiments, respectively, the basicentric coordinate system.



Figure 2. Experimental measurement of hand-arm vibrations in the soil-processing activity

The vibration transmitted to the hand shall be measured and reported for three directions of an orthogonal coordinate system. The primary quantity used to describe the magnitude of the vibration shall be the root-mean-square (rms) frequency-weighted acceleration expressed in meters per second squared ($m\ s^{-2}$). Vibration exposure is dependent on the magnitude of the vibration and on the duration of the exposure. In order to apply the guidance on health effects, the vibration magnitude is represented by the vibration total value a_{hv} :

$$a_{hv} = \sqrt[2]{a_{hw_x}^2 + a_{hw_y}^2 + a_{hw_z}^2} \quad (1)$$

where, subscripts, w - refers to frequency-weighted acceleration values, and, x, y, z - refer to the direction of translational, or rectilinear, vibration.

Daily vibration exposure is derived from the magnitude of the vibration (vibration total value) and the daily exposure duration and can be expressed with:

$$A(8) = a_{hv} \sqrt{\frac{T}{T_0}} \quad (2)$$

where, T is total daily duration of exposure to the vibration a_{hv} , respectively, T_0 is the reference duration of 8h (28.800 s).

By using an exposure points system, hand-arm vibration exposure management can be simplified. The number of exposure points, P_E , is defined by:

$$P_E = \left(\frac{a_{hv}}{2.5\ m/s^2} \right)^2 \frac{T}{T_0} \cdot 100 \quad (3)$$

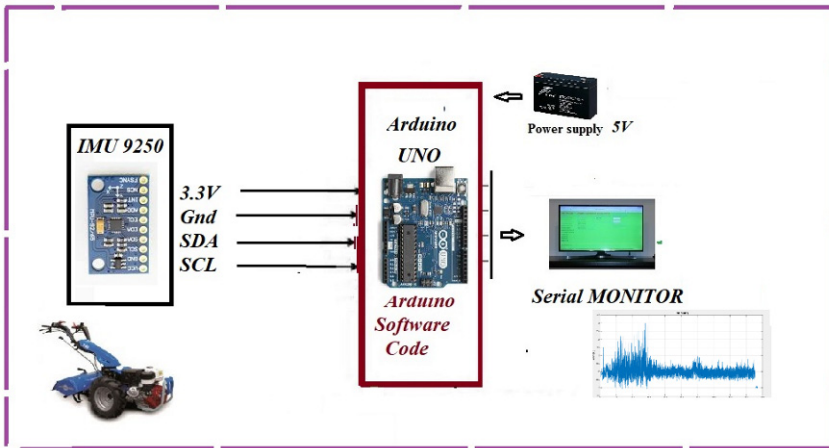


Figure 3. Block diagram of vibration monitoring system

The proposed monitoring system is presented in Figure 3. The main component of hardware section is the **Arduino UNO**, a microcontroller board based on the ATmega368, on miniature computers in a single integrated circuit. The main board can be programmed flexibly to provide specific features regarding requirement function in the intelligent system, such as data handling. In general, Arduino boards have proven to be robust enough to be accurate, simple tasks are not affected by the programming style even at beginner level. Software implementation of our vibration monitoring system uses Arduino software.

Industry of Inertial Motion sensors (IMU) are in a fast growing, mainly because they are miniaturized and require a low power supply. IMU sensors typically contain three orthogonal accelerometers, gyroscopes, and magnetometers, measuring angular velocity, acceleration and magnetic field respectively. A multi-chip module MPU 9250 developed by InvenSense Inc. (that combines a full 9DoF inertial sensor and a Digital Motion Processor in a small 3x3x1mm package), is used as the motion sensor in our research.

Micro-Electro-Mechanical Systems, or MEMS, is a technology that in its most general form can be defined as miniaturized mechanical and electro-mechanical elements that are made using the techniques of microfabrication. The MEMS accelerometer can be considered as a mass-spring system. Figure 4 illustrate block diagram of IMU 9250 module. It is composed of movable proof mass with plates that is attached through a mechanical suspension system to a reference frame.

Therefore, the measurement of an accelerometer can be modelled as (Zhi, 2015):

$$R(t) = \hat{v} - g + s_a(t) + n_a(t) \quad (4)$$

where \hat{v} represents the instantaneous linear acceleration, g represents gravitational acceleration, $s_a(t)$ and $n_a(t)$ stand for accelerometer bias and noise respectively.

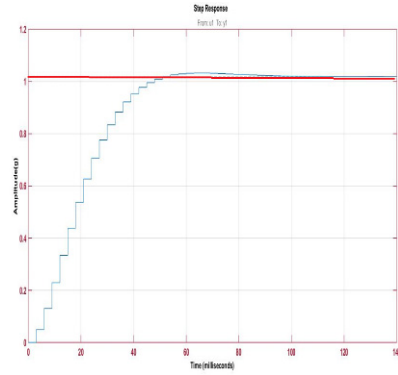
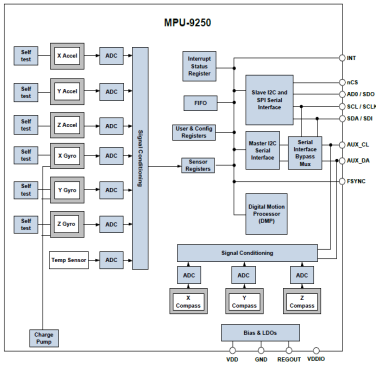


Figure 4. Block Diagram of IMU 9250 module

Figure 5. Step response of system

For communication between the Arduino and IMU sensor an I2C protocol communication (f_{SCL} , SCL Clock Frequency, 400kHz) is used. The Arduino microcontroller is connected over USB to a computer to send and receive serial data as human readable ASCII text using serial communication protocol which will be set to 115200 Bd. Data were exported in ASCII format and were loaded in MATLAB for further analyses. Transient response plots in figure 5 provide insight into the basic dynamic properties of the linear ARX model obtaining in MATLAB for purpose measurement system.

RESULTS AND DISCUSSION

To test the use of sensors, we have conducted several series of measurements to check the system and data accuracy. Accelerometers are extremely sensitive to changing the direction of movement and impact forces while gyroscopes are sensitive to temperature changes and suffer from a slow-changing bias (Ipate et al, 2015). The MPU 9250 accelerometer present a temperature drift of $\pm 0.026\% / ^\circ C$.

An important feature of the accelerometer included in the MPU 9250 is the programmable self-test function supplied by the manufacturer. In figure 6 is presented the total acceleration measured whit IMU 9250 device in calibration test. The accelerometer remains statically near 1 g because there are no other gravitational forces.

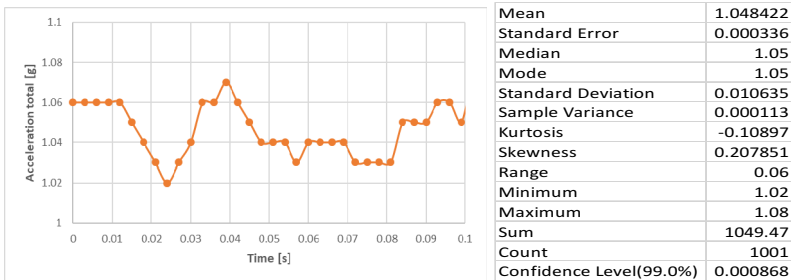


Figure 6. The measurement accuracy and drift of IMU 9250 device

Total acceleration scaled data is illustrated in figure 7. Data come from accelerometer sensors in sequence of 16 bits with the range of ($\pm 78.48 \text{ m s}^{-2}$) and a sensitivity scale factor of 4096 LSB/g. A translational orientation is given to the system and quantification of fluctuations is observed as a response.

The sample rate of the system is 168 Hz, corresponding to 0.006 seconds between every sequent data. The collected signal transformed from the time domain into the frequency domain, using Fast Fourier Transform (FFT), is shown in figure 8. The acceleration peak values found within the frequency range of 64-65 Hz in FFT diagram is clearly vibration generated by the combustion engine overloaded. Also, hand transmitted vibration along z-axis was found most significant and appeared to be more severe than those in horizontal (y-axis) and lateral (x-axis) directions under the same working conditions.

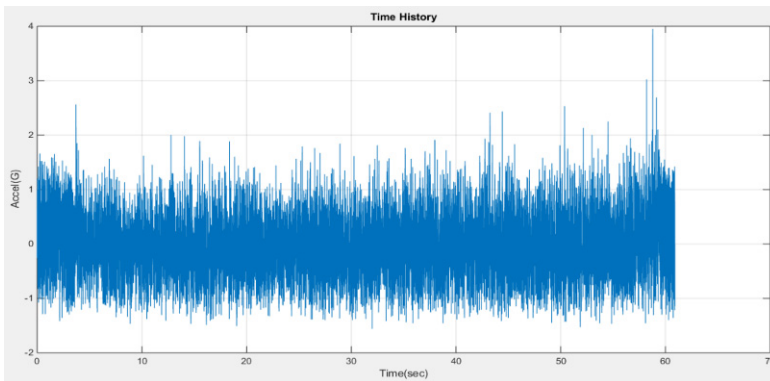


Figure 7. Total acceleration scale data

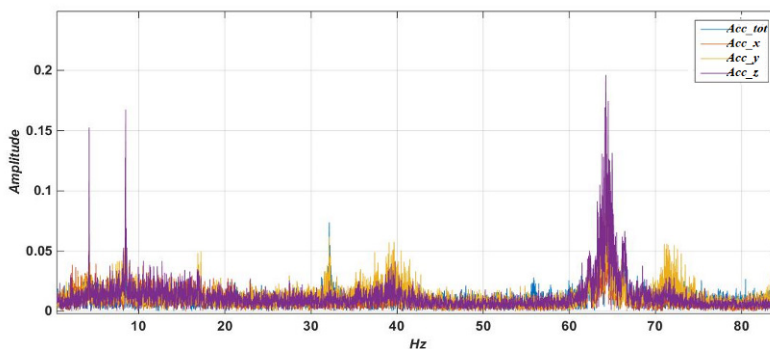


Figure 8. Data of vibrating pedestrian-tractors from accelerometers shown in the frequency domain

To evaluate the risk of exposure vibration transmitted to the hand-arm system in the soil processing activities we compare the daily vibration exposure computed whit relation (3) whit two reference values: exposure action value (EAV) of 2.5 m s^{-2} and exposure limit value (ELV) of 5.0 m s^{-2} established by the European Union (Directive 2002/44/EC) (Gomes and Savionek, 2014).

For a daily exposure duration of $T = 2$ h, representing an average exposure time for working activity, and a total vibration a_{hv} of 3.512 m s^{-2} , the daily vibration exposure $A(8)$ is 1.774 m s^{-2} , below the vibration exposure action (EAV). In this case, the value of the exposure number is 50, half of the amount corresponding to the score of the limit value for the action of exposure.

If we consider that total daily vibration exposure consists of several operations with different amplitudes of vibrations, then we must consider the individual contribution of each operation. If the vibration total values for exposure times of 1.5 h and 0.5 h (within the same working day) are 3.512 m s^{-2} and 2.783 m s^{-2} respectively, then $A(8)$ is 1.672 m s^{-2} . So, according to relation purposed in ISO 5349-1 (Annex C3) it would take over 18.44 years of exposure to vibration in the soil-processing activity with a pedestrian-controlled tractor BCS 740, so 10% of a population of workers to develop Vibration induced White-Fingers. For hand-arm measurements, ISO 5349 does not set limits for allowed doses.

CONCLUSIONS

Any employer who carries out an activity involving risks from mechanical vibration exposure must implement a number of previous and concomitant steps to carry out the work. An economic and low cost smart vibration monitoring system is proposed and implemented in this paper. It gives a basic idea of how to estimate level risk of vibration exposure and provide a direction of agricultural workers security using Arduino UNO and MATLAB software. Also, it can be said that identifying the symptoms of diseases caused by exposure to vibration is not easy, requiring knowledge, both medical and technical.

We can conclude that the results obtained with the Arduino platform have been satisfactory, it is possible to achieve a reliable data acquisition using low-cost hardware and open source software with utility both in the educational field and in the usual practical engineering activities.

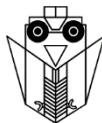
ACKNOWLEDGEMENT

The work has been funded by the Institutional Development Fund of the Ministry of National Education through the Financial Agreement CNFIS-FDI 2017-0172. The authors also thank the reviewers of the paper for the extremely useful indications that have led to significant improvements in the scientific level of the paper.

REFERENCES

- Atif, M. and Serdaroglu, S. (2011). A Measurement System for Human Movement Analysis, Chalmers University of Technology, Göteborg, Sweden, Master of Science Thesis.
- Bovenzi, M. and Betta, A. (1994). Low-back disorders in agricultural tractor drivers exposed to whole-body vibration and postural stress, *Applied Ergonomics*, Vol. 25, Issue 4, p. 231-241.
- Cuttini, M., Brambilla, M., Bisaglia, C. (2017). Whole-body vibration in farming: background document for creating a simplified procedure to determine agricultural tractor vibration comfort, *Agriculture*, ISSN 2077-0472, 7, 84; doi:10.3390/agriculture7100084.
- Gomes, H.M. and Savionek, D. (2014). Measurement and evaluation of human exposure to vibration transmitted to hand-arm system during leisure cyclist activity, *Braz. J. Biom. Eng.*, 30(4), pp. 291-300.

- Gomez, M.I., Hwang, S., Stark, A.D., May, J.J., Hallman, E.M., Pantea, C.I. (2003). An analysis of self-reported joint pain among New York farmers, *Journal of Agricultural Safety and Health* 9 (2): 143-157, ISSN: 1074-7583.
- Hassan, A.S. (2013). Hand transmitted mechanical vibrations and shocks to operators of single-axle tractor during field operations, Master of Science Disertation.
- Hendriek, C. Boshuizen, Paulien, M. Bongers, Carel, T J Hulshof (1990), Self-reported back pain in tractor drivers exposed to whole-body vibration, *International Archives of Occupational and Environmental Health* 62:109-115.
- Hettinger, T. (1956). *Der Einfluss sinusförmiger Schwingungen auf die Skelettmuskulatur*, *Int. Z. Angew Physiol*, 16, 192-197.
- Ipate, G., Voicu, Gh., Dinu, I. (2015). Research on the use of drones in precision agriculture, *U.P.B. Sci. Bull., Series D*, Vol. 77, Iss. 4, pp. 263-273.
- Manetto, G., Cerruto, E. (2013). Vibration risk evaluation in hand-held harvesters for olives, *Journal of Agricultural Engineering* 2013; volume XLIV(s2):e142, p:705-709.
- Truța, A., Arghir, M. (2010). Biomechanical notions of human body in vibrational environment, ISBN 978-606-92133-3-9, Arcadia Media, Cluj-Napoca.
- Zhi, R. (2016). A Drift Eliminated Attitude & Position Estimation Algorithm In 3D, The University of Vermont, Master of Science Thesis.
- *** Directive 2002/44 / EC of the European Parliament and of the Council from 25 June 2002 on the minimum safety and health requirements for the exposure of workers to the risks arising from physical agents (vibration);
- *** Health and Safety Guide to Work on Mechanical Vibrations <http://www.inpm.ro/files/publicatii/2013-05.07-ghid.pdf>.
- *** ISO 2631-1/1997. Mechanical vibration and shock -- Evaluation of human exposure to whole-body vibration. Part 1: general requirements.
- *** ISO 5349-1/2001. Mechanical vibration: measurement and evaluation of human exposure to hand-transmitted vibration. Part 1: general requirements.
- *** ISO 5349-2/2001. Mechanical vibration: measurement and evaluation of human exposure to and-transmitted vibration. Part 2: practical guidance for measurement at the workplace.
- *** ISO 8041/2005. Human response to vibration: measuring instrumentation.



INFLUENCE OF ATTACK ANGLE TO DRAFT FORCE VARIATION OF A FURROW OPENER AT MULCH FOIL PLANTER

Gabriel GHEORGHE*, Cătălin PERSU, Dan CUJBESCU, Marinela MATEESCU

National Institute of Research - Development for Machines and Installations designed to
Agriculture and Food Industry - INMA Bucharest, Romania

E-mail of corresponding author: gabrielvalentinghe@yahoo.com

SUMMARY

Within this paper is presented a theoretical analysis, performed in SolidWorks Simulation, of the soil trajectory over the surface of an active body organ for furrows opening mounted on an equipment which incorporates mulch film in soil. The paper also analyses the pressure distribution on the active surface of the organ. The simulation was performed for several attack angles in order to reveal their influence on both variables investigated: pressure on the active surface and soil trajectory.

Further on, we performed an experimental determination of the strain which appear on the back surface of the active body for several attack angles in order to characterize the draft force which is sustained by the body. The obtained values were compared with the theoretical pressure resulted from previously performed analysis, taking into consideration all known variables. This work was realized with the purpose to optimize: geometric characteristics (organ shape), work qualitative indicators (working width) and energy indicators (draft force).

The analysis of the results shows different deformations at the different attack angles in three different points along tool to optimize geometric characteristics. The best result was obtained to 75 degrees angle where we have an average value of $13 \mu\text{m m}^{-1}$ on the 1st mark, $17,5 \mu\text{m m}^{-1}$ on the 2nd mark and $1,8 \mu\text{m m}^{-1}$ on the 3rd mark, so is not big difference between 1st and 2nd mark so we obtain a uniform distribution of the soil at this angle.

Keywords: structural analysis, optimizing, solidworks simulation, strain gauge.

INTRODUCTION

Sowing is made at 70 cm distance between the rows and 5-8 cm depth, ensuring 15-25 kg of seeds per hectare. The technical equipment undergoing structural analysis is presented in Fig. 1 performs, in a single passage, the establishment of weeding crops simultaneously with covering the seed row with a degradable film which prevents weeds from coming out of the ground on the lane corresponding to the plant row (Gheorghe et al., 2017)



Figure 1. Equipment for sowing and applied biodegradable foil [5]

In the working process as the tractor advances, the rattler forms a furrow, the degradable foil is positioned in the groove formed and fixed in the furrow by a wheel until the cover disc covers the roughened furrow formed by the rattling and fixes the foil to the ground. At each end of the plot, the working process resumes provided that the technical equipment is placed with the backing disk at a sufficient distance to hang the foil already applied.

During the work done by the technology, wear is generated by the interaction between tillage tool and soil.

The chosen part which I have chosen to analyzed is the most active part of the applying mulching films equipment. That part will be executed after performing finite element analysis.

In this paper we will investigate how the angle and depth influence the deformations occurring in the tool that opens the furrow for incorporating the foil (Fig. 2).

A simple theoretical analysis before executing the equipment was made for a good design, but in this article there will be stuck tensiometer marks on the back of the active organ and will study the deformations that occur at different attack angles, to see which is the best angle of the active organ for the most efficient use of the equipment.



Figure 2. Equipment for applying the mulch films

Few studies were carried out on pressure distribution between soil and tillage tools, especially by means of analytical models based on the earth pressure theory (Godwin and O'Dogherty, 2007; Godwin and Spoor, 1977; Hettiaratchi and Reece, 1967; McKyes, 1985) and numerical models such as Finite Element Modelling (FEM) (Abo-Elnor, Hamilton and Boyle, 2004; Bentaher et al., 2013; Mouazen and Nemenyi, 1999), Discrete Element Modelling (DEM) (Shmulevich, 2010; Shmulevich, Asaf, and Rubinstein, 2007; Ucgul, Fielke, and Saunders, 2014), and Computational Fluid Dynamics (CFD) (Karmakar and Kushwaha, 2006). From these studies, pressure signal on a tillage tool is irregular and the pressure is correlated with soil shear strength (Elijah and Weber, 1971), working depth, and tool travelling speed (Mayauskas, 1958). Moreover, by using FEM, the higher pressure is as were found at the tool edge (Chi and Kushwaha, 1989). Accurate mathematical models are necessary to design, optimize tools because they allow the prediction of the pressure distribution over the entire tool surface in many different operating conditions. Mathematical models have to be validated and therefore more extensive experimental studies have to be carried out.

MATERIALS AND METHODS

In this experiment we used the equipment with the following features:

– Type of equipment	worn
– Power source	33,55 kW tractor
– Working width, mm	1000-1200
– Maximum number of sowing sections, pieces	2
– The distance between the sowing sections, mm	700-800
– Depth of sowing, mm	50-70
– Depth of foil embedding, mm	100-200
– The distance between plants on the row, mm	150-300
– Overall dimensions, mm:	
– length	2625

- width 1680
- height 1561
- Weight, kg 370

The first step was to stick the tensiometer marks to see how it is distributed deformation throughout actively studied organ, were mounted in the following way: the first was mounted at the base to observe deformations at maximum depth, the second one was mounted in the middle, because a lot of soil is gathering in this area and the third was mounted in the upper part to observe whether at a very high value of the angle there are deformations in that area due to cutting the soil and bringing it to the upper part of the active element (Fig. 3).

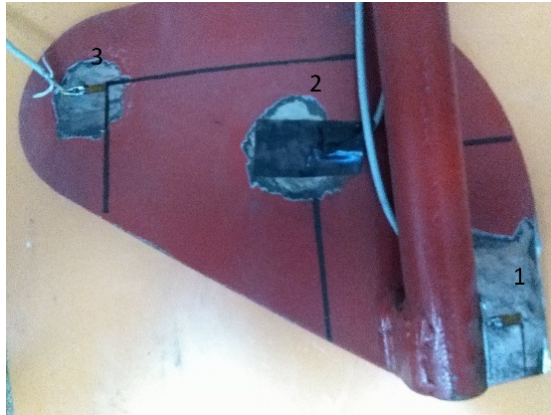


Figure 3. Positioning of the tensiometric marks

Traction resistance force, assumption of normal pressure

In the processing experimental data from the soil tillage tools, we have often used successfully the traction resistance (draft force) formula founded by Goreacikin (1965):

$$F = fG + kab + \varepsilon\rho abv^2 \quad (1)$$

where F is the draft force, f is, according to [12], a coefficient analogous to the coefficient of friction. G is the weight of the soil processing machine, k is a coefficient that characterizes the specific deformation resistance of the soil, a and b are depth and width of work, ρ is the soil volume density, v is the working speed (assumed constant) and ε , is a coefficient that depends on the shape of the active surface of the tool body.

This force was calculated to be introduced into SolidWorks Simulation, to calculate the theoretical specific deformities occurring on the studied tool with these characteristics (Table 1).

Table 1. Characteristics of the forward force

Symbol	f	G (kg)	k	$S(\alpha)=ab$	ε	ρ (kg m ⁻³)	v (m s ⁻¹)
Value	0,5	3367	35000	$S(\alpha)$	2	1100	1.11

$$F(\alpha) := f \cdot G + k \cdot S(\alpha) + \varepsilon \cdot \rho \cdot S(\alpha) \cdot v^2 \quad (2)$$

The formula (2) is customized for the equipment used in this research, this varies depending on the angle of advance of the coulter and $Sa(\alpha)$ is calculated with the formula (3) depending on α where $S10$ is area of the surface at front of the tool and the $S2p$ is area of the curved surface which come into contact with the soil.

$$Sa(\alpha) := S2p \cdot \cos(\alpha) + \frac{S10}{2} \cdot (1 + \sin(\alpha)) \tag{3}$$

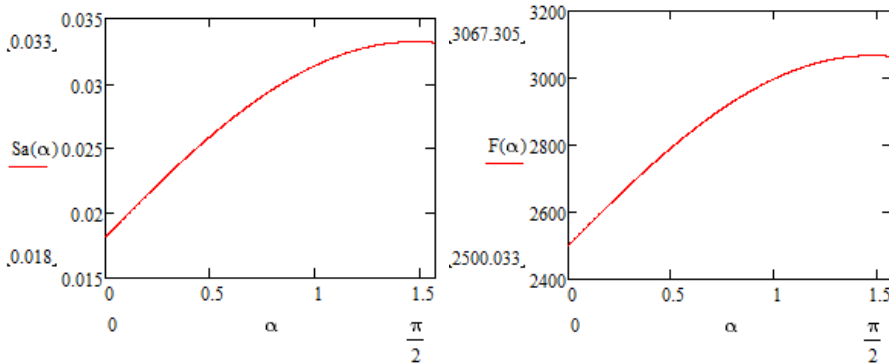


Figure 4 Variation of the area come into contact with the soil and the force of forwarding according to the angle of forwarding of the tool

RESULTS AND DISCUSSION

In order to have a higher efficiency, in FEA (finite element analysis) we used a concept of more general and simpler structure than usual. Usually in the FEA, structure (strength) means a group of bars, plates, shells and volumes (solids). To shift from its real structure to the model of computing algorithms, there is no general method to ensure the development of a unique model that approximates with an error default, known as structure to be approximated. It is generally possible for a structure to develop more models, all correct but with different performance. The model for calculating the strength of a structure shall be based on intuition, imagination and previous experience of those who do those models. There is need to effectively synthesize all available information on the structure.

After the active organ was introduced into Solid Works Simulation, were taken the following steps:

- we selected the material of tool: 65Mn10;
- we fixed the tool and we applied the calculated forces depending of the angle and to the depth of 165 mm (fig.5);
- creating mesh;
- run the simulation;
- collecting the results.

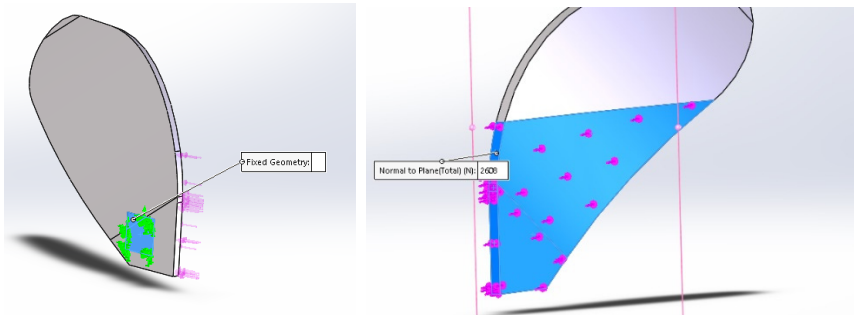


Figure 5. The steps to begin the theoretical stimulation in SolidWorks Simulation

The same study was carried out experimentally at different angles in the field where was positioned the tool at the angles of 15°, 30°, 45°, 60°, 75°, 90°, at the same depth 165 mm like in figure 6.

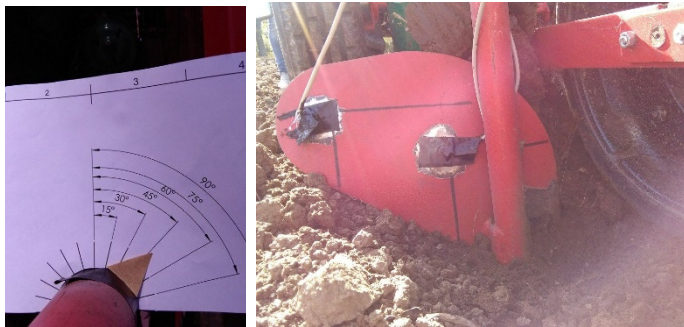


Figure 6. Pictures from the experimental study

An example of theoretical results we can see in figure 7 for an angle of 15 degrees we got for mark 1 a value of 13,76 $\mu\text{m m}^{-1}$.

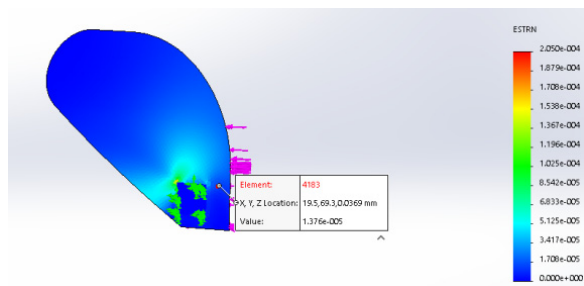


Figure 7. The results of theoretical simulation at an angle of 15 degrees with SolidWorks Simulation

After I made all theoretical simulation in SolidWorks we can compare with the results of experimental simulation (table 2), we can see if we have difference between them and to see how it influences the angle of attack of the tool the specific deformations. In figure 8,9,10 we can see graphs with specific deformations resulting from experimental research at the first 3 angles.

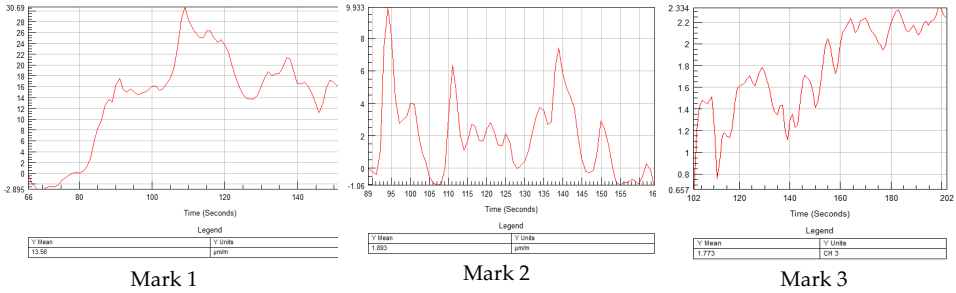


Figure 8. Specific deformations for the 15 degree of tool

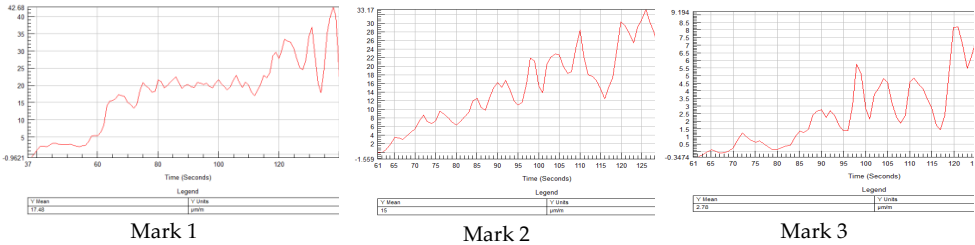


Figure 9. Specific deformations for the 30 degree of tool

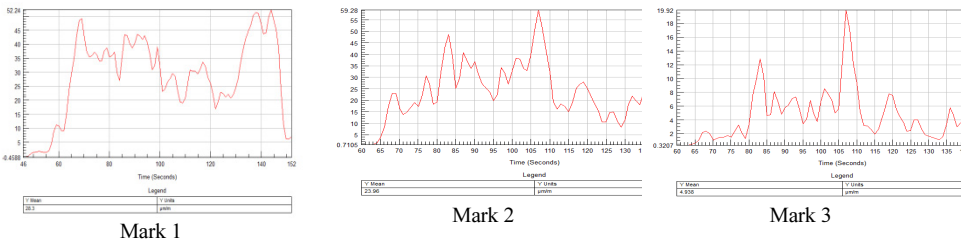


Figure 10. Specific deformations for the 45 degree of tool

Table 2. All theoretical and experimental results

α°	Mark 1		Mark2		Mark3	
	$\mathcal{E}_{theoretical}$ ($\mu\text{m/m}$)	$\mathcal{E}_{experimental}$ ($\mu\text{m/m}$)	$\mathcal{E}_{theoretical}$ ($\mu\text{m/m}$)	$\mathcal{E}_{experimental}$ ($\mu\text{m/m}$)	$\mathcal{E}_{theoretical}$ ($\mu\text{m/m}$)	$\mathcal{E}_{experimental}$ ($\mu\text{m/m}$)
15	13,76	13,56	1,421	1,893	1,850	1,773
30	15,64	17,48	10,25	15	2,05	2,78
45	23,8	28,3	19,77	23,96	3,852	4,938
60	20,84	21,06	28,86	30,53	2,154	1,131
75	12,76	13,9	15,64	18,18	1,754	1,946
90	31,82	32,44	7,94	8,388	3,421	2,523

CONCLUSIONS

According to results comparison we can see the values are approximately equal, the theoretical and experimental results on same position, so we can use theoretical simulation sometimes to get faster and less costly results.

The results show that at the 75 degrees angle, soil spreads best over the entire surface and has a very good knife trajectory because we can see at the first mark appears the lowest deformation and is the same as on the 2nd mark.

Even if to the 2nd mark at other angles beside 75 degrees show lower values for example for the angle of 15, 30 and 90 degrees, the 15 and 30 degrees do not form the furrow needed to incorporate the foil into the ground, and at the 90 degree angle the differences between marks 1 and 2 are too large and the organ will unevenly deform.

Because there are no large deformations, the tool can be optimized in the following way:

- first of all, we can change the thickness of the tool;
- secondly, we can modify the material and run simulations with other material cheaper;
- and thirdly we can modify the gauge dimensions because the trajectory is very small at all angles on the 3rd mark, so there is no need to be so long.

This methodology can stand at the bottom of future research such as the influence of speed on these deformations and in the end, we can calculate energy consumption at different attack angle.

ACKNOWLEDGEMENT

The work has been funded by Ministry of National Education and Research through the National Agency for Scientific Research, within the project entitled “Innovative technology for weeding crop establishment through mulching using degradable film”, PN 16 24 04 02.

REFERENCES

- Abo-Elnor, M., Hamilton, R., Boyle, J.T. (2004). Simulation of soil-blade interaction for sandy soil using advanced 3D finite element analysis. *Soil and Tillage Research*, 75(1), pp. 61-73.
- Bentaher, H., Ibrahim, A., Hamza, E., Hbaieb, M., Kantchev, G., Maalej, A. (2013). Finite element simulation of moldboard-soil interaction. *Soil and Tillage Research*, 134, pp. 11-16.

- Chi, L., and Kushwaha, R.L. (1989). Finite element analysis of forces on a plane soil blade. *Canadian Agricultural Engineering*, 31(2), pp. 135-140.
- [Elijah, D.L. and Weber, J.A. (1971). Soil failure and pressure patterns for flat cutting blades. *Transactions of the ASAE*, 14(4), pp. 781-785.
- Gheorghie, G., Catalin, P., Marin, E., Manea, D. (2017). Structural analysis of technical equipment for setting up row crops and applying degradable film, Proc 16th International Scientific Conference ENGINEERING FOR RURAL DEVELOPMENT, Jelgava, Latvia, pp 1233-1238.
- Godwin, R.J. (2007). A review of the effect of implement geometry on soil failure and implement forces. *Soil and Tillage Research*, 97(2), pp. 331-340.
- Godwin, R.J., and O'Dogherty, M.J. (2007). Integrated soil tillage force prediction models. *Journal of Terramechanics*, 44, pp 3-14.
- Godwin, R.J., and Spoor, G. (1977). Soil failure with narrow tines, *Journal of Agricultural Engineering Research*, 22(3), pp. 213-228.
- Goriachkin, V.P. (1965) Collected papers, Vol. I-III, Moscow.
- Hettiaratchi, D.R.P. and Reece, A.R. (1967). Symmetrical three-dimensional soil failure. *Journal of Terramechanics*, 4(3), pp. 45-67.
- Karmakar, S. and Kushwaha, R.L. (2006). Dynamic modeling of soil-tool interaction: An overview from a fluid flow perspective. *Journal of Terramechanics*, 43(4), pp. 411-425.
- Mayauskas, I. S. (1958). Investigation of the pressure distribution on the surface of a plow share in work. *Journal of Agricultural Engineering Research*, 4, pp. 186-190
- Mattetti, M., Varani, M., Molari, G., Morelli, F. (2017). Influence of the speed on soil-pressure over a plough. *Biosystems Engineering* 156, pp. 136-147.
- McKyes, E. (1985). Soil cutting and tillage. In *Developments in agricultural engineering* (Vol. 7). Amsterdam, The Netherlands: Elsevier.
- Mouazen, A.M., and Nemenyi, M. (1999). Tillage tool design by the finite element method: Part 1. Finite element modelling of soil plastic behaviour. *Journal of Agricultural Engineering Research*, 72(1), pp. 37-51
- Shmulevich, I. (2010). State of the art modeling of soil-tillage interaction using discrete element method. *Soil and Tillage Research*, 111(1), pp. 41-53
- Shmulevich, I., Asaf, Z., Rubinstein, D. (2007). Interaction between soil and a wide cutting blade using the discrete element method. *Soil and Tillage Research*, 97(1), pp. 37-50.
- Ucgul, M., Fielke, J.M., Saunders, C. (2014). Three-dimensional discrete element modelling of tillage: Determination of a suitable contact model and parameters for a cohesionless soil. *Biosystems Engineering*, 121, pp. 105-117.



KARAKTERISTIKE TRAKTORSKOG DIZEL MOTORA S DIREKTNIM UBRIZGAVANJEM PRI KORIŠTENJU RAZLIČITIH VRSTA DIZELSKOG GORIVA

Zlatko KORONC*, Dubravko FILIPOVIĆ, Goran FABIJANIĆ

Sveučilište u Zagrebu Agronomski fakultet, Zavod za mehanizaciju poljoprivrede,
Svetošimunska 25, 10000 Zagreb, Hrvatska

*E-mail dopisnog autora: zkoronc@agr.hr

SAŽETAK

Cilj ovog rada bio je istražiti utjecaj različitih vrsta dizelskog goriva na karakteristike traktorskog dizel motora. Istraživanje je provedeno na trocilindričnom dizel motoru s direktnim ubrizgavanjem nazivne snage 46 kW s tri vrste dizelskog goriva: standardni Eurodizel, premium Eurodizel (Class) i Eurodizel plavi prema OECD Code 2 pravilniku za službeno ispitivanje karakteristika poljoprivrednih i šumskih traktora. Na osnovi dobivenih rezultata može se zaključiti da nije bilo razlika u istraživanim karakteristikama dizel motora korištenjem standardnog Eurodizela i Eurodizela plavog. Korištenjem Eurodizel Class goriva ostvarena je veća prosječna snaga motora za oko 2% i zakretni moment za oko 3% u odnosu na snagu i zakretni moment ostvarenu korištenjem standardnog Eurodizela i Eurodizela plavog. Prosječna specifična potrošnja korištenjem Eurodizel Class goriva bila je manja za 7.5% u odnosu na Eurodizel plavi, a 4.6% manja u odnosu na standardni Eurodizel.

Ključne riječi: snaga, zakretni moment, specifična potrošnja goriva, satna potrošnja goriva

UVOD

U Republici Hrvatskoj su kvaliteta goriva i značajke koje se moraju kontrolirati regulirane novom Uredbom o kvaliteti tekućih naftnih goriva (NN 57/2017). Ovom se Uredbom propisuju granične vrijednosti sastavnica i značajki kvalitete tekućih naftnih goriva, kao i način utvrđivanja i praćenja kvalitete tekućih naftnih goriva. Od 2014. u Republici Hrvatskoj je na snazi norma HR EN 590:2014 koja utvrđuje zahtjeve i metode ispitivanja za dizelsko gorivo koje se prodaje i isporučuje na tržištu. Primjenjuje se na dizelsko gorivo namijenjeno vozilima s dizel motorom izvedenim za pogon na dizelsko gorivo koje sadrži do 7 % (V/V)

metilnih estera masnih kiselina (FAME). Značajne tehničke izmjene u ovoj europskoj normi u odnosu na prethodno izdanje su: ugrađena izmijenjena EN 14214 FAME specifikacija, ugrađen je poseban zahtjev povezan s ograničenjem upotrebe manganov metilciklopentadienil trikarbonila (MMT) prema zahtjevu Europske komisije, dodan je uređaj za ispitivanje paljenja goriva (EN 16144) kao zamjenska metoda ispitivanja na CFR motorima, dodana je metoda simulirane destilacije plinskom kromatografijom (GC) i uvedena je poboljšana EDXRF tehnika određivanja niske količine sumpora EN 13032 kao zamjena za EN ISO 20847. Norma sadrži i Nacionalni dodatak NA u kojem se preporučuje označavanje mjernih uređaja za prodaju goriva s količinom sumpora najviše 10 mg/kg i zahtjevi uvjetovani klimom gdje se određuju granične vrijednosti temperatura za točku filtrabilnosti (CFPP) za tri različita vremenska razdoblja (Hrvatski zavod za norme, 2014).

Iako država normama propisuje minimalnu kvalitetu koju određeni naftni derivati moraju zadovoljavati, kvaliteta naftnih derivata koji se nude na tržištu nije jednaka jer različiti dobavljači i prodavači imaju različiti raspon vrijednosti kvalitete unutar tih normi. Posljednjih su godina propisi o zaštiti okoliša značajno utjecali na formulaciju dizelskog goriva i ograničenja specifikacija. Unatoč značajnim dostignućima, emisije motora će se morati smanjivati i ubuduće, jer pravilnici koji ograničavaju emisiju štetnih tvari postaju sve stroži (Dobovišek i sur., 2009). Stroga ograničenja emisije iz vozila uvjetovanih zakonskim odredbama o emisijama onečišćujućih tvari u okoliš dovela su do nužnog uvođenja i kvalitetnijih goriva. Goriva moraju udovoljavati strogim specifikacijama kako bi sustavi za pročišćavanje ispušnih plinova bili što efikasniji i kako bi utrošak goriva u motoru bio optimalan i bez štetnih posljedica na rad motora. Međutim, uporabom tehnologija za dobivanje čistih goriva mogu se narušiti neka svojstva goriva koja u krajnjoj liniji mogu utjecati i negativno na ponašanje goriva u primjeni što zahtijeva povećanu primjenu aditiva u dizelskom gorivu (Jednačak, 2009; Fayyazbakhsh and Pirouzfahar, 2017).

Uz standardno dizel gorivo, dobavljači nude posebno formulirana goriva s modificiranim svojstvima koja nadmašuju propisane minimalne zahtjeve. Takva goriva se nazivaju premium ili class dizel, ali se koriste i drugi nazivi. Razina poboljšanja u svakoj zemlji obično se razlikuje od dobavljača do dobavljača, a može varirati i od regije do regije.

Poljoprivrednici u Republici Hrvatskoj su godinama imali problema zbog loše kvalitete plavog dizela čija je primjena u suvremenim traktorima često prouzročila kvarove i visoke troškove održavanja. Naročito su bili pogođeni vlasnici suvremenih traktora s motorima koji zadovoljavaju norme Euro 3B i Euro 4. U takvim motorima nije se smjelo ni slučajno koristiti gorivo s količinama sumpora kakve su bile u plavom dizelu, jer korištenje nekvalitetnog goriva može dovesti do skupih kvarova za čije otklanjanje su troškovi veći što su motori moderniji i sofisticiraniji. Povremeno su se kod nas provodila određena testiranja goriva i to obično u organizaciji pojedinih medija. Neka od tih testiranja su provedena prilično korektno, dok su neka bila na granici senzacionalizma pri čemu se često pribjegavalo raznim ishitrenim i neutemeljenim ocjenama koje su, umjesto da objektivno elaboriraju probleme kvalitete goriva na našem tržištu, izazivali još veću zbuđenost potrošača (Jednačak, 2008). Istraživanja vezana za utjecaj kvalitete i sastava goriva na karakteristike dizel motora provedena su u raznim zemljama od strane Yang i sur. (1999), Icingur i Altiparmak (2003), Lee i sur. (2004), Chen i sur. (2008), Sabah i Miqdam (2012). Iz tih razloga je u Zavodu za mehanizaciju poljoprivrede provedeno istraživanje karakteristika dizel motora s tri vrste dizelskog goriva koje se mogu nabaviti na tržištu, a na raspolaganju su poljoprivrednicima: standardni Eurodizel, premium Eurodizel (Class) i plavi Eurodizel kako bi se utvrdilo da li se njihovim korištenjem ostvaruju karakteristike koje odgovaraju tvrdnjama proizvođača motora.

MATERIJALI I METODE

Istraživanje karakteristika dizel motora je provedeno s tri vrste dizel goriva istog proizvođača koje je moguće koristiti za pogon traktora i samokretnih poljoprivrednih strojeva: Eurodizel (ED), Eurodizel Class (EDC) i Eurodizel Plavi (EDP). U Tablici 1. su prikazane granične vrijednosti sastavnica i značajki kvalitete dizelskog goriva koje se stavlja na tržište Republike Hrvatske kojima prema normi HR EN 590:2014 moraju udovoljavati sve vrste dizelskog goriva.

Tablica 1. Granične vrijednosti sastavnica i značajki kvalitete dizelskog goriva koje se stavlja na tržište Republike Hrvatske
Table 1. The limit values of the components and characteristics of the quality of diesel fuel placed on the market of the Republic of Croatia

Sastavnica i značajka kvalitete / Component and quality feature	Jedinica / Unit of measure	Granične vrijednosti / Limit values	Metoda ispitivanja / Test method
Cetanski broj / Cetane number		> 51,0	HRN EN ISO 5156 HRN EN 15195 HRN EN 16144 ASTM D 613 HRN EN ISO 3675
Gustoća pri 15 °C / Density at 15 °C	kg m ⁻³	< 845,0	HRN EN ISO 12185 ASTM D 1298 ASTM D 4052
Destilacija / Distillation: - 95 % (v/v) predestilirano do / predestilled up to:	°C	< 360,0	HRN EN ISO 3405 ASTM D 86
Policiklički aromatski ugljikovodici / Polycyclic aromatic hydrocarbons	% m m ⁻¹	< 8,0	HRN EN 12916 HRN EN ISO 20846
Količina sumpora / Sulfur content	mg kg ⁻¹	< 10,0	HRN EN ISO 20884 HRN EN ISO 14596 HRN EN ISO 13032 ASTM D 5453
Količina metil ester masnih kiselina / Amount of fatty acid methyl ester (FAME)	% v v ⁻¹	< 7,0	HRN EN 14078
Točka filtrabilnosti za razdoblje: / Filtration point for period: 16.4 - 30.9. / April 16. – September 30. 1.10. - 15.11. / October 1. – November 15. 1.3. - 15.4. / March 1. – April 15. 16.11 - 29.2. / November 16. – February 29.	°C	< 0 < -10 < -10 < -15	HRN EN 116

Izvor: Narodne novine 57/2017

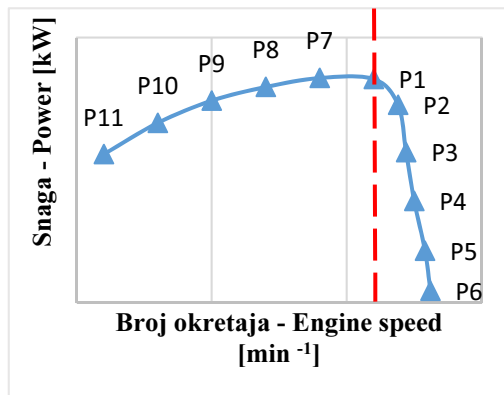
Karakteristike motora uz upotrebu tri različite vrste goriva analizirane su na dizel motoru proizvođača Same Deutz-Fahr koji je ugrađen u traktor tipa Deutz-Fahr Agroplus 310 Ecoline. Deklarirana nazivna snaga motora od strane proizvođača iznosi 46 kW, a maksimalni zakretni moment 244 Nm. Prije početka ispitivanja motor je imao 50 odrađenih sati. Ostale tehničke značajke ispitivanog motora prikazane su u Tablici 2.

Tablica 2. Tehničke značajke ispitivanog dizel motora
Table 2. Technical characteristics of the tested diesel engine

Tip motora / Engine type	Trocilindrični, četverotaktni / Three-cylinder, four-stroke
Model motora / Engine model	1000.3 WTE3
Način ubrizgavanja goriva / Fuel injection method	Direktno ubrizgavanje / Direct injection
Hlađenje / Cooling	Tekućinom / Liquid
Usis zraka / Air intake	Turbopunjač / Turbocharger
Radni volumen / Displacement	3000 cm ³
Broj ventila po cilindru / Valves per cylinder	2
Provt / Bore	105.0 mm
Hod / Stroke	115.5 mm
Omjer kompresije / Compression ratio	16:1
Visokotlačna crpka za gorivo / High-pressure fuel pump	Pojedinačna za svaki cilindar / Individual for each cylinder
Brizgaljka / Injector	S pet otvora / 5 openings
Tlak ubrizgavanja goriva / Fuel injection pressure	1200 bar

Za potrebe istraživanja provedeno je ispitivanje karakteristika motora u laboratoriju za ispitivanje motora Zavoda za mehanizaciju poljoprivrede. Motor je priključen preko priključnog vratila traktora na hidrauličku kočnicu Schenk tip U1-40 (točnost < 1%). Tijekom ispitivanja mjerena je sila kočenja, broj okretaja i satna potrošnja goriva. Satna potrošnja goriva mjerena je volumetrijskom metodom korištenjem trbušaste pipete volumena 100 ml mjerenjem vremena u kojem je utrošen poznati volumen goriva. Iz dobivenih podataka su izračunate vrijednosti za snagu i zakretni moment motora, te specifičnu potrošnju goriva. Broj okretaja motora mjeren je pomoću digitalnog mjerača broja okretaja Lutron DT 2236 (točnost ± 0,05%). Za vrijeme ispitivanja je praćena i temperatura ulja u motoru uređajem MGT 300 EVO. Podaci o okolišnim uvjetima (temperatura, relativna vlažnost i tlak zraka) potječu sa meteorološke postaje Državnog hidrometeorološkog zavoda Zagreb-Maksimir koja se nalazi u blizini laboratorija u kojem je provedeno ispitivanje. Prosječna temperatura tijekom ispitivanja iznosila je 15.2 °C, relativna vlažnost zraka 56.0 %, a tlak zraka 1019.2 hPa.

Istraživanje karakteristika dizel motora korištenjem različitih vrsti goriva provedeno je prema OECD Code 2 pravilniku za službeno ispitivanje karakteristika poljoprivrednih i šumskih traktora (OECD, 2017). Prvi dio mjerenja je obuhvatilo 6 točaka ispitivanja u regulatorskom dijelu krivulje s maksimalno aktiviranom polugom akceleratora (Slika 1).



Slika 1. Točke ispitivanja motora prema OECD Code 2
Figure 1. Testing points according to OECD code 2

Točka P1 predstavlja nazivnu (nominalnu) snagu motora, a mjeri se kod nazivnog broja okretaja. Točka P2 je snaga ostvarena kod 85 % zakretnog momenta ostvarenog u točki P1. Točka P3 je snaga ostvarena kod 75 % zakretnog momenta ostvarenog u točki P2. Točka P4 je snaga ostvarena kod 50 % zakretnog momenta ostvarenog u točki P2. Točka P5 je snaga ostvarena kod 25 % zakretnog momenta ostvarenog u točki P2. Točka P6 predstavlja karakteristike neopterećenog motora. Daljnje mjerenje je provedeno na dodatnih 5 točaka u području krivulje od nazivne snage do maksimalnog momenta mjerenim na svakih 200 okretaja motora (P7 – izmjerene vrijednosti na 2000 min⁻¹, P8 – na 1800 min⁻¹, P9 – na 1600 min⁻¹, P10 – na 1400 min⁻¹, P11 – na 1200 min⁻¹). Dobivene vrijednosti predstavljaju prosjek od 3 mjerenja provedenih u jednom satu. Statistička analiza provedena je korištenjem Excell programa.

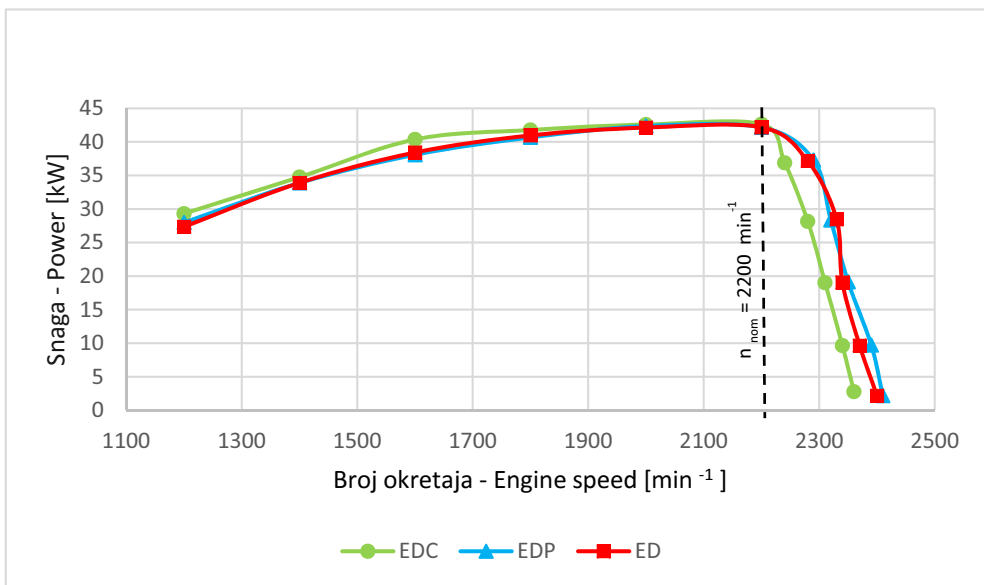
REZULTATI I DISKUSIJA

Istraživanje karakteristika dizel motora provedeno je s tri vrste goriva: Eurodizel (ED), Eurodizel Class (EDC) i Eurodizel Plavi (EDP). Karakteristike motora: snaga, zakretni moment, satna i specifična potrošnja goriva u pojedinim točkama mjerenja odnosno u funkciji broja okretaja motora za različite vrste goriva prikazane su u slijedećim tablicama i grafikonima. U tablicama su prikazane vrijednosti navedenih karakteristika motora u pojedinim točkama mjerenja, dok su u grafikonima prikazane krivulje koje prikazuju navedene karakteristike motora u funkciji broja okretaja.

Tablica 3 i grafikon 1 prikazuju ostvarenu snagu dizel motora korištenjem ED, EDP i EDC goriva. U regulatorskom dijelu krivulje (točke P1 do P6) su bile manje razlike u snazi, dok su nešto veće razlike uočene u području krivulje od nazivne snage do maksimalnog momenta (točke P7 do P11). Najveća razlika u snazi korištenjem EDC goriva u odnosu na ostale dvije vrste goriva bila je pri 1600 min⁻¹, pri čemu je korištenjem EDC goriva ostvarena 5.93% odnosno 5.05% veća snaga u odnosu na ostvarenu snagu korištenjem EDP i ED goriva. Nije bilo nikakve razlike u maksimalnoj snazi pri korištenju ED i EDP goriva. Prosječna ostvarena snaga korištenjem EDC goriva bila je veća za 1.81% odnosno 1.98% od prosječno izmjerene snage korištenjem EDP i ED goriva, dok je prosječna snaga ostvarena korištenjem ED i EDP goriva približno jednaka.

Tablica 3. Snaga dizel motora s tri vrste goriva kod različitih OECD točaka mjerenja
 Table 3. Diesel engine power with three fuel types at different OECD testing points

Snaga Power [kW]	P1	P2	P3	P4	P5	P6	P7	P8	P9	P10	P11	Prosjeak Average
ED	42,19	37,16	28,48	19,07	9,65	2,18	42,14	40,98	38,43	33,91	27,37	29,23
EDP	42,19	37,32	28,36	19,15	9,74	2,19	42,39	40,69	38,11	33,91	28,00	29,28
EDC	42,63	36,89	28,16	19,02	9,64	2,76	42,59	41,78	40,37	34,76	29,31	29,81

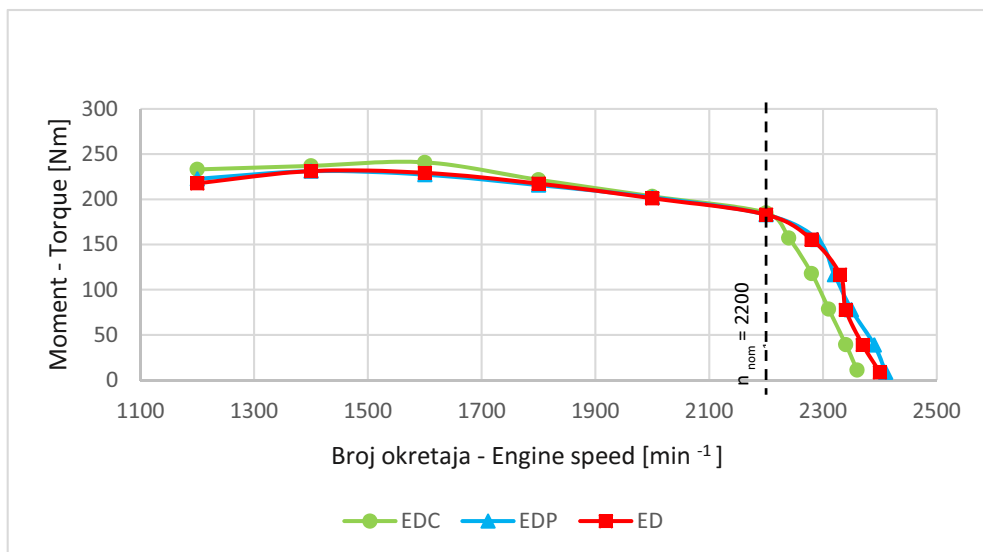


Grafikon 1. Snaga dizel motora s tri vrste goriva u funkciji broja okretaja
 Graph 1. Diesel engine power with three fuel types in function of engine speed

Tablica 4 i grafikon 2 prikazuju ostvareni zakretni moment dizel motora korištenjem ED, EDP i EDC goriva. Najveći zakretni moment korištenjem EDC goriva ostvaren je pri 1600 min^{-1} , dok je pri korištenju ostala dva goriva najveći zakretni moment ostvaren pri 1400 min^{-1} . Pri 1600 min^{-1} bila je i najveća razlika u zakretnom momentu pri čemu je korištenjem EDC goriva ostvaren 5.93% odnosno 5.04% veći zakretni moment u odnosu na korištenje EDP i ED goriva. Prosječni zakretni moment korištenjem EDC goriva bio je veći za 2.68% odnosno 2.85% od prosječnog momenta izmjenjenog korištenjem EDP i ED goriva. Prosječni zakretni moment nastao korištenjem ED i EDP goriva je približno jednak.

Tablica 4. Zakretni moment dizel motora s tri vrste goriva kod različitih OECD točaka mjerenja
 Table 4. Diesel engine torque with three fuel types at different OECD testing points

Moment Torque [Nm]	P1	P2	P3	P4	P5	P6	P7	P8	P9	P10	P11	Prosjek Average
ED	183,11	155,64	116,73	77,81	38,90	8,67	201,23	217,42	229,37	231,30	217,80	152,54
EDP	183,11	155,64	116,73	77,83	38,92	8,67	202,38	215,88	227,44	231,30	222,81	152,79
EDC	185,04	157,28	117,96	78,64	39,04	11,18	203,35	221,64	240,93	237,08	233,22	156,88

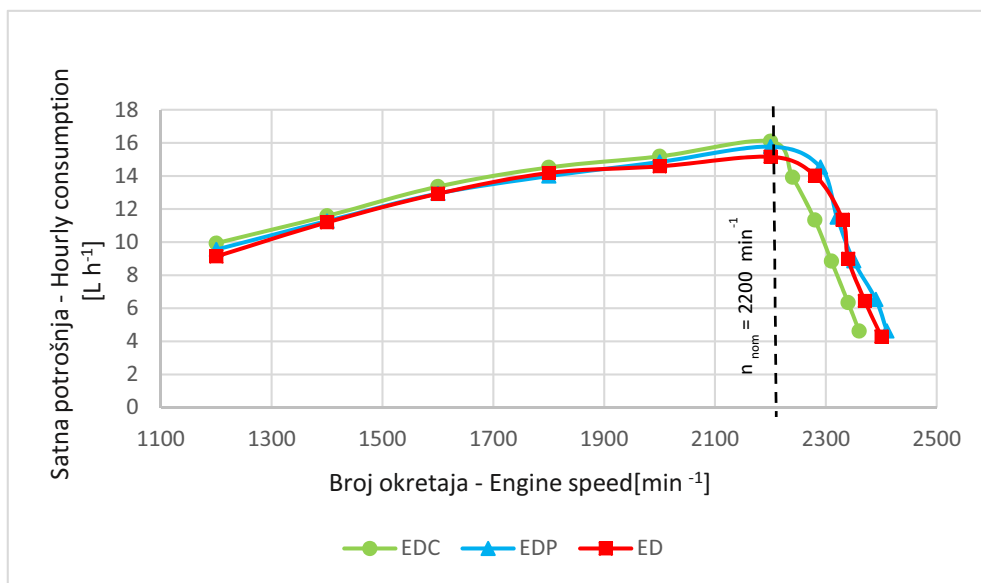


Grafikon 2. Zakretni moment dizel motora s tri vrste goriva u funkciji broja okretaja
 Graph 2. Diesel engine torque with three fuel types in function of engine speed

Tablica 5 i grafikon 3 prikazuju satnu potrošnju goriva dizel motora korištenjem ED, EDP i EDC goriva. Najveća satna potrošnja korištenjem sve tri vrste goriva izmjerena je u točki nazivne snage motora. Najmanja prosječna satna potrošnja bila je kod korištenja ED goriva, za 1.76% odnosno 2.71% manja od prosječne satne potrošnje izmjerene korištenjem EDP i EDC goriva.

Tablica 5. Satna potrošnja goriva dizel motora s tri vrste goriva kod različitih OECD točaka mjerenja
 Table 5. Hourly fuel consumption of diesel engine with three fuel types at different OECD testing points

Satna potrošnja Hourly consumption [Lh ⁻¹]	P1	P2	P3	P4	P5	P6	P7	P8	P9	P10	P11	Prosjek Average
ED	15,16	14,03	11,36	9,00	6,45	4,29	14,59	14,18	12,93	11,20	9,14	11,12
EDP	15,78	14,54	11,51	8,87	6,54	4,63	14,85	14,00	12,94	11,28	9,56	11,32
EDC	16,10	13,92	11,34	8,85	6,34	4,62	15,19	14,52	13,36	11,59	9,94	11,43

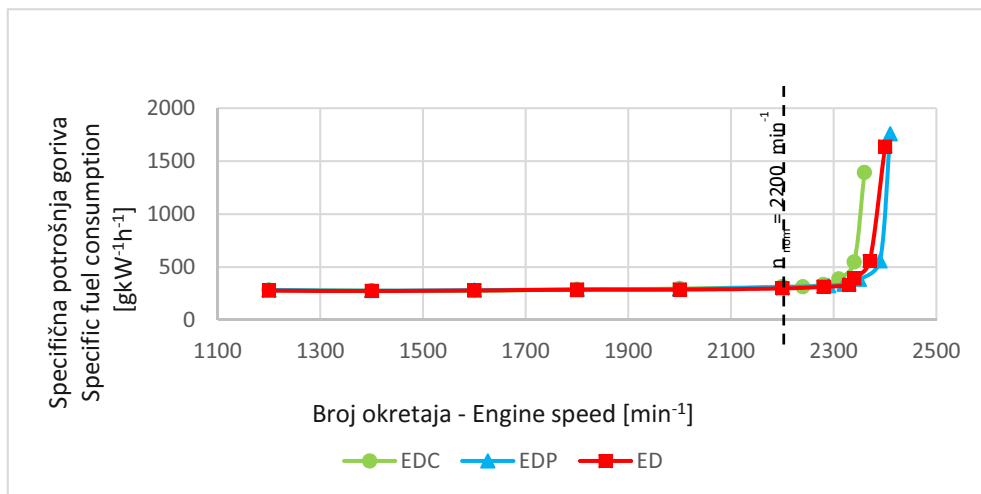


Grafikon 3. Satna potrošnja goriva dizel motora s tri vrste goriva u funkciji broja okretaja
Graph 3. Hourly fuel consumption of diesel engine with three fuel types in function of engine speed

Tablica 6 i grafikon 4 prikazuju podatke o izmjerenoj specifičnoj potrošnji ED, EDP i EDC goriva. Najmanja prosječna specifična potrošnja izmjerena je korištenjem EDC goriva i bila je manja za 7.49% odnosno 4.64% od prosječne specifične potrošnje izmjerene korištenjem EDP i ED goriva. Prosječno najveća specifična potrošnja goriva izmjerena je korištenjem EDP goriva. Prosječna specifična potrošnja korištenjem ED goriva bila je manja za 2.98% od prosječne specifične potrošnje korištenjem EDP goriva. Kod sve tri vrste goriva najmanja specifična potrošnja bila je kod maksimalnog zakretnog momenta motora.

Tablica 6. Specifična potrošnja goriva dizel motora s tri vrste goriva kod različitih OECD točaka mjerenja
Table 6. Diesel engine specific fuel consumption with three fuel types at different OECD testing points

Specifična potrošnja Spec. fuel consumpt. [gkW ⁻¹ h ⁻¹]	P1	P2	P3	P4	P5	P6	P7	P8	P9	P10	P11	Prosjek Average
ED	299,44	314,48	332,15	392,99	556,51	1638,27	288,31	288,31	280,28	275,16	278,09	449,45
EDP	311,14	324,10	337,65	385,26	558,52	1758,29	291,51	286,19	282,62	276,81	283,97	463,28
EDC	314,61	314,19	335,35	387,32	548,33	1392,26	297,10	289,53	275,74	277,69	282,42	428,60



Grafikon 4. Specifična potrošnja goriva dizel motora s tri vrste goriva u funkciji broja okretaja
Graph 4. Diesel engine specific fuel consumption with three fuel types in function of engine speed

Prema dobivenim rezultatima mjerenja može se zaključiti da nije bilo razlika u istraživanim karakteristikama dizel motora korištenjem standardnog Eurodizela i Eurodizela plavog, osim u boji koja se dodaje zbog kontrole potrošnje. Korištenjem Eurodizel Class goriva ostvarena je veća prosječna snaga motora za oko 2% i zakretni moment za oko 3% u odnosu na snagu i zakretni moment ostvarenu korištenjem standardnog Eurodizela i Eurodizela plavog. Prosječna specifična potrošnja korištenjem Eurodizel Class goriva bila je manja za 7.5% u odnosu na standardni Eurodizel, a 4.6% manja u odnosu na Eurodizel plavi. Rezultati pokazuju da se ne mogu očekivati neke značajne razlike u snazi i zakretnom momentu dizel motora korištenjem premium dizelskog goriva koje se nalazi na tržištu, ali da razlike ipak postoje. S obzirom na nešto značajniju razliku u specifičnoj potrošnji goriva i razliku u cijeni, na svakom poljoprivredniku ostaje da odluči koje će gorivo koristiti. Pri korištenju različitih vrsta goriva treba voditi računa i o utjecaju na dijelove uređaja za napajanje gorivom, prvenstveno dijelova visokotlačnih crpki i brizgaljki (Dobovišek i sur., 2009).

Jedan od najvažnijih pokazatelja kvalitete dizelskog goriva je cetanski broj čiji je utjecaj presudan za pravilno izgaranje goriva u motoru. Icingur i Altiparmak (2003) su istraživali utjecaj cetanskog broja dizelskog goriva na karakteristike dizel motora s direktnim ubrizgavanjem i utvrdili da se povećanjem cetanskog broja s 46 na 54.5 snaga motora povećala za 4%, a zakretni moment za 5%. Sabah i Miqdam (2012) su istraživali utjecaj cetanskog broja dizelskog goriva na potrošnju goriva dizel motora s direktnim ubrizgavanjem i utvrdili da se povećanjem cetanskog broja s 48.5 na 55 specifična potrošnja goriva smanjila za 12.55%. Rezultati istraživanja Chena i sur. (2008) također su pokazali relativno mali utjecaj svojstava dizelskog goriva na snagu, potrošnju goriva i proces izgaranja u testnom Euro 4 dizel motoru.

Svima je u interesu da goriva koja se koriste budu podvrgnuta permanentnoj nepristranoj kontroli kako bi kupci bili sigurni da kupuju kvalitetno gorivo, a proizvođači i dobavljači bili dodatno motivirani da takvo gorivo i isporučuju. Zato je vrlo važno da se prilikom testiranja goriva i interpretacije rezultata u obzir uzmu svi bitni i relevantni parametri kvalitete goriva

(Jednačak, 2008). Kvaliteti goriva u Republici Hrvatskoj u velikoj mjeri doprinosi Program praćenja kvalitete tekućih naftnih goriva koja se stavljaju na tržište Republike Hrvatske ili koja se koriste za vlastite potrebe (Narodne novine 120/16) koji sadrži način uzorkovanja tekućih naftnih goriva posebno za benzinske postaje i skladišta, broj i učestalost uzimanja uzoraka tekućih naftnih goriva, lokacije uzorkovanja, ovisno o količini tekućih naftnih goriva koje je dobavljač stavio na tržište Republike Hrvatske ili koje koristi za vlastite potrebe, način obavljanja laboratorijske analize uzoraka tekućih naftnih goriva te izvješćivanje o provedbi analiza.

ZAKLJUČCI

Na osnovi rezultata istraživanja provedenih s tri vrste dizelskog goriva može se zaključiti sljedeće:

- Prosječna snaga ostvarena korištenjem Eurodizel Class goriva bila je veća za 1.81% u odnosu na snagu ostvarenu korištenjem Eurodizela plavog odnosno 1.98% u odnosu na snagu ostvarenu korištenjem standardnog Eurodizela.
- Prosječni zakretni moment korištenjem Eurodizel Class goriva bio je veći za 2.68% u odnosu na zakretni moment ostvaren korištenjem Eurodizela plavog odnosno 2.85% u odnosu na zakretni moment ostvaren korištenjem standardnog Eurodizela.
- Razlike u prosječno ostvarenoj snazi i zakretnom momentu korištenjem standardnog Eurodizela i Eurodizela plavog bile su zanemarive.
- Prosječna specifična potrošnja korištenjem Eurodizel Class goriva bila je manja za 7.49% u odnosu na Eurodizel plavi, a 4.64% manja u odnosu na standardni Eurodizel.

LITERATURA

- Chen, W.M., Wang, J.X., Shuai, S.J. (2008). Effects of fuel properties on the performance of a typical Euro IV diesel engine. *Huan Jing Ke Xue* 29, 2665-2671.
- Dobovišek, Ž., Vajda, B., Pehan, S., Kegl, B. (2009). Utjecaj svojstava goriva na značajke motora i tribološki parametri. *Goriva i maziva* 48, 131-158.
- Fayyazbakhsh, A., Pirouzfard, V. (2017). Comprehensive overview on diesel additives to reduce emissions, enhance fuel properties and improve engine performance. *Renewable and Sustainable Energy Reviews* 74, 891-901.
- Hrvatski zavod za norme (2014). HRN EN 590:2014 Goriva za motorna vozila – Dizelsko gorivo – Zahtjevi i metode ispitivanja, Zagreb.
- Icingur, Y., Altiparmak, D. (2003). Effect of fuel cetane number and injection pressure on a DI Diesel engine performance and emissions. *Energy Conversion and Management* 44, 389-397.
- Jednačak, M. (2008). Zahtjevi kvalitete goriva i kontrola na tržištu. *Goriva i maziva* 47, 429-430.
- Jednačak, M. (2009). Parametri kvalitete goriva i njihovi učinci na ponašanje goriva u primjeni. *Goriva i maziva* 48, 121-130.
- Lee, S.W., Park, S., Daisho, Y. (2004). An experimental study of the effects of combustion systems and fuel properties on the performance of a diesel engine. *Proceedings of the Institution of Mechanical Engineers, Part D: Journal of Automobile Engineering* 218, 1317-1323.
- Narodne novine (2017). Uredba o kvaliteti tekućih naftnih goriva i načinu praćenja i izvješćivanja te metodologiji izračuna emisija stakleničkih plinova u životnom vijeku isporučenih goriva i energije. *Narodne novine* 57/2017, Zagreb.
- Narodne novine (2016). Program praćenja kvalitete tekućih naftnih goriva za 2017. godinu. *Narodne novine* 120/2016, Zagreb.

- OECD (2017). Standard Code for the Official Testing of Agricultural and Forestry Tractor Performance. Code 2. Organisation for Economic Co-operation and Development, Paris.
- Sabah, T.A., Miqdam, T.C. (2012). Effects of fuel cetane number on multi-cylinders direct injection diesel engine performance and exhaust emissions. *Al-Khwarizmi Engineering Journal* 8, 65-75.
- Yang, C., Kidoguchi, Y., Kato, R., Miwa, K. (1999). Effects of fuel properties on combustion and emissions of a direct-injection diesel engine. *Journal of the Marine Engineering Society in Japan* 34, 798-806.

TRACTOR DI DIESEL ENGINE PERFORMANCES USING DIFFERENT TYPES OF DIESEL FUEL

SUMMARY

The aim of this paper was to investigate the impact of different types of diesel fuel on the performances of the tractor diesel engine. The research was conducted on a three-cylinder DI diesel engine (nominal power 46 kW) with three types of diesel fuel: standard Eurodiesel, premium Eurodiesel (Class) and Eurodiesel Blue according to the OECD Code 2 for the Official Testing of Agricultural and Forestry Tractor Performance. Based on the obtained results, it can be concluded that there were no differences in the investigated diesel engine performances using standard Eurodiesel and Eurodiesel Blue. Using premium Eurodiesel (Class) fuel the average engine power was increased by about 2% and the torque by about 3% in relation to the power and torque achieved using standard Eurodiesel and Eurodiesel Blue. The average specific fuel consumption by using premium Eurodiesel (Class) was 7.5% lower than Eurodiesel Blue and 4.6% lower than the standard Eurodiesel.

Key words: power, torque, specific fuel consumption, hourly fuel consumption



ANALYSIS OF HUMAN WHOLE-BODY VIBRATION EXPOSURE ON A U650 TRACTOR

Alina OVANISOF*, Ovidiu VASILE, Maria DRAGOMIR

Department of Mechanics, University Politehnica of Bucharest,
313 Splaiul Independentei, 060042 Bucharest, Romania

*E-mail of corresponding author: alinaovanisof@yahoo.com

SUMMARY

Based on the minimum health and safety requirements for the exposure of workers to mechanical vibration-related risks, this paper presents an assessment of the level of whole-body vibration exposure for a human operator. Experimental analysis is performed on a U650 tractor used for agricultural works. Using a Matlab program, we present the assessment of vibrations for health, comfort and perception, highlighting the compliance with the minimum requirements imposed by Directive 2002/44 / EC.

Keywords: vibration, level of exposure, frequency weighting curves

INTRODUCTION

The influence of mechanical vibration on the human body has been studied in various papers without being exhausted from a scientific point of view (Alexandru, 2014; Alexandru, 2013; Biris and Arghir, 2012; Bratu, 2014; Bratu, 2013; Bratu, 2012, Bratu, 2011, Bratu, 2000; Bratu, 1990; Ciuncanu, 2015; Ciuncanu, 2013, Gillich and Praisach, 2014, Iancu et al., 2013; Murzea, 2013; Vasile, 2013). During transport, there are mechanical vibrations on the human body that do not have a positive influence, they can cause discomfort that leads to an activity that does not work in optimal working conditions or over time, may have more or less serious effects on the health of the human body subjected to these vibrations.

If the exposure is long, there are medical studies that show the following conditions:

- Osteo-musculo-articular syndrome
- Digestive disorders
- Raynaud's Syndrome
- Nervous system disorders

Try to ensure a high degree of protection and prevention of these harmful vibrations on the human body and create the best possible working conditions. Consider the position on a

chair (driver's seat / driver's seat), and the measurement directions are set, as in Fig. 1 (Directive 2002/44/EC, 2002; ISO 2631-1, 2001; Vasile, 2015).

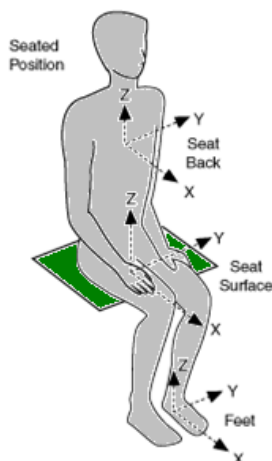


Figure 1. The coordinate system used to measure WBV (whole body vibration), for seated position

MATERIALS AND METHODS

Directive 2002/44/EC define the sets an exposure action value, above which it requires employers to control the whole-body vibration risks of their workforce and an exposure limit value above which workers must not be exposed (Directive 2002/44/EC, 2002):

- a daily exposure action value of $0,5 \text{ m s}^{-2}$ or vibration dose value (VDV) of $9,1 \text{ m s}^{-1,75}$;
- a daily exposure limit value of $1,15 \text{ m s}^{-2}$ or vibration dose value (VDV) of $21 \text{ m s}^{-1,75}$;

The ISO 2631-1 standard classifies vibration exposures into three categories:

- likely health risk zone (RMS – $0,86 \text{ m s}^{-2}$ and VDV – $17 \text{ m s}^{-1,75}$), where vibration exposure is likely to be a risk to health (in Directive it is $A(8)$ - daily exposure limit value);
- caution zone (RMS – $0,43 \text{ m s}^{-2}$ and VDV – $8,5 \text{ m s}^{-1,75}$), where vibration exposure is a potential risk to health (in Directive it is $A(8)$ - daily exposure action value);
- below the caution zone, where the vibration exposure level is considered acceptable and unlikely to be a risk to health.

An important role at reducing vibration transmitted to the human body to different types of machines and equipment he is using elastomeric materials, which are found in literature studies a wide range of vibration isolation (Alexandru, 2013; Biris and Arghir, 2012; Bratu, 2014; Bratu, 2011; Bratu, 1990), controlled generation excitation (Ciuncanu, 2015). Thus, by reducing the level of vibration transmitted to the human operator, using various solutions may reduce human exposure to vibration.

ANALYSIS OF ACCELERATIONS TRANSMITTED TO THE OPERATOR

A basic method for the evaluation of human exposure to whole-body vibration (WBV) requires that the evaluation includes measurement of the weighted root-mean-square (R.M.S) acceleration, which is calculated as the following (ISO 2631-1, 2001):

$$a_w = \left[\frac{1}{T} \int_0^T a_w^2(t) dt \right]^{\frac{1}{2}} \quad (1)$$

where:

$a_w(t)$ is the weighted acceleration as a function of time (time history) of measured signal, in meters per second squared ($m s^{-2}$)

T is the measurement duration, in seconds

The coordinate system used to measure WBV (ISO 2631-1, 2001) can be seen in Fig. 1.

The RMS continuous evaluation method takes into accounts the occasional shocks and transient vibrations using a small integration time constant. The size of vibration is defined as the maximum transient vibration value MTVV, which is the maximum value in time of $a_w(t_0)$, obtained using the following equation (ISO 2631-1, 2001; Vasile, 2013):

$$a_w(t_0) = \left\{ \frac{1}{T} \int_{t_0-T}^{t_0} [a_w(t)]^2 dt \right\}^{\frac{1}{2}} \quad (2)$$

where:

$a_w(t)$ is instantaneous frequency weighted acceleration ($m s^{-2}$)

T is the time integration of continuous mediation, in seconds

t is the time (integration variable)

t_0 is the time observation (the instantaneously time).

The maximum transient vibration value (ISO 2631-1, 2001) in $m s^{-2}$ is calculated as follows:

$$MTVV = \max\{a_w(t_0)\} \quad (3)$$

which corresponding to the maximum value of $a_w(t_0)$ read on the measurement period

Further evaluation can be carried out by means of vibration of the fourth power vibration dose is more sensitive on the peaks than the based method in Eq. 1, because basic mediation used as the fourth power instead of second power of the time acceleration evolution (ISO 2631-1, 2001). Vibration dose value VDV is measure on $m s^{-1.75}$ as is defined as:

$$VDV = \left\{ \int_0^T [a_w(t)]^4 dt \right\}^{\frac{1}{4}} \quad (4)$$

where:

$a_w(t)$ is instantaneous frequency weighted acceleration ($m s^{-2}$)

T the measurement time in seconds

Measurement of vibration (WBV) is made with portable acquisition system consist of: notebook, coupled acquisition board NI USB-9233 4-channel type of purchase (see on Fig. 2), triaxial accelerometer type 4306 B 003, Bruel & Kjaer, controlled by a virtual analyzer developed under LabView software platform ver 2011 from National Instruments. The tests were carried out at the University "Politehnica" of Bucharest, on a paved portion.



Figure 2. Photos from experimental measurements

RESULTS AND DISCUSSION

The measuring point was on the floor of the tractor. At this point, the operator works in seated position. The throttle transducer was fixed with a magnet on the tractor floor. Direction of direction X, Y - in the horizontal plane and Z in the vertical direction. Measurements were made at three speeds of 850, 1200, 1500 rpm.

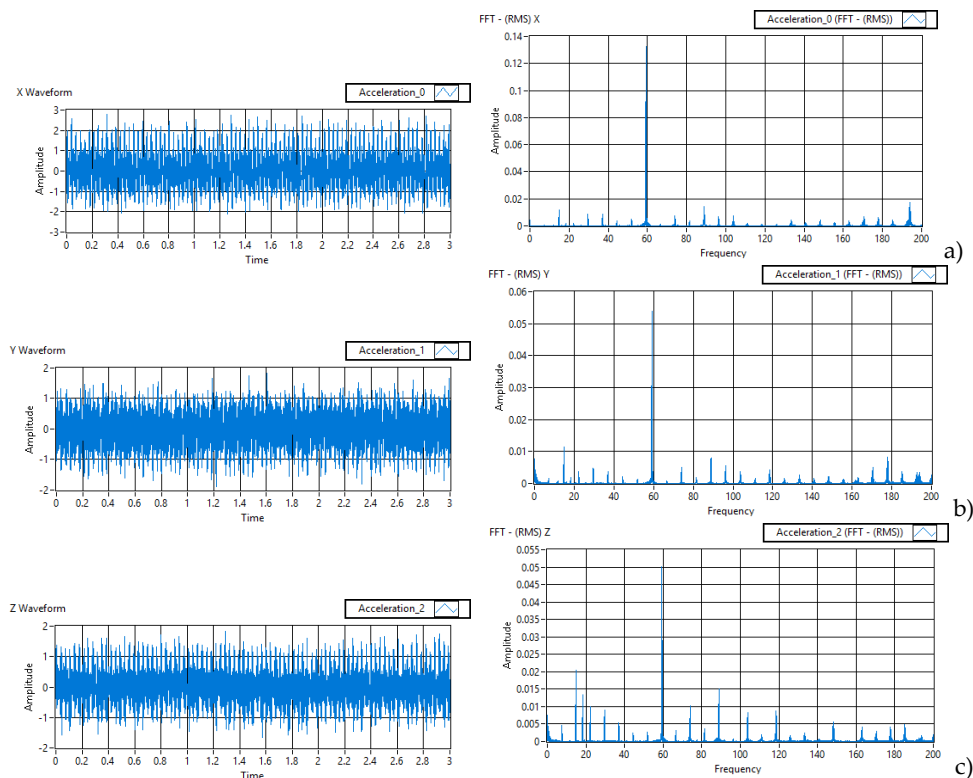


Figure 3. Vibration acceleration time history (left) and FFT spectrum analysis (on the right), in $m\ s^{-2}$ for 850 rpm, for a) X direction; b) Y direction; c) Z direction

Multiple records were performed for WBV, of which for the present study we have chosen a recording signal with a duration over 250 seconds each with simultaneous measurement on three dimensions, with 5000 samples / second sampling rate. In the appended figures Fig. 3-5, it can observe the accelerations time spectrum in the range of 0-3 s and FFT analysis on 0-200 Hz domain, if the engine is running at 850, 1200 and 1500 rpm.

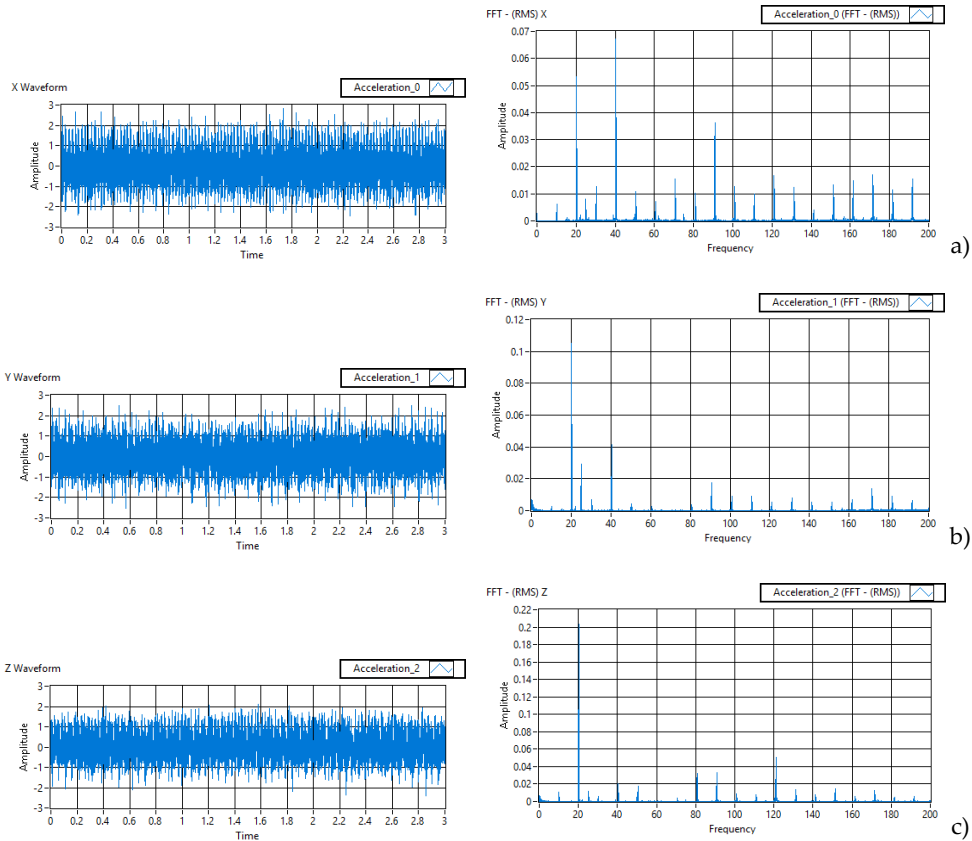


Figure 4. Vibration acceleration time history (left) and FFT spectrum analysis (on the right), in $m\ s^{-2}$ for 1200 rpm, for a) X direction; b) Y direction; c) Z direction

In the case of determining the weighted RMS acceleration, depending on the time evolution of the measured acceleration at the measuring point respectively, have been taken into account the weighting curves (Directive 2002/44/EC, 2002; ISO 2631-1, 2001): W_c and W_d for X-axis, W_d for Y-axis and the W_k for Z-axis, as shown in the Table 1, 2 and 3 corresponding to engine speeds of 850, 1200 and 1500 rpm.

Because has been registered variation in time of the acceleration, simultaneously on the threeaxis for the vibration combination of several directions, the following equation can be used (Directive 2002/44/EC):

$$a_v = \left(k_x^2 a_{wx}^2 + k_y^2 a_{wy}^2 + k_z^2 a_{wz}^2 \right)^{\frac{1}{2}} \quad (5)$$

where:

a_{wx} , a_{wy} , a_{wz} are RMS accelerations weighted to orthogonal axes X, Y and Z;
 k_x , k_y , k_z are the multiplication factors.

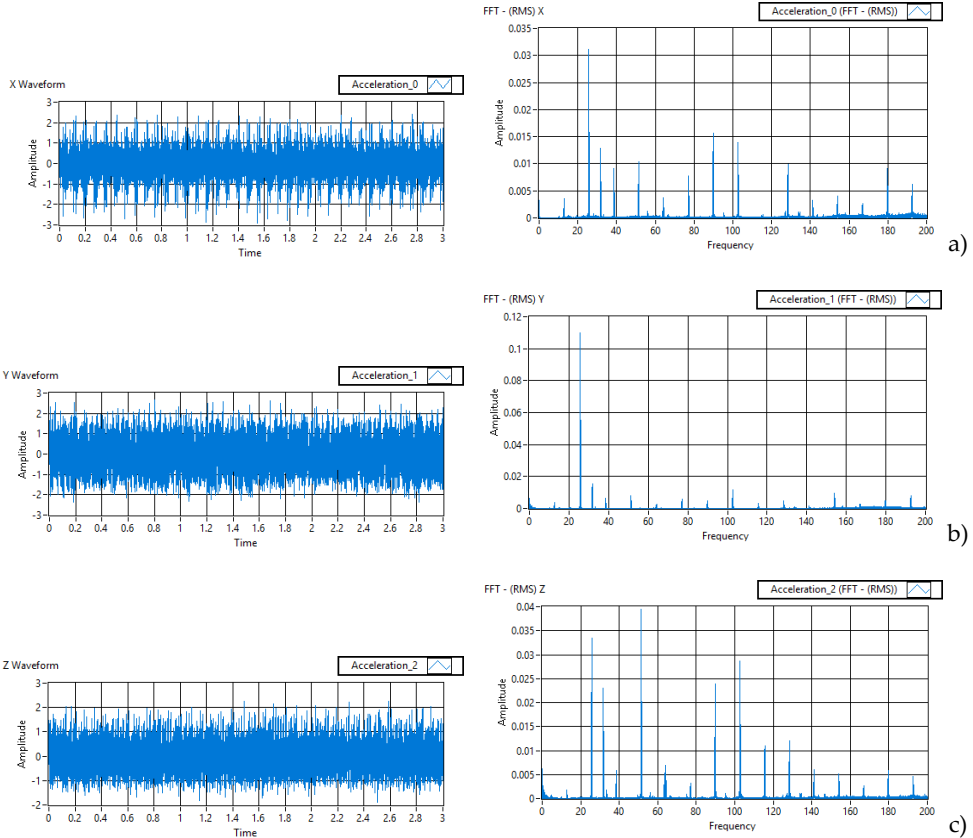


Figure 5. Vibration acceleration time history (left) and FFT spectrum analysis (on the right), in $m s^{-2}$ for 1500 rpm, for a) X direction; b) Y direction; c) Z direction

The recorded signal was implemented in a MATLAB program developed by the author, which was performed signal analysis and application frequency weighting curves corresponding to the measuring axes (X, Y and Z). The principal frequency weighting, related to health, confort and perception are given by W_k for the z direction and W_d for the x and y directions. The functions implemented in MATLAB meet the requirements to transfer functions of filters given in the ISO 2631-1 recommendation.

The root mean square (RMS) calculations were performed to calculate significant parameters to test against standardized thresholds for health risk (ISO 2631-1, 2001) confort, and perception. If daily exposure of human operator is known, ISO 2361-1 (B 3.1) gives us a health caution guidance zone threshold upper and lower limits. At an exposure duration of 96 minutes, vibration exposure below $0.75 m s^{-2}$ have not been shown to produce measurable health effects, vibration exposure in the health guidance caution zone (between 0.75 to $2.0 m s^{-2}$) indicates that caution should be taken, and vibration exposure above the $2.0 m s^{-2}$

indicates likely health risks. The measured vibration exposure within the working place located on a chassis was compared to these thresholds.

Table 1. The experimental results and calculation for 850 rpm

Axis direction	X		Y	Z
Frequency weighting curve	W_c	W_d	W_d	W_k
Mean square weighted acceleration a_w [$m\ s^{-2}$]	0.05716	0.01424	0.0178	0.06198
Maximum transient vibration value MTVV [$m\ s^{-2}$]	0.05716	0.01424	0.0178	0.06198
Vibration dose value VDV [$m\ s^{-1.75}$]	0.2611	0.06509	0.108	0.315

Table 2. The experimental results and calculation for 1200 rpm

Axis direction	X		Y	Z
Frequency weighting curve	W_c	W_d	W_d	W_k
Mean square weighted acceleration a_w [$m\ s^{-2}$]	0.03182	0.007869	0.02353	0.1468
Maximum transient vibration value MTVV [$m\ s^{-2}$]	0.03182	0.007869	0.02353	0.1468
Vibration dose value VDV [$m\ s^{-1.75}$]	0.1297	0.0322	0.108	0.5282

Table 3. The experimental results and calculation for 1500 rpm

Axis direction	X		Y	Z
Frequency weighting curve	W_c	W_d	W_d	W_k
Mean square weighted acceleration a_w [$m\ s^{-2}$]	0.02233	0.005539	0.02453	0.04863
Maximum transient vibration value MTVV [$m\ s^{-2}$]	0.02233	0.005539	0.02453	0.04863
Vibration dose value VDV [$m\ s^{-1.75}$]	0.1079	0.02695	0.2037	0.2436

Based on the values determined in Tables 1-3 and applying equation (5) according to the requirements of ISO 2631-1 for health, comfort and perception a_v is calculated for the vibration combination of three directions X, Y and Z, presented in Table 4.

Table 4. Vibration evaluation on the three simultaneous directions in terms of health, confort and perception

Engine running condition	Health	Comfort	Perception
	a_v [$m\ s^{-2}$] RMS		
850 rpm	0.069713	0.086172	0.066039
1200 rpm	0.150854	0.152041	0.148882
1500 rpm	0.060037	0.058866	0.054747
	where we have: X axis; W_d , $k=1.4$ Y axis; W_d , $k=1.4$ Z axis; W_k , $k=1$	where we have: X axis; W_c , $k=1$ Y axis; W_d , $k=1$ Z axis; W_k , $k=1$	where we have: X axis; W_d , $k=1$ Y axis; W_d , $k=1$ Z axis; W_k , $k=1$

Analyzing the results presented in Tables 1 to 3, it is observed that for the case study, the vibrations transmitted to the whole body, maximum vibration dose values (VDV) are $0.315 \text{ m s}^{-1.75}$ for 850 rpm, $0.5282 \text{ m s}^{-1.75}$ for 1200 rpm and $0.2436 \text{ m s}^{-1.75}$ for 1500 rpm. Note that all these maximum values are in the Z direction. Similarly, it is observed that in all three cases, the vibration dose value (MTVV) has maximum values in the Z direction (vertical direction, as can be seen in Fig. 2).

In the case of this study (WBV), frequency weightings used for the prediction of the effects of vibration on health, comfort, perception are W_c , W_d and W_k . These weightings are applied using the multiplying factors k , corresponding to each axis indicated in the last line of Table 4.

CONCLUSIONS

The effects of vibration on human comfort is possible to be evaluated in some environments, but that comfort level is affected by different factors including the activities being performed while subjected to vibration.

From the point of view of the Vibration Dose Value analysis, it can be seen in Tables 1-3 that in all situations the worst situation with maximum values of VDV is in the vertical direction - on the Z axis. This can also be seen in the spectral analysis graphs in Fig. 3c, 4c and 5c. However, the values obtained fall within the admissible limits laid down in Directive 2002/44 / EC - which applies to the Member States of the European Union. Depending on the human operator's work schedule and the intervals in which he works, an A (8) daily exposure assessment can also be performed.

This evaluation, conducted based on standard ISO 2631-1 have provided significant insight into the health, confort and perception as presented in Table 4. It can be seen that vibrations have a maximum effect on the human operator in the case of motor operation at 1200 rpm.

Based on these results, it can be seen that the regime with the most significant effect on the human operator is not obtained for the highest engine speed.

Vibration exposure depends on the engine speed and the weight of the trailer or the soil processing process if a plow for agricultural land processing is used. This study also provided information on the VDV spectral analysis of the U650 while operating at different speeds.

REFERENCES

- Alexandru, C. (2013). Analysis of the dynamic behavior of the antiseismic elastomeric isolators based on the evaluation of the internal dissipated energy. *Applied Mechanics and Materials*, 430, pp. 317-322.
- Alexandru, C. (2014). Influence of position angle of elastic anti-vibration elements on the transmissibility, *Romanian Journal of Acoustics and Vibration*, 11 (1), pp. 59-62.
- Biris, A. and Arghir, M. (2012). Actiunea vibratiilor induse de masinile unelte portabile asupra sistemului mana-brat, a XII a Conferinta Nationala multidisciplinara cu participare internationala Profesorul Dorin PAVEL, Sebes, pg 215-222.
- Bratu, P. (1990). Elastic bearing systems for machines and equipment, 260 pages, Technical Publishing House.
- Bratu, P. (2000). Vibration of elastic systems. Technical Publishing House, Bucharest.

- Bratu, P. (2011). The variation of the natural frequencies of road vibrator-rollers, as a function of the Parameters of Neoprene Vibration Isolation Elements. *Materiale Plastice*, 48 (2), pp. 144-147.
- Bratu, P. (2012). Evaluation of the dissipated energy in viscoelastic or hysteretic seismic isolators. *Romanian Journal of Acoustics and Vibration*, 9 (1), pp. 53-56.
- Bratu, P. (2013). Physical instability and functional uncertainties of the dynamic systems in resonance. *Applied Mechanics and Materials*, 430, pp. 32-39.
- Bratu, P. (2013). Corrective analysis of the parametric values from dynamic testing on stand of the antiseismic elastomeric isolators in correlation with the real structural supporting layout. *Applied Mechanics and Materials*, 430, pp. 305-311.
- Bratu, P. (2014). Dynamic interaction between the foundations and the unbalanced rotating machine. 21st International Congress on Sound and Vibration 2014, pp. 602-607.
- Ciuncanu, M. (2013). The influence of the excitation signal form on the evaluation of the damping characteristics of the elastomeric antiseismic isolators. Bucuresti, SISOM.
- Ciuncanu, M. (2015). Test performance evaluation for elastomeric anti-seismic devices on specialized stands with controlled generation excitation functions. 22th International Congress on Sound and Vibration, Florance, Italy.
- European Parliament and the Council of the European Union. (2002). Directive 2002/44/EC on the minimum health and safety requirements regarding the exposure of workers to the risks arising from physical agents (vibration).
- Gillich, G.R., Praisach, Z.I. (2014). Modal identification and damage detection in beam-like structures using the power spectrum and time-frequency analysis, *Signal Processing*, 96 (Part A), pp. 29-44.
- Iancu, V., Gillich, G.R., Iavornic, C.M., Gillich, N. (2013). Some models of elastomeric seismic isolation devices, *Applied Mechanics and Materials*, 430, pp. 356-361.
- ISO 2631-1:2001. (2001). Mechanical vibration and shock – Evaluation of human exposure to wholebody vibration – Part 1: General requirements.
- Murzea, P. (2013). Analysis of the behavior of large-span structures in the case of ambient vibrations considering the variety of motion possibilities, *Romanian Journal of Acoustics and Vibration*, 10 (1), pp. 39-46.
- National Instruments (2008). Overview of Human Vibration Weighting Filters. Retrieved on 29/11/2017 at <http://www.ni.com/white-paper/6957/en/>.
- Vasile, O. (2013). Dynamic Behaviour Analysis of Machines in Transient Regime on Torsional Vibration Stresses. *Romanian Journal of Acoustics and Vibration*, 10 (2), pp. 129-134.
- Vasile, O. (2015). Analysis of the Human Health and Safety Requirements to Vibration Generated Risks. *Applied Mechanics and Materials*, 801, pp. 236-241.



GRAIN PILE STRATIFICATION PROCESS ON SIEVES OF HARVESTER CLEANING SYSTEM

Gheorghe VOICU*, Magdalena - Laura TOMA, Elena - Madalina STEFAN,
Paula TUDOR, Mihaela - Florentina DUTU

University Politehnica of Bucharest, Faculty of Biotechnical Systems Engineering,
Bucharest, Romania

*E-mail of corresponding author: ghvoicu_2005@yahoo.com

SUMMARY

In the separating process of grain seeds on the cleaning system sieves of the harvesting combines, the stratification of the material on the sieves plays an important role. This phenomenon is achieved by the combined effect of the sieves oscillating motion and the airflow passing from the bottom up through the sieves holes. The results of some experimental researches related to the influence of the heap components stratification on the separating process of the seeds on the upper sieve of the cleaning system according to the parameters of the adopted working regime are presented in this paper. The phenomenon could be emphasized by colouring in different colours the seeds at the bottom and above of the material and determining the seeds distribution collected along the sieve length, underneath it. Using the regression analysis of experimental data with the Gauss distribution function, the distribution curves of the seeds collected under the sieve were plotted. The position of the maximum of these curves (horizontally and vertically) presents the influence of the working regime parameters on the heap stratification and the seed separation along the sieve.

Keywords: grain separation, stratification, gauss function, seeds losses

INTRODUCTION

Grain cereal means the mixture of seeds and other materials than grain present in the mixture after they pass through the combine trencher.

The stratification principle stays at the base of the seeds separation from the hopper that has reached the combine cleaning system. This principle relies on heap components density due to their relative movements within the layer that facilitates the displacement of the seeds through the material layer and their passage through the separation surface openings (Voicu et al., 2007; Wang et al., 1994; Zhao et al., 2011).

The heap layers separation, according to the components density, cannot take place without the action of external forces capable of weakening the inner bonds between the seeds and the other components. This is accomplished by transmitting an oscillation motion to both the heap-oscillating conveyor and the sieve block through a driving mechanism, often in a form of an articulated quadrilateral mechanism. The driving mechanism must provide certain oscillation directions as well as certain distributions and magnitudes of inertial forces along the sieves length in order to enhance the heap component stratification and thus the seed separation (Zaika, 1975; Voicu et.al., 2006; Böttinger and Fliege, 2012).

The main forces acting on the heap particles on the sieve surface are the inertial force imprinted by the sieve through its oscillation movement, which is the dynamic effect of the sieve motion on the material and the force of the air discharged by the cleaning system fan. The movement of the combine cleaning system has an influence on the relative displacement of the heap components through the speeds and accelerations it imparts to them.

Under the action of airflow and sieve oscillations, the material on the separation surface loosens so that the inner bonds between the particles decrease, which makes them move vertically into the material layer. The seeds, having a density greater than the straw particles, descends to the base of the layer in contact with the sieve and can be separated through its holes while the straw parts move to the top of the layer being removed by the air stream. The higher the airflow, the looser, therefore more stratified, the layer of material becomes.

The importance of airflow to the seed cleaning process has been highlighted by various researchers (Panasiewicz et al., 2012), the authors determining the mathematical model of particles motion equations (seeds and stalk components) in the air flow according to their speed and direction.

When passing through the material layer, the velocity of the airflow decreases, being influenced by the layer thickness (respectively the feed rate), but also by the size of the sieve holes (meaning the shutters opening degree if the sieve is Petersen or Closz type). The influence of the material feed flow on the cereals pneumatic cleaning was determined in several research papers. It was found that not only the velocity of the airflow decreases with the increase in the flow of material to be cleaned, but also its direction changes slightly (Ueka et al., 2012).

Also, the modelling and simulation of the seed separation process within the cereal combine cleaning system has been studied by other researchers including Gebrehiwot (2009), Schreiber and Kutzbach (2003), Korn et al. (2013) and Voicu et al. (2007, 2008).

The present paper aims to bring some additions to the material stratification process on the grain cleaning system sieves subjected to the simultaneous action of the sieve oscillations, but also to an ascending airflow passing through the orifices and the material layer. The main objective of the paper was to highlight the stratification phenomenon by determining the distribution of the seeds collected under the top sieve of the grain combine cleaning system, placed under and above the material layer on the sieve as well as in the main layer of the material.

MATERIALS AND METHODS

In order to track the stratification effect on the seed separation process from heap reaching the top sieve of the combine cleaning system, laboratory tests have been carried out on an experimental plant which has the characteristics of a traditional cleaning system of a Romanian cereal combine (Voicu et al., 2006).

The experiments were carried out with an autumn wheat heap of the Romanian variety Fundulea 4, in which coloured seeds were put in two distinct colours (red and blue), at the base and above the material layer on the heap oscillating conveyor. Writing ink has been used for colouring and the seeds are put separately on drying prior to use. For ease of calculation, seed mass of a certain colour was of 100 g.

The main characteristics of the material used in the experiments were: the bulk density of seeds $775 - 800 \text{ kg}\cdot\text{m}^{-3}$; the mass of 1000 seeds $38.6 - 43.5 \text{ g}$; seed humidity $11.3 - 12.5\%$; volumetric mass of straw components $62.3 - 65.9 \text{ kg}\cdot\text{m}^{-3}$; the straw/seeds ratio pp/s $0.2 - 0.3$. Most samples of this kind were performed at the oscillation frequency of 280 min^{-1} , but also at 335 min^{-1} .

The parameters studied and modified during the experimental tests were oscillation frequency f ; specific feed rate q ; mass ratio of straw/seeds pp/s ; the speed of the air flow at the fan outlet v_a ; opening of the blinds D_i .

When processing the material collected in the drawer boxes under the sieve, the coloured seeds were selected and weighed separately, the amount of seed of a particular colour in a box constituting exactly the percentage of coloured seeds collected on the respective section of the sieve.

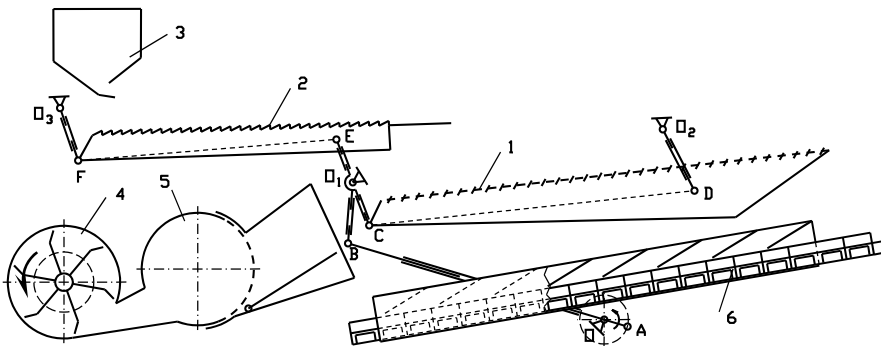


Figure 1. Schematic diagram of the experimental stand (Voicu et al., 2006)
 1. sieve with adjusted vents (Petersen); 2. oscillating conveyor; 3. feed bin with pile; 4. centrifugal fan with coil case; 5. outlet air unifier; 6. slide-in chassis for separated material gathering equipped with two sets of compartments

Based on the data obtained from the material processed from the drawer boxes below the sieve, the seed distribution curves at the bottom of the heap layer and those at the top of the layer were plotted and compared to the seed distribution of the heap main bulk collected in drawer boxes.

The maximum position of the separation curves was determined from the regression analysis of the experimental points with Gauss distribution function:

$$y = y_o + \frac{A}{w\sqrt{\pi/2}} \exp\left(-2(x - x_c)^2 / w^2\right) \quad (1)$$

where y is the percentage of seed collected in the boxes under the sieve, and x is the distance from the sieve end to the considered point (m).

At the same time, the regression equation coefficients and its parameters for each of the 7 × 3 plotted distribution curves (the dispersion σ and the theoretical curve height H), as well as the correlation coefficients χ^2 and R^2 , were determined.

RESULTS AND DISCUSSION

The seeds quantities (in percent), by assortment, collected in the boxes under the sieve are summarized in Table 1.

Table 1. The percentages of seed quantities in the general layer, at the base and above of the layer, collected in the boxes under the sieve

No. sample	Seed fraction	Seed mass under the sieve at different lengths from the sieve end, %								
		0.15 m	0.30 m	0.45 m	0.60 m	0.75 m	0.90 m	1.05 m	1.20 m	End of sieve
Working regime: $f = 280 \text{ min}^{-1}$; $q = 1 \text{ kg m}^{-1} \text{ s}^{-1}$; $v_a = 8 \text{ m s}^{-1}$; $D_j = 9 \text{ mm}$; $pp/s = 0.23$										
P1	Seeds in layer	1.0	3.0	10.6	15.6	20.0	20.8	19.7	7.1	2.2
	Seeds above	0	0	0.5	15.6	27.2	37.0	15.7	1.6	2.4
	Seeds below	2.6	2.7	2.8	17.1	22.9	34.3	14.2	2.9	0.5
Working regime: $f = 280 \text{ min}^{-1}$; $q = 1.5 \text{ kg m}^{-1} \text{ s}^{-1}$; $v_a = 8 \text{ m s}^{-1}$; $D_j = 9 \text{ mm}$; $pp/s = 0.29$										
P2	Seeds in layer	1.3	3.7	10.3	15.5	17.1	17.4	21.6	10.8	2.3
	Seeds above	0	0.7	2.1	4.5	9.1	19.1	32.7	29.0	2.8
	Seeds below	0.5	4.6	13.0	14.8	16.2	16.3	21.3	11.5	1.8
Working regime: $f = 280 \text{ min}^{-1}$; $q = 1.5 \text{ kg m}^{-1} \text{ s}^{-1}$; $v_a = 8 \text{ m s}^{-1}$; $D_j = 11 \text{ mm}$; $pp/s = 0.3$										
P3	Seeds in layer	1.7	6.8	27.6	29.4	19.5	10.0	3.7	0.9	0.4
	Seeds above	1.5	4.5	9.6	32.0	27.1	13.7	9.8	1.1	0.7
	Seeds below	1.8	7.5	28.9	30.5	22.1	7.2	2.0	0	0
Working regime: $f = 280 \text{ min}^{-1}$; $q = 1.5 \text{ kg m}^{-1} \text{ s}^{-1}$; $v_a = 8 \text{ m s}^{-1}$; $D_j = 12.5 \text{ mm}$; $pp/s = 0.24$										
P4	Seeds in layer	2.7	9.6	33.5	36.2	13.2	3.6	0.8	0.2	0.2
	Seeds above	0	2.0	19.4	33.0	38.7	5.8	0.4	0.3	0.4
	Seeds below	0.6	14.0	39.0	36.6	9.3	0.5	0	0	0
Working regime: $f = 280 \text{ min}^{-1}$; $q = 1.5 \text{ kg m}^{-1} \text{ s}^{-1}$; $v_a = 10 \text{ m s}^{-1}$; $D_j = 12.5 \text{ mm}$; $pp/s = 0.25$										
P5	Seeds in layer	2.0	7.7	33.9	36.5	14.5	3.6	1.0	0.3	0.5
	Seeds above	0	4.9	27.7	48.8	14.7	1.6	1.5	0.4	0.4
	Seeds below	3.5	4.9	45.2	35.7	8.3	2.4	0	0	0
Working regime: $f = 280 \text{ min}^{-1}$; $q = 2 \text{ kg m}^{-1} \text{ s}^{-1}$; $v_a = 10 \text{ m s}^{-1}$; $D_j = 11 \text{ mm}$; $pp/s = 0.25$										
P6	Seeds in layer	1.3	4.2	15.5	23.8	21.0	17.9	12.5	2.6	1.2
	Seeds above	0.9	1.4	3.9	21.1	25.8	22.6	16.5	6.2	1.6
	Seeds below	1.3	4.7	14.6	27.5	19.3	16.0	13.6	2.2	0.8
Working regime: $f = 335 \text{ min}^{-1}$; $q = 2 \text{ kg m}^{-1} \text{ s}^{-1}$; $v_a = 10 \text{ m s}^{-1}$; $D_j = 11 \text{ mm}$; $pp/s = 0.25$										
P7	Seeds in layer	0.2	0.8	3.1	13.9	22.6	20.8	16.8	15.8	6.0
	Seeds above	0	0	0	4.0	8.9	12.3	49.5	17.8	7.5
	Seeds below	0	0.3	1.7	12.7	27.1	22.3	17.1	14.5	4.3

From the analysis of the curves and the data in Table 1, it was found that approximately on all samples, the coloured seeds placed directly on the oscillating conveyor separated before the other seeds of the bulk mass, while the coloured seeds placed above the layer on the conveyor, have separated in greater percentage towards the rear end of the sieve after the separation of the main seed mass. However, in the material collected under the sieve, the

difference between the seed mass at the base of the material layer and the mass of the seed in the general layer is not as great as the difference between the mass of the seeds above and those in the main layer (see the values of x_c in Table 2).

The distribution curves of the separated seeds and collected under the sieve along its length are shown in Figures 2 and 3, respectively, and the regression coefficients values and the recorded curves parameters are presented in Table 2.

Table 2. Regression parameters of experimental data with equation (2)

No. sample	y_0	x_c	w	A	σ	H	χ^2	R ²
P1	-0.981	0.827	0.581	16.80	0.291	23.06	3.988	0.963
	0.045	0.845	0.328	14.94	0.164	36.28	7.354	0.973
	1.068	0.841	0.347	13.40	0.173	30.85	12.345	0.940
P2	-1.706	0.849	0.678	18.41	0.339	21.67	8.160	0.910
	1.297	1.070	0.315	13.18	0.157	33.41	12.186	0.947
	-4.025	0.831	0.790	22.76	0.395	22.98	11.286	0.871
P3	0.594	0.583	0.371	14.11	0.186	30.33	6.236	0.968
	1.632	0.681	0.331	12.55	0.165	30.29	11.080	0.943
	-0.113	0.579	0.366	15.17	0.183	33.10	4.079	0.982
P4	0.730	0.538	0.282	13.91	0.141	39.29	0.817	0.997
	-0.283	0.657	0.302	15.42	0.151	40.82	15.141	0.955
	-0.199	0.513	0.277	15.30	0.138	44.14	0.364	0.999
P5	0.707	0.543	0.278	13.94	0.139	39.95	1.456	0.995
	0.688	0.572	0.226	13.97	0.113	49.31	0.748	0.998
	1.186	0.512	0.204	13.22	0.102	51.82	5.517	0.986
P6	-1.338	0.713	0.547	17.11	0.274	24.95	4.223	0.966
	-0.293	0.807	0.456	15.49	0.228	27.11	5.585	0.965
	-1.294	0.700	0.541	17.03	0.271	25.10	12.156	0.910
P7	-1.129	0.901	0.587	17.31	0.293	23.55	6.775	0.943
	1.088	1.032	0.300	13.41	0.150	35.65	5.619	0.977
	-0.882	0.881	0.508	16.57	0.254	26.02	11.725	0.923

Thus, at sample 1, for a feed rate $q = 1 \text{ kg}\cdot\text{m}^{-1}\cdot\text{s}^{-1}$ and an air velocity at the fan outlet $v_a = 8 \text{ m}\cdot\text{s}^{-1}$, while the sieve holes opening was relatively small ($D_j = 9 \text{ mm}$) and the straw/seed ratio was $pp/s = 0.23$, the maximum of the separation curve of the seeds placed directly on the oscillating conveyor (at the bottom of the material layer) was at $\sim 0.841 \text{ m}$ from the sieve front end, while for the ones placed above the layer on the conveyor the maximum of the separation curve was about 0.845 m (the maximum of the seed separation curve from the main bulk mass was at $\sim 0.827 \text{ m}$ from the sieve front end – Fig. 2a).

At the same oscillation frequency ($f = 280 \text{ min}^{-1}$), the same velocity of the airflow ($v_a = 8 \text{ m}\cdot\text{s}^{-1}$) and the same blinds opening ($D_j = 9 \text{ mm}$), for a feed rate $q = 1.5 \text{ kg}\cdot\text{m}^{-1}\cdot\text{s}^{-1}$ and a pp/s ratio of 0.29 , the maximum of the separation curve shifted to the back end of the sieve but kept the natural order of settlement in the graph: for the seed at the base of the layer, the peak of the separation curve was about 0.831 m of the front end, while for the seeds above the heap layer, the maximum of the separation curve was at $\sim 1.070 \text{ m}$ (sample 2, Fig. 2b).

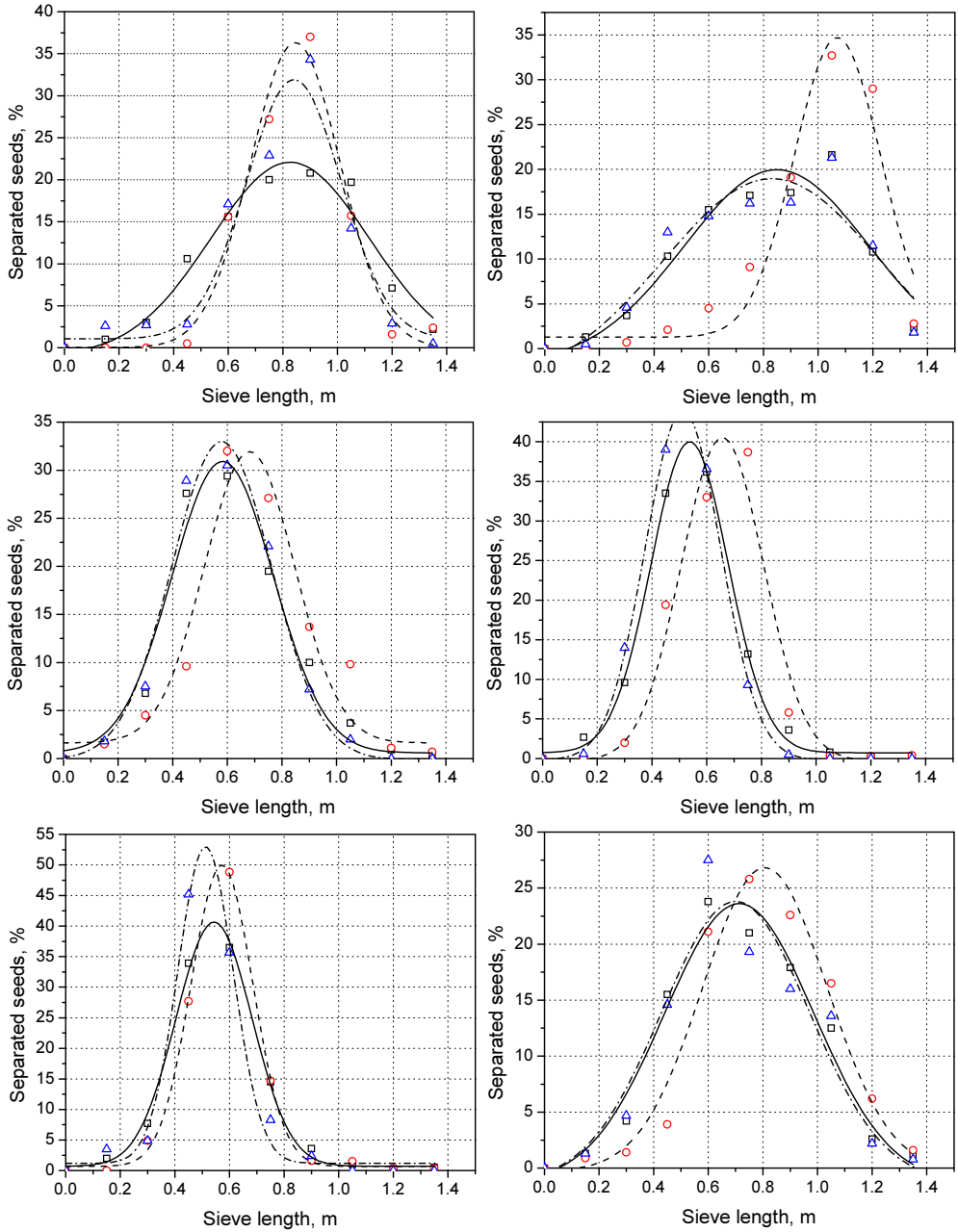


Figure 2. Seed distribution of fractions collected under sieve, along its length, at a frequency of 280 min⁻¹

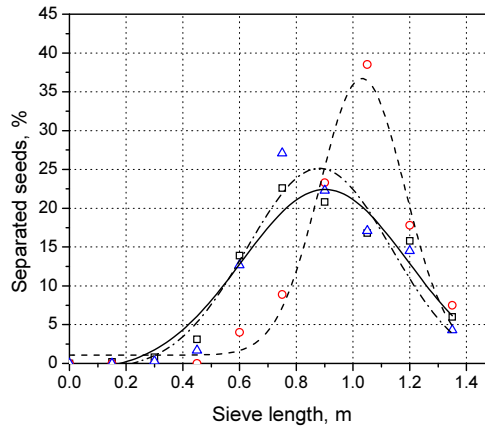


Figure 3. Seed distribution of fractions collected under sieve, along its length, at a frequency of 335 min⁻¹

By increasing the blinds opening to $D_j = 11$ mm and keeping the other parameters of the working regime relatively constant, the curve maximum of the seed separation through the holes moved towards the feeding end of the sieve, as shown in Fig. 2c (sample 3). The order of plotting the separation curves maximum was also kept this time: the maximum was at 0.557 m from the sieve front end for the seeds at the bottom and the maximum was about 0.681 m from the sieve end for the seeds at the top, while the distribution curve maximum for seed in the general layer was positioned at 0.583 m from the sieve feeding end.

As the blinds opening increases even more ($D_j = 12.5$ mm) and the ratio pp/s decreases to ~ 0.24 , keeping the supply rate $q = 1.5 \text{ kg}\cdot\text{m}^{-1}\cdot\text{s}^{-1}$, the air velocity $v_a = 8 \text{ m}\cdot\text{s}^{-1}$ and the oscillation frequency $f = 280 \text{ min}^{-1}$, the maximum of the separation curves moved accordingly to the sieve front end (sample 4, Fig. 2d), also keeping the plotting order in the graph (0.513 m the front end for the seed at the base of the layer, 0.538 m for the main seed mass, 0.657 m for the seed at the top).

Analysing the curves of Fig. 2e, recorded for the separated seeds along the sieve (sample 5), it is observed that approximately under the same conditions as the previous sample, but with a higher air velocity at the fan outlet ($v_a = 10 \text{ m}\cdot\text{s}^{-1}$), the maximum of the distribution curves moves back again to the sieve rear end for the seeds from the heap main mass and from the bottom layer, but tends to move forward for the seed at the top layer, which demonstrates that the air has an important role in dispersing the material layer on the sieve (particularly the straw parts), allowing the seed in the upper layers to pass through it more easily and to contact the sieve more quickly (the maximum of the separation curve is at ~ 0.572 m from the sieve front end for the top layer seeds, at 0.512 m for those at the base of the layer and for the ones in the main seed mass, the curve maximum is about 0.543 m from the sieve end).

When the feed rate increases to $2 \text{ kg}\cdot\text{m}^{-1}\cdot\text{s}^{-1}$, while the other parameters remain practically unchanged (Fig. 2f), the maximum of the separation curve moves back to the sieve rear end, keeping the relative order of displacement in graph for the three analysed fractions (0.700 m from the front end of the base seed, 0.713 m for the main mass seed and 0.807 m for the top seeds).

By increasing the oscillation frequency to 335 min^{-1} and keeping the other parameters of the working regime constant (sample 7), the material moves very fast on the sieve surface, its agitation increases and the maximum of the separation curves, for all three fractions, moves to the back end of the sieve. Under these conditions, the seeds in the upper layers do not have the time to pass through the material on the sieve and, as it can be seen from Fig. 3, they will be separated to a maximum percentage closer to the sieve rear end (the separation curve maximum for the top seeds is about 1.032 m from the sieve front end). Even for the seeds situated from the very beginning on the sieve at the base of the heap layer, the separation is uneven, although the maximum of the separation curve is a bit ahead ($\sim 0.881 \text{ m}$ from the sieve front end) compared to the other fractions.

As a general finding of the graph analysis of separation curves of the seeds along the sieve, it can be seen that for seed at the bottom of the layer and those of the general seed mass, the separating curve peaks are spaced closer one on the other, compared to the relative distance between the maximum separation curve for the top seed fraction and the seed mass.

This makes even more important the stratification of the material on the oscillating conveyor and on the sieve, by finding appropriate working regimes leading to a faster displacement of the seeds in the upper layers of the heap mass towards its base and to a better separation of the seeds through the sieve holes, with as little loss as possible.

It can also be said that the stratification process is complex, all the parameters of the working regime being of importance to the process. If a stronger stirring of the material on the screen is desired, for a more pronounced stratification (both by increasing the air velocity and by increasing the oscillation frequency), then it is necessary to have a longer sieve, with a larger opening of the sieve holes.

From the direct observations on the seeds collected in the boxes bellow the sieve, it was found that the percentage of shrivelled seeds (less developed seeds) was higher to the sieve rear end compared to the percentage of seeds found in boxes at the rear end. This proves once again that the influence of airflow is significant on the stratification process, the lighter particles in the upper layers contact harder and later the sieve in order to be separated through the holes.

In order to highlight this phenomenon, in some experimental samples, besides the other analysed parameters, we determined the mass of 1000 seeds from each collecting box.

It was found that at oscillation frequencies of 240 and 280 min^{-1} , at a lower feed rate ($q = 1 \text{ kg} \cdot \text{m}^{-1} \cdot \text{s}^{-1}$), the seeds with higher individual mass separated well before the seeds with lower individual mass which means that the stratification process of the material on the sieve can be made easier, the seeds with higher density reaching faster in contact with the sieve in positions allowing them to pass through the holes. The less developed seeds remaining in the heap top layers separated later through the orifices towards the sieve back end. Under these circumstances, seed losses may be of less importance because they will be mainly composed of shrivelled seed with low nutritional value.

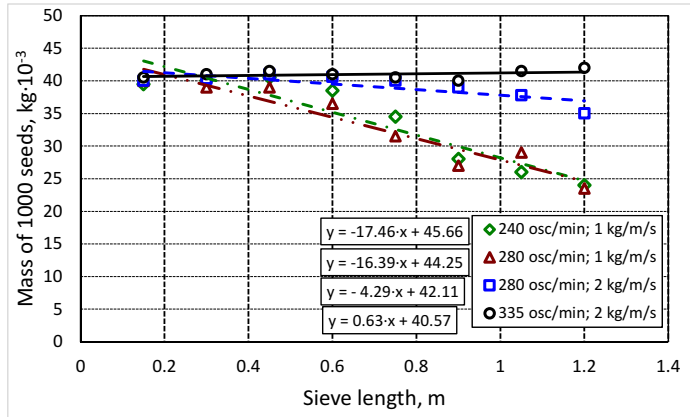


Figure 4. Weight variation of 1000 seeds per site length, depending on the working regime parameters

- o: $f = 240 \text{ min}^{-1}$; $q = 1 \text{ kg}\cdot\text{m}^{-1}\cdot\text{s}^{-1}$; $v_a = 8 \text{ m}\cdot\text{s}^{-1}$; $D_j = 11 \text{ mm}$;
- : $f = 280 \text{ min}^{-1}$; $q = 1 \text{ kg}\cdot\text{m}^{-1}\cdot\text{s}^{-1}$; $v_a = 8 \text{ m}\cdot\text{s}^{-1}$; $D_j = 11 \text{ mm}$;
- ◇: $f = 280 \text{ min}^{-1}$; $q = 2 \text{ kg}\cdot\text{m}^{-1}\cdot\text{s}^{-1}$; $v_a = 10 \text{ m}\cdot\text{s}^{-1}$; $D_j = 11 \text{ mm}$;
- △: $f = 335 \text{ min}^{-1}$; $q = 2 \text{ kg}\cdot\text{m}^{-1}\cdot\text{s}^{-1}$; $v_a = 10 \text{ m}\cdot\text{s}^{-1}$; $D_j = 11 \text{ mm}$.

CONCLUSIONS

From the above, it results that at the same oscillation frequency and at the same sieve loading, the airflow is the factor which can lead to better results with respect to the seeds separation from the heap mass by reducing the inner bonding forces of the material layer and its dispersion, which makes the top layers seeds easier to contact the sieve and to separate more quickly through the holes in the sieve shutters.

Regarding the quantity of seeds that passes beyond the sieve rear end, from the analysis of the data presented in Table 1, it is found that in all the cases studied this is much lower for the seeds at the base of the material layer, in some cases they reach to separate just before the sieve rear, while for seeds above the general material layer losses are higher than the losses of seeds in the general material layer, in most cases with almost 1.5 times over, but decreasing if the airflow rate is $\sim 10 \text{ m}\cdot\text{s}^{-1}$.

REFERENCES

- Böttinger, S. and Fliege, L. (2012). Working performance of cleaning units of combine harvesters on sloped fields. *Landtechnik* 67(1): 34–36.
- Gebrehiwot, M.G., De Baerdemaeker, J., Baelmans, M. (2009). Computational and experimental study of a cross-flow fan for combine cleaning shoes. Conference Land-technik AgEng 2009: innovations to meet future challenges, Hannover, Germany, VDIBERICHT 2060: 387–392.
- Korn, Ch., Hübner, R., Herlitzius, T., Rüdiger, F., Fröhlich, J. (2013). Numerical study of airflow in a combine cleaning shoe, *Landtechnik* 68(2): 83–87.

- Panasiewicz, M., Sobczak, P., Mazur, J., Zawislak, K., Andrejko, D. (2012). The technique and analysis of the process of separation and cleaning grain materials, *Journal of Food Engineering* 109: 603–608.
- Schreiber, M. and Kutzbach, H.D. (2003). Modelling Separation Characteristics in Combine Cleaning Shoes, *Landtechnik* 4: 236 – 237.
- Ueka, Y., Matsui, M., Inoue, E., Mori, K., Okayasu, T., Mitsuoka, M. (2012). Turbulent flow characteristics of the cleaning wind in combine harvester, *Engineering in Agriculture, Environment and Food*, 5(3): 102-106.
- Voicu, Gh., Căsândroiu, T., Toma, M.L. (2006). A multiple logistic regression statistical model to estimate grain loses on sieve cleaning system from combine, *Actual tasks on agricultural engineering* 34: 481-491.
- Voicu, Gh., Casandroi, T., Toma, M.L. (2007). Predictions regarding the influence of the material movement along the sieve on seeds separation in cleaning systems from the cereal combine, *Actual tasks on agricultural engineering* 35: 155-166.
- Voicu, Gh., Căsândroiu, T., Târcolea, C. (2008). Testing stochastic models for simulating the seeds separation process on the sieves of a cleaning system, and a comparison with experimental data, *Agriculturae Conspectus Scientificus (ACS)* 73(2): 95-101.
- Wang, Y.S., Chung, D.S., Spillman, C.K, Eckhoff, S.R., Rhee, C., Converse, H.H., (1994), Evaluation of Laboratory Grain Cleaning and Separating Equipment, Part I, *American Society of Agricultural Engineers, Transactions of the ASAE*, 37(2), 507-513.
- Zaika, P.M. (1975). Parametri granicinâh rejimov vibroseparații zernovâh smesei, *Mehanizacija i elektrifikacija sel'skogo hozjajstva* 8: 10-12.
- Zhao, Z., Li, Y., Chen, J., Xu, J. (2011). Grain separation loss monitoring system in combine harvester, *Computers and Electronics in Agriculture* 76: 183–188.



INFLUENCE OF THE OSCILLATION FREQUENCY ON THE SEPARATION PROCESS AT THE CONICAL SIEVES

Dorel STOICA^{1*}, Iulian-Claudiu DUȚU², Gheorghe VOICU²,
Mihaela-Florentina DUȚU²

¹ Mechanics Department, University Politehnica of Bucharest, no.313 Splaiul Independenței,
060042, Bucharest, Romania

² Biotechnical Systems Department, University Politehnica of Bucharest, no.313 Splaiul
Independenței, 060042, Bucharest, Romania

*E-mail of corresponding author: dorel.stoica@upb.ro

SUMMARY

This study presents the results of experimental researches on the working process and his efficiency for a sieve with external conical surface with alternative periodic motion. The sieve is suspended at the top and bottom with three elastic threads (of silk), with thread diameter $\phi 1.5$ mm and is provided with circular apertures of $\phi 4.2$ mm. Vibratory motion was obtained with an eccentric mechanism, placed horizontally and acting on tangential direction to the sieve at adjustable distance. The sieve was used for sorting of canola seeds having sizes between $\phi 1.25$ mm and $\phi 2,5$ mm, in percent of 95%.

Keywords: conical sieve, oscillation frequency, separation

INTRODUCTION

Based on the data in the table and the determinations performed, were plotted the distribution curves of material on conical sieve generatrix (according to the number of seeds collected under the sieve and beyond the edge thereof).

In order for a granular mixture can be sifted and sorted into fractions using sieves is required to exist a state of sifting of the material, so that is a relative movement between the particles and the separation surface. In another order of ideas for the particles may be sieved, two conditions must be met: first, the particles must reach on the aperture, which is achieved by the relative movement of these on the separation surface and, second, particles have sufficient time to be involved in passing through apertures (Casandriou and Voicu, 1992; Tarcolea et al., 2008).

A mixture of seeds (grains, technical plants, oilseeds, etc.), after being cleansed of impurities, is required to be sorted by size, because each fraction should be directed on a particular technological processing route or may be given a different destination (the more developed seeds can be used as seeding material, seeds with a lower degree of development can be routed for industrial processing, poorly developed seeds are used for animal feed or disposed of as waste, etc).

Before the processing of seeds and the use of it, either in milling industry, either as seeding material, they go through a complex process of cleaning and conditioning to ensure that all foreign bodies are removed from their mass (Casandroiou and Voicu, 1992).

Sorting of seeds by the particle size is carried out, generally, into separation blocks with oscillating movement. Sifting and sorting on sieve requires relative movement of the material particles on the separation surface, which is performed either by a corresponding inclination of the sieves, either by the oscillation movement of the sieve blocks (Casandroiou et al., 2008). Separation surfaces may have different shapes (plane, conical, cylindrical, parabolic), and oscillatory movement is obtained using mechanisms of different construction, either crank drive (with eccentric), or with the aid of unbalanced rotating masses, or with other mechanisms that ensure the required oscillating movement. Also, separation surfaces can be realized in the form of metal or textile braids or in the form of perforated sheets with apertures, ordinarily, elongated or circular.

Experimental research on the process of separation and sorting on sieve with oscillatory motion have been made by numerous researchers worldwide. Thus, separation process of material on sieve is influenced by the amplitude and frequency of oscillation, which provide the relative movement of material on separation surfaces. Other parameters that influence the separation are: sieve slope, angles of internal and external friction of the material, sieve apertures, average particle size (Harrison and Blecha, 1983; Letosnev, 1963; Voicu et al., 2003). Clogging of sieve apertures depends on the particle size, phenomenon investigated by R. Feller (1977). Mechanical classification of seeds with sieves is not a complete classification, each time in a fraction being found 10-20% from particles of fraction that should have separate (Elfverson and Regner, 2000).

In our paper, are presented the results of experimental research on a sieve with perforated sheet with a external conical separation surface, with angle of inclination of 8°, provided with circular apertures with a diameter of ϕ 4.2 mm, used to study the separation and sorting of the canola seeds, the sieve may be used to separate impurities from the seeds mass.

MATERIALS AND METHODS

Conical sieve is suspended with elastic threads of silk with a diameter ϕ 1.5 mm, and actuating in oscillating movement (circular alternative) was made from an electric motor through a worm adjustment and an oscillating slide. Actuation was done at a distance d (adjustable) from sieve center (in the rest position), being rigidly connected by the edge of sieve, radially, and a link arm 2 (Fig. 1).

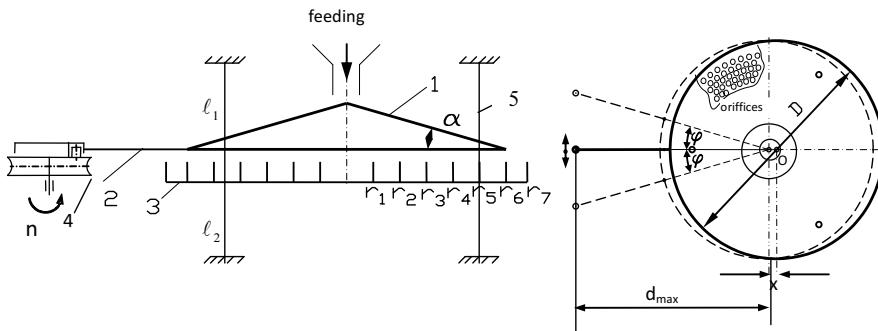


Figure 1. Scheme of conical sieve used in experiments

(1. sieve with circular apertures; 2. actuating arm; 3. material collecting box; 4. actuating mechanism with whorm wheel and oscillating slide, 5. elastic cables)

These has been linked to the lever of the oscillating slide through a coupler with helical spring in order to reduce the oscillation of sieve on radial direction of the lever 2, at the ends of the stroke of slide and. Thus, the amplitude of oscillation could be adjusted, in four steps, by changing the distance d , to obtain sieve amplitude oscillation of 3.58, 3.74, 3.91 and 4.10 mm. Also, sieve oscillation frequency could be adjusted with actuating mechanism, being used three frequencies of oscillation: 250, 520 and 790 min^{-1} (Table 1).

Diameter of conical sieve, at the bottom thereof, is of 430 mm, and the density of circular aperture on the separation surface is 2.25 aperture/ cm^2 . Length of suspension wire is $l_1 = 240$ mm, and $l_2 = 180$ mm. A detailed description of the construction of the conical sieve is shown in the papers by Stoica (2011), Stoica et al. (2011) and Stoica et al. (2013).

For experiments were used canola seeds (harvested in the south of Romania) after a storage period of about six months. The material sample mass was always the same 0.5 kg seeds.

Canola seeds humidity was about 7.65-8.05 %, determined using a thermobalance Partner MAC 110, at a drying temperature of 105oC.

Seeds had sizes between $\text{Ø}1.25\text{-}2.5$ mm, (in a proportion of more than 95%) determination which has been performed using a sieve shaker for granulometric analysis VAPO model, with sieve aperture 125 μm , and 250 μm .

Were carried out determinations at three oscillation frequency, four sieve oscillation amplitudes and three different feed rates, obtained by the position above or below of outflow opening of feed funnel, (fig. 1). The three feed rates used were: 0.020, 0.033 and 0.042 kg s^{-1} canola seeds. The outflow opening of the feeding funnel has a diameter of 25 mm.

Collecting of canola seeds under sieve was performed in a box with concentric circular compartments, having diameters: 80, 140, 200, 260, 320, 410 and 460 mm. Notification of beginning and end of material feeding was made visual, starting and stopping each time a stopwatch with digital display.

It was followed, in the main, distribution of canola seeds collected under the sieve, and loss of seeds that has passed the edge of the sieve. To estimate the coefficient of sorting seeds were performed experimental determinations by sorting on fractions of the material collected in each of the boxes under the sieve to identify the fraction with the highest percentage in the

box (sorting was done on four size classes: 1- 1.25 mm; 1.25- 1.6 mm; 1.6 – 2 mm; 2 – 2.5 mm) (Stoica et al., 2012; Stoica and Rusanescu, 2013a; Stoica and Rusanescu, 2013b).

RESULTS AND DISCUSSION

Some of the results obtained in experiments (only for $A = 3.91$ mm – which is the most determinant oscillation amplitudes, feeding rate $Q=0.033$ $kg\ s^{-1}$ and those three oscillation frequency) are presented in Table 1.

With values from Table 1 were drawn the distribution curves of seeds separated on sieve generatrix for the three values of oscillation frequency.

Estimation of the influence of oscillation frequency on the sorting process of seeds on sieve was performed by regression analysis of the experimental data (in %) with Gaussian distribution function (Stoica et al., 2011), for which have been determined the correlation coefficient χ^2 and R^2 values:

$$p_x(\%) = y_0 + P \cdot \exp\left(-\frac{(x-x_c)^2}{2w^2}\right); y_0 = 0,$$

where: $p_x(\%)$ represents the weight percentage of separated material over a range (radius) of sieve length; P , x_c and w – experimental coefficients.

In relation (1), „ P ” represents the maximum percentage of material collected in the boxes under the sieve, „ x_c ” radius of the sieve base corresponding to the maximum percentage of separated seeds (or average values determined), and „ w ” is compared to the maximum position (Anghelina et al., 2014; Rusanescu et al., 2013). These coefficients depend on the working regime parameters and are presented in Table 2.

Charts of the regression function, for the 4 size class of the seeds and the three oscillation frequencies are shown in Fig. 2.

Table 1. The amounts of separated seeds on the sieve radius base for $A=3.91$ mm, $Q=0.033$ $kg\ s^{-1}$ at three different oscillation frequencies

Nr.	The range of sieve on sample which is collected x. (m)		0	0.04	0.07	0.10	0.13	0.16	0.205	Over sieve
1	$F_1=250\ min^{-1}$	G	0	127	138	107	56	53	19	0
		%	0	25.4	27.6	21.4	11.2	10.6	3.8	0
2	$F_2=520\ min^{-1}$	G	0	136	162	91	57	25	13	16
		%	0	27.2	32.4	18.2	11.4	5	2.6	3.2
3	$F_3=790\ min^{-1}$	G	0	151	181	102	49	16	1	0
		%	0	30.2	36.2	20.4	9.8	3.2	0.2	0

From the analysis of graphs it is found approximately the same allure of distribution curves for each of the four size classes with that proper to general mixture of seeds. Parameter values x_c shows that at higher oscillation frequency separation is more quickly, while at oscillation frequency $F_1=250\ min^{-1}$ (small frequency) all four fractions is separated away from the center of sieve.

Table 2. Regression coefficients, respectively of correlation, obtained from regression analysis

Nr. sample	Size classes	Gaussian function	Equation coefficients			Corelation	
			P	x_c	w	χ^2	R ²
1	F ₁ = 250 min ⁻¹	All seed	2.726	0.078	0.089	29.238	0.844
2		Seeds with d > 2 mm	0.482	0.082	0.092	0.769	0.855
3		Seeds d=1.6 – 2 mm	1.970	0.078	0.085	16.133	0.848
4		Seeds d= 1.25 – 1.6 mm	0.152	0.084	0.106	0.093	0.775
5		Seeds d < 1.25	322.920	0.105	2.083	0.032	0.853
6	F ₂ = 520 min ⁻¹	All seed	2.853	0.067	0.064	19.849	0.943
7		Seeds with d > 2 mm	0.433	0.062	0.065	1.336	0.844
8		Seeds d=1.6 – 2 mm	2.088	0.068	0.061	8.942	0.957
9		Seeds d= 1.25 – 1.6 mm	0.146	0.065	0.071	0.090	0.889
10		Seeds d < 1.25	0.143	0.073	0.094	0.087	0.819
11	F ₃ = 790 min ⁻¹	All seed	2.695	0.065	0.058	17.236	0.952
12		Seeds with d > 2 mm	0.418	0.058	0.056	0.986	0.900
13		Seeds d=1.6 – 2 mm	1.970	0.066	0.057	8.512	0.958
14		Seeds d= 1.25 – 1.6 mm	0.139	0.060	0.061	0.077	0.916
15		Seeds d < 1.25	0.106	0.0540	0.050	0.067	0.900

Still, for a better sorting by size would require a lower frequency as shown in the charts presented, at which the maximum position of the distribution curve increases with decreasing of seeds sizes (Fig. 2; Fig. 3).

In Fig. 3 are graphically represented variations of peak positions of the separations curves for each size class at those three oscillation frequency of sieve.

It is found that for lower oscillation frequencies, seeds of small size classes are separated before the larger size classes of seeds.

At lower oscillation frequency (790 min⁻¹) separation of seeds becomes random possible due to entry into resonance of sieve and of elastic system for clamping of actuating mechanism lever.

For size class 2.2 – 2.5 mm seeds are separated closer to the feeding point of sieve as the oscillation frequency is smaller. This it is found otherwise for all size classes with a more pronounced character for the first two size classes (1 – 1.25 mm; 1.25 – 1.6 mm) (Table 2).

If at oscillation frequency of 250 min⁻¹ seeds from the third size class separates closer to the vertical axis of the sieve compared to other size classes at the other two oscillation frequency (520, 790 min⁻¹) separation of seeds begin to depart from the vertical axis of oscillation (Table 1).

Therefore we can say that for seeds with sizes under 1.5 mm separation is made closer to the axis of rotation for used sieve and that the size of sieve aperture can properly calibrate the seeds mixture for all oscillation frequency analyzed.

If it is desired an appropriate calibration for larger classes is necessary either increasing of aperture diameter, either use of sieves with apertures of stepwise increasing, either reduce of oscillation frequency.

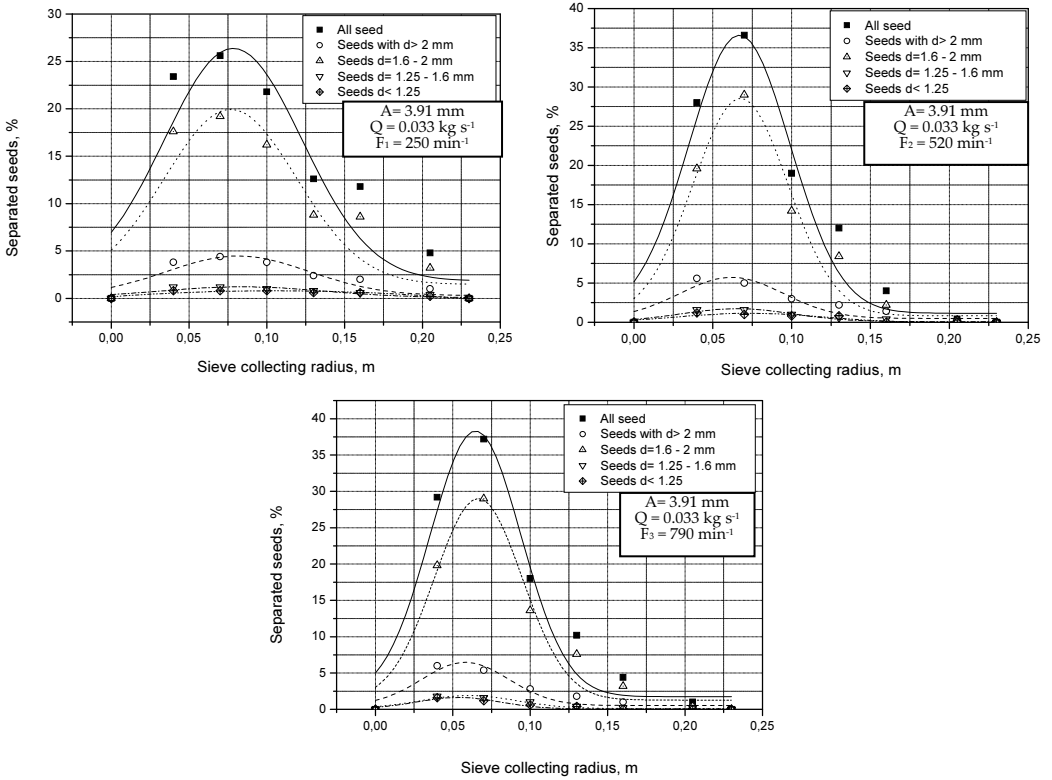


Figure 2. The regression curves of experimental data with normal distribution function, (Stoica et al., 2013)

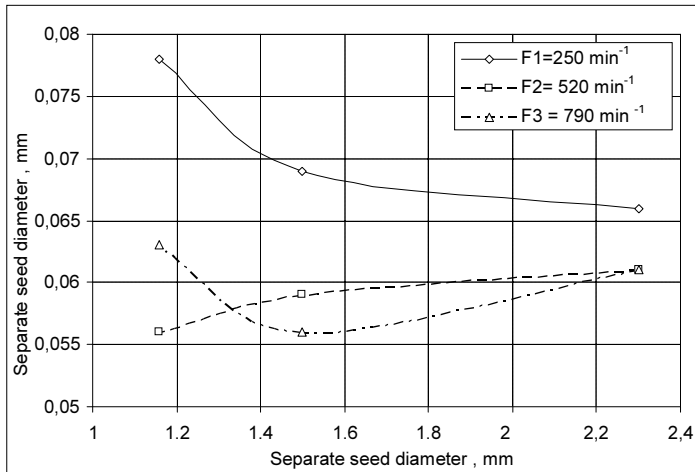


Figure 3. Variations in peak positions of separation curves for each size class at those three oscillation frequency

It should also be said that the inclination angle has a great influence on the movement of seeds, them rolling on the inclined surface of the sieve as the angle is greater. Perhaps if the angle of sieve with the horizontal would be smaller, the sorting degree of seeds would improve.

CONCLUSIONS

Conical sieve with oscillatory movement around the axis of the cone can be used successfully at separation of impurities from the mixture of cereals crops, technical of legumes, if the separation surface is appropriately selected.

Regarding the use of conical sieves for sorting by size, researches from this paper were not very conclusive, but if working regime parameters (amplitude, frequency and feeding rate) are chosen properly can be obtained good results.

It is necessary so, further research for lower oscillation frequencies and lower inclination angles of sieve in the case of sorting canola seeds on experimented sieve with apertures and also seeds of other crops.

At none of feeding rate and amplitude of oscillations, for the three oscillation frequencies used in experiments, was not found a good sorting on fractions of seeds with different sizes. Although the maximum of the separation curve is modified less for the fractions mentioned, in each compartment of the collecting box were found each time seeds of other fractions. It follows that, in the actual form of conical sieve (with apertures of the same dimensions on the entire surface), its use as equipment for sorting on fractions of different sizes is not effective. Is, so, necessary to perform apertures of different sizes on the cone generatrix, from larger to smaller size, from top to bottom.

REFERENCES

- Anghelina, Fl.V., Popescu, I.N., Bratu. V., Anghelina. C., Rusănescu, C.O. (2014). Physical-mathematical model of Lorentz factor for the integrated intensity of single crystal diffraction; Computational materials science; ISSN: 0927-0256; Volume 94: pp 234-239.
- Cășândroiu, T., Voicu Gh., Maican E. (2008). A Mathematical model for the seed loses prediction on the cleaning system sieves of the harvesting combines, Modelling and optimization in the machines building field MOCM – 14, vol.2, Romanian Technical Sciences Academy, University of Bacău.
- Cășândroiu, T., Voicu Gh. (1992). Curba de separare a materialului pe lungimea sitei superioare la sistemul de curățire al combinelor de cereale, București.
- Elfverson, C., Regnér, S. (2000). Comparative precision of grain sieving and pneumatic classification on a single kernel level, Applied Engineering in Agriculture, VOL. 16(5): 537-541.
- Feller, R. (1977). Clogging rate of screens as affected by particle size, Transactions of the ASAE: pp. 758-761;
- Harrison, H. P., Blecha, A. (1983). Screen oscillation and aperture size – Sliding only, Transactions of the ASAE: pp. 343-348.
- Letoșnev, N.M. (1963). Mașini agricole (traducere din lb. rusă). Editura Tehnică, București.
- Rusănescu, C.O., Rusănescu, M.T., Iordănescu, Fl., Anghelina, V. (2013). Mathematical relationships between alloying elements and technological deformability indexes, Journal of optoelectronics and advanced materials, Vol. 15, No. 7-8: pp. 718-723.
- Stoica, D. (2011). Contribuții la studiul fenomenelor vibratorii privind utilajele din domeniul prelucrării produselor agricole, teză de doctorat, Bucuresti.

- Stoica, D., Voicu, Gh., Ungureanu, N., Voicu, P., Carp-Ciocardia, C.D. (2011). Influence of oscillations amplitude of sieve on the screening process for a conical sieve with oscillatory circular motion, *Journal of Engineering studies and research*, Bacău: pp 83-89.
- Stoica, D., Voicu, Gh., Rusănescu, C.O. (2012). Influence of vibration amplitude oscillations on the conical sieve suspended, *Bulletin of University of Agricultural Sciences and Veterinary Medicine Cluj-Napoca. Agriculture*, volum 69, no 1.
- Stoica, D., Stanciu, G., April - June (2013). Influence the degree of sorting the separation process a conical sieve: *Digest Journal of Nanomaterials and Biostructures*, ISSN 1842 - 3582, Vol. 8, No. 2: pp. 513 – 518.
- Stoica, D. and Rusănescu C.O. (2013a). Research on the Influence of Vibration Frequency on A Conical Sieve Suspended – *Metalurgia International*, vol.XVIII, nr.3, ISSN 1582 – 2214, pp 84-86.
- Stoica D. and Rusănescu C.O., (2013b). Research on Variation of Displacements, Velocities and Accelerations at a Site Selector Blocks (Fanner) Grain - *Magazine of Hydraulics, Pneumatics, Tribology, Ecology, Sensorics, Mechatronics, "HIDRAULICA"* ISSN 1453 – 7303: pp 38-42.
- Târcolea, C., Căsandroi, T., Voicu, G., (2008). Stochastic models for simulating seed separation process on sieves, *Proceedings of the 36th International Symposium "Actual tasks on agricultural engineering"*, Opatija, Croatia: pp.293-306.
- Voicu, Gh., Căsandroi, T., Țuțuianu, G.D. (2003). Aspects regarding the powering by vibration generators with rotation masses of the classifying plane sieves blocks, *Modelling and optimization în the machines building field MOCM-9*, vol.1, Technical Sciences Academy of Romania: pp.111-116.



DESIGN AND CONSTRUCTION OF A FERTILIZER SPREADER FOR GLASS HOUSES AND GREENHOUSES

Ioan ȚENU*, Oana-Raluca COORDUNEANU, Petru CÂRLESCU, Radu ROȘCA

University of Agricultural Sciences and Veterinary Medicine "Ion Ionescu de la Brad"
Aleea Mihail Sadoveanu nr. 3, Iași, 700490, România

*E-mail of corresponding author: itenu@uaiasi.ro

SUMMARY

The continuous increase of the demand for vegetables has imposed the modernization and improvement of the agricultural machineries, both for field crops and for the crops grown in protected spaces as glass houses and greenhouses. Fertilization with solid chemical fertilizers is an important part of the growing technology; the fertilizer spreaders must achieve distribution uniformity higher than 90%. Plants grown in protected spaces need higher amounts of mineral substances and, as a result, supplementary fertilizations are needed.

The limited space available in glass houses and greenhouses does not allow the use of the universal fertilizer spreaders, imposing the design and construction of a specialized equipment, which should be mounted on two or four wheels tractors used for the mechanization of this type of crops. As a result of this requirement a specialized solid fertilizers spreader was designed and built within the agricultural machinery department of the University of Agricultural Sciences and Veterinary Medicine "Ion Ionescu de la Brad" from Iași.

The equipment has three operating sections and performs gravitational or centrifugal spreading of the fertilizers, on each row. The experimental tests, conducted in order to evaluate the distribution uniformity, proved that the spreader is achieving the necessary agro technical requirements and quality indices.

An innovative image analysis technique was used in order to evaluate the granules size distribution in the spread material. The statistical analysis confirmed the validity of this technique.

Keywords: fertilization, protected spaces, fertilizer spreader.

INTRODUCTION

The fertilization of agricultural crops is an important phase of the growing technology, being accounted with an influence of 60-70% over the production rate, while the impact of other agrotechnical factors is accounted to 30-40% (Gelings and Permenter, 2004; Stewart and Bandel, 2002).

For solid fertilizers the particle distribution over the surface unit has a tremendous importance, in order to insure equal conditions for plant development, without losses of fertilizers into the environment (Dilz and Van Brakel, 1985; Van Meirvenne and colab., 1990; Miller et al., 2009), leading to an increased consumption of fertilizers and to the reduction of crop quality and economical efficiency (Richards and Hobson, 2013).

The distribution of fertilizers in protected spaces has some specific characteristics and demands, due to the intensive characters of this type of technology; in the same time the requirements of the vegetable crops must be harmonized with the properties of the soil inside glass houses or greenhouses. An increase with 20-30% of fertilizer consumption is expected for the crops grown in protected spaces in comparison to field crops.

The general purpose fertilizer spreaders cannot be used in protected spaces; as a result, a dedicated equipment must be designed and built, considering some specific requirements: short duration of the operation, uniform spreading of the fertilizers, precise fertilizer metering, according to the requirements for the respective crop (Olieslagers et al., 1996; Suditu, 2003). Vegetable crops, in general, need larger quantities of fertilizers and water because of the larger volume of the root system; all these requirements should be accounted for when growing vegetables in protected spaces, thus avoiding any unnecessary losses (Indrea et al., 2003; Ciofu et al., 2004; Popescu, 2008).

The paper addresses two issues:

- the design, construction and testing of a specialized solid fertilizers spreader for use inside greenhouses and glass houses,
- the assessment of an innovative image analysis technique in order to evaluate the granules size distribution in the spread material.

MATERIAL AND METHOD

The research was performed within the Agricultural machinery department of the University of Agricultural Sciences and Veterinary Medicine "Ion Ionescu de la Brad" from Iași.

The equipment (fig. 1) is composed of a frame (2), running on two wheels (5), coupled with a two wheels tractor by the means of a traction bar. Three working units (4) are placed on the frame; the fertilizer is distributed by the means of the distribution devices (7 and 8). Transmission mechanisms are used in order to rotate the fertilizer metering devices (9) and the centrifugal disk (3). The equipment has an overall width of 110 cm, allowing its use inside protected spaces; the width of the spreading strip is 4-5 m.

The working units are composed of a pyramid-shaped hopper which has a folding lid at the upper part. The metering unit and stirrer are placed at the bottom end of the hopper. The metering unit is equipped with a rotating disc with holes; its motion is provided by the right side driving wheel, using the spur gear transmission (9) and the roller chain transmission (4 and 10, fig. 2). Different transmission ratios may be achieved by using different chain wheels (0.6; 0.48; 0.4). Figure 2 presents the transmission schematics.

A finger type stirrer is placed at the lower part of the hopper; it prevents the formation of vaults inside the fertilizer charge and provides a continuous flow of fertilizer towards the metering unit. The rotational motion of the stirrer is provided by the same transmission used by the metering unit.

Fertilizer spreading over the soil surface is achieved using either a gravitational device (fig. 1b) or a centrifugal one (fig. 1c).

The gravitational device is a plate with vanes (7), that ensure the uniform distribution of the fertilizer fed by the three working unit.

The centrifugal device consists of a flat rotating disc with four straight vanes, placed under the central working unit; the rotation of the disc is provided by the tractor P.T.O. via a cardan shaft and a bevel gear (3).

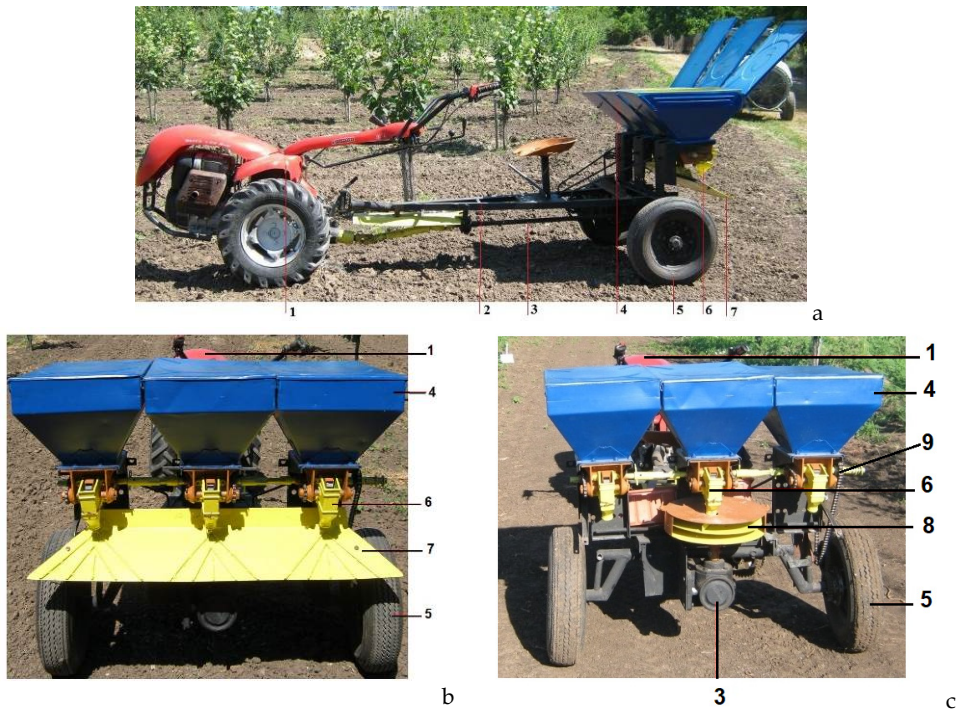
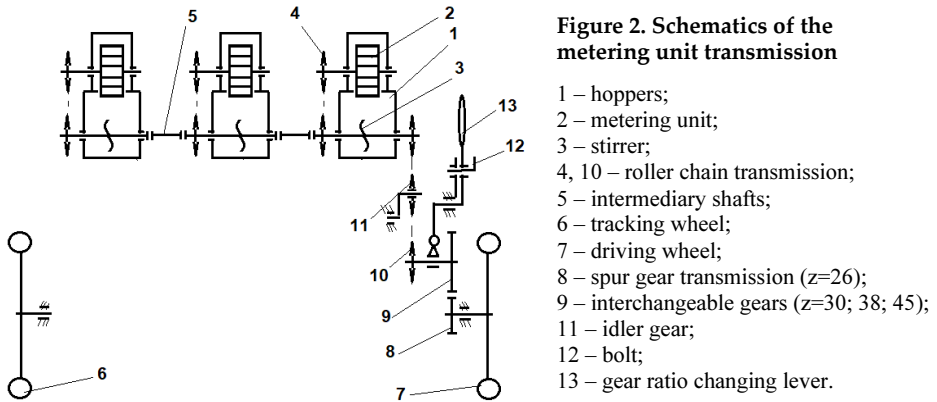


Figure 1. View of the fertilizer spreading equipment

a – general view; b – view of the gravitational spreading device; c – view of the centrifugal spreading device; 1 – two wheels tractor; 2 – frame; 3 – centrifugal disc transmission; 4 – working units; 5 – driving wheel; 6 – metering unit; 7 – spreading plate; 8 – centrifugal disc.



A two wheels tractor, type VALPADANA Blitz 120 Rev, was used during the experimental tests; the fertilizer was ammonium nitrate with 33.5% nitrogen (white granules).

The experimental tests were performed in field conditions, in a plum tree plantation, three years old, using the above mentioned spreading devices (gravitational type and centrifugal type).

The terrain was previously tilled using a rotary cultivator; soil leveling and re-compaction were then performed using a grooved roller and a plain roller (fig. 3).



Figure 3. Test field preparation
a, b – preliminary soil tillage; c – administration of fertilizers.

For the *gravitational distribution* of the fertilizer the tests were performed using the three available transmission ratios: $i_1 = 0.6$; $i_2 = 0.48$; $i_3 = 0.4$. A strip of land with a length of 103 m and a width of 3 m was covered in each test. The measurements were performed 3 m after the start line, in order to avoid the errors introduced during the transition period.

The actual test length of 100 m was divided into five areas of 20 m each in order to obtain five repetitions for each test.

A 30cm/30cm square frame was used in order to evaluate the size distribution of the fertilizer granules (fig. 4). The square frame was randomly placed on each strip (in five different locations) and was photographed in order to evaluate the number and diameter of the granules inside the delimited perimeter. As a result, 25 positions of the square frame were obtained for each test (five individual positions for each of the five repetitions).

Different forward speeds were recorded during the tests ($6.2 \text{ km}\cdot\text{h}^{-1}$, $6 \text{ km}\cdot\text{h}^{-1}$ and $6.6 \text{ km}\cdot\text{h}^{-1}$), resulting in an average speed of $6.27\pm 0.176 \text{ km}\cdot\text{h}^{-1}$.



Figure 4.
Square frame (30cm/30cm)

For the *centrifugal distribution* method a strip of land with a length of 30 m and a width of 3 m was covered in each test; as in the previous series of tests, the length was divided into three areas with a length of 10 m each, resulting in three repetitions. The rotational speed of the centrifugal disk was $n_1= 800 \text{ rev/min}$, $n_2 = 1000 \text{ rev/min}$ and $n_3 = 1250 \text{ rev/min}$, respectively; the forward speed was $v_1= 1.2 \text{ km}\cdot\text{h}^{-1}$, $v_2= 2.26 \text{ km}\cdot\text{h}^{-1}$ and $v_3= 5.08 \text{ km}\cdot\text{h}^{-1}$, respectively.

In order to evaluate the density of the fertilizer granules 10 samples of 4 g each were randomly selected. Each sample was photographed with a CANON A 490 camera. The images were analyzed using the image J software (fig. 5) and the granules were classified in five dimensional classes: 0 – 1.5 mm; 1.5 – 2 mm; 2 – 2.5 mm; 2.5 – 3 mm; 3 – 5 mm. The number of granules in each dimensional class was then counted and the percentage for each class was calculated; fig. 6 displays the average results for the 10 samples considered.

The volume of the granules was calculated for each dimensional class based on the granules diameter, assuming that their shape is spherical. The overall volume of fertilizer resulted by multiplying the volume of each granule with the number of granules in the respective class. The density was obtained as the ratio between the mass (4 g) and the overall volume.

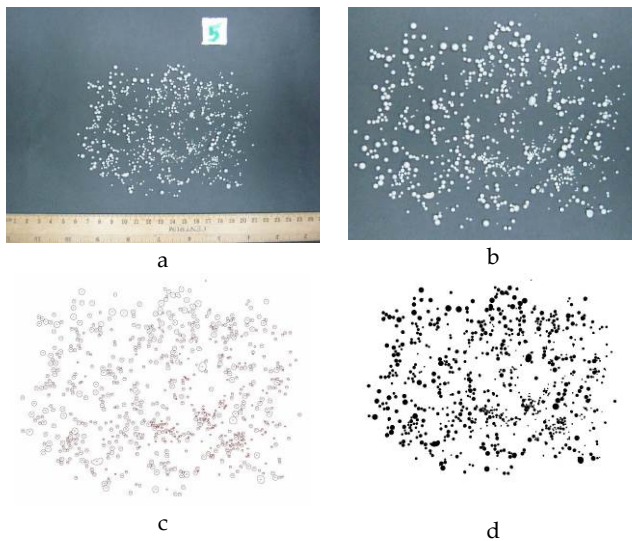


Figure 5. Image analysis using Image J
a – initial photograph;
b – detail of the initial photograph;
c, d – Image J analysis.

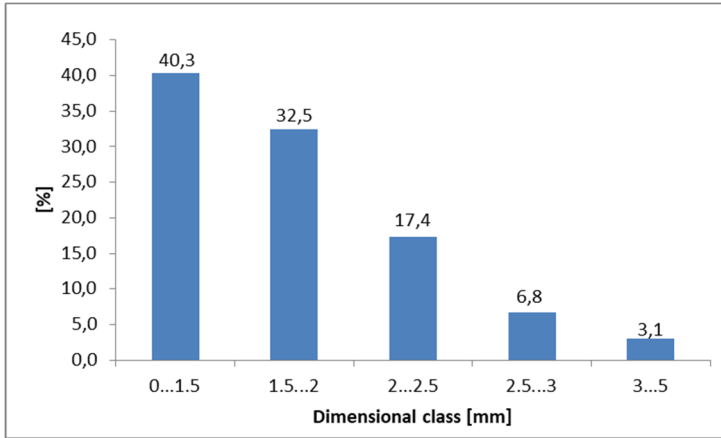


Figure 6. Dimensional classes of the granulated fertilizer

The same image processing procedure based on the Image J software was applied in order to establish the granule diameter distribution during the field tests.

In order to validate the proposed image processing technique the significance of the differences was analyzed; it was assumed that the particle size distribution should not be affected by the characteristics of the operating regime – transmission ratio, forward speed of the equipment or rotational speed of the disk.

The analysis was performed using the standard error of the difference between means and the t_{exp} parameter for the experimental data:

$$S_d = \sqrt{\frac{s_1^2 + s_2^2}{n}}, \quad t_{exp} = \frac{|\bar{X}_1 - \bar{X}_2|}{S_d}$$

where s_1 and s_2 are the standard errors for each group and \bar{X}_1 , \bar{X}_2 are the mean values for each group. The difference between the groups is considered not significant if $t_{exp} < t_{0,05}$; the $t_{0,05}$ values were calculated using the Excel TINV function, for the respective degree of freedom.

The analysis was performed for the 0-1.5 mm dimensional class, by comparing the percentage distributions for the following cases:

- a) for the gravitational distribution method: different transmission ratios, considering the individual values;
- b) for the centrifugal distribution method:
 - same rotational speed (800, 1000 and 1250 rev min⁻¹, respectively) and different forward speeds;
 - same forward speed (1.2, 2.26 and 5.08 km·h⁻¹, respectively) and different rotational speeds.

The analysis of significance was performed for a p value of 0.05; a p value higher than 0.05 meant that there was no significant difference between the variants, leading to the conclusion that the image analysis method provided trustworthy results.

The fertilizer rates were calculated using the granules average density and the overall volume, obtained on the basis of image analysis.

RESULTS AND DISCUSSION

Gravitational distribution

Fig. 7 summarizes the results regarding the dimensional distribution of the granules, for the three transmission ratios taken into account. The chart shows that the majority of the distributed granules had a diameter lower than 1.5 mm (62.6-77.0%); the granules with diameters comprised between 1.5 and 2 mm represented 15.7-22.4%. The best results were obtained for the transmission ratio $i_2 = 0.48$, with 77% of the granules in the 0-1.5 mm and the lowest percentages of granules with diameters higher than 1.5 mm.

The results referring to the significance of differences are presented in table 1. The results clearly show that there were no significant differences between the data groups, which meant that image analysis provided the same distribution of the granules size although the amounts of fertilizer that were distributed were different (table 2).

Table 2 presents the results concerning the fertilizer rate (mass per unit surface). As expected, the fertilizer rate has increased with the increase of the transmission ratio due to increase of the rotational speed of the metering devices.

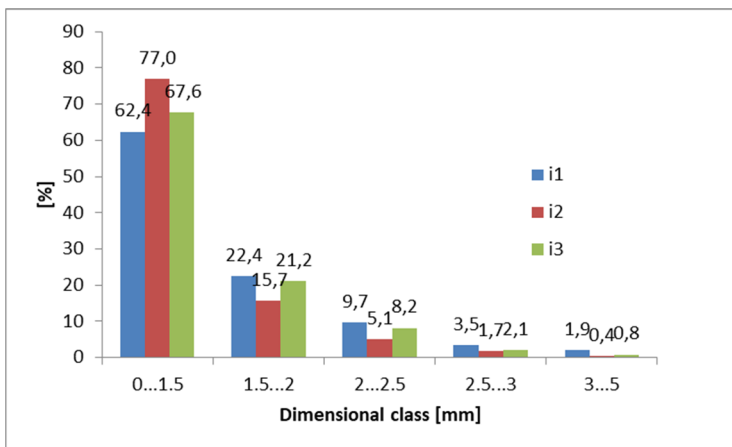


Figure 7. Granules size distribution for the gravitational method (mean values)

Table 1. Significance of the differences

Data groups	t_{exp}	$t_{0.05}$
i_1 & i_2	0,551	2,447
i_2 & i_3	1,212	

Table 2. Fertilizer rates for the gravitational method

Transmission ratios	Fertilizer rate (kg ha ⁻¹)
$i_1 = 0.60$	136.92
$i_2 = 0.48$	124.18
$i_3 = 0.40$	106.86

Centrifugal distribution

Figures 8, 9 and 10 summarize the experimental results for the three traveling speeds of the equipment and the three rotational speeds of the disk.

For the traveling speed $v_1 = 1.2 \text{ km}\cdot\text{h}^{-1}$ the percentage of granules in the 0-1.5 mm class decreased for the rotational speed of $1000 \text{ rev min}^{-1}$, while for 800 and $1250 \text{ rev min}^{-1}$ the results were not significantly different (approx. 82% of the spread granules had a diameter smaller than 1.5 mm).

For a traveling speed of $2.26 \text{ km}\cdot\text{h}^{-1}$ (v_2) the best results were obtained for 800 rev min^{-1} and $1000 \text{ rev min}^{-1}$ (approx. 80% of the spread granules had a diameter smaller than 1.5 mm); at $1250 \text{ rev min}^{-1}$ the percentage of granules with diameters lower than 1.5 mm decreased to 71.4%.

Overall, the best results were recorded for the forward speed of $5.08 \text{ km}\cdot\text{h}^{-1}$ (v_3) and a rotational speed of the distribution disk of 1250 rev/min (84.2 % of the spread granules had a diameter smaller than 1.5 mm).

The results referring to the significance of differences are presented in table 3. The data shows that, despite the different operating conditions, the use of imagine analysis method produced the same results regarding the size distribution of the fertilizer granules.

Table 3. Significance of the differences

Data groups	t_{exp}	$t_{0.05}$
v_1 & v_2	0.779	2.776
v_2 & v_3	0.531	
n_1 & n_2	0.951	
n_2 & n_3	0.328	

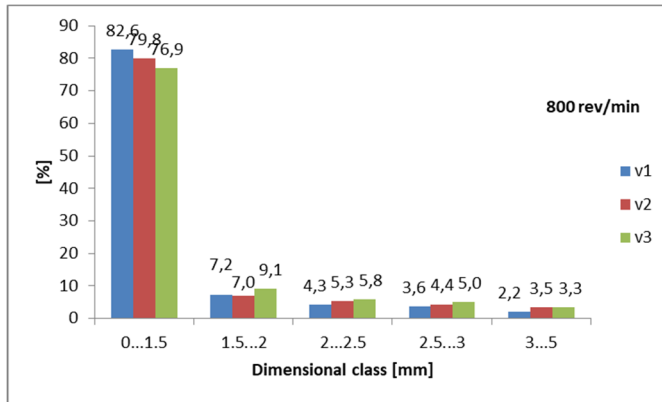


Figure 8. Granules size distribution for the centrifugal method ($n_1 = 800 \text{ rev min}^{-1}$)

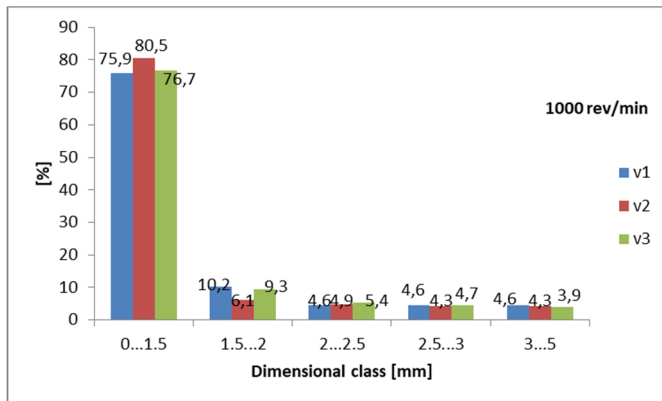


Figure 9. Granules size distribution for the centrifugal method ($n_2 = 1000 \text{ rev min}^{-1}$)

Table 4 presents the results concerning the fertilizer rate (mass per unit surface) for the centrifugal method. The fertilizer rate decreased when the forward speed was increased (because the same amount of fertilizer was distributed over a larger surface) and increased when the rotational speed of the distribution disk was increased.

For both the gravitational and centrifugal distribution methods the traveling speed affected the particle size distribution: for the gravitational distribution method, the traveling speed modifies the peripheral speed of the metering devices and thus the initial downwards speed of the particles, while for the centrifugal distribution method the overall speed of the particle results from the composition of the particle speed when leaving the distribution disk with the forward travelling speed of the equipment.

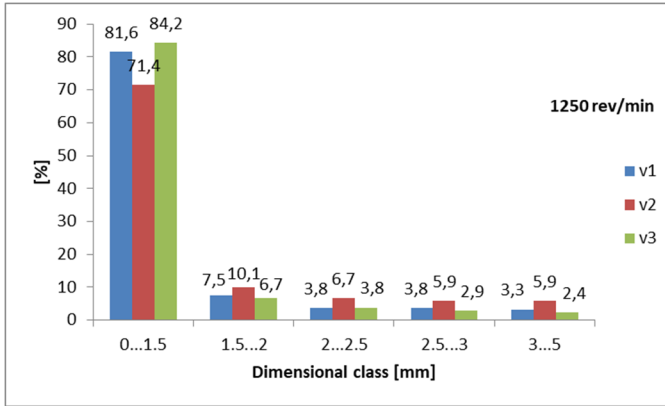


Figure 10. Granules size distribution for the centrifugal method (n₃ = 1250 rev min⁻¹)

Table 4. Fertilizer rates for the centrifugal method

Rotational speed [rev min ⁻¹]	Forward speed [km·h ⁻¹]	Fertilizer rate [kg ha ⁻¹]
n ₁ = 800	V ₁ = 1.2	40.55
	V ₂ = 2.26	33.33
	V ₃ = 5.08	22.55
n ₂ = 1000	V ₁ = 1.2	42.11
	V ₂ = 2.26	36.22
	V ₃ = 5.08	27.33
n ₃ = 1250	V ₁ = 1.2	45.33
	V ₂ = 2.26	38.88
	V ₃ = 5.08	30.11

CONCLUSIONS

- A specialized solid fertilizers spreader was designed and built. The equipment is composed of three operating sections and performed gravitational or centrifugal spreading of the fertilizers, on each row.
- An innovative image analysis technique was used in order to evaluate the fertilizer granules size distribution.
- The image analysis of the photographs was performed using the Image J software
- The proposed image processing technique was validated based on an analysis of the significance of the differences
- The analysis showed that, for a specific distribution method, there was no significant difference between the variants in terms of particle size distribution, thus confirming the validity of the image analyzing technique.

- The centrifugal distribution method provided a better uniformity in particle size distribution compared to the gravitational distribution method.
- The experimental tests proved that the spreader is achieving the necessary agro technical requirements and quality indices.

REFERENCES

- Ciofu R., Stan N., Popescu V., Chilom P., Apahidean S. Al., Horgoş A., Berar V., Lauer K. F., Atanasiu N. (2004). Treatise on the growing of vegetables (in Romanian). Ceres Publishing House, Bucharest.
- Dilz K. and Van Brakel G. D. (1985). Part I: Effects of uneven fertiliser spreading—A literature review. Proc. No. 240. York, U.K.: Intl. Fertiliser Soc.
- Gelings C.W. and Permenter K.E. (2004). Energy Efficiency in Fertilizer Production and Use. Encyclopedia of Life Support Systems (EOLSS), Developed under the Auspices of the UNESCO, Eolss Publishers, Oxford, UK, [<http://www.eolss.net>].
- Indrea D., Apahidean S. Al., Mănuțiu D.N., Apahidean, M., Sima, R. (2003). Vegetables growing (in Romanian). Ceres Publishing House, Bucharest.
- Miller P. C. H., Audsley E., Richards I. R. (2009). Costs and effects of uneven spreading of nitrogen fertilisers. Proc. No. 659. York, U.K.: Intl. Fertiliser Soc.
- Popescu V. (2008). Field and greenhouse growing of vegetables (in Romanian). MAST Publishing House, Bucharest.
- Olieslagers R., Ramon H., De Baerdemaeker J. (1996). Calculation of fertilizer distribution patterns from a spinning disc spreader by means of a simulation model. *J. Agric. Eng.Res.*, 63(2), 137-152. <http://dx.doi.org/10.1006/jaer.1996.0016>.
- Richards I. R. and Hobson R. D. (2013). Method of calculating effects of uneven spreading of fertiliser nitrogen. Proc. No. 734. York, U.K.: Intl. Fertiliser Soc.
- Stewart L. and Bandel A. V. (2002). Uniform Lime and Fertilizer Spreading. Publication EB254. Mearyland Cooperative Extension.
- Suditu P. (2003). Fertilizing equipments (in Romanian). Tehnopress Publishing House, Iași.
- Van Meirvenne M., Hofman G., Demyttenaere P., (1990), Spatial variability of N fertilizer application and wheat yield. *Fertilizer Res.*, 23 (1), 15-23, <http://dx.doi.org/10.1007/BF02656128>.



ASSESSMENT OF SOIL IMPACT AFTER USING A VIBRO-COMBINATOR

Dan VIDREAN¹, Florinel Cosmin BOJA^{1*}, Alin TEUȘDEA²,
Cristina Ioana DRAGOMIR³, Nicușor Flavius BOJA¹

¹Department Engineering and Informatics, Faculty of Economics, Informatics and Engineering, "Vasile Goldiș" Western University of Arad, Liviu Rebreanu Street nr. 91-93, 310414 Arad, Romania

²Department of Animal Husbandry and Agro-tourism, Faculty of Environmental Protection, University of Oradea, Gen. Magheru 26, 410396 BH, Oradea, Romania

³Department Forest Engineering Forest Management Planning and Terrestrial Measurements, Faculty of Silviculture and Forest Engineering, Transilvania University of Brasov

*E-mail of corresponding author: bojanicu@yahoo.com

SUMMARY

Seedbed preparation for crop establishment (sowing) is one of the most important agricultural works, as is done with high energy consumption and high costs. The quality of this work influences in large measure the germination of crop and the productivity that can be obtained per hectare. These devices are called combinators. Of all the existing combinators, the most efficient are the vibro-combinators. The advantages of using vibro-combinators are: required preparation of seedbed in difficult working conditions and preservation of moisture and total porosity and reducing of soil compression degree. Such important factors can ensure fast, uniform and early germination of seeds, these requirements standing at the basis of abundant harvests. Advanced methods of statistical analysis (univariate three-way ANOVA and multivariate analysis, PCA, Manova and HCA) began to be successfully used in recent years for the study of soil behaviour at the interaction with the working bodies. In order to carry out the research, we settled in six parcels in the plains of the West of Romania so that we could have three different types of soils which are representative for that specific area. From each profile were collected soil samples in three steps of 6, 12 and 18 cm. For each sample were performed six repetitions (N = 6). We started by measuring the particle size distribution (granulometric composition) and the main physical properties of the soil (moisture, bulk density, total porosity and soil compression degree).

Keywords: vibro-combinator, soil tillage, bulk density, total porosity, compression degree.

INTRODUCTION

Nowadays, humanity is facing a major controversy over the choice of appropriate technology of soil tillage. It is the time that is required an intelligence choice between conventional technologies (classical) for seedbed preparation, assuming an intense mechanical processing of soil, which affects soil structure and soil organic matter, and the conservative tillage technologies for seedbed preparation, which removes these disadvantages in terms of an accepted decrease of the production (Pisante et al., 2010).

Therefore, at present, there is different equipment from the ones found in classical cultivation technologies, which in single pass can achieve tillage with minimum energy consumption, thus creating optimal conditions for sowing and for obtaining higher yield without soil degradation (Benites, 2000).

The paper presents a study on the optimization of working regime of vibro-cultivators based on environmental impact assessment for use in seedbed processing. Study presents a method to determinate some physical and mechanical proprieties before and after soil tillage with aggregates consisting of tractor and vibro-cultivators, in three parcels in the plains of the West of Romania.

Vibro-cultivators are machines for seedbed preparation. They are equipped with tools sustained by elastic suspension. The elasticity of supports facilitates the oscillations of working tool – elastic support assembly. This set has a natural mode shapes which corresponds to a natural frequency of vibration (Cardei et al., 2015).

Modern agricultural operations now demand the utilization of a wide variety of equipment and specialist machinery systems, with many having rotary elements such as axles, gears, pulleys etc. With these agricultural machinery systems, which have rotary elements, uncontrolled vibrations may become an important problem to consider. When the initial 'switch-on' frequency meets with the natural frequency of a machine element in the system, undesired noise, high levels of vibration and mechanical failures may occur during operation (Celik et al., 2010; Petrescu et al., 2015).

Generally, combinator consists of a vibro-cultivator A (cultivator for total processing of soil), composed of: frame 1, coupling device at the power source 2, wheels for limiting of working depth 3, soil loosening bodies 4, and a helix harrow B, which consists of frame 5, two rod-rotors 6, and horizontality adjustment system 7 (Fig. 1). Worldwide, more and more prestigious companies have incorporated into the range of products vibro-combinators of such kind.

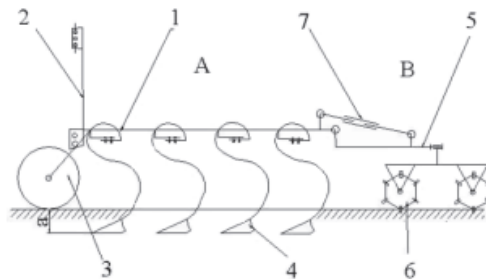


Figure 1. General scheme of a vibro-combinator (Căprioiu, 1982; Biris et al., 2015)

Deep tillage tools are one of the primary components of agricultural equipment which experience high level soil reaction forces during tillage operations. These forces may cause

plastic deformation or failure which is undesirable for tillage machines/tools. The active tillage elements of agricultural machineries require extensive studies in order to obtain a proper soil fragmentation and displacement (Petrescu et al., 2015).

MATERIALS AND METHODS

In order to obtain a global image on the impact of the new vibro-combinator (the prototype SANDOKAN 2) (table 1) in terms of the physical and mechanical properties of the soil, it was necessary to determine its properties before the passage of the equipment (in the state of the soil), and after its passage on all the three parcels and trials. These parcels will be suggestively named: soil 1, soil 2 and soil 3; and the three types of active elements (Gamma, Delta1 and Delta2) (fig. 2-3).

Table 1. Main characteristics of the prototype vibro-combinator SANDOKAN 2

No. crt.	Characteristics	MU	Values
1	Mass	kg	5670
2	Length in transport	m	6.6
3	Height in transport	m	3.95
4	Width in transport	m	2.93
5	Width of the gamma active parts, reversible chipper type	mm	35
6	Width of the delta 1 active parts, arrow type	mm	150
7	Width of the delta 2 active parts, arrow type	mm	250



Figure 2. The prototype vibro-combinator SANDOKAN 2 equipped with the three types of active elements (GAMMA, DELTA1, DELTA2)

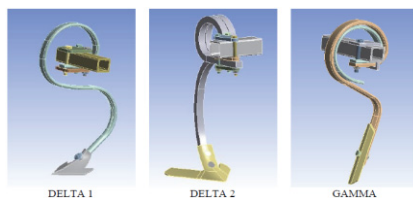


Figure 3. Geometrical models for the three active elements (Petrescu et al., 2015).

The physical properties were determined by using the method of thekopecky with a constant volume of 100 cm³, carrying out six repetitions at different depth, from 6, 12 and 18 cm (fig. 4). The methods of analysis and interpretation of the results as well as the work

procedure for the determination of the physical and mechanical properties are those indicated in the specialized literature (Boja et al., 2012; 2013).



Figure 4. Placement of the sampling rings on different depth stages

Statistical analysis. All data were subjected to univariate three-way analysis of variance (ANOVA, $P=0.05$) and done with KyPlot (Version 5.0.2, <http://www.kyplot.software.informer.com>). The ANOVA factors were: Soil (soil type), h (depth), Device (active element) and their three order interaction. The means pairwise comparisons were investigated by Tukey's post-hoc test ($P =0.05$). Multivariate analysis: principal component analysis (PCA) was performed with P.A.S.T. version 3.04 statistical software, (Palaeontology Statistics, Copyright Oyvind Hammer and D.A.T. Harper (November 2014), <http://folk.uio.no /ohammer/past/>) (Hammer et al., 2001).

RESULTS AND DISCUSSION

When analysing the granulometric curves presented in figure 5 and table 2, one can notice the fact that there was a sandy-clay-dusty texture in soil 2 and 3 encompassed in the experiment at a participation quota that scarcely varies, with the exception of the 1st soil where the particle size distribution is different: clay-dusty-sandy texture.

Table 2. Average values of the granulometric analysis at different depths of prelevation

Type of soil	Depth, (cm)	Values of the granulometric analysis (%)		
		Sand, mass percentage	Dust, mass percentage	Clay, mass percentage
SOIL 1 (S1)	6	26.2	28.6	44.8
	12	26.8	28.7	44.3
	18	27.4	28.7	44.4
SOIL 2 (S2)	6	35.7	30.2	34.5
	12	35.1	30.2	34.8
	18	35.1	30.1	34.7
SOIL 3 (S3)	6	43.4	27.8	28.5
	12	43.2	28.1	28.7
	18	43.2	28.5	25.9

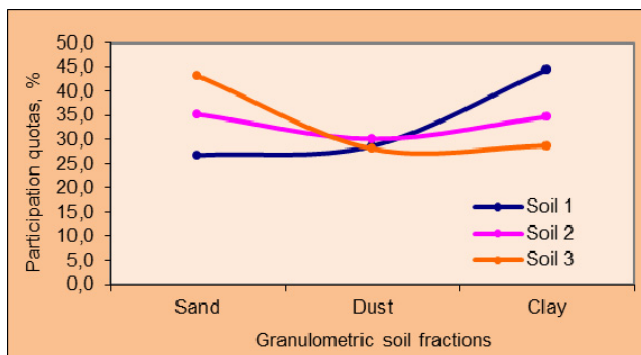


Figure 5. Granulometric curves analysis of the soils

From the analysis of the values gathered for the participation quotas of the granulometric fractions, we could infer some interesting differentiations among the three types of soil in which we tried the vibro-combinator, as follows:

- All the three types of soil that we tried on the vibro-combinator are a relatively close mix, but in different proportions among the three granulometric fractions;
- The sand fraction (gravel + fine) is predominant in the soil 3 (43,2 %);
- For the dust fraction (I + II), the differences among the three types range only for 2%, the highest value being registered on the soil 2 (30,1 %);
- The participation quotas of the clay granulometric fraction are among the biggest, varying between 28,7 % (soil 3) and 34,7% (soil 2), and reaching 44,5 % for soil 1;
- The dust granulometric fraction is almost constant for all the three types of soil.

To synthesise more efficiently the data taken and to be able to describe completely the intrinsic characteristics of the sample, it was chosen a statistic processing with the aid of the program KyPlot. The results obtained are given in Tables 3-4, to underline the variance of apparent density, soil moisture, total porosity and soil compression degree, and comparative with each types of soils and three active elements (Gama, Delta 1, Delta 2). Thus, for each types of soils included in the experiment resulted in eight statistical indicators for each technical work use a new vibro-combinator, but also witness sample. The mechanical processing of the soil through traditional and modern methods is currently questionable due to the high energy consumption and the continuous degradation of the arable horizon through erosion and excessive compaction.

It is known that the bulk density varies between 1-2 g/cm³, according to the type soil and horizon, being generally lower in the case of the soils rich in humus and in the structured soils as compared to the unstructured soils. The values of the bulk density are in tight correlation with the degree of settlement of the soil. The high bulk density means a decrease of the capacity to retain water, of the permeability, of aeration and an increase of the mechanical resistance opposed by the soil during its sampling. On the contrary, low bulk densities can reduce the bearing of the soil, making difficult the mechanized execution of the works, even the driving of the operation machinery (Spoljar et al., 2009; Spoljar et al., 2011; Boyraz and Atilgan, 2014; Boja et al., 2016; Calistru et al., 2016).

By analyzing the values of total porosity, we can say that for the first type of soil we noticed an increase of the total porosity from 40,19 %, which represents the initial state of the soil, to 44,36 % (value obtained after the working of the soil with the vibro-combinator

equipped with Gamma elements), 45,64% (with Delta 1 elements) and 45,71% (with Delta 2 elements).

The degree of settlement for the 1st type of soil presents values > 18%, which means that the soil is strongly settled for all levels of depth and after the passage with the three types of active elements of the cultivator.

The values gathered for the second type of soil varies from weakly settled (1...10%) to moderately settled (11...18%). However, it is important to specify the fact that the lowest values of the degree of settlement appeared after preparing the germination bed with the aid of the active elements Delta 2.

In the case of the third type of soil, we had negative values for this mechanical index of the soil at all depths, especially for the types of active elements, which means there is a soil moderately loose (-17...-10%) - fact that can be explained by the fact that this parcel has been annually worked.

Analysing the influence of the active elements on the different types of soils, some conclusions can be made (Table 3 and Fig. 6-10):

- in terms of apparent density values (D_a), the lowest value is found on all soil types (S1, S2, S3) when working with the active elements Delta2;
- the total soil porosity has maximum values when the vibro-combinator is equipped with the Delta2 active elements, logical situation due to the existing relation to density and porosity;
- soil moisture values reach peak values after processing with Delta2 to S1 and S2, and in S3 the maximum value of soil moisture is reached after processing with Delta1;
- the soil compaction degree has a similar humidity variation, namely: minimum values for S1 and S2 using Delta2 and in S3 following the use of Delta1.

Table 3. Results for the soil physical and mechanical properties (values are expressed as mean±st.dev.) for the interaction factor Soil*Device (CTRL, Gama, Delta1, Delta2)

Soil*Device	Soil moisture (%)	Bulk Density (g cm^{-3})	Total Porosity (%)	Soil compression (%)	Water retention ($\text{m}^3 \text{ha}^{-1}$)
S1.CTRL	19.56h±2.60	1.68a±0.09	35.45f±3.48	32.17a±6.60	423.66e±230.12
S1.Delta1	17.48i±5.34	1.48c±0.05	43.08d±1.98	17.56c±3.74	351.98f±218.78
S1.Delta2	23.69g±1.71	1.47cd±0.06	43.48cd±2.28	16.79c±4.33	436.40de±224.70
S1.Gama	17.48i±1.02	1.59b±0.18	38.85e±6.83	25.66b±13.04	350.94f±183.72
S2.CTRL	28.72c±4.93	1.47cd±0.03	43.56cd±1.14	14.00cd±2.28	543.61b±300.88
S2.Delta1	27.25f±4.14	1.42de±0.06	45.48bc±2.35	10.20de±4.67	498.61c±271.64
S2.Delta2	29.19b±4.42	1.40e±0.08	46.35b±3.24	8.50e±6.42	528.84b±298.40
S2.Gama	29.72a±6.30	1.44cde±0.04	44.62bcd±1.61	11.91de±3.22	563.18a±328.87
S3.CTRL	28.06de±5.93	1.22f±0.02	53.21a±0.93	-7.45f±1.62	447.86d±266.47
S3.Delta1	28.26d±6.01	1.19f±0.02	54.46a±0.94	-9.97f±1.66	439.36de±262.04
S3.Delta2	27.86e±5.85	1.17f±0.02	55.03a±0.91	-11.14f±1.59	427.21e±253.89
S3.Gama	28.06de±5.93	1.20f±0.02	53.83a±0.89	-8.70f±1.56	433.29de±257.97

Table 4. Results for the soil physical and mechanical properties (values are expressed as mean±st.dev.) for the interaction factor h*Device (CTRL, Gama, Delta1, Delta2)

h*Device	Soil moisture (%)	Bulk Density (g cm ⁻¹)	Total Porosity (%)	Soil compression (%)	Water retention (m ³ ha ⁻¹)
06.CTRL	19.82i±2.73	1.40cd±0.16	46.36de±6.02	8.58cd±13.78	164.47f±20.79
06.Delta1	17.68k±5.42	1.31fg±0.11	49.74ab±4.33	1.98fg±10.55	136.34g±38.22
06.Delta2	22.23h±1.30	1.29g±0.12	50.50a±4.57	0.48g±11.04	172.06f±22.18
06.Gama	19.56j±2.43	1.34efg±0.12	48.53abc±4.74	4.37efg±11.23	155.02fg±18.05
12.CTRL	26.11f±4.33	1.48ab±0.22	43.17fg±8.34	14.75ab±18.16	454.72d±54.87
12.Delta1	25.74g±4.15	1.38cde±0.14	46.98cde±5.51	7.40cde±12.67	421.79e±59.70
12.Delta2	26.86e±2.79	1.36def±0.14	47.87bcd±5.27	5.66def±12.15	435.29e±54.18
12.Gama	25.73g±6.10	1.43bc±0.21	45.03ef±8.02	11.15bc±17.30	430.53e±92.09
18.CTRL	30.40b±5.95	1.49a±0.21	42.68g±8.21	15.39a±18.29	795.94a±89.46
18.Delta1	29.58d±5.67	1.40cd±0.14	46.29de±5.50	8.41cde±13.11	731.82c±94.82
18.Delta2	31.66a±4.18	1.39cde±0.15	46.49cde±5.97	8.01cde±14.04	785.11a±83.48
18.Gama	29.96c±8.25	1.46ab±0.22	43.73fg±8.44	13.35ab±18.56	761.87b±168.46

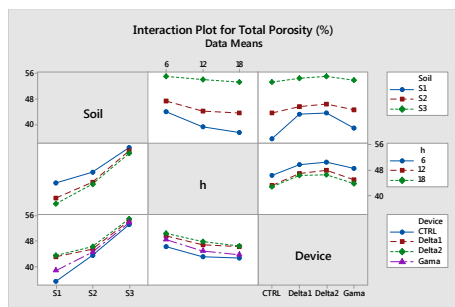


Figure 6. Interaction plot for total porosity (from three-way ANOVA) for soil types (factor Soil), depth (factor h) and active elements (factor Device).

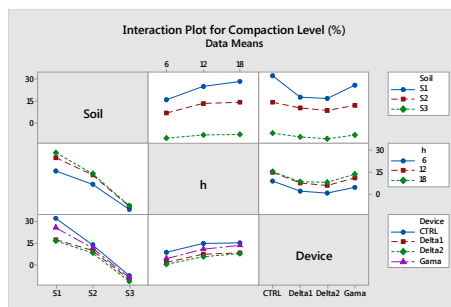


Figure 7. Interaction plot for compaction level (from three-way ANOVA) for soil types (factor Soil), depth (factor h) and active elements (factor Device).

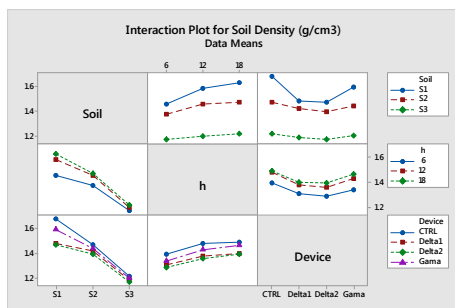


Figure 8. Interaction plot for soil density (from three-way ANOVA) for soil types (factor Soil), depth (factor h) and active elements (factor Device).

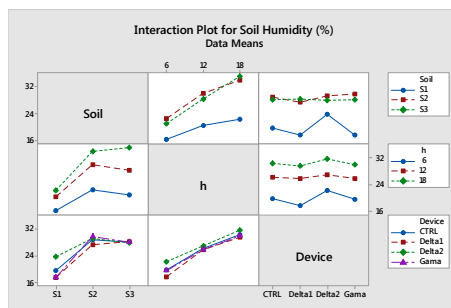


Figure 9. Interaction plot for soil humidity (from three-way ANOVA) for soil types (factor Soil), depth (factor h) and active elements (factor Device).

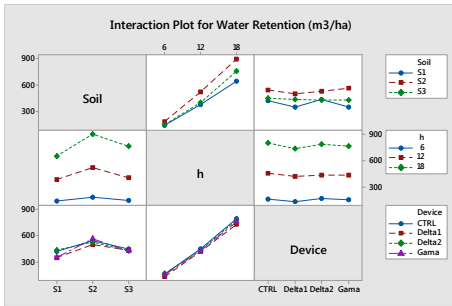


Figure 10. Interaction plot for compaction level (from three-way ANOVA) for soil types (factor Soil), depth (factor h) and active elements (factor Device).

Analysing the impact of active organisms on soil depth, some conclusions can be drawn (Table 4 and Figure 6-10):

- bulk density (D_a) records minimum values ($S1=1.47\pm0.06$; $S2=1.40\pm0.08$; $S3=1.17\pm0.02$) when using Delta2 for all three depths (6 cm, 12 cm, 18 cm);
- total porosity has an inverse variation such as that of apparent density: the highest values ($S1=43.48\pm2.28$; $S2=46.35\pm3.24$; $S3=55.03\pm0.91$) are found for all three depths when working with Delta2;
- and soil moisture values ($S1=23.69\pm1.71$; $S2=29.19\pm4.42$; $S3=27.86\pm5.85$) respect the same law that: for all three depths the maximum value occurs after processing with Delta2;
- the soil compaction degree has a similar variation, that is, the smallest values ($S1=16.79\pm4.33$; $S2=8.50\pm6.42$; $S3=-11.14\pm1.59$) are recorded at all depths when working with Delta2,
- When working with Delta2 active elements, all physico-mechanical soil indicators have optimal values (Table 4) regardless of working depth.
- the same legality is preserved (with few exceptions) and when analyzing the impacts of the active organ of the vibro-combinator on the soil types contained in the experimental field.

Multivariate analysis

To evaluate the vibro-combinators soil tillage performances were studied the variables: bulk density (g/cm^3), total porosity (%) and soil compression (%). To evaluate the soil environmental impact of the vibro-combinators were considered the variables: soil moisture (%) and water retention (m^3/ha). In order to assess simultaneously the vibro-combinators soil tillage performances and environmental impact, was involved the multivariate analysis: principal component analysis (PCA) and multivariate analysis of variance (MANOVA, $P = 0.05$). The PCA and MANOVA were done separately for each soil types S1, S2 and S3. The PCA method involved as input data the variables correlation matrix and between sample groups algorithm. The MANOVA algorithm used as input data the first two principal components (PCs) coordinates of the group samples. The group samples were described by the interaction factor Device*h (i.e. active elements*depth).

Statistical results for PCA for soil types are presented in Table 5. For all soil types the first two PCs present eigenvalues greater than unity and a cumulative percentage of explained variance greater than 95.0%. Due to this reason these PCs are sufficient to describe the experiment with statistical significance.

Table 5. Principal components analysis statistics for soil factor (PC principal component).

S1	PC	Eigenvalue	% variance
	1	3.578	71.567
	2	1.258	25.166
	3	0.163	3.2669
	4	1.22E-05	0.0002
	5	5.49E-09	1.10E-07
S2	PC	Eigenvalue	% variance
	1	4.380	87.614
	2	0.585	11.710
	3	0.033	0.673
	4	0.0001	0.002
	5	6.86E-06	0.0001
S3	PC	Eigenvalue	% variance
	1	4.239	84.793
	2	0.743	14.877
	3	0.0158	0.3172
	4	0.0006	0.0120
	5	4.01E-05	0.00080181

The PCAs biplots gathers in the same graphical representation the samples scores and variable loadings (Fig. 11-13). The sample groups are marked by points inside a convex hull and the variables are represented by vectors with the starting points in the coordinate system origin. The variable vectors end points shows the direction that describes the group highest abundance (or levels) of the corresponding variables. This means that the group samples placed in the one vector direction (marked by its end point), have high abundance/level of that variable. When the sample groups are placed in the opposite direction, they have lowest abundance/levels for that variable. Analysing Fig. 11-13, for the soil type S1, the PCA biplot prescribe.

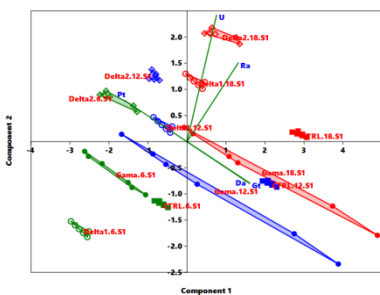


Figure 11. Principal component analysis (PCA) biplot for different depths (factor h) and for the three active elements (factor Device) for soil type S1.

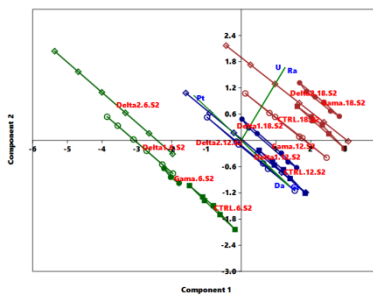


Figure 12. Principal component analysis (PCA) biplot for different depths (factor h) and for the three active elements (factor Device) for soil type S2.

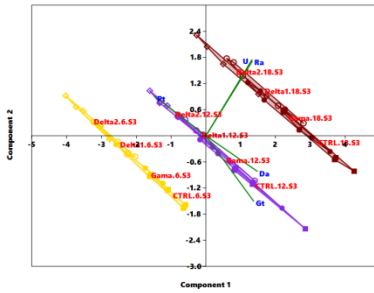


Figure 13. Principal component analysis (PCA) biplot for different depths (factor h) and for the three active elements (factor Device) for soil type S3.

Analysing Fig. 13, for the soil type S3, the PCA biplot prescribes that the best performance for soil tillage and environmental protection have all the active elements Delta1, Delta2 and Gamma for 6 cm depth. However, at other depths the studied active elements are producing environmental damages of soils that have the same properties as S3.

CONCLUSIONS

The advantages of using vibro-combinators are: perfect preparation of seedbed in difficult working conditions and preservation of soil moisture. Such important factors can ensure fast, uniform and early germination of seeds, these requirements standing at the basis of abundant harvests. The research investigated the soil tillage performances and the environmental impact of several active elements of the vibro-combinators, at certain soil depths and soil types. The multivariate analysis allowed to assess for each soil type which active elements performs both best soil tillage and environmental protection of the soils. From the technical point of view, the 6 cm depth is the most important to soil tillage for crop production. For this depth the active elements of the vibro-combinator: Delta2 and Delta1 are those that performs both best soil tillage and environmental protection of the studied soils. (Bulk density (Da) ($S1=1.47\pm0.06$; $S2=1.40\pm0.08$; $S3=1.17\pm0.02$); Total porosity ($S1=43.48\pm2.28$; $S2=46.35\pm3.24$; $S3=55.03\pm0.91$); Soil moisture ($S1=23.69\pm1.71$; $S2=29.19\pm4.42$; $S3=27.86\pm5.85$); Soil compaction degree ($S1=16.79\pm4.33$; $S2=8.50\pm6.42$; $S3=-11.14\pm1.59$)).

ACKNOWLEDGEMENTS

This work was supported by POSCCE based on 1CLT/800.024/21.05.2014 financing program.

REFERENCES

- Pisante, M., Corsi, S., Kassam, A. (2010). The Challenge of Agricultural Sustainability for Asia and Europe. *Transist. Stud. Rev.*, Springer, Vol. 17, No. 4, pp. 662-667.
- Benites, J. (2000). Manual on integrated soil management and conservation practices The Challenge of Agricultural Sustainability for Asia and Europe. *FAO Land and Water Bulletin*, No.8, pp. 1-4.
- Cardei, P., Rigon, L., Muraru, V.M., Muraru-Ionel, C., Constantin, N., David, A. (2015). A method of calculating the optimal speed of operation for vibro-cultivators. *Proceedings of 43. International Symposium, Actual Tasks on Agricultural Engineering*, vol. 43, p 211-221.

- Celik, H.K., Topakci, M., Canakci, M., Rennie, A., Akinci, I. (2010). Modal analysis of agricultural machineries using finite element method:a case study for a V-belt pulley of a fodder crushing machine. *JFAE*,8 3-4. pp. 439-446.
- Petrescu, H.A., Martin, R., Vlasceanu D., Hadar A., Parausanu I., Dan R. (2015). Modal analysis using fem of three active elements for an agricultural machine. *Proceedings of 43 International Symposium Agricultural Engineering, Actual Tasks on Agricultural Engineering*, vol. 43, pp. 201-209.
- Căproiu, Șt. (1982). *Agricultural machinery for soil tillage, seeding and crop maintenance*. Didactic and Pedagogic Publishing House, Bucharest.
- Biris, S.S.T., Bungescu, S.T., Manea, D., Boja N., Cilan, T.F., Martin, R. (2015). State of art approach to vibro-combinators soil tillage implements construction. *Proceedings of 43. International Symposium Agricultural Engineering, Actual Tasks on Agricultural Engineering*. vol. 43, p 177-188.
- Boja, N., Boja, F., Teușdea, A., Carțiș, M., Pușcaș, S. (2012). Study on the Impact of Soil Processing on Some Physico-mechanical Properties. *Journal of Environmental Protection and Ecology (JEPE)*, vol. 13, no.2A/2012, pp. 941-950.
- Boja, N., Boja, F., Teusdea, A., Dărău, P.A., Maior, C. (2013). Research regarding the uniformity of sprinkler irrigation. *JEPE*.vol. 14, no.4 / 2013, pp. 1661-1672.
<http://www.kyplot.software.informer.com>.
- Hammer O., Harper D.A.T., Ryan P. D. (2001). PAST: Paleontological Statistics Software Package for Education and Data Analysis. *Palaeontologia Electronica*, 4 (1), 9.
- Boja, N., Boja, F., Teusdea, A., Dărău, P.A., Maior, C. (2016). Soil porosity and compaction as influenced by tillage methods. *JEPE*.vol.17, no.4/2016, pp.1315-1323.
- Spoljar, A., Kistic, I., Birkas, M., Kvaternjak, I., Marencic, D., Orehovacki, V. (2009). Influence of tillage on soil properties, yield and protein content in maize and soybean grain. *JEPE*, Vol. 10, No 4, pp. 1013–1031.
- Calistru, A.E., Topa, D., Rostek, J., Puschmann, D.U., Peth, S., Horn, R., Jitareanu G. (2016). Soil physical properties and winter wheat yield as affected by different tillage systems. *JEPE*, Vol. 17, No 3, pp. 978–989.
- Spoljar, A., Kistic, I., Birkas, M., Gunjaca, J., Kvaternjak, I. (2011). Influence of Crop Rotation, Liming and Green Manuring on Soil Properties and Yields. *JEPE*, Vol.12, No1, pp.54-69.



STUDY ON ADAPTING THE PARAMETERS OF VIBRATORY TILLAGE TO THE RESONANCE FREQUENCY OF THE AGRICULTURAL SOIL

Nelus-Evelin GHEORGIȚĂ, Sorin-Stefan BIRIȘ*, Nicoleta UNGUREANU,
Sorin IORDACHE, Maria PRUNĂU

Politehnica University of Bucharest, Faculty of Biotechnical Systems Engineering, Biotechnical
Systems and Research and Development Centre, Bucharest, Romania

*E-mail of corresponding author: biris.sorinstefan@gmail.com

SUMMARY

It has already been demonstrated that draft force can be decreased by machines equipped with vibrating tools. The main issue is to reduce energy consumption. The dynamic characteristics and soil parameters depend on strain level. For best results, the frequency of vibratory tillage tools must be as close as possible to the natural frequency of the soil. The paper presents a synthesis of the theoretical researches on the possibility to adapt the constructive and functional parameters of the vibratory working tools to the own frequency of agricultural soil.

Keywords: agricultural cultivator, tillage tool, vibrations, agricultural soil

INTRODUCTION

The analysis of the literature shows that it is possible to use the vibrations in carrying out the working processes of the agricultural machines in order to fulfill at least one of the following aspects:

- reduction of energy consumption in the execution of agricultural works;
- qualitative improvement of agricultural technological processes;
- increasing the productivity of agricultural machinery;
- constructive simplification of agricultural machinery;
- the universalization of certain assemblies or subassemblies of agricultural machinery.

Active tools with elastic supports are vibrating in operation, in the longitudinal direction and sometimes in the transversal direction, having a more active effect on tillage, by increasing the crumbling degree of the soil.

The biggest part of the required drawbar work from tillage implements is caused by friction between soil and implement. Therefore, the reduction of friction forces is a reasonable possibility to lower the power requirements in tillage (Kattenstroth et al., 2011).

Different approaches to reduce the friction forces in tillage can be found in scientific publications. In the 1950's, Eggenmueller conducted experiments with mechanical vibrations at a frequency of 50 Hz. He was able to demonstrate a reduction of drawbar forces up to 80 %. One disadvantage of this system was the maximum working speed limited at 2 m s⁻¹. According to Eggenmueller (1958) an enhancement of the oscillation frequency could allow a higher working speed.

The vibratory tillage operations in the conventional tractive method have been investigated for the potential development of more effective soil cutting, the potential of the forced vibration as a promising mean for soil pulverization and reducing the draft force and machine weight (Mahmood et al., 2011).

MATERIAL AND METHOD

Unlike the rigid tines, the vibratory working tools can reduce the draft force. The reason for this reduction in draft for a flexible tine is due to lowering speed before maximum force is exerted and soil failure (Berntsen et al., 2006).

Although the resistance force of the active tool can be reduced by up to 20%, and the furrow crumbling process can be greatly improved using mechanical vibrations, their generation requires energy consumption that often exceeds this reduction. For this reason, the use of autovibrations in the soil process is attempted, primarily because the agricultural soil is not homogeneous, and is processed with active tools mounted by means of elastic elements on the cultivator frame.

The angle of soil-metal friction has a large influence on draft in model calculations. However, no great effect of metal surface roughness on the magnitude of the horizontal (draft) force was found, but mainly in the direction of the resulting force. The soil-metal friction angle is also affected by soil type and soil water content and may increase with increasing speed. Furthermore, if the soil builds up on the active tool, friction occurs between soil particles and between soil and metal (Aluko and Seig, 2000).

The interface friction angle may then be assumed to be equal to the internal friction angle of the soil (Wheeler and Godwin, 1996).

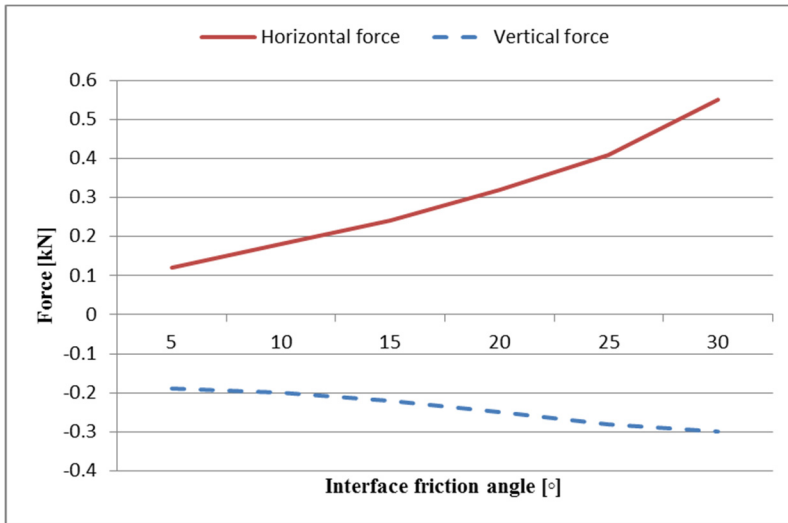


Figure 1. Horizontal (solid line) and vertical (dotted line) force for a vibratory active tool (Wheeler and Godwin, 1996)
Standard values: rake angle 30°, speed 2 m/s, working depth 0.1 m

Draft force is the component of pull in the direction of travel. It is very important to determine draft force even within short run because of wide fluctuation in soil conditions. Also it is commonly expressed as N/cm^2 of furrow slice, known or defined as specific draft, however it sometimes expressed as $12 \text{ kN}\cdot\text{m}^{-1}$ of width, and sometimes indicating the depth of cut, for tillage implements (Elamin, 1981).

We could express the draft value as in equation (Elamin, 1981):

$$F = F_0 + k \cdot v_T \quad (1)$$

where:

F —is the draft force [kN]

F_0 —static component of the draft force, independent of speed [kN]

k —a constant which value depends on type and design of implement, and soil conditions.

v_T — tractor forward speed [m/s].

Vibrating a tillage tool is an effective way of reducing the draft force required to pull it through the soil. The degree of draft force reduction depends on the combination of operating parameters and soil conditions. Thus it is necessary to optimize the vibratory implement for different conditions.

The non-stop (spring-loaded) system not only that protects the active tools from underground obstacles, but it also facilitates penetration due to vibrations caused. The presence of the spring transmits a strong oscillation or vibration type (vibratory action), allowing penetration even under extremely dry or difficult conditions. The spring tension is adjusted by a screw, and with this can also be adjusted the frequency of tools (Fig. 2) (Maschio-Gaspardo, 2015).

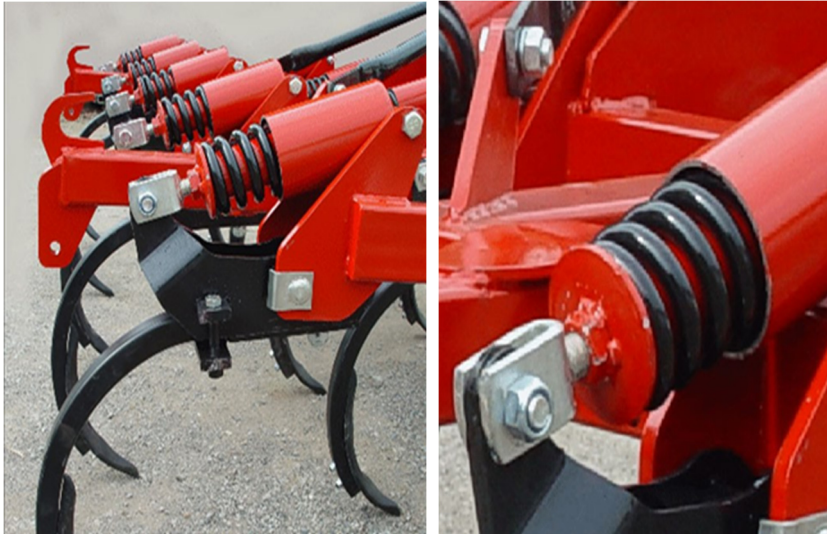


Figure 2. Elastic support equipped with spring (Non stop CH - Cultivator, 2015)

The spring tines have the advantage of being maintenance-free and having a lower draft requirement than rigid tines. In contrast to rigid tines, spring tines have a lateral flexibility and search out the path of least resistance through the soil.

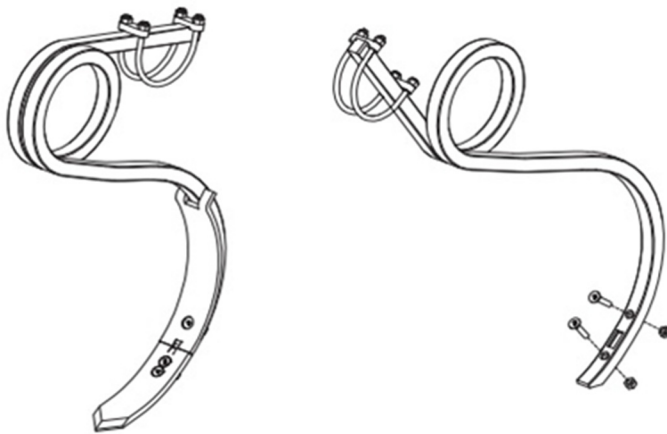


Figure 3. Flexible working tools (Tine cultivators, 2015)

From the same category of flexible working tools are straight (gamma) or delta. Gamma tools till the soil with no effective turning; this choice is optimal for retaining soil water content when operating in dry conditions like those for seeding in late summer or late spring. On the opposite, delta tines due to higher soil disturbance aerates and dries up excessively wet soils, eradicates weeds sprouted after primary tillage and buries part of crop residues (Maschio-Gaspardo, 2015).



Figure 4. Gamma and delta vibratory active tools (Maschio Gaspardo, 2015)

Rolled convex steel used in the production of vibratory tillage tools is designed to provide a maximum lifetime. Unlike standard flat steel, specially rounded corners prevent cracks. Using this special steel profile, active tillage tools are able to vibrate faster and more powerfully. High quality alloy steel ensures long lifetime of both active tools and wearing parts. Some of the tools are subjected to a special shot peen bombardment process (as illustrated in figure 5).

This ensures that any potential fatigue cracks from the shaping process are closed up, thereby increasing the tine's lifetime (Genuine tines and shares, 2016).

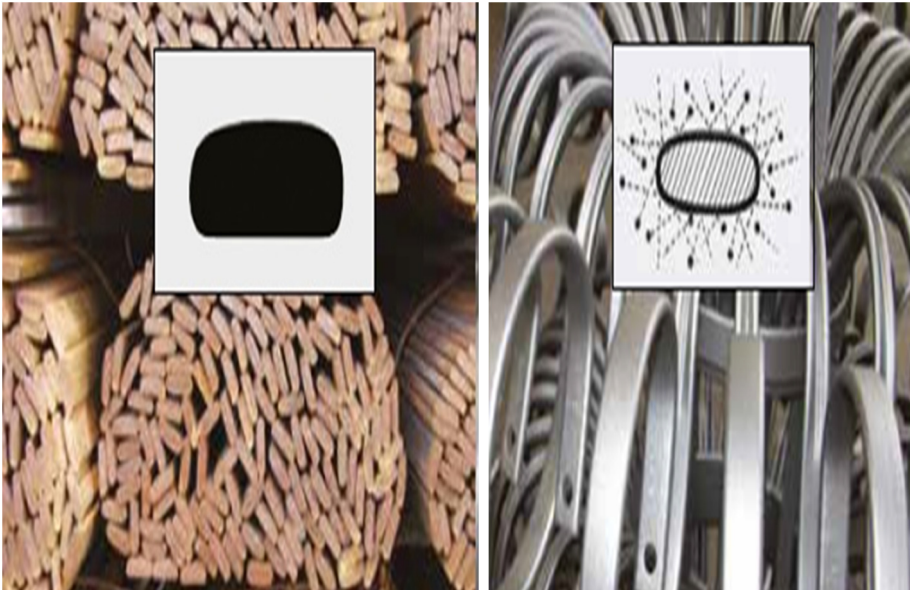


Figure 5. Rolled convex steel used in the production of vibratory tillage tools

RESULTS AND DISCUSSION

The researches highlighted that one of the most important components related to the resistance force (draft force) is the external friction between the active surface of the tool and the soil. It also results from experimental attempts that these friction forces decrease significantly when the tillage tool vibrates. On the other hand, the resistance force is significantly influenced by the constructive parameters of the tool. One of these constructive parameters is the settlement angle of the tool towards the direction of movement.

Figure 6 shows the graphical variation of the resistance force of vibrating tillage tool, for different oscillation frequencies of the tool and various angles of inclination towards the direction of movement. It can be noticed that the higher oscillation frequency of the tool is, the forces required to move the tool through the soil decrease. Also, increasing the inclination angle of the tool's active surface it results in an increase of the resistance force.

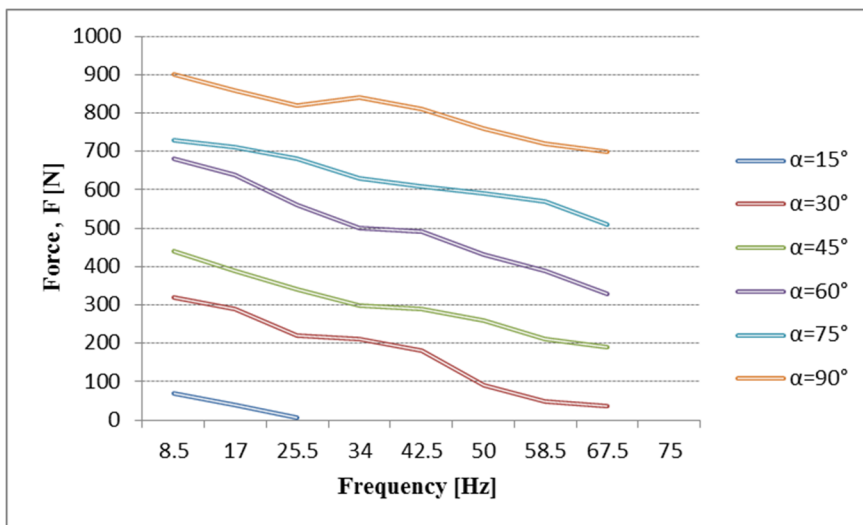


Figure 6. The dependence between resistance force and frequency (Bernaki and Haman,1967)

Future research aims to conduct laboratory tests on agricultural soil samples, which will allow the identification of the natural frequencies (resonance frequencies) for the soil and which can be correlated with the frequencies generated by the soil tillage tool (via the elastic support).

In Figures 7 and 8 are presented the values of external friction coefficient in two extreme situations: the tillage tool without oscillation and at an oscillation of 57 Hz. It can be observed a variation depending on the soil humidity and that coefficient values are higher without oscillation.

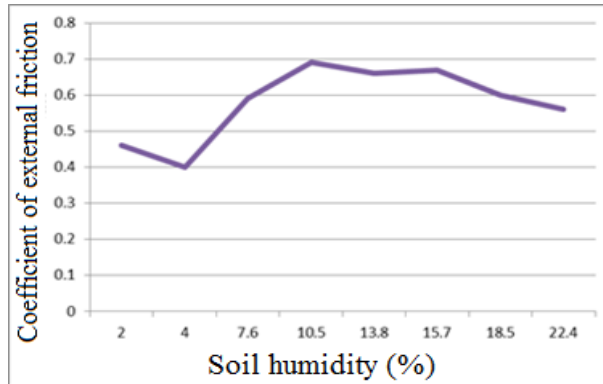


Figure 7. Values of the external friction coefficient, μ , without oscillation with different soil humidities (Bernaki and Haman,1967)

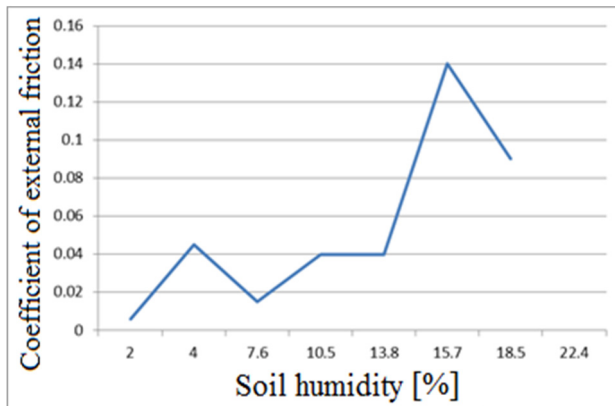


Figure 8. Values of the external friction coefficient, μ , at a frequency of 57 Hz, with different soil humidities (Bernaki and Haman,1967)

CONCLUSIONS

One of the most important aspects to be further considered is to increase the efficiency of tillage process. This can be done by finding a technical solution that allows the automatic adjustment of the constructive and functional parameters of the vibratory tillage tools to the agricultural soil's own frequency so that the efficiency is maximal.

From the experimental tests, the friction forces between the tool and the soil decrease spectacularly when the tool vibrates.

The friction forces between the tool and the soil are one of the main components of the draft force. As the oscillation frequency of the tillage tool increases, the draft force decreases (Figure 6). Soil humidity has an important role in the phenomenon that occurs at the interface between the tool and the soil. The higher the soil humidity, the greater is the adhesion forces between the tool and the soil, which results in the increase of the external friction coefficient.

As it can be seen in Figures 7 and 8, in the case of vibration of the tool, for the same soil humidity values, the overall coefficient of external friction between the tool and the soil decreases. To improve the tillage process of the self-vibrating active tools, a particularly important role is their elastic support, i.e. the global elastic constant of the support.

The challenge of future experiments is to allow the automatic adaptation of the elastic constant of the tool support so that the tool's effect on the soil to be its maximum crumbling, which is produced for tool vibration frequencies close to the soils natural frequency.

In this case, the most promising technical solutions seems to be the helical springs, used to mount the tool support, which have the possibility to automatically adjust their pre-tensioning and to provide elastic constants adapted to the required values.

ACKNOWLEDGEMENTS

This work was supported by UEFISCDI based on 25BG/2016 financing program.

REFERENCES

- Aluko, O.B. and Seig, D.A. (2000). An experimental investigation of the characteristics of and conditions for brittle failure in two-dimensional soil cutting. *Soil Till Res* 57:143–157.
- Bernaki, H. and Haman, J. (1967). *Grundlagen der Bodenbearbeitung und Pflugbau*, VEB VerlagTechnik, Berlin.
- Berntsen, R., Berre, B., Torp, T., Aasen, H. (2006). Tine forces established by a two-level model and the draught requirement of rigid and flexible tines, *Soil & tillage research*, pp.230-241.
- Eggenmüller, A. (1958). *FeldversuchemiteinemschwingendenPflugkörper*. *Grundlagen der Landtechnik* 8 H. 10, 55-95.
- Elamin, I.E.A. (2007). *Tillage, Draft and Power as Influenced by Soil Moisture Content, Tractor Forward Speed, and Plowing Depth in New Halfa Agricultural Scheme (SUDAN)*. Doctoral thesis. University of Khartoum, Faculty of Agriculture .
- Kattenstroth, R., Harms, H.H., Wurpts, W. and Twiefel, J. (2010). Reducing friction by ultrasonic vibration exemplified by tillage, *Landtechnik* 65, no. 1, *Cropping and machinery* pp. 42-44.
- Mahmood, H.F., Subhi, Q.A., Hussein, E.K. (2011), Comparison of Vibrations, Tillage Depths and Soil Properties for Moldboard and Disk Plows at Three Tillage Speeds. *Asian Journal of Agricultural Research*, pp: 90-97.
- Wheeler, P.N., Godwin, R.J. (1996). Soil Dynamics of Single and Multiple Tines at Speeds up to 20 km/h, *Soil Engineering*, pp 17.
- ***(2015) Maschio Gaspardo Catalog, Range of tine cultivators and seedbed tillers, suitable for tractors from 51 to 250 kW, pp 14.
- *** (2015) Non stop CH Cultivator, <http://www.foukas.gr>
- ***(2015) Tine cultivators, <http://www.vaderstad.com/en/tillage/tine-cultivators/swift-400-870>, pp: 61.
- ***(2016) Kongskilde, Catalog, Genuine tines and shares.



STUDY ON THE COMPACTION UNDER FRONT AND REAR WHEEL OF A 40 kW TRACTOR ON PLOWED SOIL

Nicoleta UNGUREANU^{1*}, Valentin VLĂDUȚ², Cătălin PERSU²,
Dan CUJBESCU², Marius Remus OPRESCU², Iulian VOICEA²

¹ Department of Biotechnical Systems, Faculty of Biotechnical Systems Engineering, University Politehnica of Bucharest, Splaiul Independentei Blv., no. 313, sector 6, Bucharest, Romania

² National Institute of Research - Development for Machines and Installations Designed to Agriculture and Food Industry – INMA, Ion Ionescu de la Brad Blv., no. 6, sector 1, Bucharest, Romania

*E-mail of corresponding author: nicoletaung@yahoo.com

SUMMARY

Compaction is the most dangerous type of soil degradation in the European Union and one of the major problems faced by farmers, because it affects soil quality and agricultural production. The paper aims to determine the compaction characteristics in agricultural soil, beneath the front wheel and the rear wheel of a 40 kW New Holland tractor. The experiments were carried out in real conditions, on a plowed field, in stationary regime, for different tire inflation pressures and wheel loads. The most modern system for measuring of contact pressure that is currently available (TekScan mesh pressure sensor) has been placed both at soil-tire interface and in soil depth at 0.1 and 0.2 m. By means of the I-Scan software were obtained: contact pressure, size of contact area, 2D maps of pressure distribution in the footprint and the variation of pressure over time.

Keywords: compaction, tire inflation pressure, contact area, contact pressure.

INTRODUCTION

Soil compaction is “the densification and distortion of soil by which total and air-filled porosity are reduced, causing deterioration or loss of one or more soil functions” (Van den Akker, 2008). In agricultural soil, compaction is induced by agricultural machinery and trampling of animals applying stresses larger than soil bearing capacity (Nawaz et. al., 2013). It affects soil functions and soil structure (Schjønning et. al., 2016), soil productivity, cultivation costs, crop growth, crop yield, product quality and environmental quality (Fountas et. al., 2013; Lipiec and Hatano, 2003). Compaction is mostly due to technological

errors in modern agriculture, such as the overuse of heavy agricultural machinery often on wet soils, and the intensification of cropping systems (Chen and Weil, 2011).

All mechanized farm operations, starting with seedbed preparation, fertilizer and chemical applications and finally harvesting increase the risk of degradation of agricultural soil through artificial compaction. However, compaction is not a recent phenomenon, because it existed in the form of hardpans before the advent of mechanized agriculture (Batey T., 2009). Nowadays, the risk of soil compaction increased mostly due to the significant increase of weight of agricultural machinery. In European agriculture, tractor weight increased from 3 tons (in 1940) to 7 tons (in 1998) respectively 20 tons (at present). Trucks wheel loads are of 6 tons in the front axle (with single tires) and 17 tons in the rear tandem axle (with dual tires). Sugarcane trailers (two axles with dual tires) have 10 tons load on both front and rear axles. Most wheel loads usually exceed the axle load limits proposed to prevent superficial compaction, of 6 tons on single axle and 8 tons on tandem axle (Lozano et. al., 2013). However, the extra weight of tractors, harvesters and loaded trailers has been to some extent compensated by the use of dual wheels on tractors, an increase in tire widths on harvesters, and an increase in the number of axles on trailers, all which allow reductions in tire pressures (Batey, 2009).

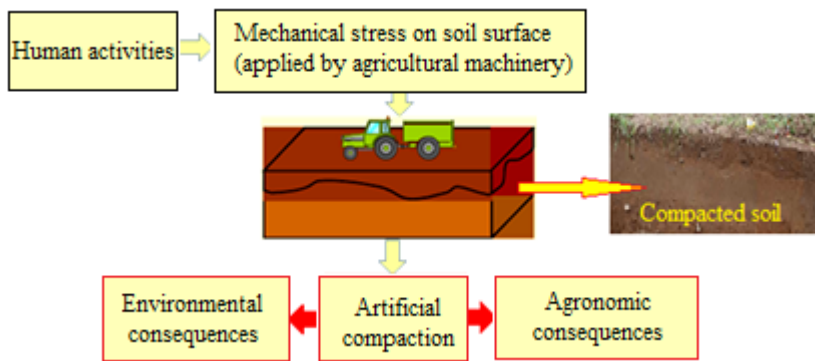


Figure 1. Diagram of the artificial compaction of soil

The depth of compaction usually varies from 100 to 600 mm but is more obvious on topsoil at a depth of about 100 mm (Ziyae and Roshani, 2012) and is greatly influenced by contact area and contact pressure.

“Contact area” is the portion of wheel or tire in contact with the soil, and is an important factor for the load capacity of the tire. “Static contact area” is the contact area between tire and a rigid or deformable surface, when the tire is loaded statically, without forwarding movement (Wulfsohn D., 2009). Tire contact area is computed by dividing the single wheel load by the tire inflation pressure. “Contact pressure” at the soil–tire interface is the axle load divided by the surface area of contact between the soil and machine (Hamza and Anderson, 2005) and is a good indicator of the potential compaction on agricultural soils. Machinery and implements fitted with tracks or larger than standard tires with low inflation pressures (radial tires) are suggested to reduce tire-soil contact pressure and to increase tractive efficiency and, thereby, the potential for compaction (Ziyae and Roshani, 2012).

Tire inflation pressure is probably the most important factor controlling compaction under wheels (Batey, 2009) because it influences the contact area and contact pressure at soil-

tire interface for a given load (Xia K., 2011). Due to higher tire inflation pressure, smaller footprint area is formed, soil deformation increases and the stress is distributed deeper into the soil, requiring remedial works such as deep loosening. Using lower tire inflation pressure, tire deformation increases, footprint area increases, contact pressure decreases, soil deformation is smaller and stress is transmitted to shallower depths (Biriş S.Şt., 2010).

Compaction due to high wheel loads is a persistent threat to soil fertility. An agricultural machinery of 4 ton wheel load can cause compaction to a depth of 300 mm, while a 10 ton wheel load can cause compaction as deep as 500 mm or more (Birkas M., 2014). Arvidsson and Keller (2007) found that tire inflation pressure has a large influence on soil stress at 100 mm depth, but has very little influence in the subsoil (300 mm and deeper). In contrast, wheel load has a large influence on subsoil stress. Increasing wheel load of about two times, contact area increases at a rate of 30-40% while if tire inflation pressure is increased by two times, contact area decreases at a rate of 70-80% (Ekinici and Çarman, 2011).

MATERIALS AND METHODS

The experiments aimed to determine the contact area and contact pressure under front and rear wheels of a 40 kW New Holland tractor, on plowed agricultural soil, in stationary regime. Soil moisture was determined using the FieldScout TDR 300 capacitive portable moisture analyzer (14.7% at soil surface, 16.3% at 0.1 m depth and 17.1% at 0.2 m depth). The distribution of contact pressure in the contact area was recorded using a mesh-type sensor (Tekscan Industrial Sensing) with minimum size of the sensitive surface 650 mm x 550 mm (Fig. 1). Prior to the experiments, the sensor was calibrated and coupled to the VersaTek Handle data acquisition system and a laptop.

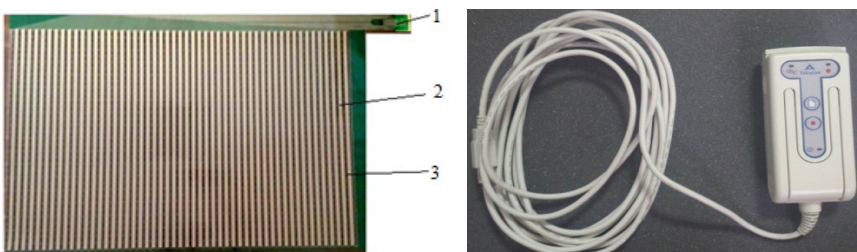


Figure 2. Tekscan sensor and VersaTek Handle data acquisition system
1 - connection to the data acquisition system; 2 - sensitive elements;
3 - connection wires between the sensitive elements

In the first set of experiments, the mesh sensor was interposed between the soil and the tire (0 m depth). With the compressor and the pressure gauge, it was adjusted and measured the inflation pressure in the front tire at 200 kPa, and the load on the front wheel was recorded using the weighing platform with electronic indicator type RW-10PRF (Fig. 3).



Figure 3. Weighing platform with electronic indicator type RW-10PRF

The tractor traveled at low speed and stationed on the sensor so that the contact area and the contact pressure could be recorded in the software. Then, the tire inflation pressure was decrease to 150 kPa and 100 kPa and the data acquisition was made (Fig. 4).



Figure 4. Aspects during field testing

The procedure was repeated for the rear wheel. The sensor was then placed in the soil at a depth of 0.1 m, respectively 0.2 m, after which it was covered with soil, and the measurements (wheel load, contact area, contact pressure) were repeated for both wheels at the three tire pressures.

RESULTS AND DISCUSSION

The results obtained from testing under the *front wheel* of the tractor are given in Table 1.

Table 1. Results obtained for the front wheel of 40 kW tractor

Soil depth (m)	Tire inflation pressure (kPa)	Wheel load (kN)	Contact area (m ²)	Contact pressure (kPa)
0	100	3.4460	0.0338	102
	150	3.4784	0.0280	124
	200	3.4215	0.0257	133
0.1	100	3.5833	0.0624	57
	150	3.6863	0.0575	64
	200	3.5598	0.0538	66
0.2	100	3.4166	0.1110	31
	150	3.5019	0.0974	36
	200	3.5637	0.0902	40

Figure 5 shows a caption from the I-Scan software for the front wheel, at 0.2 m depth, for tire inflation pressure of 100 kPa. It can be noticed from the 2D contact area that the highest contact pressure is distributed in the middle of the contact area, where tire ribs came in contact with the soil. The variation of contact pressure over time is linear.

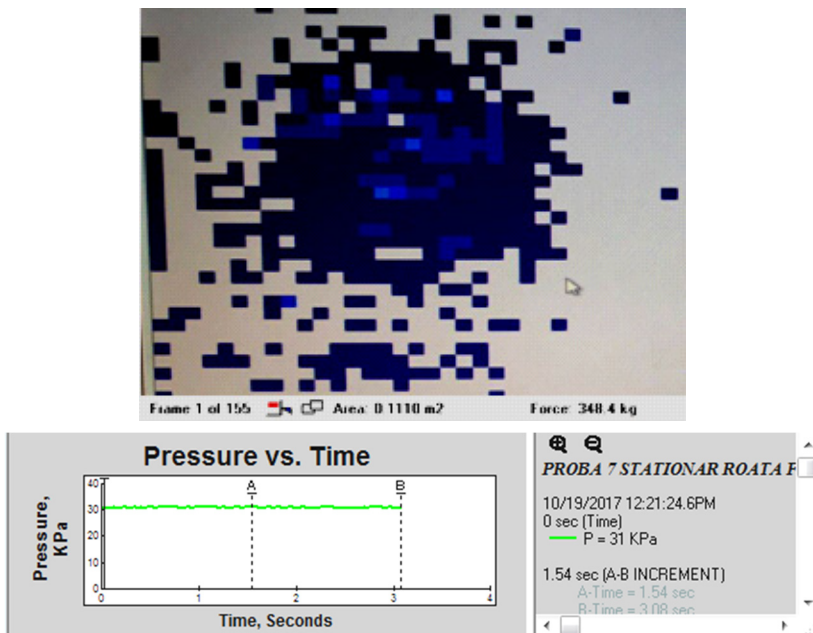


Figure 5. 2D map of pressure distribution at 0.2 m depth under the front wheel at 100 kPa tire inflation pressure

For the front wheel it was plotted the variation of contact area with soil depth, for the three inflation pressures (Fig. 6). It can be seen that at constant tire inflation pressure, the contact area increases with soil depth. Analyzing the results obtained at 100 kPa tire inflation pressure, it is observed that compared to the contact area recorded at soil surface, at a depth of 0.1 m the contact area increased 1.84 times and at the depth of 0.2 m the contact area increased 3.28 times. The same trend is found for the other tire inflation pressures.

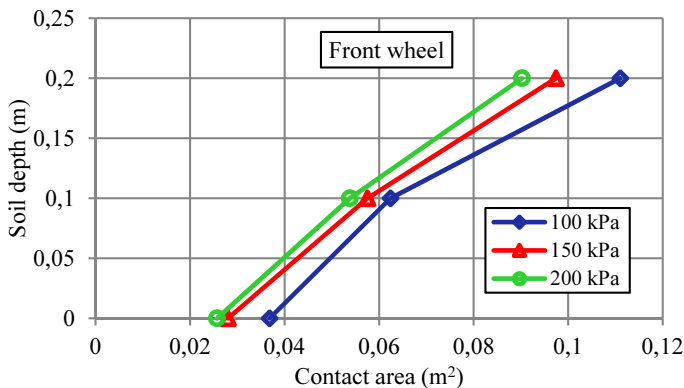


Figure 6. Variation of contact area with soil depth under the front wheel, at different tire inflation pressures

At the variation of contact area with tire inflation pressure under the front wheel of the tractor (Fig. 7) it was found that at constant depth, as tire inflation pressure increases, the contact area decreases. In this situation, the soil deforms more, stresses are distributed at higher depths and the compacted soil must be processed by deep loosening to remove the compacted layers. Nevertheless, contact areas does not change significantly at the variation of tire inflation pressure, most likely because the tire has not deformed much since its ribs are prominent and rigid.

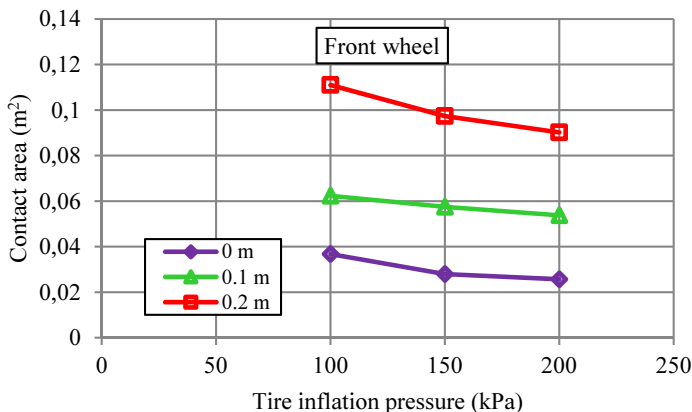


Figure 7. Variation of contact area with tire inflation pressure, at different soil depths under the front wheel

Analyzing the variation of contact pressure with soil depth at the tested tire inflation pressures under the front wheel (Fig. 8) it was found that at constant tire inflation pressure, the contact pressure decreases with soil depth.

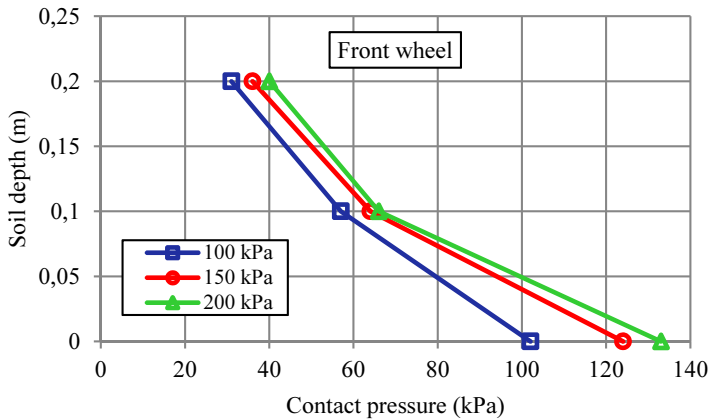


Figure 8. Variation of contact pressure with soil depth, at different tire inflation pressure under the front wheel

An increase in tire inflation pressure at constant depth resulted in the increase of contact pressure. The highest contact pressures were recorded at soil surface (between 102-132 kPa). For example, at soil surface, for 100 kPa tire inflation pressure, the contact pressure is 102 kPa, value that decreases 3.29 times at 0.2 m soil depth. This trend is observed for all inflation pressures, because under the front wheel, the contact pressure at 0.2 m decreases over 3 times in comparison to the contact pressure at soil surface.

At the testing under *rear wheel* of the tractor were obtained the results presented in Table 2.

Although larger in diameter, rear wheel was wider than front wheel by about 0.1 m, so the contact pressure is not significantly higher under the rear wheel than under the front wheel.

Table 2. Results obtained for the rear wheel of 40 kW tractor

Soil depth (m)	Tire inflation pressure (kPa)	Wheel load (kN)	Contact area (m ²)	Contact pressure (kPa)
0	100	5.5652	0.0455	122
	150	5.5594	0.0421	132
	200	5.5451	0.0366	151
0.1	100	5.7496	0.1009	57
	150	5.5751	0.0789	71
	200	5.6584	0.0757	75
0.2	100	5.9742	0.1683	35
	150	5.8389	0.1301	45
	200	5.8252	0.1133	51

For the rear wheel it was plotted the variation of contact area with soil depth, corresponding to the three inflation pressures (Fig. 9). Compared to the front wheel, in the case of the rear wheel, for the same depth and the same tire inflation pressure, larger contact areas were obtained due to higher wheel load, which led to greater tire deformations. At constant depth, by doubling tire inflation pressure, contact area decreased by about 20% at soil surface, 25% at 0.1 m depth and 33% at 0.2 m depth.

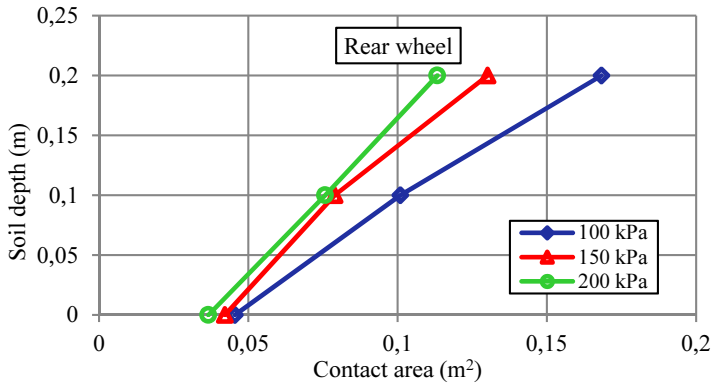


Figure 9. Variation of contact area with soil depth under the rear wheel, at different tire inflation pressures

For the rear wheel, although wheel load does not vary significantly in the tested conditions, at 0.1 m depth the values of contact area are about 2 times higher than those at soil surface, while at 0.2 m depth, contact area is 3 - 4 times higher than that recorded at soil surface.

The variation of contact area with tire inflation pressure under the rear wheel, at tested depths, is presented in Figure 10. The tests revealed that at constant tire inflation pressure, the contact area at 0.1 m depth increases 2 times compared to that at soil surface, while at 0.2 m depth the contact area increases 3 times the values at soil surface. At soil surface, the contact area does not vary significantly with tire inflation pressure, but the most visible change in the contact areas is at 0.2 m.

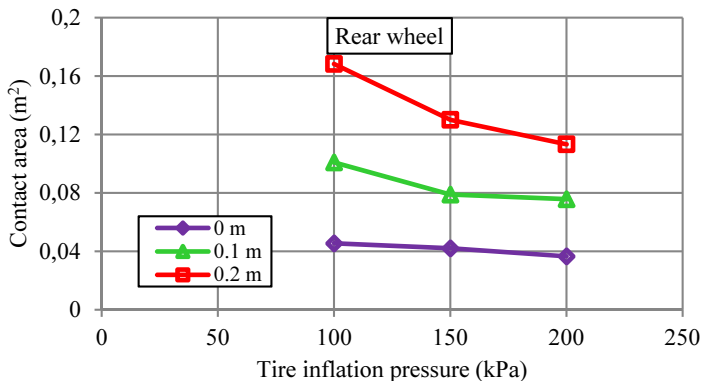


Figure 10. Variation of contact area with tire inflation pressure, at different soil depths under the rear wheel

The variation of contact pressure with soil depth at various tire inflation pressures under the rear wheel (Fig. 11) shows that the contact pressure increases with tire inflation pressure and decreases with soil depth.

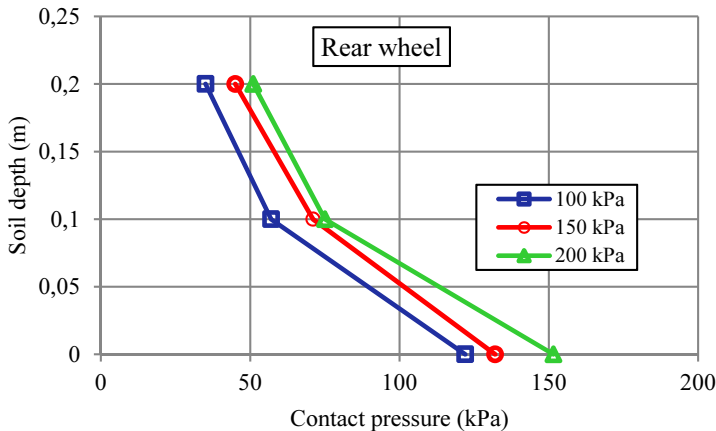


Figure 11. Variation of contact pressure with soil depth, at different tire inflation pressure under the rear wheel

At soil surface it was found that at 100 kPa tire inflation pressure, the contact pressure under the rear wheel increased by about 16% compared to that under the front wheel; at 150 kPa the increase was of 6% and at 200 kPa the increase was of 12%.

We should mention that a series of tests were also carried out in dynamic regime. However, the results that were obtained are not conclusive enough. In dynamic regime, although the time of wheel passage on the area where the sensor was mounted was quite short, it allowed the data to be recorded in the I-Scan software, but due to the unevenness of the field, the contact pressure was mainly distributed over the back edge and the outer edge of the wheel. This research topic remains of interest to the authors, and it requires further thoroughness to establish the most rigorous testing conditions (including the testing of several types of pressure sensors) for a better understanding of the phenomenon.

CONCLUSIONS

Having in view that the agricultural soil usually becomes compacted if the contact pressure exceeds 85 kPa, it can be said that under the tested conditions, for both wheels, compaction would mainly affect the topsoil (0 – 0.1 m depth), which has the advantage that it can be alleviated by superficial loosening. The layer of soil at a depth of 0.2 m is less predisposed to compaction.

Contact area is influenced by tire inflation pressure and wheel load. For both wheels, the largest contact areas were obtained at a depth of 0.2 m.

For the front wheel, by increasing tire inflation pressure from 100 kPa to 200 kPa at constant depth, the contact area decreased by 24% at soil surface, 13.7% at 0.1 m and 18.7% at 0.2 m depth. For the rear wheel, by increasing tire inflation pressure from 100 kPa to 200 kPa at constant depth, the contact area decreased by 19.5% at soil surface, 25% at 0.1 m and 32.7%

at 0.2 m depth. The increase of contact area does not necessary lead to the decrease of contact pressure in the soil, but rather to the limiting of high contact pressure in soil depth, so that the highest contact pressures are concentrated closer to the topsoil.

For both tested wheels, the recorded values of contact pressure at each depth are close because the contact area does not change significantly as tire inflation pressure varies. This is due to the fact that tire ribs are quite high and do not allow full contact of the intermediate area with the soil, regardless how small tire inflation pressure is.

ACKNOWLEDGEMENT

This work has been funded by University Politehnica of Bucharest, through the “Excellence Research Grants” Program, UPB–GEX2017, Ctr. No. 61/25.09.2017, internal number IS 25.17.03/2017 (COMP SOL).”.

REFERENCES

- Arvidsson, J. and Keller, T. (2007). Soil stress as affected by wheel load and tyre inflation pressure. *Soil Till. Res.*, vol. 96, pp. 284-291.
- Batey, T. (2009). Soil compaction and soil management – a review. *Soil Use and Management*, vol. 25, pp. 335–345.
- Biriș, S.Șt. (2010). *Mathematical modeling of soil compaction*, Printech Publishing, Bucharest, Romania.
- Birkas, M. (2014). *Book of soil tillage*. Published by Szent Istvan University Press.
- Chen G., Weil R. R. (2011). Root growth and yield of maize as affected by soil compaction and cover crops. *Soil and Tillage Research*, vol. 117, pp. 17-27.
- Ekinci, Ş. and Çarman, K. (2011). Effects on tire contact area of tire structural and operational parameters. 6th International Advanced Technologies Symposium (IATS’11), Elazig, Turkey.
- Fountas, S., Paraforos, D., Cavalaris, C., Karamoutis, C., Gemtos, T., Abu-Khalaf, N., Tagarakis, A. (2013). A five-point penetrometer with GPS for measuring soil compaction variability. *Computers and Electronics in Agriculture*, vol. 96, pp. 109-116.
- Hamza, M.A., Anderson, W.K. (2005). Soil compaction in cropping systems. A review of the nature, causes and possible solutions. *Soil & Tillage Research*, vol. 82, pp. 121-145.
- Lipiec, J. and Hatano, R. (2003). Quantification of compaction effects on soil physical properties and crop growth. *Geoderma*, vol. 116, pp. 107-136.
- Lozano, N., Rolim, M.M., Oliveira, V.S., Tavares, U.E., Pedrosa, E.M.R. (2013). *Soil & Tillage Research*, vol. 129, pp. 61-68.
- Nawaz, M., Bourrie’, G., Trolard, F. (2013). Soil compaction impact and modelling. A review. *Agron. Sustain. Dev.*, vol. 33 (2), pp. 291–309.
- Schjonning, P., van den Akker, J.J.H., Keller T., Greve M.G., Lamandé M., Simojoki A., Stettler, M., Arvidsson, J., Breuning-Madsen, H. (2016). Soil compaction. Ch 6. JCR Technical Reports – Soil threats in Europe. Status, methods, drivers and effects on ecosystem services. A review report, deliverable 2.1 of the RECARE project.

- Van den Akker, J.J.H. (2008). Soil compaction. In: Huber S., Prokop G., Arrouays D., Banko, G., Bispo, A., Jones, R.J.A., Kibblewhite, M.G., Lexer, W., Möller, A., Rickson, R.J., Shishkov, T., Stephens, M., Toth, G., van den Akker, J.J.H., Varallyay, G., Verheijen, F.G.A., Jones, A.R. (Eds.) Environmental Assessment of Soil for Monitoring: Vol. I. Indicators & Criteria. EUR 23490 EN/1, Office for the Official Publications of the European Communities, Luxembourg, pp. 107-124.
- Ziyae, A. and Roshani, M.R.. (2012). A survey study on soil compaction problems for new methods in agriculture. Intl. Res. J. Appl. Basic. Sci., vol. 3(9), pp. 1787-1801.
- Wulfsohn, D. (2009). Soil - tire contact area. Advances in Soil Dynamics. ASABE, vol. 3, pp. 59-84.
- Xia, K. (2011). Finite element modeling of tire/terrain interaction: Application to predicting soil compaction and tire mobility. Journal of Terramechanics, vol. 48, pp. 113-12.



FEM MODELLING OF MACHINERY INDUCED COMPACTION FOR THE SUSTAINABLE USE OF AGRICULTURAL SANDY SOILS

Nicoleta UNGUREANU^{1*}, Valentin VLĂDUȚ², Sorin-Ștefan BIRIȘ¹,
Gigel PARASCHIV¹, Mirela DINCĂ¹, Bianca Ștefania ZĂBAVĂ¹,
Vasilica ȘTEFAN², Nelus Evelin GHEORGHÎĂ¹

¹Department of Biotechnical Systems, Faculty of Biotechnical Systems Engineering, University Politehnica of Bucharest, Splaiul Independentei Blv., no. 313, sector 6, Bucharest, Romania

²National Institute of Research - Development for Machines and Installations Designed to Agriculture and Food Industry – INMA, Ion Ionescu de la Brad Blv., no. 6, sector 1, Bucharest, Romania

E-mail of corresponding author: nicoletaung@yahoo.com

SUMMARY

The anthropogenic compaction of agricultural soil depends mainly on the type of soil, soil moisture, wheel load, tire inflation pressure, size and shape of footprint area, contact pressure and number of passes. This paper aims to assess the depth to which soil compaction would occur, by modelling the distribution of stresses and displacements in sandy soil under wheel loads applied by an agricultural trailer. Modelling by Finite Element Method was performed in the Quickfield Student program using the 2D geometric model of plane load. For known characteristics of the soil, at various wheel loads (4.5, 13 and 21 kN) and tire inflation pressures (180, 240 and 300 kPa) were obtained the models of stress distribution in soil depth and the models of soil displacement. It was also obtained the stress in increments of 100 mm in soil depth. The models show that for 4.5 kN and 13 kN wheel loads, regardless tire inflation pressure, the topsoil would become compacted, while 21 kN wheel load, at 240 kPa and 300 kPa increases the risk of subsoil compaction.

Keywords: compaction, wheel load, tire inflation pressure, stress, displacement.

INTRODUCTION

Human interventions in the use of the world's natural resources are resulting in their degradation, with long term consequences. Soil is a vital part of every ecosystem and one of

the most important resources that we depend on, and its health is the basis for sustained food security. In terms of sustainability, soil degradation is defined as the current and/or future reduction in its capacity to perform ecosystem functions and services (including those of agro-ecosystems and urban systems) that support society and development (Lee and Schaaf, 2006).

Soil compaction is one of the twelve forms of soil degradation identified in the European Union (Stolte et al., 2016). It has natural or anthropogenic causes and it occurs when soils are subjected to stresses exceeding their strength (Khodaei et al., 2016). Most regions of the world have compacted soils, but the negative economic impact of soil compaction is most severe in the countries most dependent on agriculture for their incomes (Maheshwari, 2012). Worldwide, compaction accounts for 4% (68.3 mil. ha) of anthropogenic soil degradation, while in Europe, compaction accounts for 17% of the total degraded area (Alakukku, 2012). In Central and Eastern Europe, 25 mil. ha are lightly compacted and 36 mil. ha are severely compacted (Soil Atlas). In 2015, Romania had 6.5 mil. ha of arable soils affected by anthropogenic compaction and 2 mil. ha affected by natural compaction (Ungureanu N., 2015). The factors that influence soil compaction are presented in Figure 1.

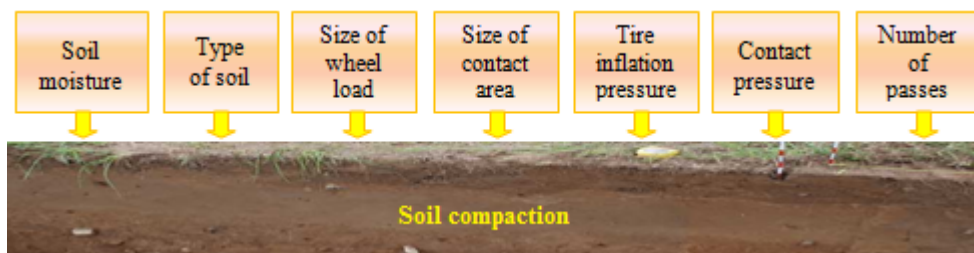


Figure 1. Factors of influence on soil compaction

In anthropogenic compaction, stress applied by agricultural machinery, often on soils with high moisture, is transmitted at different depths through the footprint, resulting in topsoil and/or subsoil compaction. Topsoil compaction (until a depth of 300 mm) reduces crop yield but it can be alleviated by tillage and soil biota (Schjønning et al., 2016). Crop yield loss of 14% was reported in the first year after repeated wheel traffic on agricultural soils in seven countries in Europe and North America (Gysi et al., 2001). Subsoil compaction (300 mm and deeper) is more persistent and the compacted layer cannot be removed by conventional tillage (Wolkowski and Lowery, 2008). The higher the wheel load, the larger is the depth at which stress is distributed in the soil. Due to the applied stress, the soil becomes compacted, and its functions and quality are affected with consequences on crop production, food sustainability and the economic stability of farmers.

Worldwide, research and technology transfer efforts have increased the awareness on soil compaction. Various pseudo-analytical models and modelling techniques can predict the response of soil to the passage of agricultural vehicles. This paper aims to obtain, by the Finite Element Method, the models of stress distribution in sandy soil for different wheel loads and tire inflation pressures and to estimate the depth of compaction in each case. Such models can be adapted for other types of soils and machinery, giving useful information to farmers and designers of agricultural machinery on the depth at which compaction would appear, helping to minimize the risk of compaction and to increase soil sustainability.

MATERIALS AND METHODS

The Finite Element Method (FEM) is actually the most advanced numerical method that idealizes the soil to an elastic-plastic material. FEM requires the generation of a large number of finite elements to obtain highly accurate results and is successfully applied to simulate the distribution of stress and displacement in soil depth.

Input parameters for FEM modelling were the properties of sandy soils, which were not determined experimentally by the authors, but their values were taken over as they were presented in the study of Gysi et al. (2001). In Romania, sandy soil is widely found in Dăbuleni - Olt County, an agricultural region intensely affected by wind erosion and drought (known as the Romanian desert). As agricultural machinery it was chosen a trailer commonly used for transport of fruits and vegetables in Dăbuleni farmlands. Other input parameters are the footprints and contact pressures determined in laboratory (Ungureanu, 2015), for various wheel loads ($Q = 4.5 \text{ kN}, 13 \text{ kN}$ and 21 kN) and tire inflation pressures ($p_i = 180 \text{ kPa}, 240 \text{ kPa}$, and 300 kPa). We should mention that data presented in this paper is part of an extended study that included various soils, loads and tire inflation pressures.

Table 1. Input parameters for FEM modelling

Soil parameters for FEM modelling		Trailer parameters for FEM modelling			
Properties	Value	Wheel load, kN	Tire inflation pressure, kPa	Footprint area, m ²	Contact pressure, kPa
Young's modulus of elasticity (E), kPa	13000	4.5	180	0.03	146
Poisson's ratio (ν), -	0.3		240	0.028	163
Cohesion (c), kPa	2		300	0.023	194
Internal friction angle (ϕ), °	32	13	180	0.066	194
Density (ρ), kg·m ⁻³	2040		240	0.056	227
Moisture (w), %	6.5		300	0.051	251
				180	0.099
		21	240	0.077	272
			300	0.073	288

Modelling by FEM was achieved in Quickfield Student program, using the 2D geometric model of plane load (Fig. 2). A volume of soil of 1 m^3 was considered, and on its surface was applied a pressure plate with the area equal to the area of footprint between the soil and tire. Over the pressure plate was applied an evenly distributed load (see the upper corner of the meshed section in Fig. 2), with the aim to simulate the action of a wheel at soil surface.

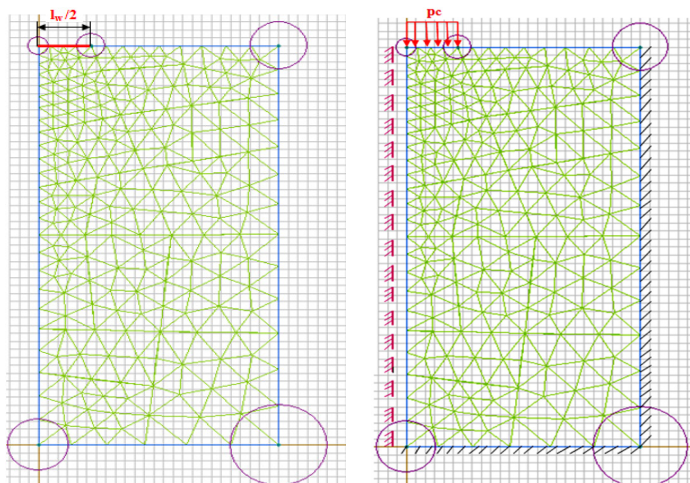


Figure 2. Meshed model of the analyzed volume of soil

Considering the same soil properties in Table 1, Gysi et al. (2001) suggested the use of unevenly distributed loads for FEM modelling of soil compaction underneath the tires of agricultural machinery, because their study revealed that stress profile was more realistic compared to that obtained for uniform load distribution. However, for simplifying reasons, in most FEM studies the load is uniformly distributed at soil-tire interface. To achieve the highest accuracy of results, the model in Figure 2 was meshed to 250 nodes, with smaller sizes of the finite elements in the area where the stress is concentrated. The mesh has been fitted with two-way fixations to allow soil movement only in the vertical direction.

RESULTS AND DISCUSSION

Although the complete stress state is very relevant for changes in soil functions due to stresses applied by agricultural machinery, most studies (including ours) are focused on the vertical component of soil stress. Future research on stress distribution should include the complete stress state.

The values of maximum and minimum stress, respectively soil displacement in the sandy soil, obtained by FEM modelling, are presented in Table 2 and Figures 3 - 8.

Table 2. Output parameters obtained by FEM modelling

Wheel load, kN	Tire inflation pressure, kPa	Maximum stress, kPa	Minimum stress, kPa	Maximum displacement, mm
4.5	180	90.6	1.88	3.06
	240	99.81	1.94	3.41
	300	98.6	1.6	3.47
13	180	124	3.0	4.91
	240	144	3.4	5.59
	300	157	3.4	5.86
21	180	137	3.3	5.37
	240	172	4.0	6.73
	300	180	4.0	6.73

In Figure 3 is presented the spatial distribution of equivalent stress by von Mises criterion, respectively soil displacement, for 4.5 kN wheel load and 180 kPa tire inflation pressure. These models correspond to a contact pressure of 146 kPa, evenly distributed in the footprint area of 0.03 m². Modelling results have shown that the maximum stress of 90.6 kPa is concentrated in the topsoil to a depth of about 150 mm. This phenomenon is due to flow and agglomeration of soil particles under the action of wheel load, which resulted in the formation of a denser layer of soil. Stress that propagate under this layer decrease with soil depth. Minimum stress is 1.88 kPa and maximum displacement is 3.06 mm.

Increasing tire inflation pressure to 240 kPa and keeping wheel load constant, for 163 kPa contact pressure and 0.028 m² footprint area, it resulted a maximum stress of 99.8 kPa (at 120 mm depth), minimum stress of 1.94 kPa and maximum soil displacement of 3.41 mm.

Figure 4 shows the models for 4.5 kN wheel load and 300 kPa tire inflation pressure, with contact pressure of 194 kPa and footprint area of 0.023 m². Maximum stress of 98.6 kPa is found at 100 mm below soil surface, minimum stress is 1.6 kPa and maximum displacement is 3.47 mm.

Figure 5 shows the distribution of equivalent stress by von Mises criterion, respectively soil displacements, for 13 kN wheel load and 180 kPa tire inflation pressure, for contact pressure of 194 kPa and footprint area of 0.066 m². Maximum stress (124 kPa) is found at 150 mm, minimum stress is 3 kPa and maximum displacement of 4.91 mm.

For 13 kN wheel load and 240 kPa tire inflation pressure were obtained 227 kPa contact pressure and 0.056 m² footprint area. The maximum stress was 144 kPa (at about 120 mm depth), minimum stress was 3.4 kPa and maximum displacement of 5.59 mm.

At 13 kN wheel load and 300 kPa tire inflation pressure (Fig. 6), it resulted a contact pressure of 251 kPa distributed in footprint area of 0.051 m². It can be seen that the highest stress of 157 kPa is found at 140 mm below soil surface, minimum stress is 3.4 kPa, and maximum soil displacement is 5.86 mm.

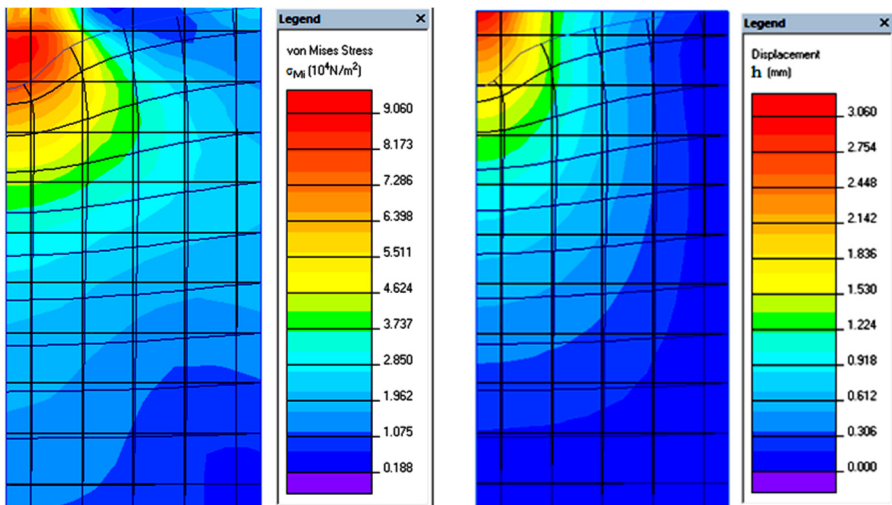


Figure 3. Stress and displacement, at 4.5 kN wheel load and 180 kPa tire inflation pressure

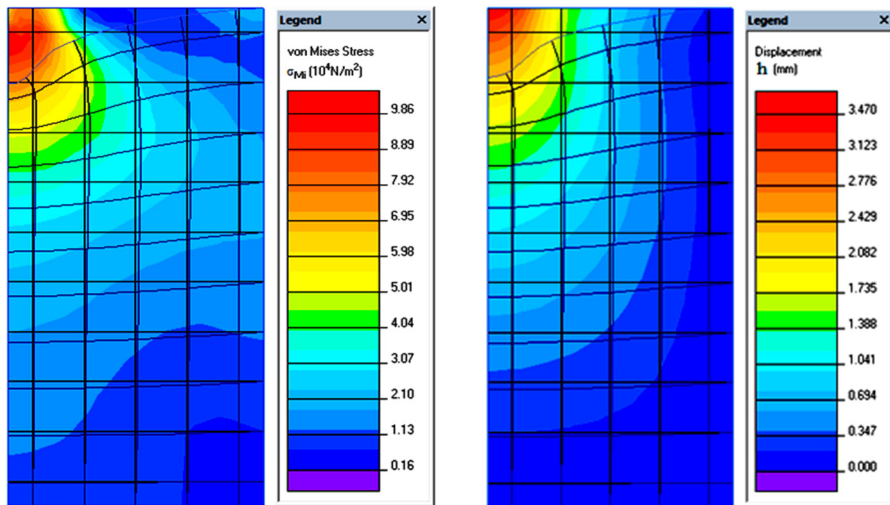


Figure 4. Stress and displacement, at 4.5 kN wheel load and 300 kPa tire inflation pressure

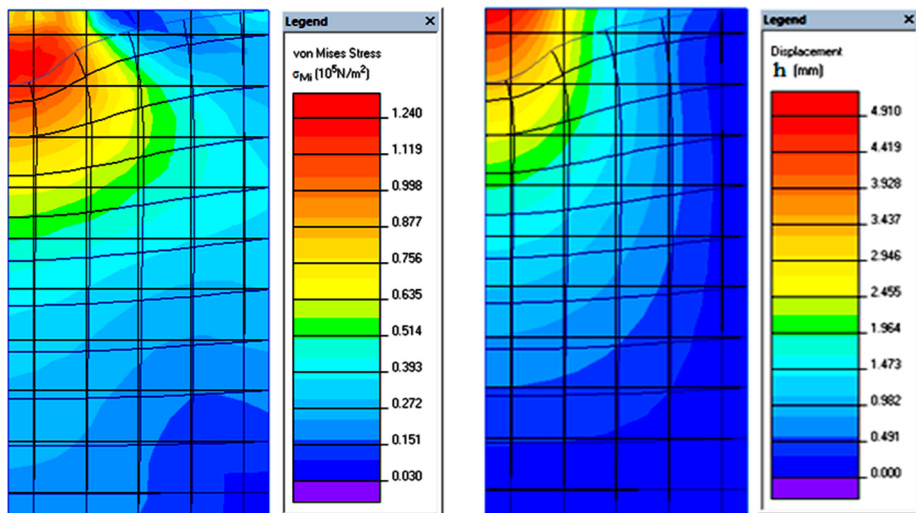


Figure 5. Stress and displacement, at 13 kN wheel load and 180 kPa tire inflation pressure

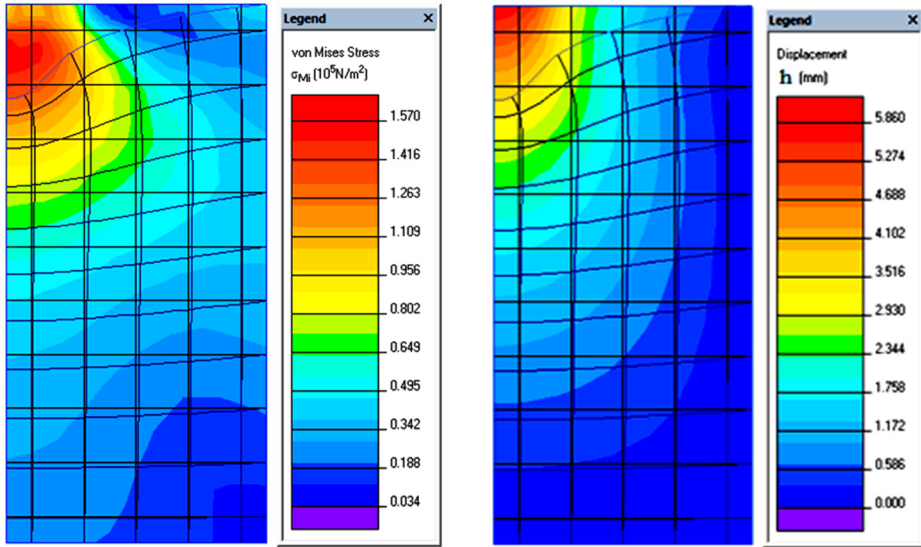


Figure 6. Stress and displacement, at 13 kN wheel load and 300 kPa tire inflation pressure

For 21 kN wheel load and tire inflation pressure of 180 kPa (Fig. 7), contact pressure of 214 kPa and footprint area of 0.099 m², maximum stress of 137 kPa occurs at approximately 150 mm depth, minimum stress is 3.3 kPa and soil displacement is 5.37 mm.

For 21 kN wheel load, 240 kPa tire inflation pressure, contact pressure is 272 kPa and footprint area 0.077 m², which resulted in a maximum stress of 172 kPa, minimum stress of 4 kPa, and maximum displacement of 6.73 mm.

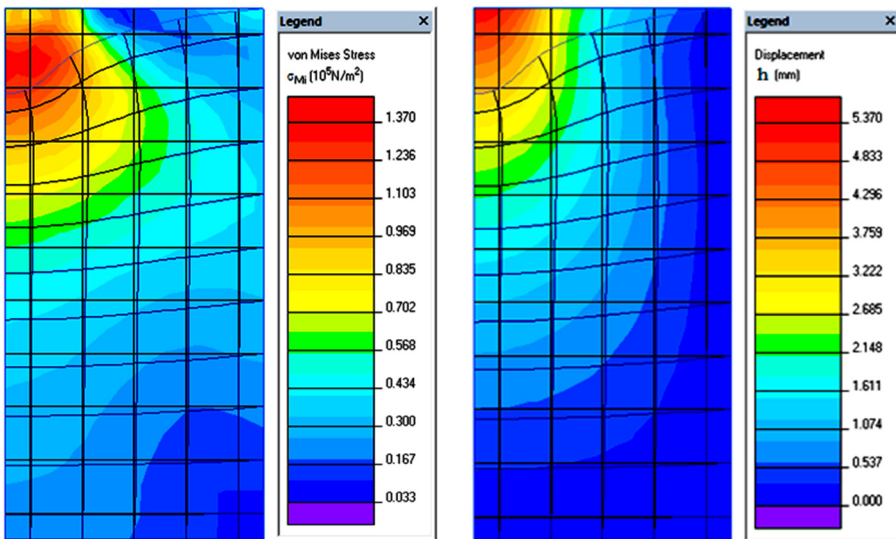


Figure 7. Stress and displacement, at 21 kN wheel load and 180 kPa tire inflation pressure

The models in Figure 8 were obtained for 21 kN wheel load and 300 kPa tire inflation pressure, for contact pressure of 288 kPa and footprint area of 0.073 m². It was found that the highest soil stress of 180 kPa is concentrated in the topsoil, the minimum stress is 4 kPa, and the maximum displacement is 6.73 mm.

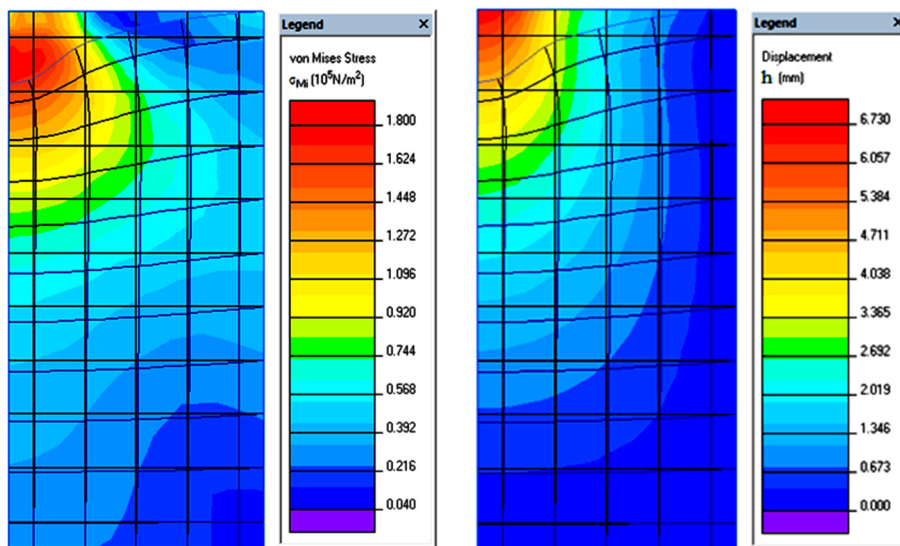


Figure 8. Stress and displacement, at 21 kN wheel load and 300 kPa tire inflation pressure

Equivalent stress by von Mises criterion, obtained by FEM modelling and distributed in the sandy soil down to 1000 mm depth, in increments of 100 mm, are summarized in Table 3.

Table 3. Variation of von Mises equivalent stress with the depth of sandy soil

Soil depth, mm	Tire inflation pressure, kPa								
	180			240			300		
	Wheel load, kN = 4.5			Wheel load, kN = 13			Wheel load, kN = 21		
Equivalent stress, kPa									
0	58.928	62.596	62.214	74.846	98.612	96.419	82.583	117.99	110.78
50	84.263	90.863	94.947	101.973	142.08	137.23	112.95	154.47	157.67
150	84.558	88.057	77.851	116.757	132.86	142.34	127.72	159.52	163.53
250	60.886	60.760	52.159	88.001	99.220	104.65	96.174	119.5	120.28
350	44.451	44.053	37.042	66.517	73.769	76.997	72.464	88.940	88.461
450	33.670	33.241	27.757	50.805	56.331	58.544	55.285	67.912	67.260
550	26.634	26.255	21.828	40.472	44.769	46.392	44.013	53.937	53.299
650	21.984	21.630	17.926	33.624	37.096	38.339	36.551	44.738	44.047
750	18.826	18.500	15.303	28.861	31.802	32.856	31.366	38.366	37.748
850	16.474	16.182	13.372	25.293	27.856	28.765	27.485	33.608	33.048
950	13.926	13.676	11.294	21.403	23.565	24.323	23.256	28.431	27.945
1000	12.818	12.587	10.392	19.708	21.696	22.390	21.413	26.176	25.724

The agricultural soil usually becomes compacted if the stress is higher than 80 kPa, resulting in the blocking of root emergence of plants (Biriş, 2010; Tekin and Okursoy, 2007). From this reasoning and in accordance with data in Table 3, we can estimate that under the studied conditions, compaction would occur thus:

- a) at 4.5 kN wheel load: for all tire inflation pressures, in the topsoil to a depth of 50-150 mm;
- b) at 13 kN wheel load: for all tire inflation pressures in the topsoil; for 180 kPa – to a depth of 50-250 mm; for 240 kPa – at 0-300 mm; for 300 kPa – at 0-300 mm.
- c) at 21 kN wheel load: in the topsoil for 180 kPa – to a depth of 0-300 mm; in the subsoil for 240 and 300 kPa – at 0-350 mm.

The few studies on stresses distribution have reported their results in a very empirical way, which makes it difficult to draw general conclusions on the influence of wheel load, tire inflation pressure, tire characteristics and soil properties (Lamande and Schjonning, 2008). Most researchers have studied the distribution of stress at soil-tire interface, obtaining different vertical stress distributions, parabolic or U-shaped, for different types of soils, loads and tires (Cui et al., 2007).

The models obtained in our theoretical study show that tire inflation pressure influences the topsoil compaction and wheel load has the most significant influence on stress distribution in the subsoil.

Similar results were obtained by Arvidsson and Keller (2007), who found that the maximum stress in the subsoil was mainly determined by wheel load, while tire inflation pressure had no significant effect on stresses measured in the subsoil.

Also, the experiments conducted on clay loamy soil by Gonzales et al. (2013) show tire behavior for 100 kPa and 325 kPa tire inflation pressure under a wheel load of 0.7 kN, corresponding to contact pressures of 100 kPa and 240 kPa. The difference in vertical stress distributed in the soil was higher in the topsoil and negligible under a depth of 80 mm. In this case the inflation pressure and contact pressure influences only the superficial layer to a depth of 80 mm. For a wheel load of 2.3 kN, the influence of inflation pressure and contact pressure reaches a depth of 140 mm. Hence, contact pressure and tire inflation pressure only influence the vertical stresses in the topsoil, where most of the compaction takes place. Below 150 mm depth, only the wheel load generates vertical stresses.

During compaction, there are not significant differences between the stresses distributed in sandy and clayey soil. Nevertheless, soil displacement is smaller on sandy soils than on clayey soils. This is confirmed by Ungureanu (2015), where FEM modelling was made considering the same agricultural trailer with the same wheel loads and tire inflation pressures, but on clayey soil, and in all situations, soil displacement was 4 times higher than in sandy soil. For example, at 4.5 kN wheel load and 300 kPa tire inflation pressure, soil displacement was 14.5 mm, while at 21 kN and 300 kPa, soil displacement was 28.1 mm.

CONCLUSIONS

The study shows that at constant tire inflation pressure, footprint area increases with increasing wheel load. The increase of footprint area does not mean a lower intensity of stress in the soil, but the concentration of stress in the topsoil.

At 180 kPa tire inflation pressure, the maximum stress decreased from 137 kPa at maximum wheel load (21 kN) to 124 kPa at 13 kN wheel load and finally to 90.6 kPa at minimum wheel load (4.5 kN). By increasing tire inflation pressure to 300 kPa, maximum stress increased to: 180 kPa at 21 kN, 157 kPa at 13 kN and 98.6 kPa at 4.5 kN wheel load.

In terms of depth, the maximum stress was concentrated to about 100-150 mm near soil surface. Smaller, but yet significant stress were distributed deeper into the soil as wheel load increased.

To reduce compaction, farmers should operate the trailer with low inflation pressures and reduced wheel loads. Thus, footprint area increases, stress is distributed at shallower depths, and compaction is easier to alleviate by loosening works.

Continuous investigations for the proper understanding of the processes involved in compaction are needed in order to maintain soil sustainability and to prevent future challenges on global food security.

ACKNOWLEDGEMENT

This work has been funded by University Politehnica of Bucharest, through the "Excellence Research Grants" Program, UPB-GEX2017, Ctr. No. 61/25.09.2017, IS 25.17.03/2017 (COMPSOL)".

REFERENCES

- Alakukku, L. (2012). Combating soil degradation. Soil compaction. Ecosystem Health and Sustainable Agriculture 1. Sustainable Agriculture (C Jakobsson, eds), The Baltic University Programme, Uppsala University, 217-221.
- Arvidsson, J. and Keller, T. (2007). Soil stress as affected by wheel load and tyre inflation pressure. *Soil & Tillage Research* 96: 284-291.
- Biriș, S. Șt. (2010). Mathematical modeling of soil compaction. Printech Publishing, Bucharest, Romania.
- Cui, K., Defosse, P., Richard, G. (2007). A new approach for modelling vertical stress distribution at the soil/tyre interface to predict the compaction of cultivated soils by using the PLAXIS code. *Soil & Tillage Research* 95: 277-287.
- Gonzales Cueto, O., Iglesias Coronel, C.E., Recarey Morfa, C.A., Urriolagoitia Sosa, G., Hernández Gómez, L.H., Urriolagoitia Calderón, G., Herrera Suárez, M. (2013). Three dimensional finite element model of soil compaction caused by agricultural tire traffic. *Computers and Electronics in Agriculture* 99: 146-152.
- Gysi, M., Maeder, V., Weisskopf, P. (2001). Pressure distribution underneath tyres of agricultural vehicles. *Transactions of the ASABE* 44(6): 1385-1389.
- Khodaei, M., Fattahi S. H., Navid H. (2016). Evaluation of FEM modelling for stress propagation under pressure wheel of corn planter. *Agricultural Engineering International: CIGR Journal* 18(3): 14-22.
- Lamande, M. and Schjonning, P. (2008). The ability of agricultural tyres to distribute the wheel load at the soil-tyre interface. *J. Terramech.* 45: 109-120.
- Lee, C. and Schaaf, T. (2006). The future of drylands. International Scientific Conference on Desertification and Drylands Research Tunis, Tunisia, Springer.
- Maheshwari, D.K. (2012). Bacteria in agrobiolgy: stress management. Springer – Verlag Berlin Heidelberg.
- Schjonning, P., van den Akker, J.J.H., Keller, T., Greve, M.G., Lamandé, M., Simojoki, A., Stettler, M., Arvidsson, J., Breuning-Madsen, H. (2016). Soil compaction. Ch 6. JCR Technical Reports – Soil threats in Europe. Status, methods, drivers and effects on ecosystem services. A review report, deliverable 2.1 of the RE CARE project.
- Soil Atlas (http://eusoiils.jrc.ec.europa.eu/projects/Soil_Atlas/Pages/115.html).

- Stolte, J., Tesfai, M., Øygarden, L., Kværnø, S., Keizer, J., Verheijen, F., Panagos, P., Ballabio, C., Hessel, R. (2016). JCR Technical Reports – Soil threats in Europe. Status, methods, drivers and effects on ecosystem services. A review report, deliverable 2.1 of the RECARE project.
- Tekin, Y., Okursoy, R. (2007). Development of a hydraulic-driven soil penetrometer for measuring soil compaction in field conditions. *Journal of Applied Sciences* 7: 918-921
- Ungureanu, N. (2015). Contributions to the modelling of artificial compaction of agricultural soil. Doctoral thesis. University Politehnica of Bucharest, Romania.
- Wolkowski, R. and Lowery, B. (2008). Soil compaction: causes, concerns, and cures, A3367 (<http://www.soils.wisc.edu/extension/pubs/A3367.pdf>).



UTJECAJ TEHNIČKIH ČIMBENIKA RASPRŠIVANJA NA ZEMLJIŠNO I ZRAČNO ZANOŠENJE TEKUĆINE U NASADU VIŠNJE

Davor PETROVIĆ*, Đuro BANAJ, Vjekoslav TADIĆ, Dario KNEŽEVIĆ,
Anamarija BANAJ

Poljoprivredni fakultet Sveučilišta J. J. Strossmayera u Osijeku, Zavod za mehanizaciju,
Vladimira Preloga 1, 31000 Osijek

E-mail dopisnog autora: pdavor@pfos.hr

SAŽETAK

U radu su prikazani rezultati istraživanja utjecaja čimbenika raspršivanja na zemljišno i zračno zanošenje tekućine u nasadu višnje s raspršivačem Agromehanika AGP 200 ENU. Istraživanje se obavlja prema ISO normi 22866 (uređaji u zaštiti bilja - metode mjerenja zanesene tekućine u poljskim uvjetima). Ispituje se utjecaj norme raspršivanja kao čimbenik A, tip mlaznica kao čimbenik B i brzina zračne struje ventilatora kao čimbenik C. Za raspršivanje i evaluaciju zanesene tekućine koristi se otopina organske boje Tartazine s koncentracijom od 4%. Filter papirići koji služe kao kolektori postavljaju se prema navedenoj normi direktno u zoni raspršivanja. Neposredno poslije svake aplikacije filter papirići se prikupljaju i spremaju na tamno i hladno mjesto. Uzorkovani filter papirići ispiru se sa 10 ml deionizirane vode u laboratorijskim uvjetima. Nakon ispiranja intenzitet obojenosti tj. valna duljina otopine očitava se sa spektrofotometrom (Varian Cary 50 UV-Visible). Sa različitim kombinacijama tehničkih čimbenika raspršivanja ostvaruju se različiti intenziteti zanošenja, kako zemljišnog, tako i zračnog zanošenja. Najveći gubitak tekućine (zanošenje) ostvaruje se sa čimbenicima $A_1B_1C_2$ (norma 250 l ha^{-1} ; mlaznica TR; zrak 3), a najmanji gubitak ostvaruje norma od 200 l ha^{-1} ; mlaznica ITR i zrak 2 (tretman $A_2B_2C_1$).

Gljučne riječi: zanesena tekućina, norma raspršivanja, brzina zraka, mlaznice, raspršivač

UVOD

Sredstva za zaštitu bilja postaju dio našeg svakodnevnog života. Nalaze se u cjelokupnom agroekološkom sustavu u poljoprivrednom zemljištu, vodotokovima, uskladištenim proizvodima. U idealnom slučaju pesticid bi trebao biti toksičan samo za ciljane organizme,

da je bio razgradiv i ekološki prihvatljiv. Nažalost nerijetko je slučaj da štetno djeluje i na bezopasne i korisne organizme. Smanjenje zanošenja tekućine izvan ciljanog prostora zaštite bilja i poboljšanje učinkovitosti aplikacije pesticida ciljevi su Europske direktive *128/2009/E2*, u kojoj se navodi da je svaka članica EU dužna donijeti akcijski plan održive uporabe pesticida.

Ovisno o intenzitetu upotrebe kemijskih sredstava za zaštitu bilja pojavljuju se kratkotrajni i dugoročni negativni učinci na okoliš Maghsoudi i Minaei (2013). Tehnologija za smanjenje zanošenja tekućine izvan ciljanog prostora zaštite bilja svodi se na proučavanje i unapređenje kvalitete raspršivanja s obzirom na veličinu kapljica, brzinu gibanja, klimatološke uvjete i niz drugih važnih čimbenika. Istraživači u ovom području suočavaju se s izazovom do koje granice je moguće optimizirati raspršivanje a da pokrivenost tretirane površine ostane optimalna, a s time i biološka učinkovitost pesticida.

Glavni cilj aplikacije zaštitnih sredstava je dobiti što ravnomjerniju pokrivenost lisne površine s optimalnim depozitom. Loša raspodjela tekućine ima za rezultat velike gubitke pesticida koji mogu smanjiti učinkovitost raspršivanja i povećati opasnost od zagađenja okoliša Verduyze i sur. (1999).

Mnogi autori bave se proučavanjem važnosti tehnike aplikacije pesticida. Brzinu zračne struje istražuju: Pergher i sur. (1997); Cunningham i Harden (1999); De Moor i sur. (2000); Wei i sur. (2016), normu raspršivanja Pergher i Petris (2008a); Tadić, V. (2013), položaj i orijentaciju mlaznica Farooq i Landers (2004), vrstu i veličinu mlaznica Zhu i sur. (2004); Derksen i sur. (2007) i brzinu gibanja raspršivača Celen i sur. (2008); Marucco i sur. (2008). Na pravilnu depoziciju sredstva za zaštitu bilja utječu razni čimbenici kao što su: struktura i oblik krošnje, fizikalno-kemijska svojstva pesticida, agroklimatološki uvjeti i primijenjena tehnika raspršivanja koje proučavaju slijedeći autori: Catania i sur. (2011); Rossel i sur. (2012); Vallet i Tenet (2013).

Tadić (2013) proučava utjecaj različitih ISO veličina mlaznica na optimalnu pokrivenost površine i intenzitet zanošenja unutar trajnih nasada, te navodi da mlaznice manjeg ISO broja ostvaruju bolju pokrivenost tretirane površine, ali zbog manje veličine kapljica ostvaruju povećano zanošenje.

Djelotvornost zračne mase prilikom raspršivanja u trajnim nasadima ovisi o brzini i geometriji zračne struje koju generira ventilator raspršivača Holownicki i sur. (2000); Panneton i sur. (2005).

Brzinu zračne struje s različitim čimbenicima podešavanja istražuju Tadić i sur. (2014); Banaj i sur. (2014). Zande i sur. (2014) navode da je zračno zanošenje tekućine 2,5 - 3 puta veće od zemljišnog zanošenja. Na udaljenosti od 5 m od zadnjeg reda stabala u trajnom nasadu zanošenje tekućine iznosilo je 11% - 23% norme raspršivanja kod nasada u punoj lisnoj masi. U istom nasadu ostvareno je smanjenje zanošenja tekućine 25% - 77% u fazi mirovanja, što pokazuje direktan utjecaj zračne struje s obzirom na stadij razvoja stabla i potrebe za prilagođavanjem izlazne brzine zraka.

Miranda-Fuentes i sur. (2015) navode da brzina zračne struje utječe na depozit unutar krošnje. Prevelika brzina zračne struje dovodi do loše pokrivenosti i prekomjernog zanošenja pesticida izvan ciljanog prostora zaštite bilja, dok nedovoljna količina zračne struje kao posljedicu ima lošu pokrivenost i depozit u gornjim slojevima krošnje. Učinkovitost aplikacije možemo definirati kao omjer depozita pesticida na ciljanom objektu raspršivanja (krošnji) i ukupne količine norme raspršivanja pesticida koji je upotrebljen. Za evaluaciju neželjeno zanesene tekućine upotrebljavaju se različite metode vizualizacije: fluorescentne i vidljive boje, vodoosjetljivi papirići. Najraširenija je upotreba fluorescentnih i vidljivih boja koje nisu opasna za ljudsku uporabu.

Brojni autori upotrebljavaju ovu vrstu boje za detekciju i evaluaciju zanesene tekućine: Zhu i sur. (2006); Nuyttens i sur. (2007); Wenneker i sur. (2008); Bjugstad i Hermansen (2009).

Za sakupljanje zanesene tekućine izvan ciljanog prostora bilja koriste se razni kolektori tj. sakupljači od različitih vrsta materijala i oblika. Istraživanja pokazuju da je filter papir najprihvatljiviji s obzirom na cijenu i učinkovitost, te se koristi u brojnim istraživanjima: De Schampheleire i sur. (2008); Godyn i sur. (2008).

Cilj istraživanja je utvrditi utjecaj različito podešenih tehničkih čimbenika raspršivanja na zemljišno i zračno zanošenje tekućine upotrebom raspršivača *Agromehanika AGP 200 ENU* u trajnom nasadu višnje te na temelju rezultata doći do saznanja koja kombinacija tehničkih parametara ostvaruje najmanje zanošenje tekućine izvan ciljanog prostora zaštite bilja.

MATERIJAL I METODE

Istraživanje je obavljeno prema *ISO normi 22866* (uređaji u zaštiti bilja - metode mjerenja zanesene tekućine u poljskim uvjetima) u nasadu višnje uzgojnog oblika popravljena piramida. U istraživanju je korišten nošeni raspršivač *Agromehanika AGP 200 ENU* (sl. 1.) opremljen sa visinskim usmjerivačima zraka visine 117 cm i širine 11 cm. Promjer ventilatora iznosi 585 mm proporcionalno podesiv u pet stupnjeva. Protok zračne struje koju iznosi cca. 12000 m³ h⁻¹ kada su lopatice postavljene u položaj 1, a postavljanjem lopatica u položaj 5 protok zračne struje iznosi cca. 32000 m³ h⁻¹. Izlazna brzina zračne struje kreće se u rasponu od 10 do 35 m s⁻¹. Najveća dopuštena brzina okretaja ventilatora je 1800 min⁻¹. Na raspršivač se postavljaju dva tipa mlaznica *TR 8002* i *ITR 8002* proizvođača *Lechler*. Raspršivač je opremljen sukladno europskoj normi *EN 13790* s tri spremnika tekućine, od kojih je glavni spremnik obujma 200 litara. Na raspršivač je instalirana klipno - membranska crpka proizvođača *Agromehanika* kapaciteta 61 l min⁻¹ (model crpke *BM 65/30* s dvije membrane) pri radnom tlaku od 30 bar. Brzina zračne struje podešava se promjenom položaja lopatica na ventilatoru.



Slika 1. Raspršivač *Agromehanika AGP 200 ENU*
Figure 1. *Agromehanka AGP 200 ENU* orchard sprayer

Standardna mlaznica *Lechler TR 8002* stvara mlaz pod radnim kutom od 80° koji je šuplje konusne izvedbe i koristi se u zaštiti voćnjaka i vinograda. Protok mlaznice iznosi 0,8 l min⁻¹ pri radnom tlaku od 3 bar. Mlaznica je izrađena od plastičnih polimera s keramičkim uloškom koji se može izvaditi iz tijela mlaznice radi čišćenja. Ovaj tip mlaznice stvara vrlo veliki broj malih kapljica koje ostvaruju dobru pokrivenost tretirane površine, sa osjetljivošću na zanošenje.

Zračno - injektorska mlaznica konusnog mlaza proizvođača *Lechler ITR 8002* posebno je konstruirana za smanjenje intenziteta zanošenja tekućine. Tijelo mlaznice izrađeno je od plastičnih polimera s keramičkim uloškom otpornim na trošenje koji je promjenjiv. Protok od 0,8 l/min ostvaruje pri tlaku od 3 bar, a kut prskanja je 80°. Ovaj tip mlaznica stvara veći promjer kapljica nego što je to slučaj kod *TR* mlaznica, što u velikoj mjeri smanjuje pojavu zanošenja tekućine. Slika 2. prikazuje nosač mlaznica na koji se postavljaju ispitivane mlaznice.



Slika 2. Lechler ITR 8002 i TR 8002 mlaznice
Figure 2. Lechler ITR 8002 and TR 8002 nozzles

Kao čimbenik *A* ispituje se norma raspršivanja. Koristi se optimalna norma raspršivanja A_1 (250 l ha⁻¹ - izračunava se prema trenutnom stanju nasada i obujmu lisne mase), te A_2 norma raspršivanja, koja se smanjuje za 30% (200 l ha⁻¹). Kao drugi tehnički čimbenik promatra se utjecaj tipa standardne mlaznice B_1 (*Lechler TR 80 02 C*) i mlaznice sa smanjenim zanošenje tekućine: *Lechler ITR 80 02 C* – čimbenik B_2 . Čimbenik C označava utjecaj zračne struje na zanošenje tekućine. C_1 označava brzinu zračne struje ventilatora izračunata prema obujmu lisne mase (3. položaj lopatica prema tehničkim specifikacijama) i brzinu zračne struje smanjene za 30 % (2. položaj lopatica prema tehničkim specifikacijama) – čimbenik C_2 .

Vremenski uvjeti tijekom pokusa prate se pomoću pokretne meteorološke stanice tvrtke *Hobo*. Prate se slijedeći čimbenici: brzina vjetera, smjer vjetera, temperatura, relativna vlažnost zraka, odnosno svi parametri koji imaju direktan utjecaj na tehničke čimbenike zaštite bilja. Tijekom istraživanja koristi se organska boja *Tartrazine* s koncentracijom od 4 % (*Acros Organics*) za bojanje tekućine s kojom se obavljala aplikacija.

Za prikupljanje zanesene tekućine kao kolektori koriste se filter papirići proizvođača *Technofil* (površine 35 cm²). Filter papirići za sakupljanje zemljišnog zanošenja tekućine postavljaju se na horizontalne nosače na površinu tla. Kolektori se postavljaju na duljinu od 20 m s razmakom od 0,5 m na prvih 10 m, dok je na drugih 10 m razmak iznosi 1 m. Mjerenje zanošenja počinje između dva stabla u redu koji se tretira. Koristi se 30 kolektora poslaganih u četiri ponavljanja (120 po tretmanu).

Filter papirići korišteni za prikupljanje zračnog zanošenja tekućine vertikalno se postavljaju na visini od 5 m sa razmakom od 0,5 m. Nosači kolektora za prikupljanje zračnog zanošenja postavljaju se na udaljenosti od 5 i 10 m od tretiranog reda. Na vertikalnom nosaču ukupno se postavlja 10 filter papirića (80 po tretmanu). Na slici 3. prikazani su vertikalno i horizontalno postavljani nosači sa kolektorima (filter papirićima).



Slika 3. Vertikalno i horizontalno nosači filter papirića
 Figure 3. Vertical and horizontal collectors for filter papers

Nakon svakog tretmana filter papirići prikupljaju se tijekom 15 min i spremaju se u hermetički zatvorene vrećice koje se odlažu na mjesto bez pristupa sunčeve svjetlosti. Za tu namjenu koriste se neprozirne plastične kutije tamne boje. Uzorkovani filter papirići u laboratoriju ispiru se sa 10 ml deionizirane vode, nakon čega se određuje koncentracija tekućine, pomoću valne duljine očitane na spektrofotometru (*Varian Cary 50 UV-Visible*). Za određivanje koncentracije tekućine pri korištenju organske boje *Tartarzina* koristi se valna duljina od 425 nm. Dobivene vrijednosti služe za izračun zanošenja ($\mu\text{g cm}^{-2}$). Brzina zračne struje mjeri se ručnim anemometrom (*Kestrel 4500BT*).

REZULTATI I RASPRAVA

Rezultati provedenog istraživanja u nasadu višnje s različito podešenim tehničkim čimbenicima raspršivanja prikazani su u tablicama 1. i 2.

Tablica 1. Zemljišno i zračno zanošenje tekućine – norma od 250 l ha⁻¹
 Table 1. Ground and air drift – spraying norm of 250 l ha⁻¹

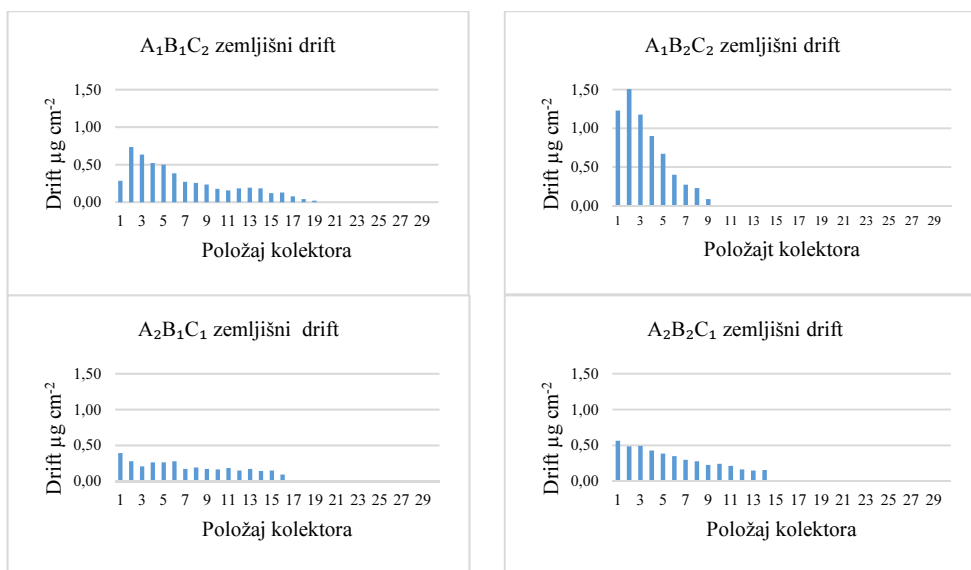
	$A_1B_1C_1$			$A_1B_1C_2$		
	Zem. drift g ha ⁻¹	Zra. drift g ha ⁻¹	10 m	Zem. drift g ha ⁻¹	Zra. drift g ha ⁻¹	10 m
\bar{X}	14,45	23,86	6,00	17,07	25,42	12,79
σ	0,13	0,85	0,36	0,87	0,95	0,82
C.V. %	0,83	10,19	16,95	4,83	10,66	18,28
	$A_1B_2C_1$			$A_1B_2C_2$		
	Zem. drift g ha ⁻¹	Zra. drift g ha ⁻¹	10 m	Zem. drift g ha ⁻¹	Zra. drift g ha ⁻¹	10 m
\bar{X}	20,47	9,86	0	21,57	12,35	0
σ	0,91	0,61	0	1,68	0,67	0
C.V. %	4,21	17,79	0	4,44	15,38	0

Tablica 2. Zemljišno i zračno zanošenja tekućine – norma od 200 l ha⁻¹
 Table 1. Ground and air drift – spraying norm of 200 l ha⁻¹

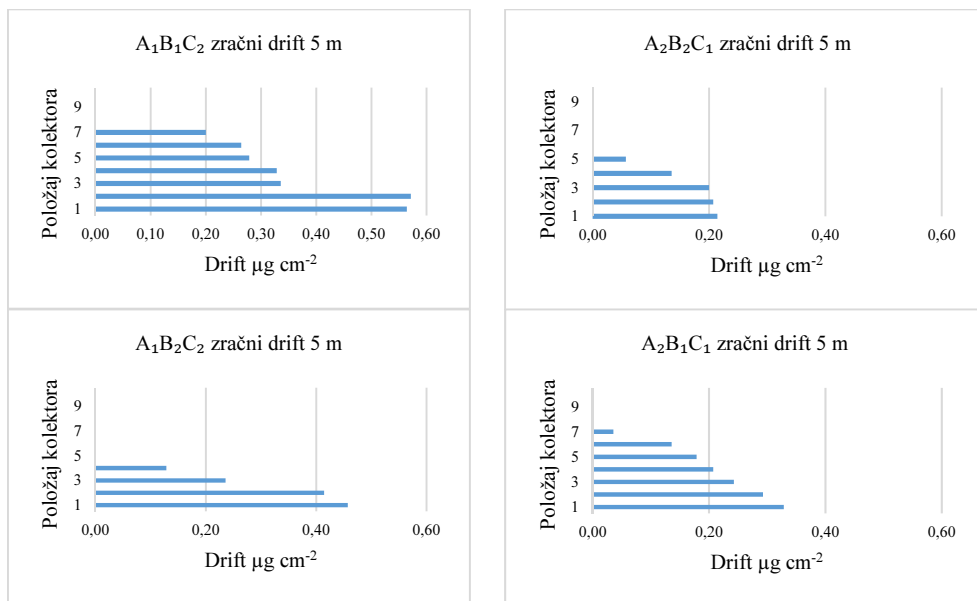
	<i>A₂B₁C₁</i>			<i>A₂B₁C₂</i>		
	Zem. drift g ha ⁻¹ 20 m	Zra. drift g ha ⁻¹ 5 m	10 m	Zem. drift g ha ⁻¹ 20 m	Zra. drift g ha ⁻¹ 5 m	10 m
\bar{X}	10,92	14,21	5,00	13,42	21,21	10,57
σ	0,82	0,25	0,17	0,78	0,61	0,63
C.V. %	7,13	5,03	9,90	5,54	8,26	16,95

	<i>A₂B₂C₁</i>			<i>A₂B₂C₂</i>		
	Zem. drift g ha ⁻¹ 20 m	Zra. drift g ha ⁻¹ 5 m	10 m	Zem. drift g ha ⁻¹ 20 m	Zra. drift g ha ⁻¹ 5 m	10 m
\bar{X}	14,80	8,14	0	16,14	8,85	0
σ	0,87	0,31	0	0,75	0,63	0
C.V. %	5,59	10,91	0	4,43	20,40	0

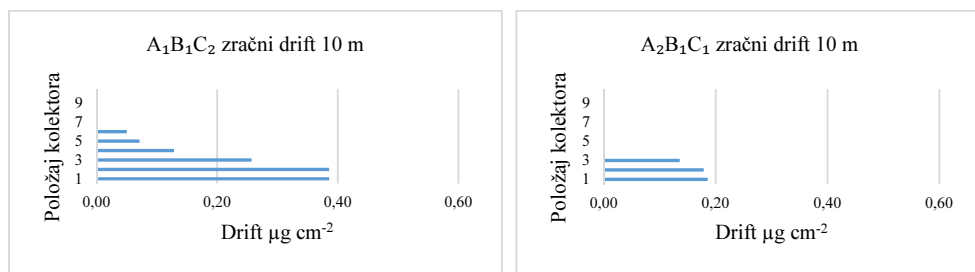
Gubitak zemljišnog zanošenja tekućine prikazuje slika 4., a slike 5. i 6. ostvarene gubitke zračnim zanošenjem tekućine na nosačima filter papira koji se postavljaju na 5 m i 10 m od sredine tretiranog reda direktno u zoni raspršivanja.



Slika 4. Zemljišno zanošenje tekućine
 Figure 4. Ground drift



Slika 5. Zračno zanošenje tekućine na udaljenosti 5 m
 Figure 5. Air drift at distance of 5 m



Slika 6. Zračno zanošenje tekućine na udaljenosti 10 m
 Figure 6. Air drift at distance of 10 m

Najveći gubitak zemljišnog zanošenja tekućine od $21,57 \text{ g ha}^{-1}$ ostvaruje se kombinacijom tehničkih čimbenika $A_1B_2C_2$ (norma prskanja 250 l ha^{-1} , 3. položaj lopatica prema tehničkim specifikacijama, mlaznice ITR), dok je najmanje zemljišno zanošenje od $10,92 \text{ g ha}^{-1}$ ostvareno tretmanom $A_2B_1C_1$ (norma prskanja 200 l ha^{-1} , 2. položaj lopatica prema tehničkim specifikacijama, mlaznice TR).

Najveći gubitak zračnog zanošenja tekućine na nosaču udaljenom 5 m od sredine tretiranog reda iznosi $25,42 \text{ g ha}^{-1}$ ostvaren je sa kombinacijom $A_1B_1C_2$ (norma prskanja 250 l ha^{-1} , 3. položaj lopatica prema tehničkim specifikacijama, mlaznice TR), a kombinacija $A_2B_2C_1$ (norma prskanja 200 l ha^{-1} , 2. položaj lopatica prema tehničkim specifikacijama, mlaznice ITR) ostvaruje najmanje zračno zanošenje od $8,14 \text{ g ha}^{-1}$ na istoj udaljenosti.

Najveće zračno zanošenje na nosaču postavljenom na 10 m udaljenosti od sredine tretiranog reda iznosi 12,79 g ha⁻¹ i ostvaruje se sa kombinacijom $A_1B_1C_2$ (norma prskanja 250 l ha⁻¹, zrak 3, mlaznice TR), dok kombinacije gdje se koristi ITR mlaznica nije zabilježeno zračno zanošenje na istoj udaljenosti ($A_1B_2C_1$, $A_1B_2C_2$, $A_2B_2C_1$ i $A_2B_2C_2$).

ZAKLJUČAK

Na temelju dobivenih rezultata mogu se donijeti sljedeći zaključci:

- Najveći sveukupni gubitak tekućine ostvaren je kombinacijom $A_1B_1C_2$ (norma 250 l ha⁻¹ mlaznica TR 3. položaj lopatica prema tehničkim specifikacijama),
- Najmanji gubitak ostvaren je s normom 200 l ha⁻¹ mlaznicom ITR i 2. položaj lopatica prema tehničkim specifikacijama (tretman $A_2B_2C_1$).

Prema obavljenom istraživanju upotreba zračno – injektorskih mlaznica tj. mlaznica za smanjenje zanošenja tekućine prilikom aplikacije u znatnoj mjeri smanjuje gubitke zaštitnih sredstava. Zračno zanošenje tekućine potpuno je reducirano, dok je zemljišno zanošenje svedeno na minimum. Smanjenje brzine i količine zračne struje kao i smanjenje norme raspršivanja pozitivno djeluje na smanjenje zemljišnog i zračnog zanošenja tekućine. Potrebno je provesti daljnja istraživanja radi uvida do koje granice je moguće smanjivanje norme raspršivanja i zračne struje ventilatora, a da se ne ugrozi biološka učinkovitost pesticida.

LITERATURA

- Banaj, Đ., Tadić, V., Petrović, D., Knežević, D., Banaj, A. (2014). Vertikalna raspodjela zračne struje raspršivača AGP 200 ENU. Proceedings of the 42nd International Symposium on Agricultural Engineering "Actual Tasks on Agricultural Engineering", Opatija, pp 167 - 177
- Bjuggstad, N., Hermansen, P. (2009). Field Measurements of Spray Drift in Strawberry. Agricultural Engineering International: the CIGR Ejournal. Manuscript PM 1048. Vol. XI, pp 1 - 13
- Catania, P., Inglese, P., Pipitone F., Vallone, M. (2011). Assessment of the wind influence on spray application using an artificial vineyard. Eur. J. Hortic. Sci., pp 102 -108
- Celen, I.H., Arin, S., Durgut, M.R. (2008). The effect of the air blast sprayer speed on the chemical distribution in vineyard. Pak. J. Biol. Sci. Vol.11: 1472 - 1476
- Cunningham, G.P. and Harder J. (1999). Sprayers to reduce spray volumes in mature citrus trees. Crop Protection, Surrey, Vol. 18: 275 - 281
- De Moor, A., Langenakens, J., Vereecke, E., Jaeken, P., Lootens, P., Vandecasteele, P. (2000). Image analysis of water sensitive paper as a tool for the evaluation of spray distribution of orchard sprayers. Asp. Appl. Biol. Vol. 57: 329 - 342
- Derksen, R.C., Zhu, H., Fox, R.D., Brazee, R.D., Krause, C.R. (2007). Coverage and drift produced by air induction and conventional hydraulic nozzles used for orchard applications. Trans. ASABE 50: 1493 - 1501
- De Schampheleire, M., Baetens, K., Nuyttens, D., Spanoghe, P. (2008). Spray drift measurements to evaluate the Belgian drift mitigation measures in field crops. Crop Protection Vol. 27: 577 - 589
- Godyn, A., Holownicki, R., Doruchowski, G., Swiechowski, W. (2008). Dual - fan Orchard Sprayer with Reversed Air-stream – Preliminary Trials, Agricultural Engineering International, The CIGR Ejournal, Manuscript ALNARP 08 007. Vol. 10.
- ISO TC 23/SC 06 N 22866:2005. Equipment for crop protection-Methods for the field measurement of spray drift.
- Landers, A., Farooq, M. (2004). Reducing Spray Drift From Orchards, New York Fruit Quarterly, Vol. 12: 3

- Holownicki, R., Doruchowski, G., Godyn, A., Swiechowski, W. (2000). Variation of spray deposit and loss with air-jet directions applied in orchards. *Journal of Agricultural Engineering Research*, Vol. 77(2): 129 - 136
- Maghsoudi, H., Minaei, S. (2013). Variable rate spraying: a methodology for sustainable development. The 1st national conference on solutions to access sustainable development in agriculture, natural resources and the environment, Iran (Tehran) In Farsi.
- Marucco, P., Tamagnone, M., Balsari, P. (2008). Study of air velocity adjustment to maximise spray deposition in peach orchards. *Agricultural Engineering International: the CIGR Ejournal*. Manuscript. X: 1-13
- Miranda-Fuentes, A., Gamarra-Diezma, J. L., Blanco-Roldán, G. L., Cuenca, A., Llorens, J., Rodríguez-Lizana, A., Gil, E., Agüera-Vega, J., Gil-Ribes, J. A. (2015). Testing the influence of the air flow rate on spray deposit, coverage and losses to the ground in a super-intensive olive orchard in southern Spain. *SuproFruit 2015 - 13th Workshop on Spray Application in Fruit Growing*, Lindau, Germany, Julius-Kühn-Archiv, 448
- Nuyttens, D., Baeten, K., De Schampheleire, M., Sonck, B. (2007). Effect of nozzle type, size and pressure on spray droplet characteristics, *Biosystems Engineering* Vol. 97: 333 - 345
- Panneton, B., Lacasse, B., Piche, M. (2005). Effect of air-jet configuration on spray coverage in vineyards. *Biosyst. Eng.* Vol. 90: 173 - 184
- Pergher, G., Gubiani, R., Tonetto, G. (1997). Foliar deposition and pesticide losses from three air-assisted sprayers in a hedgerow vineyard. *Crop Protection* Vol. 16: 25 - 33
- Pergher, G. and Petris, R. (2008a). The effect of air flow rate on spray deposition in a Guyot-trained vineyard. *Agric. Eng. Int. CIGR E J.* X: 1 - 15
- Rosell, J.R. and Sanz R. (2012). A review of methods and applications of the geometric characterization of tree crops in agricultural activities. *Comput. Electron. Agric.* Vol. 81: 124 - 141
- Tadić, V. (2013). Utjecaj tehničkih čimbenika raspršivanja na pokrivenost lisne površine u trajnim nasadima. Doktorska disertacija, Poljoprivredni fakultet, Sveučilište J.J. Strossmayera, Osijek
- Tadić, V., Banaj, Đ., Petrović, D., Knežević, D., Lukinac Čačić, J., Menđušić, I. (2014). Brzina i protok zraka s različitim tipovima raspršivača. *Agronomski glasnik*. Vol. 75, 4: 181 - 196
- Vallet, A., Tinet, C. (2013). Characteristics of droplets from single and twin jet air induction nozzles: a preliminary investigation. *Crop Protection*. Vol. 48: 63 - 68
- Van de Zande, J C., Butler Ellis, M C., Wenneker, M., Walklate, P J., Kennedy, M. (2014). Spray drift and bystander risk from fruit crop spraying. *Aspects of Applied Biology* Vol. 122: 177 - 186
- Vercruyse, F., Steurbaut, W., Drieghe, S., Dejonckheere, W. (1999). Off target ground deposits from spraying a semi-dwarf orchard. *Crop Prot.* Vol. 18: 565 - 570
- Wenneker M. and Zande J.C. (2008). Drift Reduction in Orchard Spraying Using a Cross Flow Sprayer Equipped with Reflection Shields (Wanner) and Air Injection Nozzles. *Agricultural Engineering International, The CIGR Ejournal*. Manuscript Vol. X: 1 - 10
- Wei, Q., Sanqin, Z., Weimin, D., Chengda, S., Jiang, L., Yinian, L., Jiabing, G. (2016). Effects of fan speed on spray deposition and drift for targeting air-assisted sprayer in pear orchard. *Int J Agric & Biol Eng.* Vol. 9 No.4: 53
- Zhu, H., Dorner, J., Rowland, D., Derksen, R., Ozkan H. (2004). Spray penetration into peanut canopies with hydraulic nozzle tips. *Biosystems Engineering*, Vol.87: 275 - 283
- Zhu, H., Derksen, R. C., Guler, H., Krause, C. R., Ozkan, H. E. (2006). Foliar deposition and off-target loss with different spray techniques in nursery applications. *American Society of Transactions of the ASABE. Agricultural and Biological Engineers* ISSN 0001-2351. Vol. 49(2): 325 - 334

IMPACT OF TECHNICAL SPRAYING FACTORS ON GROUND AND AIR DRIFT IN CHERRY ORCHARD

SUMMARY

In this paper, the results of impact of technical spraying factors on ground and air drift are shown by using *Agromehanika AGP 200 ENU* in a cherry orchard. The research was conducted according to *ISO 22866* norm (devices and machines in plant protection – methods of measuring drift in field conditions). The influence of flow rate is marked as factor *A*, the type of nozzle as factor *B*, and air velocity as factor *C*. For spraying and evaluation of drift, an organic color is used in concentration of 4 % (*Tartazine*). Filter papers are used for liquid collecting direct in spraying area. Immediately after each application, the filter papers are collected and stored in a dark and cold place. The sampled filter papers are washed with 10 ml of deionized water under laboratory conditions. After washing, the color intensity of dilution was analyzed at *Varian Cary 50 UV-Visible* spectrophotometer. With different combination of technical spraying factors, a different values of drift are measured, both ground and air. The highest drift was achieved with $A_1B_1C_2$ technical combination (spraying norm of 250 l ha^{-1} , *Lechler TR 8002* nozzle, and air velocity 3, while the lowest result was achieved with spraying norm of 200 l ha^{-1} , *Lechler ITR 8002* nozzle, and air velocity 2 ($A_2B_2C_1$ combination).

Key words: drift, spraying norm, air velocity, nozzles, orchard sprayer



THEORETICAL SIMULATION FOR PROTECTIVE STRUCTURE OF OPERATOR CABIN AGAINST FALLING OBJECT

Gabriel GHEORGHE^{1*}, Cătălin PERSU¹, Marian MIHAI¹, Dan CUJBESCU¹,
Sorin BIRIȘ², Edmond MAICAN²

¹National Institute of Research - Development for Machines and Installations designed to Agriculture and Food Industry - INMA Bucharest, Bd. Ion Ionescu de la Brad 6, sector 1, Bucharest, Romania

²Polytechnic University of Bucharest, Spl. Independenței 313, sector 6, Bucharest, Romania
E-mail of corresponding author: gabrielvalentinghe@yahoo.com

SUMMARY

The important evaluation criterion of the farm tractor cabs is the safety of the machine operator. The machines operating in the above mentioned areas are now sorted into the category of middle range machines. At the present time the frequent use of smaller scale and bigger scale machines in the various industry areas is common. Momentarily the evaluation criteria were unified for all machine types. Resistance tests of the cabin were done according to ISO 8083:2006 regarding devices of protection against falling objects of forestry tractors on wheels - The fulfilling of defined requirements by regulation and standards are the basic condition for certificating of reliability of safety frame of the mobile working machine.

The safety frames of the mobile working machines for the groundwork machines have to ensure the operator safety during the machine operation even in the difficult and extremely heavy working conditions. The working space of the machine operator is evaluated in the term of ability to protect the operator in the situation of rolling-over of the machine and in the situation when the object is falling to the safety frame of the mobile working machine. To declare the conformity with the regulations and standards requirements the laboratory measurements are provided on actual structure prepared for launch to the market. The laboratory measurements of the structure can be considered as the final stage of the design process, because after proving of safety frame reliability the mobile working machine can be operated from the operator's safety point of view. The requirements of minimum endurance during the tests are given by the existing regulation and standards and vary according to the machine type and the machine weight.

Keywords: SolidWorks Simulation 2016, Falling objects Protective Structure (FOPS), DLV (Deflection Limiting Volume)

INTRODUCTION

Currently protective structures for construction and mining machines are required to provide safety in case of a rollover during engineering work (ROPS - Rollover Protective Structure - ISO 3471, EN 13510:2004) and protect construction machines against falling objects (FOPS - Falling Object Protective Structures - ISO 8083:2006). In the case of mining machines safety at much higher impact energies than the ones specified by ISO 3449 must be ensured. This is dictated by the operating conditions and the danger of rock slides. In Poland standard PN-92/G-59001: 'Rock slide protective structures (RSPS). Requirements and tests is binding for mining machines (Karlinski et al., 2008). Depending on the needs, the cabin may have adjustable height, which facilitates transport and increases the field of view of the machine operator when drilling blast holes. However, such structures also cause a number of problems in adjusting the cabin to the safety requirements outlined in normative acts. The mass of such machines reaches up to 30,000 kg and when the vehicle rolls over the structure must protect the residual space defined by the Deflection Limit Volume (DLV) who simulating the operator body maximum boundaries as per ISO3164:2008 was placed inside the cabin and the cabin. This paper presents the methodology of conducting simulation tests for such units with the application of finite element (Karlinski et al., 2013). Accidents which involve a fall over object on structure are often fatal for the worker operating the mining machines. Fall over are the leading cause of work-related death in USA, where only about 70% of mining machines sold were equipped with fall over protective structures (FOPSS) (The Freeman, 1999). Each year, about 250 people are killed in mining accidents in USA (source: Centers for Disease Control and Prevention), constituting more than one-third of all production mining-related fatalities (Murphy and Yoder, 1998). The majority of fatal accidents involved mining machines without protective structures (Arana et al., 2010). Myers and Pana-Cryan (2000) compared three strategies to prevent injuries incurred as a result of mining machines overturns. The strategies were 'do nothing', 'install FOPS, and 'replace machines cabin'. They concluded that the preferred strategy in terms of cost- effectiveness was to 'install FOPS' on mining machines for which FOPS were available. FOPS in combination with a seat belt can prevent nearly all mining machine fall over objects protection (Manado et al., 2007).

A general problem in designing a falling object protective structure system is to find out the actual demands of the load, since in most cases the load is neither known nor can it be measured. This problem also occurs in the application considered in this paper where the load not only is unknown but may also change in a very fast manner by impacting on protective structure. In order to deal with this fact, the nonlinear control strategy has to be augmented by a load estimator. This is a challenging task since it is well known that the separation principle of the control of potential energy & measure or calculate kinetic energy and the estimator design does not hold for nonlinear systems. In this contribution, the stability of the deformation in protective structure design consisting of the nonlinear controller, the nonlinear load estimator and the plant model is proven by means of theory & FEA analysis (Gore and Barjinhe, 2014).

Features which are taken into account for cabin testing:

1. To fulfill the demands to sale equipment in European countries, FOPS (fall over protection) to operator cabin of any earth moving equipment is mandatory & its legal requirement.
2. Whereas design of protecting structure against FOPS is dependent upon weight of falling object & potential energy of falling object on protective structure. During impact the amount of energy get absorbed by protective structure with deformation of structure.

3. By weight consideration of falling object, the test standard & load carrying capacity of FOPS varies from equipment to equipment depend upon cabin rigidity structure provided during design of cabin.
4. If test standard & load carrying capacity of FOPS different from equipment to equipment because of weight of falling object, then design of protecting structure for operator cabin against FOPS is not similar from certain category of machine group.
5. We will see all above parameter how it affects in current operator cabin by design point of view & then what to be required to modify in current design to fulfill EU standard in problem identification (Gore and Barjinhe, 2014).

Furthermore, a protective structure can be an integral part of the operator's cabin whereby one gains such benefits as: a cost reduction, an increased operator workspace or a reduced machine height.

The testing lab performs different FOPS tests, but it is necessary to carry out theoretically simulation to observe the changes of the structure without destroying the cabin.

These tests are done with a finite element simulation program, and I have chosen the Solidworks Simulation to do this test.

Two levels of performance criteria are specified for impact protection, based on the machine end use.

a) Level I: protection against the impact of a round test object dropped from a height sufficient to develop an energy of 1,365 J. See Figure 1

b) Level II: protection against the impact of a cylindrical test object dropped from a height sufficient to develop an energy of 11,600 J. See Figure 2. (Gore and Barjinhe, 2014).

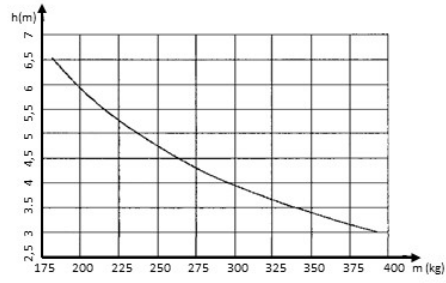
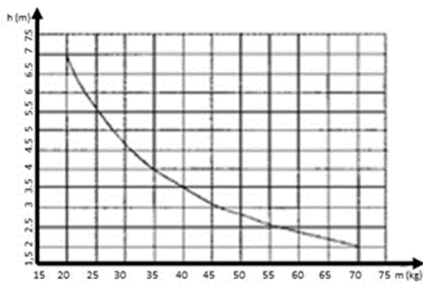


Figure 1. Energy Requirement Curve- Level I Figure 2. Energy Requirement Curve- Level II

MATERIALS AND METHODS

For this simulation for achieving the 11,600 J energy value according ISO 8083, level 2 of performance, it was used a falling object with a mass of 310.3 kg, made of steel, this being suspended at 3.91 m on top of the cabin's rooftop.

The area in which was realized the impact was determined according with ISO 8083, this being localized in the front of the rooftop.

Dimensions of falling object:

- Height: 750 mm;
- Superior diameter: 250 mm;
- Impact surface diameter: 200 mm.

After the 3D design of the cabin in the SolidWorks 2016 program, it was entered the following input data to run the simulation:

- a) cabin has been fixed on the ground without damping (fig. 3);

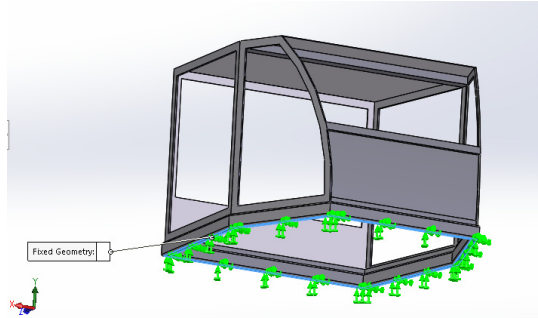


Figure 3. Fixed cabin to start the simulation

- b) it was introduced force (F) acting on the surface contact of the roof (fig. 4);

$$F = m \cdot g \cdot \Psi \quad (\text{N}) \quad (1)$$

Where:

m - mass of weight (310.3 kg);

g - gravitational acceleration ($9.81 \text{ m}\cdot\text{s}^{-2}$);

Ψ - impact multiplier where is 2.5 because we have a force applied with shock.

To check a structure stressed by shock, first we calculate the static unitary stress, static deformation (produced by the same load, if applied slowly) and impact multiplier; the dynamic unitary stress and dynamic deformation are obtained by multiplying static unitary stress, respectively static deformation by impact multiplier.

In our case there is a sudden application of a stress, without height of fall ($h = 0$), and the impact multiplier is calculated according to the equation (2).

$$\Psi = 1 + \sqrt{1 + \frac{2h}{\delta_s}} \quad (2)$$

From equation (2) results $\psi = 2$, which shows that the effect of suddenly applied stress is two times higher than the effect of a static stress applied, namely, with the value increasing slowly from zero to a final value; sudden application of a stress is also a cases of shock. The forces introduced in the calculation were multiplied by two, after measuring masses and calculating the weights, to be sure it will resist we added 0.5 to this coefficient to be sure of the strength of this cabin (Drobota et al., 1972).

According to the data we will apply a force of 7,610 N.

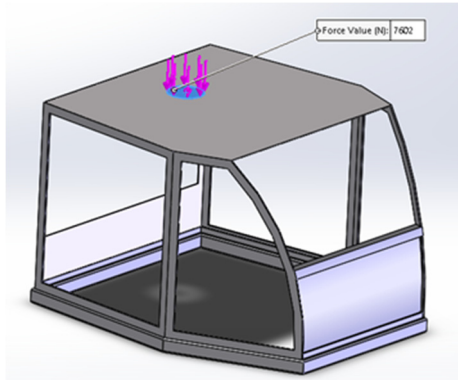


Figure 4. Application of force according to ISO 8083 (Impact surface diameter: - 200mm)

c) the material with the following characteristics has been selected (table 1);

Table 1. The characteristics of the material chosen (S275JR)

Property	Value	Units
Elastic Modulus	2.100,000,031e+011	N m ⁻²
Poisson's Ratio	0.28	N/A
Shear Modulus	7.9e+010	N m ⁻²
Mass Density	7,800	Kg m ⁻³
Tensile Strength	410,000,000	N m ⁻²
Yield Strength	275,000,000	N m ⁻²

d) before running the simulation, the last step is to creating mesh and with this step the program checks if the design was done correctly otherwise the meshing cannot be created (fig.5).

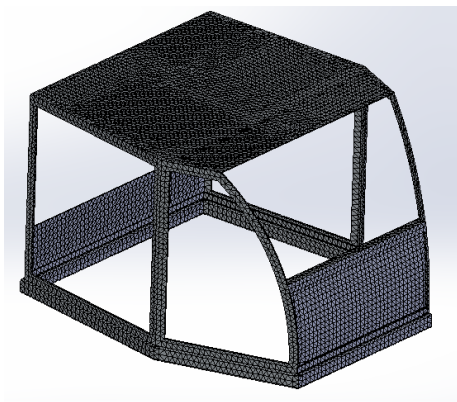


Figure 5. Meshing the structure

All four steps were analyzed for different thicknesses of the roof to see if the displacement of roof could lead to penetration of DLV (Deflection Limiting Volume), who is maxim 230 mm from DLV to the roof.

RESULTS AND DISCUSSION

We started the simulation with a roof thickness of 10 mm and resulted a displacement of 4.48 mm (Fig.6.a) and the yield strength of the material has not been reached (Fig.6.b).

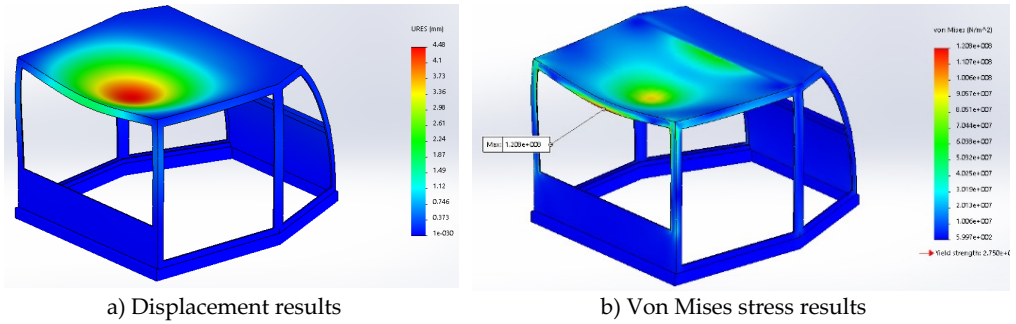


Figure 6. The results of simulation for a roof with thickness of 10 mm

We do same steps for different thickness of the roof and results are in table 2.

Table 2. The results of simulation for different thicknesses of the roof

Material	Thickness (mm)	Displacement (mm)	Von Mises max (N·m ⁻²)
S275JR	10	4.48	$1,208 \cdot 10^8$
S275JR	8	7.49	$1,421 \cdot 10^8$
S275JR	7	10.4	$1,819 \cdot 10^8$
S275JR	6	15.3	$2,407 \cdot 10^8$
S275JR	5	24.2	$3,347 \cdot 10^8$
S275JR	4	41.4	$4,807 \cdot 10^8$

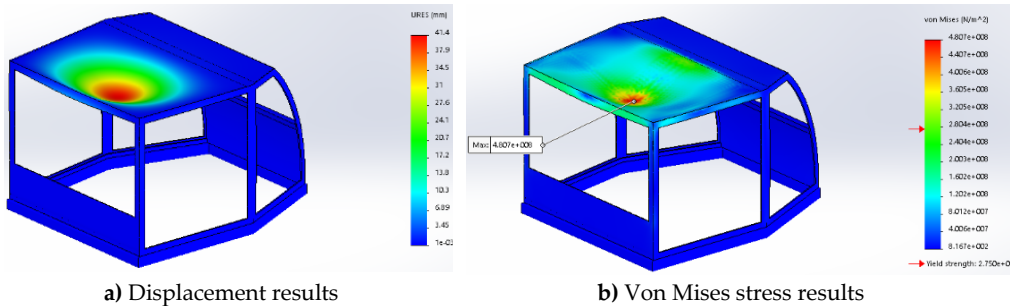


Figure 7. The results of simulation for a roof with thickness of 4 mm

The ROPS analysis performed with the solidworks simulation 2016 software provided some preliminary results that can be taken into account before building the cabin so that the experimental model is as close to the prototype as possible.

In this article, we performed the analysis at just a few thicknesses and the same material, but a manufacturer can do this analysis for what materials and sizes it wants to reach the lowest cost but also be effective in terms of resistance.

CONCLUSIONS

We can see that at thickness of the roof on 5 mm we reached yield strength for material S275JR, but not reached tensile strength that according figure 5 is $4,100 \cdot 10^8 \text{ N}\cdot\text{m}^{-2}$.

At the thickness of the roof on 4 mm (figure8) we reached tensile strength, so it's not recommended to reach a very low thickness, if we want a thickness of the roof on 4 mm, respectively reducing cabin weight, we need to change material like E335 with tensile strength ($5,500 \cdot 10^8 \text{ N}\cdot\text{m}^{-2}$) or E360 with tensile strength ($6,700 \cdot 10^8 \text{ N}\cdot\text{m}^{-2}$) with the same density.

Following the finite element analysis of the FOPS, studied in the experimental research, it was found the possibility of optimizing the manufacturing process of the protective structures by reducing the thickness of the material used in the manufacture without endangering operator safety.

ACKNOWLEDGEMENT

The work has been funded by UEFISCDI within the project entitled „Enhancement competitiveness of SC IRUM REGHIN SRL by optimization of manufacturing technology of operator protection structures, for agricultural and forestry tractor“ contract 25BG/2016.

REFERENCES

- Arana, I., Mangado, J., Arnal, P., Arazuri, S., Alfaro J.R., Jarén, C. (2010). Evaluation of risk factors in fatal accidents in agriculture. Spanish Journal of Agricultural Research, 8 no. 3, 592-598.
- Ballesteros, T., Arana, I., Ezcurdia, A.P., Alfero, J.R. (2013). E2D ROPS development & test of an automatically deployable in height & width front mounted ROPS for narrow track tractors. Bio-system engineering, vol 116, 1-14.
- Centers for Disease Control and Prevention. Retrieved at: <https://www.cdc.gov> on 20 November 2017.
- Drobotu, V., Dorobantu, M., Atanasiu, M. (1972). Materials resistance. Didactic and Pedagogic Publishing House, Bucharest.
- Gore, P., Barjibhe, R.B. (2014). Design of protective structure of operator cabin against falling object (FOPS). International journal of latest trends in engineering and technology, Vol. 3, Issue 4, ISSN: 2278-621X.
- Karlinski, J., Rusinski, E., Smolnicki, T. (2008). Protective structures for construction and mining machine operators. Automation in Construction, vol 17, 232-244.
- Karlinski, J., Ptak, M., Dzialak, P. (2013). Simulation test of roll-over protection structure. Archive of civil & mechanical engineering, vol 13, 57-63.
- Manado, J., Arana, J.I., Jaren, C. (2007). Design calculation on roll-over protection structure for agriculture tractor. Bio-system engineering, vol 96, 181-191.

- Murphy, D. J. and Yoder, A. M. (1998). Census of Fatal Occupational Injury in the Agriculture, Forestry, and Fishing Industry. *Journal of Agricultural Safety and Health*, Special Issue, 55-66.
- Pana-Cryan, R. and Myers, M.L. (2002). Cost-effectiveness of roll-over protective structures. *American Journal of Industrial Medicine*, Vol. 42, Issue S2, 68-71-
- The Freeman. (1999). *Ideas On liberty*, vol.49, no. 1.



NONLINEAR IMPACT RESISTANCE SIMULATION OF A NEWLY DESIGNED ROOF FROM AN AGRICULTURAL TRACTOR CABIN

Edmond MAICAN¹, Sorin-Ştefan BIRIŞ¹, Cătălin PERŞU², Mihaela DUȚU¹,
Mihai Gabriel MATACHE², Sorin IORDACHE¹, Călin ALFIANU³

¹ Politehnica University of Bucharest, Biotechnical Systems R&D Centre,
Spl. Independenței 313, sector 6, Bucharest, Romania

² INMA Bucharest, Bd. Ion Ionescu de la Brad 6, sector 1, Bucharest, Romania

³ SC IRUM SA, Str. Axente Sever 6, Reghin, Mureş, Romania

E-mail of corresponding author: biris.sorinstefan@gmail.com

SUMMARY

The roll over / falling object protection structure (ROPS and FOPS) of agricultural tractors increases the safety of the driver in case of collisions, tractor roll-over or cabin impact with falling objects. The protective system consists of a high resistance steel frame and a roof reinforced layer. In order to be better accepted on the EU market, a newly designed agricultural tractor or tractor cabin should pass safety tests according to Regulation (EU) No. 1322/2014. This paper presents the procedure of a nonlinear dynamic analysis and its challenges, as well as the obtained results for a protective roof structure from a new agricultural tractor cabin. The simulation takes place under the conditions provided by the above mentioned regulation, which states that the impact between a weight of a prescribed mass and shape falling from a prescribed height should not penetrate the cab ceiling or deform it up to the driver space. The simulation aims to reduce costs with experimental model manufacturing due to early identification of design flaws. CAD model was developed in Autodesk Inventor, while additional minor model changes, meshing and simulation were performed in the Ansys Workbench environment.

Keywords: FOPS, nonlinear analysis, tractor cabin, passive safety

INTRODUCTION

The Falling Object Protective Structure (FOPS) is designed to absorb the impact energy in case of accidental falling objects over the cabin, and thus to provide overhead protection and protect the tractor operator from serious injuries. According to recent studies, the number of

fatal accidents in Europe in agriculture and forestry is the highest when compared to any other sector (Kogler et al., 2015). Therefore, passing safety tests is mandatory for each newly designed agricultural tractor cabin, in order to be certified as *safety cabin*. Most reported incidents involve people next to the tractor rather than sitting in the cabin, so it could be stated that current FOPS structures are generally adequate (Robinson et al., 2013). These tests are worldwide standardized and should prove that the structure provides a certain space for the operator in the event of an accident. Therefore, specific regulations are currently in force worldwide for testing every type of machine. Within the European Union, Regulation (EU) No 1322/2014 provides the requirements for the approval of agricultural and forestry vehicles (European Commission 2014), establishing the testing procedure for both FOPS and ROPS (rollover protective structure).

This investigation aims to make a preliminary assessment of the structural response of a new FOPS cabin cover, by means of finite elements analysis. It also provides the methodology to perform a nonlinear dynamic analysis for short-duration and severe loading, involving large deformation and material failure and fragmentation. The Regulation 1322/2014 defines a safety zone for the operator, which must not be entered by the falling object or by parts of the structure during the test. It also establishes the drop test procedure and specific means to determine whether the FOPS enters the clearance zone. Following, the main testing provisions are mentioned:

- The energy to be developed by the falling object should be 1365 J;
- The standard laboratory test weight (i.e. the falling object) should be a sphere made of ductile iron or solid steel, with a diameter between 200 and 250 mm;
- The mass of the sphere should be 45 ± 2 kg; thus, all the necessary data to calculate the height from which the object is dropped are provided.

MATERIALS AND METHODS

The new cabin roof consists of three components: the upper cover, the middle structural layer, and the lower roof. Among them, the middle one is the component that is designed to sustain the loadings developed during FOPS test (Figure 1). Due to the computing resources that are necessary to make a nonlinear dynamic analysis of an assembly, with material fragmentation and interaction between components during process development, only the middle component will be analyzed.

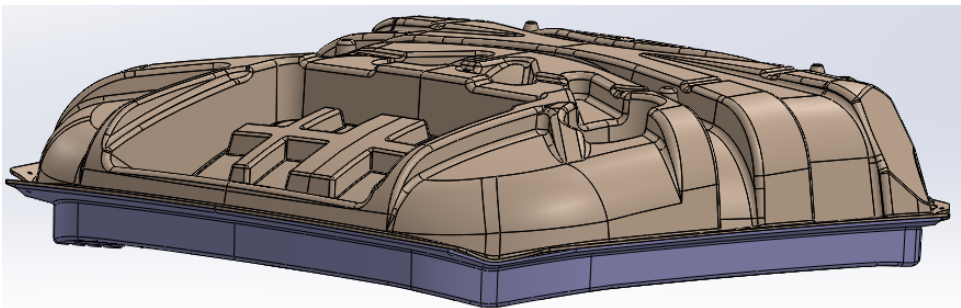


Figure 1. CAD model of the assembled mid and lower components of the tractor roof (The upper cover is not represented here)

Both the geometry of the middle component and the load are symmetrical with respect to a vertical plane containing the longitudinal axis of the cabin. Therefore, only half of the geometry will be analyzed using symmetry boundary condition. In order to have a better control of the mesh in the impact area, the component is circularly sliced in this region, thus dividing the roof and obtaining a separate volume centered around the impact point.

The component is made of LFI (Long Fiber Injection Molding) – a complex composite made of glass fiber and polyurethane, commonly used for producing large-sized structural components. Materials from this class have good impact resistance, provide adequate energy absorption, have low mass and low heat transfer coefficient (Gibson and Ashby 1999), (Linul, et al. 2014), (Şerban, et al. 2016).

Table 1 shows the physico-chemical properties of the material. Part of them were provided by the producer, while bulk modulus and shear modulus were calculated based on the existing properties, as follows:

$$\text{Bulk modulus: } K = \frac{1}{3} \frac{E \cdot G}{3G - E};$$

$$\text{Shear modulus: } G = \frac{E}{2(1+\nu)},$$

where E is tensile modulus, and ν is the Poisson’s ratio.

Poisson’s ratio was evaluated on the basis of various LFI records from databases providing mechanical properties for various materials (MatWebLLC 2017).

Table 1. LFI Plastic Grades – material properties

Property name	Material property	Notes
Density, g cm ⁻³	1.25	Average value
Tensile modulus, MPa	4300	
Bulk modulus, MPa	3583	Calculated
Shear modulus, MPa	1654	Calculated
Poissons’s ratio	0.3	
Heat deflection temperature, °C	116	
Ultimate elongation (at break) %	1.5	
Ultimate tensile stress, MPa	100	Average value
Ultimate shear stress, MPa	75	$\tau = (0.7 - 0.82)\sigma$ for this material when is close to failure
Flexural modulus, MPa	8000	at 23 °C
Glass fiber content, %	30 ± 5	Average: 30
Fiber length, mm	12.5 – 100	
Linear thermal expansion coefficient, µm/m°C	18	
Water absorption, %	0.3	at equilibrium

The CAD model was designed using Autodesk Inventor, and exported as stp file for subsequent finite elements analysis. More than 2000 surfaces were used to model the shape of the structural component of the roof. This complexity led to a number of geometry conversion errors – a well-known situation that poses difficulties when working with modules from different software packages. Tolerances and surface constrains affected the meshing process. Thus, geometry repair, cleanup, and locally redesign was necessary after the transfer process. The thickness of the component varies from 4 to 5 mm. Therefore, using

shell elements was not an option. A further step was to reduce the number of finite elements by eliminating the unnecessary details, small areas, chamfers, and edges.

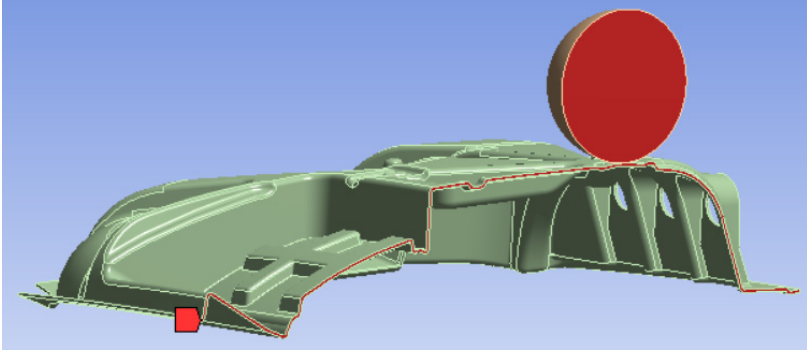


Figure 2. Symmetry plane (in red) through the structural component and impact sphere

The impact sphere was modeled in a position that simulates the initial contact with the roof, and the entire model was then dimensionally reduced to half by means of a symmetry plane (Figure 2). Because friction has a negligible effect on the magnitude of the results, frictionless contact was declared between the roof component and the sphere. The speed of the sphere is calculated based on the energy it should have when it impacts the roof:

$$v = \sqrt{\frac{2E}{m}} = 7.8 \text{ m s}^{-1}$$

where:

$E = 1365 \text{ J}$ is the energy that the sphere should have when it impacts the roof; $m = 45 \text{ kg}$, is the mass of the sphere; v is the sphere speed at the moment it contacts the roof.

Manual virtual topology was employed to group the remaining small faces into virtual cells, in order to further simplify small features and to reduce the number of elements. The procedure was also applied to larger faces, aiming to define mappable faces that can be used to obtain higher precision swept mesh elements. This objective however requires equivalent cells on the opposite side of the model (Figure 3).

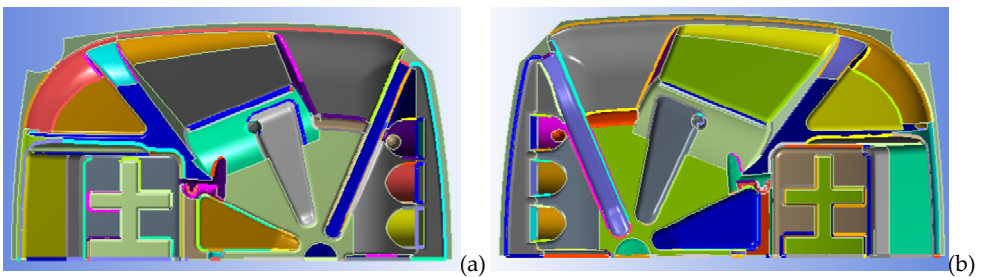


Figure 3. Virtual cells (represented through various colors) were created to reduce the number of mesh elements and to define mappable faces; a) – top view; b) – bottom view

Mesh controls were defined to better tune the mesh size in critical areas. As one can notice in Figure 4, mesh refinement was performed within the critical impact area (the circularly sliced volume) in order to obtain two layers of elements along the component thickness, this being a compromise between the available computing resources and results accuracy. A total number of 639 394 elements (146 898 nodes) were generated.

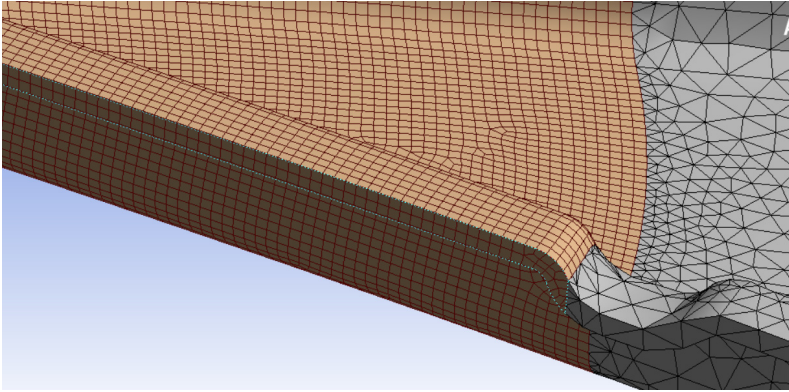


Figure 4. A circular region around the impact area was refined to obtain two layers of elements along the component thickness

Constraints were applied as displacement restrictions on the faces where the roof component is supported by the cabin chassis. Due to the significant mass of the impacting sphere, gravitational acceleration was also specified.

One important parameter to be set up for solver control is the element erosion option, which in this case is set to be based on material failure. In this respect, the geometric strain limit for erosion was deactivated. Exceeding failure criteria for a certain element will result in removing that element from the analysis. The solver was also set to double precision, and the number of output control points was increased to 100 for additional results set.

Based on an existing model of polyurethane with nonlinear characteristics from the materials library, a new nonlinear model for the LFI material was generated. The *Principal Strain Failure* model was assigned as the failure criteria. The only data required for this model are density, bulk modulus, shear modulus, maximum principal strain and maximum shear strain (values are given in Table 1). In this representation, if any element exceeds the values for Maximum Principal Strain or for Maximum Shear Strain, it will fail and will be removed from the analysis.

The solver was instructed to retain the mass and momentum of free nodes (nodes that have all connected elements eroded), in order to calculate subsequent impacts of free nodes and to solve the transfer of momentum in the system. This option also allows to check the trajectory of free pieces of material, as the Regulation 1322/2014 states that no parts of the structure should impact the operator.

Simulation time was set to 0.03s, and was calculated starting from the speed of the impact sphere.

RESULTS AND DISCUSSION

The solver took 18 hours to simulate the system behavior during the 0.03 simulation time. Because the solver does not involve equilibrium iterations, a convergence criterion is not applied to control the accuracy of the solution, and the conservation energy law is used instead. The energy error is calculated and compared to an upper allowable limit (Lee 2017):

$$\text{Energy error} = \frac{|Current\ energy - Ref.\ energy - Work\ done|}{\max(|Current\ energy|, |Ref.\ energy|, |Kinetic\ energy|)}$$

where:

Current energy is energy at a certain time; *Ref energy* is the total energy of the initial time.

Figure 5 shows the energy summary of the simulation. Because friction between sphere and roof structure was not included in the analysis, the contact energy was negative, representing 6.8% of the peak internal energy. This value is acceptable, as it does not exceed 10% of the internal energy value (LS-Dyna Support, 2017). The element hourglass mode is a zero-energy way of element deformation that will not produce strain or stress, but can interfere with the response of the structure, thus affecting the accuracy of the solution. As one can calculate from the energy summary graph, the maximum energy that is added to the system to control the hourglass mode is about 6.2% of the peak internal energy, which is also under the threshold of 10% (Lee, 2017). Once impact occurs, the internal energy is developing up to a point where elements start to erode. At this point, the system will begin to discard the internal energy of the eroded elements. As expected, the kinetic energy is decreasing after the initial contact. In view of the above observations, it can be concluded that the obtained results are reliable.

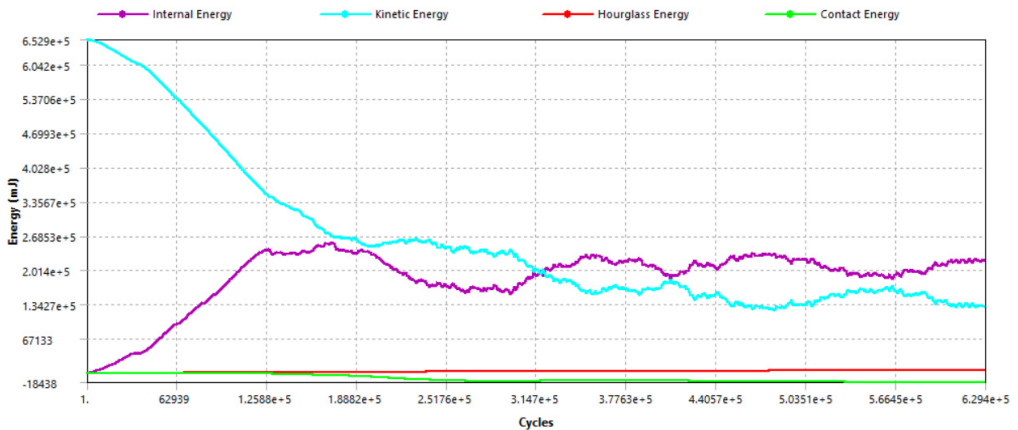


Figure 5. Energy statistics during solution output

Results show that the roof structure breaks as a result of the impact. Two video files that show the impact behavior are available at the following web addresses: isb.pub.ro/temp/Eq_stress.avi and isb.pub.ro/temp/Eq_stress_X_view.avi. Formation of stress waves and their propagation throughout the entire structure is visible. As one can also notice in figure 6, the highest stress values are recorded throughout the ribbing that starts from the impact area. The rib takes over an important part of the impact energy, channels the stress wave towards the edge of the structural roof component, and dissipates part of it laterally throughout the roof.

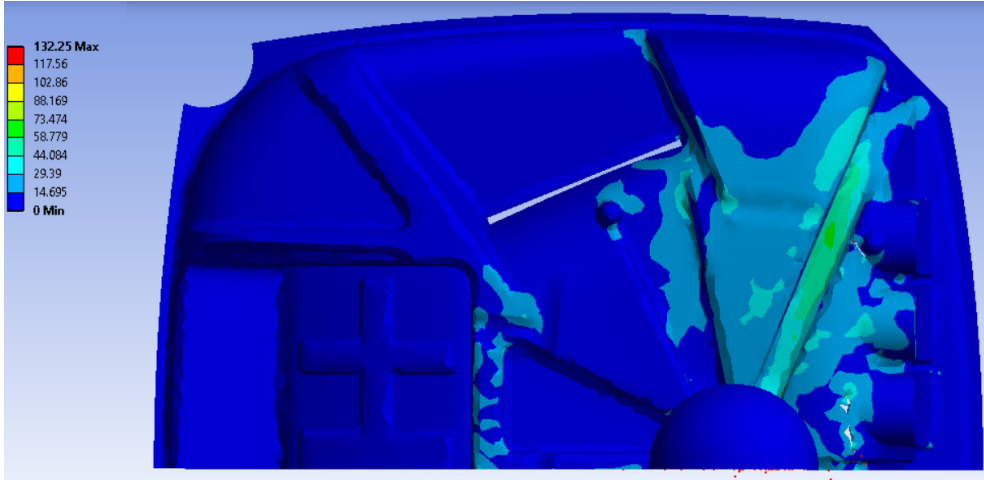


Figure 6. Stress wave propagates through the ribbing towards the edge of the roof layer, and starts to dissipate laterally throughout the entire structure (0.0057 s from the initial contact)

In order to calculate the remaining kinetic energy of the impacting sphere after it penetrates the roof, a velocity probe scoped to the sphere was inserted as part of the solution. The calculated residual speed was 2.72 m s^{-1} – a value that corresponds to a remaining kinetic energy of 166.7 Joule.

CONCLUSIONS

The simulation considers only the impact of the sphere with the structural component of the roof. The upper and lower roof covers have not been considered. Therefore, it is very likely that the residual kinetic energy of about 167 Joule would be taken over by these two components, if they were included in the simulation. On the other side, a required ultimate safety factor of at least 1.5 should be considered (Technical_Committee_B/513 2006). The main risk factors here are the statistical variation of LFI material strength, as well as geometrical deviations of the manufactured structure relative to the CAD model.

In order to improve the strength of the structural component of the roof, several measures can be taken. The simpler one consists in reinforcing the impact area and distributing the impact load on a larger surface of the roof, by adding a metal plate over the impact surface of the roof (between the upper roof and the structural component).

An additional measure implies geometric changes to the structural component. Thus, the thickness of the material in the areas that broke should be increased. This measure will force the stress waves to propagate and dissipate to less-demanded areas (towards the left side, in Figure 6). A second immediate change should be made on the right-side geometry in order to make it more flexible. Although it takes most of the energy (see the rib in Figure 6), it does not allow the stress to properly dissipate towards the more flexible left side, due to its rigidity. Therefore, the upper-right rib from Figure 6 should be enlarged and splayed as it goes towards the edge of the structure.

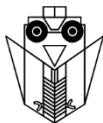
Another measure can be taken with regard to the material. A LFI polyurethane with higher values for ultimate tensile and shear stress should be selected. These conditions are generally met by materials with a glass fiber content of over 40% (MatWebLLC 2017). It is most likely that the final solution will be a combination of the previously proposed changes.

ACKNOWLEDGEMENTS

This work was carried out under the project Increasing the competitiveness of SC IRUM SA, by optimizing the manufacturing technology of the operator protection structures of the forestry and agricultural tractors, Grant 25 BG/2016, funded by MEN - UEFISCDI Romania in the frame of the National Plan for Research, Development and Innovation PNCDI III.

REFERENCES

- European Commission. (2014). Commission Delegated Regulation (EU) No 1322/2014. Official Journal of the European Union. http://data.europa.eu/eli/reg_del/2014/1322/oj.
- Gibson, L. and Ashby, M. (1999). Cellular Solids. Structure and Properties. Cambridge: Cambridge University Press.
- Kogler, R., Quendler, E., Boxberger, J. (2015). Analysis of occupational accidents with agricultural machinery in the period 2008–2010 in Austria. *Safety Science* 72: 319-328.
- Lee, H.H. (2017). Finite Element Simulations with Ansys Workbench 17 - Theory, Applications, Case Studies. SDC Publications.
- Linul, E., Șerban, D., Voiconi, T., Marșavina, L., Sadowski, T. (2014). Energy - Absorption and Efficiency Diagrams of Rigid PUR Foams. Proceedings of the 14th Symposium on Experimental Stress Analysis and Material Testing. Timisoara. 246-249.
- LS-Dyna Support. (2017). Retrieved on 06/05/2017, at <http://www.dynasupport.com/howtos/general/contact-energy>.
- MatWebLLC. (2017). MatWeb - Material Property Data. <http://www.matweb.com/>.
- Robinson, B.J., Scarlett, A.J., and Seidl, M. (2013). Development of technical requirements / performance specifications for functional and occupational safety topics of agricultural and forestry vehicles - Final Report. Transport Research Laboratory.
- Șerban, D.A., Weissenborn, O., Geller, S., Marșavina, L., Gude, M. (2016). Evaluation of the mechanical and morphological properties of long fibre reinforced polyurethane rigid foams. *Polymer Testing* 121-127.
- Technical_Committee_B/513. (2006). Mobile road construction machinery. Safety. Common requirements. BS EN 500-1:2006. Retrieved on 24/09/2017, at <http://www.shangde.org/filedown.php?id=28>



HARVESTING AND PROCESSING OF FRENCH MARIGOLD TO OBTAIN PRODUCTS WITH NEW USES

Adriana MUSCALU^{2*}, Ladislau DAVID³, Mariana BIRSAN², Ion GRIGORE²,
Ana Cristina FATU⁴, Catalina TUDORA^{1,2}

¹ University of Agronomic Sciences and Veterinary Medicine of Bucharest, Romania

² National Institute of Research - Development for Machines and Installations Designed to
Agriculture and Food Industry - INMA Bucharest, Romania

³ University Politehnica of Bucharest, Romania

⁴ Research and Development Institute of Plant Protection - ICDPP Bucharest, Romania

*E-mail of corresponding author: amuscalis@yahoo.com

SUMMARY

Medicinal plants cultivation is one of the best businesses for local farmers, due to its potential and the extremely favourable soil and climatic conditions in Romania. Mechanized harvesting can be an important premise, and in some cases even a guarantee, for producing quality and profitable medicinal plants. The lack of harvesting equipment and high labour costs make farmers cultivate these species on small and medium surfaces. This paper presents the research carried out within INMA on the mechanized harvesting technology, by cutting of French marigold. It is based on the use of low capacity equipment for small and medium surfaces. We also present a technology for French marigold processing to obtain products with new directions of application. It is about obtaining some essential oils and hydrosols (floral waters), for which preliminary tests have proven antimicrobial capacity. The results obtained allow: to evaluate the work performance of the French marigold harvesting equipment and to obtain products with new application possibilities required by organic farming.

Keywords: french marigold, technology, harvesting, processing, control

INTRODUCTION

According to W.H.O. over 75% of the world population uses medicinal plants today for basic medical needs (Si-Yuan Pan et al., 2014). The increased interest in these species was not generated only by traditional phytotherapy, but also by the fact that they are a rich source of biologically active substances. These chemical compounds that have an effect on the

metabolism of the human body are called active principles. (Grigore et al., 2016) For the pharmacodynamic action of medicinal plants, the quality of plant material, which depends largely on the harvesting time, is essential. This should coincide with the period when the accumulations of active principles in the useful parts of medicinal plants are maximal. (Muntean, 2010).

In many countries in Europe, the areas cultivated with medicinal plants have been drastically reduced, with imports being preferred (Schippmann et al., 2002). The phenomenon is the same for Romania, where although pedoclimatic conditions are particularly favourable, farmers cultivate these plants on small and medium areas.

The harvesting methods differ in relation to the useful parts of the medicinal plants that are collected and regardless of how they are carried out: manually, semi-mechanized or mechanized, the content of active principles must be affected as little as possible (Pajic et al., 2016, Martinov et al. 2007). Applying mechanized harvesting involves: the creation of new varieties of medicinal plants with the most uniform development possible, the creation of performing machines based on new harvesting techniques (Martinov et al., 2007).

Following the processing of medicinal plants, essential oils and hydrosols (floral waters) are also obtained. These are essential compounds, complex, synthesized by plants as secondary metabolites and characterized by strong odour. In nature, essential oils play an important role in plant protection, having antibacterial, antiviral, antifungal, insecticidal action; they also act against herbivores by reducing their appetite for such plants. They can attract some insects to favour pollen, seed dispersion and they can have a repellent effect (Bakkali et al. 2008).

The paper presents the technology of harvesting the medicinal plant French marigold - *Tagetes patula* L. *Compositae* family, with low capacity equipment as well as its processing technology. Following the processing of plant raw material, were obtained crude products (essential oil and hydrosol) and their antifungal capacity was tested.

MATERIAL AND METHODS

For medicinal plant harvesting, we used specialized equipment for collecting the aerial parts of French marigold plant, commonly grown in rows or strips. The harvesting equipment field of use comprises all species of medicinal and aromatic plants that are harvested as *herba*. If it is made up of stem, leaves and flowers, the collection is usually done when the plants are blooming. From some species, only the leaf stem is collected, the harvesting sometimes taking place throughout their vegetation period.

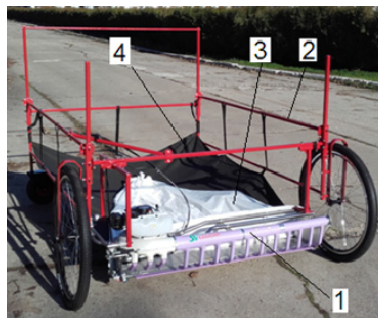


Figure 1. Medicinal plant harvesting equipment

The equipment for harvesting medicinal and aromatic plant (fig.1) consists of the following main sub-assemblies: 1 – mower; 2 – rolling chassis; 3 – collecting bag; 4 – collecting bag holder.

The main technical characteristics of the equipment are:

Mower model	SV 120 H
Mower producer	Zhejiang Kawasaki Tea Machinery CoLtd (China)
Type of cutting device	with double cutting blade
Cutting blade	horizontal 1200 mm
Mower power	heat engine T320
Engine producer	Mitsubishi (Japan)
Engine type	single cylinder, positive ignition and air cooling
Cutting height	adjustable, 40 ... 500 mm
Cutting width	1200 mm
Fuel consumption	1 ... 1,7 l h ⁻¹ (depending on the working regime)
Speed of airflow developed by the blower	15 ... 21 m s ⁻¹
Overall dimensions	
length	max 2370 mm (with swivel wheels facing rearwards)
width	1712 mm
height	1300 mm
Equipment mass	51 kg

In the working process, depending on the particularities of the crop and the species to be harvested, the working height is established and the corresponding adjustment is made. The equipment is pushed, with the engine stopped, to the end of the medicinal plant rows, being placed with the wheels in the direction of the rows so that they “cover” them. The equipment wheels run in the space between rows. Then the engine is started and shortly after, the mower is engaged. The engine “is accelerated” to about 50% of its capacity and then the equipment starts running on rows. Depending on the harvesting conditions (the desired speed, the characteristics of the medicinal plant culture), the “engine acceleration” command is activated until the satisfactory working regime is obtained.

The plant material cut by the mower is directed by the blower into the collecting bag, the air coming out through a rectangular cut, covered by a fine mesh so that the collected material is retained inside.

Because of the cutting device length, the overall dimensions and the fact that it is sometimes necessary to repeatedly drive the cutting device controls during operation, it is advisable to assume the operation by two persons.

The experimentation of the medicinal plant harvesting equipment was carried out in a French marigold culture (*Tagetes patula* L., *Compositae* family), established by planting seedlings in the spring of 2017, observing the technological links on the experimental plots of INMA Bucharest.

The essential oil and hydrosol (floral water) of French marigold (*Tagetes patula* L., *Compositae* family) used in this study was obtained from the inflorescences and tops of the harvested plants' upper branches, by hydrodistillation (entrainment with water vapors under pressure), in a pilot installation of French origin.

Culture	<i>Nanuk variety</i>
Distance between rows	60 cm
Distance between plants/row	30 cm
Bush height	39 ... 42 cm
Bush diameter	40 cm
Number of branches	5 ... 8
Inflorescence form and diameter	flower heads of 4 ... 6 cm
Maturation period	July – until the fall of frost
Weed spreading degree	approx 10%
Surface form	flat

RESULTS AND DISCUSSION

The qualitative working indexes and the energetic ones determined in the tests and the results obtained are presented in table 1.

Table 1. Qualitative working indexes

No.	Name of energetic and qualitative working indexes	U. M.	Average value
1	Number of harvested rows	pc.	2
2	Cutting (working) height	mm	230
3	Working speed	km h ⁻¹	1.2
4	Cutting process efficiency	%	84.2
5	Loss (uncut plants)	%	15.8
6	Collecting process efficiency	%	85.4
7	Loss (uncollected cut plants)	%	14.6
8	Fuel consumption	l h ⁻¹	1.62

In order to test the antimicrobial activity of French marigold essential oil and hydrosol, two entomopathogenic fungal strains were used: *Beauveria bassiana* (BbIt) and *Beauveria brongniartii* (Bbg). Fungal strains were tested in the form of aqueous conidial suspensions obtained by washing with sterile distilled water and Tween 80 (0.01%) the sporulated fungal cultures on agarose culture medium. The Petri dishes (94x16 mm), in which 20 ml of potato-dextrose-agar medium were poured, were inoculated, after solidification, with 0.5 ml of conidial suspension which was evenly distributed with a Drigalski spatula.

The effect of essential oil and hydrosol (floral water) on the vegetative growth of the two fungal strains was tested by the impregnated disc method. Approximately two hours after plaque inoculation, 5 sterile filter paper discs (6 mm Ø) were individually impregnated with the test products at the initial concentrations placed on the culture medium surface. Immediately after placement, the dishes were sealed. The control was represented by discs impregnated with sterile distilled water. Evaluation of the tested products' effect was made after 10 days of incubation at 25°C by measuring the inhibition area.

The preliminary results obtained (Fig. 2) showed that French marigold essential oil completely inhibited spore germination, both in *Beauveria brongniartii* and *Beauveria bassiana* (inhibition zone diameter ≥ 2 mm). In case of treatment with French marigold hydrosol (floral water) no areas of vegetative growth inhibition have been observed, fungal mycelia completely spanning the surface of Petri dishes both at *B. brongniartii* and *B. bassiana*.

The antifungal properties of the essential oil and hydrosol (floral water) obtained from the French marigold inflorescences tested are due to the synergistic action of the component compounds because both the oil and the hydrosol are complex mixtures of molecules. The question is whether their biological effects are the result of all the constituent molecules synergism, or the result reflects only the interaction of the main compounds, present in larger quantities. In most cases, the main compounds reflect quite well the biophysical and biological characteristics of the essential oils from which they were isolated (Ipek et al., 2005), the intensity of the effects depending only on their concentration when tested alone or included in the essential oil and hydrosol. It is possible that the activity of the main compounds is modulated by other minor compounds present in the essential oil (Franzios et al., 1997; Santana-Rios et al., 2001; Hoet et al., 2006). Several essential oil components play a role in defining perfume, density, texture, colour and especially, cell penetration capacity, lipophilic or hydrophilic attraction, fixation on cell, membranes walls and cell distribution. This last characteristic is very important because the distribution of oil in the cell determines the different types of radical reactions depending on their cell division. For biological purposes, it is more important to study essential oil and hydrosol as a whole than a few compounds, because the concept of synergism in this case seems to be significant.

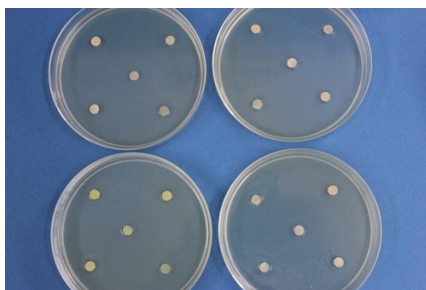


Figure 2. *Beauveria sp.* culture treated with French marigold (*Tagetes patula L.*, *Compositae family*) essential oil

CONCLUSIONS

The results showed the efficiency of medicinal plant harvesting equipment, designed to collect the herba of these species, grown on small and medium surfaces. Also, the harvesting equipment is an important premise for the development of equipment useful for small farmers, as well as for obtaining of quality products. The preliminary tests carried out revealed the antifungal activity, strongly inhibiting the French marigold (*Tagetes patula L.*, *Compositae family*) volatile oil, on two entomopathogenic fungal strains, *Beauveria brongniartii* and *Beauveria bassiana*. In the future, in order to test the complete and complex antimicrobial activity, several concentrations of French marigold volatile oil will be tested, by different test methods, on several types of phytopathogenic microorganisms. Subsequent studies to be carried out will focus on the preparation of protection natural pharmaceutical products, applicable to organic farming.

REFERENCES

- Bakkali, F., Averbeck, S., Averbeck, D., Idaomar, M. (2008). Biological effects of essential oils – A review. *Food and Chemical Toxicology* 46: 446-475.
- Franzios, G., Mirotsoy, M., Hatziapostolou, E., Kral, J., Scouras, Z.G., Mavragani-Tsipidou, P. (1997). Insecticidal and genotoxic activities of mint essential oils. *Journal Agriculture Food Chemistry* 45: 2690-2694.
- Grigore, A., Pirvu, L., Bubueanu, C., Colceru-Mihul, S., Ionita, C., Ionita, L. (2016). Medicinal plant crops-important source of high value-added products. In *Scientific Papers. Series A. Agronomy* LIX: 298-307.
- Hoet, S., Stevigny, C., Herent, M. F., Quetin-Leclercq, J. (2006). Anty-panosomal compounds from leaf essential oil of *Strychnos spinosa*. *Planta Medica* 72: 480-482.
- Ipek, E., Zeytinoglu, H., Okay, S., Tuylu, B. A., Kurkcuoglu, M., Husnu Can Baser, K. (2005). Genotoxicity and antigenotoxicity of Origanum oil and carvacrolevaluated by Ames Salmonella/microsomal test. *Food Chemistry* 93: 551-556.
- Martinov. M. and Konstantinovic M., (2007). *Harvesting in: Medicinal and aromatic crops. Harvesting, drying, and processing* (Öztekin S, Martinov M, eds.). The Haworth Press Inc., NY, USA, 56-84.
- Muntean, L. S. (2010). The use and cultivation of medicinal and aromatic plants in Romania, Hop and Medicinal Plant. *Printing House Academicpres Cluj Napoca* 1-2:34-43.
- Pajic, M., Pajic, V.I.S., Oljaca, M., Gligorevic, K. (2016). Influence of harvester type and harvesting time on quality of harvested Chamomile. *Journal of Agricultural Sciences* 61, 2:201-213.
- Santana-Rios, G., Orner, G.A., Amantana, A., Provost, C., Wu, S.Y., Dashwood, R.H. (2001). Potent antimutagenic activity of white tea in comparison with green tea in the Salmonella assay. *Mutat. Res.* 495:61-74.
- Schippmann, U., Leaman, D., Cunningham, A. B. (2002). Impact of Cultivation and Gathering of Medicinal Plants on Biodiversity: Global Trends and Issues. *Biodiversity and the Ecosystem Approach in Agriculture, Forestry and Fisheries. Satellite event on the occasion of the Ninth Regular Session of the Commission on Genetic, Resources for Food and Agriculture. Rome, 12-13 October 2002.*
- Pan, S.Y., Gao, S.H., Zhou, S.F., Yu, Z.L., Chen, H.Q., Shang, S.F., Tang, M.K., Sun, J.N., Ko, K.M. (2014). *Historical Perspective of Traditional Indigenous Medical Practices: The Current Renaissance and Conservation of Herbal Resources. Evidence-Based Complementary and Alternative Medicine* 2014.



ASPECTS OF DIGITIZATION IN AGRICULTURAL LOGISTICS IN GERMANY

Heinz BERNHARDT*, Michael MEDERLE, Maximilian TREIBER, Sascha WÖRZ

Technical University of Munich, Agricultural Systems Engineering,
Am Staudengarten 2, 85354 Freising, Germany

*E-mail of corresponding author: heinz.bernhardt@wzw.tum.de

SUMMARY

Digitization is one way to fulfil the demands on agricultural logistics. The growth in farm size and new branches mean that logistics is becoming ever more complex. A simple takeover of systems from the general logistics is not possible because of the special conditions of agriculture. First offers for digital logistics in agriculture are on the market. These are usually only for small areas and not complete chains. Often there are still difficulties with data availability and interfaces. There are first solutions for digitization in logistics across several levels of trade. These work if the partners are well organized and agree. If this confidence does not exist, digital collaboration is also difficult. A big problem that still has to be solved is data ownership and privacy.

Key words: logistic, digitalization, data management, data privacy protection

INTRODUCTION

Logistics plays a crucial role in agriculture. Between field, stable and trade many different goods have to be transported. In recent years, the importance of logistics in agriculture in Germany has increased. The quantities and distances per farm have increased. This has different causes: the growth of the farms, the reduction of the locations of trade and the biogas boom (Bernhardt, 2002; Götz, 2015).

At the same time, the demands on logistics have increased. As the consumer in Germany is very critical about food safety all goods flows from the field or stable to trade must be traceable. Logistics is no longer just about the transport and handling of the goods but also on the data belonging to the transported goods (Seufert, 2006; Folinas, 2015).

The aim of the farms is also to optimize the processes in agricultural logistics. Especially in large logistics chains e.g. the transport of 500 ha of silage maize for a biogas plant cost reduction plays a decisive role. The resource manpower must also be used optimally as it is

important for logistics processes and there are always less well-trained drivers available (Sonnen 2007; Heizinger, 2011).

All of this means that digitization in agricultural logistics is increasingly being used to solve the problems that arise. The effects can be subdivided into several areas. These are: the comparison with industrial logistics, the hardware and software used and the impact on marketing.

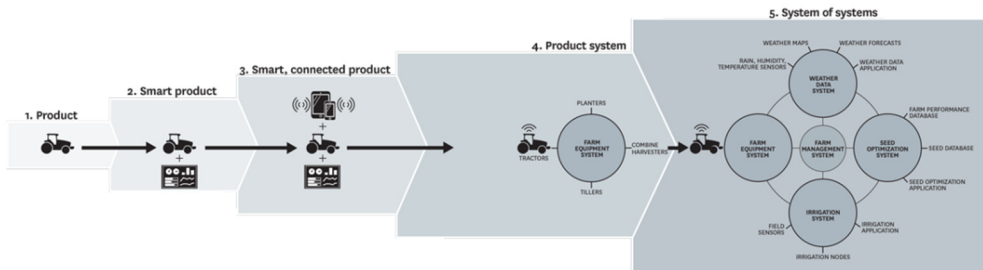


Figure 1. Data management in agriculture (Proter and Heppelmann, 2014)

Comparison of general logistics and agricultural logistics

Digitization is currently playing a crucial role in all sectors of the economy. In Germany, all these efforts are summarized under the term "Industry 4.0" which describes the complete digital networking of all production processes. It could be assumed that agriculture can directly take over the developments in the field of general logistics but it shows that agricultural logistics has considerable structural differences compared to general logistics. A key difference in agricultural logistics is that here the sources and sinks in logistics move during the process. In general logistics the starting point and target are always specified and therefore long term planning is possible. In agriculture the start point and target can move in space during the logistics process. The combine harvester, for example, moves on the field during harvesting. The precise location on the field on which it has to overload the grain onto the transport vehicle is difficult to determine previously because factors such as yield, driving patterns on the field, soil properties, the driver's operation etc. are difficult to simulate. This considerably complicates the preliminary planning as both vehicles continue to move during the reloading (Sonnen, 2006; Rusch, 2012; Heizinger, 2014; Lamsal, 2016; Wörz, 2017).

The agricultural logistics are also different in that the transport is generally carried out with tractors. Transport from the field to the road happens with the same technology. The transport vehicles must therefore be able to drive both in the field and on the public road. Therefore, it is difficult to use technology from the general logistics, optimized for the road, in agriculture. This structure of agricultural transport technology in Germany has grown historically and can only be changed with a complete change of organization and technology (Götz, 2011; Götz, 2014).

Hardware in agricultural logistics

Agricultural logistics has been marked by digitization in recent years. A good example of this is the use of navigation systems in agriculture (Kluge, 2015). For large logistics chains, such as the harvest of silo maize it is important for the transport vehicles that they are on time with the forage harvester. For this purpose, navigation systems have been used for several years. These differ from the usual systems for street navigation. For agriculture, dirt roads, bridge loads and other agricultural aspects must be marked on the maps. In addition, one-way street rules must be able to be deposited so that no two transport vehicles meet on a dirt road. Agricultural navigation systems must also be able to plan very dynamically on the basis of the harvest data since crop quantity, ground conditions or machine condition can change the distances. The variety of influencing factors make the development of special systems for agriculture difficult, which is why paper cards are often still to be found as a safety system in practice (Steckel, 2015).

Another digital system which promises advantages in logistics is yield recording in the combine harvester or forage harvester. However, both systems show that they record the data too late for direct logistics. There is no time left to plan the logistics accordingly, as the transport vehicles almost have to be at the harvester when they are collected. With the forage harvester, the yield data are sometimes used to divide the costs of transport from different farmers. More interesting for logistics is currently the development of drones or satellites for yield estimation. This data could be available early and precisely enough to even reschedule the logistics in the technology and organization used (Pauli, 2012).

Overloading makes great demands on the drivers of the harvesting vehicle or the transport vehicle, especially at night or after many hours of work. Here digitization also offers opportunities to relieve the driver. From several manufacturers systems are offered in which the track signal of the harvester is charged and transmitted by radio to the transport vehicle. The steering of the transport vehicle is thereby taken over by the harvesting vehicle and the vehicle is always kept at the same distance and speed. This is particularly advantageous for sudden evasive manoeuvres of the harvesting vehicle because this information engages directly in the steering of the transport vehicle and thus can prevent accidents caused by the reaction delay of the driver of the transport vehicle. During the filling process camera systems detect the filling of the transport vehicle and control the forage harvester to optimally load the transport vehicle.

Another important aspect for the digitization of large logistics chains in one area is that all vehicles are clearly identified. For newer harvesters, this can be done via the telematics system. Many transport vehicles and older tractors do not have this. Here is now the possibility to mark these vehicles with Bluetooth chips. This chip can be clearly recognized by the other vehicles and thus each vehicle of the chain can be identified.

In order to be able to document all data of the transport of a commodity these must be collected digitally. Two systems are currently used for this purpose. In one method all data of the goods are stored separately from the individual machines in a central cloud. In the other system, the data remain with the goods and are transferred from the harvester to the transport vehicle and then goods and data are transported together to the warehouse (Rusch, 2012). In the first system, the data is stored very quickly in the cloud, but you have to put data and goods back together properly. In the second method, the data always remain with the goods, but several transmission processes are necessary for this.

Software in agricultural logistics

The spread of digitization in agricultural logistics is well recognized by the use of farm management systems. Farm management systems document, process and analyse all information on location, process flow, technology, employees, costs, etc. of the farm. Farm management systems therefore provide ideal conditions for planning agricultural logistics (Pauli, 2015; Pavlou, 2016). The problem that always shows in practice is that although the appropriate tools for planning are available usually the planning goals cannot be formulated clearly. As an example, the infield logistics can serve here. The pattern of driving on a field e.g. when sowing, fertilizing or harvesting has a significant impact on the associated costs, working hours and effects on the soil structure (Shearer, 2015; Zhou, 2015; Sabelhaus, 2015). It is therefore close to the driving of the fields before a simulation to plan. For this purpose, products are also offered by various manufacturers. However, observations in practice show that these products are not as accepted by the farmers as the advertised savings potential suggests. An analysis of the objectives of the products shows that these are usually optimized for the longest route and the least turning operations. But these are not always the goals of the farmer. Here, the transport capacity of sugar beet harvester or slurry tanker or the location of possible overload points at the edge of the field may determine the route on the field (Mederle, 2015). To use digital tools to optimize the farm, the real goal of the individual operation must be precisely determined. This is often difficult.

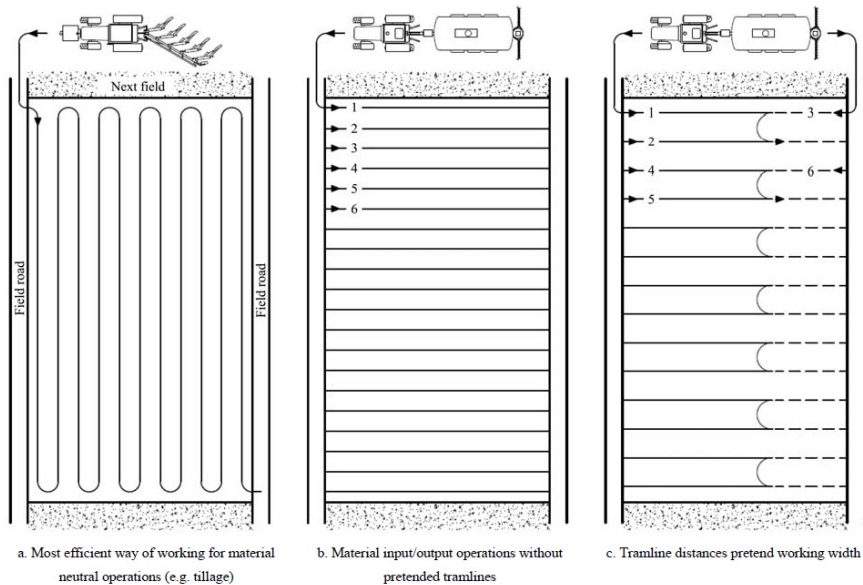


Figure 2. Different infield-strategies depending on various operations (Mederle, 2017)

The technical data for farm management systems are usually supplied from telematics systems of the machines. Originally designed purely as a display for IsoBus data, these systems today regulate the collection, processing, display, exchange and documentation of all machine data. Interfaces can also be used to exchange data from different machines. Telemetry systems are thus the basis of many products the previous chapters were

presented. But even here, agricultural practice shows that the general use and the economic benefits usually fail due to trifles. In order to transfer the system from the demonstration phase to the general usage, it has to be stable. This is difficult because German agriculture, use different radio network, have different machines with different ages in one logistic chain or different manufacturers and data standards communicate with each other. An example is the radio data transmission. There is a lot of investment to be able to transfer even more data, but especially in rural areas, the network coverage is sometimes bad. Radio network coverage in rural areas is not optimal. Depending on the network provider, it ranges from 89% to 98% in the G4 network (LTS). The average upload rates in rural areas are between 8.41 and 19.53 Mbps, for comparison in the city between 10.65 and 29.02 Mbps on average (Mandau, 2017). Even low power wide area networks such as LoRa or Sigfox do not achieve sufficient coverage in rural areas. Navigation systems for large crop chains do not work if parts of the chain are not currently visible because they cannot transmit their position (Schattenberg, 2013; Nordemann, 2015). Another difficulty is partly the capacity of the data network in the machine. Originally the IsoBus was designed to control the machine. Today, all machine data should also be sent via this data network. To make this possible, the data is compressed. But this also loses information that would be needed in farm management systems. So it would be a new own data network for this data necessary (Weltzien, 2016). Especially on small farms in southern Germany, another problem arises for the digitization of agricultural logistics. Here the machines are used for a long time. Many of these machines do not yet have the required interfaces for data exchange.

Impact of digitization on production chain partners

Logistics also plays a decisive role in trading. Here too the transfer of digital data via the individual trading stages is considered an advantage. When implementing digitization in logistics, the individual trading chains have developed very differently.

In sugar beet production, the individual fields are recorded digitally and all important information, such as grower, rowing order or storage location documented. On the basis of this data, the planning of the shared harvesters is planned. The individual harvester then reports their operating data via GSM. These data can then be used to further fine-plan and to plan the transport. When loading the transport vehicles then all the necessary data of the sugar beets are digitally transmitted and the quality data then reported back to the farmer. All harvest, transport and billing data is recorded in a central database and can be queried online by all parties involved in the process. This system is possible because in southern Germany there is only one central processor of sugar beets with nine sugar factories and one central farming community with 18 000 farmers and 137 000 ha of sugar beet acreage, which are also economically linked. Because everything is in one hand, a functioning digital agricultural logistics system for sugar beet could be established for a long time. Difficulties in the organization can thus be easily clarified. However, the system still has technical problems as discussed in the chapter Software (Gebhard, 2016).

In the digitization of grain logistics, things look quite different. Here, neither the farmers nor the traders have central organizations that can develop a common structure. Here there are only first approaches for a digital data collection in logistics at farmer and trade. These systems are not compatible with each other. When marketing, therefore, the digital data are often given by the farmer on paper to the warehouse and re-entered by this into their digital system. Both sides have not yet found an organizational structure with which they can digitally share logistics data.

CONCLUSION

Overall, the digitization of agricultural logistics in Germany is desired and also necessary. Both the condition in growing farms and the trading requirements point in this direction. The first interesting products can be found on the market. It turns out, however, that there is often still a lack of stability of the systems used. Here the agriculture which works on the area is exposed to special conditions.

An important issue that is not yet sufficiently clarified is the privacy and ownership of the data collected. Many partners have their own data as well as great interest in the data of the other partners. For fear of being cheated or exploited by others, most of them withhold their data. There is currently no structure regulating the data exchange. A shared data usage would bring economic benefits to all partners, but how these benefits have to be distributed to all just needs to be clarified.

REFERENCES

- Bernhardt, H. (2002). Schüttguttransport in landwirtschaftlichen Betrieben Deutschlands. Dissertation Justus-Liebig-Universität Giessen, Germany.
- Deeken, H., Krampe, F., Steckel, T. (2017). Verbesserung logistischer Prozesse durch Dezentralisierung von Entscheidungen, 37. GIL-Jahrestagung „Digitale Transformation - Wege in eine zukunftsfähige Landwirtschaft“, Dresden, ISBN: 978-3-88579-662-6, p. 41-44.
- Folinas, D., Aidonis, D., Manikas, I., Bochtis, D. (2015). Logistics Processes Prioritization in the Agrifood Sector, *International Journal of Agricultural Management*, 4, 72-83.
- Gebhardt, H., Kirchberger, T. (2016). Rübenanbau und Zuckererzeugung ab 2017, URL http://bisz.suedzucker.de/Downloads/Kuratoriumstagungen/Kuratoriumstagung_2016/Gebhardt_Hans-Joerg_Kirchberg_Thomas.pdf, 15.2.2017.
- Götz, S., Holzer, J., Winkler, J., Bernhardt, H., Engelhardt, D. (2011). Agrarlogistik – Systemvergleich von Transportkonzepten der Getreidelogistik; *Landtechnik*, 5, 381-386.
- Götz, S., Zimmermann, N., Engelhardt, D., Bernhardt, H. (2014). Influencing factors on agricultural transports and their effect on energy consumption and average speed. *Agric Eng Int: CIGR Journal*, Special issue 2014: Agri-food and biomass supply chains, 59-69.
- Götz, S., Zimmermann, N., Engelhardt, D., Bernhardt, H. (2015). Simulation of agricultural logistic processes with k-nearest neighbors algorithm. *Agric Eng Int: CIGR Journal*, Special issue 2015: 18th World Congress of CIGR, 241-245.
- Heizinger, V. and Bernhardt, H. (2011). Algorithmic Efficiency Analysis of Harvest and Transport of Biomass, *Journal of Agricultural Machinery Science*, Hrsg. Agricultural Machinery Association Turkey, Volume 7 Number 1, ISSN 1306-0007, p 95-99.
- Heizinger, V. (2014). Algorithmic Analysis of Process Chains in Agricultural Logistics, Dissertation, TUM München, Germany.
- Kluge, A. (2015). CLAAS Fleet View Mobile application for coordinating the transport logistics in the grain harvest, *VDI-MEG LandTechnik 2015 Hannover November 2015*, 355-358, Düsseldorf: VDI-Verlag 2015.
- Lamsal, K., Jones, P., Thomas, B. (2016). Harvest logistics in agricultural systems with multiple, independent producers and no on-farm storage, *Computers & Industrial Engineering*, 91, 129-138.
- Mandau, M. and Pauler, W. (2017). Bestes Handynetzz 2017/18: Netzabdeckung O2, Vodafone, Telekom im Test Deutschlands härtester Netztest, In: *Chip.de*, 1/18.
- Mederle, M. and Heizinger, V., Bernhardt, H. (2015). Analyse von Einflussfaktoren auf Befahrungsstrategien im Feld, 35. GIL-Jahrestagung 2013, 113-116, Geisenheim: GIL 2015.

- Mederle, M. and Bernhardt, H. (2017). Analysis of Influencing Factors and Decision Criteria on Infield-Logistics of different Farm Types in Germany, In: CIGR E-Journal, Vol 19. Issue 2, pp. 139-148.
- Nordemann, F., Tönjes, R., Pulvermüller, E. (2015). Robust Communication for Agricultural Process Management in Rural Areas How Dynamic Combination and Configuration of Communication Technologies enables robust Data Transfers in Rural Areas, VDI-MEG LandTechnik 2015 Hannover November 2015, 95-100 Düsseldorf: VDI-Verlag 2015.
- Pauli, A., Angermaier, W., Tüller, G., Bernhardt, H. (2012). Evaluierung von Dokumentationsdaten elektronischer Erfassungssysteme in der Erntelogistik von Biomasse, 32. GIL-Jahrestagung: Informationstechnologie für eine nachhaltige Landwirtschaft, 29. Februar.-1. März 2012, Freising: GIL, 2012.
- Pauli, S. (2015). Automatische Dokumentation von Warenströmen bei Transportprozessen von landwirtschaftlichen Gütern, Dissertation, TUM München, Germany.
- Pavlou, D., Orfanou, A., Busato, P., Berruto, R., Sørensen, C., Bochtis, D. (2016): Functional modeling for green biomass supply chains, Computers and Electronics in Agriculture 122, 29–40.
- Proter, M. and Heppelmann, J. (2014). How smart, connected products are transforming companies. Cambridge / Hamburg: Harvard Business Review, 03.12.2014.
- Rusch, C. (2012): Untersuchung der Datensicherheit selbstkonfigurierender Funknetzwerke im Bereich von mobilen Arbeitsmaschinen am Beispiel der Prozessdokumentation, Dissertation, TU Berlin, Germany.
- Sabelhaus, D., Schulze Lammers, P., Meyer zu Helligem, L., Röben, F. (2015). Pfadplanung von landwirtschaftlichen Fahrmanövern, Landtechnik (2015) 4, 123-131.
- Schattenberg, J., Harms, H., Lang, T., Becker, M., Batzdorfer, S., Bestmann, U., Hecker, P. (2013). Datenaustausch in mobilen Maschinenverbänden zur echtzeitfähigen Positionierung, Landtechnik (2013) 5, 359-364.
- Seufert, H. (2006). Landwirtschaft = QM Qualitätsmanagement im Lebens- und Futtermittelsektor, DLG-Verlag, Frankfurt.
- Shearer, S., Wolters, D., Root, P., Klopfenstein, A., Schroeder, B. (2015). Modeling of Grain Harvest Logistics for Modern In-Field Equipment Complements, VDI-MEG LandTechnik 2015 Hannover November 2015, 379-386, Düsseldorf: VDI-Verlag 2015.
- Sonnen, J. (2007). Simulation von Ernteprozessketten für Siliergüter. Dissertation, Humboldt-Universität zu Berlin, Germany.
- Steckel, T., Bernardi, A., Gu, Y., Windmann, S., Maier, A., Niggemann, O. (2015). Anomaly Detection and Performance Evaluation of Mobile Agricultural Machines by Analysis of Big Data, VDI-MEG LandTechnik 2015 Hannover November 2015, 349-354, Düsseldorf: VDI-Verlag 2015.
- Tian-Tian Zhang, Qiao-Yu Zhang (2015). The application of Internet of Things in the logistics of agricultural products. Design, Manufacturing and Mechatronics: pp. 558-567. https://doi.org/10.1142/9789814730518_0067.
- Warkentin, H., Steckel, T., Maier, A., Bernardi, A. (2017). Verbesserung mobiler Arbeitsprozesse mit Methoden von Big Data und Data Analytics. 37. GIL-Jahrestagung „Digitale Transformation - Wege in eine zukunftsfähige Landwirtschaft“, Dresden, ISBN: 978-3-88579-662-6, p 161-165.
- Weltzien, C. (2016). Digitale Landwirtschaft – oder warum Landwirtschaft 4.0 auch nur kleine Brötchen backt, Landtechnik, Bd. 71, Nr. 2.
- Wörz, S. (2017). Entwicklung eines Planungssystems zur Optimierung von Agrarlogistik Prozessen, Dissertation, TUM München, Germany.
- Zhou, K., Leck Jensen, A., Bochtis, D., Sørensen, C. (2015). Simulation model for the sequential in-field machinery operations in a potato production system, Computers and Electronics in Agriculture, 116, 173–186.



INCREASE OF SOIL TILLAGE EFFICIENCY WITH USING OF RTK - NAVIGATION

Nikola VAJDA, Damijan KELC*, Peter VINDIŠ, Peter BERK, Jurij RAKUN,
Denis STAJNKO, Miran LAKOTA

University in Maribor, Faculty of Agriculture and Life Sciences, Pivola 10, 2311 Hoče, Slovenia

*E-mail of corresponding author: damijan.kelc@um.si

SUMMARY

The concept of precision farming is wide, and it represent the efficiency which is achieved with the help of precision. For the navigation of field machines the RTK (Real Time Kinematic) navigation is needed. In order to verify the positive effects in practice, we used tractor Fendt 828, which was equipped with the RTK navigation system. We compared how much fuel and time we save, and the width of overlap using manual driving. The experiment was conducted on two areas of land size of 172 x 58 meters, and the two working machines wide 3 and 6 meters. When the experiment was done, we saved 15,7% of the time and 8,66 % of the fuel on a working machine of 3 meters wide, and 12,6 % of the time and 8,28% of the fuel on a working machine of 6 meters wide. The width of the overlap represent 10% of the working width of the machine, and with the method of turning, which RTK navigation allows, we save additional time. The use of precision agriculture technologies allows us to better plan and analyze the working procedures.

Key words: RTK navigation, soil cultivation, efficiency, fuel savings, precision farming

INTRODUCTION

With precise farming, we gain a better realization of plant production, and in foreign literature there is a lot of research on this topic. We know very well that the structure of land in agri-developed countries is completely different than in Slovenia, and the use of RTK-navigation comes to a different perspective than on our fragmented land. The decision was to explore the actual situation or, the usefulness of RTK technology on the structure of our land. In the task we want to check the actual saving of time and fuel, which consequently influences the reduction of variable production costs. In order to save time, we will test various ways of turning the tractor enabled by RTK technology. The purpose is also to

determine the human accuracy of driving the tractor in the field and compare it with the use of RTK precision (± 2 cm).

If we want Slovenian agriculture to become more competitive, we need to introduce modern agricultural technologies into our agricultural environment. Modern technology includes satellite navigation, which is intensively used in neighbour developed countries.

To determine the accuracy of the position less than one meter, we need a reference or base station. This may be your own mobile or permanent reference station owned by an operator and used by several users. A permanently operating reference station is permanently located where there are no disturbing factors, such as large reflecting surfaces or radio transmitters. Since the coordinates of the reference station are precisely determined, the receiver can determine observation corrections from observations and known satellite positions. Through the communication channels (GSM, UMTS, NTRIP), the reference station in the form of standardized records sends such data to mobile receivers in the field, in our case on the tractor. Using the obtained data, the receiver, together with its data from observations or corrections of the reference receiver, determines its precise position in real time (GNSS, 2017).

The receiver determines its position by measuring the distances to satellites in the universe, creating a replica of the signal it receives from the satellite, and comparing it with the signal generated in the receiver. Because the signal on the Earth is very weak, special signalling is required. The locally-determined signal receiver delays so long that the cross-fermentation function reaches full alignment with the source signal. After complete alignment, the PRN code is removed from the signal. Such signal is ready for further processing. The receiver decodes the position of satellites. The precise position of the receiver is determined by measuring the distances of the four satellites. The position is determined by the method of the smallest squares between pseudo-satellite distances. More available satellites we have, the better and more precise is the quality of locating the position (GNSS, 2017).

After we got real-time location information, leading the tractor is taken over by various sensors, computers, electric motors and hydraulics. For automatic control systems, we have various options. The system can be installed directly by the tractor manufacturer, where the hydraulic control of the steering system is carried out, which, by means of sensors of the wheel rotation angle, leads the tractor along the field. The second option is the subsequent upgrading of the tractor with navigation device where we have the option of hydraulic or electronic control of the steering. Various manufacturers offer various additional electric motors that are installed directly on the tractor's steering wheel. The price of the post-production upgrade with hydraulic steering is approximately 4500 €, and electro-steering is approximately 3000 €.

In Slovenian literature, general theoretical information dominates. Such a situation was to be expected. Technology in Slovenia is new. The investment is expensive. The practical data is still too small for the technology to expand. Most information can be found on the websites of authorized dealers or importers. One such website is Geoservis d.o.o., where we can obtain a sufficient amount of data on the operation and usability of GPS in agriculture.

Vaukana (2001) described the method of capturing spatial data using GPS technology and how to use GPS systems to accurately determine the position in the space, measure the surfaces, ranges and paths, and simultaneously monitor agricultural machines in work tasks. It also provides information on GPS operation, signals, faults, measuring instruments and software.

Kašman (2003) described in his thesis the details of the Global Information System (GPS). In the literature, he described in detail the composition of GPS, its purpose, accuracy and

mistakes. He also devoted much attention to the description of Geographic Information Systems. In the task they monitored the working procedure of ploughing and recorded satellite data with data that were later processed and used for precise calculation of the costs of ploughing. With the help of evidence, a working hypothesis was confirmed that with the aid of the GPS system, we can more accurately assess the costs of ploughing in comparison with the simulation model.

The difference between the stated accuracy indicated by the manufacturers and the actual measured accuracy was compared in one experiment in Germany. Different GPS systems were compared among each other, differing primarily in their ability to control precision. In the first treatment, a classic manual drive was compared, in the second manual drive in combination with GPS guidance, the third was autonomous driving, and in the last, fourth, autonomous driving with RTK system. At first and second treatment, the actual accuracy was worse than stated, namely, the accuracy was indicated for a manual run of 20 cm and the actual one was 22 cm. In the second treatment, the accuracy was 10 cm and the actual one was 12 cm. For the following two systems, the actual accuracy was better than indicated. In the autonomous run without RTK, the accuracy was 5 cm, the actual 3.5 cm, and the RTK 2 cm and the actual 1.2 cm. In the continuation of this research, the productivity of automatic and manual driving was demonstrated, where productivity was increased by about 8% in automatic driving, which is 0.5 ha per hour (Reckleben, 2010).

Important study was done in Austria, where three different systems were used to guide the tractor: manual driving, manual GPS-assisted driving, and automatic driving system. With the working width of 15 m and 3 m, the actual width of the working machine was compared. For a working width of 15 m, the actual working width of the hand-held vehicle was 14.29 m, for GPS assistance and manual driving 14.92 m, and for automatic driving 14.91 m. At a working width of 3 m, the actual working width of the manual drive was 2,775 m, and for GPS assistance and automatic driving 2,906 m (Landerl 2009).

In the study, Landerl (2009) studied the time needed to process parcels in the size of 3,186 ha. A hand-guided ride was compared to each other, where 29 passes were required to process the plot and 39.38 minutes, of which turning time was 8.4 minutes. With the help of the GPS system and the ring ride, 28 passages were needed, and 34.12 minutes and a turning time of 4.77 minutes. In automatic driving, 28 passes were needed. 36.05 minutes and 6.02 minutes for turning. For manual driving, the average turning time was 13.39 seconds, while using the GPS system was significantly shorter. 13.38 seconds were used on average for the autonomous driving system and 10.61 seconds for the manual hand-held GPS system. Differences in the turning time between the GPS systems were separated due to the longest distance travelled in autonomous driving. As a matter of interest, at the end of this study, it was stated that with the help of the GPS system, in addition to working area of 5 m, work surface of up to 9 ha can be processed within 12 hours (Landerl, 2009).

Landerl (2009) also tried to determine the fuel savings in the experiment. He compared the three systems. Manual-assisted steering system, manual driving with GPS and autonomous driving. During the experiment, they measured the average fuel consumption per ha. The first part considered only the actual treatment without manoeuvres at the end of the plot. This resulted in manual driving with 35,292 l / ha of GPS and at the end of the GPS autonomous drive with a minimum consumption of 34,403 l / ha. The main reason for the difference in fuel consumption was the number of transits per ha. According to research, we can say that with the help of GPS, we save fuel.

Lopez (2013) showed the savings in manual drive and RTK system in crop production. The savings in the production of silage maize with the GPS system is around 13 € / ha, 22 € /

ha of sugarcane, 22 € / ha of sugar beet and 23 € / ha for cereals. The highest hectare savings, 61 € / ha, was in the production of potatoes. They also showed average hectare savings in all the aforementioned crops, except for potatoes. Using an accuracy of 0.30 m, we can save 4-5 € / ha, with an accuracy of 0.15 m 9-12 € / ha and using the RTK system 20-23 € / ha.

The aim of our research is to examine the factors that affect the cost of producing food in the field. We will analyze how much we can save time and fuel through RTK. We estimate that between 5-12%. We estimate that manual driving is 10-20% less accurate than RTK. Additional time savings can be achieved by turning the tractor, RTK technology allows each other to process.

MATERIALS AND METHODS

The Slovenian national network The signal is the GNSS (Global Navigation Satellite System) network, which is made up of 16 uniformly distributed permanent stations throughout the country. The stations are arranged in such a way that the distance between them is less than 70 km, while the borders of the country complement the stations of the neighbouring countries (5 Austrian, 6 Croatian and 1 Hungarian). Network operation The signal is provided by the GNSS Service under the auspices of the National Geodetic Authority at the Geodetic Institute of Slovenia. Access to network data Signal is also possible through the DGPS service provided by Telekom Slovenije. In this way, we can access RTK data via the GSM (Global System for Mobile communications) network where the user needs a GSM-modem connected to a mobile server (Ministry of Environment and Space, 2016).

Geoservis d.o.o. Slovenia is the main manager of permanent GNSS stations (Figure 1), where besides own stations, they also take care of partner stations. In Slovenia there are 7 permanent stations, and in the current year 2016, 4 additional permanent stations will be installed (GNSS, 2012).

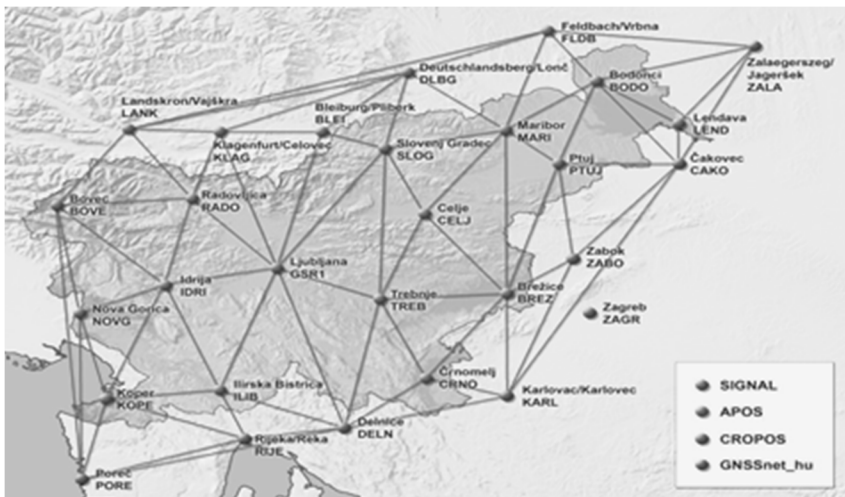


Figure 1. Reference stations of the national network Signal (GNSS Map)

The field part of the experiment was held in Sebeborci in the municipality of Moravske Toplice (Figure 2). The farm is under the home-name "Kerchmar Tabla" (GERK_PID:

1247662) and has a total area of 5.73 ha. The floors are sandy-loamy and easy to process. The previous crop in the field was corn for silage, and there was little crop residue in the field. There is no correct rectangular shape, so for the purpose of the experiment we divided it into two identical smaller parcels with dimensions of 58 mx 172 m, which represented an area of 1 ha for each of them.



Figure 2. Experimental Fields (Public MGG Graphic Data Viewer, MKGP)

In the experiment we prepared soil for soybean seeding, so that during the first round of the soil, we worked with a raspberry working width of 3 meters. The next round was followed by a fine prefabricated device with a cultivator working width of 6 meters. The experiment was carried out in such a way that, when dealing with RTK, the plot was first treated with a working connection of 3 m and later with a 6 m working connection. At the end of the field, we turned semi-circular to each other or third row. On the second plot, we carried out a manual drive, where we also first treated the parcel with a working connection of 3 meters wide and then with a working connection of 6 meters wide. At the end of the ozone we turned to classical in every kind. With the help of the tractor, we obtained basic information on the consumption, processing time, distance traveled. With the help of traffic lines recorded by tractor navigation, the number of necessary trips to the plot (GPS visualizer, 2016) was counted in the GPS Visualizer web application.

Before we started the experiment, we set the tractor and the navigation in more detail. In order to avoid deviations due to uneven working speed during the processing time, at both working widths of 3 m and 6 m for manual and autonomous RTK driving, the operating speed was set at 10 km/h with the help of the tempomat.

In the experiment, the Fendt Vario 828 (figure 3) was used, with a 6-cylinder engine of 6065 cm³ and a rated power of 203 kW (EG 97/68). The engine is equipped with the SCR (Selective Catalytic Reduction) system, where the exhaust gases are subsequently treated with AdBlue (32% urea solution), which changes the NO_x nitric oxide into non-toxic nitrogen and water. A non-stop welding gearbox is installed on the tractor, which is a hydrostatic-mechanical gear unit with distributed power transmission.



Figure 3. Fendt 828 Profi plus

We used cultivator the Cenius 3001 grinder (Figure 4) with a working width of 3 m, which is optimal for rapid soil treatment with intensive mixing of crop residues. The grip is widely used, as it enables processing from a depth of 5 cm up to 28 cm. Legs with 500 kg overload protection are installed in three types, with a total of 11 legs, and the distance between them is 81 cm.



Figure 4. cultivator Cenius 3001

In the experiment, a prefabricated pre-cultivator of the renowned Kverneland manufacturer with a working width of 6 m was used (figure 5). The total weight of the connection is 2590 kg, and for optimum performance the minimum working power of the tractor is 100 kW. The cultivator consists of 4 working areas. These are: leveling board, cylinder, s-foot and 2 rollers.



Figure 5. Kverneland TLG

The tractor we used in the experiment is equipped with the navigation of the American company Topcon and enables precision up to ± 2 cm. The navigation also includes the Topcon AGI-4 antenna, which is standardly equipped with WAAS and EGNOS, and an additional option extends to RTK precision, as was the case in our case. The antenna is thus composed of three components. The first component is an antenna or receiver, the other is a gyroscope or compass, which ensures precise movement of the tractor in case of uneven surfaces (various slopes of the tractor).

Tractor Fendt tells its users at all times of fuel consumption, time of work, distance travelled ... With this computer, for each treatment, we separately measured fuel consumption, time of parcel processing, total processing time of each parcel, including the turning at the end of the field. We also measured the total distance travelled in the processing of a particular plot for each treatment.

GPS-visualizer is a free web-based tool that is used to create maps and profiles using geographic information. The input data can be of different formats and sources. The web-based tool is versatile as it is compatible with many navigation devices. For example, we can easily remove the data from our navigation and map the route on the map; we can insert titles or simply enter the coordinates (GPS visualiser, 2016).

RESULTS AND DISCUSSION

Table 1. Data of tractor measurements with a working connection of 3 m wide

Working width 3 m (Amazone CENIUS 3001)			
	RTK	Manual drive	Difference (%)
Total time (m : s)	26 : 26	31 : 22	15,7
Processing time (m : s)	21 : 58	24 : 25	10,04
Turning time (m : s)	3 : 28	6 : 57	50,12
Distance travelled (m)	3456	3822	9,58
Fuel consumption (l)	9,5	10,4	8,66
Number of trips	20	22	10

Table 1 gives the data of tractor measurements with a working connection of 3 m wide. With this working connection we used a total of 26 minutes and 26 seconds of time to process the plot using automatic control, while we used 31 minutes and 22 seconds for manual driving. In this case, the turning time for automatic control was 3 minutes and 28 seconds, and for manual driving 6 minutes and 57 seconds. In order to process the entire experimental parcel, we transported 3456 m through RTK in 20 rounds and consumed 9.5 l of fuel. In a manual run, we carried 3822 meters in 22 rounds and spent 9.5 liters of fuel. From the obtained data, it can be understood that by using the RTK-type control with 2 centimetres accuracy, we spent 15.7% less time and 8.66% less fuel.

Table 2. Data of tractor measurements with a working connection of 6 m wide

Working width 6 m (Amazone CENIUS 3001)			
	RTK	Manual drive	Difference (%)
Total time (m : s)	13 : 46	15 : 45	12,6
Processing time (m : s)	10 : 54	12 : 15	11,03
Turning time (m : s)	2 : 52	3 : 30	18,1
Distance travelled (m)	1712	1916	10,65
Fuel consumption (l)	5,4	5,9	8,28
Number of trips	10	11	10

Table 2 shows the data of tractor measurements with a working connection of 6 meters wide. The total processing time with automatic control was 13 minutes and 46 seconds, of which we spend 2 minutes and 52 seconds for turning (table 2). In manual control mode, 15 minutes and 45 seconds were spent for the processing of the experimental parcel, 3 minutes and 30 seconds for turning the zones. We spent 12.6% less time to process the entire experimental plot. Altogether, with the help of automatic control, a total distance of 1712 m was carried out, while in the manual run 1916 m. In the RTK mode, we used 5.4 liters of fuel in 10 rounds and 5.9 liters of fuel in 11 rounds, so we saved 8.28% of the fuel.

On the basis of all the field trials we have made, with the help of RTK-navigation, the scales make important findings. Our purpose was to compare time, fuel and driving accuracy compared to manual driving. The findings show that when working with a 3 m wide working connection, with the help of RTK navigation, we saved 15.7% of the time and 8.66% of the fuel. When working with a working connection of 6 meters wide, processing

time was reduced by 12.6% and fuel savings of 8.26%. The accuracy of driving in manual driving or overlapping is presented in both cases, with a working connection width of 3 meters and 6 meters, 10% of the working width of the connection. This means that the work piece is 3 meters long and 30 cm wide and 60 cm wide with a working connection of 6 meters wide. RTK-Navigation has enabled us to turn to any other or third type, which additionally saves time and fuel.

According to the literature review and the results of measurements in the experiments carried out, we can conclude that the use of RTK navigation in the future is one of the factors in ensuring the competitiveness of agriculture and increasing the efficiency of soil treatment. The positive effects of navigation are not only evident when saving time and fuel. Due to more precise driving and precise connections associated with the navigation device, it also provides additional savings in the consumption of raw material (seeds, fertilizers, FFS). Especially because the percentage of overlap is minimal, and the application of FFS and fertilizers is very uniform. Today's lifestyle causes more and more people's stress and health problems. Because the work on agricultural holdings is a lot, people are also all day in bad conditions on the tractor. When reviewing the research, we found that using the navigation, the tractor load is reduced. With this, we have two positive effects of navigation, that is, the economics of cultivation as well as the health status of the driver. One of the negative features of RTK navigation is at present a high price and therefore an inaccessibility for smaller and medium-sized farms. As with other things, it will also take place in this area over time to lower prices and make navigation easier to access for smaller farms, which will thus increase the competitiveness of production.

Our findings are consistent with the Hege research (2014) in his study demonstrated the positive characteristics of RTK autonomous tractor driving in mechanical weed control in the production of onions and spinach.

CONCLUSIONS

Using the experiments and the results obtained, we can say that with RTK we save about 10% of the time and fuel, since the fuel consumption using RTK-navigation at a 3 m working width was reduced by 8.66%, with a working connection of 6 meters width by 8.26%. With a working connection of 3 m width, 15.7% of the time was saved and 12.6% for the working connection of 6 m width. Manual driving is less precise by 10%. We also found that the covering at the working connection of 3 meters represents about 30 cm, and at the working connection 6 meters to 60 cm. We have shown that the turning time at a working connection of 3 meters wide is reduced by 50.12% and by 18.1% at a working connection of 6 meters wide. The savings in the 3 meter work connection are even greater, as a greater number of bends were required. Increasing the number of trips also increases the time saving when turning on the end of the field. Turning time using RTK navigation is shorter, as the turning mode allows turning at a higher speed.

REFERENCES

- GNSS Geoservis (2017). Retrieved on 18. October 2017 at: <http://www.gnss.si/kako-deluje>
GPS visualiser (2017). Retrieved on 22. October at: <http://www.gpsvisualizer.com>
Hege, D. (2014). Retrieved on 11 September 2017 at: <https://www.landwirtschaft.sachsen.de/landwirtschaft/6779.htm>

- Kašman, I. (2003). Diplomsko delo - Dokumentiranje in analiza stroškov delovnega postopka z uporabo satelitske navigacije. Univerza v Mariboru.
- Landerl, G. (2009). Untersuchungen zum Nutzen und zu Genauigkeiten von GPS-gestützten Parallelfahrssystemen (Lenkhilfe, Lenkas- sistent und Lenkautomat) bei Traktoren. Wien, Universität für Bodenkultur.
- Lopez, H. (2013). Retrieved on 25. October 2017 at: <https://www.landwirtschaftskammer.de/duesse/rueckblick/pdf/2013-06-19-rentabilitaet-pf.pdf>
- Ministrstvo za okolje in prostor (2017). Retrieved on 26. October 2017 at: <http://www.gu-signal.si/node/1> (26. 10. 2017)
- Reckleben, Y. (2010). Vorzüge und Schwachstellen von Lenksystemen in der Landwirtschaft. Fachhochschule Kiel.
- Vaukan, T. (2001). Diplomsko delo - Satelitska navigacija kot osnova za geoinformacijske sisteme v kmetijstvu. Univerza v Mariboru.



CONVERGENCE OF DIFFERENT MODELS FOR THE SAME STRUCTURE IN COMPUTER AIDED ENGINEERING

Vergil MURARU*, Petru CARDEI, Sebastian MURARU,
Cornelia MURARU-IONEL, Paula CONDRUZ

National Institute of Research - Development for Machines and Installations Designed to
Agriculture and Food Industry – INMA Bucharest,
Ion Ionescu de la Brad Blv. No. 6, Bucharest, Romania
E-mail of corresponding author: virgil.muraru@gmail.com

SUMMARY

This paper presents a study regarding the convergence of different models for the same structure. Generally, the geometric models of the structure are generated in CAD (Computer Aided Design) systems. Based on geometric models, loading of the structure and the boundary conditions, different analysis models (mathematical, physical, structural, experimental, virtual, etc.) are achieved. The study method of the convergence of the models set of the same structures refers to the general study of a structural analysis problem. Through the convergence of the models set of the same structures, it is understood, first of all, an approach to the analysis problem of a structure by several models.

The minimum number of models in order to be able to apply this method is two models. When the number of the models is reduced to two, practically the method will improve (refine) the models, until the results are sufficiently "close" to a value (trend towards a limit) in terms of the chosen and used convergence estimators. The method of the convergence of the models set of the same structures involves achieving more models and each model is refined until the results are close enough, in terms of the convergence estimators defined within this method. If one or more models do not converge to the majority of the considered models, then, one will try to justify their limits, possibly by modifying some parameters, in order to bring them into a reasonable vicinity of the other models results.

The convergence demonstrates the theoretical existence of a result and contributes significantly (reducing financial and human effort) to validating results through experimental verification.

Keywords: Computer Aided Design (CAD), Computer Aided Engineering (CAE), Finite Element Analysis (FEA), structural model, convergence.

INTRODUCTION

The study method of the convergence of the models set of the same structures refers to the general study of a structural analysis problem. The convergence of the models set of the same structures is an approach of the structure analysis problem by several mathematical or physical models (experimental, eventually theoretical-empirical, structural, etc.).

The minimum number of the models able to apply this method is two. When the number of the models is reduced to two, practically, the method will refine the models, until the convergence estimators are sufficiently "close" to a limit (Muraru et al., 2017). In this case of the method of studying the convergence of structural models, a single mathematical model was sufficient for a given structural analysis problem. The model is solved by numerical methods or by analytical methods by refining the meshing or increasing the number of considered terms. In the case of approximate analytical solutions achieved, developments in various series are used, until the last two results obtained are sufficiently "close", according to the acceptance or convergence criteria based on various convergence estimators.

In the case of the convergence of the models set of the same structures, several models are being developed and each model is refined until the results in terms of the convergence estimators defined in this methodology are sufficiently close.

If one or more models do not converge to the majority of the considered models, then, one will try to justify their limits, possibly by modifying some parameters, in order to bring them into a reasonable vicinity of the other models results.

Whatever the method used, the convergence presents the existence of a quantified result and ensures a substantial reduction of the human and material effort, when the results are validated by experimental verification.

In fact, the algorithm of this method is more complicated, at least because it includes the algorithm of the methods for study the models' convergence, for each model that competes and for the method of study of the convergence, if this can be applied.

MATERIAL AND METHOD

The working algorithm of the models' convergence study method

Although impossible to be transposed on the computer totally, a working algorithm for the study method of the convergence in models for a structural analysis problem is given and presented in Fig. 1. The total transposition on the computer cannot be done because the formulation of the structural analysis problem and achieving of the mathematical models is not fully based on algorithm.

The first stage, **EMSCM 1**, of the algorithm is dedicated to the formulation of the problem. We have started with this stage, although, we could take over the problem that had been already formulated, because the mathematical models and their solving constitute the main subject of the method.

The first question to be answered in this stage refers to the possibility of modeling the phenomenon. At this stage we need to identify a category of phenomena from which the studied phenomenon is part. One must decide if there are mathematical models of this phenomenon or if these can be achieved.

At this stage, if the answer to the first question is affirmative, then, one can answer to the second question of this stage, namely, whether there already are mathematical models for the studied phenomenon?

If the answer to this question is affirmative, then, more mathematical models of this phenomenon are included in the convergence study in models. Whether there already are models for the studied phenomenon, or not, the attempt of a new model is possible.

However, before attempting a new model, it is necessary to consider the complexity of its formulation and the necessary financial and temporal effort.

In conclusion, depending on the existence of some models that have already been tested or not, we will try to achieve a structural model, complementary or mandatory. The achieving of a new mathematical model involves complex experimental problems, usually in the determination of the constitutive laws, and then a validation, at least partial of the model functionality.

In this stage is very important, when one decides how and which available models are going to be taken into the study and whether one or more new models are being achieved. The inventory of the models and the precise parameterization of each are very important. Also, it is important to know clearly which are the parameters of each model and which of the parameters can be used to improve the quality of the model.

The stage 2, **EMSCM 2** is the construction stage of the new mathematical models. This stage will take place only if the models are taken from the models archive specific to the phenomenon, whether it is an empty set or does not correspond to the user's goals.

The main concern of this stage is to achieve a solvable model through structural analysis, although the method itself refers to any kind of mathematical methods, the comparison being made only among the results that represent the same status parameters of the phenomenon physically modeled.

In the third stage, **EMSCM 3**, for each of the nm models considered in the study, an iterative process begins, by modifying one or more parameters of the model at each new iteration for each model remained in competition.

The number of iterations is not necessarily the same for all the models. If some of the models give results much different than the others, maybe inconsistent with the known experimental facts, then these can be eliminated along the way.

Essentially, at this stage, it is necessary to establish for each mathematical model entered in the competition, the set of parameters that can be varied in the convergence study process:

$$p_k^{(i)}, k = 1, \dots, nm, i = 1, \dots, np_k \tag{1}$$

Where $p_k^{(i)}$ is the parameter with index i of the model k , nm is the number of mathematical models (in this structural methodology) considered in the convergence study, and np_k is the number of parameters potentially usable in the k^{th} convergence study for the structural model.

In the fourth stage, **EMSCM 4**, included in the iterative cycle, the parameters for solving the model are chosen, as follows:

$$pr_k^{(i)}, k = 1, \dots, nm, i = 1, \dots, npr_k \tag{2}$$

where npr_k is the number of varied parameters in the iteration process of the convergence study in models for each of the nm models. The parameters taken into consideration in the iteration process, in search of the convergence are chosen from either the model parameters or from the parameters of the numerical or analytical method used in order to solve the model.

Between two successive stages of an iteration, at least one parameter of one of the structural models must be varied (not to each model, but at least one parameter must be varied to at least one of the models remained in the competition).

During the study it may be possible, even very quickly, that many convergence estimators become close or even coincide, because the models are achieved, so that, the most complex ones can include the results of the most elemental. Because of that, some of the most elementary models no longer allowed variations of model parameters in higher iterations.

The last activity of this stage consists of solving the model by methods specific to each one: analytical, approximate or numerical.

It is recommended not to extract the results that are convergence estimators until a convergence study of the respective model is performed, if it is necessary for the parameters that were not considered in the iteration from the three stages cycle.

The iteration applies separately for each model similarly to the way in which the model convergence study is performed.

In the fifth stage, **EMSCM 5**, also included in the iterative cycle, the solutions of the results of the previous stages are synthesized in the form of the convergence estimators, which are the physical dimensions that characterize the structure / phenomenon, common to all the models, because, only in the common terms one can compare the results of the mathematical models of the same structure / phenomenon.

Obviously, in this iterative grouping that includes the **EMSCM 3**, **EMSCM 4** and **EMSCM 5** stages, there is the question of choosing between two options.

- Each integral model is solved in the convergence study, if necessary, then is compared at the end;
- An iteration is achieved with the models that admit iterations, then are compared, the operation is repeating as often as necessary to meet the convergence conditions, but with a predetermined upper limit of the number of iterations, over which models that do not satisfy the convergence conditions are considered unconverging and will be eliminated.

The working strategy is an option for user.

The sixth stage, **EMSCM 6** performs the convergence test, more precisely, controls if after the last choices of the running or calculation parameters of the mathematical models, the absolute differences between the convergence estimators corresponding to each model have decreased or not below the conventional values chosen.

The models for which the convergence tests are satisfactory, pass in the seventh stage, **EMSCM 7**, where a report is organized and prepared. The models that do not pass the test, go to the **EMSCM 8** stage where one decides whether the iteration continues.

In the seventh stage, **EMSCM 7**, the results of the models that passed the test are retained, their convergence estimators concentrating within a radius range, conventionally established by the user. A report is prepared, which mandatory contains a table with the final values of all the convergence estimators corresponding to the selected models.

In eighth stage, **EMSCM 8**, the models that no longer have iterative resources or have other inconveniences are excluded. The models that have the possibility to touch the convergence and have the corresponding parametric resources are reiterated, the process being resumed for them, with the eighth stage, **EMSCM 8**.

In the ninth stage, **EMSCM 9**, the solving parameters of the models that still have the convergence potentially are modified and sent to the iterative cycle starting with stage three, **EMSCM 3**.

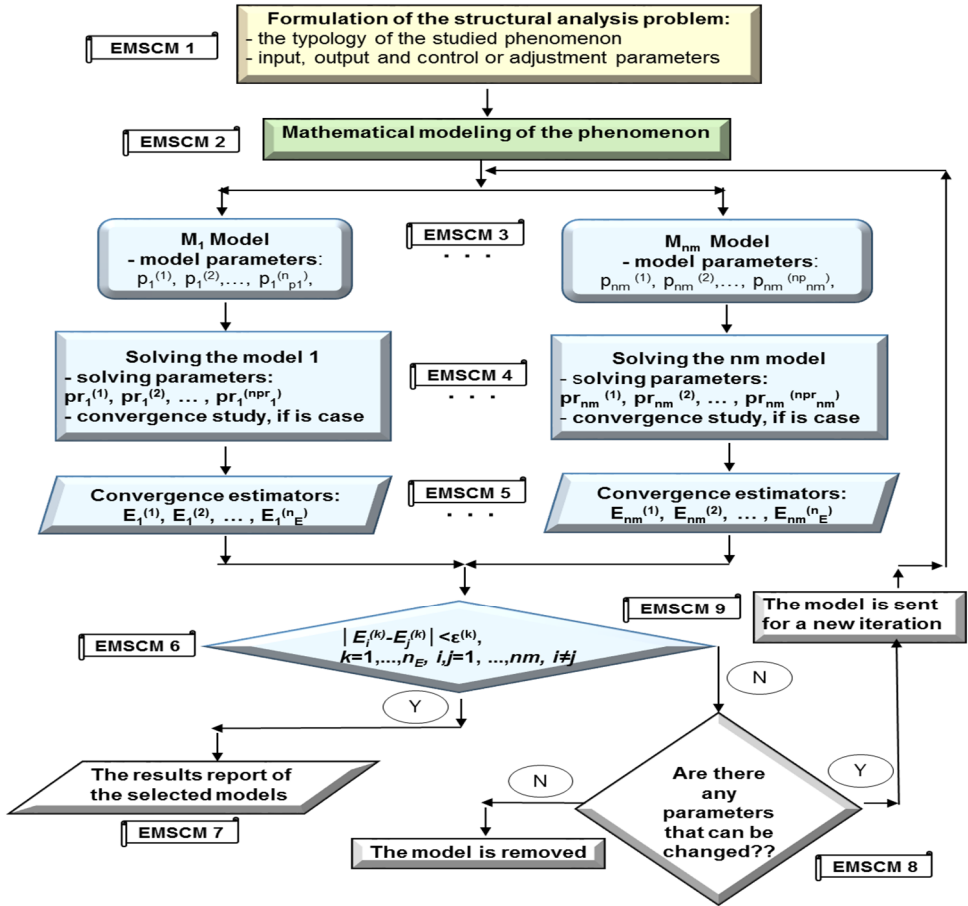


Figure 1. The general working algorithm of the method of studying the convergence in models

RESULTS AND DISCUSSIONS

Different models can be used for a structure, for example:

1. A bar with rectangular section by the length a and width b , length L , elasticity modulus $E=2.1 \cdot 10^{11} \text{ N/m}^2$, Poisson coefficient, 0.3 and the density being about 7850 Kg/m^3 . A load by the type of force with linear density on a centered delta interval is considered.

At the endpoints ($x = 0$ and $x = L$), the embedded bar will be considered.



Figure 2. The geometric scheme of the linear force density distribution on the bar

In the next numerical example solved on the basis of Timoshenko's equation, a long steel bar of 200 mm having the square cross-sectional of 10 mm is taken.

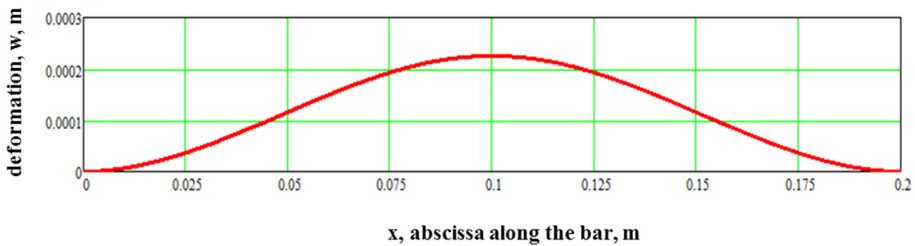


Figure 3. The variation of the w deformation (resultant relative displacements), along the deformed axis of the bar

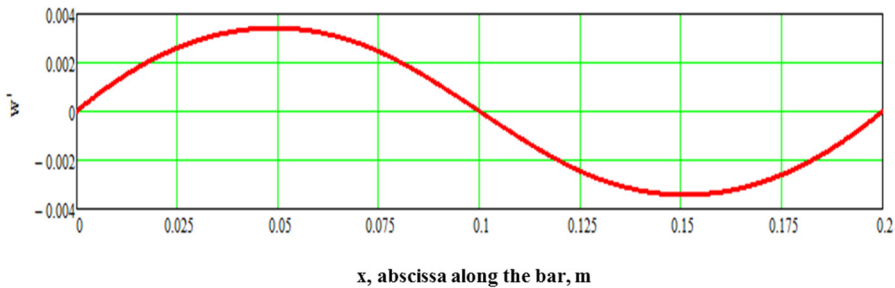


Figure 4. The variation of the specific deformation, w' , along the deformed axis of the bar

2. A model for the same problem within a FEA software:

The structural model with finite elements brings a new solution for the same problem of the bar loaded with a constant force in a portion at its center. The loading scheme is shown in Fig. 5. The structural modeling of the bar represents the subject of this paragraph and was made using 200 finite elements of BEAM3D type.

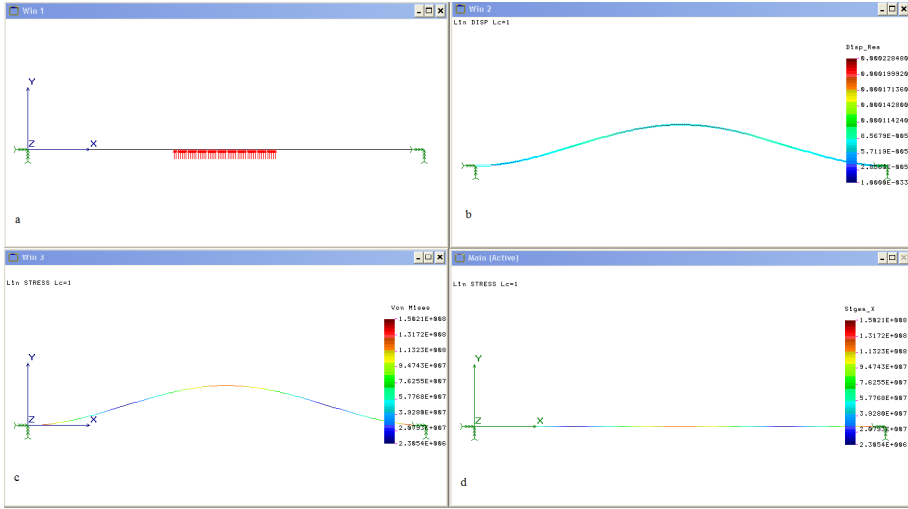


Figure 5. The solution of the bar symmetrically loaded to the origin with an uniform force, in graphical and numerical form (a-Geometry, bearing and loading of the model; b-variation of the relative resultant displacement filed along the bar; c- the distribution of the axial stress field on the deformed shape of the bar; d- the axial stress field on the undeformed shape of the bar)

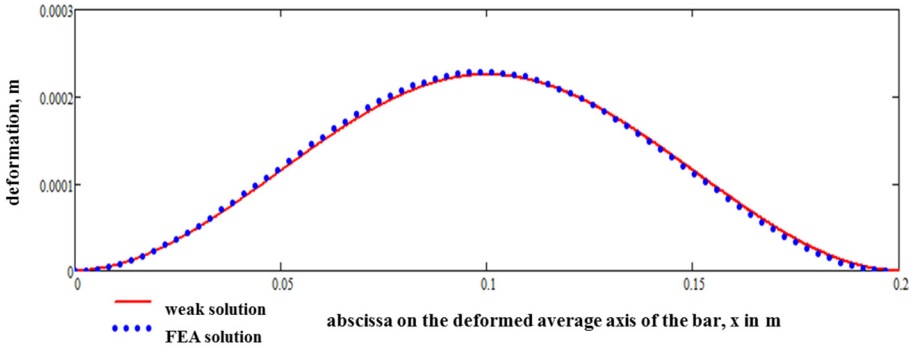


Figure 6. Comparative representation of the solution - the resultant relative displacement (deformation) previous given and the solution obtained using the finite element method, using the COSMOS / M program

The main results appear in Fig. 5, where the variation along the bar for the resulting relative displacement, respectively the axial stress are given. In Fig. 5 are also described the geometry, bearing and loading of the model. On this model, the force (1000 N intensity) is distributed in 51 central nodes. The bar is incased at the ends.

In Fig. 6 the variation of the resultant relative displacement (deformation) of the bar axis for the previous solution and for the given solution using the COSMOS / M program, based on the finite element method is graphically represented.

Similarly, the stretching of a straight metallic bar with a square section was analyzed, in order to apply the algorithm. The results of the numerically simulated models, in the terms

of the chosen convergence estimators, are given in Table 1. Six models of a structure made up of a stretched bar were taken into consideration.

Table 1. The convergence estimators synthesis

Model	Estimator 1 u_x max, relative displacement along x axis, [m]	Estimator 2 ϵ_{xx} , relative displacement at the center of the bar	Estimator 3 σ_{xx} , stress at the center of the bar [Mpa]
Elemental, continuous, Hooke model (Buzdugan, 1980)	0.00014286	0.00047619	100.000
Discret Hooke model (Tripa and Hluscu, 2006)	0.00014286	0.00047619	100.000
Timoshenko Static with axial effect model	0.00011143	0.00037143	100.000
Analytical model without model parameters, (Lazar, 1983) (De Pascalis, 2010)	0.00014286	0.00047619	117.308
3D Structural with Uniaxial Finite Elements model (Hall and Woodhead1967)	0.00014286	0.00047619	100.000
3D Structural simple model (Przemieniecki, 1968)	0.00014547	0.00047619	100.000

We remark a very good convergence of the considered models, 5 of them providing the same value, 0.00047619 (in engineering language 476.19 $\mu\text{m/m}$). At the Timoshenko model, the difference being appreciable. However, the Timoshenko model can be declared inappropriate, only after the experimental validation.

The axial stress estimator at the middle of the bar, has a value of 100 MPa in five out of six cases. Its values differ appreciably from the values for the analytical model.

From the point of view of the relative displacement estimator along the Ox axis at the end of the bar, the convergence seems to be ensured around the value of 0.14286 mm, except of the Timoshenko model. The other differences are negligible and are found in models that include the portions caught in the work benches of the stretching machine.

CONCLUSIONS

The first two stages of the algorithm may not be taken into consideration, because these are conceptual stages and are harder to be automatized.

The algorithm is not complicated, but the success of its application depends largely on the quality of the models designed for a well-defined structural problem.

The experimental verification of the models at a reduced or real scale is recommended, especially for structural issues with high safety factor.

The choice of the convergence estimators is mainly made according to the expected results to be obtained.

The convergence of the models can be assured or not. In the case of non-convergence, the models are rebuilt or the parameters in the model are changed. The models that do not converge further after they were rebuilt or after changing the parameters, are eliminated.

The algorithm can be successfully applied in virtual testing. It can lead to cost savings by saving human and material resources.

ACKNOWLEDGEMENT

This work has been done within the project “Advanced informatics and digital research of conception and development of efficient intelligence technology systems for agriculture” within the NUCLEU 2016 - 2017 Program. Code PN 16.24, founded by the Government of Romania - Ministry of National Education and Scientific Research.

REFERENCES

- Buzdugan, Gh. (1980). Materials resistance. Technical Publishing House, Bucharest.
- De Pascalis, R. (2010). The Semi-Inverse Method in solid mechanics: Theoretical underpinnings and novel applications, Doctoral theses, Universite Pierre et Marie Curie, France, Universita del Salento, Italy.
- Hall, A.S. and Woodhead, R.W. (1967). Frame Analysis. John Wiley & Sons Publishing House, New York.
- Lazar, D. (1983). Principles of continuous medium mechanics. Technical Publishing House, Bucharest.
- Muraru, V., Cardei, P., Muraru, S.L., Sfiru, R., Muraru-Ionel, C. (2017). Study regarding the convergence of the structural models in computer-aided design, Proceedings of 17th International Multidisciplinary Scientific Geoconference SGEM, Vol. 17, Albena, Bulgaria, pp 633 – 640.
- Przemieniecki, J.S. (1968). Theory of matrix structural analysis, McGraw-Hill Publishing Company, New York.
- Tripa, P. and Hluscu, M. (2006). Materials resistance. MIRTON Publishing Company, Timișoara



INTEGRATION OF WEATHER INFLUENCES INTO AN ON-FARM-ENERGY MANAGEMENT SYSTEM

Martin HÖHENDINGER^{1,2*}, Sascha WÖRZ¹, Hans-Jürgen KRIEG³,
Reinhard DIETRICH³, Lorenz FRECH⁴, Jörn STUMPENHAUSEN²,
Heinz BERNHARDT¹

¹ Technische Universität München, Lehrstuhl für Agrarsystemtechnik,
Am Staudengarten 2, D-85354 Freising, Germany

² Hochschule Weihenstephan-Triesdorf, Lehrstuhl für Landtechnik,
Am Staudengarten 1, D-85354 Freising, Germany

³ BEDM GmbH, Arthur-Piechler-Straße 1i, D-86316 Friedberg, Germany

⁴ Rudolf Hörmann GmbH & Co.KG, Rudolf-Hörmann-Straße, D-86807 Buchlohe, Germany

*E-mail of corresponding author: martin.hoehendinger@hswt.de

SUMMARY

The methods of renewable energy production show high volatility as they depend on the occurring weather impacts. In this context, the technology of Smart Grids is supposed to adjust the energy consumption depending on the occurring production.

In dairy farming, automatization and sensor based management creates this flexibilisation of working processes, additionally modern farms produce energy through photovoltaic plants and wind turbines.

An autonomous energy- and production management system, should enable a simultaneous production of energy, milk and meat, as well as consider animal welfare constraints.

Therefore, the aim of this research is, to analyse which climatic influences can have an impact on the energy production and consumption of farms. Since these influences cause a fluctuating energy supply and consumption this research shall furthermore, point out possibilities and parameters, which are usable to consider these impacts in the controlling process of the management system and the operational running in the agricultural enterprise.

A literature research is carried out, to identify the actual available systems and verify their suitability in this context.

The research shows the most important impacts of weather conditions to the energy management system. For a successful consideration of these impacts in the production and energy management system of dairy farms, adaptations and further research are.

Key words: occurring weather, Smart Grids, energy consumption

INTRODUCTION

Renewable and sustainable energy production is an important resource for energy in Germany (Wille-Hausmann, 2011). Seeing that, the availability of the new sources of energy, namely sun and wind, varies with time and place (Hammer et al., 2008) it is relevant which influences arise for the grid and the power plant from the volatile input of Energy to the grid (Wille-Hausmann, 2011). Risks arising from volatile energy production of renewable energy sources can be reduced clearly, if information for the expected energy production are supplied. Therefore, meteorological information has gained a key role in the financially viable use of these new technologies (Hammer et al., 2008).

In this context, the technology of “Smart Grids” is supposed to adjust the energy consumption depending on the occurring production (Wille-Hausmann, 2011).

In dairy farming, the requested flexibility can be realized by the automatized and sensor based management of working processes (Herd, 2014). Furthermore, modern dairy farms produce energy from biogas- and photovoltaic (PV) plants, or wind turbines. Therefore, the agricultural enterprise may play a significant role in the stabilization of energy grids, as it can be both source or sink for electric power.

An autonomous energy- and production management system, should enable a simultaneous production of energy, milk and meat, as well as consider animal welfare constraints. This aim shall be achieved by a temporally coordinated consumption and production of energy in the agricultural enterprise.

According to this, the first part of this paper shows the main features of an autonomous energy and production management system. In this system, the decision making process is determined by a plan of action in conjunction with real time and predicted data of energy production and consumption.

In the second part, weather impacts that play a role for the energy production are characterised. Further, the relevant parameters for the consideration in the system and possible solving approaches are explained.

The third part discusses, these solution approaches in the context of time horizon as well as data source and transmission

METHODOLOGY

In this research, the farmstead is assumed to be in Freising (Germany). Therefore, the weather and climate data are obtained from weather stations in Freising that are supplied of the Bavarian State Research Center for Agriculture.

The focus of this research is on climate data and weather events, as affects the energy production and consumption in an agricultural enterprise (Huber, 2015). In consequence, these effects also have an influence on the farm energy management system.

Therefore, a literature research is carried out, about weather influences and the impact they have on energy and production management system. As literature sources, the libraries of Technical University of Munich and Weihenstephan-Triesdorf University of Applied Sciences are used. Further, the online platforms Google Scholar and Web of Science are used for an online research. Special attention is paid to the parameters that are essentially important for the energy production and animal welfare. Important key words for the research were smart grid, energy management, renewable energy, wind or solar energy, forecast and weather. For the field energy consumption in conjunction with animal welfare

important keywords were, stable climate, heat stress, water supply, stable lightning and energy efficiency. Additionally, common synonyms and German translations were used in the research.

Subsequent, possibilities are discussed how these impacts can be integrated within the management system and in respect to animal welfare constraints.

ENERGY MANAGEMENT SYSTEM

An energy management system is used for systemic detection of energy flows. It forms the basis for investment decisions regarding energy efficiency. It also includes every organisational element used for the creation of an energy policy. The system also is used to establish strategic targets and attain these targets. (Kahlenborn et al., 2012)

To achieve these, there are three flexibility options along of the value chain that are generation-, storage- and load management (Scheven, 2015). Additionally, for the optimisation of an industrial production process all components and external Factors that are part of the production system should be considered (Scheven, 2015). According to this, the concept of an autonomous energy and production management system for dairy farms should be designed as an autonomic working management system that can handle the described tasks on its own. The Renewable Energy For Industry (REFI)-Model (Figure 1), developed by Scheven (2015) combines production and energy management systems for industry companies. This model works with input-parameter out of practice that are adopted individually to enterprise issues (Scheven, 2015).

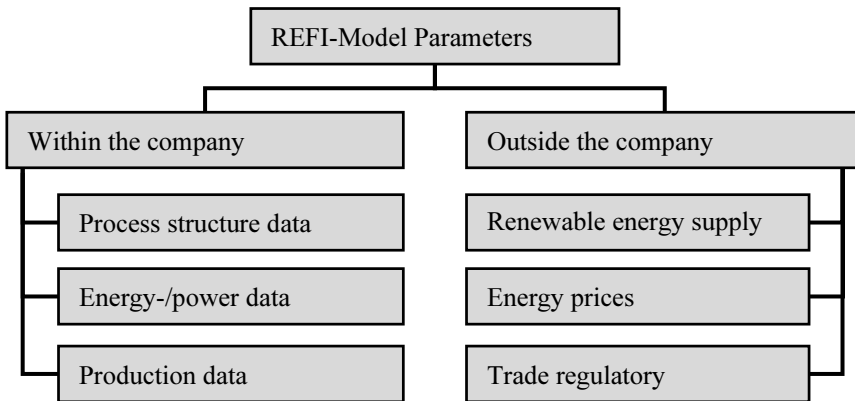


Figure 1. Relevant parameters of the REFI-Model (Scheven, 2015)

However, for application of this model on dairy farms, adoptions are necessary. Dairy farms may take a special role, as especially internal and external factors have often strong influence on the production processes and are hardly controllable factors. In this context, weather is one of the most important impact factors, as it affects the production processes and in consequence the energy production and consumption of dairy farms. These influences need to be considered in the energy management system. To achieve this, forecasts of the entire production and consumption of electric power within the agricultural enterprise are necessary (Bitsch, 2006). Therefore, it is necessary to master the relevant data flows to achieve a stable controlling system.

IMPACTS OF WEATHER

Weather is the physical condition of the atmosphere at a certain time or in a short time period at a certain place or area, these conditions are described by physical numeric parameters (Deutscher Wetterdienst, 2017).

As described, the weather conditions occurring at the location of the stable are crucial for the energy production from weather dependent power plants and the energy consumption of the dairy farms (Huber, 2015). In consequence, the energy production and the consumption of a farm varies during the year (Figure 2), this volatility rises for shorter observation periods. Uncertainties that arise from these weather influences can be compensated by the supply of precise information about the expectable production of solar and wind energy (Hammer et al., 2008). Therefore, for farms with an integrated production and energy management system the forecast of the occurring energy production at a certain time is important.

The REFI-Model uses real time quarter hours values about the feed in of wind and solar energy provided by grid operators (Scheven, 2015). To consider uncertainties from the prediction, these values are presented inclusive a possibility corridor (Scheven, 2015). As wind and solar energy use different renewable energy sources, different pieces of information are needed for the forecast of energy production. In the following, important weather influenced impacts to the energy supply and consumption in the system are characterized and explained.

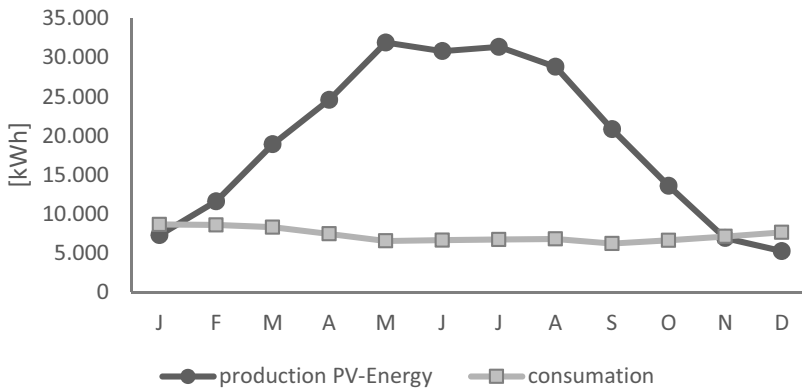


Figure 2. Monthly energy production and consumption of a 125 cows model dairy farm (Huber, 2015)

ENERGY PRODUCTION AND PREDICTION

Wind energy production

The production of wind energy depends mainly on the occurring wind speeds (Ambach and Garthoff, 2016). Therefore the prediction of the expected wind speed is an important

factor to consider during the selection of possible locations for wind turbines and the maximisation of their productivity (Ambach and Garthoff, 2016).

Solar energy production

There are three factors playing a vital role for the energy generated by a PV system. The dry-bulb temperature comprising the metrological data, the solar elevation and solar azimuth angles compromising the celestial data, and the solar radiation data (Chow et al., 2012).

In this context, the dry-bulb temperature, which is provided by public services, can be used. The solar azimuth angle is the azimuth angle of the sun. The solar elevation angle is the elevation angle of the sun, that represents the angle between the direction of the geometric centre of the Sun's apparent disk and the idealised horizon (Chow et al., 2012). Determined by the angle of impact the highest global radiation can be observed at the equator and decreases with the movement to the poles of the globe (Klett et al., 2015). Therefore, the location of the farm and the orientation of the solar panels is an important influence for the prediction of the solar power potential. In this context, Huber (2015) showed, that different orientations caused big differences in total energy production and efficiency.

For the global radiation, the prediction of cloud formation can play a key role for the improvement of this data. The forecast for global radiation in short time intervals can be obtained from satellite data, by extrapolation of the observed temporal development of considerable cloud structures. The predicted satellite picture is the basis for the calculation of the global radiation. (Hammer et al., 2008)

In this context, the Heliosat-Method is a method, for the ascertainment of the global radiation at the ground from satellite data. It is based on principal of the reflection of the solar radiation which depends mostly on the clouds degree. For this, the most important parameter is the backscatter value, which facilitates the calculation of the occurring cloud structures. (Hammer et al., 2007)

Energy consumption and animal welfare

The environmental circumstances have impacts on the climatic conditions inside of the stable. These conditions are important for animal behaviour, animal health and the productivity of dairy cows. In this context, air temperature, humidity, harmful gas content, air flow and light are important parameters for characterisation of the climatic conditions in the stable. (Haidn and Leicher, 2015)

Especially in summer months, air temperatures exceed the physiological optimum of cows (Figure 3). Cows are not negatively affected by temperatures down to -20°C . Their physiological optimum is between $+4$ and $+16^{\circ}\text{C}$, but temperatures higher than 20 or 25°C in conjunction with relative high air humidity cause heat stress (Heidenreich et al., 2005).

To prevent negative influences by the stable climate and heat stress, there are different structural and technical possibilities to regulate the climate inside the stable.

In the first place, the construction of a stable should consider appropriate ventilation openings, additionally different sizes of fans at different places can improve the air exchange (Heidenreich et al., 2005). Another possibility of cooling is a water sprinkling devices, which should be controlled by a thermostat and only work at temperatures higher than 24°C (Heidenreich et al., 2005).

Further the seasonal climate fluctuation has influences on the energy consumption of milk cooling systems, as well as water heating systems and the light system (Hermann, 2014; Pommer, 2015; Werner et al., 2016). These climatic impacts cause seasonal and daily variations in energy consumption (Figure 2) (Huber, 2015).

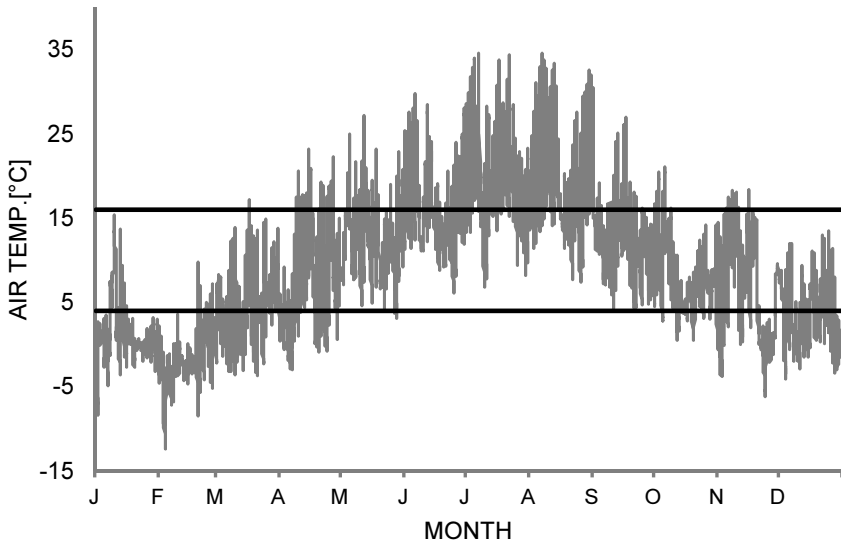


Figure 3. Air temperature trend in Freising (Bayerische Landesanstalt für Landwirtschaft, 2015) and physiological temperature optimum for cows

According to the mentioned technology, also variations of energy consumption caused by the climatic regulation systems should be considered in the management system. The basis for this could be the occurring weather conditions as well as forecasts that are integrated into the planning and controlling process. In consequence, these regulation processes need to be planned and considered in the energy consumption plan of the management system. In this context, also forecast methods for the climate inside the stable could be an approach to face these variations and to guarantee the required conditions for a high animal welfare.

Forecast horizon of weather impacts

A reliable energy supply forecast helps to prevent unexpected loads and provides vital information for decisions made on energy generation and purchase. However, energy generation prediction for photovoltaic (PV) system has been limited for years, especially concerning short-term predictions. (Chow et al., 2012)

For this reason, different forecast models have been developed that give estimates for the expected energy production. Usually, all predictions and calculations are based mainly on the forecast of the weather conditions at a certain time. (Hammer et al., 2008; Treiber et al., 2016)

The predicted weather parameters for the period between one and three days are converted into solar and wind energy performance forecasts by different processing models (Hammer et al., 2008). These forecast models depend on different parameters and calculation systems that have to be integrated into the planning and regulation processes of the management system. Additionally, there is different data used in the forecast calculation of wind energy and PV-power. According to Schierbeck et al. (2010) network operators use Day-Ahead and Intraday forecasts for marketing issues in the energy grid. The difference between the grid operators and the farms is funded in the use of these data. As grid

operators deal with many renewable power plants for the single farm especially the own energy production is important. However, this energy production is determined by local weather conditions. In this context, single clouds probably have a significant impact on the energy production. For the forecasts of grid operators many power plants of one region are considered, therefore small local weather happenings have only small influence to the grid.

In respect of the plan of action intraday forecasts give more opportunities for a detailed plan of action. In this context, Treiber et al. (2016) showed the statistical wind power forecast for an individual turbine and an entire park with a horizon of 30 min. Already Chow et al. (2012) predicted the solar energy production for real-time and up-to-20-min lapse within 95% confidence limits. These estimations shall give a sufficient basis for the management, scheduling, and dispatching operations in power systems (Chow et al., 2012). However, Chow et al. (2012) did not consider the particularities of dairy farms, therefore it is to verify, if these high temporal resolution is feasible for the energy and (the letter d was missing) production management of dairy farms. Additionally, the energy consumption of farms is influenced by the occurring weather conditions. Especially the production and storage of milk as well as the animal welfare determines a volatile energy consumption. As far as known, there is no prediction model described for the forecast of energy consumption of dairy farms. For this, the challenge is to consider the impacts of weather phenomenon on the production processes and in consequence the energy consumption.

A solving approach is given by Bitsch (2006) recommends a plan of action, which is mainly based on the energy production and is actualised in a 15 minutes time interval. This plan of action could also contain predicted values of energy consumption. The additional integration of actual values that are measured in real time contributes to the improvement of the forecast quality (Schierbeck et al., 2010). To provide these actual data an integrated weather station at the farm site could be installed.

Data supply and transmission surface

According to Bitsch (2006), the optimisation process for an intelligent decentral energy management system runs communicative in a respective network, where the individual components and units of production, consumption and storage are connected. For construction of this network e.g. LAN/WAN, ISDN, GSM with an interface port like e.g. OPC respectively XMTL with standard or dial-up connection or statistic acquisition are usable. (Bitsch, 2006)

For the reason, of high claims to the calculation capacity of a system (Wengenmayr, 2017), the complete creation of weather forecasts within the management program is not feasible.

There are different conceivable sources for information about the climatic impacts on the production of energy in the farm management system.

The first option is the integration of intraday forecasts for the energy production at a certain time. These data can be received from external providers, who update these forecasts in periodic intervals. In this case, the algorithms and calculations are outsourced, which means, that no computing power is needed for these calculations. Changes and adoptions of the prediction methods and algorithms in this model would not be able. In consequence, the planning process depends on the calculation system and data from external providers.

The second option is the integration of predicted weather parameters that are available at different weather service providers. The obtained data is transformed into a forecast for the energy production. In this case, the algorithms are part of the energy management system. This enables an easy adoption of the prediction method and algorithms, further it is easier to

consider real time data that are measured at the farm site. As mentioned before, this real time data contributes to an improved forecast.

CONCLUSIONS

It is shown that weather is an important impact factor on an integrated energy management system. In fact, it affects two important components of the production process, the energy supply and the energy consumption, it is necessary to consider these impact in the management system. To deal with these influences exact weather data, forecasts and prediction models are needed. As weather conditions are locally very variable, the forecasts models need a high temporal and local resolution. For this reason, the prediction and forecast models that are used by industry and grid operators are not appropriate for application in dairy farms. In this context, it is to verify, if a weather station at the farm site, which provides actual data gains reasonable improvements of the prediction.

For the forecast of climate inside of stables in conjunction with the external weather conditions, comprehensive research is necessary. In this context, it is to verify, how the energy consumption of each consumer is affected by the weather conditions, and if there are flexibility potentials that are usable in the management system.

ACKNOWLEDGEMENTS

The authors thank the Federal Ministry of Food and Agriculture (BMEL). The project is supported by funds of the Federal Ministry of Food and Agriculture (BMEL) based on a decision of the Parliament of the Federal Republic of Germany via the Federal Office for Agriculture and Food (BLE) under the innovation support program.

REFERENCES

- Ambach, D. and Garthoff, R. (2016). Vorhersagen der Windgeschwindigkeit und Windenergie in Deutschland. *ASTA Wirtschafts- und Sozialstatistisches Archiv*, 10, 15–36.
- Bitsch, R. (2006): Integration von erneuerbaren Energiequellen und dezentralen Erzeugungen in bestehende Elektro-Energiesysteme. *LIFIS ONLINE*, 1–15.
- Chow, S. K. H., Lee, E. W. M., Li, D. H. W. (2012). Short-term prediction of photovoltaic energy generation by intelligent approach. *Energy and Buildings*, 660–667.
- Haidn, B. and Leicher, C. (2015). Maßnahmen zur Verbesserung des Tierwohls im Milchviehstall. In: *Bayerische Landesanstalt für Landwirtschaft (ed): Milchviehhaltung – nachhaltig und zukunftsorientiert*. 1st Ed., 15–40.
- Hammer, A., Heinemann, D., Lorenz, E., Sood, A. (2008). Der Einfluss von Wetter und Klima auf die Energieversorgung. *EINBLICKE - Forschungsmagazin der Carl von Ossietzky Universität Oldenburg*, 20–21.
- Herd, D. (2014). Vernetzung von Systemen und Cloud-Anwendungen in der Nutztierhaltung. *LANDTECHNIK*, 245–249.
- Huber, C. (2015), Konzeption, Ertragsanalyse sowie Wirtschaftlichkeitsbetrachtung verschiedener dachgebundener Photo-Voltaik Anlagen für einen Modell-Milchviehstall im Rahmen des "Integrated Dairy Farming". Bachelorarbeit, Hochschule Weihenstephan-Triesdorf, Freising.
- Kahlenborn, W., et al. (2012). Energiemanagementsysteme in der Praxis: ISO 50001: Leitfaden für Unternehmen und Organisationen.

- Scheven, A. von, (2015). Flexibilitäts Optionen im industriellen Umfeld an verschiedenen Energiehandelsmarktplätzen im Smart Grid. Dissertation, Technische Universität Darmstadt, Darmstadt.
- Schierbeck, S., Graebner, D., Seming, A., Weber, A. (2010). Ein distanzbasiertes Hochrechnungsverfahren für die Einspeisung aus Photovoltaik. *Energiewirtschaftliche Tagesfragen*, 60, 60–64.
- Treiber, N. A., Heinermann, J., Kramer, O. (2016). Wind Power Prediction with Machine Learning. In: Lässig J, Kersting K, Morik K (eds): *Computational sustainability*. Springer, Switzerland, 13–29.
- Wille-Haussmann, B. (2011). Einsatz der symbolischen Modellreduktion zur Untersuchung der Betriebsführung im "Smart Grid". Dissertation, Fernuniversität in Hagen, Hagen.
- Bayerische Landesanstalt für Landwirtschaft (2015). Agrarmeteorologie Service. <http://wetter-by.de/Internet/AM/inetcntrBY.nsf/cuhome.xsp?src=4JHVFJGNW4&p1=535TN12L42&p3=2CQ7BH7901>. Accessed 1 December, 2017.
- Deutscher Wetterdienst (2017). Wetter und Klima - Deutscher Wetterdienst - Glossar - W - Wetter. <http://www.dwd.de/DE/service/lexikon/Functions/glossar.html?nn=103346&lv2=102936&lv3=103164>. Accessed 27 September, 2017.
- Hammer, A., Lorenz, E., Petrak, S. (2007). Fernerkundung der Solarstrahlung für Anwendungen in der Energietechnik. https://meetings.copernicus.org/dach2007/download/DACH2007_A_00357.pdf. Accessed 25 September, 2017.
- Heidenreich, T., Büscher, W., Cielejwsky, H. (2005). DLG-Merkblatt 336 Vermeidung von Wärmebelastungen für Milchkühe. http://2015.dlg.org/fileadmin/downloads/merkblaetter/dlg-merkblatt_336.pdf. Accessed 29 June, 2017.
- Hermann, H.-J. (2014). DLG-Merkblatt 399 Wasserversorgung für Rinder. http://2015.dlg.org/fileadmin/downloads/merkblaetter/dlg-merkblatt_399.pdf. Accessed 27 September, 2017.
- Klett, S., et al. (2015). Sonnenenergie. https://www.lfu.bayern.de/buerger/doc/uw_62_sonnenenergie.pdf. Accessed 20 September, 2017.
- Pommer, R. (2015). LfULG-Schriftenreihe, Heft 1/2015 "Energiebedarf von Melk- und Kühlanlagen". Schriftenreihe. <https://publikationen.sachsen.de/bdb/artikel/23799>. Accessed 20 November, 2017.
- Wengenmayr, R. (2017). Messen-Berechnen-Interpretieren: Wie entsteht eine Wettervorhersage? https://www.dwd.de/SharedDocs/broschueren/DE/presse/wettervorhersage_pdf.pdf?__blob=publicationFile&v=8. Accessed 17 October, 2017.
- Werner, D., et al. (2016). DLG-Merkblatt 415 Beleuchtung und Beleuchtungstechnik im Rinderstall. http://2015.dlg.org/fileadmin/downloads/merkblaetter/dlg-merkblatt_415.pdf. Accessed 27 September, 2017.



SOLUTIONS TO AUTOMATE OPERATIONAL MONITORING ACTIVITIES OF AGRO-FORESTRY TASKS

Fabrizio MAZZETTO*, Raimondo GALLO

Faculty of Science and Technology, Free University of Bozen/Bolzano,
Piazza Università 5, 39100, Bolzano, Italy

*E-mail of corresponding author: fabrizio.mazzetto@unibz.it

SUMMARY

An innovative approach for automating operational monitoring activities in agro-forestry tasks is here described and discussed. This approach can be considered as a solution for Precision Agriculture (PA) and Precision Forestry (PF) applications and can be employed as an ICT tool for the management aims for a variety of agro-environmental companies. Aim of the proposed concept is to develop a system, composed by both hardware and software units, able to collect and manage operative raw data and then to translate them into operational information that will be used in decision making processes. All the procedures will be carried out automatically, in order to ensure an objective compilation of the field activity register. Thus, the entrepreneur will have automatically updated all the operative information in a dedicated database system. All the obtained documents can then be used for certification and traceability processes if required by the procedural guideline, as well as to satisfy any other management task, including the estimation of the actual operative costs (and impacts) of the farm.

Keywords: operational monitoring, Precision Agriculture, Precision Forestry, ICT

INTRODUCTION

Operational monitoring refers to all those tasks necessary to monitor survey and report all those information required to get an overview of the working processes done to accomplish a specific activity. The operational monitoring is carried out to ensure a continuous traceability of the input of a system. In the agro-forestry sector, the assessment of these previous mentioned information is a strategical point to be monitored in order to optimize all the resources and maximize the profits.

Through the operational monitoring a large amount of useful information about the management and the logistic of each activity done by the farmer or lumberjack were collected. Indeed, thanks to this procedures information on the productivity, on the efficiency and the estimation of input and output can be done. Due to the strategical importance of the collection and elaboration of this information, combined to the growing up of dedicated ITC systems, new solutions of Farm Management Information System (FMIS) were developed and used. Fountas (2015a) considers the FMIS an electronic and IT tool suitable to generate operative information acceptable to be used by the farmer, in order to carry out decisional tasks through well-established procedures for collecting, processing and elaborating data. Nowadays all the operational data necessary for the system to perform all the processes is based on manual entry (Nikkilä et al., 2010). In theory, the operators should collect and enter all the operative data at the end of each activity or, at least, at the end of each working day. Therefore, during the job all input and output should be noted by the operator and then inserted into the FMIS. The farmers consider these tasks as high time-consuming and they do not always accomplish it for lack of time. Hence, the FMIS is filled up during the weekend or at the end of the entire operation, which leads to uncertainties and missing information due to forgetfulness.

Aim of this preliminary work is to describe the approach and the technologies developed to carry out automatic operational monitoring for three common operations in the agro-forestry sector: apple harvesting, timber yarding and motor-manual felling with chainsaw. The devices which will be described will be an active support for Precision Farming and Precision Forestry approaches. The provided system will be able to automatically collect and interpret all the operative parameters achieving management and logistic information. This automatic system will permit not only to improve the efficiency of human work but also to reduce it, by speeding up the processes of operational parameters acquisition, improving the production and motivating skilled work (Lopes and Neto 2010). In the end, this new concept of intelligent system is capable to translate ex-post or actual operative parameters into information, in order to automatically perform an objectivity compilation of the field activity register. Thus, the entrepreneur will have automatically updated all the operative information in a dedicated database system. All the obtained documents can then be used for certification and traceability processes if required by the procedural guideline, as well as to satisfy any other management task, including the estimation of the actual operative costs (and impacts) of the farm.

MATERIALS AND METHODS

The approach

The aim of this research is to develop an integrated system capable to perform an automatic operational monitoring of field activities in order to carry out an automatic compilation of the field activity registers. Hence, the final target is to develop a management tool able to reduce the stress of the farmer or the lumberjack allowing them to concentrate only on the planned operations, forgetting all the compiling procedures of documents. To achieve the research goal, different innovative hardware and software solution were developed according to the monitored operation. Generally, the proposed solution is composed by a FDL (Field-Data Logger) coupled with other sensors.

The FDL is the core of the system. It is an embedded unit with its own ID code to identify the machine on which it is installed. According to the operation, and the machines' spaces and power supply possibilities, different units were developed. Anyway, all the units are

characterized by having an accelerometer module and GNSS unit (GPS+GLONASS). Beside these, there is also a multiprocessor which drives all these components, and the connected sensor as well, and carries out a first data processing. All those embedded components are contained in a commercial or customized IP67 plastic box.

As said, the space availability and the possibility of connection to the electric system of the machine, determine the dimension and the presence of external batteries. As reported in the Figure 1, it is possible to see the different solutions developed to accomplish the experiment.



Figure 1. Here the three developed FDLs were shown: on the left the Tractor-FDL, on center the Yarder-FDL while on the right the Chainsaw-FDL. The Tractor-FDL is energy supplied by the electric circuit of the tractor, while, the others foreseen the use of external LiPo.

The embedded accelerometer has the aim to turn the datalogger automatically on when a vibration overpasses a well-determined threshold. The set threshold refers to the switching on of the machine's engine or its displacement. When the FDL is on, a warm up period for the GNSS acquisition and for the connection to the phone network (where present the GPRS module) is required (maximum 30 seconds). Data recording starts when the GNSS unit receives the satellite signals. Different fixing sampling frequency where set according to the operation to monitor (0.2 Hz field operational monitoring, 1 Hz for chainsaw monitoring and 0.5 Hz for yarding monitoring). At the same time, when the recording procedure starts, the multiprocessor synchronizes the raw data collected by the GNSS and by the other sensors.

The three FDL were connected to different sensors according to the operation to monitor and the goal to achieve.

1. Tractor-FDL: the datalogger was mounted in the tractor's cab and it was equipped with an RFID antenna in order to read the code transmitted by an active RFID transmitter installed on an implement. Thanks to the double code (datalogger+transmitter) it is possible to identify the power unit and the implement coupling, allowing the identification of *who* did *what* during a determined working session.
2. Yarding-FDL: the datalogger was mounted on the carriage and connected with a load cell. This sensor was placed in between the hook and the chockers in order to measure the weight of the load transported during the inhaul phase. These records are also linked with an automatic time study in order to obtain the productivity of the yarding operations recognizing all the elemental phases (outhaul, hook, inhaul and unhook). The challenge of the Yarding-FDL is to be able to estimate the mass of the load also in case of dragging.
3. Chainsaw-FDL: the datalogger was mounted on the top of air-filter cover. It is composed by a tri-axes accelerometer in order to monitor all the acceleration generated by the engine as well as the displacement of the equipment in the space. Then, measuring the amount of time spent at high rpm (when the chainsaw does an effective cut) it was

possible to calculate the diameter at the stump level, the diameter at DBH and finally the volume of the entire tree.

All the synchronized data are stored in a buffer memory or in a mini-SD. They can be downloaded manually through USB connection or via radio modem, if the GPRS module is present. All the collected data are then uploaded in a server. Here, a relational database management system (RDBMS) is implemented in order to store and elaborate the raw data. Here, all the stored data are organized in tables in order to be analysed by the so-called *Operational Inference Engine* (OIE). Authors considered the OIE as a set of mathematical and statistical procedures able to elaborate and translate raw data into useful information. Therefore, thanks to specifically developed algorithms, which are driven by the OIE, it is possible to interpret the raw data in order to obtain an operative monitoring of the field activities (Mazzetto et al., 2012). In chronological order, generally, the OIE analysis carries out:

- The identification of the Working Sections (WS, is considered as a sequence of activities between two switching on/off subsequent events);
- The elimination of possible fixings classified as outliers (all the records at a distance (d) higher of $d > d_{avg} \pm 2\delta$ from the collected dataset centroid);
- The classification of the different working phases (effective work, stops, breaks, auxiliary operations and maneuvers, transports and displacements, according to the monitored operation) applying algorithms based on speed, advancement direction, vibrations assessment, weight assessment, and the working pattern analysis;
- The clustering of all contiguous fixings classified as effective work into a common area;
- The synchronization of GNSS data with the data collected from the sensors to compute, according to the activities, the working coverage rate on each crop unit, the productivity (hence, also the tree volume), the worktimes occurred during the current WS as well as a summary of all the consumed inputs.

Since the OIE manages also algorithms based on spatial analysis, it is necessary to map the entire farm as well as the forest parcels boundaries.

All the computations done by the OIE are then summarized and displayed on a Web-GIS platform for an easy and quick consultation for the entrepreneur. Thus, the final user can access, through his domain and his own credentials, his personal page, in order to monitor and to check all the supervised operational parameters (Figure 2).

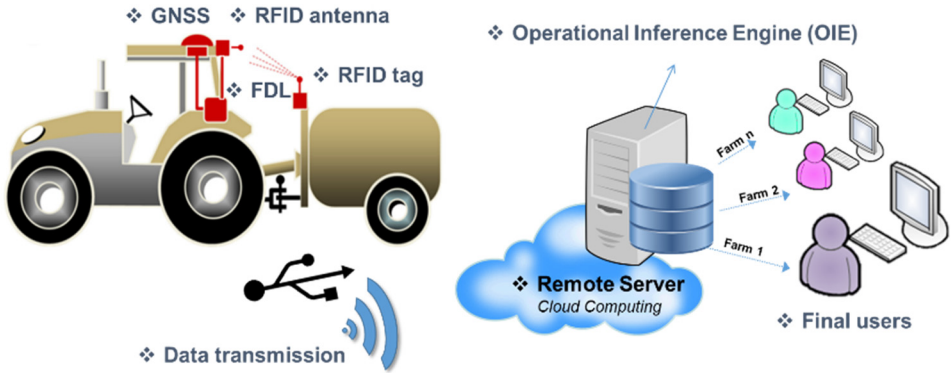


Figure 2. The conceptual model followed is reported. On the left the collection and transmission of the raw data, on the right their elaboration and consulting through a Web-GIS platform.

System validation

All the proposed systems were validated through the comparison between the time duration assessed by the OIE's elaborations and the manual survey collected for the same operations.

The Tractor-FDL was tested during harvesting operations in apple orchards. Here the operator had the task to bring empty fruit bins to the harvesting machines placed inside the inter-row of the same or different parcels, to pick up full bins and to bring them to the trailer. During this test the effective harvesting operations, stops and displacements were analysed.

The Yarding-FDL was tested during logging operations using cable cranes. Here two different tests were done: one on the capability of the system to carry out an automatic time study, while the other on the capability to assess the weight of the logged load during the inhaul. For the first test, the validation consisted in the automatic identification of the 4 typical working phases (outhaul, hooking, inhaul and unhooking), the assessment of each duration and the total number of cycles done. Meanwhile, for safety reasons, the weight assessment was done in an in-scale yarding system.

The Chainsaw-FDL was tested during motor-manual felling operations. The validation procedures consisted in the comparison of the volume calculated by the developed system with the same parameter estimated using specific single entry tables.

RESULTS AND DISCUSSIONS

Tractor-FDL

In literature only studies that describe the ontology, the data flows and the functioning of the FMIS were found (Fountas et al., 2015a, Fountas et al., 2015b, Sørensen et al., 2011), nevertheless no quantitative results to be compared with the present research were reported.

A preliminary testing of the Tractor-FDL was carried out by monitoring and evaluating 23 working sessions. During the validation the total duration of the working session, the work in field, the stops and displacement were assessed. In table 1 a summary of the surveys was reported.

Table 1. Summary of the results obtained for the manually and automatic operational monitoring. M_S and A_S refer at the manual survey and the OIE's elaborations

	Total time		Mean time		St. dev		Difference		R2
	A_S	M_S	A_S	M_S	A_S	M_S	-	%	
Working session (s)	1519,2	1517,2	66,1	66,0	49,0	49,0	-0,09	-0,1%	0,998
Work in field (s)	847,5	831,7	36,8	36,2	26,5	21,3	-0,69	-1,9%	0,827
Stops (s)	490,3	481,1	21,3	20,9	18,7	23,0	-0,40	-1,9%	0,907
Displacements (s)	181,9	204,4	7,9	8,9	4,7	8,3	0,98	11,0%	0,641

Very small differences were found from the comparison between the two methods. Indeed, considering the duration of each WS, the WF and ST the differences were lower than 2%, in absolute terms while it was equal to 11% for the displacements. In terms of minutes, these differences are equal to 0.09, 0.69, 0.40 and 0.98 for WS, WF, ST, and DS, respectively. Very good correlation values were recorded and no statistical differences were recorded between the two methods ($t > 0.05$).

The higher differences in the displacement phases can be due to a no proper identification of the phase beginning and ending calculated by the automatic survey. Indeed, the OIE assesses more fixings than the actual ones as displacements instead of work in field with the consequence of a not proper assessment. This happens because part of the field operation works carried out on the parcel border are considered displacement by the OIE, as they *jump* outside the parcel because of a GNSS drift, because of multipath or cycle slip phenomena. In this case, these points are considered as displacements by OIE's elaboration. To solve this problem a buffer zone should be applied around the field boundary to enlarge the parcel surface.

Yarding-FDL

During the preliminary studies, due to safety reasons, the testing of the Yarding-FDL was split in two different tests: the first consisted in an automatic time study, while the second in an automatic weight assessment in an in-scale system. The automatic time study trials were set in four harvesting sites of the Alpine region (North-East of Italy). During this study a total of about 41 hours (2450 min) of effective manual time study (M_TS) were performed and an amount of 228 working cycles have been detected. Out of the total working cycles detected by the automatic procedure (A_TS), 220 cycles were successfully recognized. Hence, for gross time study, Yarding-FDL recognized the 96.5% of the working cycles, as reported in Table 2.

Table 2. Summary of gross time of working cycle for each dataset. Data consider dataset with missed cycles. A_S automatic survey, M_S manual survey

	N. of cycles		Gross time		Average		St. Dev.		R2
	A_S	M_S	A_S	M_S	A_S	M_S	A_S	M_S	
Working session (s)	220	228	138535,8	138157,2	638,4	636,6	5,4	5,4	0,886
Difference (s)	8		-378,6		-1,8		-		

Some working cycles were missed due to a low number as well as a bad displacement of satellites. If the missed cycles were not considered, the differences recorded between manual and automatic time study would be below the 1%. For the analysis of the elemental time study the missed cycles have not been considered in the result's discussion (Table 3).

Table 3. Statistics of the elemental time study recorded during the cable logging working cycles. Missed cycle do not considered. A_S automatic survey, M_S manual survey

	Average (min)		St. Dev. (min)		Difference		R2
	A_S	M_S	A_S	M_S	-	(%)	
Outhaul (s)	102	102	1,01	0,99	-0,01	-1%	0,563
Hook (s)	288	294	3,48	3,59	0,12	3%	0,880
Inhaul (s)	162	156	1,40	1,38	-0,15	-6%	0,663
Unhook (s)	90	90	2,77	2,68	0,01	1%	0,930

Very good correlation values have been obtained ($R^2 > 0.8$) for both the gross and for the hook and unhook elemental phases. Lower correlation was recorded for the outhaul and inhaul probably due to the dynamic characteristic of these operations. In terms of time, the recorded difference was always lower than 10%, this means that the system is able to automatically carry out a time study analysis with an error lower than 10 seconds.

Regarding the weight assessment, the mass transported during 120 inhaul operations have been registered and collected. For each evaluation, the parameters collected were the weight and the inclination of the choker during the dragging. Indeed, the friction generated by the contact between the soil and the log generates a resistance proportional to the weight of the load. During the test, two repetitions with four different distances of tying (CK-nn%) were carried out and the estimated weight was compared with the reference weight (Table 4). The choker was tied at 2%, 5%, 10% and 20% of the total length of the log from its upper top.

Also in this test, Authors obtained very satisfactory $R^2 (>0.9)$ by the comparison between the estimated dataset and the manually measured, for both the repetitions. Given the good results obtained with the application of the two separate systems of the Yarding-FDL, further steps foresee the synchronization, and testing of both systems.

Table 4. Summary of the automatic weight assessment. In this table the results obtained by the two repetitions are reported. The average weight measured as reference was 40,2 kg.

	Repetition 1				Repetition 2			
	CK-2%	CK-5%	CK-10%	CK-20%	CK-2%	CK-5%	CK-10%	CK-20%
Average (kg)	41,4	42,2	40,2	41,7	40,8	38,4	39,5	38,6
Difference (kg)	-1,2	-2,0	0,0	-1,5	-0,6	1,8	0,7	1,6
(%)	-2,9%	-5,1%	-0,1%	-3,8%	-1,6%	4,4%	1,9%	4,0%
R2	0,980	0,990	0,996	0,995	0,981	0,965	0,990	0,948

Chainsaw-FDL

In literature are present researches where the correlation between felling time, diameter and volume assessment were studied. Nevertheless, no one of these deals with the automatic collection procedure of the raw data as well as they elaboration (Ciubotaru and Maria, 2012; Vusic et al., 2012).

The measurement of the time in which the chainsaw was working at high rpm during the WS, allows the implemented OIE, thanks to dedicated mathematical models, to calculate the diameter at the stump level and at the breast high and finally the volume of the entire tree. The comparison of this assessment was done for 9 felling operations (Table 5).

Table 5. Summary of the validated results. The comparison between the measurements collected by manual survey (M_S) and those obtained by the OIE's elaborations (A_S) are reported and compared

	Sum		Average		St. dev.		Difference		R2
	A_S	M_S	A_S	M_S	A_S	M_S	-	%	
Time study (s)	735,4	639	81,7	71,0	45,95	42,56	-10,7	-15,1%	0,909
DS (cm)	483,1	491	53,7	54,6	15,65	17,20	0,9	1,6%	0,893
DBH (cm)	361,5	353	40,2	39,2	10,80	12,30	-0,9	-2,4%	0,928
Vol (m ³)	16,58	16,49	1,84	1,83	0,99	1,12	0,0	-0,5%	0,932

Comparing the results obtained for both diameters, applying a t-test, no statistical differences were found ($t > 0.05$). Often occurred that when the FS starts with uncontrollable situations such as revving the engine or removal of the lower obstacles (branches), the estimations EFT, DST and DBH can be strongly influenced. Thanks to the very satisfactory R², next steps foresee the study of a solution capable to distinguish the felling operations from the trunk processing. In this way, the final goal will be to offer an operational monitoring device able to collect information on the processing of the entire tree. Indeed, as reported in a specific study (Fisher, 2010), by using the data collected by the accelerator it is possible to establish the chainsaw position in the space. So it is easily possible to know if the chainsaw is working in horizontal (typical position during the cutting) or vertical position (during obstacle removing).

Then, the final users can visualize and consult all the operative outputs through a Web-GIS application (Figure 3).

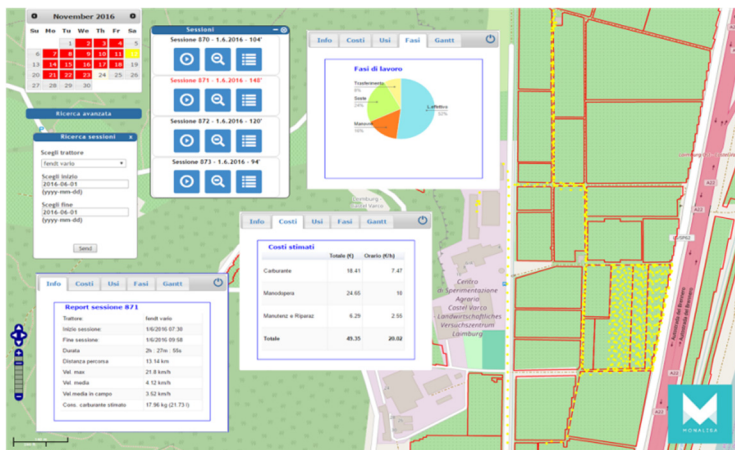


Figure 3. Example of graphical output. All the elaborations are displayed on Web-GIS tools

CONCLUSIONS

Preliminary results obtained by innovative solutions for the operational monitoring, based on the use of a field-data logger and specific sensors, as well as a dedicated OIE for data collection and interpretation, were here reported.

The developed application was tested on three operations: apple harvesting, timber logging and motor-manual felling. For all the operations, the experience has obtained very interesting and important outcomes achieving very satisfactory results in term of capability and accuracy. In general, by the comparison with manual surveys of the same operation, very low differences were found. Nevertheless, the difference always lower than 10%, is considered acceptable.

In conclusion, the positive results here obtained highlighted that the application of the proposed approach can be considered as a good and interesting tool for the automatic operational monitoring of activities in the agroforestry sector. The proposed system can be considered an innovative operational procedure for Precision Agriculture or Precision Forestry applications. Indeed, this can be a useful tool to obtain operative information for the automatic compilation of the field activity registers, suitable to be used also for certification and traceability processes. This tool can be also employed for the operative costs and input consumption estimation, applying specific estimative parameters. Further study will be planned in order to assess other field activities as well as to improve the recognition of displacement working phases.

REFERENCES

- Fountas, S., Carli, G., Sørensen, C.G., Tsiropoulos, Z., Cavalaris, C., Vatsanidou, A., Liakos, B., Canavari, M., Wiebensohn, J. and Tisserye, B. (2015a). Farm management information systems: Current situation and future perspectives. *Computers and Electronics in Agriculture*, 115, pp.40-50.

- Fountas, S., Sorensen, C.G., Tsiropoulos, Z., Cavalaris, C., Liakos, V. and Gemtos, T. (2015b). Farm machinery management information system. *Computers and Electronics in Agriculture*, 110, pp.131-138.
- Nikkilä, R., Seilonen, I. and Koskinen, K. (2010). Software architecture for farm management information systems in precision agriculture. *Computers and electronics in agriculture*, 70(2), pp.328-336.
- Lopes, D.C., Steidle Neto, A.J. (2010). Recent Advances on agricultural software: a review. *Agriculture Research and Technology*, Editors: Kristian Bundgaard and Luke Isaksen p.139-169. ISBN: 978-1-61761-488-0
- Mazzetto, F., Sacco, P. and Calcante, A. (2012). Algorithms for the interpretation of continuous measurement of the slurry level in storage tanks. *Journal of Agric. Eng.*, 43(1), p.6.
- Sørensen, C.G., Pesonen, L., Bochtis, D.D., Vougioukas, S.G. and Suomi, P. (2011). Functional requirements for a future farm management information system. *Computers and Electronics in Agriculture*, 76(2), pp.266-276.
- Ciubotaru, A., Maria, Gh.D. (2012). Research regarding structure of working time in spruce felling with mechanical chainsaw Husqvarna 365. *Bulletin of the Transilvania University of Brasov*, Vol. 5 (54) n. 1.
- Fisher, C.J. (2010). Using an accelerometer for inclination sensing. AN-1057, Application note, Analog Devices. 1-8.
- Vusic, D., Zeljko, Z., Turk, Z. (2012). Productivity of chainsaw felling and processing in selective forest of Croatia. In *Proceedings of FORMEC Conference "Forest Engineering – Concern, knowledge and accountability in today's environment"*. Dubrovnik – Croatia 2012.



ASSESSING THE QUALITY AND ENERGY INDICES OF PRECISION PLANTERS

Dan CUJBESCU^{1*}, Gheorghe BOLINTINEANU¹, Cătălin PERSU¹,
Iuliana GĂGEANU¹, Mihaela NIȚU¹, Augstina PRUTEANU¹, Gheorghe VOICU²,
Nicoleta UNGUREANU²

¹ Testing Department, INMA, Ion Ionescu de la Brad Blv. No. 6, Sector 1, Bucharest, Romania

² Department of Biotechnical Systems, University POLITEHNICA of Bucharest,
Splaiul Independentei nr. 313, Sector 6, Bucharest, Romania

*E-mail of corresponding author: dcujbescu@yahoo.com

SUMMARY

The paper presents a series of experiments to determine quality and energy indices of six row precision planters with vertical disc seed metering apparatus. The experiment was performed at 3 working velocities in 3 replications and different crops (corn, sunflower, soybean, beans). The quality indices followed were: sowing precision, unevenness of distribution on the working width, the index of achieving the sowing norm, the degree of damaging seeds, depression, unevenness of depression, exhaustor flow rate, as well as the average sowing depth and its unevenness. The energy indices determined were represented by the skidding of tractor wheels, traction power and the degree of using the engine power. The conclusions obtained from laboratory and field tests are useful in determining ways for optimizing the process of precision planters.

Keywords: sowing, planter, uniformity, depth

INTRODUCTION

Sowing precision is a significant factor in achieving a quality planting work with high yields. By being placed at evenly distributed distances, roots of future plants will develop and cover evenly the space on the sown row without being pushed outside it by a neighbouring root (Jaggard, 1990). Therefore, for determining seed spacing uniformity at three field speeds using a seed location method in the field and a laboratory method involving an opto-electronic sensor system five planter configurations were evaluated. Planter seed spacing uniformity was described using the Coefficient of Precision (CP3) measure (Panning et al., 2000). Quality and energy indices were also determined through experimental researches on a row unit, fitted with pneumatic seed metering device with

vertical distribution discs and different size orifices (Stoian and Bădescu, 2009; Molder and Marin, 2011; Marin et al., 2014). Experimental researches were conducted for monitoring the functional and economic indices of the planting work through the means of GPS system. (Păunescu et al., 2010). Seed distribution unevenness is correlated with the method through which seed reach the trench opened by the coulter (Fornstrom and Miller, 1989). Seed spacing uniformity was optimized using spherical materials and Response Surface Methodology (RSM) (Yazgi and Değirmencioğlu, 2015). A 4-row John Deere 7300 row crop planter was used to test three planter metering systems in order to improve down-the-row seed spacing (Miller et al., 2012).

MATERIALS AND METHODS

Physical-mechanical characteristics of seeds used during experimental researches are presented in table 1.

Table 1. Physical characteristics of seeds

Crt. no..	Seed type	Purity (%)	Volumetric mass (kg dm ⁻³)	MTS (g)
1.	Corn	99	0.769	378.3
2.	Sun flower	100	0.370	45.3
3.	Soybean	99.9	0.740	189.6
4.	Beans	99.8	0.719	270.3

Data regarding the characteristics of land parcels are presented in table 2.

Table 2. Parcel characteristics

Crt. No.	Index name	Characteristic
1.	Previous crop	Cereals
2.	Previous agricultural work	Autumn ploughing+ 2 harrowing +1 passing with the combiner
3.	Soil Type	Forrest reddish-brown
4.	Degree of soil grinding (%): fractions > 10 cm	-
	fractions 5-10 cm	5.6
	fractions < 5 cm	94.4
5.	Soil moisture (%): - in the 0-5 cm layer	15.9
	- in the 5-10 cm layer	17.5
	- in the 10-15 cm layer	20.2
6.	Degree of soil levelling	Without unevenness
7.	Degree of plant residues coverage	Without plant residues

In order to determine the work quality indices, during experiments, the planter was coupled with the tractor. Each experiment was performed in three repetitions. The active

element of seed metering devices with pneumatic seed distribution consists in a disc with orifices. Seed drive is made by creating a pressure difference along the orifices, and the evacuation into the trench opened by the coulter is performed forced or under the seed's own weight, due to the interruption of depression in that area along the orifices where the seeds are held.

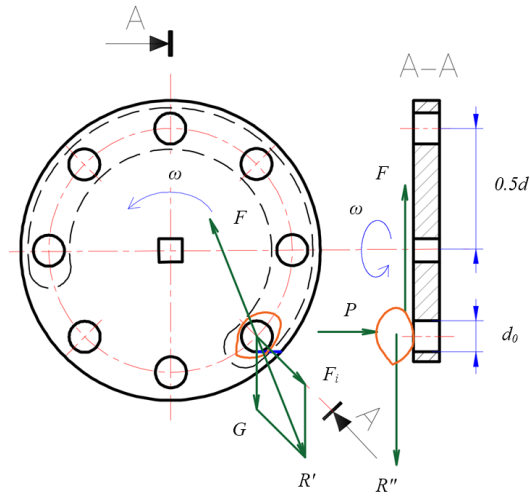


Figure 1. Forces acting on the seeds during the rotation of the vertical distribution disc with orifices having pneumatic action on seeds (G – seed weight; F_i – centrifugal force; R' – resultant of forces G and F_i ; P – force of pressing the seeds on the orifice; F – friction force between the seed and the distribution disc; R'' – resultant of forces P and F ; d_0 – diameter of the distribution disc orifice)

Seeds are driven by the distribution disc because they are pressed on the disc in front of the orifices by force P created under the action of air depression.

$$P = \frac{\pi \cdot d_0^2}{4} \cdot \Delta p \quad (1)$$

where:

d_0 - diameter of the distribution disc orifice (mm);

P - pressure exerted on the seeds (N mm^{-2}).

Forces that tend to detach the seed from the disc are represented by seed weight G and the centrifugal force F_i , giving the resultant R , whose maximum value is reached when the seed is situated in the inferior position.

Forces opposing seed detachment from the distribution disc are represented by the force P of pressing the seeds on the orifice, due to the difference in pressure on the two sides of the disc and the friction force F between the seed and the distribution disc.

For the seed not to detach from the distributor, in the most unfavourable situation, when the seed is situated in the inferior position, the following relations need to be complied with:

$$f \cdot P \geq G + F_i \quad (2)$$

$$P \cdot \frac{d_0}{2} \geq (G + F_i) \cdot \frac{l_{\max}}{2} \quad (3)$$

where:

l_{\max} - maximum seed length (mm);

f - coefficient of friction between the seeds and the distributor (-);

d_0 - diameter of distribution disc orifice (mm);

A first condition for the distribution device to function takes into consideration the minimum seed width b_{\min} and orifice diameter d_0 and is given by the relation:

$$b_{\min} > d_0 \quad (4)$$

The second operating condition of the distribution disc is constituted by the depression Δp created by the exhauster in the depression chamber, pressure that is exerted on the seeds, equal with the difference between atmospheric pressure and the pressure inside the depression chamber, whose value is given by the relation:

$$\Delta p \geq \frac{4 \cdot G}{\pi \cdot f \cdot d_0^2} \cdot \left[1 + \frac{d}{2 \cdot g} \cdot \left(\frac{\pi \cdot n}{30} \right)^2 \right] \quad (5)$$

Figure 2 presents the layout of a row unit from the planting machine used for conducting the experimental researches.

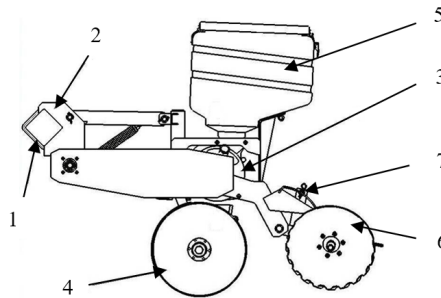


Figure 2. – Layout of the row unit used for conducting the experimental researches

(1 – support; 2 – flange; 3 – distribution device; 4 – double disc coupler; 5 – seed reservoir; 6 – discs for closing the trench; 7 – device for adjusting the sowing depth).

Precision planters accurately place single seeds or groups of seed (in nests) almost equidistant apart along a furrow. Sowing precision was determined both on stand as well as “in green” for emerged seeds. Sowing precision as number of seeds in one nest, for which were established:

- nests with one seeds (%);
- nests with multiple seeds (two, three) (%);
- nests without any seeds (empty) (%).

Sowing precision as distance between nests on row (the reference element being the theoretical interval, adjusted, between seeds in row x_{ref}), for which were established:

- distances within the interval $(0.5 - 1.5) x_{ref}$ are normal distances;
- distances smaller than $0.5 x_{ref}$ are considered as doublings;
- distances bigger than $1.5 x_{ref}$ are considered as empty spaces.

Theoretical interval, adjusted, between seeds in row x_{ref} was calculated with the following relation:

$$x_{ref} = \frac{10000 \cdot n_{seeds}}{N \cdot D_r} \quad (6)$$

where:

x_{ref} is the theoretical distance between seeds on a row (cm);

n_{seeds} is the number of seeds in a nest (-);

N is the sowing norm (plants ha⁻¹);

D_r is the distance between rows (cm).

Distribution unevenness on the working width (between planting units) is calculated using the formula:

$$e = \frac{\sqrt{\frac{\sum_{i=1}^n (N_m - N_i)^2}{n-1}}}{N_m} \cdot 100 \quad (7)$$

where:

e - distribution unevenness on the working width (%);

N_m - average number of seeds distributed by the planting units (-);

N_i - number of seeds distributed by each planting unit (-);

n - number of planting units (-).

The index of achieving the norm is calculated using the formula:

$$i = \frac{N_m}{N_r} \cdot 100 \quad (8)$$

where:

i - index of achieving the norm (%);

N_m - average number of seeds distributed by the planting units (-);

N_r - number of seeds adjusted on each planting unit (-);

The degree of seed harming was determined for large corn seeds, as follows:

- a 2.5 kg quantity of unharmed seeds was introduced in the planting units – which was driven on stand until the seed samples were completely exhausted;
- seeds harmed when passing through the distribution devices were separated and weighed;
- the degree of seed harming was calculated using the formula:

$$D_h = \frac{M_v}{M} \cdot 100 \quad (9)$$

where:

D_h – degree of harming (%);

M – mass of seeds introduced in the bunker (g);

M_v – mass of harmed seeds (g).

For determining the depression achieved on planting units, a Pitot Prandtl tube and a static pressure probe with 1 mm diameter were used. Depression was obtained by summing the two readings P_1 and P_2 compared to the equilibrium position of the manometric liquid:

$$P_S = P_1 + P_2 \quad (10)$$

Speed of revolution measured using the tachometer was 3100 rot/min at a 540 rot/min speed of the tractor's PTO.

Vacuum unevenness is calculated using the formula:

$$n_v = \sqrt{\frac{\sum_1^n (p_{sm} - p_{si})^2}{2}} \cdot 100 \quad (11)$$

where:

n_v - vacuum unevenness (%);

p_{sm} - average static pressure between tubes (mmcol. H₂O);

p_{si} - static pressure at each tube (mmcol. H₂O);

n - number of planting units (-).

For establishing the exhauster's flow rate, the dynamic pressure in the exhauster's aspiration pipe was determined. For this purpose, between the exhauster and the air distributor's body was fitted a $\varnothing = 100$ mm and 800 mm in length metallic tube provided at the half of its length with a $\varnothing = 9$ mm orifice. Measurements were made using the Pitot – Prandtl tube. Tests were conducted with the planter unfed with seeds at the distribution discs orifices and also with the planter fed with seeds at the distribution discs orifices. Based on the values obtained measuring the depression, air speed was calculated using the formula:

$$v_{air} = 4 \cdot \sqrt{P_d} \quad (12)$$

where:

v_{air} - air speed (m s⁻¹);

P_d - dynamic pressure (mm col. H₂O).

Exhauster flow rate was calculated using the formula:

$$Q = W \times S \times 3600 \quad (13)$$

where:

Q - exhauster flow rate (m³ h⁻¹);

S - section of the metallic tube (m²).

The average working depth was measured "in green" by cutting the part of the plant that is situated above soil, and afterwards digging and measuring the part of the plant that remains in the soil. Tests comprised 20 measurements in 3 repetitions on all sowed rows and for all working speeds.

Within experiments were determined the following energy indices: wheel slip (%); drawbar pull (daN); tractive power (kW); necessary PTO power (kW); degree of using the engine power (%).

Tests were conducted for three speeds in three repetitions.

Planting machine bunkers were filled up to 3/4 of their capacity.

Energy indices calculation was made using the following relations:

$$\text{Wheel slip } \delta = \frac{N_s - N_o}{N_o} \cdot 100 \quad (14)$$

where:

δ – tractor wheel slip (%);

N_s – number of drive wheels rotations on the given space when the tractor is in load (-);

N_o – number of drive wheels rotations on the given space when the tractor is not in load (-).

Tractive power:

$$P_{tr} = 360 \cdot F_{tr} \cdot v \quad (15)$$

where:

P_{tr} – tractive power (kW);

F_{tr} – drawbar pull (daN);

v – working speed (km h⁻¹).

The degree of using the engine power (%):

$$K = \frac{P_{ef}}{P_n} \cdot 100 \quad (16)$$

where:

K – degree of using the engine power (%);

P_{ef} – tractor engine necessary power for driving the aggregate (kW);

P_n – tractor nominal power (kW).

RESULTS AND DISCUSSION

Sowing precision was determined both on stand as well as “in green” on emerged plants.

Figure 3 presents the variation of sowing precision determined on stand, depending on operating speed, for all the types of seeds used in experimental researches.

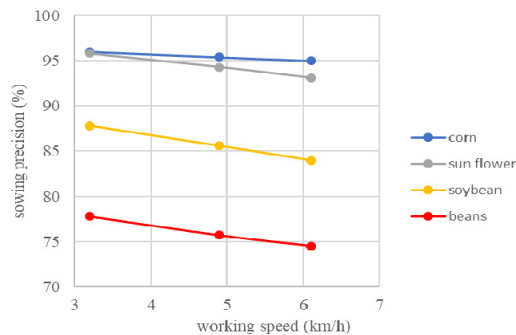


Figure 3. Variation of sowing precision determined on stand, depending on the operating speed

Table 3 shows the variation of sowing precision on stand, as distance between seeds, depending on the working speed (v).

Table 3. Variation on the stand of sowing precision as distance between seeds depending on the working speed

Crt. no.	Index name	Crop				Working speed, v_l (km h ⁻¹)
		Corn	Sun flower	Soybean	Beans	
		Sowing precision as distance between seeds (%)				
1.	Good distances (0.5 - 1.5) x_{ref}	94	94.8	85.7	76.3	3.2
		92.8	93.7	84.5	74.7	4.9
		92.2	92.2	83.9	71.6	6.1
2.	Smaller distances <0.5 x_{ref}	4.4	3.7	9.1	11.1	3.2
		2.6	4.1	9.3	11.4	4.9
		2.1	4.4	9.1	12.1	6.1
3.	Bigger distances >1.5 x_{ref}	1.6	1.5	5.2	12.6	3.2
		4.6	2.2	6.2	13.9	4.9
		5.6	3.4	7.0	16.3	6.1

Sowing precision of emerged corn plants (as number of seeds in the nest, $N=64500$ plants ha^{-1} , $D_r=70$ cm) for the adjusted speed (x_{ref}) between seeds of 22.15 cm, is shown in figure 4.

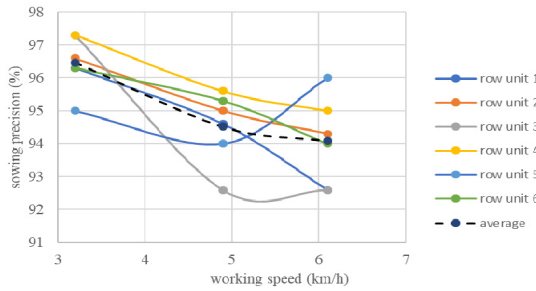


Figure 4. Sowing precision variation determined for corn seeds as number of emerged seeds for $x_{ref} = 22.15$ cm

In figure 5 are presented the distances between seeds on row for each planting unit, as well as the average distance between seeds on row depending on the operating speed for the work of sowing corn seeds for a norm of $N=64500$ plants ha^{-1} and a distance between rows $D_r=70$ cm.

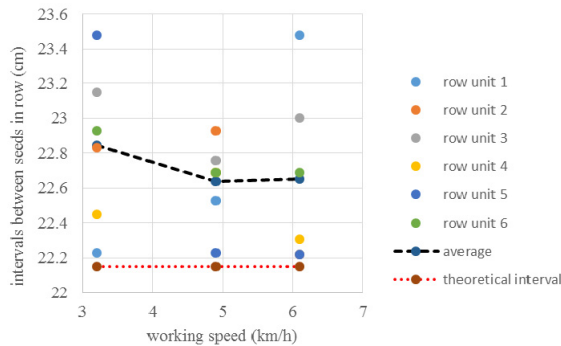


Figure 5. Variation of distance between seeds depending on the operating speed for sowing corn seeds

In table 4 are presented the results of determinations regarding distribution unevenness and index of achieving the norm for corn.

Table 4. Distribution unevenness on the working width (e) and the index of achieving the norm (i) for corn ($N=64500$ plants ha^{-1} , $v = 6.1$ km h^{-1} , $x_{ref} = 22.15$ cm)

Crt. no.	Index name	Row number						Average	e (%)
		1	2	3	4	5	6		
		Sowing precision as distance between seeds (%)							
1.	Good distances ($0.5 - 1.5$) x_{ref}	74	77	76	74	78	72	75,16	
2.	Smaller distances < 0.5 x_{ref}	22	17	10	22	20	23	19	-
3.	Bigger distances > 1.5 x_{ref}	4	6	14	4	2	5	5,84	
4.	i (%)	105	105	99	107	103	108	104.5	3.7

The results of determination regarding vacuum and vacuum variations are presented in table 5.

Table 5. Results of determinations of vacuum and vacuum variations

No. of row unit	Vacuum Δp (kPa)					
	Position of the obturation flap					
	1	2	3	4	5	6
1	2.175	2.401	3.116	3.596	3.792	3.910
2	1.999	2.303	3.292	3.577	3.978	3.851
3	2.058	2.342	3.234	3.498	3.851	3.929
4	2.097	2.420	3.185	3.547	3.831	3.998
5	2.205	2.371	3.155	3.606	3.890	3.969
6	2.116	2.322	3.243	3.479	3.939	3.978
Average (kPa)	2.107	2.359	3.204	3.550	3.880	3.939
Deviation (kPa)	0.118	0.098	0.100	0.071	0.086	0.052
Vacuum variations (%)	5.5	4.05	3.11	1.97	2.23	1.33

In figure 6 are presented the results of determinations regarding the average sowing depth and its unevenness, for a depth set at 7 cm.

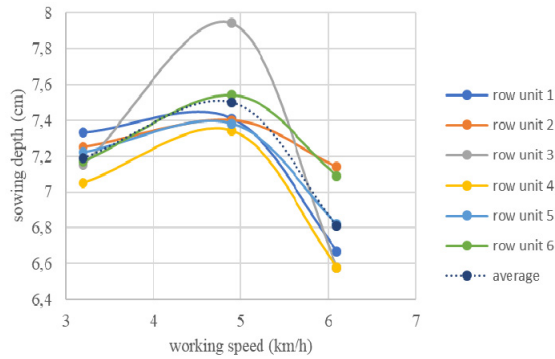


Figure 6. Sowing depth variation depending on the operating speed

Once the results from the tables and figure analysis are reviewed, it is clear that the seed spacing accuracy performance was good at a working speed of 3.2 km h^{-1} . Panning et al. (2010) reached the same result from their study when five planter configurations were evaluated for seed spacing uniformity at three working speeds using a seed location method in the field and a laboratory method involving an opto-electronic sensor system. The optimum vacuum level was 3.173 kPa . Yazgi and Degirmencioglu (2015) noticed in their study about optimization of the seed spacing uniformity of a vacuum type precision planter using spherical materials, that the optimum vacuum level goes down from 5.236 kPa to 3.26 kPa as the diameter of spherical materials increases from 4 to 6 mm.

CONCLUSIONS

The results of experimental researches suggest that the experiments conducted in the laboratory, correlated with field tests, can be useful in determining the methods of perfecting precision planters. Analyzing the results obtained is found that sowing precision (both as number of seeds in the nest as well as distance between nests on row) decreases by increasing the operating speed, a fact noted for all experimental crops: corn, sun flower, soybean, beans. It is found that the highest precision (as number of seeds in one nest) was obtained for corn crop, 96%, for an operating speed of 3.2 km h^{-1} . Also, sowing precision, as distance between seeds, decreases along with increasing the operating speed. Sowing precision is affected by the planter's capacity to place the seeds at the adjusted distance, for corn observing an increase of distances between seeds on row, compared to the adjusted distance of 22.15 cm . This was noted for all the row units. Vacuum variations between row units (another factor influencing sowing precision) had a value of 5.5% at minimum depression and 1.3% at maximum vacuum. Average sowing depth for corn plants at 6.1 km h^{-1} operating speed had the value of 7.5 cm compared to the adjusted speed of 7 cm. Energy indices determined have shown that the tractor-planter aggregate ensured a 54.9% load at a 6.1 km h^{-1} operating speed. The experimental researches conducted in the laboratory have demonstrated that they can be used to predict sowing precision in the field.

REFERENCES

- Brencu Molder L., Marin E. (2011). Experimental researches of complex technical equipment sowing corn in narrow strips. INMATEH International Symposium, ISSN: 978-973-0-11614-4, pag. 37-44
- Fornstrom K. J. and Miller S.D. (1989). Comparison of sugarbeet planters and planting depth with two sugarbeet varieties. *J. Am. Soc. Sugarbeet Technol.* 26 (3&4): 10-16
- Jaggard K. (1990). Are there too many beets in our fields? *British Sugar Beet Rev.* 58(1):6-9
- Marin, E., Bolintineanu, Gh., Sorică, C., Manea, D., Herak, D., Croitoru, Ș, Grigore, I. (2014). Scientific researches on the qualitative working indexes of the sowing body of a modern technical hoeing plants sowing equipment. *INMATEH - Agricultural Engineering*, vol. 42 (1), pp. 19-26
- Miller, E. A., Rascon, J., Koller, A., Kochenower, R. (2012). Evaluation of Corn Seed Vacuum Metering Systems. An ASABE Meeting Presentation. Paper Number: 12-1337167
- Panning, J. W., Kocher, M. F., Smith, J. A., Kachman, S. D. (2000). Laboratory and field testing of seed spacing uniformity for sugarbeet planters. University of Nebraska - Lincoln DigitalCommons@University of Nebraska – Lincoln. *Biological Systems Engineering: Papers and Publications*. 152., vol. 16(1), pp. 7-13
- Păunescu, D., Brătucu, Gh., Păunescu, S., Atanasov, A. (2010). Research regarding the use of the gps in monitoring agricultural sowing. *INMATEH - Agricultural Engineering*, vol. 31 (2), pp. 79-86
- Stoian F. and Bădescu M. (2009). Researches on the specialisation of the wide row drills for the certain crops, *INMATEH - Agricultural Engineering*, vol. 28 (2), pp. 134-138.
- Yazgi, A. and Değirmencioğlu, A. (2015). Optimization of the Seed Spacing Uniformity of a Vacuum Type Precision Seeder using Spherical Materials. *Ege Üniv. Ziraat Fak. Derg.*, 52 (3): 277-286 ISSN 1018 – 8851



DEMAND DRIVEN BIOGAS PRODUCTION BY DISCONTINUOUS FEEDING STRATEGIES

Javier LIZASOAIN^{1,2}, Jonas LEBER¹, Susanne FRÜHAUF¹,
Kwankao KARNPAKDEE¹, Bernhard WLCEK^{1,2}, Andreas GRONAUER¹,
Alexander BAUER^{1*}

¹ University of Natural Resources and Life Sciences, Department of Sustainable Agricultural Systems, Division of Agricultural Engineering, Konrad-Lorenz-Strasse 24, A-3430 Tulln, Austria

² AlpS-GmbH, Centre for Climate Change Adaptation Technologies, Grabenweg 68, A-6010 Innsbruck, Austria

*E-mail of corresponding author: alexander.bauer@boku.ac.at

SUMMARY

The increase in the energy supply coming from renewable energies is promoting the demand of flexible power production to stabilize the electrical grid. This demand could be partially met by biogas plants, providing new income opportunities for biogas operators. A discontinuous feeding regime can be used for the implementation of flexible biogas production. This paper focuses on the effect of a discontinuous feeding regime in a laboratory scale experiment based on the operating parameters used in the biogas plant Bruck/Leitha (Austria). The aim of the research was to extend the current knowledge of gas production and process stability under two discontinuous feeding strategies: one time and nine times feeding per day (1x and 9x). The results indicated that under discontinuous feeding strategies, the anaerobic digestion process, including the biogas production, was stable. The FOS/TAC values fluctuated more under the 9x feeding strategy. Moreover, the accumulation of the determined biogas rate on a gas storage tank was simulated. The discontinuous feeding (1X) could reduce the required gas storage by 11%. The results suggest that a discontinuous feeding regime could be an alternative feeding strategy for a demand driven energy supply. The reduction of the required gas storage volume of 11% does not represent a clear improvement in comparison to the existing situation in the biogas plant.

Keywords: demand-oriented energy, discontinuous feeding, gas storage, food waste, flexible biogas

INTRODUCTION

Renewable energy has become a key element in the development of future energy strategies. In 2014 the share of renewable energy in Europe reached 16 % of the gross energy consumption, which is expected to reach 20% in 2020 and 27% in 2030 (Eurostat, 2016). Some important sources of renewable energy such as sun and wind power rely on the weather conditions. In order to integrate the big fluctuations from power production and consumption and to maintain stable power grids in an efficient manner, new approaches need to be developed. For this, we need to find renewable energy systems capable to buffer the production and demand energy peaks (Huber et al., 2014). Nowadays, fossil fuel power stations using for instance natural gas, are used to buffer the energy management systems. Biogas plants could be considered as a good alternative to fossil fuel power stations (Thrän et al., 2015). The implementation of flexible biogas utilization concepts can be implemented using different technical strategies such as storage of intermediates of the biogas process, set up of additional biogas storage tanks, storage of biomethane in the gas grid or flexible feeding of the biogas reactors (Szarka et al., 2013).

All these four strategies have the potential to provide positive control power (additional capacity of the plant by activation or intensification of the power production) and negative control power (reduction or stop of power production to avoid an oversupply) (Hirth & Ziegenhagen, 2013). In 2015 the total amount of electricity produced by biogas in Europe was 60.6 TWh (EBA, 2017), which corresponds to 14.4 Mio European households. In some European countries (e.g. Germany) different policies have been developed to support flexible power generation consisting of additional payments and thus, some biogas plants have changed the base load production into flexible production. This new approach is mainly accomplished by a storage of the produced biogas, which requires considerable investments. However, the flexible feeding strategy can be implemented without considerable costs.

The anaerobic digestion systems can be adjusted to synchronize the production of biogas and its consumption in order to reduce the volume of the required gas storage tanks, which can reduce the investment costs (Barchmann et al., 2016; Mauky et al., 2015). Research on the utilization of flexible feeding systems for biogas production remains sparse. Few studies using flexible feeding strategies (ranging between one feeding every second day and several times per day) were found in the literature showing that the long-time process stability was in general terms not affected negatively (Lv et al., 2014; Mauky et al., 2015; Mulat et al., 2016). Mauky et al., (2015) even reported stable processes using an organic loading rate (OLR) of 6 Kg VS m⁻³ d⁻¹. While in some of the aforementioned trials, the feeding regime did not alter the methane production in a remarkable manner, some authors observed slightly higher methane yields up to 14% in the reactors that were fed less frequently (Mulat et al., 2016). In addition to laboratory trials, few studies have been carried out at full scale. Mauky et al., (2016) and Mauky et al., (2017) confirmed that flexible feeding did not affect negatively the long-term stability and reported that highly flexible performance is possible. Moreover, Mauky et al., (2017) demonstrated a high degree of flexibility that allowed an electricity shutdown of up to three days due to a considerable reduction of the biogas production as well as the possibility to decrease the gas storage volume up to 65%.

The aim of this study was to simulate at laboratory scale the effect of implementing a flexible feeding system in the biogas plant Bruck/Leitha (Austria) and to determine its effect on the process stability, gas production and gas quality. In addition, the required gas storage volume in the flexible feeding system was determined.

MATERIAL AND METHODS

Physico-chemical characterization

Different parameters of the feeding material and fermenter content were determined. To analyze the dry matter (DM), the feeding substrate was dried in a drying oven at 105°C until a constant weight was reached. Ash and volatile solids (VS) were expressed as the percentage of residue remaining after dry oxidation in a muffle furnace at 550°C according to Sluiter et al., (2004). The water content was determined by the Karl-Fischer titrator Mettler Toledo V20 (Columbus, Ohio, USA) using Hydranal Composite 5 and Hydranal Methanol dry from Sigma Aldrich (St. Louis, Missouri, USA). The Van Soest method (Van Soest & Wine, 1967) was applied for the determination of cellulose and hemicellulose. In addition, the content of lignin was determined using the sulfuric acid hydrolysis procedure developed by the National Renewable Energy Laboratory (NREL) (Sluiter, 2011). The FOS/TAC ratio was used as an indicator of the process stability in the reactors, as the ratio indicates the buffer capacity and therefore, the risk of acidification in a biogas plant. The elemental analysis of the samples was performed at the Microanalytical Laboratory of the University of Vienna (Austria) using the elemental analyzer EA 1108 CHNS-O (Carlo Erba, Italy). Crude fat was determined by an external laboratory (Futtermittellabor Rosenau, Austria) by dissolution with acetone and subsequent drying and back weighing of the residual material.

Biomethane potential (BMP) test

The BMP test was performed in triplicate to determine the specific biogas and methane yields of the input material according to VDI 4630 (2006), using eudiometer batch fermenters with 250 ml capacity. The input material and the inoculum were weighed out in a ratio of 1:3 based on their VS content. In every fermenter, 200 ml of inoculum were filled in. The inoculum consisted of a mixture of two inocula; one inoculum came from a previous BMP test that used steam-exploded lignocellulosic biomass, and the second inoculum was taken from a biogas plant located in Margarethen am Moos (Austria) that was mainly using agri-food residues and manure as input material. The two inocula were mixed in a 1:1 volume ratio and the resulting inoculum was sieved and diluted to around 4% DM. The mixed inoculum was stored before the performance of the BMP test for 10 days at 37 °C in order to reduce the residual gas production. No nutritional additives were added to the inoculum. As control, microcrystalline cellulose was used. The fermenters were maintained in water baths at mesophilic conditions (37.5 °C) during the tests. The productions of biogas and methane were daily monitored and all gas volumes were reported under standard conditions of 273.15 K and 101.33 kPa in liters per kilogram of volatile solids (L kg⁻¹ VS). When the volume of biogas accumulated in the eudiometers reached a minimum volume of 100 mL, the volumetric composition of biogas was analyzed with the portable gas analyzer "Dräger X-am 7000" (Dräger, Lübeck, Germany).

Semicontinuous anaerobic digestion trials

In order to identify the influence of different discontinuous feeding strategies on the anaerobic digestion performance, the biogas and methane productivity, as well as the process stability, were measured in a semicontinuous experiment according to VDI 4630 (VDI, 2006). The strategies 1x and 9x feeding per day were tested in 2 L glass fermenters with a working volume of 1.7 L. The inoculum used for starting the trial was collected from the biogas plant Bruck/Leitha and directly used in the experiment without any storage period. The trials were carried out under mesophilic conditions (37.5°C). All reactors were daily fed with an OLR of 1.4 kg VS m⁻³ d⁻¹. All input and output materials were measured and balanced in order to enable a stable working volume. To ensure a homogeneous

dispersal, the fermenters were manually stirred once per day. To preserve the feeding material from degradation, the substrate was stored at -20 °C. The biogas plant Bruck/Leitha was using waste from the agriculture and food industry as input material at the time the material was taken. The data according to process stability, and biogas and methane production was collected over 79 and 24 days, respectively. The first weeks were considered as an adaptation time to ensure stable condition under the new feeding strategies. The gas production was measured every hour by portable cameras connected to the internet. The gas volumes were reported under standard conditions of 273.15 K and 101.33 kPa, according to VDI 4630 (VDI, 2006). Biogas and methane yields were reported in liters per m³ working fermenter volume and day (L m⁻³ d⁻¹ fermenter volume). The analysis of the volumetric composition of biogas (i.e. CH₄, CO₂, O₂, H₂S, and H₂) was done once per day with the portable gas analyzer “Dräger X-AM 7000” (Dräger, Lübeck, Germany).

RESULTS AND DISCUSSION

Analysis of input material

Table 1 shows the chemical composition of the substrate which was used as feeding material. The substrate contained a high amount of water (around 80% FM). The composition’s main characteristic was crude fat, which was close to 70% DM, giving an indication of the high biogas potential. The crude protein content was around 10% DM. The amount of structural carbohydrates and lignin was much less dominant, as it could be expected from a material which is mainly composed by food waste. Moreover, the ratio C:N was 45:1.

Table 1. Chemical analysis

Water	DM	Ash	VS	Crude fat	Crude protein	Cellulose	Hemicellulose	Lignin	C:N
[% FM]		[% DM]							
79.8	20.2	5.0	95.0	69.8	9.9	5.9	4.8	2.8	45:1

Biomethane potential (BMP) test

The high fat content in the substrate become noticeable at the batch trials due to the high specific methane yield obtained (799 L kg⁻¹ VS) with a slow but efficient biomass to gas conversion as well as the existence of a high percentage of methane in the biogas (69% methane). In comparison with other input materials such as wheat and corn silage, the methane content was significantly higher. Moreover, the theoretical methane potential calculated based on the elementary analysis according to Buswell and Boyle (1967) was 963 L kg⁻¹ VS. Thus, the obtained specific methane yield reached 83% of its theoretical potential.

Semicontinuous anaerobic digestion trials

Biogas and methane yields

Figure 1 shows the impact of the feeding strategies 9x and 1x carried out in the laboratory continuous trials, as well as the average gas production recorded under continuous feeding in the biogas plant Bruck/Leitha over the whole year 2015. The average daily biogas production under the 9x and 1x feeding strategies were 1542 and 1621 L m⁻³ d⁻¹ fermenter volume, respectively. Moreover, the average daily methane production under the 9x and 1x

feeding strategies were $1082 \text{ L m}^{-3} \text{ d}^{-1}$ fermenter volume and $1140 \text{ L m}^{-3} \text{ d}^{-1}$ fermenter volume, respectively. These trials revealed a slight increase in the biogas production of 5% under the feeding strategy 1x in comparison to 9x. However, the increase did not reach the additional 14% biogas yields reported by Mulat et al. (2016). In addition to the results from the laboratory experiment, the data recorded in the biogas plant Bruck/Leitha showed average daily biogas and methane yields of $1480 \text{ L m}^{-3} \text{ d}^{-1}$ fermenter volume and $932 \text{ L m}^{-3} \text{ d}^{-1}$ fermenter volume, respectively. Despite the yields recorded in the biogas plant were lower than those obtained under the 9x and 1x feeding strategies, they cannot be directly compared since during the year, the feeding material was not strictly identical, and thus also its specific biogas and methane potentials. This can be seen in the high standard deviation caused by the annual fluctuation in the gas production. Since there can be no assurance that the content of the input material has been homogeneous over time, it is not possible to confirm that the 9x and 1x increased the yields obtained in the continuous feeding regime.

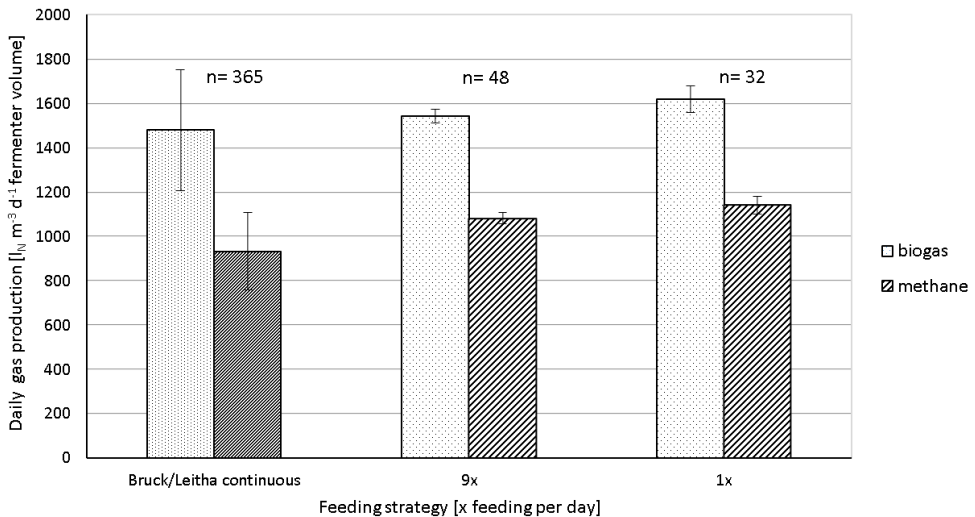


Figure 1. Daily biogas and methane production under the different feeding strategies

Process stability under the discontinuous feeding strategies

Indicators for the process stability (e.g. production of biogas, concentrations of CH_4 and CO_2 , pH and FOS/TAC values) were collected and assessed for each feeding strategy. No significant decline in the biogas production as well as no change in methane content occurred within 79 days. The average CH_4 and CO_2 content were 70% and 30% respectively. This high concentration of CH_4 that was already observed in the BMP tests of section 3.2 is common for substrates that contain a high concentration of fat (D. Deublein & Steinhauser, 2008). The study carried out by Mulat et al. (2016), which included the feeding strategies “every 2h” “1x per day” and “1x every two days”, reported similar results in the biogas composition.

In the present study, the pH value showed higher values for the 9x feeding strategies (pH 8.5) in comparison to the 1x strategy (pH 8.3). However, no substantial fluctuations could be observed in any of both feeding strategies.

The FOS/TAC ratios measured during the process were stable for both feeding strategies. The highest fluctuations were measured during the 9x feeding, with a value of 0.42 ± 0.14 . In the feeding strategy 1x, the value was 0.40 ± 0.02 , which shows to have a slightly better stabilization between the organic acids and its carbonate buffer. The measured FOS/TAC values can be catalogued as medium-high, considering that the input material contains high amount of fat and easy degradable compounds. In summation, neither flexible feeding strategy indicated a significant negative influence on the biogas and methane production. In addition, FOS/TAC concentration could point out that the 1x feeding strategy led to a slightly more stable system. However, there is no clear evidence to suggest the existence of any type of inhibition in any of the fermenters.

Gas storage capacity under continuous and discontinuous feeding

Figure 2 presents a scenario that compares the filling of the gas storage tank under continuous and discontinuous feeding strategies. As an example for the discontinuous feeding strategy, the 1x strategy was chosen, being 11:45 set as the feeding time. The 1x feeding strategy produced over 9 h (from 12:00 to 21:00) a higher amount of biogas in comparison to a continuous biogas rate. This period was taken as time span in which the whole gas storage was used for energy production. Under continuous biogas production, the gas storage level was accumulated linearly. During the gas storage (i.e. from 21:00 to 12:00), a discontinuous filling of the gas storage resulted in a lower gas storage level. This led to a required gas storage reduction of 11% even though the total production of biogas in this system is slightly higher. It is remarkable that the higher production obtained in the discontinuous feeding system did not require additional gas storage at that time. Nevertheless, the gas storage reduction obtained in the present study was lower than the obtained by Mauky et al. (2017), which could reduce the storage volume to 65%. One reason for the lower reduction observed in the present study was the lower biogas rate, which is – among other factors – influenced by the feeding material.

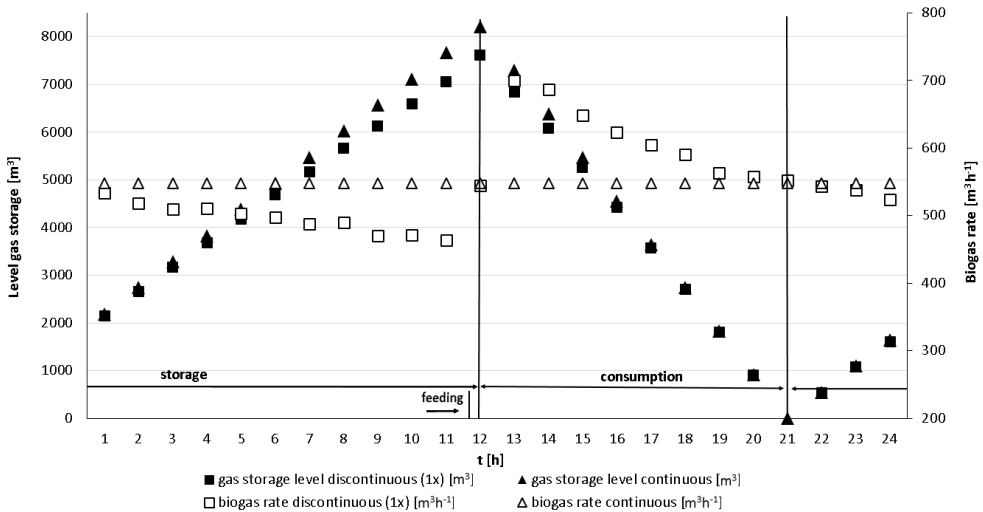


Figure 2. Simulation of the biogas storage (m^3) and biogas rate ($\text{m}^3 \text{h}^{-1}$) in the storage tank under continuous and 1x feeding strategy

CONCLUSION

With the utilization of the food residues collected by the biogas plant Bruck/Leitha, using an OLR of 1.4 kg VS m⁻³ d⁻¹ and mesophilic conditions, the results showed that the less frequent feeding strategy (1x) provided a slightly higher biogas and methane production. In addition, the study showed that this discontinuous feeding strategy can reduce the required gas storage volume by 11%. However, in comparison to other studies, this reduction is much less considerable and questions the advantage of a discontinuous feeding under these conditions. The trial showed a slightly better process stability under the less frequent feeding strategy. Therefore, the revealed results indicate that a discontinuous feeding system can be undertaken in the biogas plant Bruck/Leitha without having a negative impact on the process. Further trials using different input material and a higher OLR may improve the advantages of a discontinuous feeding system for a demand driven biogas production.

ACKNOWLEDGMENTS

The present study is part of project Bio(FLEX)Net, which is sponsored by the climate and energy foundation in the course of the energy research program.

REFERENCES

- Barchmann, T., Mauky, E., Dotzauer, M., Stur, M., Weinrich, S., Jakobi, H.F., Liebetrau, J., Nelles, M. (2016). Expanding the flexibility of Biogas plants - Substrate Management, schedule Synthesis and economic assessment, Vol. 71 (6), LANDTECHNIK, pp. 233–251.
- Eurostat (2016). Statistik der erneuerbaren Energien. Retrieved October 30, 2017 from http://ec.europa.eu/eurostat/statistics-explained/index.php/Renewable_energy_statistics/de
- Deublein, D. and Steinhauser, A. (2008). Biogas from Waste and Renewable Resources: an Introduction. Wiley-VCH Verlag GmbH, Weinheim.
- EBA - European Biogas Association (2017). Annual Statistical Report of the European Biogas Association.
- Hirth, L. and Ziegenhagen, I. (2013). Control power and variable renewables. International Conference on the European Energy Market, EEM.
- Huber, M., Dimkova, D., Hamacher, T. (2014). Integration of wind and solar power in Europe: Assessment of flexibility requirements. *Energy*, 69, 236-246.
- Lv, Z., Leite, A.F., Harms, H., Richnow, H.H., Liebetrau, J., Nikolausz, M. (2014). Influences of the substrate feeding regime on methanogenic activity in biogas reactors approached by molecular and stable isotope methods. *Anaerobe*, 29, 91-99.
- Mauky, E., Jacobi, H.F., Liebetrau, J., Nelles, M. (2015). Flexible biogas production for demand-driven energy supply - Feeding strategies and types of substrates. *Bioresource Technology*, 178, 262-269.
- Mauky, E., Weinrich, S., Jacobi, H.F., Nägele, H.J., Liebetrau, J., Nelles, M. (2017). Demand-driven biogas production by flexible feeding in full-scale – Process stability and flexibility potentials. *Anaerobe*, 46, 86-95.
- Mauky, E., Weinrich, S., Nägele, H.J., Jacobi, H.F., Liebetrau, J., Nelles, M. (2016). Model Predictive Control for Demand-Driven Biogas Production in Full Scale. *Chemical Engineering and Technology*, 39(4), 652-664.
- Mulat, D.G., Fabian Jacobi, H., Feilberg, A., Adamsen, A.P.S., Richnow, H.H., Nikolausz, M. (2016). Changing feeding regimes to demonstrate flexible biogas production: Effects on process performance, microbial community structure, and methanogenesis pathways. *Applied and Environmental Microbiology*, 82(2), 438-449.

- Schieder, D.G., A Lebuhn, M Bayer, K Beck, J Hiepp, G Binder, S. (2010). Prozessmodell Biogas – Prozessbiologie, - bewertung und Analytik. Biogasforum Bayern. Arbeitsgemeinschaft Landtechnik und landwirtschaftliches Bauwesen in Bayern e.V.. Nr.3, pp. p. 18-21.
- Sluiter, A., BRuiz, RScarlata, CSluiter, JTempleton, D. (2011). Determination of Structural Carbohydrates and Lignin in Biomass. in: Laboratory Analytical Procedure (LAP). National Renewable Energy Laboratory (2008) Technical Report NREL/TP-510-42618-revised 2011.
- Sluiter, A., Hames, B., Ruiz, R.O., Scarlata, C., Sluiter, J., Templeton, D., Energy, D.o. (2004). Determination of Ash in Biomass. National Renewable Energy Laboratory; National Bioenergy Center; Department of Energy.
- Szarka, N., Scholwin, F., Trommler, M., Fabian Jacobi, H., Eichhorn, M., Ortwein, A., Thrän, D. (2013). A novel role for bioenergy: A flexible, demand-oriented power supply. *Energy*, 61, 18-26.
- Thrän, D., Dotzauer, M., Lenz, V., Liebetrau, J., Ortwein, A. (2015). Flexible bioenergy supply for balancing fluctuating renewables in the heat and power sector—a review of technologies and concepts. *Energy, Sustainability and Society*, 5(1), 1-15.
- Van Soest, P.J., Wine, R.H. (1967). Use of detergents in the analysis of fibrous feeds. IV. Determination of plant cell-wall constituents. *Journal of the Association of Official Analytical Chemists*, 50, 50-55.
- VDI (2006). VDI 4630 - Fermentation of organic materials. Characterisation of substrate, sampling, collection of material data, fermentation tests, VDI Gesellschaft Energietechnik.



A SCALE-UP PROCEDURE FOR PROCESSING HIGH-SOLID CONTENT FOOD WASTE AND DAIRY MANURE IN A LOW TEMPERATURE ANAEROBIC DIGESTER

Bernard GOYETTE^{1*}, Rajinikanth RAJAGOPAL^{2,3}, Jean-François HINCE³, Md.
Saifur RAHAMAN²

¹Sherbrooke Research and Development Center, Agriculture and Agri-Food Canada,
2000 College Street, Sherbrooke, QC J1M 0C8, Canada

²Department of Building, Civil and Environmental Engineering, Concordia University,
Montreal, QC H3G 1M8, Canada

³Bio-Terre Systems, 4005 rue de la Garlock, Sherbrooke (Qc) J1L 1W9, Canada

*E-mail of corresponding author: bernard.goyette@agr.gc.ca

SUMMARY

Treating organic solid wastes economically is a challenge, predominantly in cold and high-altitude regions. The objective of this research was to improve the high-solids anaerobic digestion (AD) of food waste (mainly fruits and vegetable wastes [FVW]) with or without animal manure in a low-cost dry AD (DAD) system at 20-25°C. In addition, this study aimed to obtain the basic design criteria for starting up of scaled-up DAD system (100 times compared to lab-scale digester) using adapted liquid inoculum. Inoculum to feedstock ratio is being varied from 6:1 to 1:1. The organic loading rate (ORL) expressed as volatile solids (VS) and operational cycle length was varied from 0.44-2.1 kg_{VS} kg_{inoculum}⁻¹ d⁻¹ and 33-14d. Preliminary results show that methane (CH₄) production from FVW was feasible at low-temperature and specific methane yield of 0.400-0.520 L g_{VS}⁻¹ was observed even at high OLR. CH₄ conversion rates and its quality were not affected, while maintaining the operational stability (e.g. no acidification or VFA accumulations). CH₄ content reached over 60%, which shows the quality of biogas was excellent and remained almost steady. Results also suggest that DAD process at 25°C is comparatively efficient in saving heat energy and at the same time obtains the CH₄ values close to mesophilic conditions. This concept is particularly vital for cold countries facing energy constrains. Optimization study is underway to achieve ideal operating conditions.

Keywords: dry anaerobic digestion, biomass adaptation, fruit and vegetable waste, low-temperature, Methane yield

INTRODUCTION

Mining bioenergy from biomasses is an effective alternative energy resource that can be used in an environmental friendly way and requires less production energy (Zheng et al., 2012). Various biomasses derived from the carbonaceous wastes of human, livestock animals and natural resources that could be utilized as renewable energy resources. According to Environment Canada (2013), there has been growing consideration in managing the organic-fraction of the municipal waste stream in recent years. In Canada, biodegradable material such as food-waste (FW) constitutes nearly 40% of the residential waste stream; therefore diversion of organic materials is crucial to attain high diversion targets. Municipal waste (table, activated sludge, etc.) are rich in protein, fat and fiber material, and they are suitable for anaerobic digestion (AD). Currently, municipalities must pay to transport and dispose of these by-products in landfills/composting. An interesting option for municipalities would pay farmers nearby to receive and process these materials in AD bioreactors. For farmers, the co-digestion of cow manure (CM)+FW increases the recovery of green energy, production of litter for the herd and mass of organic nitrogen fertilizer for crops. Handling litter poses a significant cost on dairy operations. Thus, this paper aims to demonstrate the operational feasibility of dry anaerobic digestion (DAD) system treating CM+FW at low temperature conditions and to encourage small-scale municipalities or farmers to adopt this technology at low cost.

After the extensive research work done by Agriculture and Agri-Food Canada (AAFC) and Bio-Terre Systems (BTS) on the development of low-temperature AD system for treating high solid content wastes like solid separated animal manure and carcass (Massé et al., 2014, Rajagopal et al., 2014; Saady and Massé, 2015), focus is now put on the capacity of this new technological approach to play a capital role in the organic waste management challenges that several smaller municipalities are facing. Previous studies were performed using laboratory-scale digesters (30-120 L) to test different solid content manures with or without liquid inoculums percolation-recirculation mode of operation. It has been established that high solid AD can be successfully operates with manure up to 35% TS content (Saady and Massé, 2015). The aim of this paper was to investigate the operational capacity of the high solid low-temperature AD technology for the digestion of organic waste (food waste) as a sole feeding source with recirculation of liquid inoculums. The special emphasis was given to evaluate the biodegradation of the organic waste and the optimal operation conditions (such as OLR, cycle length) based on the organic matter reduction and methane production. To obtain this, different approaches were used such that lab-scale operations (30 L active volume) were performed in parallel and compared with a scaled-up DAD process (3m³ active volume, that is to say 100 times bigger than the lab-scale digesters) to determine its feasibility of digesting high solid content fruit and vegetable wastes (FVW) with or without solid cow manure. Liquid inoculum was used to start the pilot-scale operation and the biomass adaptation procedures (liquid to solid inoculum) were experimented.

METHODS AND MATERIALS

Experimental set-up and operation strategy

Scale-up testing is being conducted in a container-type pilot digester (8ft wide x 8 ft height x 20 ft length) developed by Bio-Terre Systems. This system is equipped with insulation, heating system, gas collection and liquid inoculum percolation-recirculation provisions. Provision was made to collect the liquid percolate using a 2" liquid collection valve located at the bottom of the container. The mixture of organic waste and solid inoculum were filled

in four numbers of plastic bin-containers, whose total capacity was 1 m³ each, primarily to ease the waste handling procedures compared to bulk loading of waste materials into the container itself. This pilot-scale container type digester can accommodate a total of 8 plastic bin-containers (i.e. total capacity of 8 m³). However, during this start-up phase of the study, four bin-containers were evenly filled with the mixture of solid inoculum and organic waste before being put in the digester container, such that a total volume of about 3 m³ of waste mixture were fed per cycle (33-14 d). The facility was also equipped with a weighing scale to measure the mass of all materials fed in to the digester. Solid inoculum, organic waste, structural agent and the final mixture were weighted for mass balance purposes. The plastic bins handling were done with a tractor, while the inoculum and organic wastes were mixed using a S70 Bobcat. The mixed material was transferred to the respective bin-containers, weighted and loaded into the pilot-scale digester. Bioreactor was then sealed for the treatment cycle length. Biogas production, temperature and pressure were monitored through on-line. Sampling of the material was done at the beginning and the end of each cycle of operation.

At the start of each cycle, liquid inoculum was added to enhance the microbial activity. The liquid leachate was collected from the container with a 4" valve and was transferred into a storage bin (1 m³) by gravity. Once or twice a week, the leachate was recirculated back to the feed mixture to maintain good humidity level and to improve the waste-biomass contact. Throughout the treatment cycle, temperature in the container bioreactor was monitored daily and the heating system was adjusted accordingly to maintain the temperature was kept between 20 and 25°C but hot summer days has bring the temperature in the headspace up to 28-29°C. Thermocouples were installed in the container and also in the organic waste mixture.

In parallel, a portion of the feed mixture was collected separately and used to fill lab-scale digesters for closer monitoring purposes. 50-L DAD digesters (30-L active volume) were operated in parallel at 25°C and gas production was monitored using by mass flow meters. The operating protocol was maintained similar to that of pilot-scale experiments.

Inoculum and feedstock sources

The liquid inoculum was obtained from an on-going semi-industrial scale bioreactor treating diluted liquid cow manure and food waste mixture at our research facility. 500-L of the liquid inoculum was taken to develop the solid inoculum, which was then mixed with 200 kg of straw bedding and 44 kg of raw solid dairy manure (without bedding, TS:19-20%). Fresh dairy cow manure was collected at the experimental farm of the Sherbrooke Research and Development Center. Feed mixture was evenly distributed into 4 bin-containers (3-m³ active volume) and was placed in the container type bioreactor for a period of 56 d primarily to allow a complete adaptation of the inoculum. A second cycle was started with the addition of solid dairy manure and straw. Afterwards, for another 106 d of reaction (caused by container modifications), co-digestion was started by the addition of a small portion of fruit and vegetable wastes (FVW). Followed to this adaptation phase, 100% of the organic loading was provided by the FVW mixture.

Raw FVW was collected from local providers, which was then weighted and grinded with a rototiller mounted on a brush cutter. It mainly comprised potato and carrots peeling, salad, potato, apple, banana, pineapple, orange, broccoli, onion, carrots and other rotten food materials. General description and specific weight of the waste was taken at every waste collection point. Overall, the proportion of fruits is slightly higher than the proportion of vegetables (51%/49%). The material was stored at 4°C before utilisation.

Sampling and analysis

For a feeding operation, a batch of about 250 kg of waste was grinded together and evenly distributed into 150-L barrels to have a more homogenous feedstock (for e.g. 6 barrels received 40 kg each of the same grinded batch). Sampling was done accordingly by taking 10% of the distributed waste into the sampling box (for e.g. 40 kg distributed per barrel; 4 kg sample). Since majority of the material was comprised of rotten food, the grinding was quite easy and the particulate size was maintained smaller than 1". For the inoculum and digested material, the sampling was done in the mixing container (steel garbage bin).

These samples were analysed for total solids (TS), volatile solids (VS), total alkalinity, volatile fatty acids (VFA) and pH (APHA, 1992). Daily biogas production was measured either by GFM mass flow meters (Aalborg, USA). Biogas composition (methane, carbon dioxide, H₂S and nitrogen) was determined with a HachCarle 400 AGCgas chromatograph (Hach, Loveland, CO). The column and thermal conductivity detector were operated at 80°C.

RESULTS AND DISCUSSION

Start-up of pilot-scale DAD and adaptation of solid biomass (Phase 1)

The initial two cycles were performed predominantly to adapt the liquid inoculum to the high solid content operation. Biogas quantity and compositions were followed to measure the biological activity. Fig. 1 presents the specific methane yield (SMY) obtained for the initial two cycles of operation. At the end of the first cycle (37 d), the dairy manure was not entirely converted into biogas since the SMY reached only 58% of the expected conversion (0.170 L_{CH₄} g_{VS}⁻¹), which indicates that residual organic material was still present in it. For that reason, the second cycle was given a longer reaction period i.e. about 127 d. At the end of second cycle, SMY obtained was about 0.244 L_{CH₄} g_{VS}⁻¹, but more importantly, the cumulative SMY for both the cycles was 0.166 L_{CH₄} g_{VS}⁻¹, which is the expected for dairy manure. For both cycles, the biogas composition was stabilized itself around 40% CH₄.

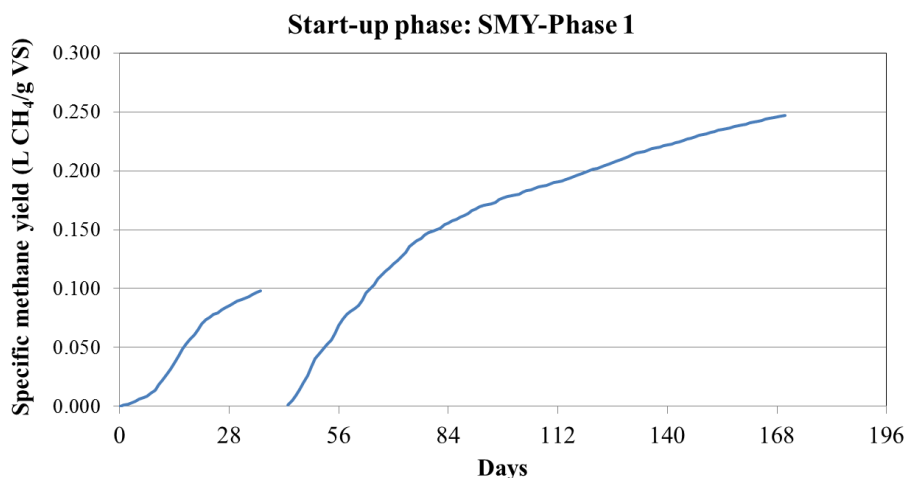


Figure 1. Start-up of DAD and solid inoculum adaptation: *Evolution of SMY*

Performance of pilot-scale DAD treating FVW waste (Phase 2: low-loading conditions)

From day 128 onwards, pilot DAD system was fed with FVW and the performance was monitored in terms of organic matter destruction, VFA accumulation, biogas concentration and its quality, and SMY. For this phase of study, the ratio of solid inoculum and food waste was maintained at 6:1 to limit the possibility of shock loading conditions to the bacteria. Organic loading rate (OLR) was maintained around 0.44-0.49 kg_{VS} kg_{inoculum}⁻¹ d⁻¹ and the results in terms of biogas and cumulative methane production, and SMY are presented in Fig. 2 (a-b). For both cycles, biogas production preceded fairly quick start-up with no lag phase after each feeding. It is to be noted that, about 77% of total biogas production was attained within 18 d and 12 d for cycle 3 (cycle length: 34 d) and 4 (cycle length: 28 d), respectively. High SMY values recorded for cycle 3 (i.e. 1.104 L_{CH₄} g_{VS}⁻¹) compared to that of cycle 4 (0.625 L_{CH₄} g_{VS}⁻¹) were probably due to the digestion of residual VS accumulated from previous cycles of operation. Thus, longer reaction period was given to cycle 3 to allow a complete digestion of the remaining VS in the bioreactor. In addition, the biogas quality measured, especially after the feeding regime was showing inconsistency because of the operation procedure. As the feeding was done in a batch mode, the bioreactor was opened at the end of each cycle in order to be loaded with a new material. Due to this, the digester's headspace was filled with ambient air, which diluted the biogas for the initial few days of a cycle. It took five days for both cycles to ramp up the biogas quality to 55% of CH₄ in the measured biogas. At the end of treatment cycles 3 and 4, the methane concentration measured was about 64% and 67%, respectively, which shows the good adaptation of biomass to the high-solid content process.

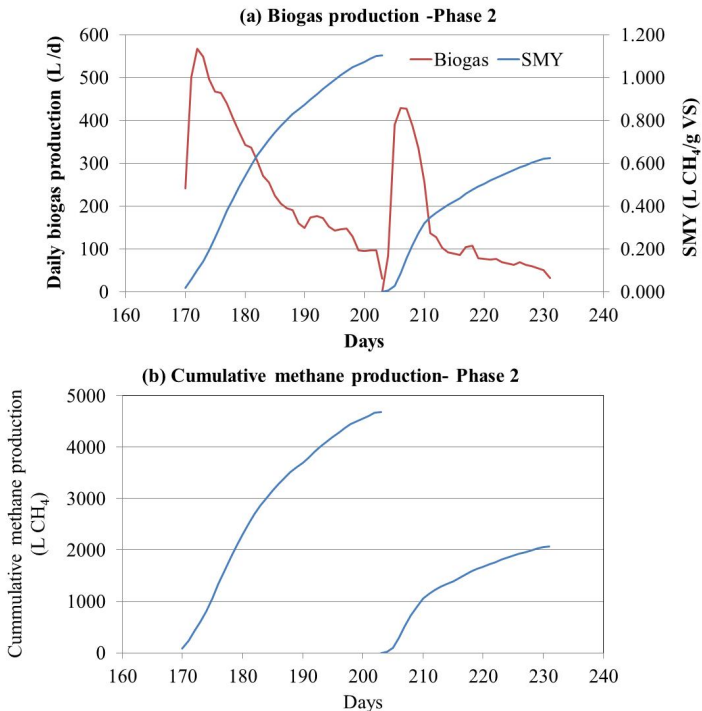


Figure 2 (a-b). Performance of Phase-2 (low OLR) DAD process: a) Biogas production and SMY evolution; b) Cumulative methane production

Performance of pilot-scale DAD treating FVW waste (Phase 3: high-loading conditions)

The purpose of this phase of study was to increase the OLR by decreasing the ratio of inoculum to feedstock, such that same size bioreactor can process more waste materials with short retention times. From day 232 onwards, the proportion of solid inoculum to dairy manure was retained at 3:1 and will eventually reduce to 1:1 ratio. The similar operating strategy was followed for this phase of study as that of Phase 2. OLR was maintained around 1.6 to 2.1 $\text{kg}_{\text{VS}} \text{kg}_{\text{inoculum}}^{-1} \text{d}^{-1}$ and cycle length was controlled at 14-16 d. Results in terms of biogas and cumulative methane production, and SMY are presented in Fig. 3 (a-b). Although, 5th and 6th cycles were operated at high OLR conditions, AD preceded fairly quick start-up with no lag phase after feeding with FVW. More than 75% of the total biogas production was attained within 7-d for both cycles. SMY values in the range of 0.400-0.520 $\text{L}_{\text{CH}_4} \text{g}_{\text{VS}}^{-1}$ were recorded. The obtained values are comparable to the AD of semi-dry mixed municipal food waste (SMY: $0.401 \pm 0.01 \text{L}_{\text{CH}_4} \text{g}_{\text{VS}}^{-1}$) [Rajagopal et al., 2017]

The short retention times and high OLR conditions seemed to have a little impact on the inoculum for the 5th cycle of operation (SMY: $0.400 \text{L}_{\text{CH}_4} \text{g}_{\text{VS}}^{-1}$) but not enough to imbalance the process. However, for the subsequent cycle, the SMY increased by 30%, which indicates the good activity of the biomass. This is confirmed by the less VFA accumulations (total content below 900mg L^{-1}) and high buffering capacity of the digester (digester pH: 7.2-7.5). pH of the substrate was acidic (4.0-4.5), but however, in the reactor it was in the neutral range. There is no sign of inhibition or nutrient deficiency at these operating conditions.

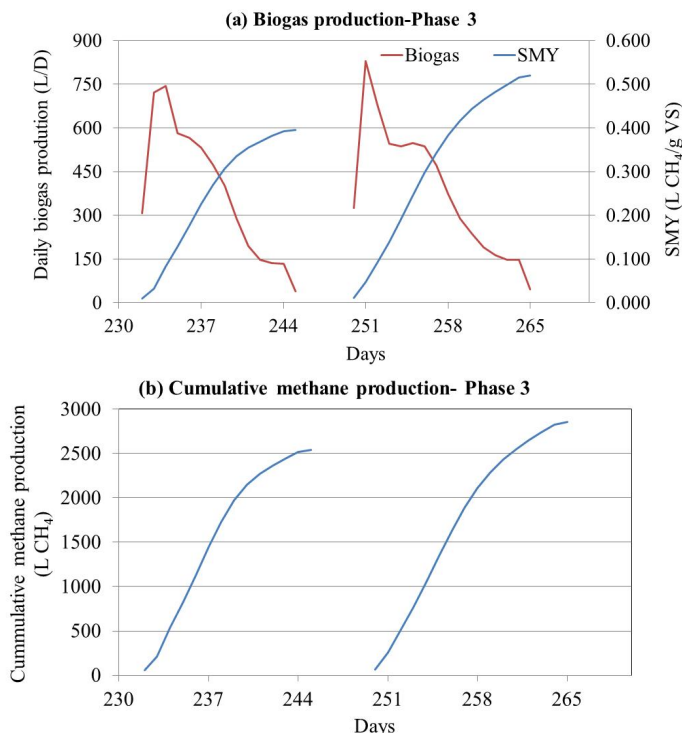


Figure 3 (a-b). Performance of Phase-3 (high OLR) DAD process: a) Biogas production and SMY evolution; b) Cumulative methane production

The calculated methane concentration for the first 4 days of both cycles was 58%. At the end of the treatment cycles, the same was increased to 66% and 63% respectively. Obtained results support the good adaptation of the biomass to the high loading operation and the short treatment cycles. Obtained results are comparable to that of lab-scale study, particularly in terms of specific methane yield (i.e. 0.4-0.5 m³ CH₄ kgvs⁻¹), and methane content of about 62-72% (detailed data not shown). The quality of biogas in the pilot-scale digester increased with time and remained almost stable thereafter and this means that the smaller size digester (in the case of DAD) is preferred as there is no waste dilution involved. This will reduce a major part in the capital investment on the construction of digesters and also suitable for cold countries. Further experiments are underway to optimise the inoculum to feed ratio, high OLRs and short treatment cycle lengths.

DAD technology: Final discussion and concluding remarks

The results of this study have been compared with data from the literature regarding different anaerobic process temperatures used in treating similar kinds of waste material. While the comparisons are intrinsically difficult as the reactor operating conditions in these studies differed, the values of SMY and the CH₄ content in biogas, yielded from the low-temperature DAD in the current study were found to be similar or marginally higher than that of mesophilic and thermophilic anaerobic digesters (Banks et al., 2011; Zhang et al., 2012). This could be mainly because (i) at lower temperature, reduced hydrolysis of complex organics have decreased the acidogenesis and thus lowered the percentage of CO₂ in the biogas and (ii) supplementary production of acetate from CO₂ and H₂ by homoacetogens and the decrease of the resulting acetate would upsurge the amount of CH₄ in the biogas (Wei et al., 2014). Most prominently, low-temperature AD is particularly well adapted to the treatment of several organic wastes because of lower free ammonia nitrogen levels than in mesophilic or thermophilic process.

Municipal food waste is a global challenge in solid waste management, especially in cold regions. It is scattered in location, non-ignorable in quantity, and non-uniform in quality. Moreover, some food waste has the tendency to acidify rapidly or lower the pH of the digester liquid. Apart from the operating temperature, this study demonstrated that solid cow manure can be used as a co-substrate provided a sufficient buffering capacity to FVW digestion by synergizing the effect of microorganisms and handling the high organic load. Further optimization will be necessary to validate and improve the performance of DAD at relatively short cycle length and high OLR. Also, economic cost analysis for larger scale digesters will be crucial for providing a sound basis for practical application of DAD process. Economic benefits are directly influenced by the amount of biogas produced, as this can replace other fuels used for cooking, heat, light, or electricity. For instance, to run a generator fueled with biogas, it is essential to have CH₄ content greater than 50% and H₂S concentration less than 1% (Lansing et al., 2008). The DAD in this study met the minimum criteria to power a generator and coupled with the quantity of methane produced; this technology could be expected to provide an economic benefit. Biogas, of about 65% methane, has a total energy potential of about 23 MJ m⁻³. Based on Statistics Canada (2010), about 35 million tons of food waste in US landfills was reported in 2010. As the calorific value of biogas is about 6 kWh m⁻³, equivalent to 0.5 L of diesel oil (Kashyap et al., 2003), this DAD technology could lead to saving of an enormous amount of fuel per year. Alternatively, biogas could be converted to electricity using a biogas powered electric generator and in such circumstances, about 2 kWh of useable electricity could be produced per cubic meter of biogas, with the rest of the energy converted into heat, which has further heating applications. Additionally, by mining CH₄ from waste for heat or electricity also reduces

direct atmospheric methane emissions and with it, GHG impact. According to the Environment Canada report (2013), diverting one ton of food waste through AD reduces GHG emissions by approximately one ton of CO₂ equivalents, as compared to landfilling.

Thus, the strength of this low-temperature DAD technology is that it provides an integrated solution to municipal and agricultural-based food waste streams without any dilutions. Specifically, DAD process offers the following benefits: (i) it operates at low temperature (20-25°C), resulting in a year-round positive energy balance, even in cold climates; (ii) it has a high process stability, ideal for municipal and agricultural solid waste applications; (iii) it offers maximal methane production utilizing a long solids retention time (SRT); (iv) it has a minimal impact from loading/feeding ambient temperature manure, even in winter; and (v) it can co-digest multiple organic waste streams or off-farm residues, using manure as the buffer.

CONCLUSIONS

This study validated the robustness of low-temperature DAD technology can be employed to treat high-solid content wastes such as dairy manure and food waste. SMY of 0.400-0.520 LCH₄ gVS⁻¹ was obtained even at high OLR (1.6 to 2.1 kgVS kg_{inoculum}⁻¹ d⁻¹) and short cycle length (14-16 d), which is comparable to the laboratory scale study. The mode of operation (process, temperature) along with the acclimation of liquid biomass to solid inoculum at step-wise increase in OLR ensured a high stabilisation of the digestion process without inhibition. Compared to higher-temperature digestion process, more energy is available for farm uses. Further research is being performed to determine the optimal operating conditions.

REFERENCES

- APHA., (1992). Standard methods for the examination of water and waste water. 18th ed. Washington DC, USA: American Public Health Association.
- Banks, C.J., Chesshire, M., Heaven, S., Arnold, R. (2011). Anaerobic digestion of source-segregated domestic food waste: Performance assessment by mass and energy balance. *Bioresour. Technol.* 102, 612-620.
- Environment Canada (2013). Technical Document on Municipal Solid Waste Organics Processing. ISBN:978-1-100-21707-9. (Viewed online on September 2017).
http://www.compost.org/English/PDF/Technical_Document_MSW_Organics_Processing_2013.pdf
- Kashyap, D.R., Dadhich, K.S., Sharma, S.K. (2003). Biomethanation under psychrophilic conditions: a review. *Bioresour. Technol.* 87, 147-53.
- Lansing, S., Botero, R.B., Martin, J.F. (2008). Waste treatment and biogas quality in small-scale agricultural digesters. *Bioresour. Technol.* 99 (13), 5881-5890.
- Massé, D.I., Saady, N.M.C., Rajagopal, R. (2014). Psychrophilic dry anaerobic digestion of high solids content dairy manure: long-term operation. *Biological Engineering Transactions* 7(3): 99-112.
- Rajagopal, R., Massé, D.I., Saady, N.M.C. (2014). Low-temperature anaerobic co-digestion of swine carcass and swine manure: Impact of high swine carcass loading rate. *Transactions of the ASABE* 57 (6), 1811-1816.
- Rajagopal R, Bellavance D, Rahaman S. (2017). Psychrophilic anaerobic digestion of semi-dry mixed municipal food waste: For North American Context. *Process Safety and Environmental Protection* 105, 101-108.

- Saady, N.M.C., Massé, D.I. (2015). A start-up of psychrophilic anaerobic sequence batch reactor digesting a 35 % total solids feed of dairy manure and wheat straw. *AMB Expr* 5:55.
- Statistics Canada (2010). Human Activity and the Environment: Annual Statistics 2009. <http://www.statcan.gc.ca/pub/16-201-x/2009000/part-partie1-eng.htm> (accessed 10/02/2017).
- Wei, S., Zhang, H., Cai, X., Xu, J., Fang, J., Liu, H. (2014). Psychrophilic anaerobic co-digestion of highland barley straw with two animal manures at high altitude for enhancing biogas production. *Energy Convers. Manage.* 88, 40-48.
- Zhang, Y., Banks, C.J., Heaven, S. (2012). Anaerobic digestion of two biodegradable municipal waste streams. *J. Environ. Manage.* 104, 166-174.
- Zheng, Y.H., Wei, J.G., Li, J., Feng, S.F., Li, Z.F., Jiang, G.M., Lucas, M., Wu, G.L., Ning, T.Y. (2012). Anaerobic fermentation technology increases biomass energy use efficiency in crop residue utilization and biogas production. *Renew. Sust Energy Rev* 16: 4588–4596.



USPOREDBA ENERGETSKIH ZNAČAJKI PŠENICE SORTE „KRALJICA“ S NEREGISTRIRANOM SORTOM „BRKULJA“

Mateja GRUBOR¹, Ana MATIN^{1*}, Nikola BILANDŽIJA², Vanja JURIŠIĆ¹,
Ivan KOPILOVIĆ³, Tajana KRIČKA¹

¹ Sveučilište u Zagrebu Agronomski fakultet Zavod za poljoprivrednu tehnologiju, skladištenje i transport, Svetosimunska 25, 10000 Zagreb, Hrvatska

² Sveučilište u Zagrebu Agronomski fakultet, Zavod za mehanizaciju poljoprivrede, Svetošimunska 25, 10000 Zagreb, Hrvatska

³ AGRO CIBALAE d.o.o., Vinkovci, Hrvatska

*E-mail dopisnog autora: amatin@agr.hr

SAŽETAK

Poljoprivredna i šumska biomasa je danas najzastupljenija sirovina za proizvodnju zelene energije i koristi se oko 65% od ukupne proizvodnje iz obnovljivih izvora. Jedna od najzastupljenijih ostataka poljoprivredne proizvodnje je slama pšenice. Temeljem toga cilj ovoga rada je utvrditi potencijalne količine slame i energetske karakteristike pšenice sorte „Kraljica“ i nove, neregistrirane sorte „Brkulja“. Karakteristike prikazane u radu su fizikalna svojstva (masa, visina, prinos), strukturna svojstva (sadržaj celuloze, hemiceluloze i lignina), fizikalno - kemijska svojstva (voda, pepeo, fiksirani ugljik, hlapive tvari, gorive tvari, koks), sadržaj elementarnih spojeva (ugljik, vodik, dušik, sumpor i kisik) te energetska svojstva (gornja i donja ogrjevna vrijednost) za obje sorte. Sorta „Brkulja“ istaknula se visinom biljke od oko 1,5 m, a sorta „Kraljica“ sa oko 0,5 m. Time je gotovo 3 puta viša od biljke sorte „Kraljica“. Masa stabljike sorte „Brkulja“ bila je 2,4 g dok je masa sorte „Kraljica“ iznosila 0,6 g, što masu stabljike pšenice „Brkulja“ čini 4 puta većom od mase stabljike sorte „Kraljica“. Energetska vrijednost obje sorte kretala se oko 16 MJ kg⁻¹. Zbog kvalitetnih energetske karakteristike, poglavito sorte „Brkulja“ dio slame pšenice (30-50%) može se između ostalog koristiti za proizvodnju toplinske i/ili električne energije te u proizvodnji biogoriva druge generacije.

Gljučne riječi: biomasa, pšenica, energetske karakteristike

UVOD

Biomasa se prema Direktivi 2001/77/EC definira kao biorazgradivi dio proizvoda, otpada i ostataka iz poljoprivrede (uključujući biljne i životinjske supstance), šumarstva i drvne industrije, kao i biorazgradivi dio industrijskog i komunalnog otpada. Pod pojmom biomasa podrazumijevaju se različite vrste organskog materijala, s energetsom vrijednošću koja je podložna pretvorbi u gorivo ili neposredno u toplinu.

Biomasa je obnovljivi izvor energije koji je u posljednje vrijeme stekao relevantnost kao alternativni izvor energije fosilnim gorivima. Važan je izvor energije za ljude bez obzira na razvijenost civilizacije. Kroz izgaranje biomase, čovječanstvo je počelo zadovoljavati potrebe grijanja i električne energije. Nadale, biomasa ima prednost da se može pretvoriti u čvrsta, tekuća ili plinovita biogoriva mehaničkim, fizičkim, toplinskim ili biološkim procesima (Montero i sur., 2016).

Pretvorba biomase u korisne oblike energije moguća je korištenjem različitih procesa pretvorbe. Izbor procesa ovisi o tipu, svojstvima i količini raspoložive biomase, željenom krajnjem obliku energije, standardima okoliša te isplativosti samog postupka. Najzastupljeniji oblik pretvorbe biomase u energiju je proces izravnog izgaranja. Dizajn i princip rada sustava za izgaranje biomase oslanjaju se na značajne karakteristike biomase, naime, ogrjevnu vrijednost, vlagu, sadržaj pepela i elementarni sastav (Chun-Yan, 2011). Ogrjevna vrijednost biomase i goriva dobivenih iz biomase jedno je od značajnih svojstava goriva koje definira gustoću energije tih goriva (Uemura i sur., 2010; Peng i sur., 2015). Također je važno za proračune dizajna ili numeričke simulacije sustava toplinskih pretvorbi za biomasu (Sheng i Azevedo, 2005). Zbog toga se obavlja fizikalno-kemijska karakterizacija biomase.

Biomasa obuhvaća širok spektar sirovina za proizvodnju energije, a jedna od značajnijih ratarskih kultura za proizvodnju biomase je slama pšenice, koja se definira kao ostatak generiran u proizvodnji pšenice. Bogat je, obnovljiv i relativno jeftin lignocelulozni materijal, a struktura slame sastoji se od celuloze, hemiceluloze i lignina (Guerra i sur., 2012). To je biomasa s visokim sadržajem energije, moguća je za upotrebu u proizvodnji električne i/ili toplinske energije te pretvorbi u biogoriva.

U pravilu su odnosi mase zrna i slame kod žitarica približno jednaki. Na 100 tona pšenice, masa slame i ostalog neiskorištenog dijela biljke je oko 100 tona (Jukić i sur., 2006).

Trenutačni pad proizvodnje pšenice odrazio se na količinu slame. Također, provedene selekcije pšenice sa niskom stabljikom, zbog polijeganja iste na polju, dovelo je do još manje količine slame. Istovremeno na tržištu Europske Unije zbog sve većih zahtjeva za slamom javlja se manjak istih te se dodatno javila potreba za pšenicom viših i debljih karakteristika slame, a da se kod toga ne smanji prinos.

Posljednjih godina zbog sve veće potražnje za slamom rađeni su pokusi na novoj sorti, nastaloj na poljima tvrtke „Agro Cibalae“, koja je prilagođena zahtjevima novih potraživanja. Temeljem navedenog cilja rada je utvrditi potencijalne količine slame, fizikalna svojstva (masa, visina, prinos), strukturna svojstva (sadržaj celuloze, hemiceluloze i lignina), fizikalno - kemijska svojstva (voda, pepeo, fiksirani ugljik, hlapive tvari, gorive tvari, koks), sadržaj elementarnih spojeva (ugljik, vodik, dušik, sumpor i kisik) te energetska svojstva (donja i gornja ogrjevna vrijednost) pšenica sorte „Kraljica“ i nove, neregistrirane sorte radnog naziva „Brkulja“.

MATERIJALI I METODE

Istraživanje je provedeno na standardnoj sorti pšenice "Kraljica" te na novoj neregistriranoj sorti radnog naziva "Brkulja" uzgojenih u Ivankovu, Hrvatska na poljima tvrtke „Agro Cibalae“, gdje su obuhvaćena i poljska mjerenja (prinos i sastavnice prinosa). Sklop sadnje navedenih kultura iznosio je 700 biljaka po m².

Laboratorijske analize biomase provedene su na Zavodu za poljoprivrednu tehnologiju, skladištenje i transport na Sveučilištu u Zagrebu Agronomskom fakultetu.

Poljska istraživanja

Poljska mjerenja obuhvatila su određivanje prinosa i fizikalnih karakteristika istraživanih pšenica kao i sakupljanje uzoraka za laboratorijske analize. Biomasa je uzorkovana u skladu s Pravilnikom o metodama uzorkovanja i kontroli kvalitete 99/2008 (NN, 2008).

Laboratorijska istraživanja

Laboratorijske analize obuhvatile su određivanje negorivih i gorivih svojstva, ogrjevne vrijednosti te lignoceluloznog sastava. Kod toga su korištene metode za udio vlage, odnosno suhe tvari (HRN EN 18134-2:2015) u laboratorijskoj sušnici (INKO, Hrvatska), udio dušika (HRN EN ISO 16948:2015) na elementarnom analizatoru Vario MACRO (Elementar, Njemačka), udio pepela (HRN EN ISO 18122:2015) te udio koksa (CEN/TS 15148:2009) u mufolnoj peći (Nabertherm, SAD) i udio fiksiranog ugljika (EN 15148:2009) računski. Nadalje, udio ugljika i vodika (HRN EN ISO 16948:2015) te sumpora (HRN EN ISO 16994:2015) na na CHNS analizatoru (Elementar, Njemačka), dok se kisik izračunao računski kao ostatak C, H, N, S elemenata, kao i udio hlapljivih tvari sukladno EN 15148:2009. Gornja ogrjevna vrijednost određena je pomoću metode EN 14918:2010 u adijabatskom kalorimetru (IKA, Njemačka), dok se donja ogrjevna vrijednost dobije računski. Određivanje udjela celuloze, hemiceluloze i lignina provedeno je modificiranom standardnom metodom ISO 5351-1:2002.

REZULTATI I RASPRAVA

Pokusima križanja sorata na poljima tvrtke „Agro Cibalae“ dobivena je sorta pšenice značajno većih prinosa zrna i slame u odnosu na standardne sorte pšenice. U tablici 1. Prikazana su fizikalna svojstva svojstva pšenice "Kraljica" i pšenice "Brkulja". Pšenica "Brkulja" istaknula se sa 4 puta većom masom stabljike te 3 puta većom visinom biljke, što povećava njen energetski potencijal u odnosu na standardnu sortu pšenice "Kraljica".

Tablica 1. Fizikalna svojstva pšenice "Kraljica" i pšenice "Brkulja"
Table 1. Physical Properties of "Queen" wheat and "Brkulja" wheat

Parametri analize Analysis parameters	Pšenica Kraljica Queen wheat	Pšenica Brkulja Brkulja wheat
Fizikalna svojstva/ Physical properties		
Masa klasa (g)/ Spike weight (g)	1,50	5,6
Masa stabljike (g)/ Stem weight (g)	0,67	2,4
Visina biljke (cm) / Plant height (cm)	56	146
Teoretski prinos stabljike (t ha ⁻¹)/ Theoretic stem yield (t ha ⁻¹)	4,7	16,8

Slama pšenice koristi se u proizvodnji druge generacije biogoriva i ubraja se u sirovine lignoceluloznog sastava prosječne vrijednosti 40 – 60% celuloze, 20 – 40% hemiceluloze te 10 – 25% lignina (USDoE, 2004). Montero i sur. (2016) navode kako na strukturalna svojstva iste kulture utječe sorta, vrsta tla te klimatski uvjeti, tako oni u slami pšenice navode 57,09% celuloze, 16,81% hemiceluloze i 19,10% lignina dok Demirbas (2001) navodi 33,82% celuloze, 45,20% hemiceluloze i 20,98% lignina. Dobiveni rezultati, prikazani u tablici 2., nalaze se u spomenutim granicama sa nešto višim sadržajem celuloze.

Tablica 2. Strukturalna svojstva slame pšenice "Kraljica" i pšenice "Brkulja"
Table 2. Structural properties of "Queen" wheat straw and "Brkulja" wheat straw

Parametri analize Analysis parameters	Pšenica Kraljica Queen wheat	Pšenica Brkulja Brkulja wheat
Strukturalna svojstva (%) / Structural properties (%)		
Celuloza / Cellulose	54,18	53,26
Hemiceluloza/ Hemicellulose	13,53	11,84
Lignin / Lignin	24,85	23,16

Kako bi se prikazao energetske potencijal biomase potrebno je utvrditi njezina fizikalno-kemijska svojstva (udio vode, pepela, fiksiranog ugljika, hlapivih tvari, gorivih tvari i koks). Stoga je u tablici 3. prikazan fizikalno kemijski sastav proučavanih sorti pšenice.

Tablica 3. Fizikalno - kemijska svojstva slame pšenice "Kraljica" i pšenice "Brkulja"
Table 3. Physico-chemical properties of "Queen" wheat straw and "Brkulja" wheat straw

Parametri analize Analysis parameters	Pšenica Kraljica Queen wheat	Pšenica Brkulja Brkulja wheat
Fizikalno-kemijska svojstva (%) / Physico-chemical properties (%)		
Voda / Water	9,35	9,51
Pepeo / Ash	7,59	9,84
Cfikisani / C _{fixed}	9,99	4,39
Hlapive tvari / Volatile matter	73,07	76,26
Gorive tvari / Combustible matter	83,06	80,65
Koks / Coke	18,78	15,94

Količina vode u biomasi negativni je čimbenik te smanjuje ogrjevnu vrijednost biomase jer se dio topline troši na njeno isparavanje (Francescato i sur. 2008.). Ross i sur. (2008.) navode optimalni sadržaj vode u biomasi između 10% i 15%. Dobiveni rezultati od 9,35% za slamu pšenice "Kraljica" i 9,51% za slamu pšenice "Brkulja" čine slamu pšenice proučavanih sorti optimalnom za sve oblike termokemijske konverzije biomase u gorivo (izravno sagorijevanje, piroliza) pa se može reći da je, s aspekta sadržaja vode, istraživana biomasa dobra sirovina za proizvodnju energije.

Jedna od glavnih čimbenika kvalitete biomase je sadržaj pepela u njoj i što je količina pepela veća kakvoća goriva, poglavito krutog, je manja. Ebeling i Jenkins (1985) navode sadržaj pepela u slami pšenice od 8,9%, Demirbas (2004) navodi sadržaj pepela od 13,7% dok je vlastitim istraživanjem utvrđen sadržaj pepela 7,59% za slamu pšenice "Kraljica" i 9,51% za

slamu pšenice "Brkulja". Pretpostavlja se da je do razlike dobivenih rezultata došlo zbog sortnih karakteristika pšenice.

Sadržaj koka i fiksiranog ugljika u biomasi smatraju se pozitivnim svojstvima biomase jer predstavljaju količinu energije izgaranjem određene količine biomase (Garcia i sur., 2012). Slama pšenice "Kraljica" sadrži 9,99% fiksiranog ugljika i 18,78% koka, a slama pšenice "Brkulja" sadrži 4,39% fiksiranog ugljika i 15,94% koka što slamu pšenice "Kraljica" čini nešto kvalitetnijom za proces izravnog sagorijevanja. Montero i sur. (2016) utvrdili su u slami pšenice sadržaj fiksiranog ugljika od 14,72%, Demirbas (2004) 21,4%, dok García i sur. (2014) utvrđuju sadržaj fiksiranog ugljika 18,20%.

Izgaranjem se biomasa razgrađuje na hlapljive plinove i kruti ostatak te je za nju specifično da ima visok postotak hlapljivih tvari (oko 80%) što joj smanjuje energetska vrijednost (Quaak i sur., 1999). Sukladno tome i u obje sorte pšenice utvrđen je visoki postotak hlapljivih tvari te je on za sortu "Kraljica" iznosio 73,07%, dok je za sortu "Brkulja" iznosio 76,26%.

Nadalje, na energetska potencijal utječe i elementarni sastav biomase (tablica 4.). S ekološkog stajališta dušik i sumpor utječu na povećanje stakleničkih plinova te se smatraju kritičnim elementima u biomasi. Također, energetska vrijednost smanjuje i sadržaj kisika u biomasi. Ugljik je osnovni i najvažniji element svih vrsta goriva i određuje njegovu kvalitetu te što ga je više energent je kvalitetniji. Vodik uz ugljik čini osnovni sastav svakog goriva i povećani udio vodika poboljšava kvalitetu goriva (Vassilev i sur., 2010).

Tablica 4. Elementarni sastav slame pšenice "Kraljica" i pšenice "Brkulja"
Table 4. Elemental composition of "Queen" wheat straw and "Brkulja" wheat straw

Parametri analize Analysis parameters	Pšenica Kraljica Queen wheat	Pšenica Brkulja Brkulja wheat
Elementarni sastav (%) / Elemental composition (%)		
Ugljik / Carbon	42,53	42,77
Vodik / Hydrogen	5,56	5,65
Dušik / Nitrogen	0,38	0,45
Sumpor / Sulfur	0,29	0,24
Kisik / Oxygen	51,25	50,90

Iz tablice 4. vidljivo je da obje sorte imaju slični elementarni sastav. Dobiveni rezultati u suglasju su s rezultatima Huang i sur (2009), Naik i sur. (2010) te Demirbas (2004). Jedino se razlikuje povećani sadržaj kisika (oko 51%) što Lewandowski i sur. (2003) objašnjavaju činjenicom da veći sadržaj celuloze ima višu koncentraciju kisika te se time smanjuje i ogrijevna vrijednost biomase. Ogrijevna vrijednost istraživanih sorata prikazana je u tablici 5. Korištenje biomase kao goriva prilikom proizvodnje toplinske i električne energije zahtijeva znanje o njezinoj ogrijevnoj vrijednosti. Ogrjevna vrijednost je temeljni parametar za određivanje sadržaja energije u gorivu (Jenkins i sur., 1998).

Tablica 5. Energetska svojstva slame pšenice "Kraljica" i pšenice "Brkulja"
Table 5. Energy properties of "Queen" wheat straw and "Brkulja" wheat straw

Parametri analize Analysis parameters	Pšenica Kraljica Queen wheat	Pšenica Brkulja Brkulja wheat
Energetska svojstva (MJ kg ⁻¹) / Energy properties (MJ kg ⁻¹)		
Gornja ogrjevna vrijednost / Higher heating value	16,11	16,02
Donja ogrjevna vrijednost / Lower heating value	14,90	14,79

Iz tablice 5 vidljivo je da obje sorte pšenice imaju sličnu ogrijevnu vrijednost. Gornja ogrijevna vrijednost kretala se oko 16 MJ kg⁻¹, dok se donja ogrijevnu vrijednost kretala između 14,8 i 14,9 MJ kg⁻¹što je u skladu s dostupnim podacima za polj. biomasu (Jenkins i sur., 1998.).

ZAKLJUČAK

Temeljem istraživanja moguće je zaključiti sljedeće:

- Veću energetska iskoristivost slame pšenice moguće je postići selekcijom sorata sa većom visinom i debljinom stabljike, čime bi se osigurala veća količina slame po hektaru. Takvim osobinama istaknula se nova sorta pšenice „Brkulja“ s teoretskim prinomom slame od 16,8 t ha⁻¹.
- Istraživane sorte pšenice sličnih su energetska karakteristika te se obzirom na svoja fizikalno-kemijska i energetska svojstva mogu koristiti za proizvodnju toplinske i/ili električne energije te u proizvodnji biogoriva druge generacije.

ZAHVALA

Ovo istraživanje provedeno je u okviru VIP projekta „Potencijal proizvodnje zelene energije iz ostataka ratarske proizvodnje“ te projekta Hrvatske zaklade za znanost, br. 3328, “Converting waste agricultural biomass and dedicated crops into energy and added value products – bio-oil and biochar production”.

LITERATURA

- Chun-Yan, Y. (2011). Prediction of higher heating values of biomass from proximate and ultimate analyses. *Fuel* 90:1128-32.
- Demirbas, A. (2001). Relationships between lignin contents and heating values of biomass. *Energy Convers Manag* 42:183-8.
- Demirbas, A. (2004). Combustion characteristics of different biomass fuels. *Progress in energy and combustion science*, 30(2), 219-230.
- Ebeling, J. M. and Jenkins, B. M. (1985). Physical and chemical properties of biomass fuels. *Transactions of the ASAE*, 28(3), 898-0902.
- Francescato, V., Antonini, E., Bergomi, L. Z. (2008). Priručnik o gorivima iz drvne biomase. Regionalna energetska agencija Sjeverozapadne Hrvatske.

- García, R, Pizarro, C, Lavín, A, Bueno, J. (2014). Spanish biofuels heating value estimation. Part II: proximate analysis data. *Fuel*, 117:1139-47.
- García, R., Pizarro, C., Lavín, A. G., Bueno, J. L. (2012). Characterization of Spanish biomass wastes for energy use. *Bioresource technology*, 103(1): 249-258.
- Guerra, E, Portilla, O, Jarquín, L, Ramírez, J, Vazquez, M. (2012). Acid hydrolysis of wheat straw: a kinetic study. *Biomass Bioenergy* 6:346-55.
- Huang, C, Han, L, Yang, Z, Liu, X. (2009). Ultimate analysis and heating value prediction of straw by near infrared spectroscopy. *Waste Manag*, 29:1793-7.
- Jenkins, B.M., Baxter, L.L., Miles, Jr. T.R., Miles, T.R. (1998). Combustion properties of biomass. *Fuel Processing Technology*. 54: 17-46.
- Jukić, Ž., Krička, T., Ćurić, D., Voća, N., Matin, A., Janušić, V. (2006). Mogućnosti korištenja komine masline u proizvodnji energije. *Krmiva*, 48(2), 77-80.
- Lewandowski, I., Clifton-Brown, J.C., Andersson, B., Basch, G., Christian, D.G., Jorgensen, U., Jones M.B., Riche, A.B., Schwarz, K.U., Tayebi, K., Texeira, F. (2003). Environment and harvest time affect the combustion qualities of *Miscanthus* genotypes. *Agronomy Journal*, 95: 1274 – 1280.
- Montero, G., Coronado, M.A., Torres, R., Jaramillo, B.E., García, C., Stoytcheva M., Valenzuela, E. (2016). Higher heating value determination of wheat straw from Baja California, Mexico. *Energy*, 109, 612-619.
- Naik, S, Goud, V, Rout, P, Jacobson, K, Dalai, A. (2010). Characterization of Canadian biomass for alternative renewable biofuel. *Renew Energy*, 35:1624-31.
- Narodne novine (2008). Pravilnik o metodama uzorkovanja i ispitivanja kvalitete sjemena, ministarstvo poljoprivrede, ribarstva i ruralnog razvoja, 99/2008.
- Peng, T., Cheng, Z., Ji, X., Qing-Yan, F., Gang, C. (2015). Estimation of higher heating value of coal based on proximate analysis using support vector regression. *Fuel Process Technol* 138:298-304.
- Ross, C. J. (2008). *Biomass Drying and Dewatering for Clean Heat and Power*. Northwest CPH Application Center. USA.
- Sheng, C and Azevedo, J. (2005). Estimating the higher heating value of biomass fuels from basic analysis data. *Biomass Bioenergy*; 28: 499-507.
- Uemura, Y., Omar, W., Tsutsui, T., Subbarao, D., Yusup, S. (2010). Relationship between calorific value and elementary composition of torrefied lignocellulosic biomass. *J Appl Sci* 10(24):3250-6. Asian Network for Scientific Information.
- USDoE - U.S. Department of Energy (2004). *Understanding Biomass as a Source of Sugar and Energy*. Biomass Program.
- Vassilev, S.V., Baxter, D., Vassileva, C.G., Andersen, L.K. (2010). An overview of the chemical composition of biomass. *Fuel*, 89: 913-933.

COMPARISON OF ENERGY PROPERTIES OF WHEAT VARIETY „KRALJICA“ WITH UNREGISTERED VARIETY „BRKULJA“

ABSTRACT

Agricultural and forest biomass is today the most widely used raw material for the green energy production and its use is about 65% of total renewable sources production. One of the most common agricultural production remains is wheat straw. Based on this, the aim of this paper is to determine straw potential and energy properties of "Kraljica" wheat variety and new, unregistered "Brkulja" variety. Characteristics presented in the paper are physical properties (mass, height, yield), structural properties (cellulose, hemicellulose and lignin content), physical and chemical properties (moisture, ash, fixed carbon, volatile substances, combustible matter, coke content), elemental compounds content (carbon, hydrogen, nitrogen, sulfur and oxygen content) and energy properties (higher and lower heating values) for both varieties. Variety "Brkulja" pointed out the plant height of about 1.5 m, and the variety "Queen" with about 0.5 m. This is almost 3 times higher than the height of the "Queen" variety plant. The stem mass of the "Brkulja" variety was 2.4 grams, while the mass of the "Queen" variety was 0.6 grams, which makes the mass of "Brkulja" wheat stems four times higher than the mass of the "Queen" variety plant. The energy value of both varieties ranged around 16 MJ kg⁻¹. Due to the high energy characteristics quality, especially the "Brkulja" variety, part of the wheat straw (30-50%) can be used, inter alia, for the production of heat and/or electricity and in the second generation biofuels production.

Key words: biomass, wheat, energy characteristics



POSSIBILITIES FOR INTRODUCTION OF WOOD GAS GENERATOR ON A FAMILY FARM – SLOVENIA CASE STUDY

Denis STAJNKO^{1*}, Miran LAKOTA¹, Damijan KELC¹, Rajko BERNIK²

¹ University of Maribor, Faculty of Agriculture and Life Sciences, Chair for Biosystem Engineering, Pivola 10, 2311 Hoče, Slovenia,

² University of Ljubljana, Biotechnical, Jamnikarjeva 101, 1000 Ljubljana, Slovenia

*E-mail of corresponding author: denis.stajnko@um.si

SUMMARY

According to the EU climate action at least 40% cuts in greenhouse gas emissions (base 1990 levels), at least 27% share for renewable energy and at least 27% improvement in energy efficiency must be targeted till the year 2030. In 2015 the share of renewable energy represented 23% in Slovenia with a tendency of stagnation, thus the use of additional renewable sources need to be introduced into the subvention scheme. Since 58% of the Slovenian territory is covered by a forest, wood has been traditionally used in households, especially for space and water heating, but less for electricity production in combined wood gas heat and power (CHP) facilities. The use of wood gas that serves as a fuel is an old manner of energy consumption, which was used during the Second World War for the mobility needs. Since then the systems have been progressed as much as in stability as in adaptability. In this case study we are focusing on the systems for obtaining wood gas from wood chips and its application in the system for co-production of the heat and power (CHP). We focused on a micro-cogeneration system with the nominal electrical power of 28kW suitable for a family farm, and calculated the costs of investment with different subvention and different working hours scenarios, respectively. According to the average heating requirements, which amount only 21.000 kWh, the installation of the CHP system on a small farm is too expensive for the profitable investment. Moreover, it was also found out that the expenses of investment should be less than 385 EUR for one MWh of electrical energy if the farmer could receive a state subvention.

Keywords: cogeneration systems, CHP, wood biomass, gasification, subvention

INTRODUCTION

In 2014, EU countries have agreed on a new 2030 Framework for climate and energy, including EU-wide targets and policy objectives for the period between 2020 and 2030. These targets aim to help the EU achieve a more competitive, secure and sustainable energy system and to meet its long-term 2050 greenhouse gas reductions target. The cost of meeting the targets does not substantially differ from the price humans will need to pay in any case to replace ageing energy system. The main financial effect of decarbonisation will be to shift our spending away from fossil fuel sources and towards low-carbon technologies. Targets for 2030 include; a 40% cut in greenhouse gas emissions compared to 1990 levels, at least a 27% share of renewable energy consumption and at least 27% energy savings compared with the business-as-usual scenario (Energy Strategy, 2015).

As it is visible from Fig. 1, the current share of renewables in gross final energy consumption for 2015 EU member countries differ significantly i.e. from 6% in Malta to 54% in Sweden, whereby Slovenia with the share of 23% produced more as the EU average, but still 4% down to the goal in 2030. Since in the last few years a tendency of stagnation might be detected from the reports, new additional renewable sources need to be introduced into the subvention scheme (EUROSTAT, 2015).



Figure 1. Share of renewables in gross final energy consumption, 2015 and 2020 (%) (EUROSTAT, 2015).

The most typical feature of the Slovenian landscape is its forests, which cover as much as 58% of the national territory (Forest Service of Slovenia for 2004), which represents the third place in Europe after Sweden and Finland. Annually, more than one million m³ of wood has been traditionally used in 30% of individual households, especially for space and water heating, but less for electricity production in combined wood gas heat and power (CHP) facilities (Krajnc et al, 2007).

CHP also known as cogeneration is an efficient clean and reliable approach to generate power and thermal energy from a wood gas. In comparison to traditional wood use, CHP can greatly increase the facility's operational efficiency, decrease energy costs, while at the

same time the emission of greenhouse gases and PM10 particles can be significantly reduced (Knoef, 2005).

In Slovenia, utilization of wood and wood waste for energy purposes has been practically at the same level after 2009, when the maximum electricity production (232.4 GWh or 15.68% of renewable sources) was recorded. Contrary, traditional use of wood has been rising slightly at the same time. Besides, economic crisis between 2009 and 2014 decreasing reference costs of electricity effected the total amount of electricity produced from CHP. Thus, in 2015 all 17 wood biomass generation devices (power stations, co-incineration and cogeneration, Table 2) generated only 52 GWh or 12.41% of renewable electricity, for which 9.71% of state stimulation funds were paid. The average price of wood biomass power plants was 136.19 EUR/MHW, while the average price of co-incineration power plants was 69.21 EUR/MHW (Borzen, 2016).

Table 1. Differences in Reference Costs of Electricity in 2009 and 2015 (Slovenian Authorities, 2016)

	RCE 2015 (€ MWh _{el} ⁻¹)					
	2009			2015		
CHP PF	<50 kW	<1 MW	<5MW	<50 kW	<1 MW	<5MW
CHP<4000 hour	238.59	157.53	123.24	183.92	121.93	87.58
CHP>4000 hour	180.75	127.00	99.57	140.55	101.85	75,35

Table 2. Electricity produced from RES generating plants and CHP for wood biomass in 2015 (kWh) (Borzen, 2016)

Size category	<50 kW	50-1000 kW	1-10 MW
Size (MWe)	0.472	0.722	3
Number of facilities	10	2	1
Annual Operating Hours (h anno ⁻¹)	7,500	7,500	7,500
Specific Investment (€ kW _{el} ⁻¹)	4,450	5,000	3,200
Maintenance (% investment)	2.0	2.0	2.0
Operation (% investment)	0.8	0.8	0.8
Insurance (% investment)	1.2	1.2	1.2
Labour	1	1	3
Only electricity (%)	22.8	27.5	17
Only heat (%)	56.3	36.2	53

The purpose of our study was two to check the existing wood cogeneration systems available in Slovenia for the use on family farms. Secondly we want to explore whether it is worthwhile to invest in a viable heating system for the supply of electricity on average large farms.

MATERIAL AND METHODS

Combined wood gas heat and power facility

This type of power plant produces electricity and thermal energy by gasifying the woodchips, which are first transported from biomass feeder to gasifier (Fig. 2).

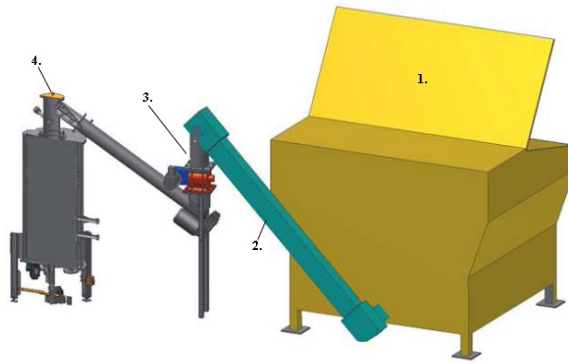


Figure 2. Transport of biomass from biomass feeder (1), dosing screw (2) and cell lock (3) to gasifier (4) (Bobanec, 2014).

The wood gasification is a pyrolysis process of producing wood gas under high temperature ($> 1100\text{ }^{\circ}\text{C}$) and minimal oxygen ($<0.5\%$) conditions from dry biomass with 12-15% water content. The result is a very clean gas almost without tar, which consists about 17% of hydrogen 25% of carbon monoxide and 2% of methane and has a temperature between 500 and 600 $^{\circ}\text{C}$ at the exit of the gasifier. The gas is first introduced into the primary heat exchanger, where it is cooled to 200 $^{\circ}\text{C}$ and thus becomes suitable for filtration (Fig. 3). This is followed by dry cleaning of the dust particles with a filter from the fabric. From the dust filter, the gas is driven forward to a wet scrubber, where even the smallest impurities are removed. The secondary heat exchanger then cools the wood gas to the ambient temperature, which is a proper condition for further use in the engine. In the cleaning device that has been connected to the gasification process a soot and coal can be separated furthermore. When burning, product gas emissions are only water vapor and carbon dioxide which has bound itself to the wood.

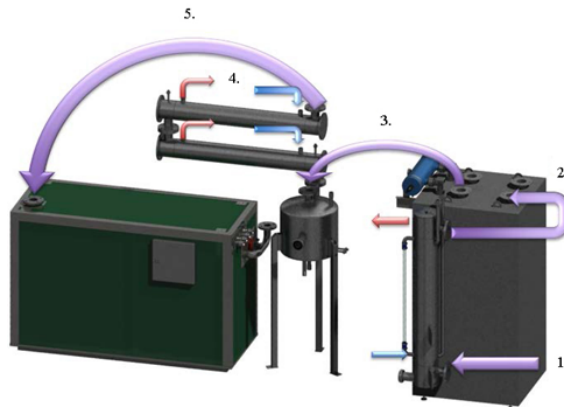


Figure 3. Cooling and purification of gas. 1. Primary heat exchanger, 2. Woven dust filter, 3. Wet scrubber, 4. Secondary heat exchanger, 5. CHP unit (Bobanec, 2014).



Figure 4. Volter 30 CHP facility before installation on the farm (Artim, 2014).

Cogeneration system Volter 30

In the following paragraph we will describe the Volter 30 cogeneration system (Table 3, Fig. 4), which serves as basis for calculating the economic viability of the system on the farm. With 28 kW electricity and 70 kW heat power it represents one of the smallest commercially available CHP units on wood biomass in Slovenia.

Table 3. Technical parameters of the Volter 30 (Artim, 2014).

Generator output	28 kW
Thermal output	70 kW
Efficiency – electricity	23 %
Efficiency – heat	57 %
Efficiency – total	80 %
Temperature of heating circle	60 – 80 °C
Generator	asynchronous
Annual service	7.500 hours
Maintenance interval	7 days
Lifespan	15 years

Support to electricity from renewable energy sources and combined heat and power installations

The support scheme for the production of electricity from renewable energy sources RES and combined heat and power CHP installations is necessary for promoting the investment in the ‘green energy’ in all EU membership countries due to the very high input cost. Accordingly, CHP installations can be divided into the following size classes:

1. micro: nominal electrical power of less than 50 kW,
2. small: nominal electrical power less than 1 MW,
3. medium-low: nominal electrical power of 1 MW up to and including 5 MW
4. medium-high: nominal electrical power of more than 5 MW up to and including 25 MW,
5. large - lower: rated power over 25 MW up to and including 50 MW,
6. large - higher: nominal electric current exceeding 50 MW up to 200 MW,
7. production facilities of rated power of 200 MW and more.

The second most important parameter includes the number of operating hours, which groups the CHP according to the number of operating hours in the reporting period or in the calendar year into two groups:

1. production plants that operate up to 4,000 hours in high-efficiency cogeneration and high-power electricity; referring to CHP production plants, where the operation is seasonal (heating season),
2. production installations which operate more than 4,000 hours in high-efficiency cogeneration and high-power electricity; referring to CHP generating plants for which the operation is not connected with the heating season.

Support height

According to the novel 'Decree on Amendments and Supplements to the Decree on Support for Electricity', produced in high-efficiency cogeneration of heat and power (Official Gazette of the Republic of Slovenia, No. 76/2009), a new statement was adopted, which says, that CHP generating plants are not eligible for support if the reference costs of electricity generation in a production facility exceed:

- a) for a CHP production plant operating up to 4,000 hours: with a nominal electrical power of less than 1 MW: 385 EUR MWh⁻¹
- b) for a CHP production plant operating more than 4,000 hours: with a nominal electrical power of less than 1 MW: 260 EUR MWh⁻¹.

The amount of operational support, which shall make profit at guaranteed purchase was determined on the basis of reference costs, which consist of variable and unchangeable reference costs.

$$\text{Reference costs} = \text{fixed reference costs} + \text{variable reference costs} \quad (1)$$

Fixed part of the reference costs is methodologically determined every 5 years or more, if the investment costs and other investment parameters change significantly. They are determined on the basis of investment costs and operating costs.

Variable reference costs are determined only for those RES generating plants where the input fuel represents the financial cost. Variable reference costs are changed annually on the basis of a change in the reference market price of electricity and input energy products - they are determined by the Energy Agency of the Republic of Slovenia (MG, Ministrstvo za gospodarstvo, 2009, ApE, 2016).

The case study was estimated on the data received from the family farm lying in the Pomurje region and has a registered basic agricultural and forestry activity. The main building is already heated by wood biomass for which about 18 m³ of dry mixed logs, 45-55 cm in length is burned in the family furnace. Annually it operates up to 600 operating hours, for heating of 400 m² of surfaces. The farm owns a forest that produces wood for heating.

RESULTS AND DISCUSSION

Calculation of the amount of support

The investment costs of the cogeneration system on wood gas is representing in table 4. As seen the costs is probably too high for the majority of Slovenian family farmers to invest in such a project without a bank credit and state support in the way of guaranteed purchase of electricity.

Table 4. Investment costs of the cogeneration system on wood gas.

Investment	€
CHP unit Volter 30	200.000
Installation, commissioning and transport	5.000
Construction costs - plate, storage room	20.000
Installations, el. attachments, ...	10.000
El. connection to the network	5.000
Project documentation	10.000
Unforeseen expenses	1.000
Total	251.000

Table 5 shows the breakdown of economic parameters needed for calculating the height of state operational support. The operating calculation was made for operation with 3,500 and 5,500 hours per year, respectively. We made operating calculations without the costs of the loan, at the selling price of wood chips 18 € nm⁻³ and fuel consumption 30 kg wood h⁻¹. In total 525 nm³ wood chips is spent for 3,500 working hours and 825 nm³ for 5,500 working hours, respectively.

EUR MWh⁻¹ in case the device operates more than 4,000 hours. This means, that the investor would be entitled to state support at 50% lower investment costs.

Table 5. Economic parameters of investment in the Volter 30 facility.

		3500 operating hours	5500 operating hours
Economic parameters of the investment			
Price of wood biomass	€ nm ⁻³	18.00	18.00
Price of heat	€ MWh _t ⁻¹	38.64	38.64
Investment	mio €	0.251	0.251
Specific investment	€ kW _{el} ⁻¹	8.964	8.964
Discount rate	%	12%	12%
Amortization	years	10	10
Maintenance	% inv.	3.2%	3.2%
Costs of insurance	% inv.	1.2%	1.2%
Operating costs	% inv.	0.8%	0.8%
Operation process			
Fuel consumption	nm ³ anno ⁻¹	525	825
Electricity	MWh anno ⁻¹	98	154
Useful heat	MWh anno ⁻¹	242.87	381.65

As seen, all results of calculating the CHP device for the model farm was obtained from the methodology for setting the reference costs, which are divided into economic parameters of the investment, operation process, costs, revenues, reference costs of electricity, prices for the guaranteed purchase of electricity and calculated support. At 3,500 hours of operation, the difference between revenues and expenses i.e. profit amounts to 49,447 €, which comes from annual heat production amounts to 242.87 MWh and 98 MWh electricity production. Since the annual return on investment costs (ROI) is 21.57% it would take 4.63 years for the

total return on investment costs. On the other side, at 5,500 operating hours the profit amounts to 56,950 €, given that 381.65 MWh of heat and 154 MWh electricity is produced. On that way, the annual return on investment costs (ROI) is 22.64% of the return on investment costs, so it would take 4.41 years i.e. 0.22 year less than at 3,500 hours of operation for the total return on investment costs. The most important criteria for receiving the support represents the height of the reference costs of electricity, which in case of 3,500 working hours amounts to 586.86 € MWh⁻¹ and 421.75 € MWh⁻¹ for 5,500 working hours, respectively (Table 6). This means that the investment in the CHP plant (Volter 30) is not eligible for support, since the reference costs of electricity generated by wood gas exceed 385 EUR MWh⁻¹ for a CHP production plant operating up to 4,000 hours. Also, the costs of the investment exceeds 260

Table 6. Calculation of the support for the Volter 30 facility.

		3500 operating hours	5500 operating hours
Costs			
Costs of wood	€ anno ⁻¹	9.450	14.850
Maintenance	€ anno ⁻¹	8.000	8.000
Insurance. management	€ anno ⁻¹	3.012	3.012
Operating costs	€ anno ⁻¹	2.008	2.008
Depreciation and costs of capital	€ anno ⁻¹	44.427	44.427
Total annual costs	€ anno ⁻¹	66.897	72.297
Revenues			
Revenue total	€ anno ⁻¹	66.897	79.697
Heat revenues	€ anno ⁻¹	9.384	14.747
Revenue electricity	€ anno ⁻¹	57.513	64.950
Market price	€ anno ⁻¹	3.608	6.003
Required support	€ anno ⁻¹	53.905	58.947
Reference cost of electricity			
Revenue/electricity	€ MWh _{el} ⁻¹	586.86	421.75
Prices for the guaranteed purchase of electricity			
Market price	€ MWh _{el} ⁻¹	36.81	38.98
Guaranteed purchase should be	€ MWh _{el} ⁻¹	586.86	421.75
State support is delivered			
Limit reference cost	€ MWh _{el} ⁻¹	<385.00	<260.00

CONCLUSIONS

Annually, more than one million m³ of wood has been traditionally used in Slovenian individual households, especially for space and water heating. Combined wood gas heat and power (CHP) facilities represent an efficient clean and reliable approach to generate power and thermal energy from a wood gas, with important reduction of the CO₂ and PM10 particles emissions. In our case study, a possibility of introduction a micro cogeneration systems on an average Slovene farm was explored and whether it would be worthwhile to invest for heating system and the supply of electricity in the public grid. A Volter 30, with 28

kW electricity and 70 kW heat power one of the smallest and less expensive (251,000 €) CHP units, was selected for a case study for calculating the economic viability of the system on operating calculation with 3,500 and 5,500 working hours per year, respectively. The reference cost of electricity, which in the first case amounts to 586.86 € MWh⁻¹ and 421.75 € MWh⁻¹ in the second one, exceeded the legible reference costs of electricity generation in micro CHP units. Namely, the investor would be entitled to state support only with the maximum 385 EUR MWh⁻¹ for a CHP production plant operating up to 4,000 hours and maximum 260 EUR MWh⁻¹ in case the device operates more than 4,000 hours. The possible enhancement of the economics would be probably reached at 7,500 hours working capacity. However, in that case the majority of Slovenian farms do not have enough demands for heating (greenhouses, barns, households) thus it should be released in the environment, which also means additional environmental burden.

ACKNOWLEDGEMENTS

The authors also acknowledge the vital contributions made by Jernej Bobanec and a Volter 30 distributor in Slovenia, Artim d.o.o., for supporting the Volter 30 CHP unit data.

REFERENCES

- ApE, (2016). Agencija za prestrukturiranje energetike. Biomasa , <http://www.ape.si/>, (Acceded, 5 May 2016).
- Artim, (2014). Tehnična dokumentacija sistema Volter 30, <http://www.volter.si/> (Acceded, 15 May 2016).
- Bobanec, J. (2014). Uporaba kogeneracijskega sistema na lesni plin na kmetiji: diplomsko delo. Maribor, 43 p.
- Borzen, (2016). Izvajanje podporne sheme za električno energijo proizvedeno iz OVE ali v visoko učinkoviti SPTE – obdobjno poročilo (elektronski vir). <http://www.nas-stik.si/Portals/0/Content/2015-12M-CP-objava.pdf>, (15. maj 2016).
- Energy Strategy 2015, Framework for climate and energy, <http://ec.europa.eu/energy/en/topics/energy-strategy-and-energy-union/2030-energy-strategy> (Acceded, 9th December 2016)
- EUROSTAT, Renewable energy statistics, (2015). [http://ec.europa.eu/eurostat/statistics-explained/index.php/File:Share_of_renewables_in_gross_final_energy_consumption,_2015_and_2020_\(%25\)_YB17.png#filelinks](http://ec.europa.eu/eurostat/statistics-explained/index.php/File:Share_of_renewables_in_gross_final_energy_consumption,_2015_and_2020_(%25)_YB17.png#filelinks), (Acceded, 9th December 2016)
- Knoef, H.A.M. (2005). Handbook Biomass Gasification. The Netherlands, BTG Biomass technology group BV: 400 p.
- Krajnc, N., Piškur, M., Medved, M., Krajnc, R. (2007). Gozd in les - razvojna priložnost Slovenije Ljubljana, Silva Slovenica, 2 p.
- MG - Ministrstvo za gospodarstvo (2009). Metodologija določanja referenčnih stroškov sproizvodnje z visokim izkoristkom (elektronski vir), http://www.mg.gov.si/fileadmin/mg.gov.si/pageuploads/Energetika/Sprejeti_predpisi/Met_RS_SPTE_2009.pdf.
- Official Gazette of the Republic of Slovenia, No. 76/2009. Uredba o spremembah in dopolnitvah Uredbe o podporah električni energiji, proizvedeni v sproizvodnji toplote in električne energije z visokim izkoristkom, stran.
- Slovenian Authorities (2016). State Aid SA. 41998 (2015/N) – Slovenia, 29 p.



LACCASE ENZYME PRODUCTION AND BIOMASS GROWTH IN LIQUID CULTURES OF WOOD-DEGRADING FUNGAL STRAINS

Mariana FERDEȘ, Mirela DINCĂ*, Bianca ZĂBAVĂ, Gigel PARASCHIV,
Mariana MUNTEANU, Mariana IONESCU

Department of Biotechnical Systems, University Politehnica of Bucharest,
Splaiul Independentei no. 313, Sector 6, Romania
E-mail of corresponding author: mirela_dilea@yahoo.com

SUMMARY

Five fungal strains namely *Pleurotus ostreatus*, *Polyporus squamosus*, *Lentinula edodes*, *Hypsizygus tessulatus* and *Flammulina velutipes*, known for wood-degrading enzymes biosynthesis were assessed in order to produce laccase in liquid culture media. The laccase is involved in the treatment of environmental pollutants and in the pretreatment of biomass used in bioethanol or biogas biosynthesis as renewable sources of energy. The tested strains were isolated from edible mushroom mycelia or they were selected from the laboratory culture collection. These fungi belong to the phylum Basidiomycota and are known for their enzymatic activity of lignin oxidation used in degradation of biomass and other polyphenolic compounds like different industrial dyes. The fungal strains were analyzed in a first stage by screening methods in terms of the laccase and hydrolases production. The fungi were cultivated in liquid media on an orbital shaker, at 25 °C, 150 rpm for 10 days. The laccase activity, pH, nutrient consumption and final fungal biomass were analyzed in all samples.

Key words: wood-degrading fungi, laccase, biomass

INTRODUCTION

Nowadays, there is a large interest in laccase production because of their potential use in detoxification of pollutants and in bioremediation of phenolic compounds. The use of laccases in processes of treatment or removal of environmental and industrial pollutants and in pretreatment of lignocellulosic material for biofuels production is due to their high efficiency and selectivity. Numerous researches and studies have been carried out in order to discover new microbial strains and to improve the production of laccases by modification of

growth conditions, use of inducers and cheaper substrates such as agricultural and food by products (Mabrouk et al., 2010; Viswanath et al., 2014).

Laccases (benzenediol: oxygen oxidoreductases, EC 1.10.3.2) are part of broad group of polyphenol oxidases. Laccase is a dimeric or tetrameric glycoprotein and usually contains four copper atoms per unit of protein (multicopper oxidases). These enzymes catalyze the oxidation of substrates with reduction of oxygen to water. They are able to oxidize polyphenols, methoxy-substituted phenols, aromatic diamines, and a range of other compounds (Bourbonnais et al., 1990; Brijwani et al., 2010; Mate et al., 2015; Afreen et al., 2016).

Laccases are increasingly being used in a wide variety of industrial oxidative processes such as delignification, dye bleaching, pulp and paper processing, prevention of wine discoloration, production of chemicals from lignin, waste detoxification and textile dye transformation, plant fiber modification, ethanol production, biosensors, biofuel cells etc.

Lignin represents a major component of wood and the second most common renewable organic polymer on earth (Mabrouk et al., 2010; Kumar et al., 2011; Schroyen et al., 2017).

In 1883 Yoshida described the laccase extracted from the exudate of the Japanese laquer tree *Rhus vernicifera*. A few years later, in 1896, laccase was found in fungi for the first time by both Bertrand and Laborde (Kunamneni et al., 2007; Li et al., 2008).

Laccases are enzymes ubiquitous in distribution and are found in plants, fungi and in some bacteria. In fungi they are produced by ascomycetes, basidiomycetes, deuteromycetes, but not by zygomycetes. In higher plants laccases have been identified in trees, cabbages, turnips, beets, apples, asparagus, potatoes, pears, and various other vegetables. The role of laccase is different in higher plants and fungi. In plants, laccase is involved in lignification process, whereas in fungi laccases catalyses many reactions like delignification, sporulation, pigment production, fruiting body formation and plant pathogenesis (Kunamneni et al., 2007).

Recently bacterial laccases have also been characterized from bacteria such as *Azospirillum lipoferum*, *Bacillus subtilis*, *Streptomyces lavendulae*, *S. cyaneus* and *Marinomonas mediterranea* (Kunamneni et al., 2007).

Laccases are produced by a large variety of fungi. Numerous studies refer to the synthesis of laccases in ascomycetes such as *Aspergillus*, *Penicillium*, *Curvularia* and wood-degrading ascomycetes *Trichoderma* and *Botryosphaeria*. Basidiomycetes yeast like *Cryptococcus neoformans* produces a true laccase capable of oxidation of phenols and aminophenols (Brijwani et al., 2010). Wood-degrading fungi belonging to Basidiomycetes and a related group of litter decomposing saprophytic fungi are known to produce higher quantities of laccases (Kuhar et al., 2014). Enzyme production and the oxidation of ABTS by *Pleurotus ostreatus*, *Flammulina velutipes*, *Gloeophyllum trabeum*, *Coniophora puteana* and *Laetiporus sulphureus* were reported (Brijwani et al., 2010). The white-rot basidiomycetes are the most efficient degraders of lignin and also the most widely studied (Kunamneni et al., 2007). The white-rot fungi produce lignin enzymes able to decompose the wood, namely lignin peroxidase, manganese-dependent peroxidase and veratryl alcohol oxidase. Moreover, they can synthesize other hydrolytic enzymes which enhance the action of laccases acting synergistically, such as glucosidases, cellulases, amylases, proteases, xylanases etc (Vrsanska et al., 2016).

Laccases can be synthesized either as extracellular or intracellular enzymes and it was suggested that the intracellular laccase functioned as a precursor for extracellular laccase as there were no differences between the two laccases (Kunamneni et al., 2007).

In the last decades the low cost production of laccases represents a high interesting area of research. These enzymes are synthesized during secondary metabolism as inducible or constitutive enzyme. The production of laccase depends on the nutrients (carbon and nitrogen sources, inducers, copper) and on the culture parameters. The inducers increase the production of laccase by providing contact with compounds that may naturally elicit a stress response and further increase production. Laccases are produced in liquid cultures of microorganisms or in solid state fermentation systems (Afreen et al., 2016).

The aim of this study was to evaluate the laccase production of five fungal strains belonging to Basidiomycetes cultivated in submerged, shaken culture.

MATERIALS AND METHODS

Fungal strains and screening for laccase and hydrolases activity

Five edible fungal strains were assessed in terms of laccase and hydrolase production, namely: *Pleurotus ostreatus* (oyster mushroom), *Polyporus squamosus* (dryad's saddle), *Hypsizygus tessulatus* (hon shimeji), *Flammulina velutipes* (enoki flower) and *Lentinula edodes* (shiitake) from the culture collection of Microbiology laboratory, Faculty of Biotechnical Systems Engineering.

The fungal strains were cultivated on Potato Dextrose Agar (potato extract 4.0 g L⁻¹, glucose 20.0 g L⁻¹, agar 15.0 g L⁻¹) and kept at 4 °C until used.

The fungi were characterized in terms of enzyme production through semiquantitative analysis using specific media in Petri dishes. Amylases were assessed in a medium containing soluble starch as a carbon source. Adding Lugol solution, the zone of hydrolysis remained uncoloured, whereas the non-hydrolysed starch was coloured dark blue. The proteolytic enzymes were highlighted on a nutrient medium with casein; the clarification of agar was due to the hydrolysis of casein around the colonies. The lipolytic fungi produced an opaque zone due to the formation of calcium salts in a nutrient agar supplemented with Tween 80 and CaCl₂. Cellulolytic colonies hydrolysed the cellulose contained in the culture medium and produced a clarified hydrolysis zone (Guiraud et al., 1980). The biosynthesis of laccases was assessed on Potato Dextrose Agar supplemented with 0.04% guaiacol. The reddish brown zones around fungal colonies are due to the oxidation of guaiacol to a coloured product (Kalra et al., 2013; El Monsséf et al., 2016).

The enzymatic indices defined as the ratio of the diameter of hydrolysis zone and the diameter of colony has been calculated.

Cultivation of fungi in liquid media

The fungal strains were cultivated in a 500 mL Erlenmeyer flasks containing 200 mL malt extract 17 g L⁻¹, on a rotary shaker (Thermoshake, Gerhardt), at 25 °C for 10 days. Laccase production, consumption of substrate, pH and biomass accumulation were assessed.

Guaiacol assay method for laccase assay

Laccase activity was analysed using guaiacol (Sigma Aldrich) as substrate. The intense brown color development due to oxidation of guaiacol can be correlated to laccase activity. Guaiacol (10mM) in sodium acetate buffer (10 mM, pH 5.4) was used as substrate. The reaction mixture contained 3 mL acetate buffer, 1 mL guaiacol and 1 mL enzyme source. The enzyme blank contained 1 mL of distilled water instead of enzyme source. The mixture was incubated at 30 °C for 15 min and the absorbance was read at 470 nm using a UV-VIS spectrophotometer T90+ PG Instruments. Enzyme activity was expressed as enzyme units

(U), defined as the amount of enzyme required to oxidize 1 micromole of guaiacol per minute. The laccase activity in U/mL is calculated using following formula:

$$EA = \frac{A \times V}{t \times v \times \epsilon}$$

where:

- EA = enzyme activity (U)
- V = total mixture volume (mL)
- v = enzyme volume (mL)
- t = incubation time (min)
- ϵ = molar absorption coefficient of oxidized guaiacol product ($26.6 \text{ mM}^{-1} \text{ cm}^{-1}$) at 470 nm (Dawson et al., 1986).

The final values of pH and total dry biomass were determined in the fungal cultures. After 14 days of incubation the filtered wet biomass was weighed and the percent of dry matter was determined at 103 °C using a thermobalance (Kern RH 120-3).

All assays were carried out in triplicate.

RESULTS AND DISCUSSION

Five edible fungal strains have been selected in order to assess the laccase production, namely *Pleurotus ostreatus* (oyster mushroom), *Polyporus squamosus* (dryad's saddle), *Hypsizygus tessulatus* (hon shimeji), *Flammulina velutipes* (enoki flower) and *Lentinula edodes* (shiitake). These Basidiomycetes are traditionally cultivated as edible mushrooms on wood substrate of agricultural by-products.

The selected fungi can be grown in liquid media to produce laccase enzyme and hydrolases involved in substrate decomposition but, in the same time, an edible biomass with high nutritional value can be obtained.

The fungal strains were characterized in terms of laccase and hydrolases production through screening methods in Petri dishes on specific media. The qualitative assessment of enzymes production, expressed as enzymatic indices (diameter of highlighted zone / diameter of colony) is presented in table 1.

Table 1. Enzymatic indices of fungal species

Fungal stain	Enzymatic indices (diameter of highlighted zone / diameter of colony), mm mm ⁻¹				
	Laccase index	Amylase index	Protease index	Lipase index	Cellulase index
<i>Pleurotus ostreatus</i>	40/8	0	30/10	23/4	12/7
<i>Polyporus squamosus</i>	6/10	0	20/16	0	0
<i>Flammulina velutipes</i>	23/18	0	30/28	15/12	0
<i>Hypsizygus tessulatus</i>	5/11	20/10	35/15	10/6	0
<i>Lentinula edodes</i>	14/25	0	0	0	7/3

Each species has produced at least two enzymes on solid media, but the largest amounts of laccase were synthesized by *Pleurotus ostreatus*, *Flammulina velutipes* and *Lentinula edodes* strains which had a higher value of laccase index (fig. 1).

Amylase enzyme was produced only by *Hypsizygos tessulatus* and proteolytic enzyme by all strains except *Lentinula edodes*. Cellulolytic enzymes were synthesized by the colonies of *Pleurotus ostreatus* and *Lentinula edodes*.



Figure 1. Laccase production by a) *Pleurotus ostreatus* b) *Flammulina velutipes* c) *Lentinula edodes* on Potato Dextrose Agar supplemented with guaiacol

The production of laccases in malt extract broth on the rotary incubator was assessed in the filtrate of cultures. The results are presented in figure 2. For each fungus, the production of laccases seems to start on the fourth day, when the enzyme activity was between 0.58 U mL⁻¹ for *Flammulina velutipes* and 1.31 U mL⁻¹ for *Pleurotus ostreatus*. The laccase accumulated in the liquid medium until the tenth day, when *Flammulina velutipes* and *Pleurotus ostreatus* produced the highest amounts of laccase, 4.64 U mL⁻¹, respectively 8.7 U mL⁻¹.

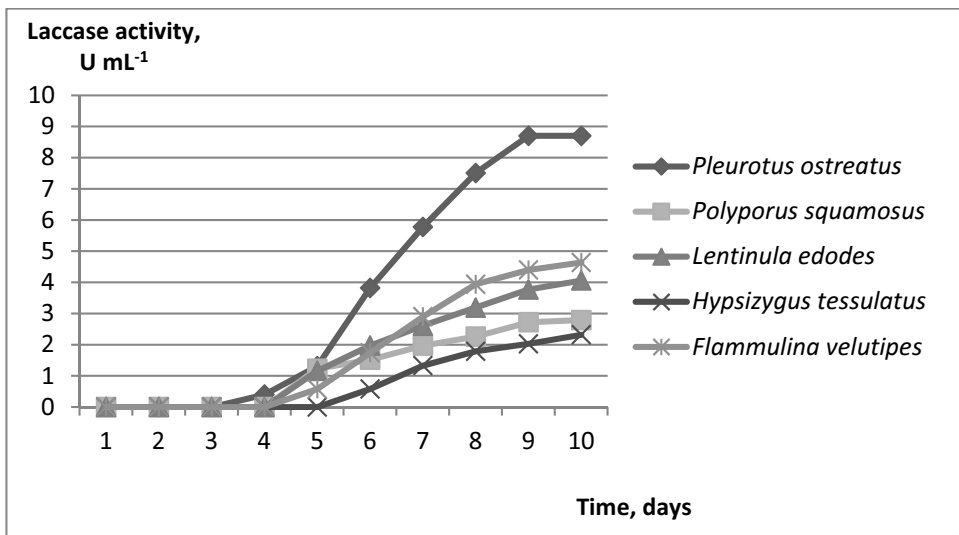


Figure 2. Laccase activity in cultures of *Pleurotus ostreatus*, *Polyporus squamosus*, *Lentinula edodes*, *Hypsizygos tessulatus* and *Flammulina velutipes*

Recent studies demonstrated that laccases are synthesized during secondary metabolism as inducible or constitutive enzyme (Afreen et al., 2016).

In accordance with this research, the laccase activity as shown in figure 2 started after the lag phase, in the fourth day. This fact could be explained by the late growth of fungal biomass in these culture media containing malt extract. The production of laccase is known to depend on the nutrients and on the culture parameters.

In this study, the fungal strains were assessed in terms of extracellular laccase production. According to Kunamneni et al., (2007), laccases can be synthesized as extracellular or intracellular enzymes and it was suggested that the intracellular laccase is a precursor for extracellular laccase, as there are no differences between the two enzymes. *Pleurotus ostreatus* synthesizes at least nine isoenzymes that differ in their catalytic properties, structure, and biosynthesis conditions (Kon K., 2009).

In table 2, pH, sugar concentration (refractometric) and fungal biomass after 10 days are presented. The initial pH of culture medium was about 6.0 and the final values of pH varied depending on the species. The yield of biomass production (dry biomass/substrate consumption) x 100 was calculated.

Table 2. pH, sugar concentration and dry biomass in fungal cultures after 10 days

Fungal strain	pH after 10 days	Sugar concentration (%)	Dry biomass (g L ⁻¹)	Yield (%)
<i>Pleurotus ostreatus</i>	4.89	1.2	2.5	50
<i>Polyporus squamosus</i>	7.45	0.5	4.8	40
<i>Flammulina velutipes</i>	5.47	0.9	4.0	50
<i>Hypsizygus tessulatus</i>	6.13	0.8	4.2	46
<i>Lentinula edodes</i>	6.16	0.9	3.9	49

Because the enzyme synthesis is correlated with the fungal biomass, the value of enzyme activity related to dry biomass was calculated as the ratio of enzyme activity and dry biomass (fig. 3).

The obtained results for the laccase activity in liquid cultures were correlated with the values of laccase indices assessed on Potato Dextrose Agar supplemented with guaiacol. The highest production of laccase was shown in the culture of *Pleurotus ostreatus*, followed by *Flammulina velutipes* and *Lentinula edodes*.

Using suitable culture media containing inducers for enzyme activity and appropriate nutrients for each species, the laccase and biomass production should be improved.

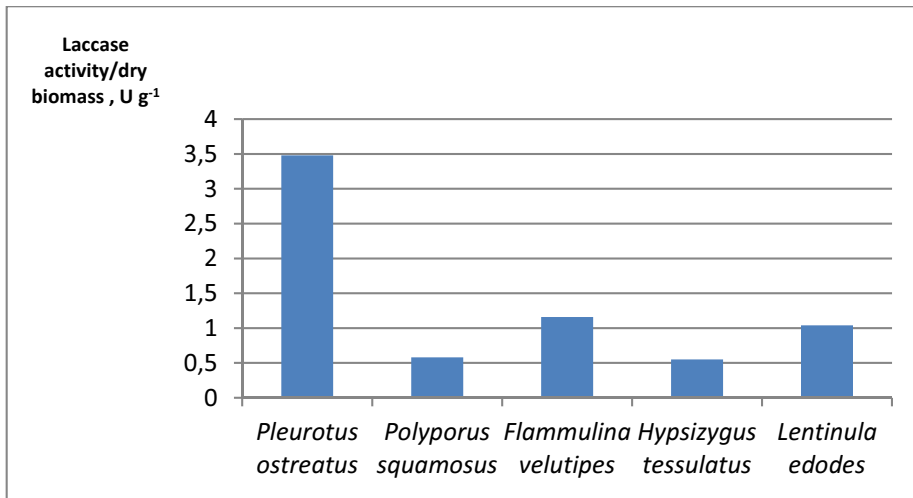


Figure 3. Laccase activity related to dry biomass in fungal cultures after 10 days

After the separation of fungal biomass, purification of laccases from culture media is not difficult because laccase is an extracellular enzyme and the fungal biomass can be easily removed (Kon K., 2009).

CONCLUSIONS

Production of laccases using wood-degrading fungal species represents an interesting perspective for environmental and industrial applications.

Five fungal strains namely *Pleurotus ostreatus* (oyster mushroom), *Polyporus squamosus* (dryad's saddle), *Hypsizygus tessulatus* (hon shimeji), *Flammulina velutipes* (enoki flower) and *Lentinula edodes* (shiitake) were assessed in terms of laccase and biomass production. The cultures were carried out on a rotary shaker, at 25 °C, 150 rpm, 10 days, in malt extract medium. The analysis of enzyme activity and fungal growth demonstrated that all tested wood-degrading fungi were able to produce laccase in submerged culture.

The highest extracellular laccase activity was found in liquid culture of *Pleurotus ostreatus*, *Flammulina velutipes* and *Lentinula edodes*. These edible mushrooms should be grown in appropriate liquid media both for laccase production and biomass for food industry.

REFERENCES

- Afreen, S., Anwer R., Singh, R.K., Fatma, T. (2016). Extracellular laccase production and its optimization from *Arthrospira maxima* catalyzed decolorization of synthetic dyes. Saudi Journal of Biological Sciences, <https://doi.org/10.1016/j.sjbs.2016.01.015>
- Bourbonnais, R., Paice, M.G. (1990). Oxidation of non-phenolic substrates: An expanded role for laccase in lignin biodegradation. *FEBS Letters* 267 (1): 99-102
- Brijwani, K., Rigdon, A., Vadlani, P.V. (2010). Fungal laccases: Production, function, and applications in food Processing. *Enzyme Research*. Art. ID 149748, 10 pages [doi:10.4061/2010/149748](https://doi.org/10.4061/2010/149748)

- Dawson R.M.C., et al. (1986) Data for Biochemical Research, 3rd ed. Oxford University Press New York
- El Monssef, R.A., Hassan, E.A., Ramadan, E.M. (2016). Production of laccase enzyme for their potential application to decolorize fungal pigments on aging paper and parchment. *Annals of Agricultural Science*. 61(1): 145–154
- Guiraud J., Galzy P. (1980). L'analyse microbiologique dans les industries alimentaires. Les Editions de l'Usine Nouvelle-Paris
- Kalra, K., Chauhan, R., Shavez, M., Sachdeva, S. (2013). Isolation of laccase producing *Trichoderma* spp. and effect of pH and temperature on its activity. *Int. J. Chem. Environ. Technol.* 5 (5): 2229–2235
- Kon, K. (2009). *Advances in Fungal Biotechnology* Ed. Mahendra Ray, I. K. International Pvt Ltd
- Kuhar, F., Papinutti, L. (2014). Optimization of laccase production by two strains of *Ganoderma lucidum* using phenolic and metallic inducers. *Rev Argent Microbiol* 46: 144 - 149
- Kumar, V.V., Kirupha, S.D., Periyaraman, P., Sivanesan, S. (2011). Screening and induction of laccase activity in fungal species and its application in dye decolorization, *African Journal of Microbiology Research*. 5(11): 1261-1267
- Kunamneni, A., Ballesteros, A., Plou, F.P., Alcalde, M. (2007). Fungal laccase – a versatile enzyme for biotechnological applications *Communicating Current Research and Educational Topics and Trends in Applied Microbiology*. Ed. Méndez-Vilas, 233-245
- Li, A., Zhu, Y., Xu L., Zhu, W., Tian, X. (2008). Comparative study on the determination of assay for laccase of *Trametes* sp. *African Journal of Biochemistry Research* 2 (8): 181-183
- Mabrouk, A.M., Kheiralla, Z.H., Hamed, E.R., Youssry, A., El Aty, A. (2010). Screening of some marine-derived fungal isolates for lignin degrading enzymes (LDEs) production. *Agriculture and. Biology Journal of North America* 1(4): 591-599
- Mate, D.M., Alcade, M. (2015). Laccase engineering: from rational design to directed evolution. *Biotechnol Adv.* 33(1): 25 - 40
- Schroyen, M., Van Hulle, S.W.H., Holemans, S., Vervaeren, H., Raes, K. (2017). Laccase enzyme detoxifies hydrolysates and improves biogas production from hemp straw and miscanthus. *Bioresource Technology* 244: 597–604
- Viswanath, B., Rajesh, B., Janardhan, A., Kumar, A.P., Narasimha, G. (2014). Fungal laccases and their applications in bioremediation. *Enzyme Research*. Vol. 2014, Article ID 163242, 21 pages <http://dx.doi.org/10.1155/2014/163242>
- Vrsanska, M., Voberkova, S., Langer, V., Palovcikova, D., Moulick, A., Adam, V., Kopel, P. (2016). Induction of laccase, lignin peroxidase and manganese peroxidase activities in white - rot fungi using copper complexes. *Molecules* 21:1553, doi:10.3390/molecules21111553.



LIGNOCELLULOSIC BIOMASS PRETREATMENT BY HYDROLYTIC FUNGAL STRAINS

Mirela DINCĂ^{1*}, Mariana FERDEȘ¹, Bianca ZĂBAVĂ¹, Gigel PARASCHIV¹,
Nicoleta UNGUREANU¹, Valentin VLĂDUȚ², Georgiana MOICEANU¹

¹Department of Biotechnical Systems, Faculty of Biotechnical Systems Engineering, University Politehnica of Bucharest, Splaiul Independentei Blv., no. 313, sector 6, Bucharest, Romania

²National Institute of Research - Development for Machines and Installations Designed to Agriculture and Food Industry – INMA, Ion Ionescu de la Brad Blv., no. 6, sector 1, Bucharest, Romania

E-mail of corresponding author: mirela_dilea@yahoo.com

SUMMARY

The most used lignocellulosic substrates for biofuels production include crop residues such as corn stalks, wheat straws, animal manure or dedicated energy crops. The main components of lignocellulosic materials are cellulose, hemicelluloses and lignin which is the most recalcitrant component of the plant cell wall (the higher the proportion of lignin, the higher the resistance to chemical and enzymatic degradation), in this case pretreatment being very important. In this paper it was investigated the efficiency of four types of fungi, namely *Aspergillus niger*, *Aspergillus oryzae*, *Sporotrichum pulverulentum* and *Trichoderma harzianum* on lignocellulosic substrate consisting of wheat straw, corn stalks and sawdust. The fungal strains were tested by cultivation in Petri dishes for determination of the following exoenzymes: laccase, amylase, cellulase, protease and lipase. To assess the suitability and profitability of fungal pretreatment, laboratory tests consisted of determination of total soluble solids (TSS), pH, sugar content, substrate's mass reduction and dry matter were conducted before and after samples pretreatment. Also, microscopic analyses were done. The tested biomass was firstly pretreated by physical (milling) in order to improve its biodegradability. It has been shown that *Sporotrichum pulverulentum* had the best performance on the tested biomass.

Keywords: lignocellulosic biomass, pretreatment, fungi, hydrolytic enzymes

INTRODUCTION

One of the main drawbacks of lignocellulosic biomass conversion into simple sugars is the resistance of lignin degradation. Thus, pretreatment is a crucial step in the conversion of

lignocellulosic biomass to fermentable sugars and biofuels (Wan and Li, 2012). There are five categories of pretreatments: mechanical, chemical, thermal, thermo-chemical and biological. However, these methods can induce important additional costs for biomass processing (Rouches et al., 2016). However, some studies reported that biological pretreatment of lignocellulosic biomass is very promising due to mild operating conditions and low operational costs and also because it is environmentally friendly (Sindhu et al., 2016; Liu et al., 2017). Biological (enzymatic) treatment of the lignocellulosic substrate can enhance the digestibility by reducing cellulose crystallinity, increasing substrate porosity, and solubilizing cellulose, hemicellulose and lignin (Shrestha et al., 2017). The most studied biological pretreatment of lignocellulosic biomass focusses on filamentous fungi and enzymatic hydrolysis pretreatments. In the case of enzymatic hydrolysis, the enzymes are produced by fungi, like *Trichoderma* and *Aspergillus* genus (Song et al., 2013; Singhvi et al., 2014).

To degrade the lignocellulosic biomass, the fungi are using extracellular enzymes that form a hydrolytic system that produces hydrolases – responsible for polysaccharide degradation and a ligninolytic system which degrades lignin and opens phenyl rings. The ligninolytic system comprises three important oxidizing enzymes, such as: lignin peroxidase, manganese peroxidase and laccase. It must be noted that not all fungi produce all these enzymes (Sanchez, 2009). The biodegradation of lignocellulosic biomass occurs under the synergistic action of microbial consortium including various bacteria and fungi. Using bacteria and fungi for the biodegradation of lignocellulosic biomass increases adaptability, improves enzymatic saccharification efficiency and pH value can be controlled during sugar utilization (Kalyani et al., 2013).

It was reported that in order to improve the efficiency of degradation, biological pretreatment may be combined with thermal, chemical or physical treatment. Particle size reduction by milling is the most used physical method for improving the digestibility by increasing the specific surface area of the tested feedstock (Mustafa et al., 2017).

The aim of this paper is to assess the effect of fungal pretreatment combined with milling on the lignocellulose biomass degradation.

MATERIALS AND METHODS

Fungal strains

Fungal cultures of *Aspergillus niger* (AN), *Aspergillus oryzae* (AO), *Sporotrichum pulverulentum* (SP) and *Trichoderma harzianum* (TH) were grown on Potato Dextrose Agar in tubes at 25 °C for 7 days. These strains were chosen from different genera of fungal species known for their ability to produce enzymes that are able to degrade the lignocellulosic substrates. Next, fungus mycelium from each tube was mixed with sterile water and transferred into 500 mL sterile Erlenmeyer flasks containing 300 mL of Potato Dextrose Broth medium, closed with a cotton plug. Then, the flasks were incubated on the orbital incubator Thermoshake Gerhardt for 72 h at 28 °C with agitation, the mixing rate being set at 150 rpm.

At the same time, fungal strains were tested by cultivation in Petri dishes for determination of the following exoenzymes: laccase, amylase, cellulase, protease and lipase.

Amylases were assessed in a medium containing starch as carbon source. Adding Lugol solution, the zone of hydrolysis remains white, whereas the non-hydrolysed starch was coloured dark blue. The proteolytic enzymes were highlighted on casein containing medium;

the clarification of agar was due to the hydrolysis of casein around the colonies. The lipolytic fungi produced an opaque zone due to the formation of calcium salts in a nutrient agar supplemented with Tween 80 and CaCl₂. Cellulolytic colonies hydrolysed the cellulose contained in the culture medium and produced a clarified hydrolysis zone (Guiraud et al., 1980). The biosynthesis of laccases was assessed on Potato Dextrose Agar supplemented with 0.04% guaiacol. The reddish brown zones around fungal colonies are due to oxidation of guaiacol to a coloured product (Kalra et al., 2013; El Monsséf et al., 2016). The enzymatic indices defined as the ratio of the diameter of hydrolysis zone and the diameters of colony were calculated.

All the fungal strains were obtained in the Microbiology Laboratory from Faculty of Biotechnical Systems Engineering, Romania.

Feedstock preparation

The wheat straw (WS), corn stalks (CS) and sawdust (SD) used in this study were collected from a farm in Teleorman county, Romania, in summer – autumn 2016. Particle size of the substrate is an important factor affecting the performance of fungal pretreatment, because larger particle size makes it harder for the fungi to penetrate into cellulosic biomass. In this case, tested biomass was grinded at 1 mm using the laboratory mill Pulverisette 19.

4.5 g of each tested substrate (wheat straw, corn stalks and sawdust) were mixed with 300 ml of water in a 500 mL Erlenmeyer flask and then autoclaved for 15 min at 121 °C. After flasks cooled at room temperature, the substrate was inoculated with 10 mL of the four types of fungus suspension that were previous incubated. During incubation, each Erlenmeyer flask was covered with a cotton plug in order to reduce humidity loss and to prevent contamination. Control flasks were prepared in the same manner, but only water was added instead of inoculum.

All flasks were incubated in the orbital incubator (Fig. 1a) for two weeks at 28 °C and the mixing rate was set at 150 rpm.

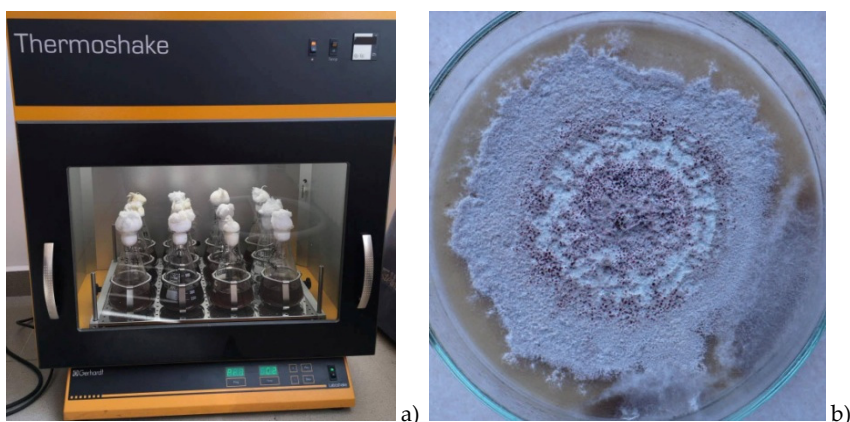


Figure 1. Erlenmeyer flasks in orbital incubator a) and *Sporotrichum pulverulentum* culture in Petri dish b)

Methods of analysis

The evaluation of fungal pretreatment on lignocellulosic biomass was done by analyzing and interpreting the following parameters: reduction of substrate mass, determination of total soluble solids (TSS), pH, sugar content and dry matter.

Samples analysis was done by collecting samples from each Erlenmeyer flasks in different days of the degradation process (days 1, 5, 9, 14).

After incubation, the solid part from each flask was separated from the liquid part in order to conduct the laboratory tests. The dry samples were weighed and the mass was compared to initial mass to determine the total solids biodegradation. The masses of samples after incubation included the associated fungal biomass which could not be separated from the solids. This caused an overestimation of the residual masses of substrates.

The content of TSS was measured using an ABBE refractometer and the dry matter content was determined with a KERN RH 123 – 3 thermobalance.

The pH of the liquid samples taken at certain intervals of time was determined using a pH meter type Hanna.

In each case sugars concentration was measured using the method in which is used the 3,5-dinitrosalicylic acid (DNS) (Miller, 1959). The absorbances were measured at 540 nm using the T92+ UV VIS spectrophotometer, PG Instruments.

Microscopic analyses were done using a Bel Photonics microscope in order to observe the biomass structure before and after biological pretreatment.

RESULTS AND DISCUSSION

According to Yeh et al. (2010), milling can significantly reduce the particle size and the degree of crystallinity for lignocellulosic materials, and consequently it can improve their enzymatic hydrolysis. In our study, all the samples were grinded at 1 mm.

The characteristics of untreated wheat straw, corn stalks and sawdust are shown in Table 1.

Table 1. Characteristics of untreated biomass

	Corn stalks (CS)	Wheat straw (WS)	Sawdust (SD)
pH	7.15	7.82	6.79
TSS, %	0.06	0.04	0.04
Dry matter, %	16.11	32.61	37.78
Sugar content, mg mL ⁻¹	0.402	0.305	0.381

During the biological pretreatment, the content of TSS (%) had insignificant values (between 0.04% and 0.08%), indicating the consumption of substrate for cell growth and maintenance.

Dry matter content, total dry biomass after 14 days of incubation and mass loss are presented in Table 2.

Table 2. Characteristics of fungal treated biomass

Sample	Type of fungi	Dry matter – DM, %	Dry biomass after 14 days – DB, g	Mass loss, g
	Wheat straw - control	32.61	3.62	-
	Corn stalks - control	16.11	3.24	-
	Sawdust - control	37.78	3.64	-
1	Sawdust + SP	35.38	3.44	0.2
2	Corn stalks + SP	11.02	2.20	1.04
3	Wheat straw + SP	15.77	3.08	0.54
4	Wheat straw + AO	13.45	3.57	0.05
5	Corn stalks + AO	11.30	3.53	0.04
6	Sawdust + AO	26.56	3.59	0.05
7	Sawdust + AN	24.57	3.61	0.03
8	Wheat straw + AN	18.74	3.44	0.18
9	Corn stalks + AN	12.98	3.18	0.06
10	Wheat straw + TH	20.89	3.43	0.19
11	Corn stalks + TH	14.82	2.83	0.41
12	Sawdust + TH	22.50	3.48	0.16

where: SP = *Sporotrichum pulverulentum*, AO = *Aspergillus oryzae*, AN = *Aspergillus niger* and TH = *Trichoderma harzianum*

Mass loss was determined according to equation 1:

$$Mass\ loss\ [g] = control_{mass} - DB \quad (1)$$

In Figure 2 are represented the highest values obtained for sugar content in Erlenmeyer flasks inoculated with *Sporotrichum pulverulentum* and *Trichoderma harzianum*. For example, sugar concentration in corn stalks samples has increased from the initial value of 0.402 mg mL⁻¹ to 0.479 mg mL⁻¹ after 216 hours and to 0.589 mg mL⁻¹ after 336 hours in the case of *Sporotrichum* culture, respectively to 0.443 mg mL⁻¹ and to 0.6 mg mL⁻¹ for *Trichoderma* culture.

Determination of sugar concentration in the tested substrate can provide important information on the decomposition of lignocellulosic biomass. Sugars were accumulated in cultures due to decomposition of lignocellulosic substrate, but in the same time it can be used for fungal mycelium growth.

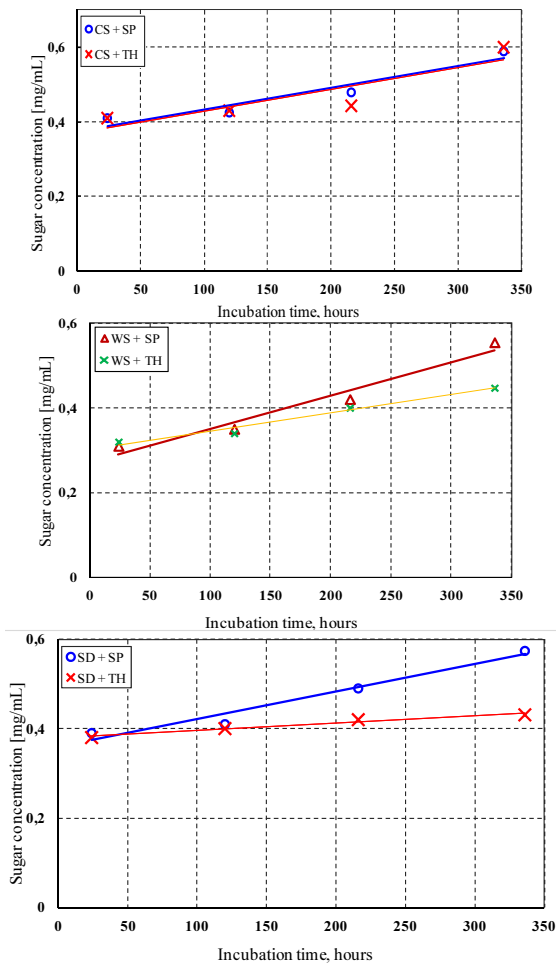


Figure 2. Sugar concentration for best degraded substrate

where: CS+SP = Corn stalks + *Sporotrichum pulverulentum*, CS+TH = Corn stalks + *Trichoderma harzianum*, WS+SP = Wheat straw + *Sporotrichum pulverulentum*, WS+TH= Wheat straw + *Trichoderma harzianum*, SD+SP = Sawdust + *Sporotrichum pulverulentum*, SD+TH = Sawdust + *Trichoderma harzianum*

The pH values presented in Figure 3 didn't show significant differences compared to the initial values, the maximum value being recorded in the case of corn stalks treated with fungal strains, to about 8 units.

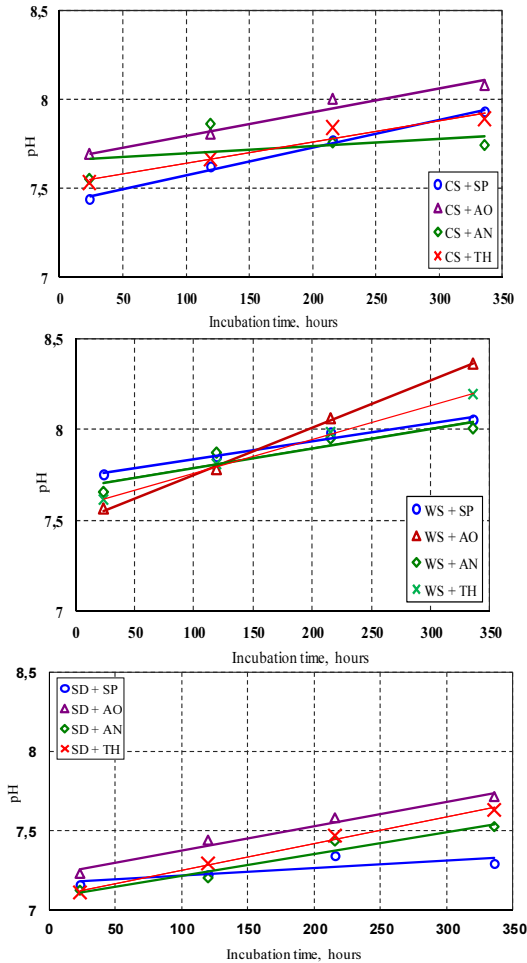


Figure 3. Variation of pH with time of incubation, for each tested substrate

where: CS+SP = Corn stalks + *Sporotrichum pulverulentum*, CS+AO = Corn stalks + *Aspergillus oryzae*, CS+AN = Corn stalks + *Aspergillus niger*, CS+TH = Corn stalks + *Trichoderma harzianum*, WS+SP = Wheat straw + *Sporotrichum pulverulentum*, WS + AO= Wheat straw + *Aspergillus oryzae*, WS+AN = Wheat straw + *Aspergillus niger*, WS+TH = Wheat straw + *Trichoderma harzianum*, SD+SP = Sawdust + *Sporotrichum pulverulentum*, SD+AO= Sawdust + *Aspergillus oryzae*, SD+AN = Sawdust + *Aspergillus niger*, SD+TH = Sawdust + *Trichoderma harzianum*

Lignin is known to be the primary obstacle to cellulose digestibility. Our results indicate that enzymatic hydrolysis of corn stalks, wheat straw and sawdust is enhanced by *Sporotrichum pulverulentum* (highest values of sugar concentrations). Tirado – Gonzales et al. (2016), also reported that *Sporotrichum pulverulentum* had the best activity on corn stover hybrids degradation.

Saha et al. (2016) evaluated 26 white – rot fungal strains, among which *Sporotrichum pulverulentum*, on corn stover to improve the efficiency of enzymatic hydrolysis. The presented results showed that hemicellulose losses from corn stover treated with *Sporotrichum pulverulentum* was more than 50%.

In Figure 4 is presented the mass loss that is attributed due to releasing of smaller molecules from polymeric substrate in the presence of selected fungal strains. The highest value was recorded in the case of corn stalks samples treated with *Sporotrichum pulverulentum* and *Trichoderma harzianum*.

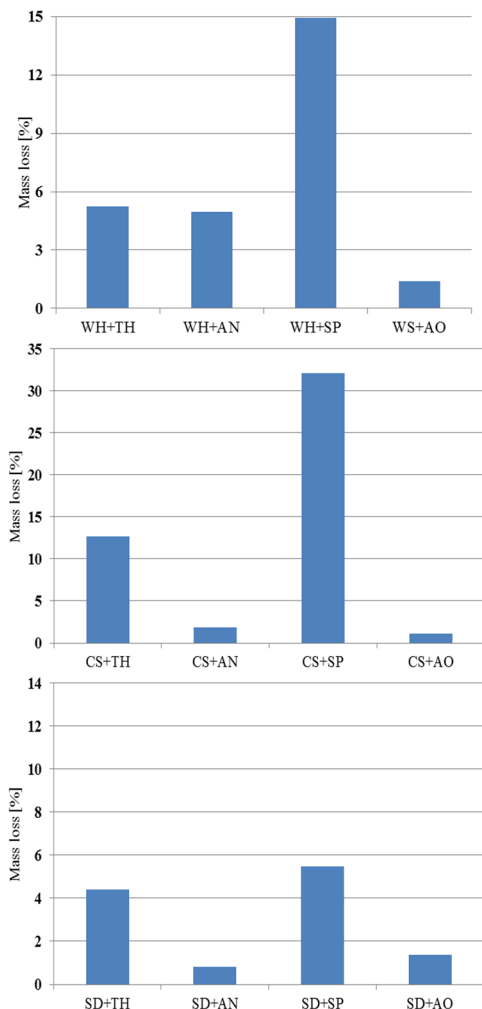


Figure 4. Mass loss for each substrate after 14 days of incubation

where: WS+TH = Wheat straw + *Trichoderma harzianum*, WS+AN = Wheat straw + *Aspergillus niger*, WS+SP = Wheat straw + *Sporotrichum pulverulentum*, WS + AO = Wheat straw + *Aspergillus oryzae*, CS+TH = Corn stalks + *Trichoderma harzianum*, CS+AN = Corn stalks + *Aspergillus niger*, CS+SP = Corn stalks + *Sporotrichum pulverulentum*, CS+AO = Corn stalks + *Aspergillus oryzae*, SD+TH = Sawdust + *Trichoderma harzianum*, SD+AO = Sawdust + *Aspergillus oryzae*, SD+SP = Sawdust + *Sporotrichum pulverulentum*, SD+AN = Sawdust + *Aspergillus niger*

Figure 5 presents some microscopic images for tested biomass before (a – Corn stalks, b – Wheat straw and c - Sawdust) and after 14 days of biological treatment with *Sporotrichum pulverulentum* (SP) (d – Corn stalks +SP, e – Wheat straw + SP, f – Sawdust + SP). As shown in Figures 5a, b, c the surface of the untreated sample seems to be smooth and compact, indicating a rigid and highly ordered surface structure.

Following the qualitative testing of the fungal strains, it was shown that *Aspergillus* species have produced amylases, laccases and proteases and *Sporotrichum pulverulentum* had produced laccases and cellulases.

Shawky et al. (2011), tested *Trichoderma* and *Aspergillus* fungal genera on rice straw and corn stalks. They reported that *Trichoderma koningii* BTS120, *Aspergillus niger* BTS149 and *Aspergillus tubingensis* BTS83 culture were the best producer of extracellular cellulases and hemicellulases in liquid culture.

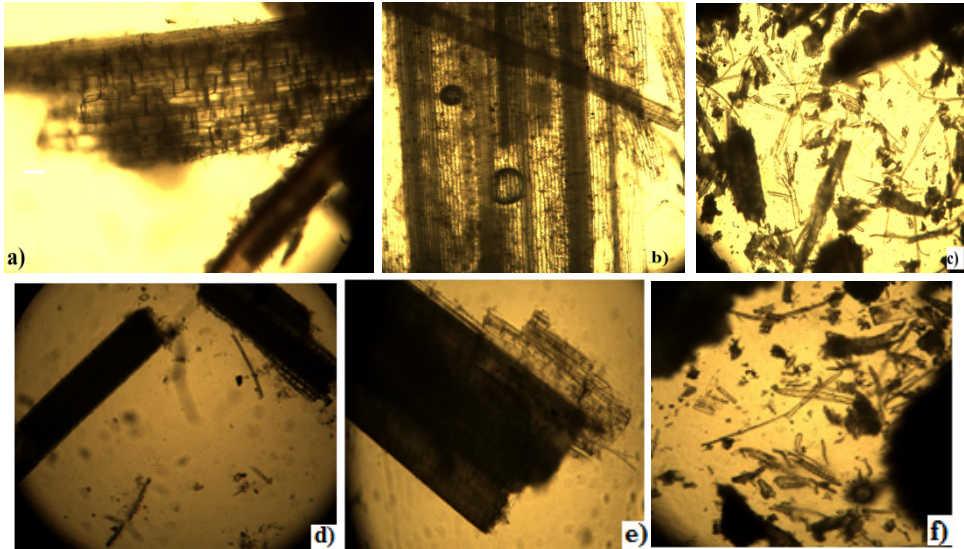


Figure 5. Tested biomass before and after biological treatment with *Sporotrichum pulverulentum*

Yu et al. (2009) reported that lignin in biomass is one of the major barriers to enzymatic hydrolysis and that lignin removal can increase pore size in the substrate and provide more accessible surface area to cellulose.

CONCLUSIONS

In the near future, lignocellulosic biomass is expected to become one of the most important renewable energy resources, to prevent global warming and the depletion of conventional fossil fuel.

Fungi are the most promising organisms for pretreatment of lignocellulosic biomass, as they can efficiently metabolize lignin in a variety of lignocellulosic materials.

In this paper, the treatment of lignocellulosic materials represented by corn stalk, wheat straw and sawdust with fungal strains has shown that in the presence of *Sporotrichum pulverulentum* and *Trichoderma harzianum* was recorded a significant mass loss of vegetal biomass with the release of sugars. The results showed that from the three tested substrates, most easily degradable in the presence of fungi was corn stalks and hardest degraded was sawdust. In 1991, Tsoumis (1991) found a high content of lignin, up to 34% in sawdust and in 2011, Shawky et al. (2011) found a content of lignin of about 16% in corn stover. However, the content of lignin from vegetal material is dependent of the plant species.

From all the tested microorganisms, *Sporotrichum pulverulentum* had the highest degradation activity of the substrate, followed by *Trichoderma harzianum*.

REFERENCES

- El Monssef, R.A., Hassan, E.A., Ramadan, E.M. (2016). Production of laccase enzyme for their potential application to decolorize fungal pigments on aging paper and parchment. *Annals of Agricultural Science* 61: 145–154.
- Guiraud J. and Galzy P. (1980). *L'analyse microbiologique dans les industries alimentaires*. Les Editions de l'Usine Nouvelle-Paris.
- Kalra, K., Chauhan, R., Shavez, M., Sachdeva, S. (2013). Isolation of laccase producing *Trichoderma spp.* and effect of pH and temperature on its activity. *International Journal of ChemTech Research* 5: 2229–2235.
- Kalyani, D., Lee, K.M., Kim, T.S., Li, J., Dhiman, S.S., Kang, Y.C., Lee, J.K. (2013). Microbial consortia for saccharification of woody biomass and ethanol fermentation. *Fuel* 107: 815 – 822.
- Liu, X., Hilgsmann, S., Gourdon, R., Bayard, R. (2017). Anaerobic digestion of lignocellulosic biomasses pretreated with *Ceriporiopsis subvermispora*. *Journal of Environmental Management* 193: 154-162.
- Miller, G.L. (1959). Use of Dinitrosalicylic Acid Reagent for Determination of Reducing Sugar, *Anal. Chem.* 31: 426 – 428.
- Mustafa, A.M., Poulsen, T.G., Xia, Y., Sheng, K. (2017). Combinations of fungal and milling pretreatments for enhancing rice straw biogas production during solid-state anaerobic digestion. *Bioresource Technology* 224: 174–182.
- Rouches, E., Herpoël-Gimbert, I., Steyer, J.P., Carrere, H. (2016). Improvement of anaerobic degradation by white-rot fungi pretreatment of lignocellulosic biomass: A review. *Renewable and Sustainable Energy Reviews* 59: 179–198.
- Saha, B.C., Qureshi, N., Kennedy, G.J., Cotta, M.A. (2016). Biological pretreatment of corn stover with white-rot fungus for improved enzymatic hydrolysis. *International Biodeterioration & Biodegradation* 109: 29 – 35.
- Sanchez, C. (2009). Lignocellulosic residues: Biodegradation and bioconversion by fungi. *Biotechnology Advances* 27 (2): 185 – 194.
- Shawky, B.T., Mahmoud, M.G., Ghazy, E.A., Asker, M.M.S., Ibrahim, G.S. (2011). Enzymatic hydrolysis of rice straw and corn stalks for monosugars production. *Journal of Genetic Engineering and Biotechnology* 9: 59 – 63.
- Shrestha, S., Fonoll, X., Kumar Khanal, S., Raskin, L. (2017). Biological strategies for enhanced hydrolysis of lignocellulosic biomass during anaerobic digestion: current status and future perspectives. *Bioresource Technology* doi: <http://dx.doi.org/10.1016/j.biortech.2017.08.089>.
- Singhvi, M.S., Chaudhari, S., Gokhale, D.V. (2014). Lignocellulose processing: a current challenge. *RSC Advances* 4(16): 8271 – 8277.
- Sindhu, R., Binod, P., Pandey, A. (2016). Biological pretreatment of lignocellulosic biomass – An overview. *Bioresource Technology* 199: 76–82.
- Song, L., Yu, H., Ma, F., Zhang, X. (2013). Biological pretreatment under non-sterile conditions for enzymatic hydrolysis of corn stover. *BioResources* 8 (3): 3802 – 3816.
- Tirado-Gonzalez, D.N., Jáuregui-Rincón, J., Tirado-Estrada, G.G., Martínez-Hernández, P.A., Guevara-Lara, F., Miranda-Romero, L.A. (2016). Production of cellulases and xylanases by white-rot fungi cultured in corn stover media for ruminant feed applications. *Animal Feed Science and Technology* 221: 147-156.
- Tsoumis G. (1991). *Science and technology of wood: structure, properties and utilization*. Verlag Kessel, Thessaloniki.
- Wan, C., Li, Y. (2012). Fungal pretreatment of lignocellulosic biomass, *Biotechnology Advances* 30: 1447–1457.
- Yeh, A.I., Huang, Y.C., Chen, S.H., (2010). Effect of particle size on the rate of enzymatic hydrolysis of cellulose. *Carbohydr. Polym.* 79: 192–199.
- Yu, H., Guo, G., Zhang, X., Yan, K., Xu, C. (2009). The effect of biological pretreatment with the selective white-rot fungus *Echinodontium taxodii* on enzymatic hydrolysis of softwoods and hardwoods. *Bioresource Technology* 100 (21): 5170 – 5175.



DETERMINING EFFICIENT MIXTURES OF BIOMASS FOR PELLET PRODUCTION

Simina MARIS^{1,2*}, Lavinia Maria CERNESCU², Stefan-Alfred MARIS¹,
Doina DARVASI², Titus SLAVICI^{1,2}

¹Politehnica University of Timisoara, Romania Mechanical Engineering Faculty, Department for Mechanical Machines, Equipment and Transportation, Mihai Viteazul, No.1, Timisoara, Romania

²Ioan Slavici University of Timisoara, Faculty of Economics.
A.P.Podeanu No. 144, Timisoara, Romania

E-mail of corresponding author: siminamaris@gmail.com

SUMMARY

In the field of energy production technology, a special interest is held by biofuels. Fuels from popular types of biomass have well known calorific values, determined by the chemical concentration of dry mass, in particular the amount of C, H, S and O contained. However, the resulting fuel contains noxes whose amount is related mainly to the content of Cl, N and S in dry mass. A good mixture of biomass should produce pellets with as high as possible calorific value, while the noxes remain lower than the accepted international maximum values. Also, the price of biomass as raw material should be taken into account, as it is determinant for the price of the finite product. In order to address these requests formulated by a small company in Romania, we elaborated an algorithm and implemented a software solution which, given a certain type of biomass, computes the most fitting recipes (as mixtures of two types of biomass) in terms of increased calorific value, low emission of noxes and price of raw material.

Key words: biomass, high calorific blends, low noxes emission, software solution

INTRODUCTION

In a previous work Maris et al. (2017) have computed the calorific value for different mixtures of biomass available in western Romania. The current paper presents an algorithm and the subsequent software solution we developed in order to determine efficient mixtures of biomass and their production costs in the particular case of a Romanian microenterprise which is set out to produce solid biofuel in the form of pellets.

Solid biofuel obtained from renewable resources became increasingly used in Europe in the last decade. As each European country assumed to produce a certain ratio of total heating and cooling supply from renewable sources, Romania's target was 22% until 2020. However, this ratio was already surpassed by 2015 (REN21). While EU remains the main producer of wood pellets, and the price of renewable energy used for heating per MJ is lower than the price of electrical energy per MJ used for heating, the demand of wood pellets for heating at European level still exceeds their production (Stolarski et al., 2016, USDA Foreign Agricultural Service, 2017).

Between 2011 and 2013, EU Commission devised a set of policies concerning the quality of clean air in Europe (COM 2013). As the energy sector was identified as the main source of air pollution, new regulations were adopted in order to limit the effects of industrial plants on the atmosphere. Thus, each EU country must implement a National Air Pollution Control Programme in order to meet the reduction commitments for 2020 and 2030. This refers to the reduction of sulphur dioxide, nitrogen oxides, dust and other toxic volatile compounds, such as chlorine compounds. Since it is essential to reduce the pollution in order to comply with the EU regulations, the biofuels used for energy should be composed of materials for which the amount of noxes would not surpass the accepted values.

From this perspective, the Romanian private microenterprise SC ANDREI SLAVICI SRL, founded in 2012, has set out to produce wood pellets and briquettes for heating. The company is a spin-out of the Ioan Slavici Foundation for Culture and Education with the purpose of commercial valorization of the scientific research results and since 2015 is a member of the Cluster for Environment and Renewable Energy Sources WESTTIM (MERWT). One of the objectives of the company is to produce pellets for heating from innovative materials and mixtures. Their main interest is to produce pellets that yield a higher calorific value, while complying with the EU regulations, in order to address the increasing demand-supply ratio and in the meantime to reduce the production costs as much as possible.

EU regulations (EN 14961, EN 14961-4) impose different values of noxes for different types of solid biofuels:

Thus, determining the mixture of two biomass types with the highest yielding calorific value, while the noxes remain lower than a certain limit leads to finding the solution of a linear optimization problem. Linear optimization, or linear programming, represents a method to achieve the best outcome of a certain mathematical model, for which the requirements are specified as linear relationships. The method is used for project selection, production planning, product mixtures (Chen et al., 2011). Ryan et al., 2014 and Quijano-Aviles et al., 2016 pointed out the usage of linear programming for determining some optimized food products. Lee and Kim, 2017 used a mixed-integer linear programming technique in order to elaborate a feasibility study for biomass-derived energy production. However, up to our knowledge, this technique is yet to be applied to determine an optimal mixture of biomass for which the highest calorific value is achieved, while the noxes remain under certain limit values.

Table 1. Classes of solid biofuels, their corresponding standards for noxes and possible origin for the biomass (EN 14961, EN 14961-4)

Class	N (%,wt. cont.)	S (%,wt. cont.)	Cl (%,wt. cont.)	Origin of biomass
A1	-	-	-	Whole trees without roots (excluding short rotation coppice) Stemwood Logging residues, deciduous, stored Chemically untreated wood residues
A2	-	-	-	Whole trees without roots (excluding short rotation coppice) Stemwood Logging residues, deciduous, stored Chemically untreated wood residues
B1	1.0	0.1	0.05	Chemically untreated wood residues Forest plantation and other virgin wood (excluding stumps/roots and bark)
B2	1.0	0.1	0.05	By-products and residues from wood processing industry (can include also chemically treated material e.g. glued, laminated, painted wood) Used wood

The aim of this paper is to present the software solution we devised for SC ANDREI SLAVICI SRL (algorithm and user interface) in order to address their need of obtaining pellets of a higher calorific value, while maintaining the noxes in the limits imposed by the EU regulations. The algorithm is a brute-force algorithm, which is well applicable for our purposes, especially because we already have a database with the properties of the raw materials. The user interface will be used in order to estimate the annual production and forecast the incomes, based on the materials which are available in the area in a specific year.

MATERIALS AND METHODS

Currently, the chemical composition for different types of biomass is known (Hartmann, 2013, Krajnc, 2015). The calorific value c was computed based on the Mendeleev formula (Hardy, 2011):

$$c = 0.339 C + 1.029 H + 0.109 S - 0.109 O$$

where C , H , S , O represent respectively the weight content of carbon, hydrogen, sulphur and oxygen in the dry mass of wood. The price for the raw materials was computed in Romanian Lei and then converted to EUR, based on the exchange rate 1 EUR = 4,59 ROL. The price for raw materials is based on the prices listed by the National Forestry Directorate – Romsilva for woods (Romsilva 2017), National Agency for Fiscal Administration – ANAF (ANAF 2017) for crops and Pitesti National Coal Company (SNC Pitesti 2017) for coal.

For mixtures of two biomass types, of mass (in kg), m_1 respectively m_2 , and with the mass concentrations of a certain chemical element $C\%_1$ respectively $C\%_2$, the total concentration of that element in the final mixture will be:

$$C\%_{tot} = \frac{m_1 C\%_1 + m_2 C\%_2}{m_1 + m_2}$$

Of course, this formula is applicable to any chemical elements present in the two biomass types. The price per kilogram of a mixture can be obtained from the prices per kilogram of the two components in a similar way to its chemical composition. Assuming that the price per kilogram of the two components is p_1 , respectively p_2 , the price (in EUR) of one kilogram of mixture is

$$p_{tot} = \frac{m_1 p_1 + m_2 p_2}{m_1 + m_2}$$

A database was constructed containing information about the EU standards, chemical composition of various biomass types and their price (in EUR) per kilogram.

Further, we will refer only to the B1 class of biomass and the computations will reflect the limits for noxes imposed by this class: N content of maximum 1%, S - maximum 0,1% and Cl - maximum 0,05% in dry content.

The algorithm we devised is presented below:

Inputs

two types of biomass, 1 and 2

Outputs

If there is a mixture of the two types of biomass for which the amount of noxes is between the limits

- the mass ratio of the mixture with the higher resulting calorific value,
 - the calorific value of the resulting mixture,
 - the price per kilogram for the raw material
 - the chemical composition of the raw material
- else
- an error message.

Algorithm

1. search the database for the maximum values for the chemical elements N,S,Cl
2. search the database for the maximum value of the mixture mass, M_{max} .
3. set the initial value for the calorific value of the mixture as equal to zero
4. for the mass of the first biomass type m_1 varying from 1 to M_{max}
5. and for the mass of the second biomass type m_2 varying from m_1 to M_{max}
6. compute the concentration for each chemical element in the mixture
7. if the concentration of N, S or Cl is above the limits then go to 9
8. if the calorific value of the mixture is greater than the previous computed calorific value, retain the values of m_1 and m_2 and the parameters computed (i.e., chemical composition of the mixture, calorific value of the mixture, price per kilogram of the raw material)
9. increase m_1 and repeat from 4
10. if the calorific value is 0 return an error message (e.g., "The level of noxes for the chosen mixture is too high according to the standards")
11. else return the mass ratio $m_1:m_2$ of the mixture, the price per kilogram, the calorific value for the mixture and its chemical composition

The amount of biomass taken into account is chosen such that the sum of the two masses remains lower than a certain maximum value (in our case $M_{max}=500$ kg).

In evaluating the operating costs we used as a model the current situation at SC ANDREI SLAVICI SRL – which refers to a pelletization line which can process at least 900 kg/h, consumes 300kW/h and for which 2 workers and 2 staff members are employed.

Other costs (e.g., transportation, advertising the products, etc.) were not taken into account.

The algorithm was implemented in Visual Basic for Excel, a component of Microsoft Office. Microsoft Excel is widely-used software and thus the usage of our software solution does not require additional costs for an end-user already using Microsoft Excel.

RESULTS AND DISCUSSION

As for the implementation of the algorithm we used the specifications for B1 class of biomass, first the available biomass should be classified according to these specifications. Table 2 presents the biomass that does not fit into the B1 category and Table 3 presents the biomass which fits into the B1 category. Due to the specific conditions in Romania, where hemp is still not cultivated on large scale, the price for hemp strains could not be determined.

Table 2. Biofuels for which N,S,C1 exceed the B1 standards, their net calorific value and their price (in EUR/kg) (source: Hartmann, 2013, Krajnc, 2015)

Biofuel	Calorific value	Price of raw material
-	(MJ/kg)	(EUR/kg)
Hemp (strains)	17,077	N/A
Hay from meadows	17,195	0,01
Hay from parks	14,227	0,01
Sunflower (straw)	15,410	0,04
Wheat (grain)	16,588	0,09
Wheat (straw)	16,814	0,04
Wheat (whole plant)	17,245	0,04
Coal	29,232	0,09
Lignite	24,918	0,08
Miscanthus	17,953	0,04
Barley (straw)	17,568	0,04
Fescue	15,846	0,04
Corn (strains)	16,414	0,04
Raigras (rye grass)	17,253	0,04
Rape (grains / cake)	25,335	0,24
Rape (straw)	17,707	0,04
Rye (grains / cake)	17,294	0,10
Rye (straw)	17,392	0,04
Rye (whole plant)	17,794	0,04
Triticale (grains)	16,286	0,11
Triticale (straw)	16,185	0,04
Triticale (whole plant)	16,248	0,04

Table 3. Biofuels for which N,S,Cl do not exceed the B1 standards, their net calorific value and their price (in EUR/kg) (source: Hartmann, 2013, Krajnc, 2015)

Biofuel	Calorific value	Price of raw material
	(MJ/kg)	EUR/kg
Bark (coniferous wood)	19,081	< 0,01
Beech (with bark)	17,693	0,02
Spruce (with bark)	18,658	0,01
Poplar	17,679	0,01
Willow	17,420	0,01

While the contents in N, S and Cl of cereals and coals are higher than the EU regulations for B1-type of solid biofuel, wood has lower noxes levels. However, the largest calorific values are characteristic for coals and rape (cake / grains).

Thus, a mixture of the materials in Table 2 leads to an amount of noxes greater than the one admitted by the B1 standard. Mixtures that are within the limits of the B1 standard contain a material from Table 2 (cereals or coals) and a material from Table 3 (woods).

The mixtures for which the N, S and Cl amounts does not exceed the B1-category standards present different mass ratios. However, a special situation occurs when the mass ratio is equal to either 1:499 or 499:1. While these mixtures respect the standards and are valid from the point of view of the algorithm, the material corresponding to a mass of 1 holds a very small influence on the calorific value of the material corresponding to a mass of 499, this influence being on the order of thousandths. Thus, these mixtures do not present an interest from the practical point of view.

Table 4 presents the highest yielding B1-category mixtures of biomass for which the mass ratios are $m_1:m_2$, with m_1 and m_2 different from 1 and 499.

It can be observed from Table 4 that the 58:3 mixture of coniferous bark and lignite, respectively the 168:3 mixture of coniferous bark and coal have the lowest prices per kg of raw material, of less than 0,01 EUR/kg. The highest prices belong to mixtures of 98:29 spruce with bark and rape (grains/ cake), respectively 245:65 beech with bark and rape (grains/cake), of 0,06 EUR/kg, respectively 0,07 EUR/kg. To these prices are added the costs of utilities (electricity and water) and salaries of the staff, which amount to 0,08 EUR/kg.

Thus, the production price varies between at least 0,08 EUR/kg (for coal mixtures) and 0,15 EUR/kg (for rape grains / cake mixtures).

Table 4. Highest yielding mixtures for solid biofuels in the B1 category, their net calorific value and the price per kg (in ROL/kg)

Mass ratio [kg : kg]	Mixture	Calorific value (MJ/kg)	Price of raw material (EUR/kg)
98:29	Spruce (with bark) + Rape (grains / cake)	20,182	0,06
51:174	Lignite + Spruce (with bark)	20,077	0,02
147:26	Bark (coniferous wood) + Rape (grains / cake)	20,021	0,04
17:168	Coal + Spruce (with bark)	19,629	0,02
58:3	Bark (coniferous wood) + Lignite	19,368	< 0,01
58:17	Beech (with bark) + Lignite	19,330	0,04
245:65	Beech (with bark) + Rape (grains / cake)	19,295	0,07
168:3	Bark (coniferous wood) + Coal	19,259	< 0,01
69:290	Lignite + Poplar	19,070	0,02
147:29	Poplar + Rape (grains / cake)	18,940	0,05
168:17	Beech (with bark) + Coal	18,753	0,03
55:290	Lignite + Willow	18,615	0,02
23:280	Coal + Poplar	18,556	0,02
23:147	Rape (grains / cake) + Willow	18,491	0,04
11:168	Coal + Willow	18,146	0,01
85:22	Beech (with bark) + Miscanthus	17,746	0,03
23:85	Miscanthus + Poplar	17,737	0,02
145:22	Beech (with bark) + Rye (whole plant)	17,706	0,03
145:23	Poplar + Rye (whole plant)	17,695	0,01
105:11	Beech (with bark) + Rape (straw)	17,694	0,03
210:23	Poplar + Rape (straw)	17,682	0,01
23:85	Miscanthus + Willow	17,534	0,01
145:23	Willow + Rye (whole plant)	17,471	0,01
23:210	Rape (straw) + Willow	17,448	0,01
23:175	Barley (straw) + Willow	17,437	0,01

Figure 1 depicts the graphical interface for the algorithm. The user picks a material from the first list ("Materialul 1") and one from the second list ("Materialul 2") and press the button on the right ("Gaseste reteta!" – i.e., "Find the recipe!"). The software computes the mixture with the highest calorific value and returns the recipe, its calorific value, the price per kg and the chemical composition. In the case of a negative response, the software returns a message, "NU EXISTA SOLUTIE VALIDA (care sa respecte norme)" – i.e., "THERE IS NO VALID SOLUTION (with respect to the standards)" and does not list any calorific value, price of chemical composition.

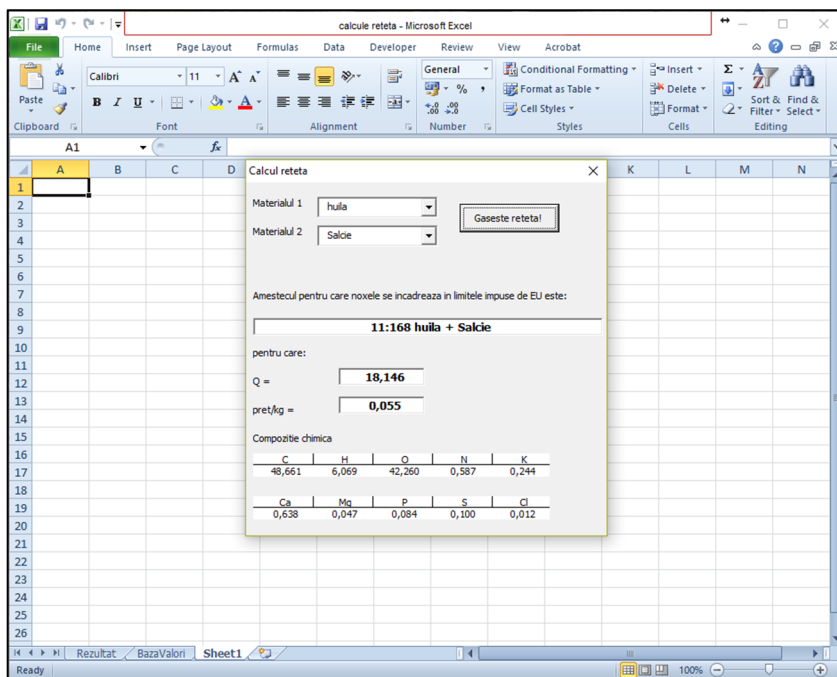


Figure 1. Graphical interface for the algorithm in case of a positive response (Excel 2010, authors' elaboration)

The brute-force algorithm we used is reliable, due to the fact that the total mass of the mixture cannot exceed 500 kg and the masses of the two individual components are non-negative integers. Thus, for each input of two raw materials, 499 cases are considered and verified (corresponding to mass ratios from 1:499 to 499:1).

Our approach is also slightly different from classical linear programming examples. This is because, instead of manually inputting two sets of data (corresponding to two types of raw materials), the inputs can be chosen from a database in which a finite number of raw materials is stored (in our case, 27 types of biomass) and also the number of possibilities to be checked is limited (in our case, 499 possibilities).

While this type of problem can be easily solved using the Solver add-in of Excel (Chandrakantha, 2011, Ayo and Ehiabhi, 2014), the Solver add-in requires that the numerical coefficients of the problem (in our case the chemical composition of the two raw ingredients, their prices per kg and their calorific value) together with the constraints (in our case the upper limit values for noxes) are manually inputted into the algorithm. Thus, there is a risk of bias which could influence the results. The user interface we devised allows the user to choose the two raw materials by name only, while the algorithm searches the existing database for the data needed in the computations. Thus, the risk of bias is minimized.

CONCLUSIONS

The current paper described an algorithm used to compute high-yielding calorific value mixtures with respect to a certain EU standard. The constants used during the computations (i.e., the chemical composition of dry matter, the maximum amount of N, S and Cl, and the maximum combined mass of the components) can be modified as needed. The user interface of the software can also be modified as needed (e.g., translated, completed with further details).

The main advantages of using our software solution are:

- the possibility of scientifically planning the production in order to obtain pellets with a higher calorific value, with respect to the maximum amount of noxes admitted by EU standards
- the costs of implementation for our solution are practically inexistent

With minimal changes, the algorithm and the software solution we developed can be used as a forecasting tool for pellets plants. Thus, a plant manager will be able to perform an accurate cost-benefit analysis and choose the most convenient solution available for his case.

REFERENCES

- ANAF, (2017). Medium prices for different types of crops https://static.anaf.ro/static/10/Anaf/AsistentaContribuabili_r/Judete_PreturiAgricole_2017.htm (accessed 02.10.2017)
- Ayo, A.S., Ehiabhi, T.A. (2014). Modeling Linear Programming Problem Using Microsoft Excel Solver. *Nigeria Journal of Business Administration*. 2014;12(1&2):163-79.
- Chen, D.S., Batson, R.G., Dang, Y. (2011). *Applied integer programming: modeling and solution*. John Wiley & Sons; 2011 Sep 20.
- Chandrakanth,a L. (2011). Using Excel Solver in optimization problems. In *Electronic Proceedings of the Twenty-third Annual International Conference on Technology in Collegiate Mathematics*. Denver, Colorado, March 17-20 2011 Mar 17 (p. 42)
- COM, (2013). A Clean Air Programme for Europe. <http://eur-lex.europa.eu/legal-content/EN/TXT/PDF/?uri=CELEX:52013DC0918&from=EN> (accessed 04.10.2017)
- EN 14961 (2010). Solid biofuels – Fuel Specification and classes, Part 1 – General requirements. CEN (European Committee for Standardization). January 2010.
- EN 14961-4 (2010). Solid Biofuels - Fuel Specifications And Classes - Part 4: Wood Chips For Non-Industrial Use. CEN (European Committee for Standardization). January 2010.
- Hardy, T. (2011). Combustion and fuels – tutorials [viewed 10.09.2017]. Available at: http://fluid.wme.pwr.wroc.pl/~spalanie/dydaktyka/combustion_mpe/combustion_mpe_tutorials.pdf
- Hartmann, H. (2013). *Handbuch Bioenergie-Kleinanlagen 2013* (3rd edition). Sonderpublikation des Bundesministeriums für Ernährung, Landwirtschaft und Verbraucherschutz und der Fachagentur Nachwachsende Rohstoffe, Gülzow (DE) 192 S., ISBN 3-00-011041-0, September 2013.
- Krajnc, N. (2015). *Wood Fuels Handbook*, Food and Agriculture Organization of United Nations, Pristina, ISBN 978-92-5-108728-2.
- Lee, M. and Kim, J. (2017). Feasibility study and benefit analysis of biomass-derived energy production strategies with a MILP (mixed-integer linear programming) model: Application to Jeju Island, Korea. *Korean Journal of Chemical Engineering*, 13:1-5.
- Nenu, P.F., Maris, S.A., Slavici, T. (2017). Optimization of renewable energy supply. *Actual Tasks on Agricultural Engineering, Proceedings of the 45th International Symposium on Agricultural Engineering*, Opatija, Croatia, 21-24 February, 459-464.

- Quijano-Aviles, M.F., Franco-Agurto, G.L., Suárez-Quirumbaym, K.B., Barragán-Lucas, A.D., Manzano-Santana, P.I. (2016). Linear programming formulation of a dairy drink made of cocoa, coffee and orange by-products. *Emirates Journal of Food and Agriculture*, 28(8):554.
- REN21 (2015). *Renewables 2015 Global Status Report*, Paris (REN21 Secretariat) ISBN 978-3-9815934-6-4.
- Romsilva, (2017). List of reference prices for woods for 2018. <http://www.rosilva.ro/files/content/bucuresti/Preturidereferinta2018.pdf> (accessed 02.10.2017).
- Ryan, K.N., Adams, K.P., Vosti, S.A., Ordiz, M.I., Cimo, E.D., Manary, M.J. (2014). A comprehensive linear programming tool to optimize formulations of ready-to-use therapeutic foods: an application to Ethiopia. *The American journal of clinical nutrition*. 2014 Dec 1;100(6):1551-8.
- SNC Pitesti (2017). Pitesti National Coal Company <http://snc-pitesti.ro/> (accessed 01.10.2017).
- Stolarski, M.J., Krzyżaniak, M., Warmiński, K., Niksa D. (2016). Energy consumption and costs of heating a detached house with wood briquettes in comparison to other fuels, *Energy Conversion and Management* 121: 71–83.
- USDA Foreign Agricultural Service (2017). EU biofuels annual 2017. Gain report no. NL7015, https://gain.fas.usda.gov/Recent%20GAIN%20Publications/Biofuels%20Annual_The%20Hague_EU-28_6-19-2017.pdf , 2017 (accessed 03.10.2017).



COMPARISON BETWEEN MISCANTHUS AND WILLOW ENERGY CONSUMPTION DURING GRINDING

Georgiana MOICEANU^{1*}, Mihai CHIȚOIU¹, Gheorghe VOICU¹,
Gigel PARASCHIV¹, Valentin VLĂDUȚ², Iulia GĂGEANU², Mirela DINCĂ¹

¹Department of Biotechnical Systems, University Politehnica of Bucharest,
Splaiul Independentei no. 313, Sector 6, Romania

²INMA Bucharest, Romania

*E-mail of corresponding author: moiceanugeorgiana@gmail.com

SUMMARY

Biomass cannot be consumed in its initial form because is hard to work with, it has a high volume, biomass transport is difficult, so it needs to be chopped/shredded. The energy consumption required for these operations is usually higher than the one necessary for the main operation. Experimental research done in the paper shows the differences between the energy consumption obtained when grinding *miscanthus* stalks and willow (*salix viminalis*). Experiments were done using a hammer mill equipped with an electric motor power of 22 kW and with 4 types of hammers, at different revolutions speed and considering similar experimental conditions. Speed revolution applied was 2400, 2550, 2700, 2800 and 3000 rpm. The experimental research revealed that hammer type A had an energy consumption lower than the other types when grinding *miscanthus* (an average of 55 kJ/kg), while for grinding willow the lowest energy consumption registered were for type B and C hammers (an average of 35 kJ kg⁻¹). Rotors revolution speed is an important element in reducing energy consumption, one step hammer showing a reduced energy consumption for revolution speeds between 2500 – 2700 rpm for grinding biomass out of *miscanthus*, while the two and three steps hammer presented lower energy consumption either for lower speed of revolution (2400 -2550 rpm) or higher speed of revolution (2850 -3000 rpm) considering the size of sieves orifices. It has to be said that the size of the sieves orifices was smaller for willow than for *miscanthus* for the grinding process. Using a value or another for revolution speed as well as different size of sieves orifices is done only by knowing the grinded material destination.

Key words: *Miscanthus x Giganteus*, *Salix Viminalis*, energy consumption, hammer mill, chopping

INTRODUCTION

In order to counter-act the effects of global warming and loosen the pressure on fossil fuels, scientists are constantly searching for environmental friendly sources for bio-renewable energy.

Biomass, which is an abundant source for creating pellets and briquettes, seems to be the most likely candidate as a constant source of renewable energy. Throughout recent decades, well-established machinery such as hammer mills, knife mills, balls mills, needle mills, shredders, linear knife grids, and disk attrition mills have been available for biomass size reduction (Igathinathane et al., 2009)

Hammer mills are amongst the most popular equipment used for biomass comminution, as a preparation process for pelletizing, but the high energy demand of this process is a constant problem in the pellet work flow.

The design process of hammer mills is highly important. Design must be realized taking factual working conditions into consideration, meaning the material type used for grinding and the drive kinematic regime. For a hammer mill crusher, with 100 kg h⁻¹ capacity and 750 rpm speed, verification with the Pro-E modelling software and the FEA model developed in Ansys, we could see an effective working cycle of approximately 167 hours (continuous). Verification was realized on the basis of drive shaft deflection, but also for the entire hammer rotor (Vijaya Kumar, 2013).

A major challenge for improving feedstock supply–conversion efficiency is to increase bulk (and therefore energy) density, flowability and digestibility of biomass feedstock. Biomass mechanical size reduction (comminution) can aid to increase the bulk density, and improve flowability and digestibility. To enhance packing density of biomass and produce pellets and briquettes, for instance, biomass feedstock has to be ground into 3–8 mm particles before compacting the material into a denser product (Mani et al., 2004). The use of hammer mill in milling provides a cheap, efficient and flexible milling process that can provide wide range of particulates and has been used in the study of grinding process of various biomaterials (Hill and Pulkinen, 1988), grinding of biomass and biomaterials is energy consuming and influences the cost of downstream production process (Searcy et al., 2007).

Hammer mills have achieved merit because of their ability to finely grind a greater variety of materials than any other machine. Scientist Himmel et al observed that total specific energy for size reduction of wheat straw using 1.6 mm hammer mill screen was twice that for a 3.2 mm screen. They used an indirect method of measuring electric power with a wattmeter and corrected with power factors, though motor efficiency was unaccounted (Himmel et al., 1985).

The literature reported that the energy consumptions of feedstock size reduction mainly depends on machine parameters such as motor speed, material storage capacity of the mill chamber, as well as cutting mechanism such as knife, hammer, ball or disk mills; material throughput characteristics; initial biomass form and properties (e.g. moisture content, temperature, chemical composition, etc.); and (iv) particle size and shape requirement of the final product (Bridgeman et al., 2010).

The grinding rates and energy requirements for the hammermilling process are influenced by a number of variables. These variables include the characteristics of the grains, the screen, the aspiration system, the hammer type and condition, and the feeding method of the hammermill (Kupritz, 1967).

An important parameter for hammer mill experimental data analysis is the specific grinding energy. Kayode and Koya (2013) showed that there is a linear correlation between

grinding energy and machine-material parameters, shaft speed, the feed rate and material bio-stiffness (in experimentation process were Palm kernel and coconut shells). Experimental verification showed that the used models adequately predicted comminution energy and was in accordance with Rittinger's classical theory.

Work reported by Agriculture Canada (1971) revealed that comparative grinding efficiencies for different thicknesses of hammers change with hammer tip speed. At the lowest speed tested, 3.18 mm hammers ground more efficiently than 1.59 mm hammers, but this relationship did not persist over the entire speed range. The increase in energy consumption was amplified as the tip speed was increased. Unfortunately, the reference did not give screen diameter or resultant particle size.

Average particle size and tip speed are known to be in aversely related, i.e. a higher tip speed results in a finer grind, all other things being equal (Rothwell and Southwell, 1986). However, results did not show any effect of the hammer tip speed on grinding quality of the grain. Since the two hammer types were not exactly the same length, the comparison of the thicknesses of the hammers, on an energy and economic basis, should take into account the effect they have on the grinding quality of the grain.

The degree of material grinding and specific grinding energy is usually used for mill qualitative indices verification. Choosing the right machine for grinding a specific material is achieved through parameter analysis correlated with material feed rate. Analysing the size of grinded particles is usually realized using the Rosin-Rammler model and other models (ex. Rosin-Rammler-Sperling-Bennet). It was experimentally proven that, for grinding cinnamon and coriander spices, hammer mills give the best performance. Analysed parameters during experiments were degree of uniformity in size and statistical average diameter of ground products, mean sizes of ground particles, Bond's work index, specific energy consumption for grinding, and flow (Tangirala et al., 2014).

Particle optimum dimension and biomass densification degree are very important factors, leading to a compromise between the cost of size reduction (grinding) and densification through compression and the efficiency in storage, transportation, as well as conversion. Experimental results for grinding and densification of *miscanthus* and switchgrass, incorporated in a system-level optimization model Bio Feed, showed that 4–6 mm was the optimal particle size for both *miscanthus* and switchgrass, mean costs being approximately 55 \$·Mg⁻¹, for *miscanthus* and \$·Mg⁻¹ for switchgrass (Shastri et al., 2013).

In the present paper, we researched the effect of motor speed on the energy consumption of a hammer mill grinding *miscanthus* plant and willow, using different speeds.

MATERIALS AND METHODS

In order to determine the energy consumption during grinding a Hammer mill MC 22 was used in this paper. Experiments were done at the National Institute of Research - Development for Machines and Installations Designed to Agriculture and Food Industry. The material was grinded through hitting and shearing between hammers mounted on the hammer disk and counter knives. Material used for testing is formed from *miscanthus* and willow crops.

Testing *miscanthus* and *salix viminalis* (willow) samples was done using sieves of different orifice sizes, four types of knives (A, B, C and D) and a rotor speed which was varied with the help of a frequency converter from 50 Hz (3000 rpm); 47.5 Hz; 45 Hz; 42.5 Hz and 40 Hz. Every sample subjected to grinding was weighted and then grinded material was analyzed.

Also, both *miscanthus* and willow has dimensions of about 12,5cm before fine grinding with hammer mill MC 22.

The samples moisture content was measured before grinding and had values above 8.52%, but the medium moisture content was about 10.3%. The four types of knives used for grinding are presented in figure 2.



Figure 1. Hammer mill MC 22

1. hammer mill; 2. exhauster; 3. cyclone with support and dust collector bag; 4. grinding material evacuation vent; 5. electric motor; 6. grinded material.

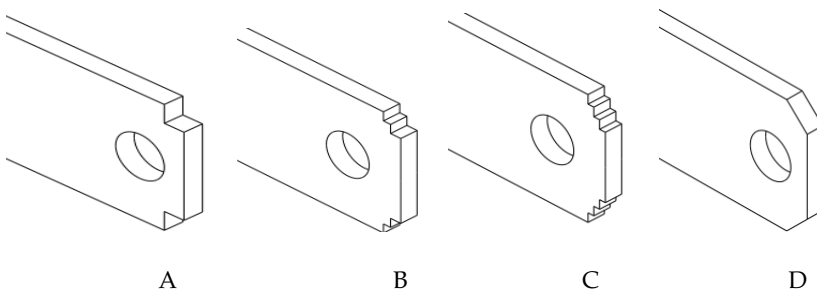


Figure 2. Four types of hammer used for testing (A – one step hammer; B – two steps hammer; C- three steps hammer; D – triangle hammer)

RESULTS AND DISCUSSION

For type B hammer – two steps hammer the result obtained after experimental research are being presented in Table 1. The conditions were similar for both materials for all testing times. The obtained results were processed with the help of Excel program in order to realize the variation graphs of energy consumption. Based on the results the energy consumption variation in correlation to the rotor speed for each knife was drawn.

As it can be seen from figure 3 the correlation coefficient was higher for *miscanthus* samples than for willow. The energy consumption recorded for *miscanthus* had the higher value for 25 mm sieve orifices and a revolution speed of 3000 rpm. Also, the values of energy consumption were medium for 16 mm sieve orifices for both crops.

The curves drawn for the energy consumption were best shown by using polynomial regression analysis for both *miscanthus* and willow (*salix viminalis*). Another fact than it can

be mentioned is that the correlation between energy consumption and rotor speed revolution is best shown for *miscanthus* sieve 25 mm and willow 10 mm sieve.

For type A hammer it can be seen that for *miscanthus* biomass there is a minimum point of energy consumption, for each of the 3 sieves used in correlation with hammer mill speed of revolution, this point moving on revolution axis considering the sieve orifices dimensions. The same thing cannot be said about *salix viminalis* which presents random variations for the energy consumption, especially for 16 mm sieve. Our recommendation for both crops would be using the 10 mm sieve because in this situation the energy consumption during grinding could be optimized in correlation to rotor speed of revolution.

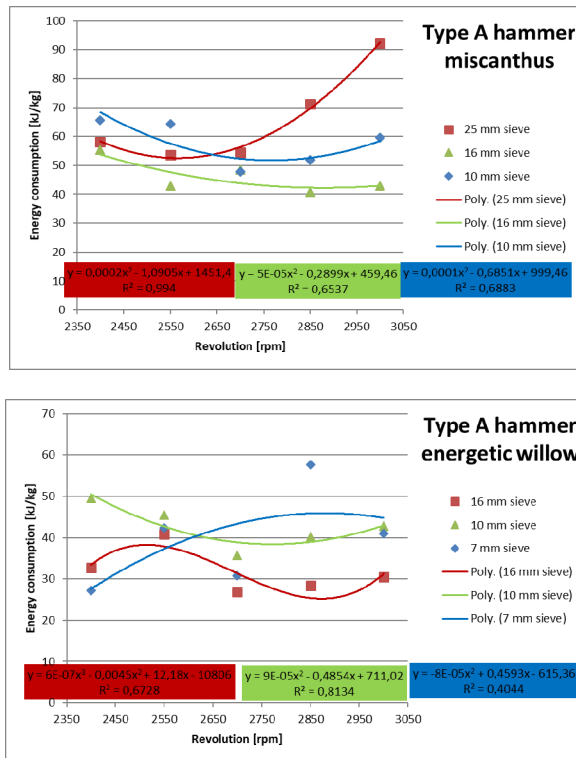


Figure 3. Energy consumption variation curve for type A hammer

Regarding the values for energy consumption it can be mentioned that for type A hammer the biggest value recorded for energy consumption for *miscanthus* samples was 92.21 kJ kg⁻¹ and the biggest value for type B hammer was 104.28 kJ kg⁻¹. Analyzing energy consumption resulted after grinding willow showed that the highest value for type B hammer was recorded for a 7 mm sieve and was 47.73 kJ kg⁻¹, meanwhile for type A hammer was 57.61 kJ kg⁻¹ for a 10 mm sieve. In order to better see these correlations variation curves were drawn and are presented in figure 4.

Table 1. Energy consumption (kJ/kg) obtained during experimental tests for knife type B

Sieve, mm	Miscanthus					Sieve	Willow				
	Rotor speed, rpm						Rotor speed				
	3000	2850	2700	2550	2400		3000	2850	2700	2550	2400
25	63.23	52.13	55.42	78.44	56.52	16	94.96	72.36	88.2	67.11	96.52
16	114.29	102.14	76.84	80.86	48.45	10	44.03	33.11	29.6	25.59	28.7
10	94.96	72.36	88.2	67.11	96.52	7	34.12	33.42	29.17	35.95	28.37

As it can be observed the correlation coefficient had values between 0.41 and 0.91 for *miscanthus* samples and 0.46 and 0.98 for willow. Also in both cases 16 mm sieve was the one that showed best the correlation between energy consumption and speed revolution.

For type B hammer it can be seen a minimum energy consumption for both *miscanthus* and *salix viminalis* for 10 mm sieve respectively 16 mm sieve and a rotors speed of revolution between 2500–2700 rpm. The other cases can be convenient in certain situations which can be concrete work conditions. For both types of biomass, hammer type B could be used in a minimum energy consumption situation with $\phi 10$ mm sieve respectively $\phi 7$ mm sieve at 2900 rpm.

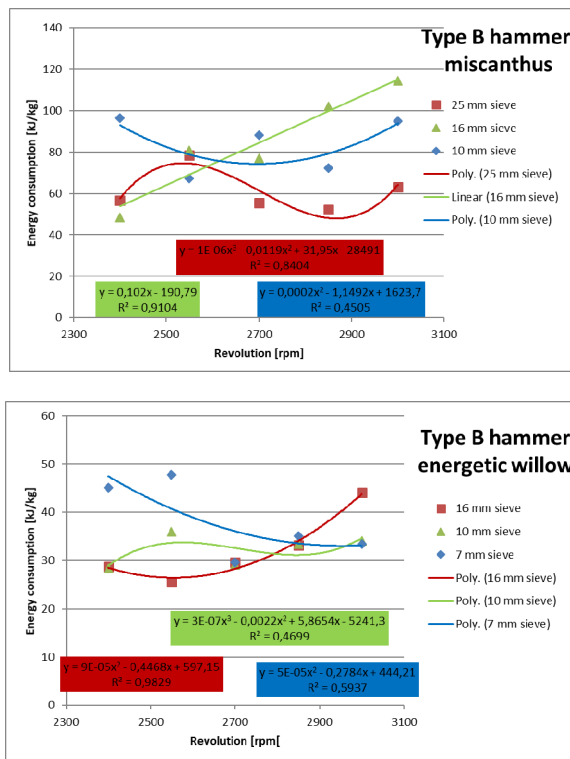


Figure 4. Energy consumption variation curve for type B hammer

Applying the same principal type C hammer was analyzed. Correlation coefficient R^2 showed a better correlation between parameters for 25 mm sieve for *miscanthus* and 16 mm sieve for willow. The energy consumption registered for willow for type C hammer presented a slightly higher value than type B hammer but about the same average value with type A hammer. For *miscanthus* it can be said that energy consumption recorded was higher for type C hammer than for A and B hammer. For *miscanthus* the value than stands out is 102.83 kJ kg⁻¹, the highest that was obtained for $\phi 10$ mm sieve and 3000 rpm. Comparing the energy consumption for all three sieves for *miscanthus* it reveals that for $\phi 25$ mm sieve the values were the smallest and for $\phi 10$ mm sieve the highest. For willow $\phi 16$ mm sieve had a medium value for energy consumption lower than $\phi 7$ mm sieve that had a medium value higher.

Considering type C hammer there are many convenient usage situations for all type of sieves, but it is obvious that a sieve with orifices dimensions bigger presents a minim of energy consumption. It is necessary to know the grinded biomass destination in order to choose correctly the sieves orifices dimensions, in this case the rotor speed of revolution being between 2500–2900 rpm, with small exceptions.

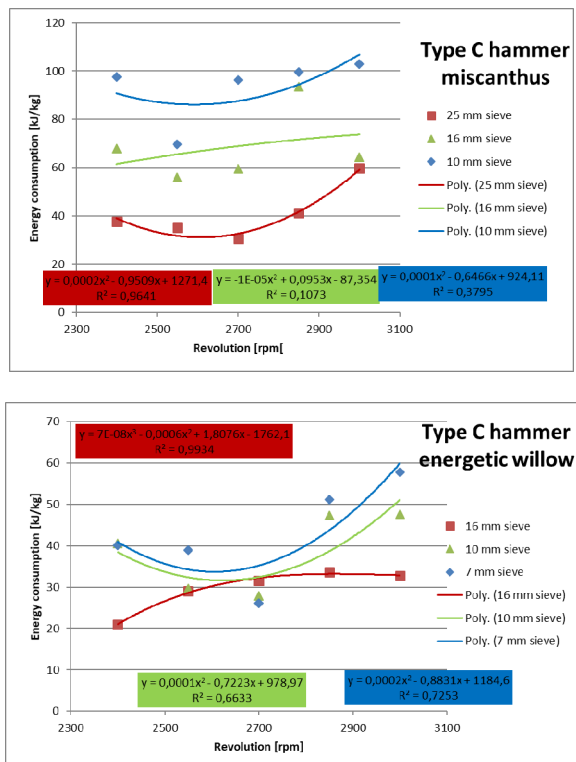


Figure 5. Energy consumption variation curve for type C hammer

Applying regression analysis on results obtained for type D hammer (triangle hammers) the variation graphs were drawn. As it can be seen from figure 6 the function used was

polynomial regression except for willow 7 mm sieve where data were best correlated with linear regression analysis. The curves resulted showed for example for *miscanthus* 10 mm sieve that the curve is concave which means that energy consumption recorded the highest value for a speed revolution of 2700 rpm.

Considering willow, the values for $\phi 16$ mm sieve presented increased value energy consumption from a speed revolution of 2400 rpm to 3000 rpm.

For type D hammer energy consumption variation in correlation to rotor speed of revolution, the most convenient sieves are $\phi 16$ mm sieve for *miscanthus* respectively $\phi 10$ mm sieve for *salix viminalis* (willow), as it can be seen from figure 6.

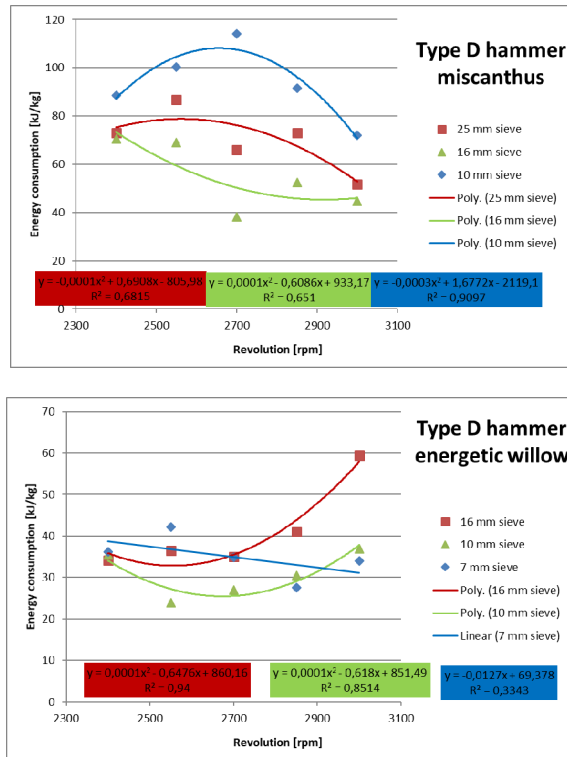


Figure 6. Energy consumption variation curve for type D hammer

Considering literature date in paper (Bitra et al., 2009) authors studied grinded process of switchgrass, wheat straw, corn stover with an instrumented hammer mill. Direct energy inputs were determined for hammer mill operating speeds from 2000 to 3600 rpm for 3.2 mm integral classifying screen. Total specific energy (kJ kg^{-1}) was defined as size reduction energy to operate the hammer mill plus that imparted to biomass. Total specific energy for switchgrass, wheat straw, and corn stover grinding increased by 37, 30, and 45% from 114.4 kJ kg^{-1} , 125.1 kJ kg^{-1} , and 103.7 kJ kg^{-1} , respectively, with an increase in hammer mill speed from 2000 to 3600 rpm for 90° - hammers (Bitra et al., 2009).

Considering data from specialty literature and it can be said that energy consumption resulted after grinding process was higher for type D hammer and lower for type A hammer for *miscanthus* samples. Applying a similar analysis on willow it can be said that the highest value of energy consumption was obtained for type C hammer and lower for type D hammer.

CONCLUSIONS

Hammer mills are usually used for agricultural biomass or energetic biomass grinding. Our experiments mainly targeted *miscanthus* biomass grinding and *salix viminalis* grinding, harvested with harvesting equipment, using a hammer mill with 1-1.5 tones h⁻¹ capacity (grinding hey biomass and corn stems), with a 22 kw engine and four types of hammers, at different revolution speeds.

Type A hammer presented a minimum for consumed grinding energy, at speeds of 2500-2700 rpm for biomass and *miscanthus*, no matter what sieve was used (ex. between 2700-2850 rpm for ϕ 16 mm and ϕ 10 mm and between 2400-2700 rpm for ϕ 7 mm sieve).

Using the type B hammer requires a careful choice for hammer rotor speed in relation to the sieve used, in order to have low energy consumption. For *miscanthus* biomass, we recommend the use of ϕ 25 mm sieve for speeds of 2700–2850 rpm, respectively a ϕ 10 mm sieve for speeds of approximately 2550 rpm. Using a ϕ 16 mm sieve is recommended only for low speeds (2400 rpm). In the case of willow biomass grinding we recommend the use of a ϕ 16 mm sieve for speeds of 2400-2550 rpm, or ϕ 7 mm for speeds of 2850-3000 rpm. The choice must take into consideration grinded biomass future destination.

Type C hammer is recommended to be used for average speeds, disregarding the sieve used, in the case of *miscanthus* grinding, as well as willow grinding, but only for small orifice sieves (ϕ 7 mm or ϕ 10 mm).

Type D hammer is our least recommendation, due to random variation in energy consumption in relation to the rotor speed and sieve used for experimentation.

In conclusion, choosing one hammer type over another, as well as the sieve, are realized taking into consideration future destinations for the grinded biomass (either for pellet processing, for obtaining briquettes, or for direct use).

Also, a conclusion that can be mentioned is that, for *miscanthus* biomass, energy consumption was slightly greater than in the case of *salix viminalis*. The highest value for specific energy consumption was recorded at 114.3 kJ kg⁻¹, for *miscanthus* biomass (using B and D hammer types), and the lowest value of 23.9 kJ kg⁻¹ was recorded for *salix viminalis* (using type C hammer, and a ϕ 16 mm sieve).

Our experimental results can be used by biomass grinding equipment users and designers in order to evaluate and propose better hammers for hammer mills, with edges that positively influence the grinding process (a smaller figure in energy consumption for a better grinding degree).

ACKNOWLEDGEMENT

This work was partially supported by the strategic grant POSDRU/159/1.5/S/137070 (2014) of the Ministry of National Education, Romania, co-financed by the European Social Fund – Investing in People, within the Sectoral Operational Programme Human Resources Development 2007-2013 and by a grant of the Romanian National Authority for Scientific

Research and Innovation, CNCS/CCCDI –UEFISCDI, project number PN-III-P2-2.1-BG-2016-0266, within PNCDI III, project entitled "Optimizing the composition of biomass mixtures for obtaining high quality pellets", ctr. 24 BG / 2016.

REFERENCES

- Bitra, V.S.P., Womac, A.R., Chevanan, N., Miu, P.I., Igathinathane, C., Sokhansanj, S., Smith, D.R. (2009). Direct mechanical energy measures of hammer mill comminution of switchgrass, wheat straw, and corn stover and analysis of their particle size distributions, *Powder Technology*: 193, 32–45.
- Bridgeman, T.G., Jones, J.M., Williams, A., Waldron, D.J., (2010). An investigation of the grind ability of two torrefied energy crops. *Fuel* 89, 3911–3918.
- Hill B, Pulkinen DA (1988). A study of pellet durability and pelleting efficiency in the production of dehydrated alfalfa pellets. Saskatchewan Dehydrators Association. New York, Springer.
- Himmel, M., Tucker, M., Baker, J., Rivard C., Oh, K., Grohmann, K. (1985). Comminution of biomass: hammer and knife mills, *Biotechnol. Bioeng. Symposium*, vol. 15, 39–58.
- Igathinathane, C., Womac, A.R., Sokhansanj, S., Narayan, S. (2009) Size reduction of high- and low-moisture corn stalks by linear knife grid system. *Biomass Bioenergy* 33, 547–557.
- Kayode, O. and Koya, O.A. (2013). Modeling the comminution energy requirements of two hard nut shells by hammer milling, *International Journal of Research in Engineering and Technology (IJRET)* 2(5): 235-239.
- Kumar, E.V. (2013). Design and analysis of rotor shaft assembly of hammer mill crusher, *International Journal of Engineering and Management Research* 3(2): 22-30.
- Kuprits. Y.N. (1965). *Technology of Grain Processing and Provender Milling*. (transl. from Russian, 1967). U.S. Department of Commerce, Springfield, Virginia.
- Mani, S., Tabil, L.G., Sokhansanj, S. (2004). Grinding performance and physical properties of wheat and barley straws, corn stover and switchgrass. *Biomass Bioenergy* 27, 339–352.
- Rothwell, T.M., P.H. Southwell. (1986). Modification and testing of a feed mill to reduce energy consumption and increase productivity. Report#2, Contract File #34SZ.01916-4-EC68. Engineering and Statistical Research Center, Agriculture Canada, Ottawa, ON;
- Searcy. E, Flynn. P, Ghafoori. E, Kumar. A (2007). The relative cost of biomass energy in transportation. *Application of Engineering in Agriculture*. pp. 136-140: 639-652.
- Tangirala, A.S., Charithkumar, K., Goswami, T.K. (2014). Modeling of size reduction, particle size analysis and flow characterisation of spice powders ground in hammer and pin mills, *International Journal of Research in Engineering and Technology* 3(12): 296-309.
- Shastri, Y.N., Miao, Z., Rodríguez, L.F., Grift, T.E., Hansen, A.C., Ting, K.C. (2014). Determining optimal size reduction and densification for biomass feedstock using the BioFeed optimization model. *Biofuels, Bioproducts and Biorefining* 8(3): 423-437.



EFFECTS OF UV-C IRRADIATION UPON THE REFERENCE STRAINS OF SOME FOOD- ASSOCIATED MICROORGANISMS

Cristian SORICĂ^{1*}, Mariana FERDES², Ion PIRNĂ¹, Valentin VLĂDUȚ¹ Elena
SORICĂ¹, Ion GRIGORE¹

¹ National Institute of Research - Development for Machines and Installations Designed to
Agriculture and Food Industry – INMA, Ion Ionescu de la Brad Blv. No. 6, Sector 1 Bucharest,
Romania

² University Politehnica of Bucharest, Splaiul Independentei No. 313, Sector 6 Bucharest, Romania

*E-mail of corresponding author: cri_sor2002@yahoo.com

SUMMARY

Within this paper are presented experimental researches on the possibility of using non-ionizing ultraviolet radiation UV-C to decrease the microbiological load existing on the external surfaces of horticultural products. Four microbial reference strains often associated with food (bacterial strains: *Escherichia coli* ATCC 11229, *Bacillus subtilis* subsp. *Spizizenii* ATCC 6633 and fungal strains: *Aspergillus niger* ATCC 15 475, *Fusarium oxysporum* MUCL 791) were irradiated to test the efficiency of UV-C decontamination performed by an installation for the decontamination of external surfaces of horticultural products. Due to the lethal mutations caused by UV-C radiations, in all cases the CFU/mL values were lower than the control. Also, it has been found that with a proper adjustment of the speed and distance from the UV-C source, it can be obtained an optimum configuration that will supply a maximum efficiency of the installation, in the given conditions.

Keywords: microbial populations, post-harvest treatment, UV-C radiation.

INTRODUCTION

Consumed fresh, fruits and vegetables, can be carriers of some optional pathogenic microorganisms such as bacteria, yeasts, molds, coming from soil, water, air, and other environmental sources. These microorganisms can cause either loss of horticultural products in the storage process, due to the postharvest decay process, or food-borne diseases with direct effects on consumer human health.

The presence of air, high humidity, and higher temperature during storage, increases the chances of spoilage. The most common spoilage is caused by different types of molds, some of those from genera *Aspergillus*, *Fusarium*, *Penicillium*, *Phytophthora*, *Alternaria*, *Botrytis*. A large number of molds produce toxic substances designated mycotoxins, as secondary metabolites. Some are mutagenic and carcinogenic, some display specific organ toxicity, and some are toxic by other mechanisms (Ray and Bunia, 2008).

Aspergillus is widely distributed and contains many species responsible for postharvest decay of fresh fruits including apples, pears, peaches, citrus, grapes.

Fusarium molds are associated with rot in citrus, apples, potatoes, and grains. Among the bacterial genera, species from *Pseudomonas*, *Erwinia*, *Bacillus* and *Clostridium* are most important.

Escherichia coli is a Gram negative, facultative anaerobic bacterium, belonging of *Enterobacteriaceae*. Many strains are nonpathogenic, but some of them are pathogenic to humans and animals and are involved in foodborne diseases.

Bacillus are cells aerobes or facultative anaerobes. All species form endospores with high resistance to radiation and heat. The genus *Bacillus* includes many species, some of which are important in foods, because they can cause foodborne disease and food spoilage. *Bacillus* is present in soil, dust and plant products, especially spices. Many species and strains can cause food spoilage.

Yeasts from genera *Saccharomyces*, *Candida*, *Torulopsis*. and *Hansenula* are associated with fermentation of some fruits, such as apples, strawberries, citrus fruits and dates (Jay et al., 2005).

In order to limit these losses, there have been used treatments with synthetic fungicide substances, whose residues remain on the surface of horticultural products, after the treatment. These residues are considered a potential threat to consumer health and especially children (Kasim and Kasim, 2007). Many outbreaks of gastroenteritis have been associated with the consumption of contaminated horticultural products (Franz and Van Bruggen, 2008). In order to reduce microbial contamination, there have been used widely, chlorine-based cleaning systems, being a significant interest in developing methods for safe and efficient decontamination of horticultural products (Hinojosa et al., 2013). Several alternative disinfectants (including hydrogen peroxide, organic acids and ozone) have been tested to reduce bacterial populations (Allende et al., 2006; Silveira et al., 2008; López-Gálvez et al., 2009).

Conventional thermal methods of food sterilization are unsuitable for fruits and vegetable destined for fresh consumption because of the heat which cause inevitable changes of color, smell, flavor and a loss of nutritional value (Perni et al., 2008).

Conventional antimicrobial treatments for fresh produce rely on chemical compounds and physical contact to inactivate and remove bacterial contamination. Recent research has identified a number of energy-based alternative technologies to improve the safety of fresh and fresh-cut fruits and vegetables: ultraviolet radiation, electron-beam irradiation, technology with pulsed visible light and technology with cold plasma. In some cases, such as UV light, these technologies have a substantial database of information regarding the use in other domains, and can be adapted to use with fresh produce. In other cases, such as with electron-beam irradiation, advances in technology need new researches. Other technologies, such as pulsed visible light and cold plasma, are newer areas of research that hold promise as antimicrobial processes which can reduce the viability of bacterial pathogens on fresh produce. Within the methods earlier mentioned, a special potential has the use of non-ionizing ultraviolet radiation UV-C. The wavelength range that varies between 200 and 280

nm, which is considered lethal to most types of microorganisms, affects the DNA replication of these microorganisms (Bintsis et al., 2000; Char et al., 2010). Non-Ionizing UV radiation can cause breaks of molecular chemical bonds and can induce photochemical reactions. The biological effects of UV radiation depends on the wavelength and the exposure time. UV-C ultraviolet radiation is already successfully used in various fields such as medicine (decontamination of air and medical instruments), environment (wastewater treatment), packaging industry (decontamination of packaging for various food products) etc. Worldwide, there are initiatives in using this method for decontaminating the outer surfaces of food products. As a postharvest treatment on fresh produce, UV-C irradiation has been proven beneficial to reduce respiration rates, control rot development and delay senescence and ripening in different whole or fresh-cut fruits and vegetables, such as apples, citrus, peaches, watermelon, grape berries, tomatoes, lettuce, baby spinach and mushrooms (De Capdeville et al., 2002; Lamikanra et al., 2005; Allende et al., 2008; Artés-Hernández et al., 2010; Escalona et al., 2010; Jiang et al., 2010; Fava et al., 2011; Manzocco et al., 2011).

According to existing studies in the field, among the most common microorganisms that can contaminate horticultural products, with adversely affect on storage or human health, are shown in table 1. For the destruction of these potentially pathogenic microorganisms, it is recommended to apply certain doses of UV-C radiation.

Table 1. Potentially pathogenic microorganisms and recommended doses (American Air & Water®; ClorDiSys Solutions)

Microorganism	UV-C radiation dose [$m \cdot W \cdot s \cdot cm^{-2}$] necessary for the destruction of	
	90 %	99 %
BACTERIA		
Bacillus anthracis	4.52	8.70
Bacillus subtilissubsp. spizizenii ATCC 6633	24	35
Clostridium tetani	13.00	22.00
Escherichia coli ATCC 11229	7	8
Mycobacterium tuberculosis	6.20	10.00
Salmonella enteritidis	4.00	7.60
Shigella dysenteriae	2.20	4.20
Staphylococcus aureus	2.60	6.60
MOLDS		
Aspergillus flavus	60.00	99.00
Aspergillus niger	132.00	330.00
Penicillium expansum	13.00	22.00
Rhizopus nigricans	111.00	220.00
Fusarium oxysporum	33.3	66.6
YEASTS		
Saccharomyces spores	8.00	17.60

The researches undertaken and presented within this paper, focuses on the evaluation of the germicidal effect of UV-C radiation against four representatives test strains cultivated in slants on appropriate nutritive media.

MATERIALS AND METHOD

For this study, it was used a new technical equipment - Installation for the decontamination of external surfaces of horticultural products, IDPH. This equipment is suitable for round shape fruits and vegetables or at least having a symmetry axle: apricots, apples, peaches, pears, plums, nectarines, cherries, sour cherries, strawberry, raspberry, peppers, tomatoes, mushrooms etc. The installation (fig. 1), is composed of the following main assemblies: frame - pos. 1, transport system - pos. 2, upper casing - pos. 3, lower casing - pos. 4, UV-C module - pos. 5, collection table - pos. 6, supply cuvette - pos. 7 and gearmotor - pos. 8. The main characteristic of the transport system is that it performs not only the transportation of the product along the installation but also the rotation of it around an axis perpendicular to the direction of advance. This characteristic assures a homogenous distribution of the UV-C radiation upon the exterior surfaces of the products. The main technical characteristics of the decontamination installation are presented in table 2.

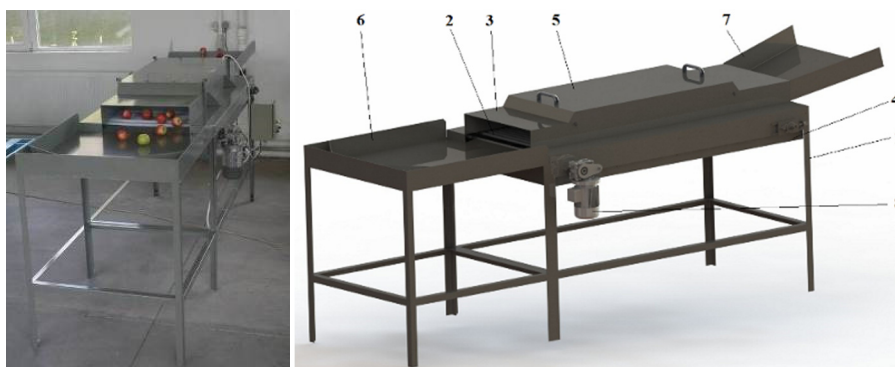


Figure 1. Installation for the decontamination of external surfaces of horticultural products, IDPH, (physical model – left side; 3D model – right side) (NUCLEU Research Program, 2014)

Table 2. The main technical characteristics of the decontamination installation

Dimensions (LxWxH)	3420x1215x1340 mm
Length of the transport system	1500 mm
UV Generator type	discharge lamps at low pressure mercury vapor
The wavelength of the emitted radiation	253.7 nm (UV-C)
Power of the UV-C lamps	55 W / pcs.
Number of UV-C lamps	5 pcs.

The bacterial and fungal strains were obtained from the Laboratory of Microbiology, Faculty of Biotechnical Systems Engineering, University Politehnica of Bucharest. Two strains of bacteria (*Escherichia coli* ATCC 11229 and *Bacillus subtilis subsp. spizizenii* ATCC6633) and two strains of molds (*Aspergillus niger* ATCC 15 475 and *Fusarium oxysporum* MUCL 791) were used. The microorganisms were cultivate in slants on appropriate nutritive media and maintained at 4°C.

In order to evaluate the germicidal effect of UV-C radiation against the four test strains, the fresh cultures were used to obtain appropriate decimal dilutions. The bacterial strains were tested on Nutrient agar and the fungal strains on Potato Dextrose Agar, in Petri dishes. Volumes of 0.1 ml cells suspension in sterile water were spread in a uniform manner on the agar surface. Immediately, the inoculated cultures were exposed to the action of UV-C radiation. The installation was prepared for three different working regimes, by varying the frequency of the supply current of the gear-motor, through the frequency converter currently existing within the automation installation (5 Hz, 25 Hz and 50 Hz). For each of the three different working regimes, there were performed determinations at different distances from the source of radiation (40 mm, 50 mm, 60 mm, 70 mm for *Escherichia coli* ATCC 11229 and *Bacillus subtilis* subsp. *spizizenii* ATCC6633 and 50 mm, 75 mm, 100 mm and 125 mm for *Aspergillus niger* ATCC 15 475 and *Fusarium oxysporum* MUCL 791). For these distances, there were determined the average intensities of UV-C radiation using a set of tools, sglux brand, Germany, comprising of the following elements: an intensity sensor for ultraviolet radiation, calibrated for the UV-C spectrum (UV Sensor "UV-Water-D"), a communication interface between the sensor and the laptop ("DIGIBOX" - CAN-to-USB converter) and a data acquisition software for the radiation intensity and air temperature, based on LabView programming environment ("DigiLog").

After the UV-C exposure at different working regimes and distances from the source of radiation, bacterial cultures were incubated at 30°C and the fungal cultures at 25°C in darkness, to allow the growth. After the time required to grow (48 hours for bacteria and 5 days for molds) the CFU/mL were estimated.

RESULTS AND DISCUSSION

After carrying out the experimental researches using the installation for the decontamination of external surfaces of horticultural products, there were achieved a series of results regarding the qualitative indices of the decontamination installation. These determinations were performed in order to calculate the UV-C radiation doses applied by the installation for each of the specific situation given by the combination between the working regimes and distances from the source of radiation. The UV-C radiation doses are important for the evaluation of the effects of UV-C irradiation upon the considered reference strains. These results are presented in Table 3.

Table 3. UV-C dose capable of being applied by the equipment

Distance from the source of radiation [mm]		125	100	75	70	60	50	40
Average intensity of UV-C radiation [$W \cdot m^{-2}$]		52.87	55.53	57.41	61.66	60.44	64.03	66.84
UV-C dose for various working regimes [$m \cdot W \cdot s \cdot cm^{-2}$]	5 Hz	131.43	138.04	142.72	153.29	150.26	159.17	166.17
	25 Hz	21.41	22.49	23.25	24.97	24.48	25.93	27.07
	50 Hz	8.56	8.99	9.29	9.98	9.78	10.36	10.82

Although it is known that the variation of radiation intensity is inversely proportional to the distance from the source of radiation, the value determined for the distance of 60 mm

appears not to comply with this law. This is due to specific geometric conditions regarding the position of the radiation deflector within the installation, which, for a distance slightly below 70 mm, obstructs the radiation from the adjacent lamps, affecting the radiation intensity measured in that position, as the sum of radiation intensities from adjacent sources in accordance with the superposition principle.

Some aspects during samples treatment with UV-C radiation, are shown in Figures 2.

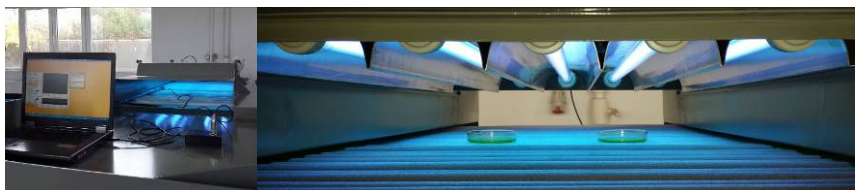


Figure 2. Aspects during samples treatment with UV-C radiation (NUCLEU Research Program, 2014)

Figure 3 presents the control samples for *Aspergillus niger* and *Fusarium oxysporum*, samples that was not treated with UV-C radiation. Figure 4 shows the best results obtained with UV-C irradiation treatment, also for *Aspergillus niger* and *Fusarium oxysporum*.

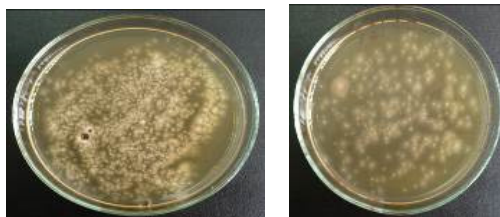


Figure 3. Control samples (*Aspergillus niger* – left and *Fusarium oxysporum* - right) (NUCLEU Research Program, 2014)



Figure 4. UV-C treated samples (*Aspergillus niger* – left and *Fusarium oxysporum* - right) - best results (NUCLEU Research Program, 2014)

The variation of the surviving units depending on the irradiation dose, for all the analyzed microorganisms except *Aspergillus niger*, is presented in the figure 5.

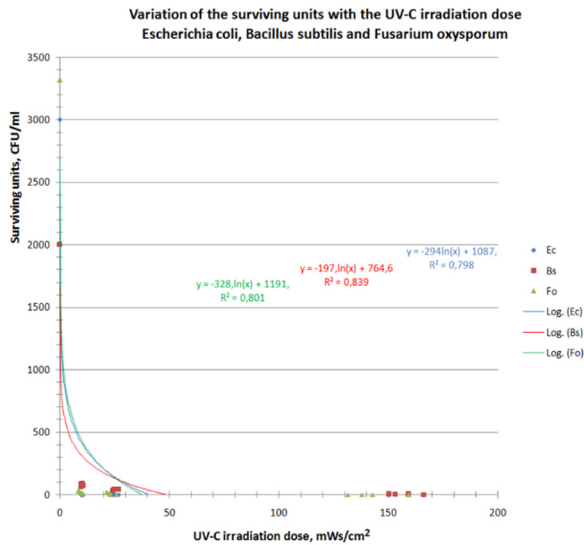


Figure 5. Variation of the surviving units with the irradiation dose, for *Escherichia coli*, *Bacillus subtilis* and *Fusarium oxysporum* (NUCLEU Research Program, 2014)

The variation of the surviving units depending on the irradiation dose, for *Aspergillus niger*, is presented in the figure 6.

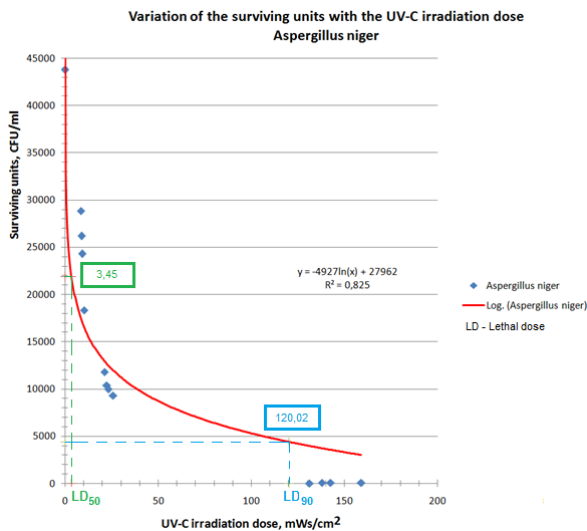


Figure 6. Variation of the surviving units with the irradiation dose for *Aspergillus niger* (NUCLEU Research Program, 2014)

Using the regression equations obtained from the processing of the experimental data, it has been calculated the LD50 and LD90 (Lethal Dose – LD“X” represents the dose at which “X”% of the units were destroyed). The results were as following:

Table 4. The Lethal Doses for the analyzed microorganisms

	Lethal dose [$m \cdot W \cdot s \cdot cm^{-2}$]			
	<i>Escherichia coli</i>	<i>Bacillus subtilis</i>	<i>Fusarium oxysporum</i>	<i>Aspergillus niger</i>
LD50	0.25	0.30	0.24	3.45
LD90	14.54	17.57	13.72	120.02
LD99	36.42	43.80	34.12	266.80

Aspergillus niger proved to be more resistant than the other strains of microorganisms considered. Analyzing the graphs in Figure 5 and 6 and data in Table 4 (obtained using the regression equations from the processing of the experimental data), it can be seen that for all microorganisms analyzed, at a minimum dose of $8.56 m \cdot W \cdot s \cdot cm^{-2}$ (the minimum UV-C dose capable of being applied by the equipment – Table 3), corresponding to the 125 mm distance from the radiation source and a frequency of 50 Hz for the supply current, the surviving units percent obtained was well below 50 %.

For a surviving units percent of 10 % - reduction log 1 CFU/mL (for *Escherichia coli*, *Bacillus subtilis* and *Fusarium oxysporum*), a minimum dose of $17.57 m \cdot W \cdot s \cdot cm^{-2}$ is required (Table 4), corresponding to a working regime characterized by the supply current frequency of 25 Hz and a distance of 125 mm from the radiation source (from Table 3 the minimum dose that is higher than the necessary dose - $17.57 m \cdot W \cdot s \cdot cm^{-2}$ is $21.41 m \cdot W \cdot s \cdot cm^{-2}$). In order to obtain the same 10 % surviving units percent, in case of *Aspergillus niger*, a minimum dose of $120.02 m \cdot W \cdot s \cdot cm^{-2}$ is required, corresponding to a working regime characterized by the supply current frequency of 5 Hz and a distance of 125 mm from the radiation source ($131.43 m \cdot W \cdot s \cdot cm^{-2}$).

It seems that for a 1 % surviving units percent - reduction log 2 CFU/mL, a dose obtained at the previous setting is sufficient for *Escherichia coli*, *Bacillus subtilis* and *Fusarium oxysporum* but *Aspergillus niger* needs a higher dose ($266.80 m \cdot W \cdot s \cdot cm^{-2}$) which can not be supplied by the equipment in a single passing. Still, analyzing the raw data obtained (not the ones obtained using the regression equations – which have values well above the real experimental data, in the right side of the graphs in Figure 6) it seems that the previous working regime (supply current frequency of 5 Hz; distance of 125 mm from the radiation source and the dose $131.43 m \cdot W \cdot s \cdot cm^{-2}$) is sufficient to obtain a 1 % surviving units percent - reduction log 2 CFU/mL in a single passing for all the analyzed microorganisms, including the more resistant *Aspergillus niger*.

Similar results have been obtained by Manzocco (2011) who studied the effect of UV-C light treatments on fresh-cut apple, confirming the germicidal effect with 1-2 log reduction in total viable counts. Also, he showed that treatments at an intensity exceeding $1.2 kJ \cdot m^{-2}$ ($120 m \cdot W \cdot s \cdot cm^{-2}$) had detrimental effects over the cells of the surface apple tissue.

CONCLUSIONS

Among the available methods for safe and efficient decontamination of horticultural products, the use of UV-C irradiation has a great potential and might be a viable solution, as a postharvest treatment on fresh produce.

From the experimental data it results that due to the lethal mutations caused by UV-C radiations, in all cases the CFU/mL values were lower than the control. Also, it has been found that with a proper adjustment of the speed and distance from the UV-C source, it can be obtained an optimum configuration that will supply a maximum efficiency of the tested decontamination installation.

REFERENCES

- Allende, A., Mcevoy, J.L., Luo, Y.G., Artes, F., Wang, C.Y. (2006). Effectiveness of two side UV-C treatments in inhibiting natural microflora and extending the shelf-life of minimally processed "Red Oak Leaf" lettuce. *Food Microbiol.* 23: 241–249.
- Allende, A., Selma, M.V., López-Gálvez, F., Villaescusa, R., Gil, M.I. (2008). Role of commercial sanitizers and washing systems on epiphytic microorganisms and sensory quality of fresh-cut escarole and lettuce. *Postharvest Biol. Technol.* 49: 155–163.
- Artés-Hernández, F., Robles, P., Gómez, P., Tomás-Callejas, A., Artés, F. (2010). Low UV-C illumination for keeping overall quality of fresh-cut watermelon. *Postharvest Biol. Technol.* 55: 114–120.
- Bintsis, T., Litopoulou-Tzanetaki, E., Robinson, R. (2000). Existing and potential applications of ultraviolet light in the food industry – a critical review. *J. Sci. Food Agric.* 80: 637–645.
- Char, C., Mitilinaki, E., Guerrero, S., Alzamora, S.M. (2010). Use of high intensity ultrasound and UV-C light to inactivate some microorganisms in fruit juices. *Food Bioprocess Technol.* 3: 797–803.
- De Capdeville, G., Wilson, C.L., Beer, S.V., Aist, J.R. (2002). Alternative disease control agents induce resistance to blue mold in harvested 'red delicious' apple fruit. *Phytopathology* 92: 900–908.
- Escalona, V.H., Aguayo, E., Martínez-Hernández, G.B., Artés, F. (2010). UV-C doses to reduce pathogen and spoilage bacterial growth *in vitro* and in baby spinach. *Postharvest Biol. Technol.* 56: 223–231.
- Fava, J., Hodara, K., Nieto, A., Guerrero, S., Alzamora, S. and Castro, M. (2011). Structure (micro, ultra, nano), color and mechanical properties of *Vitis labrusca* L. (grape berry) fruits treated by hydrogen peroxide, UV-C irradiation and ultrasound. *Food Res. Int.* 44: 2938–2948.
- Franz, E. and Van Bruggen, A.H.C. (2008). Ecology of *E. coli* O157:H7 and *Salmonella enterica* in the primary vegetable production chain. *Crit. Rev. Microbiol.* 34: 143–161;
- Hinojosa, A., Silveira, Ac., Ospina, M., Char, C., Saenz, C., Escalona, Vh. (2013). Safety of Ready-to-Eat Watercress Using Environmentally Friendly Sanitization Methods. *Journal of Food Quality.* 36: 66–76.
- Jay, J. M., Loessner, M. J., Golden, D.A. (2005). *Modern Food Microbiology*, Springer Science.
- Jiang, T., Jahangir, M., Jiang, Z., Lu, X., Ying, T. (2010). Influence of UV-C treatment on antioxidant capacity, antioxidant enzyme activity and texture of postharvest shiitake (*Lentinus edodes*) mushrooms during storage. *Postharvest Biol. Technol.* 56: 209–215.
- Kasim, M.U. and Kasim, R. (2007). *Tarim Bilimleri Dergisi-Journal of Agricultural Sciences.* 3: 413–419.
- Lamikanra, O., Kueneman, D., Ukuku, D., Bett-Garber, K.L. (2005). Effect of processing under ultraviolet light on the shelf life of fresh-cut cantaloupe melon. *J. Food Sci.* 70: C534–C539.

- López-Gálvez, F., Allende, A., Selma, M.V., Gil, M.I. (2009). Prevention of *Escherichia coli* cross-contamination by different commercial sanitizers during washing of fresh-cut lettuce. *Int. J. Food Microbiol.* 133: 167–171.
- Manzocco, L., Pieve, S. D., Bertolini, A., Bartolomeoli, I., Maifreni, M., Vianello, A. Nicoli, M.C. (2011). Surface decontamination of fresh-cut apple by UV-C light exposure: Effects on structure, colour and sensory properties. *Postharvest Biol. Technol.* 61:165–171.
- Manzocco, L., Da Pieve, S. and Maifreni, M. (2011). Impact of UV-C light on safety and quality of fresh-cut melon. *Inn. Food Sci. Emerg. Technol.* 12: 13–17.
- Mari, M., Neri, F., Bertolini, P. (2010). *Postharvest pathology - Book Series: Plant Pathology in the 21st Century*, 119-135.
- Perni, S., Liu, D.W., Shama, G., Kong, M.G. (2008). Cold atmospheric plasma decontamination of the pericarps of fruit. *J. Food Prot.* 71: 302-308.
- Ray, B. and Bunia, A. (2008) - *Fundamental Food Microbiology*, CRC Press.
- Silveira, A.C., Conesa, A., Aguayo, E., Artes, F. (2008). Alternative sanitizers to chlorine for use on fresh-cut "Galia" (*Cucumis melo* var. *catalupensis*) melon. *J. Food Sci.* 73(9): M405–M411.
- Tests conducted by Light Sources Inc - Orange, CT and verified by American Ultraviolet Company - Lebanon, IN. (2014), American Air & Water®, Inc., UV Irradiation Dosage Table, Retrieve at <http://www.americanairandwater.com/uv-facts/uv-dosage.htm>.
- Ultraviolet Light Exposure Dosage. (2014), ClorDiSys Solutions, Inc. of Lebanon, New Jersey, Retrieve at <http://www.clordisys.com/pdfs/misc/UV%20Data%20Sheet.pdf>.



CHANGES IN PHYSICAL AND CHEMICAL CHARACTERISTICS OF COFFEE BEANS AFTER THERMAL PROCESSING BY ROASTING

Tajana KRIČKA¹, Mateja GRUBOR^{1*}, Ivana TADIĆ², Vanja JURIŠIĆ¹,
Ana MATIN¹

¹ Department of Agricultural Technology, Storage and Transport, University of Zagreb
Faculty of Agriculture, Svetosimunska 25, 10000 Zagreb, Croatia

² Ministry of Agriculture, Ulica grada Vukovara 78, 10000 Zagreb, Croatia

*E-mail of corresponding author: mgrubor@agr.hr

SUMMARY

This work investigates the two most popular coffee cultivars (*Coffea arabica* and *Coffea canephora*) exposed to thermal processing of conduction drying by roasting at temperatures of 170 and 190 °C for 15 and 30 minutes air velocity in front of the coffee bean layer was 1 m/s. In order to determine how roasting temperature and time influence the characteristics of beans of both cultivars, physical properties (length, width, thickness and sphericity) and chemical properties (moisture, ash, and fat) of beans were study before and after toasting. The tests were performed according to the standard ISO methods, and for roasting a laboratory roaster with temperature and air rate control was used.

The obtained results corroborate that the dimension and sphericity of coffee bean increase in both cultivars, regardless of the roasting time and temperature. Also, moisture and oil contents significantly diminish in relation to temperature and time, while ash content is not influenced by roasting. All data were statistically analysed.

Key words: chemical characteristics, coffee beans, physical characteristics, roasting

INTRODUCTION

Coffee is one of the most widespread and popular beverages in the world. The name "coffee" is one of those rare and popular notions that are well known and equally appreciated in all parts of the world. The estimate is that around 2.25 billion cups of coffee are being drunk daily in the world today (Ponte, 2002).

It is a confirmed fact that this beverage is of Arabic origin and that some Arabic tribes were first to use coffee. It is believed that the Arabs started to brew peeled coffee beans sometimes around 1000 AD. That beverage was very much different from the coffee drink as we know today. The written sources give evidence that coffee was used by the mid-15th century in South Arabia, in Yemen's Islamic Sufi monasteries (Ilies, 2007).

The coffee production and trade have been increasing at a very high rate in recent times, especially for the last 50 years. Coffee is being grown in more than 50 countries and total world production amounts to about 8 million tons of green beans annually. However, since almost every country has a specific style for preparing coffee, the way of consumption of coffee differs from one country to another. The average world consumption is 4.8 kilograms per capita. In the European Union the average consumption is 5.8 kg (Šimunac, 2004).

Two most important commercial varieties of the species *Coffea* L. are known as *Coffea arabica* (Arabica coffee) and *Coffea canephora* (Robusta coffee). With their respective subspecies these two varieties have the highest share in the world production and consumption and the biggest economic importance. The other two varieties that are much less grown and used are *Coffea liberica* (Liberica) and *Coffea dewevrei* (Excelsa) (ICO, 2011).

In terms of production, export, industrial treatment and mass consumption the most important cultivars are *Coffea arabica* (Arabica) and *Coffea canephora* (Robusta coffee). The *Coffea arabica* bushes give good quality and highly valuable beans and, with a 61% share, this is the leading variety in the coffee production. Second to it is *Coffea canephora* (robusta) with a share of 39%, followed by *Coffea Liberica* and *Coffea Excelsa*, which have less importance in the global coffee production (ICO, 2011).

The composition of the green beans depends on cultivar and on soil texture and type. In order to enhance the chemical composition and enable their long-time use, coffee beans are subjected either to sun drying or to thermal processing by conduction drying in roasters.

The drying process significantly affects the quality of coffee and consequently the prices of final products (Illy and Viani, 1995).

Depending on coffee cultivar, bean quality and place of cultivation, there are different grades of coffee quality. Chemical analysis of caffeine in mature coffee beans is a measure for evaluation of the quality of coffee (Belay, 2011).

Thermal treatment is a procedure of subjecting a raw material to elevated temperature for a certain period of time with or without adding water steam. The energy that heats the material may be either direct heat, transferred from the site or from a high-temperature medium, or indirect heat obtained by converting another energy form (pressure) (Katić, 1997).

The process of drying includes simultaneous transfer of heat and moisture, at rates which depend on given conditions and production procedures and on characteristics of the material being treated. During this process moisture is always removed from the material surface in form of water steam. Generally, drying implies application of heat on the treated material by use of external heat source (Mujumdar, 2000).

Technological drying is the continuation and finalisation of natural ripening of a raw material, which was not possible by natural drying because of adverse weather conditions. In order to achieve as long-time and efficient storage as possible this process must be focused on preserving the quality of raw material (Sauer, 1992).

In the last few years, different procedures are being developed for preparation and treatment of products with primary aim to enhance their quality and digestibility. One of such procedures is conduction drying – roasting.

Roasting as a process is a procedure where products undergo thermal treatment. The process implies a number of physical and chemical changes, including heat exchange, chemical reactions and desiccation (Mujumdar, 2000).

In the production of premium quality coffee, care during the harvest and post-harvest procedures, such as processing, drying and storage, are vital elements for marketing of this commodity and for boosting producers' yield (Borem et al., 2013).

Roasting is the most efficient way to prepare beans for storage. Storage is considered as one of the crucial factors for preserving the quality of final product, meeting demand between the harvests, and ensuring the best market price for producers (Ribeiro et al., 2011).

Therefore, this work is focused on processing of beans of *Coffea arabica* (Arabica) and *Coffea canephora* cultivars (Robusta) through conduction drying by roasting at two temperature levels for two different times (at 170°C and 190°C; for 15 and 30 minutes). The aim is to determine whether the drying temperature and time have influence on qualitative, i.e., physical (volume, sphericity) and chemical (moisture, ash, and fats) properties of the composition of beans before and after roasting.

MATERIALS AND METHODS

Materials

The beans of two cultivars, *Coffea arabica* (Arabica) and *Coffea canephora* syn. *Coffea robusta* (Robusta) were used in the investigation.

Treatment

The drying process was conduction by use of a laboratory roaster („Seting inžinering“, Delnice, Croatia). The drying was carried out at air temperatures 170°C and 190°C and drying times were 15 and 30 minutes, air velocity in front of the coffee bean layer was 1 m/s.

The roaster consists of a housing with door and an 800 x 800 mm perforated plate. Hot air is sucked out of the roaster by an axial fan. Three PT 1000 probes are installed for measuring the air temperature at the roaster's entrance and exit. Initially the air temperature control is manual and then switched to automatic. Air speed after passing of the air through the sample layer is measured with a digital anemometer. The anemometer is Testo, Model 400, made in UK. The reading range of the digital anemometer is from 0.3 to 30 m/s, with accuracy of ± 0.2 m/s. The air rate, i.e., control of blower is also manual, by use of a phase shifting transformer. The set temperature was measured by a PT 1000 probe, just before the air flew through the sample.

Physical characteristics of coffee beans

The main values (length, width and thickness) of the selected bean samples after quartering, were determined by a slide gauge Digital Caliper 0-150 mm. The values were taken in 40 replications in both coffee cultivars, both in the natural samples and in those samples that were subjected to conduction drying by roasting at temperatures 170°C and 190°C for two different times (30 and 15 minutes).

The sphericity coefficient shows how shape of a body is similar to sphere. It is determined according to the Mohsenin equation (1970).

Chemical characteristics of coffee beans

Moisture content in coffee beans is determined according to protocol (HRN ISO 6673:1999) in laboratory dryer. Drying of the samples was conducted in a lab dryer (INKO ST-40, Croatia) with adjustable temperature control in a range from 40 to 240°C according to protocol. Accuracy of measurement is $\pm 0.1^\circ\text{C}$, and useful volume is 20 L.

Ash content is determined according to protocol (HRN ISO 1575:2001) in muffle furnace Nabertherm B170 (Lilienthal, Germany). Ash content in coffee beans was determined (for natural coffee beans samples and roasted beans samples) at temperature of 550°C in duration of 5 hours and 30 minutes.

Crude fats content is determined according to protocol (HRN ISO 6492:2001). Crude fats content in coffee beans (for natural beans samples and roasted beans samples) was determined on an extraction unit Soxhlet R 304 (Behr Labortechnik GmbH, Germany).

Statistical analysis

After collecting the data of laboratory research, the statistical analysis of the obtained data was carried out, in order to establish the differences due to the variety, temperature and roasting time for each variable. For this purpose, a statistical model which includes the effects of varieties, temperature and roasting time, as well as the effects of their interactions (cultivar x roasting temperature, variety x roasting time, roasting time x roasting temperature, variety x roasting temperature x roasting time) was made.

Model of this three-factorial experiment (cultivar x roasting temperature x roasting time = 2 x 4 x 4) was analyzed for each treatment using the statistical software package SAS version 9.1 (SAS Institute, Cary, NC, USA) using GLM procedures and Tukey test of multiple comparison with the level of significance $P \geq 0.05$.

RESULTS AND DISCUSSION

The results of the investigation whose aim was to determine how convection drying by roasting at two temperature levels for two different times (170°C and 190°C; 15 and 30 minutes) influence the changes of qualitative, i.e., physical and chemical properties of coffee beans are shown in Tables 1 to 4. The investigation was carried out on naturally dried coffee beans and beans dried through thermal processing. The cultivars that were used in this investigation are *Coffea arabica* (Arabica coffee) and *Coffea canephora* (Robusta coffee).

Physical properties of coffee beans before and after roasting

Coffee beans can have different shape and size (length, width and thickness) and these physical characteristics are conditioned by cultivar's properties and agro-meteorological conditions for growth and development of plants, which consequently influence the development and formation of fruits. As the results presented in Tables 1 and 2 show, the values regarding bean volume (length, width, thickness) and sphericity increase after thermal processing by roasting regardless of cultivar, temperature and time and they significantly diverge.

Table 1. Volume (length, width and thickness) and sphericity of naturally dried coffee beans

Cultivar	Length (mm)	Width (mm)	Thickness (mm)	Sphericity (%)
Arabica	5.52b±1.11	3.40 b±0.62	2.75 b±0.67	67.51a±0.38
Robusta	6.50 a±0.72	5.63 a±0.56	4.00a±0.33	66.54 a±0.54

Different letters within a column indicate significant differences at 5% level.

Table 2. Volume (length, width and thickness) and sphericity of roasted coffee beans

Parameters	Length (mm)	Width (mm)	Thickness (mm)	Sphericity (%)
Kultivar				
Arabica	9.04b±1.16	7.43a±0.80	3.65b±0.65	69.13a±5.99
Robusta	9.52a±0.78	7.35a±1.13	4.24a±0.69	70.16a±6.60
Temperature				
170°C	9.08b±1.17	7.42a±1.20	3.8b±0.85	69.87a±7.89
190°C	9.48a±0.79	7.36a±0.74	4.06a±0.57	69.42a±4.20
Time				
15 minute	9.09b±1.04	7.13b±1.02	3.68b±0.66	68.16b±6.19
30 minute	9.47a±0.95	7.67a±0.90	4.22a±0.70	71.14a±6.10

Different letters within a column indicate significant differences at 5% level.

In other raw materials these values generally decrease after drying, while coffee is specific in this regard as coffee beans increase with drying, which is in accordance with the investigation results obtained by Alessandrini et al. (2008), Bicho et al. (2011) and Ostervelda et al. (2003). In the investigations by Alessandrini et al. (2008), Bicho et al. (2011) and Osterveld et al. (2003) it was observed that the increased dimensions of thermally processed bean is a result of an intensive increase of bean volume (expansion of beans), which is an influence of internal transformations of gases occurring in the beans undergoing thermal processing because the application of hot air leads to a slight release of gases such as CO₂, CO and a part of moisture which is lost during the bean dehydration process.

Given the tendency of bodies to proximate to a sphere with 100% sphericity, coffee as a raw material has a 70% sphericity and, thus, falls under the category of raw materials with good physical characteristics and in line with the investigation results obtained by Severe et al. (2010) and as such it has high storage usability. Severa et al. (2010), report that in both naturally dried and thermally processed beans of Arabica and Robusta cultivars, sphericity values range from ca 70.87% to as much as 73.64%.

Pending on climate conditions, relief and types of soils and on geographical origin, the appearance and flavour of coffee as well as properties of fruit and bean largely vary. As it is already known, the development of plant and fruit and, therefore, the formation of beans are strongly influenced by weather conditions during bean ripening and final measures in processing and treatment of beans. All these procedures are reflected on chemical composition, structure and appearance of beans. The composition of green coffee bean primarily depends on plant species and, only secondly, on composition and type of soil. Therefore, physical characteristics of coffee beans depend on the conditions for plant

development, cultivar, fruit formation, harvest time and method, and conditions of processing, storage and transport.

Chemical properties of coffee beans before and after roasting

Table 3. Content of moisture, dry matter, ash and fats in naturally dried coffee beans

Cultivar	Moisture _{dm} (%)	Dry matter (%)	Ash (%)	Fat (%)
Arabica	9.25b±0.05	90.75a±0.05	4.22b±0.02	11.34 a±1.38
Robusta	9.383a±0.07	90.62 a±0.07	4.50a±0.03	7.79 a±0.14

Different letters within a column indicate significant differences at 5% level.

The results given in Table 3 show that naturally dried beans of both cultivars significantly diverge and that their moisture content is lower than indicated by Pittia et al. (2001) and Rivera et al. (2011). Pittia et al. (2001) in their investigations found the moisture content in natural beans of Arabica cultivar of 11.45%, and in Robusta cultivar of 11.26%. Riveraa et al. (2011) report that natural Arabica beans contain around 12% moisture.

However, the moisture content expectedly depends on year of cultivation.

Thermal processing of beans of both cultivars included two roasting times and temperature levels (170°C for 15 and 30 minutes; 190°C for 15 and 30 minutes) which is shown in Table 4.

Table 4. Content of moisture, dry matter, ash and fats in roasted dried coffee beans

Parameters	Moisture _{dm} (%)	Dry matter (%)	Ash (%)	Fat (%)
Cultivar				
Arabica	3.50a±0.44	96.50a±0.44	4.44b±0.13	10.94a±0.84
Robusta	2.97a±0.82	97.03b±0.87	4.62a±0.07	5.55b±2.08
Temperature				
170°C	3.199a±0.645	96.80a±0.64	4.51a±0.11	8.20a±3.28
190°C	3.273a±0.831	96.73a±0.83	4.55a±0.16	8.29a±3.17
Time				
15 minute	3.587b±0.789	96.41b±0.79	4.51a±0.16	8.17a±3.66
30 minute	3.884b±0.465	97.12a±0.47	4.56a±0.11	8.32a±2.72

Different letters within a column indicate significant differences at 5% level.

It is evident that the values for moisture and fats decrease, while roasting does not affect ash content. Casal et al. (2005) report that in beans of Arabica cultivar thermally processed at 160 °C the moisture content is 5.1%, at beans processed at 180 °C it is 4.0%, while beans processed at 200 °C contain 2.4% moisture. In beans of Robusta cultivar the moisture content in beans thermally processed at 160 °C is 5.3%, at 180°C it is 4.4%, while at 200 °C it is 2.4% in total dry matter. There is not observed significant differences in ash and fat content during roasting.

The post-roasting results for fats content are in accordance with Casal et al., 2005, as and the values for ash content are in accordance with the investigations by Franco et al., (2005). Franca et al. (2005) state that the average ash content in beans thermally processed at temperatures from 120 °C to 200 °C is 3.90% - 4.42% of total dry matter. Casal et al. (2005) state that the crude fats content in Arabica beans thermally processed at 160 °C is 11.2%, at 180 °C it is 10.9%, and at 200 °C it is 10.2% in total dry matter. In beans of Robusta cultivar the crude fats content in beans thermally processed at 160°C is 7.1%, at 180 °C it is 7.6%, and beans processed at 200 °C contain 6.6% crude fats content in dry matter.

CONCLUSION

Based on the results from these investigations on influence of conduction drying on chemical and physical characteristics of coffee beans of the cultivars Arabica (*Coffea arabica*) and Robusta (*Coffea canephora*), the following can be concluded:

- By observing physical characteristics of coffee beans during thermal processing of conduction drying by roasting it was found that with increasing temperature and roasting time beans increase in volume (length, width, thickness) and sphericity.
- By observing the changes of chemical characteristics of coffee beans of both cultivars during thermal processing of conduction drying by roasting it was determined that increased temperature and roasting time do not have significant influence on moisture, ash and crude fates contents, while at shorter roasting time there are minor diversions in changes of chemical characteristics of beans of both coffee cultivars.

REFERENCES

- Alessandrini, L., Romani, S., Pinnavaia, G., Rosa, D. M. (2008). Near infrared spectroscopy: An analytical tool to predict coffee roasting degree. *Analytica Chimica Acta*. 625: 95–102.
- Belay, A. (2011). Some biochemical compounds in coffee beans and methods developed for their analysis. *International Journal of the Physical Sciences*. 6(28): 6373-6378.
- Bicho, C. N., Leitão, A. E., Ramalho, C. J., Alvarenga, B. N., Lidon, C. F. (2011). Identification of nutritional descriptors of roasting intensity in beverages of Arabica and Robusta coffee beans. *International Journal of Food Sciences and Nutrition*. 62(8): 865–871.
- Borém, F.M., Ribeiro, F.C., Figueiredo, L.P., Giomo, G.S., Fortunato, V.A., Isquierdo, E.P. (2013). Evaluation of the sensory and color quality of coffee beans stored in hermetic packaging, *Journal of Stored Products Research*. 52: 1-6.
- Casal, S., Mendes, E., Oliveira, B. M. P. P., Ferreira, A. M. (2005). Roast effects on coffee amino acid enantiomers. *Food Chemistry*. 89: 333–340.
- Franca, A. S., Mendonça, C. F. J., Sami, D. O. (2005). Composition of green and roasted coffees of different cup qualities. *Lebensmittel Wissenschaft und Technologie (LWT)*. 38: 709 – 715.
- ICO (International Coffee Organization, England) (2011). All about coffee: Ten steps to coffee. 18: 24 – 35.
- Ilies, A. (2007). *Little Coffee Book*. Silverback Books Inc. San Francisco, United States.
- Illy, A. and Viani, R. (1995). *Espresso Coffee: The Chemistry of Quality*. Academic, London.
- Katić, Z. (1997). *Drying and dryers in agriculture*, book Multigraf, Zagreb. (in Croatian)
- Mohsenin, N.N. (1970). *Physical properties of plant and animal material*. Gordon and Breach, New York.
- Mujumdar, A.S. (2000). *Mujumdars' Practical Guide to Industrial Drying: Principles, Equipmena and New Developments*, Exergex Co., Monteral.

- Osterveld, A., Voragen, A.G. J., Schols, A. H. (2003). Effect of roasting on the carbohydrate composition of *Coffea arabica* beans. *Carbohydrate Polymers*. 54: 183–192.
- Pittia, P., Dalla, M. R., Lericis, C. R. (2001). Textural changes of coffee beans as affected by roasting conditions. *Lebensmittel Wissenschaft und Technologie (LWT)*. 34: 168 – 175.
- Ponte, S. (2002). "The 'Latte Revolution'? Regulation, Markets and Consumption in the Global Coffee Chain". *World Development (Elsevier Science Ltd.)*. 30:1099–1122.
- Ribeiro, F.C, Borém, F.M., Giomo, G.S., Ribeiro De Lima, R., Ribeiro Malta, M., Figueiredo, L.P. (2011). Storage of green coffee in hermetic packaging injected with CO₂. *Journal of Stored Products Research*. 47: 341-348.
- Riveraa, W., Velasco, X., Gálveza, C., Rincóna, C., Rosalesb, A., Arangob P. (2011). Effect of the roasting process on glass transition and phase transition of Colombian Arabic coffee beans. *11th International Congress on Engineering and Food: Food Science*. 00: 000 – 000.
- Sauer, D. B. (1992). *Storage of cereal grains and their products*. American Association of cereal Chemists, Inc. St, Paul, Minnesota, USA.
- Severa, L. (2010). Different approaches for coffee bean shape and contour determination. *Journal of Food Physics* Vol. 13. International society of food physicists. Budapest.
- Šimunac, D. (2004). *Book about coffee*. Grafem, Zagreb. (in Croatian)



UTJECAJ SORTE I RAZNOLIKOSTI VLAGE NA FIZIKALNA SVOJSTVA SJEMENA ULJANE REPICE

Ranko KOPRIVICA¹, Jan TURAN², Biljana VELJKOVIĆ^{1*},
Dušan RADIVOJEVIĆ³, Nikola BOKAN¹, Dragan ĐUROVIĆ¹,
Dragoslav ĐOKIĆ⁴, Igor BALALIĆ²

¹ Agronomski fakultet Čačak, Univerzitet u Kragujevcu, Cara Dusana 34 Čačak, Srbija

² Poljoprivredni fakultet, Univerzitet u Novom Sadu, Trg Dositeja Obradovića 8 21000, Srbija

³ Poljoprivredni fakultet, Univerzitet u Beogradu, Nemanjina 6 Zemun 11080, Srbija

⁴ Institut za krmno bilje, Krusevac, Globoder 37251, Srbija

* E-mail dopisnog autora: biljavz@kg.ac.rs

SAŽETAK

Istraživana su fizikalna svojstva tri standardne sorte uljane repice pri različitoj vlazi sjemena koja varira 6,04% - 21,17% za sortu Banačanka, 5,82% - 20,90% za sortu Jasna i 5,98% - 20,46% za sortu Slavica. Rezultati istraživanja pokazuju da je masa 1000 sjemena povećana sa 4,18 g na 4,94 g sorte Banačanka, sa 4,74 g na 5,61 g sorte Jasna i sa 4,11 na 4,81 g sorte Slavica. Volumen sorte Jasna iznosio je 4,72 mm³ - 5,49 mm³ i bio je značajno veći od sorte Banačanka 4,07-4,93 mm³ i sorte Slavica 4,12-4,81 mm³. Gustoća sjemena je smanjena ovisno od vlage sjemena i varirala je kod sorti Banačanka 1023,18 - 996,97 kgm⁻³, Jasna 1009,31 - 992,70 kgm⁻³ i Slavica 1012,96 - 992 kgm⁻³. Za sve tri sorte uljane repice poroznost je povećana s porastom vlage sjemena. Poroznost sjemena sorti Jasna (35,97-38,43%) je veća od Banačanka (35,42-38,23%) i Slavica (35,19-37,07%). Hektolitarska masa varira s različitom vlagom sjemena 665,82 - 615,84, 646,24 - 611,22, 656,57 - 624,66 kgm⁻³ za sorte Banačanka, Jasna i Slavica redom. Statički kut nasipanja povećan je za sorte Banačanka, Jasna i Slavica u rasponu 22,96° - 28,05°, 24,64° - 29,66° i 24,63° - 29,61°, s povećanjem vlage sjemena. Najveću vrijednost dinamičkog kuta stošca imala je sorta Jasna (20,32-25,90°), zatim sorta Slavica (21,03-25,58°), dok je najniži kut bio kod sorte Banačanka (19,22-24,66°). S porastom vlage sjemena povećava se koeficijent trenja. Koeficijent statičkog trenja sorti Jasna i Slavica veći je u odnosu na sortu Banačanka.

Ključne riječi: uljana repica, sjeme, vlaga, fizikalna svojstva

UVOD

Uljana repica se uzgaja na površini od oko 36 milijuna hektara i jedna je od četiri najvažnije uljane kulture na svijetu, pored soje, palme i suncokreta. Prema statističkom uredu Republike Srbije za razdoblje od 2005. do 2015. godine, u Republici Srbiji se uzgaja uljana repica u prosjeku 11.089 ha s urodom od 2,5 t ha⁻¹.

Procesi dorade, skladištenja i očuvanja sjemena ratarskih biljaka temelje se na primjeni različitih tehnoloških operacija koje se izvode na temelju razlika u fizikalnim karakteristikama sjemena (vlaga, oblik, dimenzija, sferičnost, masa 1000 sjemenki, volumen pojedinog sjemena, poroznost mase sjemena, zapreminske-hektolitarske mase, vlastite gustoće, statičkog i dinamičkog kuta unutrašnjeg trenja - kut slobodnog pada, statički koeficijent vanjskog trenja po poznatoj plohi) Babić i Babić, (2007). Bez poznavanja fizikalnih svojstava sjemenskih usjeva danas je nezamislivo konstruirati strojeve za sjetvu, berbu, transport i projektiranje skladišta, opremu za sušenje i preradu sjemena. Istraživanja mnogih autora pokazuju da se fizikalna svojstva sjemena uljane repice mijenjaju ovisno o sadržaju vlage u sjemenu i od njega ovisi kvaliteta sjemena na temelju kojih se utvrđuju parametri za proces sušenja, skladištenja i dorade (Razavi i sur., 2009, Izli i sur., 2009).

Za praktičnu primjenu u projektiranju i kontroli strojeva, postavljen je cilj istraživanja da se odredi utjecaj različitih razina vlage na procjenu promjena u osnovnim fizikalnim svojstvima sjemena uljane repice.

MATERIJALI I METODE

Za mjerenje fizikalnih svojstava koristili su se neoštećena i čista sjemena bez prisutnosti stranih primesa sorte Banačanka, Jasna i Slavice sa vlagom od 6%, 11%, 16% i 21%. Početni sadržaj vlage zrna je određen korištenjem standardne metode sušenja u sušnici. Dovođenje vlage do željene razine vlage sjemena postiže se dodavanjem određene količine destilirane vode u zrnju prema metodi (Calisir i sur., 2005, Razavi i sur., 2009, Izli i sur., 2009).

Volumen određenog broja sjemena određuje se izravnom metodom nalijevanja sjemena tekućinom čiste destilirane vode na temelju koje se izračunava volumen pojedinačnog sjemena (Babić i Babić, 2007, Lončarević 2011, Mehandžić Stanišić, 2013, Jukić i Koceva Komlenić, 2017).

Poroznost zrnaste mase određena je također izravnom metodom nalijevanja tekućine (Babić i Babić, 2007, Razavi i sur., 2009, Izli i sur., 2009, Lončarević, 2011, Mehandžić Stanišić, 2013).

Nasipna masa-gustoća (hektolitarska gustoća, volumna masa) određena je metodom koju navodi (Razavi i sur., 2009, Lončarević, 2011). Na temelju mjerenja dviju fizikalnih svojstava nasipne gustoće mase i poroznosti, izračunata je gustoća zrna po metodi (Mehandžić Stanišić, 2013). Masa od 1000 zrna određena je na uređaju za automatsko brojanje Elmor S3, a zatim utvrđena masa zrna mjerenje na analitičkoj vagi. Statični i dinamički kut unutarnjeg trenja (kut stošca) određen je metodom (Babić i Babić, 2007, Razavi i sur., 2009, Izli i sur., 2009, Lončarević, 2011) pomoću šupljeg zarubljenog lijevka (kupole - konusa) i ploče poznatog promjera. Dinamički kut unutarnjeg trenja - kut konusa (kut punjenja) nastaje dok je rasuti materijal u pokretu, što se u praksi događa tijekom manipulacije. Stoga, za praksu, dinamički kut unutarnjeg trenja je važniji od statičnog kuta unutarnjeg trenja. Za eksperimentalno određivanje koeficijenta statičkog vanjskog trenja, korišten je poseban mehanički uređaj Tribometar T1, koji funkcionira na principu kose ravni i trenja po poznatoj plohi s preciznošću od 0,02 (Radonjić i sur., 2011).

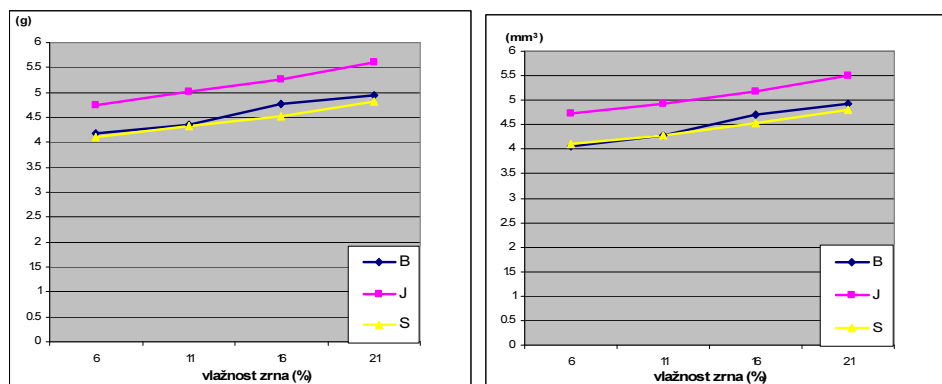
REZULTATI I RASPRAVA

Vlažnost sjemena uljane repice varira ovisno o stupnju zrelosti, vlažnosti zraka tijekom i poslije žetve. Kada je vlaga uljane repice poznata, zna se kako ju pravilno skladištiti odnosno treba li ju sušiti.

Istraživanje fizikalnih svojstava provedeno je na vlazi sjemena uljane repice sorti Banačanka 6,04%, 11,44%, 16,03% i 21,17%, Jasna 5,82%, 11,15%, 15,91% i 20,90%, i Slavica 5,74%, 11,11%, 15,97% i 20,84%.

Kod svih sorti uz povećanje vlage sjemena na svim razinama, težina od 1000 sjemenki je povećana. Najveću masu 1000 zrna imala je sorta Jasna od 4,74g do 5,61g, a najmanju sorta Slavica od 4,11 g do 4,81g pri najnižoj i najvišoj vlazi sjemena (Sl. 1).

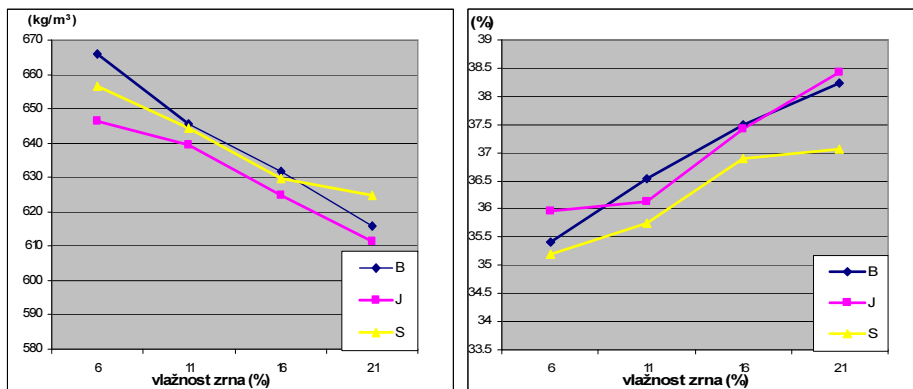
Prosječni volumen pojedinačnog sjemena sorte Jasna bio je znatno veći (4,72-5,49 mm³) u odnosu na sortu Banačanka (4,07-4,93 mm³) i Slavicu (4,12-4,81 mm³) na najnižoj i najvišoj vlazi sjemena (slika 2). Povećanje volumena sjemena sorte Jasna posljedica je veće veličine (krupnoće sjemena) koje apsorbira više tekućine u odnosu na druge dvije sorte. Rezultati istraživanja o utjecaju povećanja vlage na povećanje volumena sjemena repice su u skladu s rezultatima Calisir i sur. (2005), Razavi i sur. (2006) i Izli i sur. (2009). Moguće male razlike u vrijednostima volumena sjemena istraženih sorti su posljedice varietalnih svojstava i agroekoloških uvjeta uzgoja.



Slika 1. i 2. Utjecaj vlage sjemena na masu 1000 zrna i volumen sjemena
Figure 1. and 2. Influence of seed moisture on thousand-seed weight and seed volume

Vrijednost nasipne gustoće - mase (volumne mase, gustoće mase, hektolitarske mase) svih sorata smanjuje se s povećanjem vlage sjemena od 6%, 11%, 16% do 21%. Smanjenje nasipne gustoće u sorti Banačanka iznosi od 665,82 kg m⁻³ do 615,84 kg m⁻³, Jasna sorte od 646,24 kg m⁻³ do 611,22 kg m⁻³, a sorte Slavica s 656,57 kg m⁻³ na 624,66 kg m⁻³ (Slika 3). Slični rezultati dobiveni su za nasipnu gustoću sorti Banačanka (654,50 kg m⁻³) i Slavicu (661,50 kg m⁻³) u proizvodnoj godini 2009/2010 od strane Vujaković i sur. (2015).

Prema vlastitim istraživanjima, vlaga sjemena značajno je utjecala na vrijednosti nasipne gustoće ($p \leq 0.01$), što je u skladu s Razavi i sur. (2006), Duc i sur. (2008), Szot (2008), Habzavi i sur. (2009), Razavi i sur. (2009), Izli i sur. (2009).



Slika 3. i 4. Utjecaj vlage sjemena na hektolitarsku-nasipnu masu i poroznost sjemena
Figure 3. and 4. Influence of seed moisture on bulk density and seed porosity

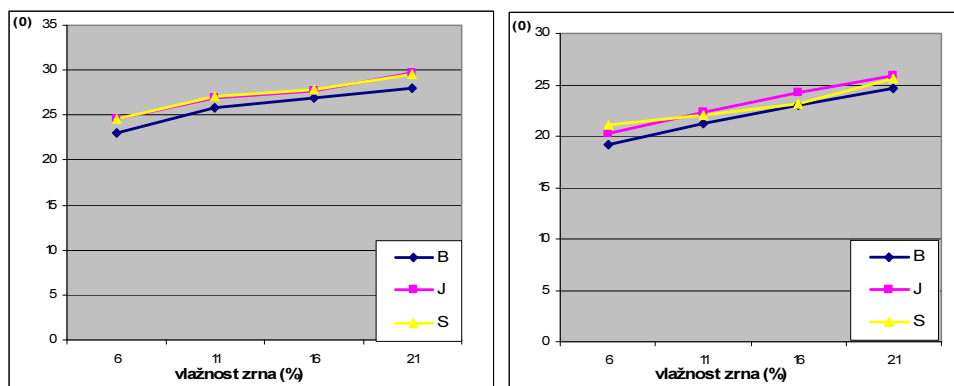
Linearno s povećanjem sadržaja vlage sjemena, nasipna gustoća se smanjuje kao rezultat povećanog sadržaja vode i smanjenog sadržaja suhe tvari u ukupnom volumenu sjemena. Promjena volumena zrna zbog oteklina rezultira manje zrna u istoj jedinici volumena.

Najmanji poroznost sjemenske mase sorte Slavica varirao je od 35,19% do 37,07% i značajno se razlikovao od vrijednosti sorti Jasna (35,97% -38,43%) i Banačanka (35,42% -38,23%) (sl. 4.). Sorta Jasna ima veće sjeme, pa između njih postoji veći prazni prostor i veću poroznost sjemenske mase. Rezultati istraživanja o utjecaju sorte zrna i vlage na poroznost mase zrna usporedivi su s onima iz Calisir i sur. (2005), Razavi i sur. (2006), Szot (2008), Izli i sur. (2009). Zabilježeno je značajno smanjenje gustoće sjemena s povećanom vlagom sjemena samo na najnižoj i najvišoj razini. Gustoća sjemena sorte Banačanka smanjena je s 1023,18 k g m⁻³ na 996,97 k g m⁻³, sorte Jasna od 1009,31 k g m⁻³ do 992,70 k g m⁻³ i sorte Slavica od 1012,96 k g m⁻³ do 992,70 k g m⁻³ u sadržaju od 6% i 21%. Relativno smanjenje gustoće sjemena s povećanjem udjela vlage u sjemenu može se pripisati laganom povećanju mase sjemena u odnosu na povećanje volumena, zbog većeg udjela vode u njemu, a manji udio suhe tvari. Vrijednosti gustoće sjemena su skladu s rezultatima Izli (2009), Hazbavi i sur. (2009) i Razavi i sur. (2006).

Statični i dinamički kutovi unutarnjeg trenja pokazuju sipkost sjemenske mase, a ta veličina uzima u obzir trenje između sjemena i drugih sastojaka. Statični i dinamički kut unutarnjeg trenja (punjenja), - kut konusa - stošca, kojeg napravi zrna masa pri slobodnom padu značajna je u proračunu korisnog prostora ćelija silosa i komore, proračunu opterećenja na zidove i podove skladišta (Jukić i Koceva Komlenić, 2017).

Vrijednosti statičkog kuta stošca kreću se od 22,96° sorata Banačanka, od 24,64° do 29,66° sorte Jasna i od 24,63° do 29,61° Slavica na najnižem i najvišem sadržaju vlage sjemena (Sl. 5).

Povećanje sadržaja vlažnosti zrna povećava se i statički kut stošca što također zaključuju autori Krička i sur. (1998), Krička i sur. (1999), Hong i sur. (2008), Szot i sur. (2007), Szot (2008), Razavi i sur. (2006), Izli i sur. (2009). Najmanji kut stošca sorte Banaćanka se značajno razlikovao od ostalih dviju sorti. Najveći kut stošca izmjeren je u sorti Slavica. To se može tumačiti činjenicom da je ova sorta imala sitnije sjeme, tako da je povećana kontaktna površina i kohezivnost između sjemena i njegove bolje prilagodbe na konusu- stošcu. Ovisno o porastu sadržaja vlage sjemena od 6% do 21% vrijednosti dinamičkog kuta stošca varirao je od 19,22° do 24,66° sorti Banaćanka, od 20,32° do 25,90° Jasna i od 21,03 do 25,58 i Slavica (slika 6). Dinamički kut unutrašnjeg trenja - kut konusa povećava se s porastom vlage u sjemenu, konstatuju rezultati istraživanja Sot i sur. (2007), Hong i sur. (2008) i Szot (2008).



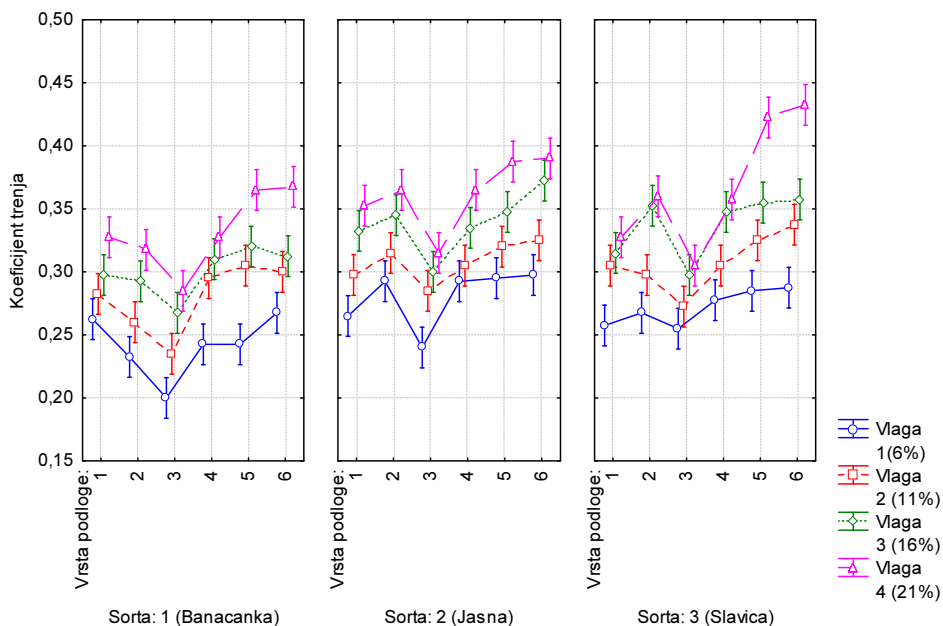
Slika 5. i 6. Utjecaj vlažnosti zrna na statički i dinamički kut unutrašnjeg trenja (nasipanja), - kut stošca

Figure 5. and 6. Influence of seed moisture on the static and the dynamic angle of repose

Statički koeficijent vanjskog trenja sorte Jasna (0,322) i Slavica (0,321) su znatno veći od sorte Banaćanka (0,288) na svim ploham i vlage sjemena osim na plohi od pocinčanog lima pri sadržaju vlažnosti zrna sa 6%.

Kod svih ploha bez obzira na sortu statički koeficijent vanjskog trenja se značajno povećava sa porastom vlage sjemena. Neovisno od sorte i vrste plohe, najmanji statički koeficijent vanjskog trenja (0,264), postupno se povećao s 0,298 (11%) na 0,325 (16%) kako bi se postigla najveća vrijednost (0,354) pri najvećem sadržaju vlage u sjemenu od 21% (Sl. 7).

Koeficijent vanjskog trenja se povećava s povećanjem udjela vlage u sjemenu zbog veće prisutnosti vode u sjemenima i kohezijskim silama. Prema rezultatima istraživanja Razavi i sur. (2009), statički koeficijent vanjskog trenja na različitim ploham povećava se nelinearno s povećanjem vlage u sjemenu.



Plohe: 1- pocinčani lim, 2- čelični lim, 3- nehrđajući čelični lim, 4- aluminijski lim, 5- plastika, 6- šper ploča

Slika 7. Statički koeficijent vanjskog trenja u zavisnosti od interakcije vrste plohe, sorte i vlage sjemena

Figure 7. Static coefficient of external friction depending on the interaction of the type of surface, variety and moisture of the seed

Na svim razinama vlage sjemena, najviši statički koeficijent vanjskog trenja nalazi se na plohi od šper ploče (0,284-0,397) i plastične (0,274-0,392), a zatim na plohi od aluminijske (0,271-0,350), čelične (0,264-0,347) pocinčanog lima (0,262-0,336) i najmanji na limu od nehrđajućeg čelika (0,232-0,302). Ovakav redoslijed je posljedica hrapavosti površina plohe, pa je najmanji statički koeficijent vanjskog trenja sjemena svih sorti zabilježen na glatko poliranoj površini lima od nehrđajućeg čelika. U istraživanju (Izli i sur., 2009, Calisir i sur., 2005) redoslijed statičkog koeficijenta vanjskog trenja je isti kao u našem istraživanju za plohe šper ploče, limova čelika, aluminijske i lima od nehrđajućeg čelika. Rezultati vlastitih istraživanja su u saglasju s rezultatima Hong i sur. (2008) za statički koeficijent vanjskog trenja za plohe plastike, pocinčanog lima i lima nehrđajućeg čelika.

ZAKLJUČAK

Na temelju poznate početne vlage sjemena utvrđuju se parametri i duljina procesa sušenja zrna. Tijekom skladištenja zrna u skladištima, praćenjem vlage i stanja sjemena poduzimaju se određeni tehnološki postupci kako bi se očuvala njegova kvaliteta.

Rezultati istraživanja pokazuju da su vrijednosti fizikalnih svojstava repice sorte Banačanka, Jasna i Slavice varirale ovisno o sorti i vlazi sjemena (6%, 11%, 16% i 21%).

Utvrđeno je da se s porastom vlage sjemena linearno povećava masa 1000 sjemena, volumen, poroznost, statički i dinamički kut unutrašnjeg trenja-kut stošca, statički koeficijent vanjskog trenja na šest različitih ploha, a da se smanjuje nasipna-hektolitarska masa i gustoća zrna.

Vrijednosti fizikalnih svojstava razlikuju se ovisno o sorti. Sorta Jasna imala je najveću masu od 1000 sjemena i volumena pojedinačnog sjemena, a najmanji nasipnu-hektolitarsku masu i gustoću sjemena u odnosu na druge dvije sorte. Sorta Jasna ima nižu hektolitarsku masu, što se može objasniti činjenicom da je sjeme znatno veće, pa tim ima više međuprostora između sjemena. Uz povećanje vlage sjemena poroznost sorte Jasna je povećana i nije se razlikovala od sorte Banačanka. Najvjerojatnije je da je sorta Jasna imala nešto veću poroznost mase sjemena zbog morfološke strukture i oblika sjemena. Najviši statički koeficijent unutrašnjeg trenja-kut stošca izmjeren je u sorti Slavica, što se također može očekivati jer ova sorta ima najmanje sjeme što povećava kontaktnu površinu i koheziju između sjemena. Sorta Jasna ima veći dinamički koeficijent unutrašnjeg trenja-kut stošca u odnosu na sortu Slavica, ali s povećanjem vlage sjemena, ta se razlika smanjuje. Sjemena povećane vlage imaju bolju koheziju između sebe, postanu ljepljiva i povezana. Utvrđeno je da se povećanjem vlage sjemena koeficijent vanjskog trenja povećava. Najveći koeficijent vanjskog trenja nalazi se na plohi šperploče i plastike, zatim na plohi aluminijska, čelika, pocinčanog lima i najmanji na limu od nehrđajućeg čelika. Sorte Jasna i Slavica imale su veći koeficijent statičkog vanjskog trenja u usporedbi s sortom Banačanka.

ZAHVALA

Rad je dio istraživanja na projektu br.31051 pod nazivom Unapređenje biotehnoških postupaka u funkciji racionalnog korištenja energije, povećanja produktivnosti i kvaliteta poljoprivrednih proizvoda financiran od strane Ministarstva prosvete, nauke i tehnološkog razvoja Republike Srbije.

LITERATURA

- Babić M. i Babić Lj. (2007). Fizičke osobine poljoprivrednih materijala. Autorizovana predavanja. Poljoprivredni fakultet, Novi Sad, 1-38.
- Calisir S., Marakoglu T., Ogut H., Ozturk O. (2005). Physical properties of rapeseed (*Brassica napus oleifera* L.). Journal of Food Engineering 69: 61–66.
- Duc L.A., Han J.W., Hong S.J., Choi H.S., Kim Y.H., Keum D.H. (2008). Physical properties of rapeseed (I). Journal of Biosystems Engineering 33(2): 101-105.
- Hazbavi I. i Minaei S. (2009). Determination and investigation of some physical properties of seven variety rapeseed. Iranian Journal of food science and technology Vol.5, No 4: 21-28.
- Hong S.J., Hon J.W., Kim H., Kim Y.H., Keum D.H., Duc. L.A (2008): Physical properties of rapeseed (II) Agricultural process and food engineering Vol.33 No. 3: 173-178.
- Izli N., Unal H., Sincik M. (2009). Physical and mechanical properties of rapeseed at different moisture content. Int. Agrophysics, 23: 137-145.
- Jukić M. i Koceva Komlenić D. (2017). Skladištenje žitarica i proizvodnja brašna (Fizikalna svojstva zrna i zrnene mase) Poljoprivredno tehnološki fakultet Osijek http://studenti.ptfos.hr/Diplomski_studij/Skladištenje_zitarica_i_proizvodnja_brasna/1_SZPB_uvod_16_17.pdf, (pristupljeno Rujan, 2017).
- Krička T., Pliestic S., Jakopović E., Preprotnik S. (1998). The influence of moisture on physical properties of wheat and maize kernels, soybeans and rapeseed. Krmiva 40 No. 2, pp.55-61.

- Krička T., Jukić Ž., Voća N., Miletić S. (1999). Komparativna analiza sušenja sjemena uljane repice "00" kultivara Silvia i "00" kultivara Diana, Karola, Semu 910201, Semu 93-10 i Lirajet. Poljoprivredna znanstvena smotra vol 64 No.2, pp. 113-121.
- Lončarević V. (2011). Uticaj vlažnosti na fizičke osobine i životnu sposobnost semena soje (*Glycine max.* (L.) Merr.). Doktorska disertacija, Poljoprivredni fakultet Novi Sad, Srbija.
- Mehandžić Stanišić S. (2013). Uticaj fizičkih osobina na kvalitet semena ratarskih useva. Doktorska disertacija, Poljoprivredni fakultet Novi Sad, Srbija.
- Radonjić S., Baralić J., Dučić N. (2011). Određivanje statičkog koeficijenta trenja korišćenjem tribometra. 6. Međunarodni simpozijum tehnologija, informatika i obrazovanje za društvo učenja i znanja. TIO 6 Tehnički fakultet Čačak, 3-5 jun 2011, Zbornik radova str.636-641 www.ftn.kg.ac.rs/konferencija/tio6/radovi.html.
- Razavi S., Yeganehzad S., Sadeghi A., Ebrahimzadeh SH., Niazmand A. (2006). Some physical properties of Iranian varieties of canola seeds. Iranian food science and technology research. Vol. 2 No. 1 pp. 53-61.
- Razavi S., Yeganehzad S., Sadeghi A. (2009). Moisture Dependent Physical Properties of Canola Seeds J. Agric. Sci. Technol. Vol. 11: 309-322.
- Szot B., Tys J., Stepniewski A., Rudko T. (2007). Określenie zmienności właściwości fizycznych i jakości nasion mieszańców rzepaku jarego. Sympozjum Naukowe "Jakość Środowiska, Surowców i Żywności", Lublin, 30.03.2007, s. 111-112.
- Szot B. (2008): Estimation of basic physical properties of spring rape seed Acta Agrophysica, 12(1): 191-205.
- Vujaković, M., Marjanović-Jeromela, A., Jovičić, D., Marinković, R. (2015). Dependence of rapeseed quality and yield on density, variety and year of production. Ratarstvo i povrtarstvo 52 (2): 61-66.

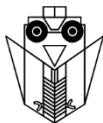
PHYSICAL PROPERTIES OF OIL RAPESEED KERNELS AT DIFFERENT MOISTURE CONTENT AND VARIETES

SUMMARY

The physical properties of the three common cultivars were evaluated as a function of seed moisture content, which varied from 6.04 - 21.17%, from 5.82 - 20.90% and from 5.98 - 20.46% in 'Banaćanka', 'Jasna' and 'Slavica', respectively. Results of thousand-seed weight increased from 4.18 g to 4.94 g in 'Banaćanka', from 4.74 g to 5.61 g in 'Jasna', and from 4.11 to 4.81 g in 'Slavica'. The seed volume of 'Jasna' ranged between 4.72 mm³ and 5.49 mm³, and it was significantly higher than that of 'Banaćanka' and 'Slavica' (4.07 - 4.93 mm³ and 4.12 - 4.81 mm³, respectively). The bulk density of 'Jasna' seeds was significantly lower than in other cultivars. Depending on seed moisture content, seed density decreased from 1023.18 kgm⁻³ to 996.97 kgm⁻³ in 'Banaćanka', from 1009.31 to 992.70 kgm⁻³ in 'Jasna', and from 1012.96-992 kgm⁻³ in 'Slavica'. Porosity increased with increasing seed moisture content in all cultivars. The porosity of 'Jasna' seeds (35.97-38.43%) was higher than that of 'Banaćanka' (35.42-38.23%) and 'Slavica' (35.19-37.07%) seeds. At different seed moisture levels, bulk density varied from 665.82 to 615.84 kgm⁻³ in

'Banaćanka', from 646.24 to 611.22 kgm⁻³ in 'Jasna', and from 656.57 to 624.66 kgm⁻³ in 'Slavica'. The static angle of repose in 'Banaćanka', 'Jasna' and 'Slavica' ranged from 22.96 ° to 28.05 °, from 24.64 ° to 29.66 ° and from 24.63 ° to 29.61° at moisture contents increasing. The dynamic angle of repose was highest in 'Jasna' (20.32-25.90°), followed by 'Slavica' (21.03-25.58°), and lowest in 'Banaćanka' (19.22-24.66°). Increasing seed moisture content was found to increase the friction coefficient. The static friction coefficient of cvs. 'Jasna' and 'Slavica' was higher than for 'Banaćanka'.

Key words: rapeseed, seed, moisture content, physical properties



RESEARCHES OF MASS AND HEAT TRANSFER OF AN INNOVATIVE VERTICAL DRYER

Petru Marian CÂRLESCU^{1*}, Vlad Nicolae ARSENOAIA¹, Ioan ȚENU¹,
Adriana Teodora MUSCALU², Mariana Silvia BÂRSAN²

¹Department of Pedotechnics, University of Agricultural Sciences and Veterinary Medicine Iași,
Sadoveanu 3, Iași 700490, Romania

²INMA Bucharest, Ion Ionescu de la Brad Blv. No. 6, Sector 1, Bucharest, Romania

*E-mail of corresponding author: pcarlescu@yahoo.com

SUMMARY

Drying of agricultural seeds is important during storage for a longer time period. Convective drying is accomplished with heat input from the drying agent passing through a porous layer of agricultural seed, taking up a certain amount of moisture. An uneven distribution of the seed layer temperature during drying results in overheating in some regions and underheating in other regions, leading to uneven seed drying.

The paper aims to determine the optimum thickness of the seed layer from a new vertical drier so that the temperature gradient in the layer is as uniform as possible. Determining the temperature profile in the seed layer can optimize hot air flow and energy consumption.

Over time, several mathematical models have been developed for the heat and mass transfer that takes place during the drying process, treating the seed layer as a solid body. By applying a heat and mass transfer model in a porous seed layer, the temperature field was simulated in three consecutive layers of thickness with 100 mm each.

Validation of the proposed mathematical model for the porous seed medium was achieved by measuring the seed temperature at several positions in the dryer.

The results obtained by simulation and experiment gave an optimum seed layer of 100 mm thick with an uniform gradient temperature.

Key words: numerical simulation, heat transfer, drying process, corn seeds.

INTRODUCTION

By the drying process the corn seeds lose a quantity of moisture until they reach the constant moisture to which they can be stored without suffering any loss of quality.

Typically, this drying process takes place convectively by means of a heat transfer hot air which penetrates the porous corn layer by taking up an amount of moisture which is eliminated in the atmosphere. If the heat required for drying is not recovered from the used hot air, the energy consumption increases. In order to reduce energy consumption and reduce drying time, it is necessary that the temperature distribution be as uniform as possible in the seed layer need to be dried.

Knowing the temperature distribution in the corn layers indicate overheating or unheating areas and can layer a uniform temperature. By knowing the temperature profile in the layer of corn can be optimized the air flow and temperature in the layers.

Many mathematical models have been developed to simulate the heat and the moisture transfer in the aerated bulk stored grains. The models were obtained at relatively low temperatures and low humidity to grain.

The partial differential equation models for wheat storage with aeration were developed by Metzger and Muir (1983) and Wilson (1988).

The models simulated forced convective heat and moisture transfer in vertical direction, but the model was not validated. Other authors (Chang *et al.*, 1993, 1994) and (Sinicio *et al.*, 1997) developed a rigorous model to predict the temperature and moisture content of wheat during storage with aeration, and found that prediction result is in reasonable agreement with observed data. The authors Sun and Woods (1997), Jia *et al.* (2001), Andrade (2001) and Devilla (2002) simulated the temperature changes in a wheat storage bin respectively, but, the moisture changes were not done. The authors Iguaz *et al.* (2004) developed a model for the storage of rough rice during periods with aeration.

Two models of the phenomenon of mass and heat transfer in a bed of grains was developed and analyzed (Thorpe, 2007). Based on model and simulation of CFD (Thorpe, 2008; Zhang *et al.*, 2016) developed and validated by experimental measurements of temperature transducers introduction the theoretical model at different points in a grain silo. The models proposed by the authors were introduced and air product temperature of less than 30°C, and two-dimensional simulations were performed.

The aim of this paper is to propose the mathematical modeling of mass and heat transfer in a cylindrical dryer with three layers of grain seeds. CFD simulation for the proposed dryer model was made with FLUENT software.

MATERIALS AND METHODS

In the drying process corn seeds from the hybrid DKC 4717 were used.

Experimentally, a three-layer concentric seed dryer was designed and developed to study temperature and moisture content distribution in order to improve the qualitative indices of corn seeds subject to preservation, Fig. 1 a. The internal deflectors of the dryer have the role of uniformity the hot air, on the height of the layer.

The experimental dryer is provided with a series of sensors for monitoring the temperature, humidity and velocity parameters of the hot air.

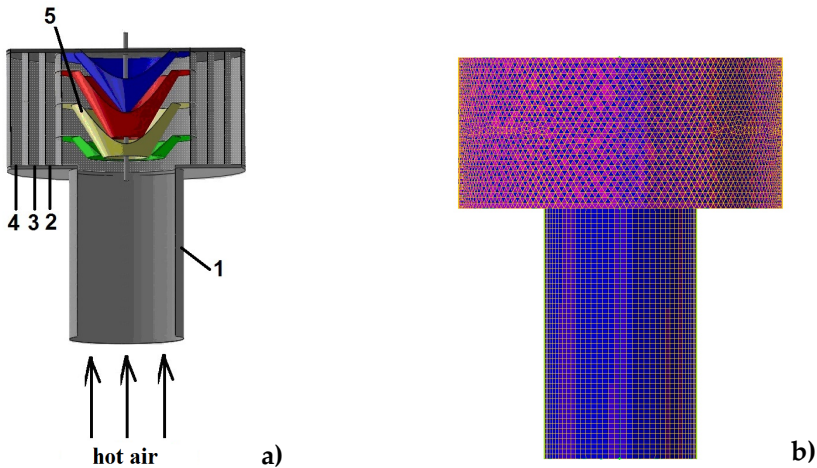


Figure 1. Geometry of the three-layer dryer and deflectors: a) section view; b) hybrid mesh (1 heat duct; 2 first seed layer; 3 second layer, 4 third layer, 5 deflectors).

The sensors used in the laboratory drier were subsequently used in the innovative vertical dryer model with heat recovery with an optimal thickness of the seed layer, Fig. 2 a, b.

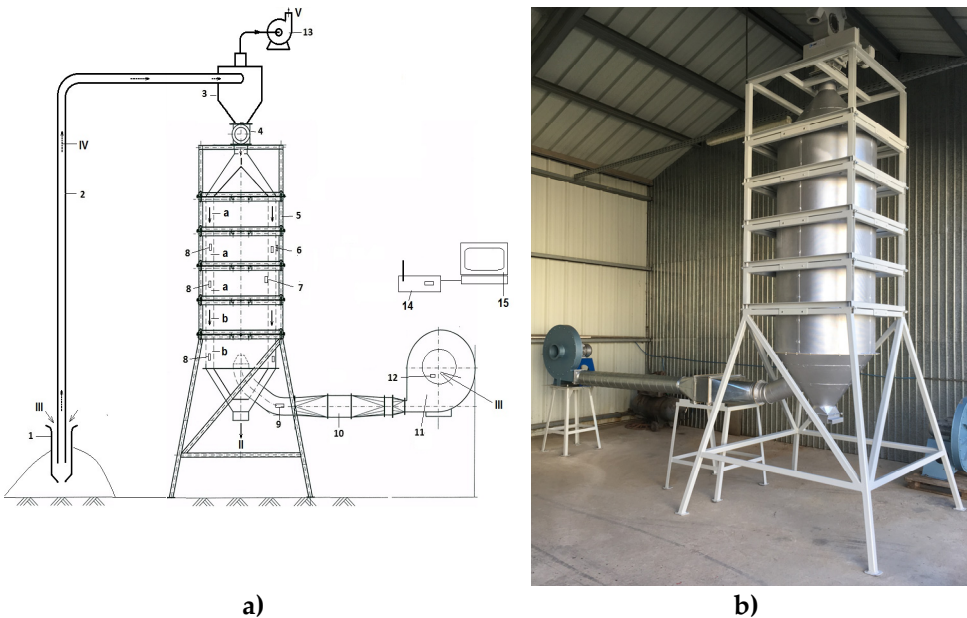


Figure 2. Innovation vertical dryer with heat recovery: a) dryer scheme; b) dryer construction (1 seed feed device; 2 pipe; 3 seed-air separator, 4 air lock, 5 vertical drier, 6 wireless sensor hot air used; 7 wireless sensor hot air; 8 temperature sensor inside the dryer; 9 velocity sensor; 10 air heater battery, 11 fan; 12 wireless sensor; 13 pneumatic fan; 14 wireless device; 15 PC; I wet seeds; II dried seeds; III air; IV mixed air seeds; V air; a drying section; b cooling section).

The temperature and humidity of the product were determined by K- type sensors (measuring range -40°C to $+400^{\circ}\text{C}$, accuracy $\pm 0.3^{\circ}\text{C}$) located in each of the three layers. Additionally, the moisture and temperature of the hot air prior to penetration into the corn seed layer and after, were monitored by means of some DLPTH1 moisture and temperature sensors (measuring range 0°C to $+100^{\circ}\text{C}$, accuracy $\pm 0.1^{\circ}\text{C}$; 0 to 100% RH, accuracy $\pm 0.1\%$ RH). Corn seed moisture content was recorded at constant time intervals using a Grain Moisture Meter Tester MD-7822 (measuring range -10°C to $+60^{\circ}\text{C}$, accuracy $\pm 2^{\circ}\text{C}$; 2 to 30% RH, accuracy $\pm 1\%$ RH).

Determination of porosity in the seed layers was performed with the 3D SKYSCAN 1172 micro CT scanner and related software. The hot air velocity at the inlet and outlet of the dryer was monitored using the TROTEC TA 300 hot wire anemometer (measuring range 0.1 ms^{-1} to 30 ms^{-1} , accuracy $\pm 0.1\text{ ms}^{-1}$). Information obtained by the sensors is numerically transferred and graphically represented on a computer by means of a graphics card. The research method has been developed by mathematical modeling of mass and heat transfer phenomena in corn seed layers based on a series of data obtained by experiment on the laboratory model and verified on the innovative vertical dryer model with heat recovery. The physical drying phenomenon that occurs in the corn layers obeys the law of conservation. However, to solve such a diversity of problems the equations that govern heat and mass transfer are expressed in very general terms and they do not model heat and mass transfer in the corn bulks during corn self drying. As a result, they have to be tailored to suit corn drying applications. To date, making the modifications to the standard CFD (Computational Fluid Dynamics) software appears to have been a stumbling block for most corn-dry technologists. This physical phenomenon is described mathematically by a partial differential equation of general form:

$$\frac{\partial(\rho_a\phi)}{\partial t} + \nabla(\rho_a v\phi) = \nabla(\Gamma\nabla\phi) + S\phi, \quad (1)$$

where: Φ is the quantity of interest which in this case is the energy or moisture content of the intergranular air, ρ_a is the density of air, v is the superficial or Darcian velocity of the air as opposed to the average velocity of the air flowing between the corn kernels, Γ is the effective diffusion coefficient of Φ through a bed of corn, t is time, ∇ is the del operator, $S\phi$ is a source term.

Eq. (1) refers to a differentially small region of corn and this implies that the properties have been averaged over some finite volume, otherwise they would be discontinuous at the boundaries of the corn kernels and intergranular air.

The variable, Φ , in the generalised transport Eq. (1) can also represent energy. In the case of porous media, such as a bulk of corn, the enthalpies of the fluid (air) and solid (corn kernels) phases must be considered. The computer software used in this work solves an enthalpy balance by Eq. (2)

$$\left((\rho_a \varepsilon c_a + \rho_s (1 - \varepsilon)) \left(c_s + c_w W + \frac{\partial H_w}{\partial T} \right) \right) \frac{\partial T}{\partial t} + c_a \nabla(\rho_a v T) = = k_{\text{eff}} \nabla^2 T + S_{\text{en}}, \quad (2)$$

where: c_a , c_s and c_w are the specific air heats, corn and liquid water, respectively, ρ_s is the density of corn kernels on a dry basis, ε - void fraction of the layer of corn (we assume that value 0,15) , W - corn moisture content , H_w - is the integral heat of corn wetting, T - temperature, k_{eff} is the effective thermal bulk conductivity of corn ($0.167\text{ W/m}^2\text{K}$), S_{en} is the

thermal source term that results from heat being liberated or extracted from the corn when they adsorb or desorb moisture.

It has been demonstrated that $\partial H_w/\partial T$ is negligibly small for corns compared with the specific heat of moist corn and it can be ignored (Thorpe, 2007). A feature of FLUENT software is that the specific heat of the porous zone must be entered as a constant, but in this application the term equivalent to specific heat, i.e. $C_g + C_w W + (\partial H_w/\partial T)$, varies with moisture content. For the simulation presented here we assume that the start value of the corn moisture content, W , is 0.157, which corresponds to a moisture content of 25% wet basis and the corn has a temperature of 21 °C. The source term, S_{en} , takes the form

$$S_{en} = -h_s (1 - \varepsilon) \rho_s \frac{\partial W}{\partial t}, \quad (3)$$

where: h_s is the sorption heat of water on the corn.

It has been obtained (Hunter, 1989) that the ratio of the heat of sorption to the latent heat of vaporisation, h_v , of free water is given by

$$\frac{h_s}{h_v} = 1 + \frac{p_{sat}}{r} \frac{dT}{dp_{sat}} \frac{dr}{dT}. \quad (4)$$

Hunter provides the following empirical relationship between the saturation vapour pressure of water and temperature (Hunter, 1987)

$$p_{sat} = \frac{6 \cdot 10^{25}}{(T + 273.15)^5} \exp\left(-\frac{6800}{T + 273.15}\right). \quad (5)$$

The relative humidity, r , of the intergranular air is defined as in Eq. (6), where p_{sat} is the saturation vapour pressure of free water.

$$r = \frac{p}{p_{sat}}. \quad (6)$$

where: p vapour pressure of water vapour may be expressed in terms of the humidity, w , of the intergranular air by

$$p = \frac{w p_{atm}}{0.622 + w}. \quad (7)$$

where: p_{atm} is atmospheric pressure. Differentiation and inversion of Eq. (5) results in

$$\frac{dT}{dp_{sat}} = \left(\frac{T + 273.15}{p_{sat}} \right) \left/ \left(\frac{6800}{T + 273.15} - 5 \right) \right. \quad (8)$$

and

$$\frac{dr}{dT} = \frac{Ar}{(T + C)^2} \exp(-BW_e). \quad (9)$$

where: A , B and C are empirical constants widely used to sorption isotherm proposed by Chung and Pfost (1967) and for this case assume the values of (921.69, 18.077 and 112.35).

The corn layers constitutes a porous medium and FLUENT software accounts for the resistance to air flow by adding a source term, S_i , to the standard momentum transport equation. S_i as the pressure gradient along a bed of corn uniformly aerated in the i -th direction with air with a velocity v_i . It takes the form

$$S_i = - \left(\sum_{j=1}^3 D_{ij} \mu v_j + \sum_{j=1}^3 C_{ij} \frac{\rho_a}{2} |v| v_j \right), i = 1, 2, 3 \quad (10)$$

where: μ is the intergranular air viscosity, v_j represent the components of the velocity in all three dimensions, ρ_a is the air density, v is the superficial or Darcian velocity of the air as opposed to the average velocity of the air flowing between the corn kernels, D_{ij} is tensor component what represent the Darcian or viscous resistance, C_{ij} is tensor component what represent inertial resistance. The empirical coefficients D_{ij} , C_{ij} can be related to those in the FLUENT software Eq. (11).

$$D_{ij} = \begin{cases} R_h / \mu; & i = j = 1, 2, \\ R_v / \mu; & i = j = 3, \\ 0; & i \neq j, i = 1, 2, 3, j = 1, 2, 3. \end{cases} \quad C_{ij} = \begin{cases} 2 \cdot S_{h0} / \rho_a; & i = j = 1, 2, \\ 2 \cdot S_v / \rho_a; & i = j = 3, \\ 0; & i \neq j, i = 1, 2, 3, j = 1, 2, 3. \end{cases} \quad (11)$$

The components of the resistance in these two directions and resistance terms in the horizontal direction can be designated as R_h and S_{h0} , and those in the vertical direction R_v and S_v . Two orthogonal horizontal directions are designated by the indices 1 and 2, and the vertical direction has the index 3.

This is implemented in FLUENT by introducing temperature of 30 °C the air viscosity and density, respectively $18.37 \cdot 10^6$ Pas and 1.191 kgm^{-3} . Using these values, we find that $D_{11}=D_{22}=1.833 \cdot 10^8$, $D_{33}=2.037 \cdot 10^8$ and $C_{11}=C_{22}=18371$, $C_{33}=26767$.

The aim of this paper is to illustrate how a standard CFD package may be modified so it can be used to simulate heat and moisture processes that occur during corn drying process. The features that apply specifically to bulk dry corn are accommodated by User-Defined Functions (UDF-s) written in a high-level computer language such as C and introduce in the FLUENT software.

Pre-processing as a first step in CFD simulation is achieved by creating the drying zone geometry and meshes it with the GAMBIT software. The geometry is discretization with hybrid mesh and 938,000 elements, Fig. 1 b.

For both the drying and CFD simulation experiment the corn seeds with an initial moisture content of 25% were used in the three layers and the porosity index determined experimentally by CT scan of a volume of 68.7 cm^3 with a number of 78 seeds of corn was 34.5%. The drying velocity used in both experiment and simulation was 2 ms^{-2} and the temperature was 40°C and 70°C, respectively. The process of calculating the drying of the corn seeds for both used temperature used temperatures was about 4 hours.

The initial conditions imposed for corn seeds in the two CFD experimental and simulation variants have shown in Table 1.

Table 1. Initial conditions imposed for corn seed processing

Layers	X (kg vap. H ₂ O/kg dry prod.)	Density ρ (kg·m ⁻³)	Specific heat c_p (J·kg ⁻¹ ·K ⁻¹)	Conductivity k (W·m ⁻¹ ·K ⁻¹)	Porosity index ϵ (-)
I, II, III	0.156	615	1679	0,158	0.34...0.38

For processing in the FLUENT software, in addition to boundary conditions defined in pre-processing, the conditions in Table 2 was added.

The boundary condition of the hot air used was imposed as (outflow type) a free discharge into the environment, atmospheric pressure ($101325 \text{ Pa} = 1 \text{ atm}$).

Table 2. Boundary conditions for the CFD simulation

Boundary sections	Status	Boundary conditions
		Fluid
Inlet hot air	normal	$u = \text{constant}$
Outlet hot air used	open	$p = 0$
Wall dryer	close	$\frac{\partial u}{\partial n} = 0$ (n – normal to the surface)

Overpressure was considered null ($p = 0$). The air flow through the deflector walls and air duct was considered null. The conditions for solving the equation systems for simulating the vertical dryer are shown in Table 3.

Table 3. Terms of solving differential equations

Terms of solving differential equations	Algorithm/Scheme	Order
Velocity-pressure coupling	Simple	-
Pressure		1
Moment		1
Mesh equations	upwinding (meshing scheme)	1
H ₂ O		1
Air		1
Energy		1

For the stability of the calculation flow of air applications was under-relaxation following factors: pressure - 0.3; moment - 0.7; density - 1; turbulent kinetic energy - 0.8; turbulent dissipation rate - 0.8; turbulent viscosity - 1.

CFD simulation was performed with the Ansys FLUENT software using the TYAN workstation (2XCPU-Intel Xeon 3.33GHz; RAM- 16GB DDR3 2600).

RESULTS AND DISCUSSION

CFD simulation post-processing follows the presentation of the main parameters of interest in the color scheme of the corn seed drying process. Parameters are presented, for each computation node, in the form of temperature fields or by showing the flow of air through current lines depending on its velocity and temperature. The post-processing was done for the three corn seed layers following the temperature and moisture content distribution in the seed layers. The temperatures for the two simulated drying variants were 313 K (40°C) and 343 K (70°C).

In the first variant, with a hot air input, the temperature of 313 K (40°C) on the longitudinal section of the three-layer corn seed dryer, the average temperature of the heat air decreases progressively from the layer I, which first contacts the hot air with 311 K (38°C)

at the second layer with 305 K (32°C), reaching the third layer at an average temperature of 301 K (28°C) until the end of the drying process. The temperature gradient distribution on the three layers has shown in Fig. 3a.

The distribution of the absolute moisture content of the corn seeds in the three seed layers of the dryer shows a lower mean value in the first layer of 0.001 (kg of water vapor/kg of dry product) (11.6%), a higher value in the second layer 0.005 (kg water vapor/kg dry product) (12%) and the highest value in the third layer of 0.11 (kg of water vapor/kg of dry product) (22%).

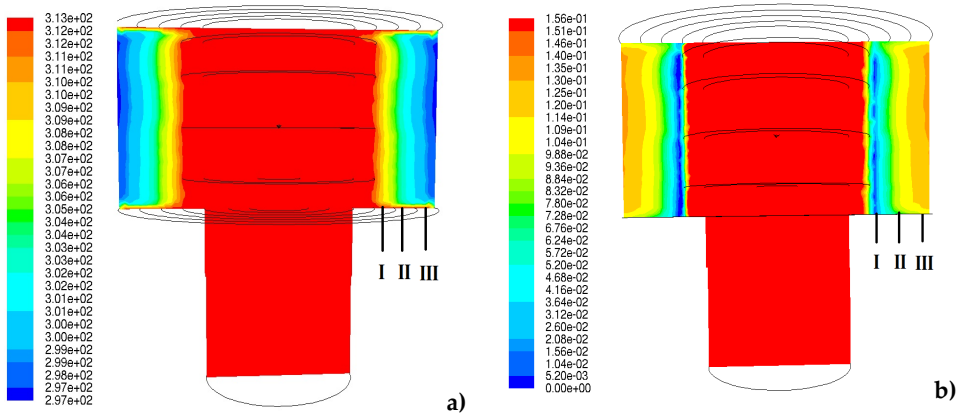


Figure 3. Vertical dryer: a) the temperature field K; b) the absolute moisture field kg water vapors/kg dry product. I first layer; II second layer, III third layer. ($v=2 \text{ m}\cdot\text{s}^{-1}$; $T=313 \text{ K}$)

The gradient of absolute moisture content distribution in the three layers of corn seeds has shown in Fig. 3b. Inside the dryer, the red color is the starting quantity of 0.156 (kg of water vapor/kg of dry product) corn seed moisture, which in this case has no physical significance because hot air circulates inside. CFD simulation was done unsteady and the results presented are at the end of drying, after 65 minutes.

By experiment, at the end of the drying process, both the moisture content and temperature in the three layers of corn seeds decrease unevenly in the radial direction as follows: the first layer 11.5% and 35°C, the second layer 11.7% and 30°C, the third layer 14% and 29,3°C.

In the second version of the CFD hot air simulation, entering the temperature of 343K (70°C) on the longitudinal section of the dryer, the average temperature decreases progressively from the first layer by 338K (65°C), to second layer by 318K (45°C), reaching the third layer at an average temperature of 308K (35°C) until the end of the drying process. The temperature gradient distribution on the three layers has shown in Fig. 4a.

The distribution of the absolute moisture content of the corn seeds in the three seed layers of the dryer shows a lower mean value (the equilibrium moisture) in the first layer of 11.5%, a higher value in the second layer of 0.0058 (kg water vapor/kg dry product) (17%) and the highest value in the third layer of 0.104 (kg of water vapor/kg of dry product) (21%).

The gradient of absolute moisture distribution in the three layers of corn seeds has shown in Fig. 4b. Inside the dryer, the red color is the starting quantity of 0.156 (kg of water vapor/kg of dry product) corn seed moisture, which in this case has no physical significance

because hot air circulates inside. CFD simulation was done unsteady and the results presented are at the end of drying after 27 minutes.

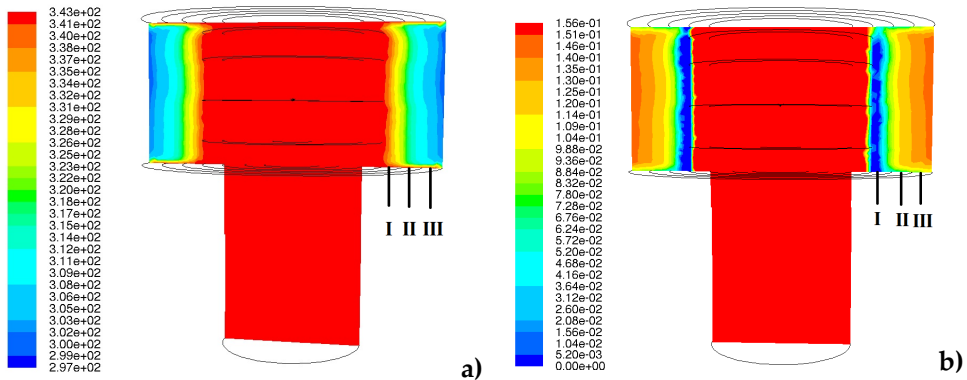


Figure 4. Vertical dryer: a) the temperature field K; b) the absolute moisture field kg water vapors/kg dry product. I first layer; II second layer, III third layer. ($v = 2 \text{ m}\cdot\text{s}^{-1}$; $T = 343 \text{ K}$)

According to the experiment, at the end of the drying process, the moisture content and temperature in the three layers of corn seeds decreases unevenly in the radial direction as follows: the first layer 9.8% and 68.2°C, the second layer 18.4% and 4.1°C, the third layer 19.9% and 38.3°C.

The innovative vertical dryer model has a single layer with a thickness of 0.1 m. The experimentally measured parameters for this dryer at 40°C were temperature and moisture. In the seed layer, at the end of drying, an average moisture content of 11.9% and an average temperature of 32°C were obtained. The temperature and moisture of the first layer of the cylindrical dryer with three layers differ with 0.4% for moisture and 3°C for the temperature, compared to the temperature and moisture in the layer of the innovative vertical dryer. The difference between laboratory ambient temperature (22°C) and the one outside (15°C) where the two tests were made, could be the explanation for the temperature difference that occur in seed layer.

CONCLUSIONS

The corn seeds are irregularly dried in the three layers of the dryer, leading to an over-drying of the first layer and keeping a high percentage of moisture in the outer layer of the dryer.

The moisture and temperature differences between the first and the last layer seeds are 10.4% and 10°C respectively, when the hot air temperature is 40°C, while for hot air temperature of 70 °C, the recorded differences are 9.5% and 30°C.

In the three-layers vertical dryer, the average temperature and moisture differences recorded between CFD simulation and experiment differ by 1°C and 4.05% for a hot air temperature of 40 °C, and 3.25 °C and 2.9% for a hot air temperature of 70°C.

By mathematical modeling of mass and heat transfer and using experimental data, CFD simulation results in an optimal layer thickness of corn in the dryer of 0.1 m.

Compared with the temperature and humidity in the innovative vertical dryer layer, the differences in temperature and moisture in the first layer of the three-layers cylindrical dryer were of 0.4% for moisture and 3 °C respectively for temperature.

ACKNOWLEDGEMENTS

This work was supported by a grant of the Romanian National Authority for Scientific Research and Innovation, CNCS/CCCDI – UEFISCDI, project number PN-III-P2-2.1-PED-2016-1357, within PNCDI III, contract no.18PED/2017.

REFERENCES

- Andra, de E.T. (2001). Simulacao da variacao de temperatura em milho armazenado em silo metalico. Tese de doutorado em Engenharia Agricola. Minas Gerais: Imprensa Universitaria, Universidade Federal de Vicosa, Brasil.
- Chang, C. S., Converse, H. H., Steele, J. L. (1993). Modeling of temperature of rain during storage with aeration. *Trans. Am. Soc. Agric. Engrs.*, 36, 2: 509-519.
- Chang, C. S., Converse, H. H., Steele, J. L. (1994). Modeling of moisture content of grain during storage with aeration. *Trans. Am. Soc. Agric. Engrs.*, 37, 6: 1891-1898.
- Chung, D.S., Pfost, H.B. (1967). Adsorption and desorption of water vapor by cereal grains and their products. (I) Heat and free energy changes of adsorption and desorption. *Transactions of the American Society of Agricultural Engineers* 10: 549-555.
- Devilla, I.A. (2002). Simulacao de deterioracao de distribuicao de temperatura umidade em uma massa de graos armazenados em silos com aeracao. Tese de doutorado em Engenharia Agricola. Minas Gerais: Imprensa Universitaria, Universidade Federal de Vicosa, Brasil.
- Dieter, B. and Karl S. (2006). Heat and mass transfer. Springer-Verlag, Berlin.
- Hunter, A.J. (1987). An isostere equation for some common seeds. *Journal of Agricultural Engineering Research* 37: 93-107.
- Hunter, A.J. (1989). On the heat of sorption of paddy rice. *Journal of Agricultural Engineering Research* 44: 237-239.
- Iguaz, A., Arroqui1, C., Esnoz, A., Virseda, P. (2004). Modeling and simulation of heat transfer in stored rough rice with aeration. *Biosystems Engineering*, 89, 1: 69-77.
- Jia, C. C., Sun, D. W., Cao, C. W. (2001). Computer simulation of temperature changes in a wheat storage bin. *J. Stored Prod. Res.*, 37: 165-167.
- Metzger, J. F. and Muir, W. E. (1983). Computer model of two dimensional conduction and forced convection in stored grain. *Canadian Agricultural Engineering*, 25, 2: 119-125.
- Sinicio, R., Muir, W.E., Jayas, D.S. (1997). Sensitivity analysis of a mathematical model to simulate aeration of wheat stored in Brazil. *Postharvest Biol. Technol.* 11: 107-122.
- Sun, D.W. and Woods, J. L. (1997). Simulation of the heat and moisture transfer process during drying in deep grain beds. *Drying Technology*, 10, 15: 99-107.
- Tannehill, J. C., Anderson, D. A., Pletcher R. H. (1997). *Computational fluid mechanics and heat transfer*, Taylor and Francis.
- Thorpe, G.R. (2007). Heat and moisture transfer in porous hygroscopic media: two contrasting analyses. *Fifth International Conference on Heat Transfer, Fluid Mechanics and Thermodynamics*, Sun City, South Africa.

- Thorpe, G.R. (2008). The application of computational fluid dynamics codes to simulate heat and moisture transfer in stored grains. *Journal of Stored Products Research* 44: 21-31.
- Wilson, S.G. (1988). Simulation of thermal and moisture boundary layers during aeration of cereal grain. *Mathematics Comp. Simul.* 30: 181-188.
- Zhang, L., Chen, X., Liu, H., Peng, W., Zhang, Z., Ren, G. (2016). Experiment and simulation research of storage for small grain steel silo. *Int J Agric & Biol Eng.*, 9,3:170-178.
- *** Ansys-Fluent. User Guide. 2010.



CFD SIMULATION OF AN INNOVATIVE VERTICAL DRYER FOR AGRICULTURAL SEEDS DRYING

Petru Marian CĂRLESCU^{1*}, Ioan ȚENU¹, Radu ROȘCA¹,
Adriana Teodora MUSCALU², Nicolae Valentin VLĂDUȚ²

¹Department of Pedotechnics, University of Agricultural Sciences and Veterinary Medicine Iași,
Sadoveanu 3, Iași 700490, Romania

² INMA Bucharest, Ion Ionescu de la Brad Blv. No. 6, Sector 1, Bucharest, Romania

*E-mail of corresponding author: pcarlescu@yahoo.com

SUMMARY

Artificial drying of agricultural seeds ensures conditions for their preservation while by reducing the water content of seeds, it is possible to keep them for long periods of time, without the need of complex storage facilities. During the drying process, both moisture and a significant amount of heat are lost, resulting in high energy consumption. Recovery of lost heat from the used drying agent was achieved in an innovative model of the vertical dryer so that the energy consumption of the drying process was reduced.

The development of the Computational Fluid Dynamics (CFD) technology and software has made it possible to design and simulate an innovative vertical dryer model with heat recovery for agricultural seed, to achieve uniform seed temperature distribution and to reduce energy consumption. CFD simulation has the advantage of testing the flow of heat agent and assessing the temperature distribution within the vertical dryer before introducing the agricultural seeds into it.

The paper presents a comprehensive method of CFD simulation in the heat recovery dryer, where the mathematical models of heat transfer and the hot air flow, the distribution of the temperature of the drying agent and the temperature in the seed layer are presented simultaneously in two or three dimensions.

The results obtained by the CFD simulation of the dryer have an error of $\pm 5\%$ against the experimental determinations, which is an accepted level in the heat transfer field.

Keywords: drying, vertical dryer, agricultural seeds, CFD simulation.

INTRODUCTION

Grain seeds are a component part of human nutrition and global production growth, as a result of market demand, makes them an important product. Each year about 60 million tonnes of grain are damaged by environmental factors. According to the FAO (Food and Agriculture Organization of the United Nations), there is an annual loss of over 20% of the world's grain harvest, most of it due to the spread of fungi, mildew and insect activity.

Drying is the most widely used method of preserving grain seeds. Drying reduces the water content and increases the concentration of soluble substrates to values that ensure the stability and preservation of cereal seeds. During the drying process, both moisture and a significant amount of heat are lost, resulting in high energy consumption (Dieter and Karl, 2006; Incopera et al., 2007). The recovery of the heat lost from the drying agent used in the cereal seed drying process is a means by which the total energy consumption can be reduced.

The development of the Computational Fluid Dynamics (CFD) technology and software has made it possible to design and simulate an innovative vertical dryer model with heat recovery for agricultural seed, to achieve uniform seed temperature distribution and to reduce energy consumption. CFD simulation has the advantage of testing the flow of heat agent and assessing the temperature distribution within the vertical dryer before introducing the agricultural seeds into it.

Over time, several mathematical models have been developed for heat and mass transfer in porous media such as grain seed layers. Many models were obtained at relatively low temperatures and low humidity to grain. The partial differential equation models for wheat storage with aeration were developed by (Metzger and Muir, 1983) and (Wilson, 1988). The models simulated forced convective heat and moisture transfer in vertical direction, but the model was not validated. Other authors (Chang et al., 1993; Chang et al., 1994; Sinicio et al., 1997) developed a rigorous model to predict the temperature and moisture content of wheat during storage with aeration, and found that prediction result is in reasonable agreement with observed data. The authors Sun and Woods, (1997), Jia et al., (2001), Andrade (2001) and Devilla (2002) simulated the temperature changes in a wheat storage bin respectively, and however, the moisture changes were not done. The authors Iguaz et al. (2004) developed a model for the storage of rough rice during periods with aeration. Two models of the phenomenon of mass and heat transfer in a bed of grains was developed and analyzed (Thorpe, 2007; Thorpe, 2008).

The paper presents a comprehensive method of CFD simulation in the heat recovery dryer, where the mathematical model of heat transfer, the distribution of the temperature of the drying agent and the temperature in the seed layer are presented simultaneously in two or three dimensions.

MATERIALS AND METHODS

Designing the innovative vertical dryer for agricultural seeds requires several steps: sketch, CFD simulation, 3D drawing, execution and functional testing.

If the results of the process correspond to the initial requirements of the project (a high energy efficiency vertical grain dryer), the project is implemented. If these requirements are not met, the process is resumed from the start.

The CFD simulation method aims to solve the problems of the flow of heat and the heat transfer inside the vertical drier. Numerical CFD simulation papers offer three stages: pre-processing, processing and post-processing (Hirsch, 1992; Tannehill et al., 1997). In the pre-

processing step the 3D modeling of the vertical drier is carried out, followed by the meshing of the dryer volume in a finite number of elements (volumes) and the introduction of boundary conditions. At the processing step, the flow model is chosen according to Navier-Stokes equations and the heat transfer energy equation. The calculations are done in this stage as well. In the post-processing step the results obtained after the model calculations are processed and the results are obtained in graphical form. According to the described steps, CFD simulation of the vertical drier requires definition of geometry. The innovative vertical dryer model with heat recovery for seed grain drying has complex execution geometry (Fig. 1), but for CFD simulation it is simplified so that it is possible to define and visualize the internal flow regions of the drying, and heat transfer (Fig. 2).

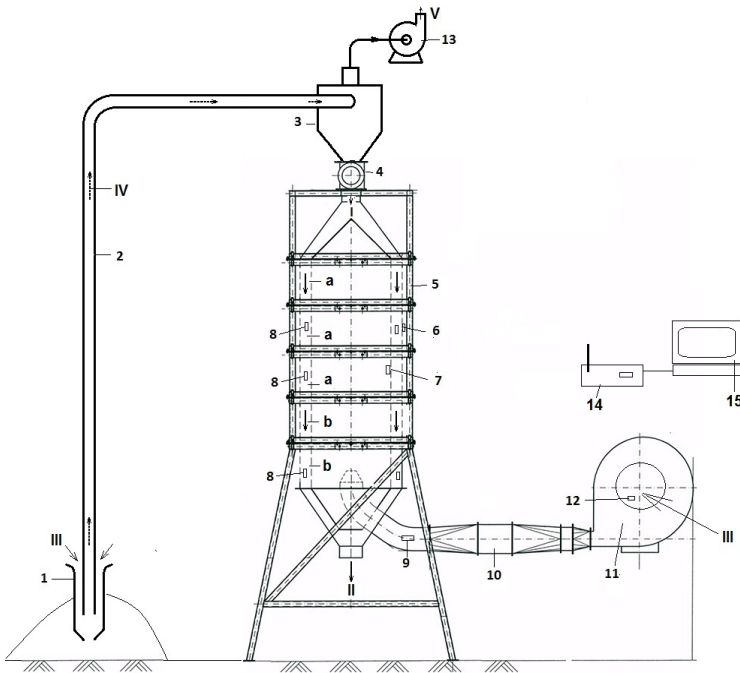


Figure 1. Innovation vertical drier with heat recovery

- 1 seed feed device; 2 pipe; 3 seed-air separator, 4 air lock, 5 vertical drier, 6 wireless sensor agent used; 7 wireless sensor agent; 8 temperature sensor inside the dryer; 9 velocity sensor; 10 air heater battery, 11 fan; 12 wireless sensor; 13 pneumatic fan; 14 wireless device; 15 PC; I wet seeds; II dried seeds; III air; IV mixed air seeds; V air; a drying section; b cooling section.

The dimensions of the dryer used in CFD simulation are identical to those in the actual model to be built, and the simplifications to the vertical drier geometry do not influence the physical phenomena that occur during the drying process. The detailed dimension are shown in Table 1.

Table 1. Dimensions of the vertical dryer model with heat recovery used in the CFD simulation

Dimensions	Unit - m
Height dryer	3
Diameter dryer	1
Grain layer thickness	0.1
Height drying/cooling sections	0.4
Diameter warm air inlet for drying	0.2

A grid independence study was carried out with three different mesh densities with mesh sizes varying from 1,500,000; 5,670,000 to 8,358,000. A mesh density of 5,670,000 cells (volumes) was optimal for good simulation and reasonable computational time. The optimizing of the meshing has the purpose to avoid errors occurring in calculation stage. Meshing of the vertical dryer model with heat recovery was of the unstructured type with tetrahedral elements at quality 0.8, developed with Gambit v. 2.2.30 software, shown in Fig. 3.

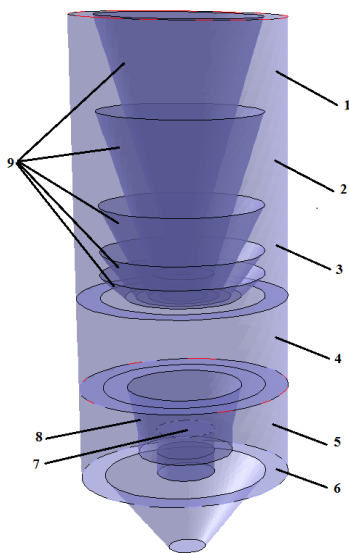


Figure 2. Vertical drier geometry for CFD simulation
1, 2, 3 drying sections; 4, 5 cooling sections; 6 grain seed layer; 7 warm air inlet for drying; 8 nozzle; 9 deflector cones.

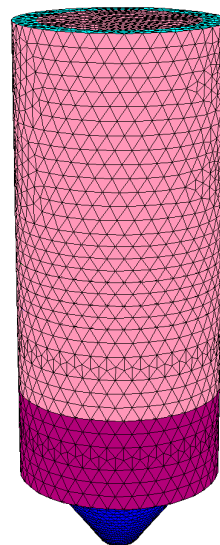


Figure 3. Tetrahedral mesh model of the vertical drier geometry.

In the step of processing the turbulent $k-\epsilon$ model was used, which is a standard model in CFD simulation for modeling hot air flow within the vertical dryer. The $k-\epsilon$ standard model is the "full" of turbulence simplest model. It is turbulence shape with two transport equations, which allows independent assessment of the turbulent velocity and length scale of turbulence. This model works well technically in a wide variety of fluid flow. Values k

turbulent kinetic energy dissipation rate and ε are obtained from the transport system of equations:

$$\rho \frac{Dk}{dt} = \frac{\partial}{\partial x_i} \left[\left(\mu + \frac{\mu_t}{Pr_k} \right) \frac{\partial k}{\partial x_i} \right] + G_k + G_b - \rho \varepsilon - Y_M \tag{1}$$

and

$$\rho \frac{D\varepsilon}{Dt} = \frac{\partial}{\partial x_i} \left[\left(\varpi + \frac{\mu_t}{Pr_\varepsilon} \right) \frac{\partial \varepsilon}{\partial x_i} \right] + C_{1\varepsilon} \frac{\varepsilon}{k} (G_k + G_{3\eta} C_b) - C_{2\varepsilon} \rho \frac{\varepsilon^2}{k} \tag{2}$$

where: ρ - density of the air; μ - viscosity air; $x_{i,j,k}$ - considered as a remote position; t - time; G_k - term generation turbulent kinetic energy; G_b - the term that takes into account the effect of buoyancy; Y_M - the term that takes into account the effect of compressibility. Pr_k and Pr_ε - turbulent Prandtl numbers for k and ε respectively.

The kinetic energy per unit mass is given:

$$k = \frac{1}{2} \overline{u_i u_i} \tag{3}$$

The term generation turbulent kinetic energy is:

$$G_k = -\rho \overline{u_i u_j} \frac{\partial u_j}{\partial x_i} \tag{4}$$

where: $u_{i,j}$ - the fluctuant air velocity on direction i, j and average component respectively.

The term buoyancy in this case is neglected because it is considered that the density varies with temperature or otherwise and gravity forces also appear neglecting. The effect of compressibility on turbulence occurs at higher flow velocity of sound, resulting in the neglect to the present model. The calculation is done with the relationship for turbulent viscosity:

$$\mu_t = \rho C_\mu \frac{k^2}{\varepsilon} \tag{5}$$

Equations (1, 2) of the obtained system will vary depending on certain terms and imposed assumptions.

The mathematical model for heat transfer is given by the energy equation based on the first principle of thermodynamics of energy conservation. The abbreviated form of this equation is:

$$\rho \frac{DU}{dt} = \frac{\partial Q}{\partial t} + k \nabla^2 T + \Phi \tag{6}$$

where: U is the internal energy, t time, Q term heat source, k coefficient of thermal conductivity, T temperature, Φ the term dissipation.

Depending on the nature of the physics governing air movement, one or more terms may be neglected. In the step of processing, the mathematical models are used to define the purpose of obtaining the flow field of the vertical dryer and the trajectory of the hot air, from the set of equations and equations describing physical properties of substances. The FLUENT simulation create an algorithm that is based on a mathematical model, which in addition is added to the contour conditions defined in the pre-processing has shown in Table 2.

Table 2. Boundary conditions for the CFD simulation

Boundary sections	Status	Boundary conditions
		Fluid
Inlet hot air	normal	$u = \text{constant}$
Inlet fresh air	open	$p = 0$
Outlet hot air used	open	$p = 0$
Wall dryer (cones, nozzle, etc.)	close	$\frac{\partial u}{\partial n} = 0$ (n – normal to the surface)

The air velocity on the hot air inlet section is considered to be constant with values ranging from 0.1 to 6.9 m·s⁻¹. The boundary condition of the hot air used was imposed as (outflow type) a free discharge into the environment, atmospheric pressure (101325 Pa = 1 atm). Overpressure was considered null ($p = 0$). The air flow through the deflector walls and air duct was considered null. The conditions for solving the equation systems for simulating the vertical dryer are shown in Table 3.

Table 3. Terms of solving differential equations

Terms of solving differential equations		Algorithm/Scheme	Order
Velocity-pressure coupling		Simple	-
Mesh equations	Pressure	upwinding	1
	Moment	(meshing scheme)	1
	Turbulent kinetic energy		1
	Turbulent dissipation rate		1

When connecting velocity-pressure parameters between equations of continuity and time was performed using SIMPLE algorithm (Patankar and Spalding, 1972; Vandoormaal and Raithby, 1984). The meshing pressure and other conservation equations were used for meshing upwind scheme (velocity value u is "transported" to the edge of the volume relative to local velocity purposes) first order (Fluent 2010). It was used in the simulation scheme linear (first order kinetics) for solving the equation of pressure in order to maintain the stability of the final solution. All the simulations carried out were steady. Flow regime for the simulation is tested in order to obtain a steady state of convergent evolution residues. Density and viscosity of air were considered constant for a given temperature (25°C) with the conditions of boundary. For the stability of the calculation, air flow parameters were under-relaxation following: pressure - 0.3; moment - 0.7; density - 1; turbulent kinetic energy - 0.8; turbulent dissipation rate - 0.8; turbulent viscosity - 1. The convergence of the solution through the stationary server was performed using the coefficients of the sub-relaxation time of 0.35 to 0.5 for the equations of turbulence. The convergence criterion used for all variables was imposed solutions to the value of 0.001. The number of iterations required for convergence equations system solutions in the processing was 863. Processing subjected model simulation was performed with TYAN Workstation (Intel Xeon 2xCPU-3.33 GHz; RAM – 16GB DDR3 2600). The numerical solution tends to converge when analytic solution and the mesh step tend to zero. A numerical solution converges if the values of variables in the field of computing nodes tend to approach the exact solution. Also, the process of solving

numerical errors is considered stable if not growing significantly discreet solution otherwise the result is not real.

RESULTS AND DISCUSSION

The solver produces a map of the distribution of all the variables throughout the domain. This result must be processed so that it can be easily reported, visualized and analyzed. This is the main purpose of the post-processing task, which is essential for comprehensive evaluation of the simulation. Usual outcomes of post-processing for visualization are temperature and velocity maps, pathlines, etc. The post-processor can also give information about the instantaneous value of all variables at certain positions in the domain, and can perform balances and numerical calculations. Simulation describes the temperature distribution in the innovative vertical dryer model with heat recovery for agricultural seed. Temperature transducers can be placed at different points in this vertical dryer, but can not be so numerous that to draw a precise temperature profile in both horizontal and vertical section of the dryer. CFD simulation allows description of the temperature field at any point of the vertical dryer.

The temperature gradient distribution on the drier vertical section has shown in Fig. 4.

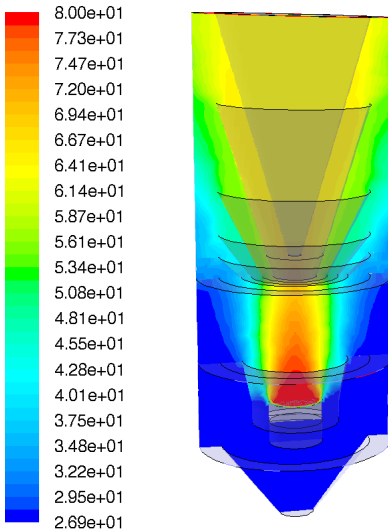


Figure 4. Temperature field on the vertical section of the dryer (°C)

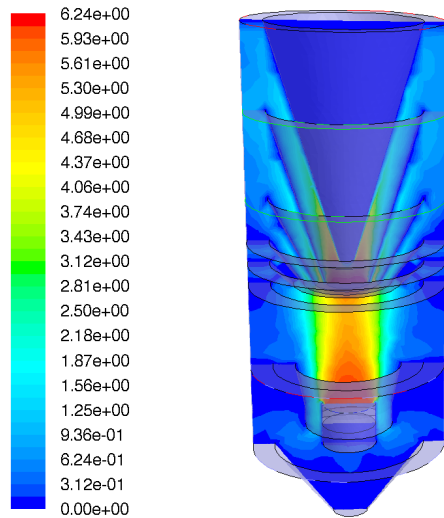


Figure 5. Velocity field on the vertical section of the dryer (m·s⁻¹)

The two regions can be distinguished vertically from the dryer: the upper drying region where the average temperature is 53°C, decreasing from top to bottom, and the cooling region at the bottom where the temperature is 27°C. The temperature in the hot air inlet area for drying is 80°C. Experimentally, a temperature transducer was introduced into the three drying regions, and after 25 minutes of operation, the temperature obtained in the drying region was 48.6°C, and in the cereal seed cooling region was 23.3°C. Thus the differences obtained with the simulation are reduced and can be explained by the thermal inertia due to

the mass transfer (humidity) to the environment which leads to the temperature decrease by a few degrees. The introduction of the nozzle at the bottom of the dryer in the immediate vicinity of the hot air supply duct makes it possible to obtain two vertically regions with different temperatures for the drying and cooling of the grain seeds.

By the introducing of the five cones inside the dryer, the air velocity distribution in the three drying zones becomes uniform, and the velocity vector is oriented from the inside of the dryer to the outside, Fig. 5. In the two cooling regions at the bottom of the dryer, the nozzle insertion makes it possible to orient the velocity vector from the outside to the interior, by absorbing cold air from the atmosphere to cool the grain layer.

The air velocity at the inlet of the dryer is $6 \text{ m}\cdot\text{s}^{-1}$, and in the grain layer it is between 1 and $2 \text{ m}\cdot\text{s}^{-1}$.

The distribution of the pathlines inside the vertical drier has shown in Fig. 6. This shows the role of the deflector cones and the nozzle inside the drier. By introducing the nozzle at the bottom, the section between the hot air duct and the lower nozzle wall decreases, causing a drop in the pressure. This pressure drop leads to the absorption of air in the atmosphere through the two lower regions of the dryer, which leads to the cooling of the cereals. With the cooling of the seeds, some of the heat accumulated by them through the drying process is recovered and reintroduced into the dryer's overall circuit, by mixing it with the hot air from the heater battery. The hot air mix pathlines from the bottom of the dryer are distributed evenly over the entire height of the three drying zones by means of the five cones. The highest temperature is distributed at the top of the dryer.

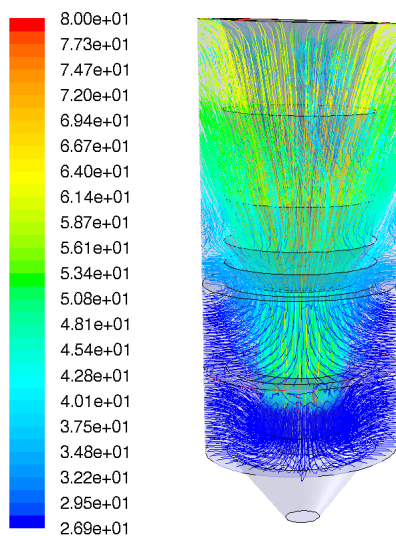


Figure 6. Temperature pathlines in the vertical dryer ($^{\circ}\text{C}$)

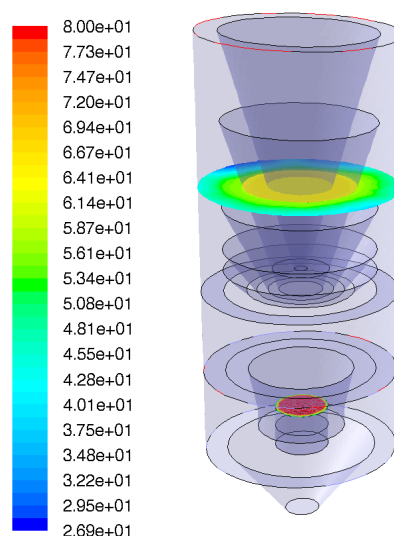


Figure 7. Temperature field on the cross section in the drying region of the dryer ($^{\circ}\text{C}$)

By cross-sectioning the dryer at the various height elevations shown in (Fig. 7), the temperature distribution in the hot air inlet region of the air heater battery has shown. In the drying region the distribution of the average temperature of 53°C in the grain seed layer was observed.

The ability to segment both the longitudinal and transversal vertical dryer by CFD simulation makes it possible to analyze the temperature and velocity fields and the pathlines and gives a 3D image of the distribution of cooling and heating/drying streams in the dryer. This makes possible to optimize the interior design of the dryer by varying the number of cones, their position and angle of inclination as well as the bottom section of the nozzle. The FLUENT software enables a functional optimization by introducing a large number of variants for input parameters (hot air velocity and temperature).

The results of the heat transfer inside the dryer are comparable to those in the literature and Fluent guide specifications.

Vertical grain dryers, currently available on the market, have an internal construction without additional devices to guide airflows to the grain layer and research in this field is at the beginning.

CONCLUSIONS

The paper presents the CFD simulation of an innovative vertical dryer for drying grain seeds, where the temperature and velocity field is presented. Temperature obtained by the CFD simulation of the vertical dryer have an error of $\pm 5\%$ against the experimental determinations, which is an accepted level in the heat transfer field. The temperature profile in seed layer resulting from the CFD simulation are presented with a high degree of accuracy. Both experimental and simulation were unsteady performed on a 3D geometry vertical dryer. The CFD simulation for drying allows large variations of temperature and velocity for hot air inlet.

ACKNOWLEDGEMENTS

This work was supported by a grant of the Romanian National Authority for Scientific Research and Innovation, CNCS/CCCDI – UEFISCDI, project number PN-III-P2-2.1-PED-2016-1357, within PNCDI III, contract no.18PED/2017.

REFERENCES

- Andra, de E.T. (2001). Simulacao da variacao de temperatura em milho armazenado em silo metalico. Tese de doutorado em Engenharia Agricola. Minas Gerais: Imprensa Universitaria, Universidade Federal de Vicosa, Brasil.
- Chang, C. S., Converse, H. H., Steele, J. L. (1993). Modeling of temperature of rain during storage with aeration. *Trans. Am. Soc. Agric. Engrs.*, 36, 2: 509-519.
- Chang, C. S., Converse, H. H., Steele, J. L. (1994). Modeling of moisture content of grain during storage with aeration. *Trans. Am. Soc. Agric. Engrs.*, 37, 6: 1891-1898.
- Devilla, I.A. (2002). Simulacao de deterioracao de distribuicao de temperatura umidade em uma massa de graos armazenados em silos com aeracao. Tese de doutorado em Engenharia Agricola. Minas Gerais: Imprensa Universitaria, Universidade Federal de Vicosa, Brasil.
- Dieter, B. and Karl S. (2006). Heat and mass transfer. Springer-Verlag, Berlin.
- Iguaz, A., Arroqui1, C., Esnoz, A., Virseda, P. (2004). Modeling and simulation of heat transfer in stored rough rice with aeration. *Biosystems Engineering*, 89, 1: 69-77.
- Incopera D. and Bergman T. (2007). Fundamentals of heat and mass transfer. John Wiley and Sons, New York.

- Hirsch, C. (1992). Numerical computation of internal and external flows, John Wiley and Sons, New York.
- Jia, C. C., Sun, D. W., Cao, C. W. (2001). Computer simulation of temperature changes in a wheat storage bin. *J. Stored Prod. Res.*, 37: 165-167.
- Metzger, J. F. and Muir W. E. (1983). Computer model of two dimensional conduction and forced convection in stored grain. *Canadian Agricultural Engineering*, 25, 2: 119-125.
- Patankar, S.V. and Spalding, D.B. (1972). A calculation procedure for heat, mass and momentum transfer in three-dimensional parabolic flows", *Int. J. Heat Mass Tran.* 14: 1787-1806.
- Sinicio, R., Muir, W.E., Jayas, D.S. (1997). Sensitivity analysis of a mathematical model to simulate aeration of wheat stored in Brazil. *Postharvest Biol. Technol.* 11: 107-122.
- Sun, D.W. and Woods, J.L. (1997). Simulation of the heat and moisture transfer process during drying in deep grain beds. *Drying Technology*, 10, 15: 99-107.
- Tannehill, J. C., Anderson, D. A., Pletcher R. H. (1997). *Computational fluid mechanics and heat transfer*, Taylor and Francis.
- Thorpe, G.R. (2007). Heat and moisture transfer in porous hygroscopic media: two contrasting analyses. *Fifth International Conference on Heat Transfer, Fluid Mechanics and Thermodynamics*, Sun City, South Africa.
- Thorpe G.R. (2008). The application of computational fluid dynamics codes to simulate heat and moisture transfer in stored grains. *Journal of Stored Products Research* 44: 21-31.
- Vandormaal, J.P., Raithby, G.D. (1984). Enhancements of the SIMPLE method for predicting incompressible fluid flows. *Numer. Heat Trans.* 7: 147-163.
- Wilson, S.G. (1988). Simulation of thermal and moisture boundary layers during aeration of cereal grain. *Mathematics Comp. Simul.* 30: 181-188.
- *** Ansys-Fluent. User Guide. 2010.
- *** FAO - <http://www.fao.org/home/en/>



ENERGY INDICES OF AN EQUIPMENT DURING FAST FREEZING OF BERRIES

Cristian SORICĂ^{1*}, Marian VINTILĂ², Valentin VLĂDUȚ¹, Mihai MATACHE¹,
Elena SORICĂ¹, Ion GRIGORE¹

¹ National Institute of Research - Development for Machines and Installations Designed to Agriculture and Food Industry – INMA, Ion Ionescu de la Brad Blv. No. 6, Sector 1 Bucharest, Romania

² Institute of Research and Development for Industrialization and Marketing of Horticultural Products "HORTING", Intrarea Binelui Street, No.1A, sector 4, Bucharest, Romania

*E-mail of corresponding author: cri_sor2002@yahoo.com

SUMMARY

In the period after harvesting or manufacturing, food undergoes a number of changes under the influence of external or internal factors. These factors worsen the quality, ultimately leading to total depreciation of the products. In order to preserve perishable food and extend the permissible storage and marketing period, one of the best methods of using artificial cold is freezing. One of the modern freezing techniques is that of cryogenic freezing using liquid carbon dioxide (CO₂) or liquid nitrogen (N₂) as a cooling substance. The research presented in the paper aims to determine the energetic indexes of an experimental model of fast freezing equipment with liquid nitrogen, both in automatic and manual operating mode. Three species of berries, namely red currants, blueberries and raspberries, were used in experimental research. The results reveal that the application of an aggressive freezing regime leads to fissures and cracks in fruit epidermis and pulp, leading to a qualitative depreciation of the frozen product. Although the rating of energetic indexes is inferior in the case of the automatic operation mode, compared to the manual one with continuous purging of liquid nitrogen, the quality of the frozen products is superior to that obtained in the manual mode.

Keywords: perishable food, cryogenic freezing, fast freezing equipment

INTRODUCTION

On the technological food chain, between harvesting (or production) and consumption, product losses can reach between 30-80% of total production, depending on the nature of the product, its marketing, climatic conditions, etc (Tofan, 2005; Toivonen et al., 2014). The main

causes of these losses are: mechanical actions (structure degradation by crushing), drying processes, aging (especially in the case of fruit) and degrading action of pests (microflora, rodents, birds, etc.) (Dimitriev, 2012).

A perishable product is the product that is susceptible to altering, changing its properties and composition. Essentially, all food products are perishable, namely, in the period after harvesting or manufacturing, they are subjected to a series of changes under the influence of external or internal factors. These changes in the composition and properties of food products (nutritive, organoleptic, physicochemical and commercial) occur under the action of three major categories of modifying agents: microbiological (microorganisms), biochemical and physicochemical (Niculita, 1998; Niculita et al., 2006). Changes in composition and attributes of food products initially lower the organoleptic, commercial, nutritional values and, ultimately, can lead to the complete depreciation of the respective product, rendering it inappropriate for consumption or dangerous for human health (Tofan, 2005).

In food products of plant origin, microorganisms are mainly represented by bacteria, moulds and yeasts. Changes of microbiological nature include the following phenomena: moulding, fermenting, decay and product altering by pathogenic and toxicogenic germs (Niculita, 1998; Niculita et al., 2006). According to the temperature level at which their metabolism is optimal, the microorganisms are divided into three categories: thermophile ($t_{min} = 45^{\circ}\text{C}$ –for thermophilic microorganisms), mesophile ($t_{min} = 10^{\circ}\text{C}$ - for mesophilic microorganisms) and psychrophile ($t_{min} = -10^{\circ}\text{C}$ –for psychrophilic microorganisms).

Cooling a product at temperatures below $+10^{\circ}\text{C}$ respectively below -10°C and keeping it at these temperatures leads to the total inhibition or elimination of mesophilic and psychrophilic microorganisms metabolism and, consequently, to diminishing or eliminating their effects on the attributes of the respective product (Porneala and Balan, 2003). Storage at low temperatures is widely used as a post-harvest treatment applied to delay the degradation of vegetables and fruit maturation (Aghdam and Bodbodak, 2014). It is mainly done by two methods: refrigeration and freezing.

The increase of preservability obtained by freezing (also ensuring the conditions required for frozen storage) is based on the effects of low temperatures to strongly slow or completely inhibit microorganism development, reduce or stop metabolic processes in living products and reduce chemical and biochemical reactions. Taking into account the minimum temperature levels of psychrophilic microorganisms multiplication, the maximum freezing temperature of foodstuffs is generally considered to be -10°C . Below this temperature, the development of microorganisms is practically negligible (Porneala and Balan, 2003).

In general, freezing occurs at temperatures between -18°C and -40°C . Depending on the temperature at which it occurs, one of freezing method is also fast freezing carried out at temperatures of -30°C ... -35°C and lasting up to 24 hours. The structural changes that occur in the frozen product depend on the size of the ice crystals formed. Slow freezing produces large crystals that lead to the detachment and damage of cells and tissues. By thawing, the hydrophilic colloids in the cells can no longer rehydrate to the initial state before freezing, causing large cellular juice losses. By fast and ultrafast freezing the best results are obtained.

One of the modern freezing technique is cryogenic freezing that uses liquid carbon dioxide (CO_2) or liquid nitrogen (N_2) as cooling substance (Fellows, 2017). Compared to conventional freezing techniques, the cryogenic method has the following advantages: fast freezing, inhibition of bacterial growth, limited dehydration, considerable reduction of quantitative losses, optimal preservation of nutritional value, maintenance of food products' appearance and taste.

The research presented in the paper aims to determine the energetic indexes of an experimental model of fast freezing equipment with liquid nitrogen, both in automatic and manual operating mode.

MATERIALS AND METHOD

Three species of berries bought from the market, namely red currants (Fig. 1A), blueberries (Fig. 1B) and raspberries (Fig. 1C), were used in the experimental research.



Figure 1. Species of berries used in the experimental research

For berries ultrafast freezing an experimental model of discontinuous operation freezing equipment with liquid nitrogen, ECR-0, intended for cryogenic freezing of different food products, developed by INMA Bucharest within the sectoral research programme was used (Fig.2).



Figure 2. Fast freezing equipment – ECR

The equipment is provided with temperature sensors that allow monitoring and permanent control of process parameters, namely: type K Thermocouple (chromel–alumel), probe diameter $\phi 1.5$ mm, measuring range $-100^{\circ}\text{C} \dots +30^{\circ}\text{C}$, allows temperature measurement in the centre of the product; type K Thermocouple, with temperature transfer element, measuring range $-100^{\circ}\text{C} \dots +30^{\circ}\text{C}$, allows temperature measurement on the external surface of

the product; thermal resistance, type TTR Pt 100, measuring range $-200^{\circ}\text{C}\dots+30^{\circ}\text{C}$, allows temperature measurement inside the freezing chamber. The chamber is provided with an access door, thermal insulated and provided with two sealing gaskets and de-icing resistances to prevent ice formation and to facilitate access to the chamber at the end of the freezing cycle. The locking system is provided with two clamps and a handle to obtain a uniform and firm closing. In order to achieve a forced convection of the atmosphere in the chamber in order to improve the thermal transfer from the product to the thermal agent, a fan was provided inside the chamber. The equipment allows operation in two working modes, namely: automatic operation mode, with setting the chamber temperature limit at which ventilation starts (in this case -30°C) and liquid nitrogen purging stops; manual operation with continuous liquid nitrogen purging.

In order to prepare for the experimental research, the following activities were carried out: for each berry species, the average mass of a berry as an average of five random weighings of the product mass was determined, the average height and the maximum equatorial diameter of the berries corresponding to each sample of the three species were measured. The mass of each sample was set at 125 g.

Considering the geometric shape of the three species fruits, the smallest distance between the thermal centre and the outer surface of the product was calculated. Assuming that the plant tissue of the product is homogeneous, having constant thermal properties throughout its mass, it is considered that the thermal centre coincides with the mass centre of the product. For regular geometric shapes, the thermal centre (CT) coincides with their geometric centre. The smallest distance between the thermal centre CT and the outer surface of the product is noted with δ_0 and is an important parameter for determining the freezing rate (Fig.3). For red currants and blueberries, δ_0 was approximated by $h/2$ and for raspberries it was approximated by $h'/2$.

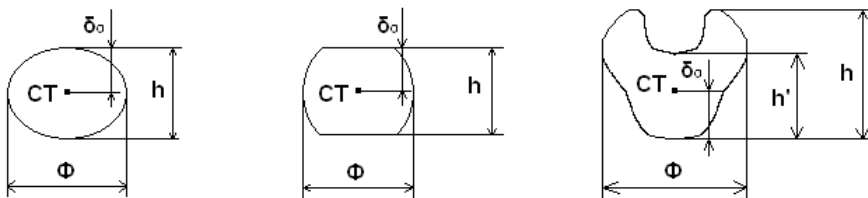


Figure 3. Dimensional characteristics according to the geometric shape of the analysed product

The freezing process is considered complete when the temperature in the product thermal centre reaches -15°C . The parameters followed during the freezing process were as follows: mass of the liquid nitrogen container used for freezing; freezing time from 0°C to -15°C ; total freezing time. Following the processing of experimental data, the following energy indexes were determined: average linear freezing rate; liquid nitrogen consumption for a freezing cycle. To characterize a freezing process in terms of cooling intensity, we consider as criterion the average linear freezing rate given by the relation:

$$w_m = \frac{\delta_0}{\tau_0}, [\text{cm}\cdot\text{h}^{-1}] \quad (1)$$

where: δ_0 is the smallest distance between the thermal centre and the outer surface of the product, [cm]; τ_0 - the freezing time from a uniform initial temperature of 0°C to the temperature to be achieved in the thermal centre, [hours].

Depending on the average freezing rate, w_m , the International Institute of Refrigeration (IIR, 2006) recommends the following classification of freezing methods: slow freezing ($w_m < 0.5 \text{ cm}\cdot\text{h}^{-1}$), fast freezing ($w_m = 0.5 \dots 3 \text{ cm}\cdot\text{h}^{-1}$), very fast freezing ($w_m = 3 \dots 10 \text{ cm}\cdot\text{h}^{-1}$) and ultrafast freezing ($w_m = 10 \dots 100 \text{ cm}\cdot\text{h}^{-1}$).

Liquid nitrogen consumption for a freezing cycle was determined by the difference between the mass of the liquid nitrogen container before and after the freezing process was completed.

RESULTS AND DISCUSSION

Following the processing and interpretation of the experimental data, the following results were obtained regarding the characterization of the three species of berries used:

Table 1. The characteristics of the species of berries used for experimentation

No.	Characteristic	UM	Value of parameters determined in the tests		
			Red currants	Blueberries	Raspberries
1.	Sample mass	g	125	125	125
2.	Average mass of a berry fruit	g	0.982	2.178	3.396
3.	Berries maximum equatorial diameter, Φ (average of five random measurements)	mm	11.72	16.51	20.24
4.	Berries average height, h	mm	11.22	13.20	h=14.15 h'=4.46
5.	The smallest distance between the thermal centre and the outer surface of the product, δ_0	mm	0.561	0.660	0.223

Process temperatures, during the freezing process, are determined by direct reading on the touch screen of the command and control panel (Fig.4).

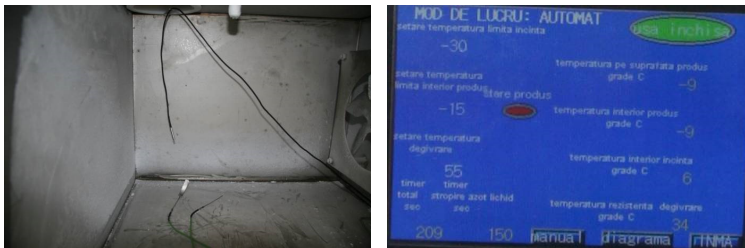


Figure 4. Determination of process temperatures using sensors specially intended for this purpose

Freezing times were determined by calculation respectively by direct reading from the total timer display at the end of the freezing process, as follows: the freezing time from 0°C to -15°C was determined by the difference between the total time at the end of the freezing process (-15°C) and its display when the temperature reached 0°C in the product's thermal

centre; the total freezing time was determined by direct reading of the total timer display at the end of the freezing process. Aspects from the determination of liquid nitrogen consumption are shown in Figure 5.



Figure 5. Determination of liquid nitrogen consumption by weighing

The followed parameters during the freezing process and the energetic indexes of fast freezing equipment are shown in Table 2.

Table 2. The parameters of the freezing process and the energetic indexes

No.	Characteristic	U.M.	Value of parameters determined in the tests		
			Red currants	Blueberries	Raspberries
Automatic operation mode					
1.	Freezing time from 0°C to -15°C	s	85	252	175
2.	Total freezing time	s	137	338	292
3.	Average linear freezing rate for an operating cycle with the chamber limit temperature set to -30°C	cm h ⁻¹	23.76	9.43	4.59
4.	Liquid nitrogen consumption for an operating cycle with the chamber limit temperature set to -30°C	kg	0.96	1.3	1.02
Manual operation mode					
1.	Freezing time from 0°C to -15°C	s	42	39	46
2.	Total freezing time	s	82	68	70
3.	Average linear freezing rate for an operating cycle, with continuous purging of liquid nitrogen	cm h ⁻¹	48.08	60.92	17.45
4.	Liquid nitrogen consumption in case of continuous purging	kg	1	0.82	0.88

Total freezing time, in the case of automatic operation mode, registered a minimum value for red currants and maximum for blueberries. In the case of manual operation mode, the total freezing time registered a minimum value for blueberries and maximum for red currants. Total freezing time was shorter in the case of manual operation mode.













The average linear freezing rate for an automatic operation cycle registered values corresponding to a very fast freezing process for blueberries and raspberries, and corresponding values for an ultrafast freezing process in the case of red currants.

The average linear freezing rate was much higher in the case of manual operation mode for all species of berries used.

Liquid nitrogen consumption, in the case of automatic operation mode, registered a minimum value for red currants and maximum for blueberries. In the case of manual operation mode, liquid nitrogen consumption registered a minimum value for blueberries and maximum for red currants. Liquid nitrogen consumption, as a whole, was lower in the case of manual operation mode.

Liquid nitrogen consumption varies directly proportional to total freezing time, in all analysed cases.

Table 3. Aspect of the samples before and after freezing

Description	Samples aspect during the experimentation		
	Red currants	Blueberries	Raspberries
Automatic operationmode			
Before freezing			
After freezing			
Manual operation mode			
Before freezing			
After freezing			

Although the liquid nitrogen consumption appears to be relatively higher in the automatic operation mode, the total freezing time is longer and the average linear freezing rate is lower, the quality of the frozen products is superior to the one obtained in the manual operation mode with continuous purging of liquid nitrogen.

After the visual analysis of the state of frozen products' outer surface, it was found that in the case of red currants and blueberries, fissures and cracks appeared in fruit epidermis and pulp during freezing in manual operation mode with continuous purging of liquid nitrogen. Raspberry fruits reacted better, with no deterioration of the outer surface condition.

Allan-Wojtas et al. (1999) demonstrated that faster freezing rates in liquid nitrogen produced frozen blueberries with better quality. Although rapid freezing was associated with an improved internal microstructure of individual berries, it also caused a fracture on the berry skin as a consequence of thermal shock.

Delgado and Rubiolo (2005) have used strawberries subjected to different freezing conditions, ranging from slow to fast freezing. High freezing rates resulted in fruits with better structure, since the rapid seeding and growth of ice crystals did not damage the cell walls and ice was primarily formed inside the cells. Reducing the freezing rates affected the shape of the cells, and there was evidence of ice growing in the extracellular environment. Even slower freezing rates resulted in a loss of membrane integrity with extracellular freezing, cell collapse, and water loss.

Although fast freezing is regarded as the best technique to maintain the texture of frozen products, Chassagne-Berces et al. (2009, 2010) demonstrated that very fast rates (submerging in liquid nitrogen) led to loss of firmness due to freeze cracking.

CONCLUSIONS

In the period after harvesting or manufacturing, food undergoes a number of changes under the influence of external or internal factors. These factors worsen the quality, ultimately leading to total depreciation of the products. In order to preserve perishable food and extend the permissible storage and marketing period, one of the best methods is using artificial cold.

Storage at low temperatures is widely used as a post-harvest treatment applied to delay the degradation of vegetables and fruit maturation.

The increase of preservability obtained by freezing is based on the effects of low temperatures to strongly slow or completely inhibit microorganism development, reduce or stop metabolic processes in living products and reduce chemical and biochemical reactions.

One of the modern freezing technique is cryogenic freezing that uses liquid nitrogen (N₂) as cooling substance. Compared to conventional freezing techniques, the cryogenic method has the following advantages: fast freezing, inhibition of bacterial growth, limited dehydration, considerable reduction of quantitative losses, optimal preservation of nutritional value, maintenance of food products' appearance and taste.

Although cryogenic fast freezing is regarded as the best technique to maintain the texture of frozen products, the use of a very aggressive freezing regime (submerging in liquid nitrogen) leads to fissures and cracks in fruit epidermis and pulp, as a consequence of thermal shock, leading to a qualitative depreciation of the frozen product.

Better results are obtained by using of an automatic operation mode for the cryogenic fast freezing process, alternating the continuous purging of liquid nitrogen with the ventilation of liquid nitrogen vapours, which conducts to an increase of quality of the frozen products.

REFERENCES

- Aghdam, M.S. and Bodbodak, S. (2014). *Food Bioprocess Technol.* Volume7, Issue 1, pp. 37-53, Springer US, p-ISSN1935-5130, e-ISSN 1935-5149, <https://doi.org/10.1007/s11947-013-1207-4>.
- Allan-Wojtas, P., Goff, H.D., Stark, R., Carbyn, S. (1999). The effect of freezing method and frozen storage conditions on the microstructure of wild blueberries as observed by cold-stage scanning electron microscopy. *Scanning*, vol. 21, 334–347.
- Chassagne-Berces, S., Fonseca, F., Citeau, M., Marin, M. (2010). Freezing protocol effect on quality properties of fruit tissue according to the fruit, the variety and the stage of maturity. *LWT Food Sci. Technol.*, vol. 43, 1441–1449.
- Chassagne-Berces, S., Poirier, C., Devaux, M.F., Fonseca, F., Lahaye, M., Pigorini, G., Girault, C., Marin, M., Guillon, F. (2009). Changes in texture, cellular structure and cell wall composition in apple tissue as a result of freezing. *Food Res. Int.*, vol. 42, 788–797.
- Delgado, A.E. and Rubiolo, A.C. (2005). Microstructural changes in strawberry after freezing and thawing processes. *LWT Food Sci. Technol.*, vol. 38, 135–142.
- Dimitriev, V. (2012). *The Basics of Refrigeration Technology–lecture cycle*, Technical University of Moldova Publishing House, Chisinau.
- Fellows, P.J. (2017). *Food Processing Technology. Principles and Practice (Fourth Edition)*, Woodhead Publishing Series in Food Science, Technology and Nutrition, chapter 22-Freezing, Pages 885–928, ISBN: 978-0-08-101907-8, <https://doi.org/10.1016/B978-0-08-100522-4.00022-5>.
- IIR, *Recommendations for the processing and handling of frozen foods*, 2006.
- Liang, D., Lin, F., Yang, G., Yue, X., Zhang, Q., Zhang, Z., Chen, H. (2015). Advantages of immersion freezing for quality preservation of litchi fruit during frozen storage. *LWT Food Sci. Technol.*, vol. 60, 948–956.
- Niculita P. (1998). *Refrigeration technique and technology in agri-food fields*, Didactic and Pedagogical Publishing House R.A, Bucharest, ISBN 973-30-5719-3.
- Niculita, P., Popa, M., Belc, N. (2006). *Bioengineering and food biotechnology*, vol. I, Ed. Academiei Romane, Bucuresti, ISBN (10) 973-27-1349-6.
- Porneala, S. and Balan, M. (2003). *Use of artificial cold - electronic course*, Todesk Publishing House, ISBN: 973.8198-64-X.
- Sectoral Research Program of the Ministry of Agriculture and Rural Development, ADER 16.2.1: *Researches on thermal, physical properties, heat and mass transfer coefficients of horticultural products for the optimization of freezing technologies applied on cold chains*, 2015 – present.
- Tofan, I. (2005). *Cold chain of perishable food products*, Agir Publishing House, Bucharest.
- Toivonen, P., Mitcham, E., Terry, L. (2014). *Postharvest Care and the Treatment of Fruits and Vegetables*. In: Dixon G., Aldous D. (eds) *Horticulture: Plants for People and Places*, Volume 1. Springer, Dordrecht, p-ISSN978-94-017-8577-8, e-ISSN978-94-017-8578-5, pp 465-483, https://doi.org/10.1007/978-94-017-8578-5_13.



INFLUENCE OF INPUT FLOW OVER GRAIN MILL EFFICIENCY UTILISATION

Lucian V. FECHETE TUTUNARU^{1*}, Nicolae FILIP¹, Elena Mihaela NAGY²,
Mihai MATACHE²

¹ Department of Automotive Engineering and Transportation, Technical University of Cluj-Napoca, B-dul Muncii 103-105, Romania

² National Institute of Research - Development for Machines and Installations Designed to Agriculture and Food Industry - INMA Bucuresti, Romania

* E-mail of corresponding author: lucian.fechete@auto.utcluj.ro

SUMMARY

The paper presents the influences of input flow over productivity and energy consumption for a small grain mill, used to produce feed for animals. Through grinding in a mill, different grains and vegetables are used as coarse flour. Due to various mechanical properties of those input materials, the mill, in case of under or over feed through manual operated feed control mechanism is not optimally running. An investigation of different input flow of materials is conducted to find the optimal position of the feed mechanism in a non-automated version of the feeder. For that the productivity of the mill is determined and consumed electrical energy is measured and compared in order to establish an efficient strategy in order to operate the mill.

Key words: energy consumption, grain mill, coarse flour

INTRODUCTION

Grinding, in general, is the most important and energy-consuming processes in food industry. About 60-75% of energy in industrial processing is spent on grinding (Danciu et al., 2009).

According to Mohsenin N.N only about 1% of grinding energy is transformed into receiving a new surface (Mohsenin N.N,1986).

The amount of energy consumed during the grinding process depends on the type of mill applied, the mill settings and on the physical and chemical properties of grain and the degree of grinding (Dziki and Laskowski, 2002; Dziki, 2008; Fang et al., 1998; Greffeuille et al., 2007; Scanlon and Dexter, 1986; Wiercioch et al., 2008).

Kernel hardness has the most significant influence on the energy consumption of grain grinding. Hard wheat requires more energy for grinding than soft wheat (Dziki et al., 2012; Greffeuille et al., 2007;).

Different studies have dealt especially with the correlation between the effect of different properties of cereal grain (hardness of kernel, moisture content, ash content in grain and vitreousness of grain, etc) and energy consumption.

The aim of this study was to investigate if the tested mill is efficiently used and to study the influence of input flow on the energy efficiency of the grain mill

MATERIALS AND METHODS

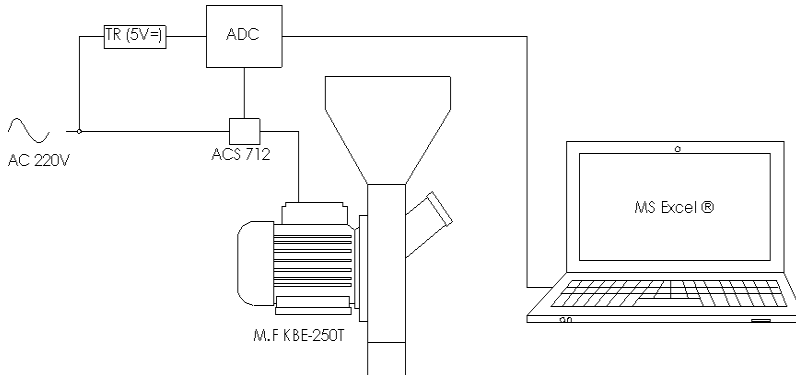
The experiment was carried out with wheat grain, ARIESAN varieties, harvested three months before, having a moisture below 14%. The wheat grains were grind in a universal household M.F KBE-250T mill, manufactured by a company named TONI (fig.1). This is a hammer mill with four lines of hammers, having five hammers in each line. The mill is powered with a 2.5 kW electric motor at 3000 rpm. The productivity of the mill, specified by the producer, is 180 kg·h⁻¹, depending on the characteristics of the grain. The mill is equipped with a shutter plate dosing mechanism, but to increase the productivity this mechanism was modified. To allow the introduction of more material we built a bigger opening tangential to the movement direction of the hammers. This mechanism has a maximum of 8x4.75 cm opening. The mill can be equipped with different diameter holes sieves, commercially available. For our research we used three sieves having a diameter of 1.5; 2.5 and 4.5 mm holes.



Figure 1. Modified universal household M.F KBE-250T mill

During the milling operation the energy consumption of the mill and also the duration of the milling for a constant amount of grains were determined in each measurement. Measurements were made for each sieve, having the shutter plate opened from 1 to 8 cm, three times for each opening, so that totally 3x8x3=72 measurements were made. For each

measurement a constant amount of 1750 grams of grain was used. This means a total of 126 kg of milled wheat.



Figureb 2. DAQ measurement system

The measurements (fig.2) were made using ACS712, a Hall effect current sensor type. This was serially connected with the electric motor of the mill and the power source. This sensor has an analog voltage output, which is converted into a digital signal in the Analog-Digital Converter module based on Atmega 328 microcontroller. The resulted digital outputs were directly acquired and then processed in a MS Excel® file.

For each test, the following sequence was repeated:

- the same amount of grains was put in the hopper;
- start recording of DAQ system (time and absorbed current, data acquiring frequency 1 Hz) ;
- start the electrical motor, wait for idle regime;
- open the shutter plate to the selected 8 position from 0 to 8 cm with a step of 1 cm (mill is grinding);
- wait until grinding is finished;
- stop the electrical motor, stop and save DAQ system file.

RESULTS AND DISCUSSION

The results obtained for each sieve and repetition were automatically recorded in Excel application. An example recorded for the sieve with 1.5 mm diameter holes is presented in fig. 3.

It can be noted from the above figure the main components of the recorded signal respectively, the starting current which is higher than 8.5 A (limit value measured by the current sensor), then the current corresponding to the idle functioning regime, followed by the raise of the current corresponding to the opening of the distributor plate. After all the grains have entered into the mill current values are lowering due to smaller amount processed until the idle current is reached and the motor is stopped. Time periods recorded, in seconds, were processed based on current variations and were calculated as the period for which the mill is functioning in load – milling time, the time for which the mill is decreasing

the current after all material from hopper was gravitationally entered into the mill, until the idle operation regime – ending time and the start time, the time for which the mill is starting to grind after it was started.

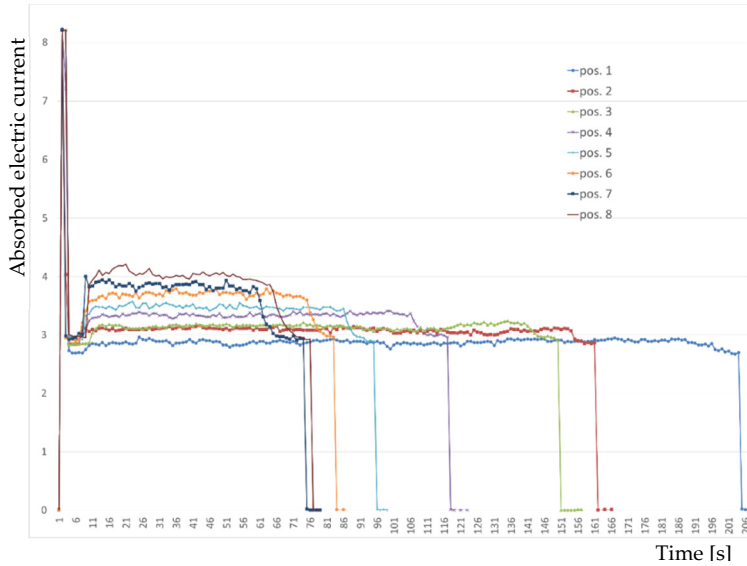


Figure 3. Current variation vs. distributor position for 1.5 mm diameter sieve

The current variations for each position of the shutter plate of the distributor mechanism are clearly revealed and the maximum, minimum and average values were extracted from the data series in table 1. The mode and median values were presented as statistic indicators of the measurements quality. Based on milling time and the grain quantity processed by the mill the input flow was calculated. Also, the mill absorbed electrical energy was calculated through integration of the current during the milling time. Two specific efficiency indicators were calculated, specific current and specific energy, by reporting the current respectively the absorbed energy to the corresponding input flow of grains into the mill.

Based on data from table 1 the variation of the current (I) and time (T) recorded for the three sieves with 1.5, 2.5 and 4.5 mm diameter are presented in fig. 4. It can be seen that the current variation with the position of the distributor plate is increasing almost linearly from an idle current of 2.69 A to a maximum recorded of 4.21 A, values that correspond to an absorbed power of the electrical motor from 645 W in idle time to 1010 W in maximum recorded load time. Taking into consideration the initial value of the supply area under the hopper was 19.6 cm², and the value was raised by cutting an additional 18.4 cm² in order to increase the input flow, the maximum current of 5.2 A stated by the mill manufacturer was not reached.

Table 1. Measured and calculated values of the mill main energy indicators

Sieve	Position	Inlet Area [cm ²]	Input flow [kg·h ⁻¹]	I _{max} [A]	I _{av} [A]	I _{min} [A]	Mode	Median	Energy [Wh]	10 ⁻³ · I _{av} /Input flow [A·h·kg ⁻¹]	10 ⁻³ · Energy/Input flow [W·h ² ·kg ⁻¹]	milling time [s]	ending time [s]	start time [s]
1.5 mm	1	4.7	35.4	2.96	2.88	2.76	2.89	2.89	32.95	81.40	930.93	178	17	10
	2	9.4	43.5	3.16	3.09	3	3.09	3.09	28.79	71.05	662.74	145	9	13
	3	14.1	48.5	3.24	3.15	3.04	3.15	3.17	26.34	64.94	543.55	130	10	14
	4	18.8	67.7	3.41	3.34	3.25	3.34	3.37	19.86	49.29	293.14	93	15	14
	5	23.5	81.8	3.57	3.47	3.33	3.47	3.45	17.31	42.44	211.51	77	10	10
	6	28.2	94.0	3.79	3.68	3.57	3.7	3.73	15.58	39.17	165.69	67	9	14
	7	32.9	118.9	4	3.81	3.73	3.84	3.84	12.77	32.08	107.45	53	15	10
	8	37.6	137.0	4.21	4.04	3.85	4.03	4.02	12.13	29.49	88.54	46	21	10
2.5 mm	1	4.7	30.73	2.94	2.86	2.78	2.89	2.87	37.65	93.07	1225.12	205	8	10
	2	9.4	39.13	3	2.92	2.86	2.92	2.92	30.25	74.69	773.06	161	13	13
	3	14.1	45.00	3.07	2.98	2.85	3.03	2.99	26.89	66.32	597.56	140	9	10
	4	18.8	59.43	3.31	3.15	3.03	3.11	3.12	21.33	52.98	358.89	106	11	10
	5	23.5	80.77	3.48	3.38	3.29	3.37	3.37	17.06	41.86	211.22	78	17	11
	6	28.2	91.30	3.7	3.53	3.41	3.47	3.52	15.8	38.68	173.05	69	12	11
	7	32.9	101.61	3.92	3.73	3.5	3.71	3.73	15.01	36.71	147.72	62	12	11
	8	37.6	108.62	4.09	3.88	3.65	3.89	3.89	14.63	35.72	134.69	58	12	9
4.5 mm	1	4.7	49.61	2.86	2.77	2.64	2.75	2.78	22.64	55.81	456.39	127	9	9
	2	9.4	86.30	2.99	2.91	2.78	2.9	2.9	13.74	33.67	159.21	73	5	9
	3	14.1	112.50	3.03	2.91	2.85	2.92	2.91	10.6	25.88	94.22	56	6	7
	4	18.8	131.25	3.21	3.07	2.83	3.05	3.07	9.6	23.36	73.14	48	7	13
	5	23.5	143.18	3.17	3.12	2.98	3.13	3.12	8.96	21.76	62.58	44	6	13
	6	28.2	170.27	3.59	3.25	3.15	3.22	3.24	7.89	19.07	46.34	37	8	13
	7	32.9	252.00	3.56	3.37	3.24	3.34	3.365	5.6	13.39	22.22	25	11	10
	8	37.6	315.00	3.59	3.49	3.37	3.47	3.48	4.68	11.08	14.86	20	9	8

In the same time the period needed to grind the mass of 1.75 kg of grain, for the three sieves was decreasing from a maximum of 178 seconds to 20 seconds, almost 9 times difference, for the 8 position used of distributor shutter plate. A second degree polynomial equation can express the variation of milling time, for first two sieves, with more than 99% confidence and for the last one the 4.5 mm with 91% confidence.

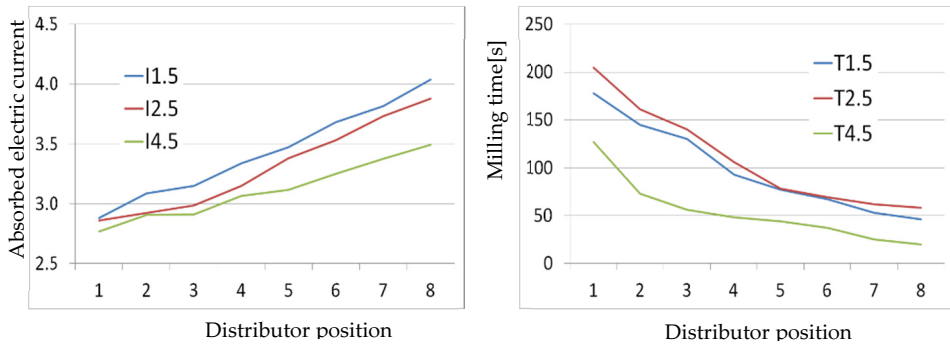


Figure 4. Current and milling time variation vs. distributor position for all 3 sieves

Regarding the electrical energy consumption of the motor and grains input flow, its variation with the 8 position of the shutter plate is presented in fig. 5. It can be seen that the allure of the curves are similar to that of the milling time due to the fact that time has an important contribution in integration equation. This way, the energy values calculated are between 4.7 and 33 W·h for the grinded mass of 1.75kg. Also, the variation of the input flow which can be stated to have the same value as mill productivity is ranging from 30.7 to 315 kg·h⁻¹.

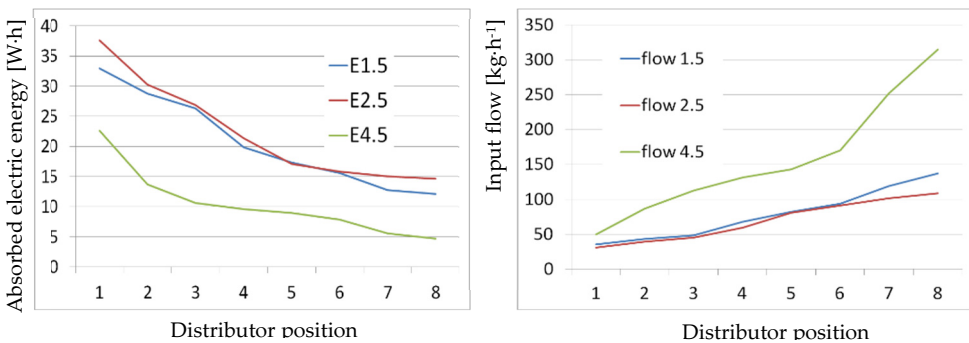


Figure 5. Energy absorbed and input flow variation vs. distributor position for all 3 sieves

The graphical representation of the two specific energy indicators (fig. 6), current and absorbed energy reported to grains input flow shows almost similar curvature with different magnitude for the two graphs. It can be seen that both these two indicators are decreasing with the increase of input flow due to smaller time needed to grind the specified grain mass. In the same time the decreasing is asymptotic approaching to a limit also due to milling time which is limited by the movement of the grinded volume present inside the mill and not passed through the holes of the sieve.

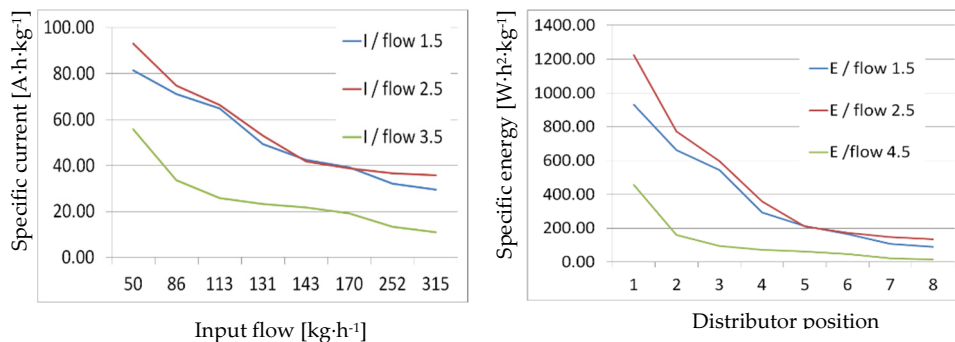


Figure 6. Specific current and energy variation for all 3 sieves

From the graphical representations presented can be seen that with the increase of the supply opening of the mill, the shutter plate, the productivity is increased. This is due to the fact that the shutter plate act as a bottleneck and more time is needed for the grains to pass from the hopper inside the mill. That concludes that the more input flow the higher the mill productivity and higher energy efficiency. But, in the same time, with the increase of the input flow, an increase of the supply current is recorded which is limited by the constructive characteristics of the electrical motor. For the analyzed case of the KBE-250T mill, can be seen that producer has limited the productivity either as a way to protect the electric motor (overheating) or as a poor design. Nevertheless, by modifying the mill in order to increase the input flow, an increase in productivity was acquire of max.75% (for the sieve with 4.5mm hole) without reaching the motor maximum current. Taking into consideration that different grains that are commonly used in animal feeding have different mechanical resistance to breaking and therefore different energy requirement to grind, a device can be design to allow to control the input flow based on absorbed current and/or motor temperature.

CONCLUSIONS

A common animal feeding mill was investigated from the perspective of energy utilization by varying its distributor plate position and sieve holes diameter. The variables measured were absorbed current of the electrical motor and mill functioning time. Through calculus the input flow/productivity was determined as well as consumed electrical energy. The results showed that for the investigated mill, the electrical motor is not efficiently used and several modifications were made in order to increase the energy efficiency as well as mill productivity. Based on the stated a device is proposed to be design in order to automate the supply of the mill with grains in order to minimize the human intervention/errors in the supply process.

REFERENCES

- Danciu, I., Danciu, C., Banu, I., Vaduva, M., Mester, M. (2009). Researches regarding the grinding resistance of the wheat grain. *Journal of Agroalimentary Processes and Technologies*, 15(3):393-395.
- Dziki, D. and Laskowski, J. (2002). Wpływ wielkości ziarna na wybrane właściwości pszenicy. *Inżynieria Rolnicza*, 5(38): 337-344.

- Dziki, D. (2008). The crushing of wheat kernels and its consequence on the grinding process. *Powder Technology*, 185(2): 181-186.
- Fang, Q., Haque, E., Spillman, C.K., Reddy, P.V., Steele, J.L. (1998). Energy requirements for size reduction of wheat using a roller mill. *American Society of Agricultural Engineers*, 41(6):1713-1720.
- Greffeuille, V., Abecassis, J., Barouh, N., Villeneuve, P., Mabile, F., Bat, L'Helouac'h, C., Lullen-Pellerin, V. (2007). Analysis of the milling reduction of bread wheat farina, physical and biochemical characterization. *Journal of Cereal Sciences*, 45(1): 97-105.
- Mohsenin, N.N. (1986). *Physical properties of plant animal materials. Structure, physical characteristics and mechanical properties.* New York: Gordon and Breach Science Publisher.
- Scanlon, M.G. and Dexter, J.E. (1986). Effect of smooth roll grinding conditions on reduction of hard red spring wheat farina. *Cereal Chemistry*, 63(5): 431-435.
- Wiercioch, M., Niemiec, A., Romański, L. (2008). Wpływ wielkości ziarniaków pszenicy na energochłonność ich rozdrabniania. *Inżynieria Rolnicza*, 5(103): 367-372.



ASPECTS REGARDING THE FLOW OF THE MIXTURE FLOUR-WATER AT DIFFERENT TEMPERATURES, THROUGH SMALL DIAMETER CHANNELS

Mariana-Gabriela MUNTEANU*, Gheorghe VOICU, George IPATE,
Nelus Evelin GHEORGHÎĂ, Gabriel-Alexandru CONSTANTIN,
Iulian-Claudiu DUTU, Irina-Aura ISTRATE

University Politehnica of Bucharest, Faculty of Biotechnical Systems Engineering,
Splaiul Independentei Blv., no. 313, sector 6, Bucharest, Romania

*E-mail of corresponding author: munteanumaya@yahoo.com

SUMMARY

Taking into account the importance of the rheological properties of food mixtures in manufacturing processes, this paper focuses on the flow of flour-water fluids at different temperatures. During flour mixing, flour proteins bind water causing swelling of gliadin and glutenin. At the same time, although it is considered a minor component, starch contributes indirectly to the change in the consistency of the mixtures. Among other things, the most important property of starch is its gelatinization. Gelatinization takes place by exposing flour-water flour samples to a temperature above 60°C. The paper generally refers to the flow through small holes and two lengths of mixtures of 100 ml of water and 14 g of wheat flour at different temperatures (27, 40, 50, 65°C). It has been found that there are changes in the strength force of piston force of the device used in experiments depending on the temperature of the mixture and the length and diameter of the flow hole. Thus, for higher temperatures, the resistance force tends to increase, regardless of the length and diameter of the flow channel, since the starch granules swell and worsen the flow through the channel. If the length of the flow channel decreases, then the strength force encountered by the piston also decreases, the force values falling within 1.5- 5 N. The results presented in the paper can be useful to the specialists and workers in the field of agro-food processing, on the technological flow of manufacturing.

Keywords: starch, gelation, viscosity, pressure, flow rate, the strength of resistance

INTRODUCTION

The purpose of preparing starch-rich products (pasta, cereals, potatoes, etc.) is to transform the starch into a digestible form by the so-called gelatinization process (Fasano et al., 2011). Starch $C_6H_{10}O_5$ is a polysaccharide which structurally consists of amylose and amylopectin (22-28% and 78-72%, respectively, for wheat starch) (Gerits et al., 2015; Encyclopædia Britannica, 2017). The starch granules appear as water-insoluble semi-crystalline (Gerits et al., 2015). The physicochemical properties of starches depend on the botanical source from which they are isolated. The major botanical and commercial sources of starches are cereals, tubers, roots, and legumes. There were published numerous comparisons of the physicochemical and functional properties of starch from different cultures and it has been found that cereal starches contain a significant amount of phospholipids (Li et al., 2014).

Gelatinization involves the breakage of intermolecular bonds and the aggregation of water molecules (Fasano et al., 2011). Evidence of the loss of an organized structure includes irreversible granule swelling, loss of birefringence, and crystallinity (Li et al., 2014). Such a process requires a sufficiently high temperature and also sufficiently high moisture content. It is believed that the threshold temperature for gelatinization is a linear function of the moisture content. However, this can be true only within some moisture range, because the process does not take place at all if not enough water is available. Water penetration occurs even at room temperature (although very slowly and with no gelatinization) and is greatly facilitated in boiling water (Fasano et al., 2011).

The initial rise temperature provides an indication of the minimum temperature required to gelatinize a given sample, which can have implications for the stability of other components in a formula, and also indicate energy costs (Sopade et al., 2006).

However, in most food systems the actual temperature at which starch gelatinizes is less important than those properties that depend on swelling, such as pasting behaviour and rheological properties of the partially or fully swollen starch granules. The properties of the starch-water system will, of course, be different if the swollen granules are dispersed mechanically to give a uniform gel (Tester and Morrison, 1990). Also, the swelling of the starch granules is accompanied by increased viscosity of the fluid (Tofană, 1997).

Final viscosity is the most commonly used parameter to define sample quality, as it indicates the ability of the material to form a viscous paste or gel after cooking and cooling (Sopade et al., 2006).

For many fluids, the viscosity depends only on the state parameters (temperature and pressure) and does not depend on the stress requirements to which the fluid is subjected (deformation stress and deformation rate) (Dynamics of fluids, 2017).

In order to explain the flow behaviour of real fluids, the flow between two flat and parallel plates is considered to be a real fluid. Movement of the layers is determined by the friction forces between the fluid layers, friction forces being caused by the molecular cohesion (Dynamics of fluids, 2017).

In many processes of the food industry are necessary thickened liquids to be processed, and transported on longer or shorter trail. In the bakery / pastry industry there are flour mixtures that have to be mixed, processed or transported through channels. Their flow is influenced by both the concentration in the flour and the temperature of the mixture, knowing that the hydrated flour particles worsen the flow, and at temperatures above 60 °C the starch granules begin the gelatinization.

The aim of this paper was to present the flow through the small diameter channels of a flour-based fluid mix at several working temperatures under the influence of a piston pump pressure, tests simulating the flow of fluids on the basis of the flour through the mold holes (eg wafers, pancakes, cakes, muffins, etc.).

MATERIALS, METHODS AND PROCEDURES - THEORETICAL ASPECTS

Experimental research was conducted at the Faculty of Biotechnical Systems Engineering from the University Politehnica of Bucharest. For the experiments, wheat flour type 650 and drinking water were bought from commerce. The single sample composition was prepared from 100 ml of water and 14 g of wheat flour with a particle diameter of less than 100 μm and with an ash content of 0.65%.

For temperature variation, each sample of the mixture was heated separately in a Berzelius flask, placed on an electric hob. The hob is equipped with a magnet that has the role of homogenizing the sample throughout the heating process (figure 1). Flour-water mixture was warmed with 4-6 $^{\circ}\text{C}$ more than the temperature at which they were measured, because it took into account the loss of temperature during the trial use. After the sample reached the set temperature, it was inserted into the cylinder provided with a plunger and a flow channel, which was then mounted on the support bracket of the apparatus used for the tests. The amount of the mixture introduced into the cylinder was about 40 ml.

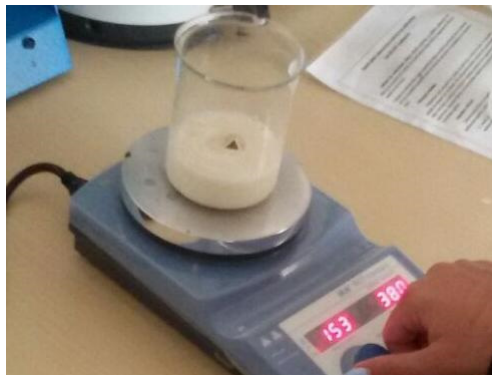


Figure 1. Sample heating

To perform a comparative analysis of resistance forces to press the piston device used in the experiments according to the temperature and length of the orifice flow, and to demonstrate that the rate of flow of fluid through the channel diameter d varies depending on the pressure inside the reservoir, the Hounsfield mechanical test apparatus was used, using a 1000 N force cell (Figure 2). The device used, during the experiments, was equipped with support for the cylindrical reservoir (of diameter D) provided with a flow channel and a pushing piston.

The piston displacement speed was kept constant at a value of 60 mm / min⁻¹ for a 60 mm piston stroke.

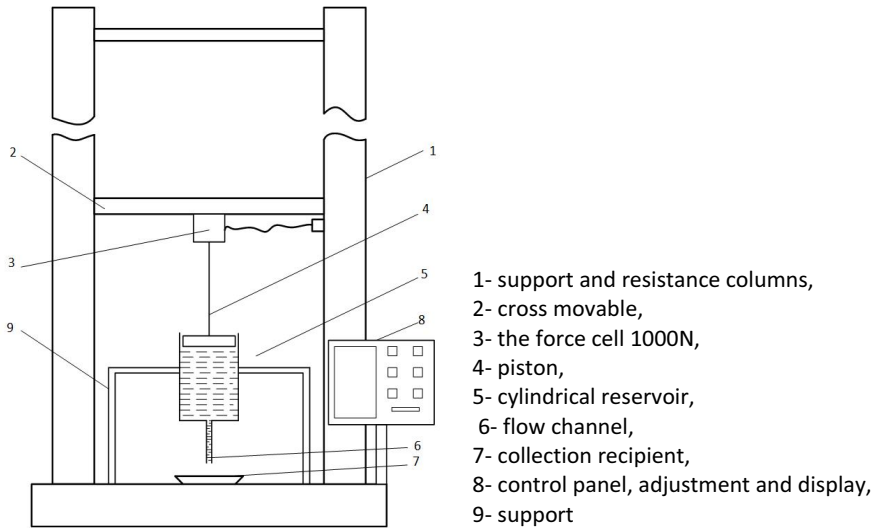


Figure 2. The Hounsfield device

For each sample mixture were performed three measurements. Two measurements for the flow channel of length $l = 53$ mm and the hole diameter $d = 0.838$ mm and a measurement channel flow length $l = 10$ mm and the hole diameter $d = 2$ mm.

Using the QMAT software installed on the computer connected to the test machine, the force curves for each sample were recorded (27° , 40° , 50° , 65° C), and each curve was retrieved in Excel, giving so, information about the strength force. An example of the force curve extracted from the QMAT program for the sample temperature of 65° C can be seen in Figure 3. The values of the compressive strength for each mixture sample using the flow channel $l = 53$ mm and the hole diameter $d = 0.838$ mm, were mediated (the arithmetic mean in the Excel program of the two determinations was calculated), and with these values, the average values of the force of the pressing force were restored. (figure 4).

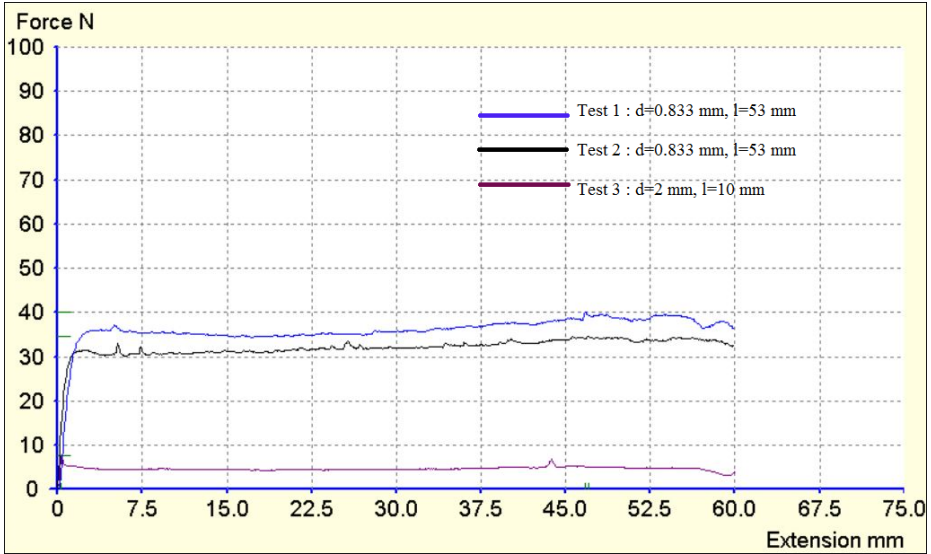


Figure 3. Image extracted during testing the sample at temperature of 65° C

To highlight the fact that the flow rate of the fluid through the pipe, v_2 , with diameter d varies depending on the pressure inside the cylinder, the list of physical sizes involved was determined: h_1 (the height of the liquid layer between the piston and the pipe end), h_2 (height from the end of the pipeline to the randomly chosen point), v_1 (Hounsfield machine speed), p_1 (tank pressure), p_2 (needle pressure). To this, is adds the density of the liquid ρ and the gravitational acceleration g .

$$\text{The law that we seek will be as: } v_2 = f(p_1) \tag{1}$$

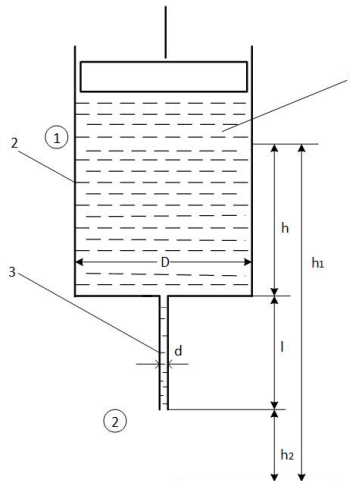


Figure 4. The reservoir with flow channel (1-piston, 2- cylinder, 3- flow channel)

$$p = \frac{F}{S} \Rightarrow p_1 = \frac{4F_1}{\pi D^2} \tag{2}$$

where P pressure is equal to the ratio of the force F acting normally and evenly distributed over a surface and S is the area of that surface and v_2 the flow rate of the fluid through the pipe (Gabor, 2011).

Knowing that the flow of the mixture has a level shift (height) and if the reference plan is considered at a distance h_2 from the base of the flow channel, then Bernoulli's law, $p_1 + \frac{\rho v_1^2}{2} = p_2 + \frac{\rho v_2^2}{2}$, deduced from the theoretical change in the kinetic energy applied to the fluid becomes (Bârlea, 2015):

$$p_1 + \frac{\rho v_1^2}{2} + \rho g h_1 = p_2 + \frac{\rho v_2^2}{2} + \rho g h_2 + P_{h\ 1-2} \tag{3}$$

$$p_1 - p_2 = \frac{\rho}{2}(v_2^2 - v_1^2) - \rho g h_1 + P_{h\ 1-2} \tag{4}$$

where: $P_{h\ 1-2}$ represents the hydraulic losses calculated between points 1 and 2, that is, at the entry into the pipe and along it. Due to the exit of the mixture from the pipe, p_2 is equal to zero ($p_2 = 0, h_2 = 0$), then the equation (4) becomes:

$$p_1 = \frac{\rho}{2}(v_2^2 - v_1^2) - \rho g h_1 + P_{h\ 1-2} \tag{5}$$

$$p_1 = \frac{\rho}{2}v_2^2 - \frac{\rho}{2}v_1^2 - \rho g h_1 + P_{h\ 1-2} \tag{6}$$

With equation (6) rearranged, the velocity v_2 of fluid flow can be determined with:

$$v_2^2 = \frac{2}{\rho}(p_1 + \frac{\rho}{2}v_1^2 + \rho g h_1 - P_{h\ 1-2}) \tag{7}$$

$$v_2^2 = \frac{2P_1}{\rho} + v_1^2 + 2gh_1 - \frac{2}{\rho}P_{h\ 1-2} \tag{8}$$

$$v_2 = \sqrt{\frac{2P_1}{\rho} + v_1^2 + 2gh_1 - \frac{2}{\rho}P_{h\ 1-2}} \tag{9}$$

RESULTS AND DISCUSSION

After experimental determinations were obtained the results shown in Table 1 and the charts from Figures 5 and 6 processed using MS Excel. From the values curve, the values of the compressive strength of force in which it varies for the four types of mixture were selected by direct view. These are presented in Table 1.

Table 1. Variation of the resistant pressing force at different temperatures

Channel type	Force [N]	Temperature			
		27°C	40°C	50°C	65°C
l=10 mm	Max.	1.5	2.8	3	5.1
d=2 mm	Min.	0.8	1.8	2.1	4.9
l=53 mm	Max.	5.1	4.8	5.8	37.0
d=0.838 mm	Min.	3.2	4.4	5.1	33.5

From the analysis of the charts from Figure 5, it has been found that the pressing resistance force of device piston increased with temperature rise and with modifying of length and diameter of the flow channel.

From the direct observation of the curves in Figure 6, there are no significant differences between the resistance values of the flow through the channel at 27 °C and 40 °C (the two curves almost overlap). There is a small difference between the values of resistance force at temperature of 50°C compared with values from temperature of 27° and 40°C, respectively, there are very large differences between the values of the resistant force to the temperature of 65°C versus values from temperature of 27°C, 40°C and 50°C.

For the sample with the temperature of 65 °C, the highest increase in force was recorded, both for the flow through the channel $l = 10$ mm and $d = 2$ mm, and for the flow through the channel with the dimensions $l = 53$ mm and $d = 0.838$ mm, which means that the swelling of the starch granules led to increased resistance.

It can be concluded that gelling of starch granules significantly influences the flow through the channels (especially through narrow channels), and the extruded or injected machines must be adapted to the working temperatures (respectively the actuating power must be higher when working at higher temperatures greater than 60°C). This is much more sensitive to long narrow channels because track losses are influenced by the l / d ratio.

However, even at the small lengths of the drainage channel, there are noticeable differences between the strength curves, which increase with the temperature.

The aforementioned can also be seen from the analysis of the values of the minimum and maximum strengths at each of the four temperatures for each of the two channels, presented in Table 1.

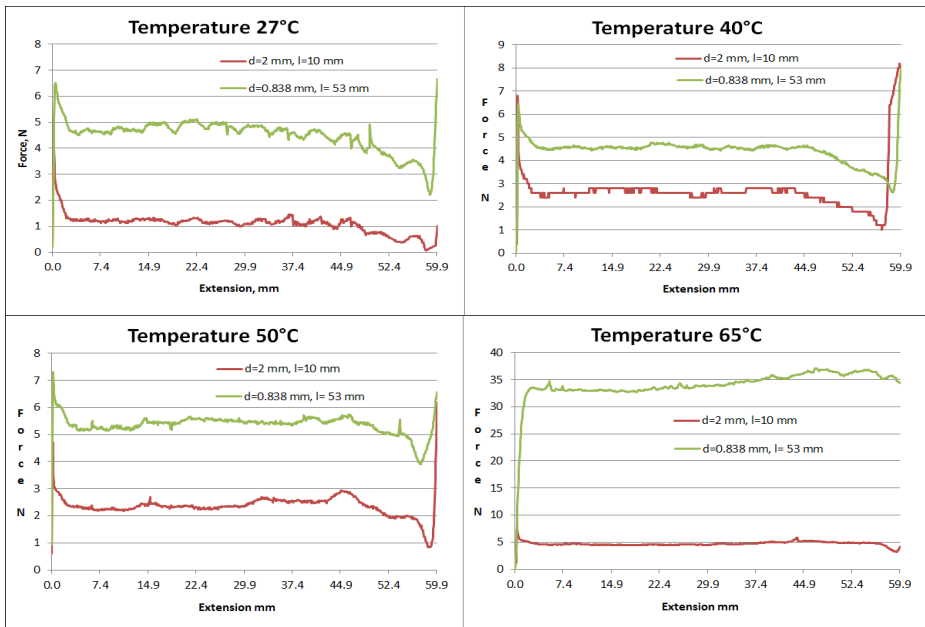


Figure 5. Variation of piston pressing resistant force the four types of mixture which have undergone flow tests through channels of different sizes

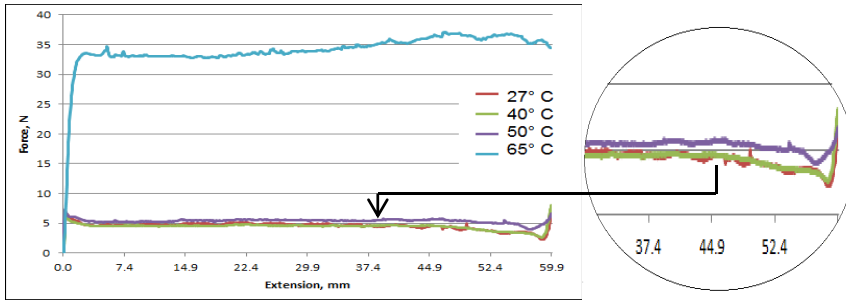


Figure 6. Variation of piston pressing resistant force the four types of mixture flowed through the channel $l = 53$ mm and $d = 0.838$ mm

CONCLUSIONS

It can be argued that the temperature of the flour-water fluids is a very important parameter when flowing through narrow channels, the strength of the flow resistance being as higher as the temperature is.

Our results show that resistant force values falls within the limits 1.15 N, at temperature of 27°C and 5 N at 65°C (average values), for a flow channel with dimensions $d=2$ mm and $l=10$ mm, respectively between 8.15 N at temperature of 27°C and 35.25 N at 65°C (average values) for the flow channel with dimensions $d=0.838$ mm and $l=53$ mm.

Also, the geometry of the channel influences the flow of said fluids, both our results and those from the specialty literature suggest that as smaller the diameter of the channel is, as higher the strength is, irrespective of the flour-water fluid mixture temperature.

Thus, the flow resistance force presents mean values between 1.5 N for the channel with $d = 2$ mm and $l = 10$ mm and 4.15 N for the channel with $d = 0.838$ mm and $l = 53$ mm at 27 °C or between 5 N for the channel with $d = 2$ mm and $l = 10$ mm and about 35 N for the channel with $d = 0.838$ mm and $l = 53$ mm at 65 °C. A working temperature of 65 °C adversely affects the flow in the sense that the resistance forces are much higher, these being influenced by the gelling of ammonium granules.

The results presented in the paper can be useful for both the pastry machine designers and the machine users and processors in the bakery and pastry industry (waffles, cookies, glazes).

ACKNOWLEDGEMENT

This work has been funded by Executive Unit for Financing Higher Education, Research, Development and Innovation – UEFISCDI, under PNCDI III- Programme 2, Subprogramme 2.1 – Transfer project to the economic operator (PTE-2016), Submission code PN-III-P2.1-PTE-2016-0077, Financial efficiency (HEE) electro hydraulic equipment (EHE) for multifunction vehicles (MFV), project acronym ECHIPEFEN, Project main domain: 3. Energy, Environment and Climate Change, Subdomain:3.1. Energy.

REFERENCES

- Bârlea, M. (2015). *Physics for Hurried Students*, Technical University of Cluj-Napoca, Cluj-Napoca, România, U.T. Press Cluj-Napoca, Fluid Dynamics, ISBN 978-606-737-090-4
- Dynamics of fluids, available at http://www.vitan.ro/Ingineria_Proceselor_I/II-Dinamica_fluidelor.ppt. (15.10.2017).
- Encyclopædia Britannica (2017), <https://www.britannica.com/science/starch>.
- Fasano, A., Primicerio, M., Tesi, A. (2011). A Mathematical Model For Spaghetti Cooking with Free Boundaries, *NHM* 6 (1): 37-60.
- Gabor, A. (2017). *Physics CourseII*, University Babeş-Bolyai, Cluj-Napoca.
- Gerits, L. R., Pareyt, B., Delcour, J.A. (2015). Wheat starch swelling, gelatinization and pasting: Effects of enzymatic modification of wheat endogenous lipids, *LWT - Food Science and Technology*, <http://dx.doi.org/10.1016/j.lwt.2015.02.035>.
- Li, S., Zhang, Y., Wei, Y., Zhang, W., Zhang, B. (2014). Thermal, Pasting and Gel Textural Properties of Commercial Starches from Different Botanical Sources, *Bioprocess Biotechniq*, 4: 161, DOI: 10.4172/2155-9821.1000161.
- Sopade, P.A., Hardin, M., Fitzpatrick, P., Desme, H, Halley, P. (2006). Macromolecular Interactions During Gelatinisation and Retrogradation in Starch-Whey Systems as Studied by Rapid Viscosity Analyser, *International Journal of Food Engineering*, 2: Iss. 4, Article 7. DOI: 10.2202/1556-3758.1074.
- Tester, R.F. and Morrison W. R. (1990). Swelling and gelatinization of Cereal Starches. I. Effects of Amylopectin, Amylose, and Lipids, *American Association of Cereal Chemists, Inc.*, 67(6):551-557.
- Tofană, M. (1997). *Course in Food Chemistry and Additives in Food Industry*, Cluj-Napoca, University of Agricultural Sciences and Veterinary Medicine of Cluj-Napoca.



APPLICATION OF ULTRASOUND IN WINEMAKING PROCESS

Alina MĂRGEAN*, Vasile PĂDUREANU, Mirabela Ioana LUPU

Transilvania University of Braşov, Food and Tourism Faculty, Engineering and Management in
Food and Tourism Department, 148 Castelului Street, 500014, Braşov, România

*E-mail of corresponding author: alinamargean@yahoo.com

SUMMARY

Ultrasound has been used as a successful tool in food industry but only in the last years its benefits started to be analyzed and implemented in processing, among which winemaking. Even though several studies have been performed regarding how ultrasound is influencing the extraction, fermentation or ageing, the subject is still of interest. Ultrasound offers the potential for improving existing processes and the developing of new process options. The demand for good quality wines has encouraged the use of ultrasound technology in winemaking process, consecutive to the research that shows ultrasound can play an important role in food technology in processing, preservation and extraction. This review summarizes the application of high and low intensity ultrasound in winemaking process in order to reveal whether this tool might be a feasible method for improving the quality in winemaking process.

Key words: ultrasound, winemaking, fermentation, maturation

INTRODUCTION

A product rich in phenolic compounds that have antioxidant properties, wine is an important component in many traditions. The crucial factors during winemaking include grape quality and variety, winemaking process and practices, wine storage (Clodoveo et al., 2016, Di Lorenzo et al., 2016).

Traditionally, red wine is made starting from crushing and destemming grapes, and the must remaining in contact with skins and seeds lead to starting the maceration. During this period, the extraction of the coloring and tannic components into the future wine takes place in the presence of alcohol produced during fermentation. When the macerating period ends, the fermented must is separated by skins and seeds using a press and the alcoholic

fermentation can continue until the parameters of the chosen wine are reached. Afterwards, spontaneously or through inoculation of selected lactic acid bacteria strains wine may undergo malolactic fermentation that confer a rounder and fuller mouthfeel to the wine. Then, the stage of wine ageing follows and consists in maturation in oak barrels (oxidative aging) and bottling (reductive aging). Also, clarification processes had to be carried out (Clodoveo et al., 2016).

Food industry became aware of the importance in implementing new technologies that study and monitor properties of food during processing as a reaction to consumers demand for higher quality and food safety products. Nowadays, the industry is searching for innovative techniques that might enhance or complement the conventional practices.

Ultrasound is such an emerging, efficient, environment friendly, green technology and the methods upon which ultrasound applications are based on include direct application to the product, coupling with the device and submerge in an ultrasonic bath (Chemat et al., 2011).

In winemaking, high frequency ultrasound can be used for monitoring and accelerating the fermentation processes. Another potential use of ultrasound in winemaking is for the improved extraction of coloring matter and the tannins from the initial processing of the fruit. The bacteria and yeast plays an important role in the winemaking process. High power ultrasound may be used to control wine spoilage organisms (Luo et al., 2012). Also, the ultrasound treatment on wine lees accelerates the protective colloids release (Cacciola et al., 2013). Ultrasound might be employed as a method to change the physicochemical properties of red wine including the electric conductivity, total phenolic compounds and chromatic characteristics and might be used to accelerate the ageing process of the wine with a longer effect on the evolution of both, color characteristics and phenolic compounds of wine during storage (Ferraretto et al., 2013, Martin and Sun, 2013, Ferraretto and Celotti, 2016, Zhang et al., 2016, Bautista-Ortin et al., 2017).

PRINCIPLE AND MECHANISM OF ULTRASOUND

Ultrasound is sound waves with frequencies higher than the upper audible limit of human hearing (16–20 kHz). In the food industry, the sound ranges employed can be divided into high frequency diagnostic ultrasound and low frequency ultrasound. High frequency diagnostic ultrasound (above 100 kHz) is a non-destructive technique and causes no physical or chemical alterations. They are successfully used for monitoring of food processes. The low frequency ultrasonic waves (18 – 100 kHz) are capable of altering material properties: physical disruption, acceleration of chemical reactions (Dolatowski et al., 2007). Into a liquid, ultrasound achieves chemical and physical effects, while the mechanical effects lead to increasing the extraction of nutraceutical components and disrupt or damage the cellular membrane (Jiranek et al., 2008, Clodoveo et al., 2016). Ultrasound assisted extraction is a simple and efficient alternative to conventional extraction techniques. The enhancement in extraction obtained by using ultrasound is mainly attributed to the effect of acoustic cavitations produced in the solvent by the passage of an ultrasound wave (Wang et al., 2008). The forces generated by acoustic cavitations determine the mechanism responsible for the ultrasonic deactivation effect. The application of ultrasound through intracellular cavitations determines a bactericidal effect in liquid foods (Dolatowski et al., 2007).

In food processing, the application of ultrasound includes freezing/crystallization, drying, degassing, extractions, induction of oxidation/reduction reactions, enzyme inactivation, filtration and defoaming (Jiranek et al., 2008, Chemat et al., 2011).

ULTRASOUND IN WINEMAKING PROCESS

In the literature, the latest research showed the potential uses of ultrasound in winemaking including: reducing the fermentation time and increasing the extraction of phenolic compounds (Sacchi et al., 2005, Vilku et al., 2008, Tiwari et al., 2010, Tudose-Sandu-Ville et al., 2012, Coletta et al., 2013, Bautista-Ortin et al., 2017), controlling a variety of wine spoilage organisms (Jiranek et al., 2008, Luo et al., 2012), or wine maturation and ageing (Ferraretto and Celotti, 2016, Zhang et al., 2016). However, when applying ultrasound in winemaking process, changes in aroma profile and sensory properties of beverages might occur, like a slight “burnt” flavor, or a slight metallic character (Nolan, 2016).

During the winemaking, the ultrasound variables are power, frequency, exposure time, amplitude and temperature (Clodoveo et al., 2016, Zhang et al., 2016). The properties of the medium, treatment parameters and ultrasound parameters are critical processing factors (Dolatowski et al., 2007, Jiranek et al., 2008).

The main stages during traditional winemaking are fermentation and maturation or ageing (Di Lorenzo et al., 2016, Zhang et al., 2016). However, the process starts with the maceration on the skins that is enhancing the extraction of the color and active compounds (Di Lorenzo et al., 2016). Thus, improving extraction using ultrasound during maceration is of great interest to increase their quantity (Coletta et al., 2013).

During the harvest time, the wineries are trying to reduce the maceration time and consequently the quality of the wine would be influenced. Alternatives to accelerate the reactions within the wine and to enhance the extraction of phenolic compounds includes ultrasound, pulsed electric field and high voltage electrical discharges, while the variables includes fermentation temperature, thermovinification, must freezing, enzyme treatments and extended maceration (Sacchi et al., 2005, Martin and Sun, 2013, Bautista-Ortin et al., 2017).

Recently, Bautista-Ortin et al. (2017) studied the application of high power ultrasound (HPU) on reducing the maceration time and increasing the extraction of phenolic compounds from red grapes. They observed that the treated must (2500 W, 28 kHz) had the highest values for phenols, anthocyanins and color intensity and a double concentration of the tannin. They also reported that the ultrasound treatment facilitated the extraction of phenolic compounds from the crushed grapes. In their opinion, the application of ultrasound might be an optimizing technique that allows wineries to reduce the maceration time while keeping the same quality characteristics of the wines.

On the other hand, Tudose-Sandu-Ville et al. (2012) studied the phenolic compounds in Merlot wines obtained through different technologies, including ultrasound. They found that the phenolic extraction was not increased after ultrasound maceration (2000W, 35 kHz, 15 min.) and the quantities of anthocyanins and tannins in the wine were low. Moreover, the influence of ampelotechnical practices and winemaking technologies on phenolic composition and sensory characteristics of red wines have been assayed by (Coletta et al., 2013). They observed that ultrasound treatment on destemmed grapes (37 kHz, 150 W, 15 min at 30 °C) improved the extraction of all phenolic compounds, especially anthocyanins and lead to improved sensory characteristics of wine.

Color, as the easily recognized aspect of a quality red wine together with the astringency, hardness and flavor are influenced by phenolic compounds (Sacchi et al., 2005, Tudose-Sandu-Ville et al., 2012). Phenolic compounds that are located in skins, pulp and seeds of grapes are partially extracted during winemaking (Coletta et al., 2013) and include non-flavonoids and flavonoids among which anthocyanins are responsible for sensory properties

and for chemical stability and tannins that entail astringency (Martin and Sun, 2013, Di Lorenzo et al., 2016).

Other studies (Tiwari et al., 2010) explored effects of amplitude level and treatment time on anthocyanins and color parameters. Varying the amplitude level (24.4–61.0 μm) and treatment time (0–10 min) at a constant frequency of 20 kHz and pulse durations of 5 s on and 5 s off, the authors concluded that a high degree of anthocyanin retention was found in grape juice, considering thus this technique as a preservation one for processing of fruit juice products where is desired a high retention of anthocyanins.

Also, Vilku et al. (2008) showed that ultrasonic technology improves the extraction of polyphenols, anthocyanins, aromatic compounds, polysaccharides and functional compounds. High values of amplitude and longer times of treatment lead to a significant increase of catechins (Ferraretto and Celotti, 2016). Ghafoor and Choi (2009) found that compared with other extraction methods ultrasound shortened the extraction time. The optimum extraction conditions for total phenols were 53.14% ethanol concentration, 46.03 °C extraction temperature and 24.03 min extraction time and 53.06% ethanol, 50.65 °C temperature and 25.58 min time for maximum antioxidant activity.

Other authors, Cacciola et al. (2013) observed that the ultrasound treatments on wine lees (5 min and 60 % amplitude and 3 and 5 min at 90 % amplitude) lead to greater effects in terms of colloids and proteins due to an increased release of colloids from the yeast. They concluded that the effects of using ultrasound for few minutes can be comparable to traditional aging on lees by obtaining a rapid extraction of macromolecules from the yeast lees.

Also, Jiranek et al. (2008) mentioned ultrasound technology as potential application during different stages of winemaking process for reduction of spoilage organisms and enhancing extraction of color and flavor compounds. Applying 20 min exposure to HPU influenced the viability of almost all organisms – yeast and bacteria commonly associated with wine spoilage, with different response of genus. Cell numbers decreased for all yeast and bacteria studied, except *Pediococcus* sp. (Luo et al., 2012). However, it was suggested that yeast cells are more susceptible to the effects of cavitations while bacteria are more resistant (Chandrapala et al., 2012).

Cho et al. (2006) reported that compared to conventional solvent extraction, the application of ultrasound-assisted extraction in grape skin can enhance the recovery of functional compounds up to 30% and also prevents the possible chemical degradation of targeted compounds (Wang and Weller, 2006).

Wine ageing consist in maturation that is an oxidative ageing that takes place in tanks or barrels and bottling that is a reductive ageing (Martin and Sun, 2013). Traditional ageing in barrels has some disadvantages including time needed, high cost, thus innovative winemaking and ageing technologies are currently assayed. Ferraretto and Celotti (2016) evaluate the effect of HPU in wine aging. The authors reported that after the treatment (20 kHz frequency, 1, 3 and 5 min. time and 51, 102 and 153 μm amplitude), the anthocyanins suffered no negative consequences, confirming thus their stability. Also, an increase in tannic compounds was observed. The results obtained by the authors suggested that the HPU uses might accelerate the aging process of wines with best results in young, well-colored wines.

Other assays evaluate the influence of ultrasound on physicochemical parameters of red wine (Zhang et al., 2016). By variation of power (120, 150, 180, 210, 240, 270 and 300 W), frequencies (45, 80 and 100 kHz), exposure time (20, 40, 60, 80 and 100 min.) and temperature (20 °C, 30 °C, 40 °C, 50 °C and 60 °C), they concluded that ultrasound can change some physicochemical properties of red wine. The significantly changes were observed on the

concentration of total phenolic compounds and electrical conductivity and the suggested parameters were 240 W, 80 kHz, 20 °C and 80 min. However, the exposure time seem to be the main factor that leads to changes in red wine.

CONCLUSIONS

Ultrasound technique has been used by the 1960' in the industry and it still is a subject of interest for enhancing or complements the conventional or traditional practices. Ultrasound has been assayed on different stages of the winemaking with different aims including accelerating chemical reactions and increase extraction of the compounds from grape to must. However, in the winemaking, most of the researchers have been carried out experiments at laboratory scale, where the conditions assayed were still limited and thus the results were not standardized related to operating conditions and makes the comparison within studies difficult.

Despite the results that demonstrated the potential application of this emerging technique in winemaking, the complete effect of ultrasound is still to be assayed due to some undesirable reactions or effects that might occur, like off odors in wine. Still, the application of ultrasound in winemaking represents a possibility to optimize maceration, fermentation and maturation stages.

REFERENCES

- Bautista-Ortin, A.B., Jimenez-Martinez, M.D., Jurado, R., Iniesta, J.A., Terrades, S, Andres, A., Gomez-Plaza, E. (2017). Application of high-power ultrasounds during red wine vinification. *International Journal of Food Science and Technology* 2017.
- Cacciola, V., Batllò, I. F., Ferraretto, P., Vincenzi, S., Celotti, E. (2013). Study of the ultrasound effects on yeast lees lysis in winemaking. *European Food Research and Technology*, 236(2): 311–317.
- Carrera, C., Ruiz-Rodriguez, A., Palma, M., Garcia-Barroso, C. (2012). Ultrasound assisted extraction of phenolic compounds from grapes. *Analytica Chimica Acta*, 732: 100–104.
- Chandrapala, J., Oliver, C., Kentish, S., Ashokkumar, M. (2012). Ultrasound in food processing – Food quality assurance and food safety. *Trends in Food Science and Technology*, 26: 88-98.
- Chang, A. C., Chen, F. C. (2002). The application of 20 kHz ultrasonic waves to accelerate the aging of different wines. *Food Chemistry*, 79(4): 501–506.
- Chemat, F., Zill-e-Huma, Khan, M.K. (2011). Applications of ultrasound in food technology: Processing, preservation and extraction. *Ultrasonics Sonochemistry* 18: 813–835.
- Clodoveo, M.L., Dipalmo, T., Rizzelo, C.G., Corbo, F., Crupi, P. (2016). Emerging technology to develop novel red winemaking practices. *Innovative Food Science and Emerging Technologies* 38: 41-56.
- Coletta, A., Trani, A., Faccia, M., Punzi, R., Dipalmo, T., Crupi, P., Gambacorta, G. (2013). Influence of viticultural practices and winemaking technologies on phenolic composition and sensory characteristics of Negroamaro red wines. *International Journal of Food Science and Technology*, 48(11), 2215–2227.
- Di Lorenzo, A., Bloise, N., Meneghini, S., Sureda, A., Tenore, G.C., Visai, L., Arciola, C.R., Daglia, M. (2016). Effect of Winemaking on the Composition of Red Wine as a Source of Polyphenols for Anti-Infective Biomaterials. *Materials*, 9(5), (316). DOI:10.3390/ma9050316.
- Dolatowski, Z.J., Stadnik, J., Stasiak, D. (2007). Applications of ultrasound in food technology, *Acta Sci. Pol. Technol. Aliment.* 6(3): 89–99.

- Ferraretto, P., Cacciola, V., Ferran Batlo, I., Celotti, E. (2013). Ultrasound application in winemaking: grape maceration and yeast lysis. *Italian Journal of Food Science*, 25, 160–168.
- Ferraretto P. and Celotti, E. (2016). Preliminary study of the effects of ultrasound on red wine polyphenols. *CyTA - Journal of Food*, DOI: 10.1080/19476337.2016.1149520.
- Ghafoor, K. and Choi, Y. H. (2009). Optimization of ultrasound assisted extraction of phenolic compounds and antioxidants from grape peel through response surface methodology. *Journal of the Korean Society for Applied Biological Chemistry*, 52: 295–300.
- Heras-Roger, J., Díaz-Romero, C., Darias-Martín, J. (2016). A comprehensive study of red wine properties according to variety. *Food Chemistry* 196: 1224–1231.
- Jambrak, A.R. and Vukušić, T. (2016). State of the Art of the Use of Ultrasound in the Beverage Industry (I) Effects on Beverages (II) Effects on Microorganisms. In: *Application of ultrasound in the beverage industry*. (J.F.G. Martin eds), Nova Science Publishers New York, 1-32.
- Jiranek, V., Grbin, P., Yap, A., Barnes, M., Bates, D. (2008). High power ultrasonics as a novel tool offering new opportunities for managing wine microbiology. *Biotechnol Lett* 30:1–6.
- Knorr, D., Zenker, M., Heinz, V., Lee, D.U. (2004). Applications and potential of ultrasonics in food processing. *Trends in Food Science & Technology*, 15(5): 261–266.
- Knorr, D., Froehling, A., Jaeger, H., Reineke, K., Schlueter, O., Schoessler, K. (2011). Emerging technologies in food processing. *Annual Review of Food Science and Technology*, 2: 203–235.
- Luo, H., Schmid, F., Grbin, P.R., Jiranek, V. (2012). Viability of common wine spoilage organisms after exposure to high power ultrasonics. *Ultrason. Sonochem.* 19: 415–420.
- Martin, J.F.G., Zhang, Q.A., Feng, C.H. (2016). Ultrasound for Accelerating the Wine Ageing Process from Physicochemical Point of View. In: *Application of ultrasound in the beverage industry*. (J.F.G. Martin eds), Nova Science Publishers New York, 89-110.
- Martin, J.F.G. and Sun, D.W. (2013). Ultrasound and electric fields as novel techniques for assisting the wine ageing process: The state-of-the-art research. *Trends in Food Science & Technology*, 33(1): 40–53.
- Mason, T. J., Paniwnyk, L., Lorimer J. P. (1996). The uses of ultrasound in food technology. *Ultrasonics Sonochemistry*, 3(3): S253–S260.
- Nolan, D. (2016) Ultrasound for accelerating the wine ageing process: A winetaster's view. In: *Application of ultrasound in the beverage industry*. (J.F.G. Martin eds), Nova Science Publishers New York, 111-114.
- Ojha, K.S., Mason, T.J., O'Donnell, C.P., Kerry, J.P., Tiwari, B.K., (2017). Ultrasound technology for food fermentation applications. *Ultrasonics Sonochemistry* 34: 410–417.
- Popescu, C., Postolache, E., Rapeanu, G., Bulancea, M., Hopulele, T. (2010). The dynamics of oxidative enzymes during the white winemaking. *Annals of the University "Dunarea de Jos" of Galati-Fascicle VI. Food Technology*, 34(1): 25–31.
- Ribereau-Gayon, P., Dubourdieu, D., Doneche, B., Lonvaud, A. (2000). Biochemistry of alcoholic fermentation and metabolic pathways of wine yeasts. *Handbook of Enology. The microbiology of wine and vinifications*. Vol. 1: 51–74. New York: John Wiley & Sons.
- Sacchi, K., Bisson, L.F., Adams, D.O. (2005). A review of the effect of winemaking techniques on phenolic extraction in red wines. *American Journal of Enology and Viticulture*, 56: 197–206.
- Tao, Y., Zhang, Z., Sun, D. W. (2014b). Experimental and modeling studies of ultrasound-assisted release of phenolics from oak chips into model wine. *Ultrasonics Sonochemistry*, 21(5): 1839–1848.
- Tiwari, B.K., Patras, A., Brunton, N., Cullen, P. J., O'Donnell, C. P. (2010). Effect of ultrasound processing on anthocyanins and color of red grape juice. *Ultrasonics Sonochemistry*, 17(3): 598–604.
- Tudose-Sandu-Ville, Ș., Cotea, V.V., Colibaba, C., Nechita, B., Niculaua, M., Codreanu, M. (2012). Phenolic compounds in merlot wines obtained through different technologies in Iași Vineyard, Romania. *Cercetari agronomice in Moldova*, 45(4): 89–98.

- Vilkhu, K., Mawson, R., Simons, L., & Bates, D. (2008). Applications and opportunities for ultrasound assisted extraction in the food industry—A review. *Innovative Food Science & Emerging Technologies*, 9(2): 161–169.
- Zhang, Q.A., Shen, Y, Fan, X.H., Martin, J.F.G, (2016). Preliminary study of the effect of ultrasound on physicochemical properties of red wine. *CyTA – Journal of Food*, Vol. 14(1): 55–64.



FLOTATION SYSTEM FOR AGRICULTURAL WASTEWATER TREATMENT

Mihai Gabriel MATACHE^{1*}, Corina MOGA², Cristina COVALIU³,
Iulian VOICEA¹, Catalin PERSU¹

¹National Institute of Research - Development for Machines and Installations Designed to Agriculture and Food Industry - INMA Bucharest, 6, Ion Ionescu de la Brad, Bucharest, Romania

²DFR Systems Ltd, 46, Drumul Taberei, Bucharest, Romania

³Politehnica University of Bucharest, 313, Splaiul Independenței, Bucharest, Romania

*E-mail of corresponding author: gabimatache@yahoo.com

SUMMARY

Taking into consideration the climate changes which have conducted to large periods of drought in summer and winter time in areas which usually didn't suffer from this phenomenon, a more sustainable approach to water management techniques has to be followed. This mean that every resource available for water should be used. In this approach, agricultural wastewater (milking parlour from dairy farming wastes, wastewater from slaughtering activities, washing of vegetables, etc) could be an important source for irrigation process. These agricultural waste waters are contaminated with several types of pollutants (pesticides, organic contents, antibiotics, pathogenic agents etc.) which have to be removed before getting into the field as irrigation water. In this paper, we discuss the technical aspects of a flotation system which is integrated within the final stage of a wastewater treatment plant for agricultural farms for removing the final small sized colloidal substances from water. In order to achieve greater purity degrees for the output water in function of the colloidal particles size we designed a flotation system consisting of a pressurized capsule with a maximum operating pressure of 10 bar. The capsule provides air bubbles with variable size which will adhere to the colloidal particles and will get them to form a foamy substance on the surface of the wastewater treatment tank. The air bubble size is regulated by the working pressure of the pressurized capsule, thus providing flexibility to the wastewater treatment plant in order to extract the majority of the remaining colloidal particles from the water.

Keywords: flotation system, agricultural wastewater, climate changes

INTRODUCTION

Our society is faced with increasing quantities of wastewater generated from various industries, farms and household use, but also with climate changes and population growth in the last decades that lead to higher water requirements for human, animal consumption but also for crop irrigations. These issues cause environmental problems, in terms of increased soil and groundwater contamination, and have led to the enforcement of stricter regulations limiting the pollution caused by these wastewaters. Therefore, new and more efficient technologies were developed in order to ensure better treatment and purification.

Dissolved air flotation (DAF) systems are among the most common and highly efficient methods used for treating wastewater and removing even the finest suspended particles (oils, animal fat and residues, solids, etc.). The operating principle of DAF systems consists in passing dissolved air through the aqueous solution (wastewater), leading to the formation of small bubbles that adhere to the suspended particles in water, decreasing their density and transporting them to the surface where they form a layer of foam which can be easily removed (Rubio et al., 2002; Torrealba Cartajena, 2007; Habibzadeh and Gurbanov, 2010; Saththasivam et al. 2016).

The efficiency of treating wastewater using dissolved air flotation systems is influenced at a great extent by the structure, stability and distribution of air bubbles, but also by their dynamic and capacity to move the unwanted particles toward the surface of the aqueous solution (Dickinson et al., 2004; Wang, 2007; Wang et al, 2010; Farrokhpay, 2011).

Therefore, in order to obtain an efficient wastewater treatment, it is necessary to have an adequate air pressure generation system that ensures the control over air flow rate, air bubble rising velocity and has a low power consumption.

The compressed air pressure for generation of the air microbubbles is one major parameter for controlling air solubility in a DAF unit and is an important factor in flotation operation. The total volume and size of air bubbles produced on depressurization is proportional to the process pressure, the flow rate, and the fluids temperatures. Large air bubbles are produced at lower pressures and higher fluids temperatures. More efficient colloidal particles removal is obtained with smaller air bubbles due to their lower rising speeds and thus increased time contact and a higher bubble surface area. A DAF system is suitable to separate solids of similar densities and sizes, which cannot be achieved by other types of separations based on gravity alone. It is very effective for particles below 100 μm , which are too small for gravity separation by sedimentation. The lower size limit for flotation separation is approximately 35 μm , although particles as small as 1 μm can be separated.

The paper addresses the technical aspects of a dissolved air flotation system of a wastewater treatment plant designed for small and medium size agricultural farms. A pressurized capsule with a maximum operating pressure of 10 bar was designed to provide air bubbles with variable size that will adhere to the colloidal particles in the aqueous solution and transport them to the surface of the treatment tank where they are removed by a surface skimmer. The system offers farmers a solution to be able to reuse the water consumed during various processes (wastewater from animal raising and slaughtering activities, washing of vegetables, etc.) for other activities, such as irrigation, with reduced efforts and costs.

Dissolved air percentage in the water is of great importance in optimizing the engineering design and operating parameters of a dissolved air flotation system, for the separation of solids from a liquid. Within this paper we discuss the means through which the percentage of gas dissolved in water could be increased, in order to obtain greater purities for the

effluent waters which thus will get suitable to be further used for irrigation. The experiments were developed using wastewater from a poultry farm loaded with chicken feathers residues which are extremely hard to separate through other treatment methods.

MATERIALS AND METHODS

For a gas mixture (air) in contact with the surface of a liquid (water), the amount of gas which will dissolve into solution is proportional with the partial pressure of that gas. For a gas mixture, Henry's law could predict the quantity of each gas which will be dissolved into the solution. However, different gases have different solubility, so this affects the final results. Solubility of air in water can be expressed as a solubility ratio:

$$S_{air} = \frac{m_{air}}{m_{water}}, \quad (1)$$

where:

S_{air} = solubility ratio

m_{air} = mass of air (kg)

m_{water} = mass of water (kg)

Air solubility in water follows Henry's Law - "the amount of air dissolved in a fluid is proportional to the pressure in the system" - and can be expressed as:

$$c = \frac{P}{k}, \quad (2)$$

where

c = solubility of dissolved gas

k = proportionality constant depending on the nature of the gas and the solvent

P = partial pressure of gas (Pa)

The oxygen solubility in water is higher than the solubility of nitrogen. Air dissolved in water contains approximately 35 – 36 % oxygen compared to 21% in air.

The DAF type wastewater treatment stage used during experiments consisted mainly of a pressurized capsule, with a capacity of 0.3 m³, which provided the air-water mixture to a final stage settling tank of 24 m³. The imposed flow rate for the DAF unit was of 100 litres per hour. The capsule was fed with tap water and compressed air, and the air-water mixture was directed through a system with nozzles at the bottom of the settling tank. The automation unit of the DAF allowed us to control the pressure and the temperature within the capsule as also the output flow from the capsule. The temperature control of the fluids inside the capsule is an innovative aspect of the research, since usually fluids are used at environment temperature. The temperature was controlled using an industrial cooler which had a heat exchanger inside the capsule, with a working range between 5 – 40°C. The control philosophy of the pressurised capsule involved maintaining a steady level of water in the middle of the capsule's height, with a cushion of compressed air above.

Experiments were performed with the DAF unit in function, setting up the working pressure and the working temperature within the pressurized capsule. The working pressure for the experiments was chosen to be in range of 3-7 bar, because of the expected bubble size (between 20-100 µm) suitable for chicken feathers residues. The temperature was set up between 5 and 25°C, because colder temperatures imply higher gas solubility and our goal was to obtain higher concentrations of gas in water, which meant a larger number of air bubbles in the settling tank.



Figure 1. Pressurized capsule within the DAF circuit

The experiments performed have investigated the process of dissolving the air within the water mass fed to the capsule, in function of the controlled working pressure and the temperatures of the used fluids: water and air. The introduced air, under the pressure, is dissolved inside the water mass. This stage is followed by a depression to the atmospheric pressure after releasing the mixture in the settling tank.

In order to perform the experiments, we made a derivation from the output of the capsule to a transparent pipe, thus providing the necessary air-water mixture for the measurements to be taken. The 150 cm long vertical transparent plastic air dispersion cylinder was attached at the base. An inlet tube rose from the base up to 13 cm above the interior base where there was an air-water dispersion nozzle which supplied the mixture air -water.

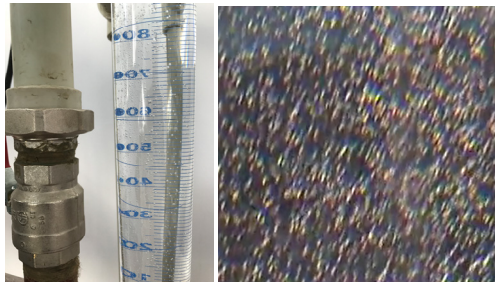


Figure 2. Air dispersion cylinder (left) and 5x zoomed image of bubbles (right)

We measured the concentration of the dissolved oxygen together with the mean dimensions of the formed bubbles. Gas concentration was determined using an Oxygen portable meter ProfiLine Oxi 3205 fitted with a galvanic oxygen sensor CellOx.

Mean bubble dimensions and rising speeds were measured using a high-speed recording camera, Phantom V10.0, series V 630, set to record at 1000 frames/ second fitted with a Canon macro MP-E 65mm f/2.8 objective. The software used for recording was Phantom Camera Control Application (<https://phantom-service.force.com/?section=PCCSoftware>). The pictures were afterwards processed using the software NI Vision Builder AI, in order to calculate their mean diameter. We measured up to 1000 bubbles for each experiment and computed their mean diameter, assuming that they all had a spherical shape.

We structured the experiments for 5 working pressures and 5 temperatures in order to get the optimum parameters for the flotation process. Afterwards, we performed measurements

of the effluents' purity from the settling tank after flotation treatment, which was fed with wastewater from poultry farm having chicken feathers residues within. This type of particles is very hard to be removed from farm wastewater, as they do not react chemically, they go through screen filters or clog them and they have various sizes.

RESULTS AND DISCUSSION

The results obtained for the dissolved oxygen concentration in the output mixture are presented in table 1.

Table 1. Dissolved oxygen concentration

Crt. no. Working pressure (Pa)	Fluid temperature (°C)				
	5	10	15	20	25
	Dissolved Oxygen (mg·l ⁻¹)				
300000	35.24	31.32	28.33	25.9	23.88
400000	46.99	41.77	37.78	34.53	31.85
500000	58.73	52.21	47.22	43.17	39.81
600000	70.48	62.65	56.66	51.8	47.77
700000	82.23	73.09	66.11	60.43	55.73

As expected, the best results were obtained for highest working pressure and lowest temperature, with a maximum concentration of 82.23 mg·l⁻¹, which accounts for approximately 231 mg·l⁻¹ dissolved air in water.

Furthermore, we analysed the average diameter of the obtained bubbles. In figure 3 we present one processed image obtained for the rising bubbles during the experiment at 5 °C and 5 bar working pressure. The processing consisted in applying several filters to the raw image which resulted in coloured blue bubbles. The image was previously calibrated using a physical calliper for comparison.



Figure 3. Processed air bubbles image and the performed calibration

In the next diagram, we present the evolution of bubble diameter with the working pressure, using the mean values obtained after image processing.



Figure 4. Evolution of bubble size with the working pressure

The bubble sizes varied between 20 and 85 μm in diameter, but for every working pressure we calculated an average diameter based on 1000 bubbles per experiment. As it can be seen in figure 4, the average bubble size decreases together with the increase of the working pressure, but from 4 bar and above the tendency to decrease is not significant, which is consistent with data obtained by (Mooyoung et al, 2002), who found a threshold pressure at around 3.5 bar from which the bubbles size doesn't decrease anymore.

Since the DAF unit together with the settling tank represent the tertiary stage in a wastewater treatment plant, we conducted the experiments with $650 \text{ mg}\cdot\text{l}^{-1}$ suspended solids wastewater, 25% being loaded with chicken feathers residues. In table 2 are presented the results obtained for different temperatures of the air-water mixture, which was fed at the bottom of the settling tank. The results were obtained averaging measurements performed during 8 hours of settling through flotation.

Table 2. Suspended solids after flotation treatment

Working pressure (Pa)	Fluid temperature ($^{\circ}\text{C}$)				
	5	10	15	20	25
	Suspended solids ($\text{mg}\cdot\text{l}^{-1}$)				
300000	226.97	223.97	218.74	218.25	217.27
400000	223.98	234.64	212.22	218	218.92
500000	217.47	219.98	211.96	216.24	217.73
600000	215.5	218.22	212.37	214.2	216.4
700000	212.52	215.58	210.97	210	215.38

Observing the gathered data, we see that the overall decrease of suspended solids within the treated water was around 66% of the initial value. The efficiency obtained for suspended solids removal is slightly lower than that of 77% obtained by (Koivunen J. and Heinonen-Tanski H., 2008), a fact that could be explained by the different characteristic of the studied wastewaters and the different settling times. Also, comparing our obtained data with the study performed by (Ross C. C. et al., 2000) who obtained an effluent value of 263 mg·l⁻¹ for the total suspended solids on a poultry wastewater treatment plant endowed with a DAF system, we can conclude that our obtained values are consistent with similar works from the same domain. The best efficiency of solid particles removal was obtained for the highest working pressure within the DAF system, 7 bar, at 15 °C temperature of the air-water mixture.

CONCLUSIONS

Taking into consideration the results presented above, because of the threshold that appeared in bubble average size after a pressure of 4 bar within the pressurized capsule, even though the effectiveness of wastewater treatment is slightly increased, it is not worth to further raise the pressure, due to bigger energy consumption. Furthermore, analysing the temperatures at which the cleaning process of water was optimum, we identified a 15°C temperature for which the water had the least amount of suspended matter after flotation treatment. The result is sort of confusing since the amount of dissolved air in water is bigger at lower temperatures. One of the reasons that could explain the phenomenon is that we didn't take into consideration the effect of the temperature of wastewater from the settling tank which was the same with that of the environment.

Also, for all experiments, the quantity of chicken feather after treatment was reduced by around 91%, thus making controlled DAF systems a proper solution for the stated issue.

ACKNOWLEDGEMENT

This work was supported by a grant of the Romanian National Authority for Scientific Research and Innovation, CNCS/CCCDI – UEFISCDI, project number PN-III-P2-2.1-PTE-2016-0183 (APIFLOT-II), contract no. 25PTE/2016, within PNCDI III.

REFERENCES

- Dickinson, E., Ettelaie, R., Kostakis, T., Murray, B.S. (2004). Factors Controlling the Formation and Stability of Air Bubbles Stabilized by Partially Hydrophobic Silica Nanoparticles, *Langmuir* 20: pp. 8517–8525.
- Farrokhpay, S. (2011). The significance of froth stability in mineral flotation – A review, *Advances in Colloid and Interface Science*, Volume 166, Issues 1–2: pp 1-7.
- Habibzadeh, Y. and Gurbanov, K.B. (2010). Effect of using dissolved air flotation system on industrial wastewater treatment in pilot scale. *Fizika (Baku)*, ISSN 1028-8546, v. 16(1): 68-74.
- Koivunen, J., Heinonen-Tanski H. (2008). Dissolved air flotation (DAF) for primary and tertiary treatment of municipal wastewaters. *Environ Technol.* 2008 Jan;29(1):101-9. DOI: 10.1080/09593330802009410.
- Mooyoung, H., Park, Y., Lee, L., Shim, J. (2002). Effect of pressure on bubble size in dissolved air flotation. *Water Science and Technology: Water Supply.* 2. 41-46.

- Ross, C.C., Smith, B.M., Valentine, G.E. Jr. (2000). Rethinking dissolved air flotation (DAF) design for industrial pretreatment. WEF and Purdue University Industrial Wastes Technical Conference.
- Rubio, J., Souza, M.L., Smith, R.W. (2002). Overview of flotation as a wastewater treatment technique, *Minerals Engineering* 15: 139–155.
- Saththasivam, J., Loganathan, K., Sarp, S. (2016). An overview of oil–water separation using gas flotation systems. *Chemosphere* 144: pp. 671–680.
- Torrealba Cartajena, J.G. (2007). Determination of Air Flotation Parameters to Perform Solid Liquid Separation Treatment in an Activated Sludge Treating Grease Waste by Promoting Filamentous Bacteria. Master's Thesis. University of Tennessee, USA.
- Wang, L.K., Shammas, N.K., Selke, W.A., Aulenbach, D.B. (2010). Gas Dissolution, Release, and Bubble Formation in Flotation Systems. *Handbook of Environmental Engineering, Volume 12: Flotation Technology*, Edited by: L. K. Wang et al., DOI: 10.1007/978-1-60327-133-2_2, Springer Science + Business Media.
- Wang, L.K. (2007). Emerging flotation technologies. In: Wang LK, Hung YT, Shammas NK (eds) *Advanced physicochemical treatment processes*, Humana Press, Totowa, NJ, pp 449–484.
- <https://phantom-service.force.com/?section=PCCSoftware>.



EXPERIMENTAL RESEARCHES ON THE QUALITY OF SORTING PROCESS OF MEDICINAL PLANTS

Augustina PRUTEANU*, Valentin VLĂDUȚ, Mihai MATAACHE,
Mihaela NIȚU

National Institute of Research - Development for Machines and Installations for Agriculture and
Food Industry - INMA Bucharest / Romania

*E-mail of corresponding author: pruteanu_augustina@yahoo.com

SUMMARY

The paper presents the quality of the sorting process expressed by the degree of separation on sorts with different sizes of dried and chopped medicinal plants (nettle, respectively thyme). The experimental researches were conducted on a chopped plant sorter, using oscillating plane sieves with different mesh sizes, different feed rates and different revolution speeds of the mechanism for actuating the sieves.

The experimental results obtained from sorting the two medicinal plants were processed and interpreted using polynomial regression functions.

Keywords: medicinal plants, sorting process; flat vibrating sieves

INTRODUCTION

Most developing countries are endowed with vast resources of medicinal and aromatic products plants. These plants have been used over the millennia for human welfare in the promotion of health and as drugs and fragrance materials. This close relationship between man and his environment continues even today as a large proportion of people in development countries still live in rural areas. Furthermore, these people are excluded from the luxury of access to modern therapy, mainly for economic reasons. About 80% of the population of many developing countries still use traditional medicines for their health care (De Silva T., 1997).

Stinging nettle (*Urtica dioica* L.), figure 1, is a perennial herbaceous plant belonging to the Urticaceae family. It is a well-known and common species, spread in temperate and tropical zones of Europe, Asia and America, adapted to a variety of climatic conditions. Stinging nettle is a perennial, monoecious plant, flowering and fruiting in summertime. Its stems and leaves are covered by stinging trichomes containing a fluid which causes blistering when entering the skin (Di Virgilio N. et al., 2015). Nettle, presents: elongated horizontal rhizomes,

from which start from the subterranean stolons: the aerial stem develops from the stolons has 4 obvious edges and is hairy, generally unblemished, empty inside; leaves are oppositely-disposed, triangular-ovate limb of 4-7 cm length and half wide, serrate edge with big teeth, with both sided haired; elongated petiole of lower leaves (almost the same as the limb), reduced petiole of upper leaves; flowers are placed in inflorescences located at leaves armpit, with 3-6 big white flowers, corolla having up to 2 cm, with upper lip shaped as a helmet, and the lower one as spoon (Ardelean A. et al., 2008).



Figure 1. Nettle (*Urtica dioica*) (Upton R. et al., 2013)

Products from stinging nettle could be used for: fibre production, in the food and feed sector and in the cosmetic/pharmaceutical sector. *Urtica dioica* L. has a high nutritive value, containing several beneficial compounds such as: vitamins A, D and C, proteins, minerals calcium, iron, potassium, manganese, choline, amines, carotenoids, anti-oxidant chlorophyll, and 5-hydroxytryptophan. Stinging nettle plant extracts contained 6.8% palmitic, 1.1% stearic, 3.6% oleic, 20.2% linoleic, and 12.4% linolenic acid, respectively (Di Virgilio N. et al., 2015). Actions of nettle herb extracts are: anti-inflammatory, local analgesic, antioxidant, diuretic, galactagogue, anti-allergenic, rubefacient, counter-irritant, nutritive and hemostatic (Upton R. et al., 2013).

The genus *Thymus* belongs to the family Lamiaceae and consists of between 300 and 400 species, but the main horticultural species are: *Thymus vulgaris* L., *Thymus serpyllum* L (Babović N. et al., 2013). *Thymus serpyllum* L., figure 2, has ascending stem of 3-5 centimetres height; the leaves are small, linear and aromatic, elliptic-ovate or round, flat, non-serrate, with petioles, pubescent; flowers are placed in circles, grouped in inflorescences or racemes; they are purple or pink and cyclamen, rarely white with cylindrical bell-shaped calyx with five teeth, three upper short teeth and two lower long teeth, short pubescent floral tube, having the external part of corolla with ovate edged four-angular upper lip (Ardelean A. et al., 2008).

Essential oils are highly volatile liquids obtained from various plant materials (flowers, buds, seeds, leaves, branches, bark, herbs, trees, fruits, roots and other parts of plants). Thyme (*Thymus serpyllum* L.) is a popular remedy for both conventional medicine. It is used as antiseptic, aromatic, expectorant, stomach, antispasmodic, carminative and preservative substance. Wild Thyme is a constituent of many herbal preparations made in pharmacies and in the pharmaceutical industry thanks to its pharmacodynamic effects. It is widely used in

medicine, pharmacy, food industry, cosmetics, alcoholic and the non-alcoholic beverage industry as well as the paints and varnishes industry (Babović N. et al., 2013).



Figure 2. Thyme (*Thymus serpyllum* L.) (Ardelean A. et al., 2008)

The study (Sonmezdag A. S. et al., 2016) characterize volatile, aromatic and phenolic compounds of wild thyme. A total of 24 the compounds were identified and quantified in the *Thymus serpyllum*. Terpenes was qualitative and quantitative the most volatile in the sample. Fragrance extract dilution analysis (AEDA) was first used for determining the aromatic compounds. In total, 12 aromatic compounds were detected in the aromatic extract of GC-MS-Olfactometry and terpenes were the most abundant compounds. 18 phenolic the compounds were identified and quantified in *T. serpyllum*. Luteolin 7-O-glucoside, luteolin and the rosmarinic acid was the most abundant phenolic in this case medicinal herbs.

Technology of processing the medicinal plants comprises the following technological processes: harvesting, conditioning, chopping, separation on dimensional fractions and extraction or tea packing (Păun G et al., 2011).

Separation according to size is the most used method of sorting medicinal plants chopped in bulk, namely when they do not preserve the chosen minced dimension and non-homogenous mixtures of vegetal matter result. Equipment performing the separation of non-homogenous vegetal mixtures per varieties has as main working part the flat or cylindrical screen. (Oztekin S. et al., 2007).

During the technological process of separation, obtaining the homogenous size fractions (sorts), depends on the following factors: number of sieves, sieve dimensions (length, width), sieve mesh dimension, physical and mechanical characteristics of vegetal material minced, inclination angle of sieves, material feeding rate, amplitude and number of rotations of sieve driving mechanism, that sets several types of movements (Ene G., 2005).

In the paper (Yang Y., 2007) the authors describe two basic sieve motions, which are involved in separation applications: oscillation in a vertical plane or in a horizontal plane. Figure 3 shows oscillation in vertical plane, which results in the vertical movement of particles on the screen surface enabling them to pass through the sieve apertures. The speed of oscillation and the amplitude of throw can be adjustable. ASTM standard (E11-95) sieve separation has this vertical motion. Figure 4 shows the oscillation in horizontal motions that result in the horizontal movement of particles on the sieve surface. Compared with vertical

sieve motions, horizontal sieve motions cause particles to push each other through the sieve apertures.

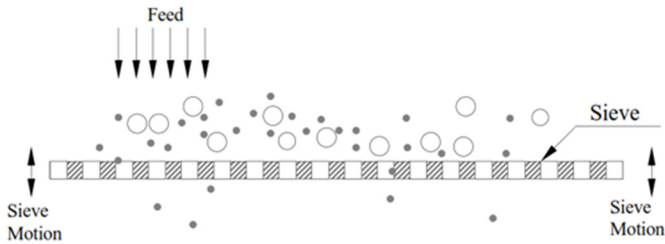


Figure 3 - Sieve oscillation in vertical plane (Yang, Y., 2007)

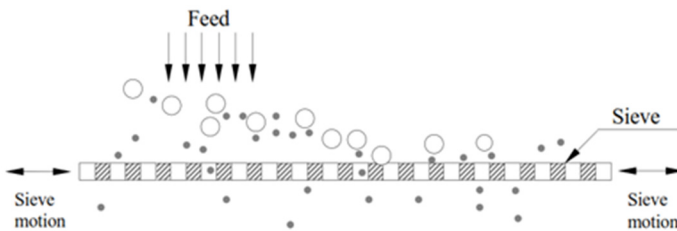


Figure 4. Sieve oscillation in horizontal plane (Yang Y., 2007)

The current paper presents the experimental and theoretical researches related to obtaining a maximum sorting degree appropriate for certain varieties of medicinal plants: nettle, and thyme, under certain conditions of work (sieve mesh dimensions, screen apertures, material feeding rate and number of rotations of sieve driving mechanism).

MATERIALS AND METHODS

The plant material used in the experiments, nettle (*Urtica dioica*) and wild thyme (*Thymus serpyllum* L.) was harvested from the spontaneous flora of Romania and identified by morphological and biological characteristics (Chifu et al., 2002; Ardelean A. et al., 2008) of the species. The herb was dried naturally in the shade, until it reached the storage moisture content (maximum 13%), cleaned of foreign bodies (inorganic materials or other plants, injured parties) under the provisions of (Romanian Pharmacopoeia, 1993; European Pharmacopoeia, 2005), and then was chopped in loose using the TIMATIC grinder for medicinal plants, adjusted to the size of 4 mm for nettle and 2 mm for thyme.

The experimental researches were conducted on a dimensional sorting equipment for chopped plants, existing in operation within INMA Bucharest, whose design scheme is shown in figure 5. This equipment is provided with 9 frames with sieves, having different hole sizes, used in sets of two or three, depending on the requirements. Sieve tilting was fix in three fix points: 12.1° , 13.3° and 14.7° depending on plant type, and also on the removal of other unwanted parts of the plants.

The bedframe of the sieves (pos. 2) is supported on a frame made of welded laminated profiles (pos. 8) through rubber dampers (pos. 10). The drive of the equipment is made with two vibrating drives (pos. 6) mounted on symmetrically welded plates outside the bedframe.

The feeding of sorter with material is made using an inclined conveyor belt, which discharges the plant material in the center of the feeding hopper and hence on its upper sieve where the separation process takes place. Mass (M) of sorter flow (Q_{alim}) was uniformly distributed on conveyor surface and was adjusted knowing that the band length is of 6 meters and conveyor speed (v) is of 0.04 m/s. For each experiment, the plant fragments separated through the screen holes were collected in the box mounted below sieve C with large.

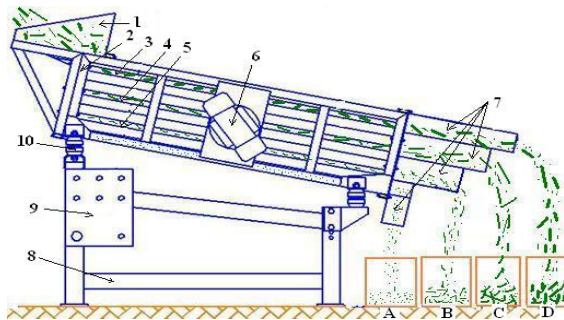


Figure 5. Scheme of the equipment for sieving medicinal plants (Pruteanu A. et al., 2017)

1 – feeding hopper; 2 – bed frame; 3,4,5 – sieves with square holes of varying sizes (pos. 3 sieve with large holes, pos. 4 sieve with medium holes and pos.5 sieve with small holes); 6 – vibrating drive; 7 – outlets; 8 – frame; 9 – control panel; 10 – rubber dampers; A, B, C, D – collector boxes

Three feed rates were used in the experiments (0.0166 kg s^{-1} , 0.0125 kg s^{-1} and 0.0083 kg s^{-1}) and three revolution speeds of the mechanism for actuating the sieves (1000 RPM, 900 RPM and 800 RPM), sieve tilting angle fix at $\alpha = 12.1^\circ$. During the tests, three wire screens with square holes disposed in increasing order according to holes size, were used. The sieve holes size has been chosen after performing the dimensional analysis of fragments chopped so that they were placed as it follows: 2.0 - 4.0 - 5.6 mm for nettle and 1.4 - 2.0 - 3.0 mm for thyme.

An experimental determination was performed as it follows:

- one box for collecting the vegetal fragments was mounted at each of the four output openings of sieves;
- a mixture of chopped vegetal fragments was fed on conveyor's band;
- first, the sorter was put into operation, then the conveyor band and sieves were supplied with vegetal matter, letting it to go along the sieves length up to the discharge areas; then, the material flew uniformly through the four exhausting openings;
- chronometer was put into operation and covers of vegetal fragments collecting boxes were drawn;
- chronometer was stopped after 30 seconds and the vegetal matter suitable to a certain variety, from each box was weighed;
- experimental flow (q) is total mass of material (M_t) sorted by sieves during time $t = 30 \text{ s}$.

Degree of sorting (G_s) is expressed in percentages (%) and is defined as the ratio between the quantity of fragments from each collecting box (group I, group II, group III, group IV) and quantity of fragments from the four collecting boxes.

Interpretation of outcome was made for the desired group II by nettle and group I for thyme, by representing functions with multiple variables, situation when the dependent variable (percentage of group II and group I), depends, at the same time, on several independent variables, x_1 respectively x_2 , replaced one after another, so that: $x_1 = n$, $x_2 = q$, resulting in one polynomial function of II degree with two variables, having the general form shown in equation (1), (Păunescu et al., 1999):

$$f(x_1, x_2) = a_0 + a_1 \cdot x_1 + a_2 \cdot x_2 + a_3 \cdot x_1^2 + a_4 \cdot x_1 \cdot x_2 + a_5 \cdot x_2^2 \quad (1)$$

For processing the experimental data, an experimental fragmented testing program for 9 experiments, within Mathcad program, given by values of independent and dependent variables for each experiment.

RESULTS AND DISCUSSION

Values of experimental data characterizing the sorting process by sorter on 4 size groups, are presented in table 1 for nettle and in table 2 for thyme.

Table 1. Experimental results regarding the sorting of nettle fragments

Flow rate Q_{nim} [kg s ⁻¹]	Revolutions on speed, n [RPM]	Sieve angle, α [°]	Time, t [s]	Mass Group M1 [kg]	Mass Group M2 [kg]	Mass Group M3 [kg]	Mass Group M4 [kg]	Total mass M_t [kg]	Experimental flow, q [kg s ⁻¹]
0.0166	1000	12.1	30	0.055	0.275	0.094	0.074	0.498	0.0166
	900	12.1	30	0.073	0.280	0.061	0.049	0.463	0.0154
	800	12.1	30	0.078	0.253	0.049	0.037	0.418	0.0139
0.0125	1000	12.1	30	0.037	0.220	0.071	0.021	0.350	0.0117
	900	12.1	30	0.055	0.222	0.049	0.049	0.374	0.0125
	800	12.1	30	0.054	0.195	0.037	0.035	0.322	0.0107
0.0083	1000	12.1	30	0.038	0.149	0.050	0.011	0.249	0.0083
	900	12.1	30	0.047	0.158	0.032	0.004	0.241	0.0080
	800	12.1	30	0.046	0.140	0.029	0.012	0.227	0.0076

Table 2 - Experimental results regarding the sorting of thyme fragments

Flow rate Q_{nim} [kg s ⁻¹]	Revolutions on speed, n [RPM]	Sieve angle, α [°]	Time, t [s]	Mass Group 1 [kg]	Mass Group 2 [kg]	Mass Group 3 [kg]	Mass Group 4 [kg]	Total mass [kg]	Experimental flow, q [kg s ⁻¹]
0.0166	1000	12.1	30	0.346	0.041	0.102	0.008	0.497	0.0166
	900	12.1	30	0.295	0.037	0.112	0.008	0.410	0.0150
	800	12.1	30	0.228	0.049	0.119	0.009	0.405	0.0135
0.0125	1000	12.1	30	0.232	0.034	0.102	0.006	0.374	0.0125
	900	12.1	30	0.237	0.024	0.086	0.004	0.351	0.0117
	800	12.1	30	0.188	0.037	0.098	0.003	0.326	0.0109
0.0083	1000	12.1	30	0.172	0.022	0.051	0.004	0.249	0.0083
	900	12.1	30	0.147	0.028	0.050	0.004	0.229	0.0076
	800	12.1	30	0.114	0.030	0.066	0.003	0.213	0.0071

Degree of sorting (G_s) was calculated with mass of fragments presented in tables 3 and 4.

In order to determine the optimum sorting degree for group II for nettle and group I for thyme, a mathematical modelling in Mathcad program has been achieved, by which, after having imposed linear restrictions of n and q , that showed the value interval of independent variables, the coefficients and form of polynomial function of IInd degree with two variables were calculated.

Linear restrictions values framed between a minimum value and a maximum value:

$$800 \text{ RPM} = x_{1min} \leq x_1 = n \leq x_{1max} = 1000 \text{ RPM}$$

$$0.0080 \text{ kg s}^{-1} = x_{2min} \leq x_2 = q \leq x_{2max} = 0.0166 \text{ kg s}^{-1} \quad (2)$$

Thus, it resulted the function and function coefficients replaced as:

$$G_{s(n,q)} = -92.727 + 0.334 \cdot n + 1.635 \cdot q - 1.824 \cdot 10^{-4} \cdot n^2 - 8.526 \times 10^{-4} \cdot n \cdot q - 0.06 \cdot q^2 \quad (3)$$

After defining the normal equation system, the correlation coefficient $R^2 = 0.795$, was calculated. In figure 6 is presented the function's graphic.

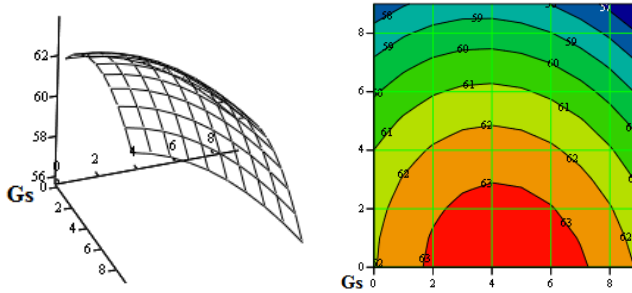


Figure 6. Variation of nettle sorting degree according to revolution speed and feeding rate

In figure 7 are presented the experimental values of sorting degree comparing to theoretical values, calculated by the polynomial regression function for each test.

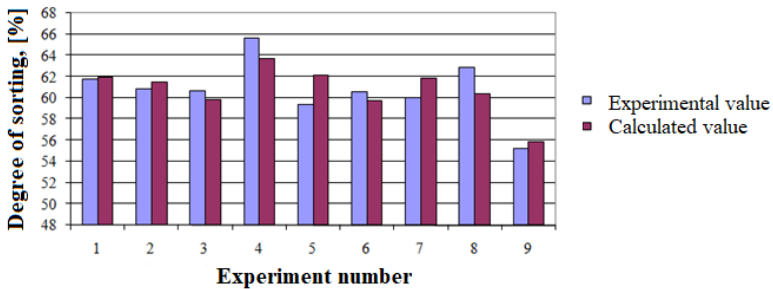


Figure 7. Degree of sorting for group II for nettle

In figure 7, it can be noticed that the differences between the values experimentally obtained and those calculated for nettle sorts II are small 0.16 % for $n = 800$ RPM and $q = 0.0081 \text{ kg s}^{-1}$ and big 2.74 % for $n = 900$ RPM and $q = 0.0125 \text{ kg s}^{-1}$.

The following operation consisted in taking 10 values from the imposed interval and determining the variation of sorting degree depending on experimental flow rate (figure 8) and revolution speed of sieve driving mechanism (figure 9).

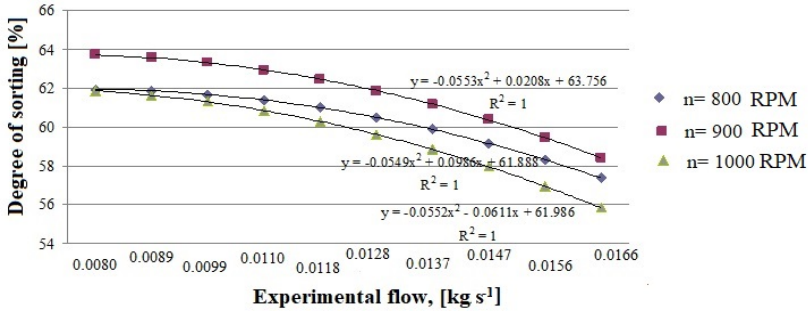


Figure 8. Variation of sieve experimental flow rate for nettle

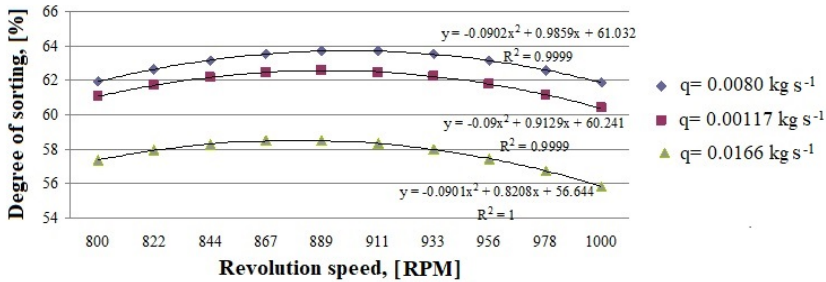


Figure 9. Variation of sorting degree depending on sieve driving mechanism, for nettle

For sieve tilting angle of 12.1° the maximum value of sorting degree was $G_s \text{ max} = 63.71 \%$, for independent variables values: $n = 900$ RPM and $q = 0.0080 \text{ kg s}^{-1}$ and minimum value is $G_s \text{ min} = 55.85 \%$, for independent variables values: $n = 1000$ RPM and $q = 0.0166 \text{ kg s}^{-1}$.

It was repeated the same process for I for thyme. Linear restrictions were

$$800 \text{ RPM} = x_{1\text{min}} \leq x_1 = n \leq x_{1\text{max}} = 1000 \text{ RPM}$$

$$0.0071 \text{ kg s}^{-1} = x_{2\text{min}} \leq x_2 = q \leq x_{2\text{max}} = 0.0166 \text{ kg s}^{-1} \quad (4)$$

Thus, it results the function and replaced coefficients, as:

$$G_{S(n,q)} = -337.937 + 0.818 \cdot n + 1.838 \cdot q - 3.969 \cdot 10^{-4} \cdot n^2 - 4.65 \times 10^{-3} \cdot n \cdot q - 0.114 \cdot q^2 \quad (5)$$

After defining the system of normal equations, the correlation coefficient $R^2 = 0.924$, was calculated. The function graphic representation is given in figure 10:

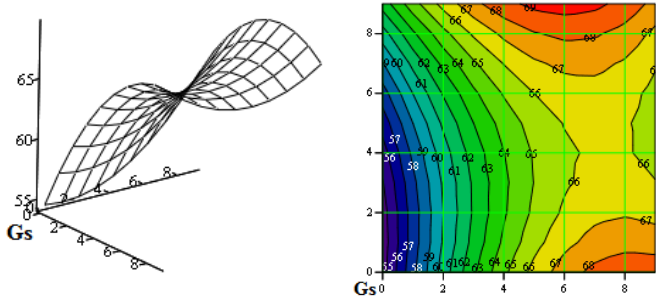


Figure 10. Variation of thyme sorting degree for sort I depending on revolution speed and sieve experimental flow rate

Figure 11 presents the experimental values of sorting degree comparing to theoretical values, for each test.

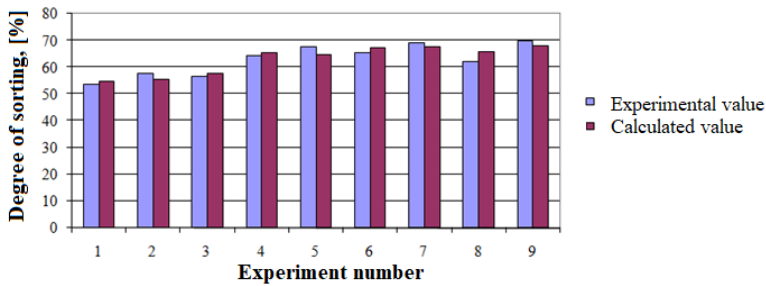


Figure 11. Degree of sorting for group I for thyme

From figure 11 it can be noticed the differences between the values experimentally obtained and those calculated for group I for thyme are small 1.08 % for $n= 800$ RPM and $q= 0.0071$ kg s^{-1} ; $n= 900$ RPM and $q= 0.0076$ kg s^{-1} and big 3.54 % for $n= 1000$ RPM and $q= 0.0125$ kg s^{-1} .

The following step was to take 10 values from the imposed interval and determine the variation of sorting degree depending on experimental rate (figure 12) and revolution speed of sieve driving mechanism (figure 13).

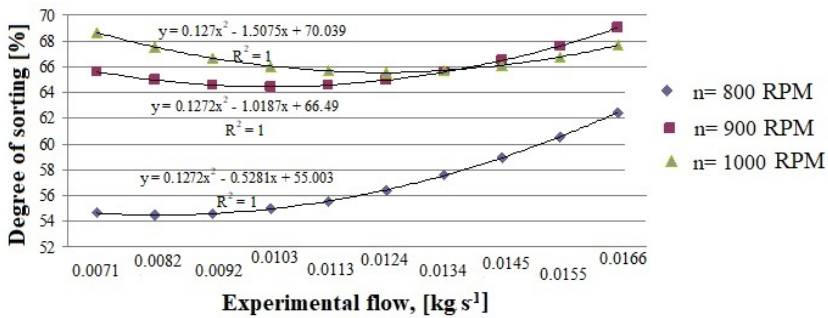


Figure 12. Variation of sorting degree depending on sieve experimental rate, for thyme

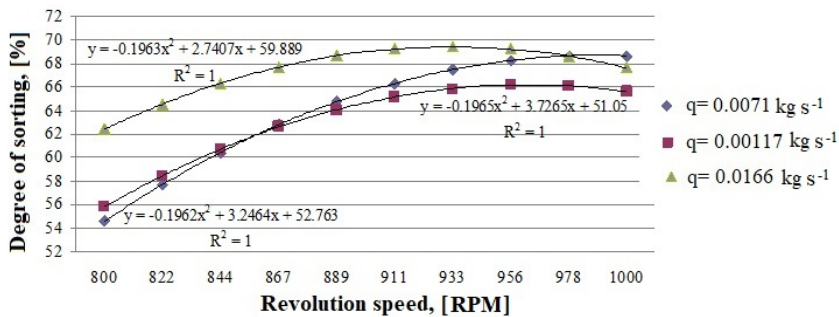


Figure 13. Variation of sorting degree depending on revolution speed of sieve driving mechanism, for thyme

For sieve inclination angle of 12.1° the maximum value of sorting degree was $G_s \max = 69.46\%$, for independent variables values: $n = 933$ RPM and $q = 0.0166$ kg s⁻¹ and minimum value $G_s \min = 54.46\%$, for independent variables values: $n = 800$ RPM and $q = 0.0082$ kg s⁻¹.

CONCLUSIONS

The experimental and theoretical results of this paper have emphasized the following conclusions:

- medicinal plants are considered natural remedies and are a real help in treating different illnesses and maintaining human health;
- medicinal plants contain bioactive substances with therapeutic role, being consumed as tea, pills, tinctures, syrup, extracts, etc;
- plant may be used as such or vegetative parts of it may be used, for example: root, stem, leaves, flowers, seeds, herb (aerial part above the soil);
- among the multitude of medicinal plants existing in spontaneous or cultivated flora in Romania, the most important are the nettle and thyme; thyme contains tannins (12-14 %), essential oil, rosmarinic acid, etc, and thyme is rich in essential oil, especially thymol and carvacrol, generally used as medicine;

- medicinal plants processing is performed with specialized equipment, separation being extremely important and being achieved with flat oscillating screens; there are many factors that influence the separation among which the most relevant are: dimensions of sieve holes and size of chopped plants, material feeding rate, revolution speed of sieve driving system and sieve inclination angle;
- nettle dried and chopped in bulk at 4.0 mm, was separated on sieves whose hole size is growing, thus: 2.0 - 4.0 - 5.6 mm; for sieve inclination angle of 12.08° the maximum value of sorting degree was $G_s \max = 63.71 \%$, for values of independent variables: $n = 900$ rot/min and $q = 0.0080$ kg/s;
- dried thyme chopped in bulk at 2.0 mm size was separated on sieves whose holes are disposed such as: 1.4 - 2.0 - 3.0 mm, for sieve inclination angle at 12.08° the maximum value of sorting degree was $G_s \max = 69.46 \%$, for values of independent variables: $n = 933$ rot/min and $q = 0.0166$ kg/s;
- variation of parameters chosen for plant sorter has been correlated to polynomial function of II-degree with two variables, deviations being insignificant.

Efficiency of a medicinal plant separation can be achieved at a high level if the working regime parameters are appropriately chosen and separation of sorted plants with homogenous dimensions is important for producing high quality phyto-therapeutic products.

ACKNOWLEDGEMENT

This paper was financed by support of National Agency for Scientific Research and Innovation, NUCLEU Programme, no. 8N/09.03.2016, Ad. Act nr.1/2016, Project PN 16 24 03 03 - "Innovative technology and equipment for increasing the quality of plant raw material obtained from medicinal and aromatic plants, in the view of elaborating competitive organic products".

REFERENCES

- Ardelean, A. and Mohan, Gh. (2008). Medicinal Flora of Romania, Editura All Publishing, Bucharest, ISBN 978-973-571-838-1.
- Babović, N., Dražić, G., Petrović, S. (2013). Obtaining active ingredients from aromatic plants during the processing of wild thyme (*Thymus serpyllum* L.), Journal on Processing and Energy in Agriculture, Biblid: 1821-4487 17; 2; p 89-92 UDK: 633.88.
- Chifu, T., Mânzu, C., Zamfirescu, O., Şurubaru, B. (2002). Guide for practical works of Systematic Botany, Univ., Al. I. Cuza" Publishing, Iaşi.
- De Silva, T. (1997), Industrial utilization of medicinal plants in developing countries, Medicinal plants for forest conservation and health care, Global Initiative For Traditional Systems (Gifts) Of Health Food And Agriculture Organization Of The United Nations, NON WOOD FOREST PRODUCTS, No. 11, Rome, , ISBN 92-5-104063-X, pp. 34-50.
- Di Virgilio, N., Papazoglou, E.G., Jankauskiene, Z., Di Lonardo, S., Praczyk, M., Wielgusz, K., (2015). The potential of stinging nettle (*Urtica dioica* L.) as a crop with multiple uses, Industrial Crops and Products, 68, pp. 42-49, (<http://dx.doi.org/10.1016/j.indcrop.2014.08.012>)
- Ene, G. (2005). Equipment designed to class and sort solid polydisperse materials, Editura Matrix Rom Publishing, Bucharest.
- Oztekın, S. and Martinov, M. (2007). Medicinal and aromatic crops: harvesting, drying and processing, Editura Haworth Press, United States and Canada.

- Păun, G., Gheorghe, O., Diaconu, M. (2011). Advanced processing of medicinal plants (Course), MedPlaNet Project, pp. 41-43.
- Păunescu, I. and David, L. (1999). Experimental research bases of biotechnical systems, Printech Publishing, Bucharest.
- Pruteanu, A., Vlăduț, V., Matache, M., Muscalu, A., Ungureanu, N. (2017). Characterization of chicory herb (*Cichorium intybus*) of separation process on length of flat vibrating sieves, Proceedings of the 45th International Symposium "Actual Tasks on Agricultural Engineering", Opatija – Croatia, ISSN 1848-4425, 2017, p. 339-350.
- Sonmezdag. A.S., Kelebek, H., Selli, S. (2016). Characterization of aroma-active and phenolic profiles of wild thyme (*Thymus serpyllum*) by GC-MS-Olfactometry and LC-ESI-MS/MS, J Food Sci Technol 53(4), pp. 1957–1965, (DOI 10.1007/s13197-015-2144-1).
- Upton R. (2013). Stinging nettles leaf (*Urtica dioica* L.): Extraordinary vegetable Medicine, Journal of Herbal Medicine, 3, pp. 9-38.
- Yang, Y. (2007). Image and Sieve Analysis of Biomass Particle Sizes and Separation after Size Reduction, Master's Thesis, University of Tennessee, (http://trace.tennessee.edu/utk_gradthes/201).
- *** – European Pharmacopoeia (2005). The Fifth Edition.
- *** – Romanian Pharmacopoeia (1993). The Xth Medical Edition, Bucharest.



STUDY OF AN AUTOMATIC OLIVES SORTING SYSTEM

Roxana Mihaela BABANATIS MERCE, Theoharis BABANATSAS,
Stefan MARIS, Dumitru TUCU*, Oana Corina GHERGAN

Department for Mechanical Machines, Equipment and Transportation, Politehnica University
Timisoara, Mihai Viteazu Street No. 1, Timisoara, Romania

*E-mail of corresponding author: tucusalix@gmail.com

SUMMARY

The paper presents the results of study of an automatic selection system for olives. During the harvesting of olives, mechanical or automatic, the olives can be black (the ripe olives on tree), or green (the olives that are unripe). It is important to select the black olives from the green olives. After this stage we must select, in both case black and green, the olive that are good for consumer, and the other olives which are good for processing oil. This selection is based on colors and image recognition. Because the green olives have different nutrition facts and differed acidity on oil, the storage is separately for the green, and black, such step being very important. The paper proposes an original method for recognition ripe olive from unripe olive based on color. For study was used an image recognition system based on colors from olives that was picked manual. It was analyzed the accurate of results from this experiment to determine the optimal parameters.

Key words: green olive, black olive, unripe olive, ripe olive, image recognition, nutrition.

INTRODUCTION

Modern agricultural operations include also the sorting systems with high automation systems. In olive industry, after harvesting, the olives are deposited in a storage area. Because after harvesting the olives continue too ripe, becomes necessary the quickly separation of the black olives from green olives, and, optional, can be separated the olives that are good for consumer from the olives that are good for oil processing (Riquelme, 2008).

Automating sorting systems for olives have a very high importance in the global market economy. Shakers are one of the most used machines for mechanical harvesting in olive

orchards (Tombesi et al., 2017). Olives must be sorted and stored in optimal conditions, so as to avoid their deterioration (Peri, 2014). For this purpose, we used a transportation conveyor system with optical recognition system, sensors, integrated in the sorting system. Actually, on the market there are some expensive olive sorting systems. In present study we tested the accuracy of digital color sensors to pick-up olives in different conditions and different speed of conveyor transporter. The main objective was to create a better and cheaper olives sorting system that can work based on digital optical sensors without scanner and optical recognition system (Tucu, 2014).

MATERIALS AND METHODS

To create the automatic sorting system of olives it must keep in mind that's its need to separate the ripe olives (black) from unripe olives (green), because they have different nutrition factors and acidity (Peri, 2014). Also, from this step we can separate the olives fruit that are good for consumer from all the others olives that are good for oil processing. This step is optional because the final recipient can be producers of olives or olive oil.

The schematic structure, that includes the optical recognition system that will separate the olives by color, is presented in Figure 1. In the first step the automatic system must sorting the black olives from the green olives (Xynoset al., 2014). In the next step (that is optional), the optical system will separate the olives that are good for consumer (1-green olives and 3-black olives), from the olives that are only good for oil processing (2-green olives and 4-black olives).

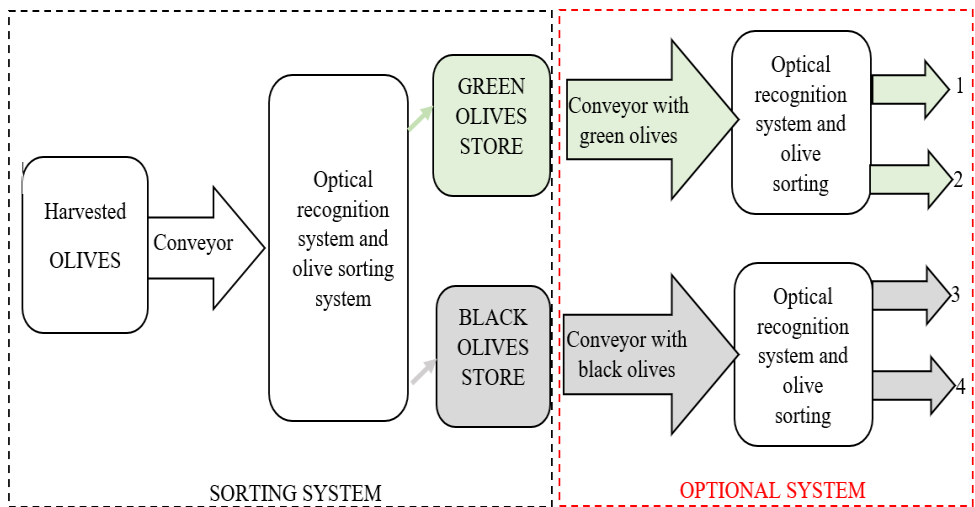


Figure 1. Schematic structure of automatic storage system for separating olives

The method to detect damaged olive fruit that would be benefit for both, consumers and producers of olives and olive oil, is demonstrated with near-infrared spectroscopy system (Hassan et al., 2011; Moschetti et al., 2016).

In our experiment we used only black and green olive and we focused on the first step, were we sort the green olives from the black.

For this reason, we have had created an experimental prototype stand (Figure 2), that can automatic sort olives based on colors with the digital optical sensors. The olives are transported in front of the pick-up device with a belt conveyor which have adjustable speed. The optical sensor for detection the green olives are positioned to read from vertical on the belt and the sensor for detection the black olives are positioned to read from horizontal on the belt. The pick-up system device is based on a push up hydraulic system, because we can control better the speed and the force for pushing the olives.

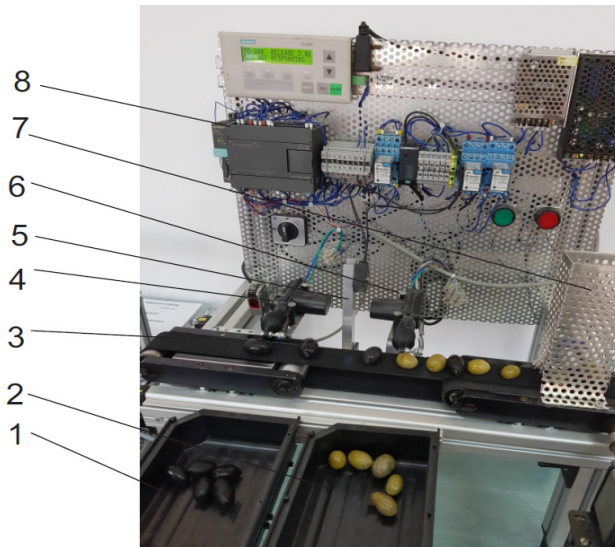


Figure 2. Experimental stand for sorting olives

The main components of the experimental stand of sorting system, according to Figure 2: 1, 2 – collected box; 3 – conveyor belt; 4, 5 – digital color sensors; 6 – pick up dispositive; 7 – olive supply point; 8 – main board.

To determine the accuracy in recognizing of the olives with the digital color sensors we did tests under different conveyor speed and distance between olives. We used 30 black olives and 30 green olives and the position on conveyor belt was randomly selected.

In the first experiment the distance between olives was about 0.05 m and the speed $0.0025 \text{ m}\cdot\text{s}^{-1}$. In the next experiments we have modified the speed to $0.005 \text{ m}\cdot\text{s}^{-1}$ and, in the same conditions, for the values 0.015, 0.02, 0.03, 0.04 and $0.05 \text{ m}\cdot\text{s}^{-1}$. In the second part of experiments, we repeat the test keeping the speed at $0.0025 \text{ m}\cdot\text{s}^{-1}$ and the next values of distance between olives: 0.03, 0.01 and 0 m.

Each time, were determined the accuracy of olive selection, A_{os} , by the equation:

$$A_{os} = \frac{\text{selected olives}}{\text{total cooresponding olives}} \times 100, [\%]$$

Also, we need to determinate the delay time between the moment when the digital color sensor detects the olive and the moment when the pick-up system push the olive in the special collected box. Base on this time we create the length between the point where digital optical sensor detect the olive and the point where the pick-up system works.

RESULTS AND DISCUSSION

The experimental data, for the accuracy in each condition were centralized in Table 1.

Table 1. Optical recognition accuracy at olives images

Distance between the olives [m]	Speed of displacement [m s ⁻¹]	Accuracy on green olives [%]	Accuracy on black olives [%]
0.05	0.0025	100	100
	0.005	100	100
	0.01	100	100
	0.015	100	100
	0.02	100	100
	0.03	99	99
	0.04	98	97
	0.05	95	94
0.03	0.0025	100	100
	0.005	100	100
	0.01	100	100
	0.015	100	100
	0.02	99	99
	0.03	99	98
	0.04	98	96
	0.05	94	93
0.01	0.0025	100	100
	0.005	100	100
	0.01	99	99
	0.015	98	98
	0.02	97	96
	0.03	94	92
	0.04	91	87
	0.05	84	79
0	0.0025	100	100
	0.005	99	98
	0.01	97	94
	0.015	93	88
	0.02	86	80
	0.03	83	71
	0.04	78	60
	0.05	63	48

Based on the experimental data from table no.1, in figure 3 was represented the relation between: distance between olives (green-G and black-B), band speed and accuracy.

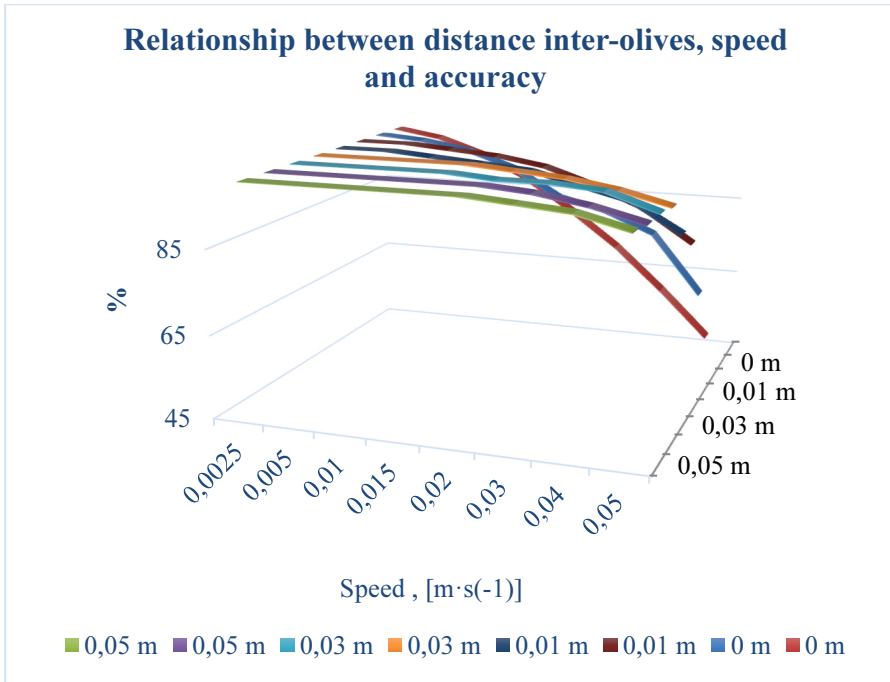


Figure 3. Experimental stand results

The first variable was the distance between olives with randomly colors (black and green) from 0.05 m to 0 m, and the second variable was the transportation speed from $0.0025 \text{ m}\cdot\text{s}^{-1}$ to $5 \text{ m}\cdot\text{s}^{-1}$.

The results indicate that the influences of transportation speed on the detected errors regardless of distance between olives could damage the accuracy of selection process, or the productivity (if the band speed are less than $5 \times 10^{-3} \text{ m}\cdot\text{s}^{-1}$, the solution could be applied without restrictions, the accuracy is more than 98 %).

At $0.04 \text{ m}\cdot\text{s}^{-1}$ speed, the productivity on each band will be around 12 kg/hour (considering media on 240 olives/kg, and minimum accuracy at 97 %).

The proposed solution could be improved if the system includes a distributor feeder for supply the olives at 0.05 m equal distances.

Another test was made by modified the distance between sensor and pick-up system based on delay time 0.0765 s.

But when we increase the speed, 0.03, 0.05 or more $\text{m}\cdot\text{s}^{-1}$ appears read errors from the optical sensors. These errors are caused from the delay time between the moment when olive is in conveyor in front of optical sensor and the moment when the pick-up select the olive.

Such system can insure acceptable accuracy of separation process, not at high level generated by the use of NIR (eg. Gozman et all, 2013), or NIRS (Cayuela, Jose A. et all, 2017), but at substantially lower costs, very advantageously for small farms.

CONCLUSIONS

It is very important to create an automatically olives sorting system. With this sorting system, it can better manage all the olives process (Tucu et al., 2006). The test in different conditions showed that such system can make an automatic selection between black and green olives, in conditions of low costs. The optimum distance between olives is around 0.05 m (too much, means decreasing of productivity), and the optimum of speed is around 0.04 m·s⁻¹. If the sensors' quality (and price), increases, the optimum could be improved by increasing the speed.

Another option could be made by the simultaneously use of two or more digital optical sensors for the corrections of these errors (future study).

REFERENCES

- Cayuela, J.A. and Garcia, J.E. (2017). Sorting olive oil based on alpha-tocopherol and total tocopherol content using near-infra-red spectroscopy (NIRS) analysis. *Journal of Food Engineering*, Vol. 202, p. 79-88.
- Guzmán, E., Baeten, V., Fernández-Pierna, J.A.F., García-Mesa, J.A. (2013). Infrared machine vision system for the automatic detection of olive fruit quality. *Talanta*, Elsevier, Vol. 116, p. 894-898.
- Hassan, H. E., El-Rahman, A. A. Abd, Attia, M. M. (2011). Color Properties of Olive Fruits During Its Maturity Stages Using Image Analysis. 8th International Conference on Laser Applications (ICLA), Cairo, Egypt.
- Moscetti, R., Haff, R. P.; Monarca, D. (2016). Near-infrared spectroscopy for detection of hailstorm damage on olive fruit. *Postharvest Biology and Technology*, Elsevier Science Amsterdam, Netherlands, Volume 120, pp 204-212.
- Peri, C. (2014). Olive handling, storage and transportation. Wiley-Blackwell, Italy.
- Peri, C. (2014). The extra virgin Olive Oil Handbook. Wiley-Blackwell, Italy.
- Riquelme, M.T., Barreiro, P., Ruiz-Altisent, M., Valero, C. (2008). Physical Properties Laboratory and Advanced Technologies in Agrofood (LPF-TAG). *Journal of Food Engineering*, Elsevier Science Amsterdam, Netherlands, Volume 87, Issue 3, pp371-379
- Tombesi, S., Poni, S., Palliotti, A., Farinelli, D. (2017). Mechanical vibration transmission and harvesting effectiveness is affected by the presence of branch suckers in olive trees. *Biosystems Engineering*, Volume: 158, Pages: 1-9.
- Tucu, D., Rotarescu V., Bordeasu I. (2006). Considerations on the relationship between product quality and milling system in plastic recycling. *Materiale Plastice*. Volume: 43 Issue: 4, pp 308-311.
- Tucu, D. (2014). Controlled stems cutting module for src nurseries. Actual tasks on agricultural engineering, *Proceedings*. Book Series: Actual Tasks on Agricultural Engineering-Zagreb, Volume: 42 Pages: 397-404.
- Xynos, N., Papaefstathiou G., Gikas E., Argyropoulou A., Aligiannis N., Skaltsounis A.L. (2014). Design optimization study of the extraction of olive leaves performed with pressurized liquid extraction using response surface methodology, pp 273-305.



CARBON FOOTPRINT OF FINAL WHEAT PRODUCTS FROM FAMILY FARMS

Viktor JEJCIC^{1*}, Fouad AL-MANSOUR², Tomaz POJE¹

¹ Agricultural institute of Slovenia, Hacquetova ulica 17, 1000 Ljubljana, Slovenia

² Jozef Stefan Institute, Jamova cesta 39, 1000 Ljubljana, Slovenia

*E-mail of corresponding author: viktor.jejcic@kis.si

SUMMARY

Carbon footprint of final wheat products like bread and bakery products, expressed as carbon dioxide equivalent ($\text{kg CO}_2 \text{ eq. kg}^{-1}$) is determined as a sum of Green House Gases emissions (GHG) from wheat production on different sizes of family farms with different production methods (conventional, integrated and organic) and GHG emissions of wheat processing in final products (bread and bakery products). Carbon footprint ($\text{kg CO}_2 \text{ eq. kg}^{-1}$) of final wheat products includes emissions of GHG from the crop production (emissions from primary energy consumption, fertilizers use, etc.), internal and external transport, drying, storage and wheat processing in bread and bakery products. Analysis of energy use in wheat production on different farm sizes and farm production methods was made. It was estimated that carbon footprint ($\text{kg CO}_2 \text{ eq. kg}^{-1}$) of final wheat products – bread and bakery products, depend on the method of farm production (conventional, integrated and organic production) and farm size. Carbon footprint $\text{kg CO}_2 \text{ eq. kg}^{-1}$ of final wheat products from the wheat production and processing of wheat in bread and bakery products is the lowest in conventional, followed by integrated and the highest in organic farm production. Emissions $\text{kg CO}_2 \text{ eq. kg}^{-1}$ of final wheat products - bread and bakery products (wheat production and its processing in bread and bakery products) are declining with the farm size (highest are on small farms and lowest on bigger farms).

Keywords: wheat production, energy use, GHG emissions, bread and bakery products

INTRODUCTION

Currently the concentration of CO_2 in the atmosphere is the highest in the last 800,000 years. It is noted that since the beginning of the industrial revolution at the 18th century, the concentration of CO_2 in the atmosphere from 278 ppm achieved highest value in current decade (global averaged CO_2 levels passed 400 ppm in year 2015) with 43 % increase

in comparison with pre industrial levels. It's worrying that concentration of CO₂ now rose by 2 ppm or more per year, Levels at Mauna Loa Observatory had already climbed to 406.42 ppm (ESRL, 2017). The annual mean rate of growth of CO₂ in a given year is the difference in concentration between the end of December and the start of January of that year. It represents the sum of all CO₂ added to, and removed from the atmosphere during the year by human activities and by natural processes. Human activities are responsible for almost all of the increase in greenhouse gases in the atmosphere over the last 150 years (IPCC - Summary for Policymakers, 2007). Increase in atmosphere concentration of CO₂ was caused by human activities, primarily by the burning of fossil fuels (coal, oil and natural gas) and added contributions like deforestation, agriculture activities, changes in land use, etc. Modern agriculture in most parts of world has become increasingly dependent on fossil fuels. In mechanized working operations the use of mineral diesel fuel is predominant. Also fossil fuels - oil and natural gas have high shares in present time in drying different agricultural crops and processing it into final products like food, fibres, biofuels, etc. The dominant share of direct energy use on U.S. farms is fuel (including diesel and gasoline) to run machinery for field operations such as planting, tilling and harvesting; to dry crops; for livestock use; and to transport goods, (Beckman et al., 2016). Direct energy uses on farms with crops production in EU is dominantly depending on fossil fuels (Al Mansour et al., 2016). Different studies have reported, that the use of mineral diesel fuel for various agricultural operations require to consider the average values as measured values for fuel consumption (l ha⁻¹ or kg ha⁻¹), it can be very variable due to different conditions in agricultural production like soil characteristics, machine type and settings, working speeds, harvest amount, plot size and form, etc. (Dalgaard, 2001; Handler, 2012; Jejčić et al., 2014). The most useful unit for fuel consumption in most of the farming field operations is consumption of fuel per hectare, since it enables the comparison between different farms and years (Jokiniemi et al., 2012). The aim of organic agriculture is to augment ecological processes that foster plant nutrition yet conserve soil and water resources. The combustion of mineral diesel fuel in engines of tractors or other propelled farm machines in various working operations of mechanized agricultural production emits greenhouse gases expressed in the unit kilogram of carbon dioxide - equivalent (kg CO₂ eq. kg⁻¹). From the pollutants discharged into the atmosphere in the combustion of mineral diesel oil, the most environmentally harmful are: carbon dioxide (CO₂), carbon monoxide (CO), nitrogen oxides (NO_x), particulate matter (PM).

The use of energy is defined as fossil energy measured in MJ. Energy use is defined as the net energy used in the production of agricultural products until they are sold and leave the farm or used as feed in livestock (Dalgaard et al., 2001). The use of energy can be divided in direct energy and indirect energy used in the production of agricultural products. Direct energy (EU_{direct}) represents the energy input in agricultural production, which can be directly converted into energy units (mineral diesel fuel, lubricants, energy from LPG or CNG for additional drying, electricity for postharvest processing, etc.). Indirect energy ($EU_{indirect}$) is the energy that is consumed in the production of inputs used in the production of agricultural products, but these entries cannot be directly converted to energy units (machinery, fertilizers, pesticides, etc.). Total energy for the production of agricultural products can be represented by the equation (1).

$$EU_{crops} = EU_{direct} + EU_{indirect}$$

$$EU_{crops} = (EU_{diesel} + EU_{other}) + EU_{indirect} \quad (1)$$

In the case of mechanized production, mineral diesel fuel is used for tractors with connected farm implements and self-propelled agricultural machinery, which means that EU_{direct} is combustion of the mentioned fuel in engines of farm machines. For calculation of

total GHG emission generated in the combustion process of internal combustion engines, the CO₂ emissions and emissions from other GHG have to be determined, which causes the effect of greenhouse gases. This quantity is expressed in unit kilogram of carbon dioxide - equivalent (kg CO₂ eq.). Emissions of GHG from combustion of mineral diesel fuel are estimated at 3.18 kg CO₂ eq. kg⁻¹ or 2.67 kg CO₂ eq. l⁻¹ (Guidelines to Defra/DECC's, 2012).

The aim of the research was determination of carbon footprint of final products from wheat (bread and bakery products). Carbon footprint of final products from wheat was determined on the basis of measurements of energy consumption in different agricultural operations, fertilizers input, etc., in conventional, integrated and organic production and later in processing wheat products in bread and bakery products.

MATERIALS AND METHODS

Energy consumption in the wheat production

In the energy analysis all intakes (direct energy use) are broken in energy which is fully consumed in the production period. Inputs of energy over a longer period of production time (more than crops season) or indirect energy (for production of tractors and farm machines as well as energy for the production of mineral fertilizers, pesticides, etc.), were not taken into account. The energy consumption in a mechanized agricultural production is defined as the energy from mineral diesel fuel, to be used in the implementation of various mechanized working operations. The total energy consumed to produce a crop yield per area of one hectare was determined by adding the energy consumption of each energy input (2).

$$E_{prod} = E_{st} + E_f + E_p + E_h + E_{it} + E_d \quad (2)$$

E_{prod} = total energy used for wheat production (MJ)

E_{st} = energy for primary and secondary soil tillage

E_f = energy consumption for fertilizing

E_p = energy consumption for plant protection

E_h = energy consumption for harvesting

E_{it} = energy consumption for internal transport

E_d = energy consumption for additional crops drying

For production of wheat, an analysis for conventional, integrated and organic production has been made. All three mentioned types of production typically have primary and secondary soil tillage, seeding, fertilization, care and crops protection, harvesting, internal transportation and additional drying of the wheat. Energy consumption in the aforementioned production is determined in the course of working operations with the tractor implements (aggregate - tractor + connected machine) for primary and secondary tillage, seeding, fertilization, care, plant protection, etc. Consumption of mineral diesel fuel in the working operations with the tractors aggregated with different implements and self-propelled farm machines at work (harvesters) was measured on different family farms in Slovenia (10 farms). For measuring of energy consumption defined were three family farm sizes. Small farm is with up to 10 ha of arable land, medium farm with more than 10 ha and up to 50 ha of arable land, and big farm is with more than 50 ha of arable land.

Fertilizers and pesticides use

In model calculations we also made different scenarios for using fertilizers in conventional, integrated and organic production. The use of mineral fertilizers is provided in conventional production. In the integrated production the use of mineral fertilizers and

organic manure in a ratio of 80% of mineral and 20% of organic fertilizers is provided. For organic farming the use of organic fertilizers (manure or slurry) is provided. For fertilizer spreading, use of spreaders for mineral fertilizers and manure spreaders (integrated and organic farming) is provided. For organic farming the use spreaders for organic fertilizers (manure or slurry) is provided.

For crops protection, pesticides that are used in conventional and integrated production (in the paper is valued only direct energy or energy for powering tractors with implements - sprayers for applying pesticides) are provided. In organic production, only plant protection products, which are permitted in the mentioned production, are provided. Replacement of herbicides is done with the usage of mechanical methods for weed control (tractor implements - special harrows for removing weeds).

Wheat yields

For wheat yields SURS data (Slovenian statistic agency, average for the last ten years) are used. In the organic farming lower wheat yields are provided in comparison with conventional and integrated farm production of wheat. In conventional, integrated and organic farming mainly the same working operations with mechanization are used, the difference is in the use of machinery for fertilizing and plant protection. The fuel consumption in organic production is slightly higher because the use of the machines for spreading of manure and slurry application is intended (both type of machines have greater energy consumption, compared to the machines for spreading of mineral fertilizers).

Total energy for production and processing

The case of wheat production and processing wheat in final products is presented (bread and bakery products) for conventional, integrated and organic wheat production, for three sizes of farms (small, medium, large) and two types of soil tillage and seeding.

Total energy used in the production of wheat is added to the total energy used for processing wheat into final wheat products (bread and bakery products). The sum of the two energies is the total energy used for the final wheat products (3).

$$E_{finprod} = E_{prod} + E_{proc} \text{ (MJ)} \quad (3)$$

$E_{finprod}$ = total energy of the final food product (bread and bakery products)

E_{prod} = total energy used in wheat production

E_{proc} = total energy consumed in processing wheat grain into final product

$$E_{proc} = E_{cle} + E_{mf} + E_{fc} + E_{it} + E_{bp} \quad (4)$$

E_{proc} = total energy used in processing wheat grain into final products (MJ)

E_{cle} = energy for cleaning the wheat grain

E_{mf} = energy for milling wheat grain in flour

E_{fc} = energy for flour cleaning

E_{it} = energy for internal transport of flour

E_{bp} = energy for baking bread or other bakery products

After completion of milling wheat grain into flour, temporary storage and transport flour to bakery for processing it into final bakery products follows.

RESULTS AND DISCUSSION

Carbon footprint of agricultural crops production and its processing present the basics for the estimation of the carbon footprint of final food products (bakery products, vegetable oils, animal food, etc.). The calculation of the carbon footprint for wheat final product is based on a calculation of the total greenhouse gas emissions – GHG, resulting from the production of crops (in paper is presented case of wheat) on a defined field area, since the start of production until harvest, storage and submission to the final consumer or producer of final products. As the basic unit for calculating GHG emissions from production area of 1 ha of arable land was selected. The direct energy used (fossil fuel, electricity and other energy) for 1 ha of arable land is determined and the amount of the annual crops yield on it for production of crops and processing it in final products.

In the paper a method for calculation of carbon footprint of bakery products (bread and other bakery products) for different farm sizes (small, medium, large) for the production of wheat and for three production types (conventional, integrated and organic) is presented. Carbon footprint includes all greenhouse gases in the production of wheat and its processing into finished wheat products (bread and bakery products).

Emissions of GHG are expressed in kg CO₂ eq. kg⁻¹ of the final wheat product (emissions from the production of wheat are added to emissions from processing wheat in the bread and bakery products) and presented in table 1.

We estimated that carbon footprint of final wheat products (bread and bakery products) expressed in kg CO₂ eq. kg⁻¹ declining with the size of the farm, the method of the secondary soil tillage and type of sowing. The lowest carbon footprint is for final wheat products (bread and bakery products) from conventional production, followed by integrated and organic production on family farms.

Table 1. Carbon footprint of final wheat products

	Emissions of CO ₂ (kg eq. kg ⁻¹)								
	Seeding in soil tilled in primary tillage with ploughs and secondary tillage with rotary tillers			Seeding in soil tilled in primary tillage with ploughs and secondary tillage with cultivators			Direct seeding in soil		
	Small farm	Medium farm	Large farm	Small farm	Medium farm	Large farm	Small farm	Medium farm	Large farm
Conventional wheat production on farm	0,131	0,128	0,125	0,129	0,127	0,124	0,119	0,117	0,115
Integrated wheat production on farm	0,148	0,144	0,141	0,147	0,143	0,14	0,136	0,133	0,131
Organic wheat production on farm	0,201	0,195	0,189	0,198	0,192	0,186	0,179	0,175	0,171
Final products from conventional wheat production (sum of CO ₂ emissions from production and processing in bread and bakery products)	1,307	1,301	1,295	1,303	1,298	1,293	1,283	1,279	1,275
Final products from integrated wheat production (sum of CO ₂ emissions from production and processing in bread and bakery products)	1,341	1,333	1,327	1,339	1,331	1,324	1,317	1,311	1,307
Final products from conventional wheat production (sum of CO ₂ emissions in production and processing in bread and bakery products)	1,447	1,434	1,422	1,441	1,429	1,417	1,403	1,395	1,387

CONCLUSIONS

Analysis of carbon footprint of final wheat products (bread and bakery products) was made. Carbon footprint of final wheat products (bread and bakery products), expressed as carbon dioxide equivalent ($\text{kg CO}_2 \text{ eq. kg}^{-1}$) is determined as a sum of Green House Gases emissions (GHG) from wheat production on different sizes of family farms with different production methods (conventional, integrated and organic) and GHG emissions of wheat processing in final products (bread and bakery products). Carbon footprint ($\text{kg CO}_2 \text{ eq. kg}^{-1}$) of final wheat products includes emissions of GHG from the crop production (emissions from primary energy consumption, fertilizers use, etc.), internal and external transport, drying, storage and wheat processing in bread and bakery products.

Carbon footprint of final food products includes emissions of GHG from the crop production (emissions from primary energy consumption, fertilizer use, etc.), internal and external transport, drying, storage and crops processing in final products. Total emissions of $\text{kg CO}_2 \text{ eq. kg}^{-1}$ of final wheat products are presented as a sum of all emissions from wheat production (with included internal transport, drying and storage) and a sum of emissions of wheat processing in final products (bread and bakery products). We found that total emissions of $\text{kg CO}_2 \text{ eq. kg}^{-1}$ of final wheat products (bread and bakery products) depend on the type of production (conventional, integrated and organic). Total emissions $\text{kg CO}_2 \text{ eq. kg}^{-1}$ of final wheat products from the agricultural production of wheat and processing of it into bakery products are the lowest in conventional production, followed by integrated and highest in organic production (emissions from wheat production are added emissions from processing wheat in bread and bakery products). Results showed that total emissions $\text{kg CO}_2 \text{ eq. kg}^{-1}$ of final wheat products like bread and bakery products are also declining with the farm size. Estimated carbon footprint of agricultural final wheat products will enable optimization of different working operations with farm machines and in processing wheat, for more economical production and lowering carbon footprint of final agricultural products from family farms in future.

ACKNOWLEDGEMENTS

The authors would like to thank the Slovenian Research Agency (ARRS) and the Slovenian Ministry of Agriculture, Forestry and Food (MKGP) for funding the targeted research project "The environmental footprint of agriculture and food industry and technological measures for the reduction thereof in the future".

REFERENCES

- Al-Mansour, F. and Jecic, V. (2016). A model calculation of carbon footprint of agricultural products: The case of Slovenia, *Energy* 1 – 9, www.elsevier.com/locate/energy
- Beckman, J., Borchers, A., Carol Jones, A. (2013). Agriculture's Supply and Demand for Energy and Energy Products, Economic Research Service, Economic Information Bulletin, number 112, USDA, 9
- Dalgaard, T., Halberg, N., Porter, J.R. (2001). A model for fossil energy use in Danish agriculture used to compare organic and conventional farming, *Agriculture, Ecosystems and Environment* 87, Elsevier, p. 51 – 65,
- ESRL–Earth System Research Laboratory. (2017). Global Monitoring Division, Mauna Loa Observatory (MLO), Hawaii, USA

- Guidelines to Defra/DECC's GHG Conversion Factors for Company Reporting. (2012). AEA for the Department of Energy and Climate Change (DECC) and the Department for Environment, Food and Rural Affairs (Defra)
- Handler, F. and Nadlinger, M. (2012). Trainer handbook, D 3.8 Strategies for saving fuel with tractors, EU project Intelligent Energy Europe, Efficient 20, IEE/09/764/SI2.558250
- IPCC - Summary for Policymakers. In: *Climate Change 2007: The Physical Science Basis*. (2007). Contribution of Working Group I to the Fourth Assessment Report of the Intergovernmental Panel on Climate Change [Solomon, S., D. Qin, M. Manning, Z. Chen, M. Marquis, K.B. Averyt, M. Tignor and H.L. Miller (eds.)]. Cambridge University Press, Cambridge, United Kingdom and New York, NY, USA
- Jejcic, V. and Al-Mansour, F. (2014). Carbon footprint of conventional and organic crop production, Actual Tasks on Agricultural Engineering: proceedings of the 42nd International Symposium on Agricultural Engineering, Opatija, Croatia, 25-28th February 2014
- Jokiniemi, T., Rossner, H., Ahokas, J. (2012). Simple and cost effective method for fuel consumption measurements of agricultural machinery, Agronomy Research, Biosystem Engineering Special Issue 1, 97



THE EFFECT OF DRIP IRRIGATION ON POTATO YIELD AND QUALITY

Jaroslav ČEPL^{1*}, Pavel KASAL¹, Milan ČÍŽEK¹, Andrea SVOBODOVA¹,
Václav MAYER², Daniel VEJCHAR²

¹ Potato Research Institute, Dobrovskeho 2366, Havlickuv Brod, Czech Republic

² Výzkumný ústav zemědělské techniky Praha, Drnovská, Praha 6 – Ruzyně, Czech republic

*E-mail of corresponding author cepl@vubhb.cz

SUMMARY

The aim of this research was verification of drip irrigation effect on potatoes under conditions of higher regions in the Czech Republic. Potato Research Institute in Havlíčkův Brod realized a project directed to evaluation of new technological procedures for effective water management under drought conditions between 2016 and 2017. Growing technology using drip irrigation combined with fertigation was verified. After the planting irrigation pipes were put under the soil surface on the ridge top. Two cultivars differing in vegetation duration were used for planting – early cultivar Monika and medium-early cultivar Jolana. Eight variants of irrigation combined with N fertilization were established. A technique for irrigation management was determined based on soil conditions. Nitrogen fertilization during season was done in two variants: 120 kg N ha⁻¹ prior to planting and 60 kg N ha⁻¹ at planting + 60 kg N ha⁻¹ in four irrigation rates (15 kg N ha⁻¹ for each). In the trials an effect of irrigation on all studied factors was detected. Potato yield was significantly increased in variants with irrigation compared to non-irrigated variants. There were no differences found between full and split N rate application. Drip irrigation increased volumetric soil moisture on optimal level for potato plant growth. A device was constructed for burying drip pipes under soil surface on the ridge top, which could be also used for pipe extraction after haulm desiccation before potato harvest.

Key words: drought, climatic changes, potato, drip irrigation, yield, fertigation, cultivar,

INTRODUCTION

Weather conditions have the highest impact on potato production size (Levy and Coleman, 2014). In recent years, weather conditions have been characterized by fluctuations above the long-term normal. In higher regions of the Czech Republic, where the potato

production is the highest, temperatures exceed the long-term normal and precipitation is slightly below average and has uneven distribution. In decisive stages of growing season precipitation does not ensure optimum for potato growth and development. This could be solved by irrigation, which has been necessary for early potatoes in drier regions of the Czech Republic with altitudes below 100 m using surface spraying. However, the decisive part of potato production is located in higher regions with altitudes around 400 m, where water deficit is becomes a limiting factor under climate change. Potatoes are highly sensitive to water stress, especially in early and medium developmental stages, when water shortage results in yield reduction and potato quality impairing (Wohleb et al. 2014). On contrary, toward the end of the growing season consequences of drought are not so significant (Lynch et al. 1995). Harris (1992) defines a linear relation between potato yield and precipitation during growing season, when potato yield was 140 kg ha⁻¹ increased with every mm of precipitation. Now, it is important to solve water supply also in higher potato production regions of the Czech Republic.

More effective irrigation technique than surface spray, which has limitations and shortages, is the basic measure (Shock, et al. 2013). Drip irrigation has been seen as very efficient system and has been widely used especially in Israel, where due to this type of irrigation the value of products grown by local farmers has been increased for 1600 % in 65 years (Tal, 2016). Drip irrigation has many advantages, there are no effects of unfavourable weather, such as strong wind or high temperature causing rapid soil drying, and this technique enables common application with fertilizers close to the plants (Zhou et al., 2015).

MATERIALS AND METHODS

The trial was established in 2016 and 2017 on the fields of Potato Research Station Potato of Research Institute Havlíčkův Brod located at altitude of 465 m. The soil type was cambisol, pseudogley and medium sandy loam. Two potato cultivars (early 'Monika' and medium-early 'Jolana' were planted at spacing of 750 x 290 mm. Planting dates were 26.4. in year 2016 and 10.5. in 2017). Eight irrigation variants were established in four replications and for each variety combined with N fertilization (Tab.1). Trial plot size was 20.9 m² (2.25 m x 9.3 m) with 96 plants based on randomized complete block system.

For subsurface drip irrigation STREAMLINE 16060 pipes were used, with distance between drippers 500 mm and performance of 1.05 l ha⁻¹ (i. e. with parameters 2.79 l ha⁻¹m⁻² = 2.79 mm h⁻¹). Pipes were buried in the depth of 30-40 mm under the soil surface on the ridge top.

Soil moisture for irrigation rate calculation was separately measured for each irrigation variant using VIRRIB sensor. Specific moisture, with that irrigation was automatically started, is given in Tab. 1.

Irrigation rate was uniform – 10 mm. The number of irrigation rates and total water amount is given in Tab. 2. Nitrogen fertigation during growing season was done using YaraLiva Calcinit (15.5% calcium salt peter) in four irrigation rates (15 kg ha⁻¹ each) from the stage of flower-bud initiation to full flowering (phenological stage 55 – 80 based on international BBCH scale). Fertigation was done in the stage of potato crop elongation (BBCH 80). For fertigation Dosatron D3 was used, mixing the fertilizer solution with irrigation water based on the set concentration. In the non-irrigated variant with fertilization during growing season N rate was broadcasted in the same fertilizer at once on the soil surface. In time of crop flowering (BBCH 60) total crop state (Tab. 4) was evaluated on a point-scale (1-9).

During growing season (in July and August) soil samples by using soil cylinders were taken from the variants 1-4 for determination of volumetric soil moisture in the depth of 100 and 200 mm. During growing season potato crops were assessed (Tab. 5). Harvest was performed on 21.10. in 2016 and on 18.10. in 2017.

Simultaneously with field trials a device was constructed (Figure 5), able to bury pipes under the ridge surface and extract them prior to harvest, when aggregated with tractor.

Table 1. Variants of the field trial

Variant	Irrigation under volumetric soil moisture	N fertilization prior to planting (kg ha ⁻¹)	N fertigation (kg ha ⁻¹)
1	No irrigation	120	-
2	15%	120	-
3	20%	120	-
4	25%	120	-
5	No irrigation	60	60
6	15%	60	60
7	20%	60	60
8	25%	60	60

Table 2. Number of irrigation rates and total applied water amount in the years 2016 and 2017

Variant	2016 year		2017 year	
	Irrigation rates	Total water amount (mm)	Irrigation rates	Total water amount (mm)
1	0	0	0	0
2	6	55	10	96
3	10	99	14	136
4	17	163	24	243
5	0	0	0	0
6	6	55	10	96
7	10	99	14	136
8	17	163	24	243

Climatic conditions (Tab. 3) in 2016 were characterized by higher mean monthly air temperatures compared to the long-term mean. Precipitation was 64 % less during growing season compared to the long-term mean. Beginning of the growing season 2017 was characterized by markedly colder and rainy spring. In April 273.5 % of long-term precipitation was recorded. Total precipitation amounts in 2017 exceeded the limit of the long-term mean also in other months; only precipitation in August was strongly below the long-term mean. Considering temperatures, the growing season was specified as extraordinary above normal; however, high temperature fluctuations were recorded in all evaluated months.

Table 3. Weather conditions during the growing season (2016 and 2017)

Indicator	April		May		June		July		August		September	
	2016	2017	2016	2017	2016	2017	2016	2017	2016	2017	2016	2017
Monthly temperature normal (°C)	7.3		11.6		15.2		16.5		16.4		12.3	
Monthly mean temperature (°C)	7.8	6.9	13.6	14.0	17.4	18.4	18.9	18.7	17.4	19.3	16.2	11.2
Monthly precipitation normal (mm)	42.5		76.3		91.4		80.9		86.6		48.2	
Monthly precipitation amount (mm)	24.2	116.1	45.8	81.4	68.8	102.2	112.2	103.5	27.8	17.4	10.9	63.4

Statistical assessment was done using variance analysis in STATISTICA CZ programme version 10.0 MR1.

RESULTS AND DISCUSSION

Evaluations (Tab. 4) done during crop flowering (BBCH 80) indicated that total crop state expressed by 9-point scale (1 = the worst state, 9 = the best state) was dependent on tested variants. Irrigated variants tendentially showed more favourable values than non-irrigated variant, but it was completely only valid for the year 2017.

Table 4. Total crop state in BBCH 80

Year	Cultivar	Point	Variant							
			1	2	3	4	5	6	7	8
2016	Monika	1-9	8.6	8.6	9.0	9.0	8.8	8.6	9.0	9.0
	Jolana	1-9	7.4	8.2	8.6	8.4	8.8	8.2	8.0	8.6
2017	Monika	1-9	7.8	8.4	9.0	9.0	6.6	7.2	8.6	8.6
	Jolana	1-9	7.4	8.0	8.6	9.0	6.8	7.2	8.6	8.2

In 2016 potato yield (Fig. 1) of the cultivar 'Monika' increased with irrigation water rate. Under conditions of full N rate applied prior to planting (120 kg ha⁻¹) potato yield was increased by 18.9 % between non-irrigation (var. 1) and the lowest irrigation level (var. 2). In variant 3 a significant difference was 32.3 % and 49.3 % with the highest irrigation level (var. 4). At the same time, it was found that split N rate (60 kg ha⁻¹ prior to planting and 60 kg ha⁻¹ in fertigation) had no impact on potato yield. For cultivar 'Jolana' similar trends were recorded in this year. Potato yield was increased compared to non-irrigated variant 1 by 15.0 (var.2), 22.3 (var. 3) and 47.5 % (var.4) between mentioned variants and a significant difference was only determined in the variant of the highest irrigation level (var.4).

Statistically significant differences were not determined between cultivars; however, Fig. 1 shows that cultivar Monika with shorter growing duration had tendency to a better response to irrigation.

In 2017 (Fig.2) the highest differences were found between tested variants for cultivar 'Monika', a significant yield increase compared to non-irrigated variant was 57.3 medium (var. 3) and 59.3 % high irrigation (var. 4). The medium-early cultivar 'Jolana' did not respond so intensively; a yield increase compared to non-irrigated variant 1 was only 11.9 (var.2), 22.5 (var.3) and 25.86 % (var.4). It was probably due to the higher precipitation rate in 2017 and the higher available soil moisture for later-maturing variety. Similarly as in 2016 it was found that split N rate (60 kg ha⁻¹ prior to planting and 60 kg ha⁻¹ in fertigation) had no impact on potato yield. In this year, statistically significant differences were also not recorded between cultivars.

Highly significant differences were found for cultivars between years (Figs. 3 - 4). The year 2016 had statistically significantly higher potato yield compared to 2017 42.2% for Monika and 39.1 % for Jolana. Lower potato yield in 2017 was probably caused by late planting date, since high precipitation in April 2017 made early planting impossible.

It can be concluded that irrigations alone were highly positive as regard as potato yields; however, common application of N with drip irrigation was not positive (Figs. 1-2). Variants with split N application did not differ from potato yield level of variants with full N rate application prior to planting. Most data in literature show usefulness of N fertigation. Rolbiecki et al. (2015) found that drip irrigation significantly increased the marketable potato yield from 17.4 to 36.3 t ha⁻¹ (109 %), the weight of a tuber and the number of tubers per plant. Nitrogen fertigation through drip system increased potato yield by 5.9 t ha⁻¹ (25 %). Ghiyal et al. (2017) found that when fertigation applied on every 3rd day with the application of nitrogen 120 kg ha⁻¹ was found significantly superior to all other tested combinations (the experiment comprising of four levels of nitrogen, i.e., 90,120, 150 and 180 kg ha⁻¹ and three fertigation frequencies, i.e., every 3rd day, every 6th day and every 9th day). Probably it would be more effective to split N rate into all fertigation rates in lower amounts than 4 x 15 kg N ha⁻¹. Zhou et al. (2015) followed plant needs, when based on the model of nutrient state in drip irrigation they always supplied 20 kg N ha⁻¹. In total, the authors supplied 100 kg N ha⁻¹ compared to usual rate of 120 kg ha⁻¹; however, yield results were not significant. Similarly, Li and Liu (2017) found that potato yield and commodity rate of fertigation treatments (drip irrigation and integration of water and fertilizer) was significantly higher than the other treatments: non-treated control (C), sprinkler irrigation and fertilizer split application (SI), drip irrigation and fertilizer split application (DI). The yield was 49.07, 27.94 and 14.91% increased compared to C, SI and DI, commodity rate was 19.41, 10.36 and 4.72 % increased compared to C, SI and DI.

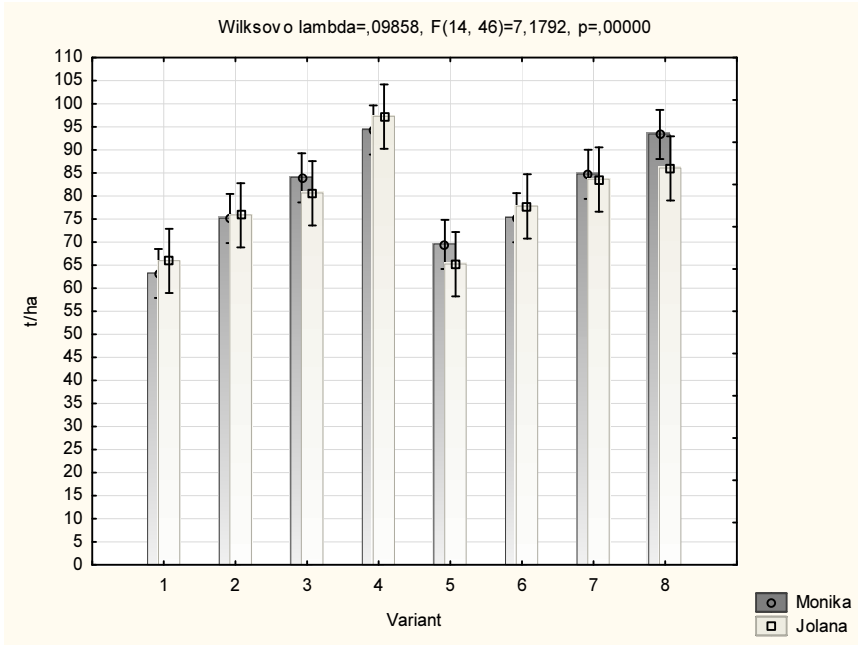


Figure 1. The effect of variants on potato yield in 2016

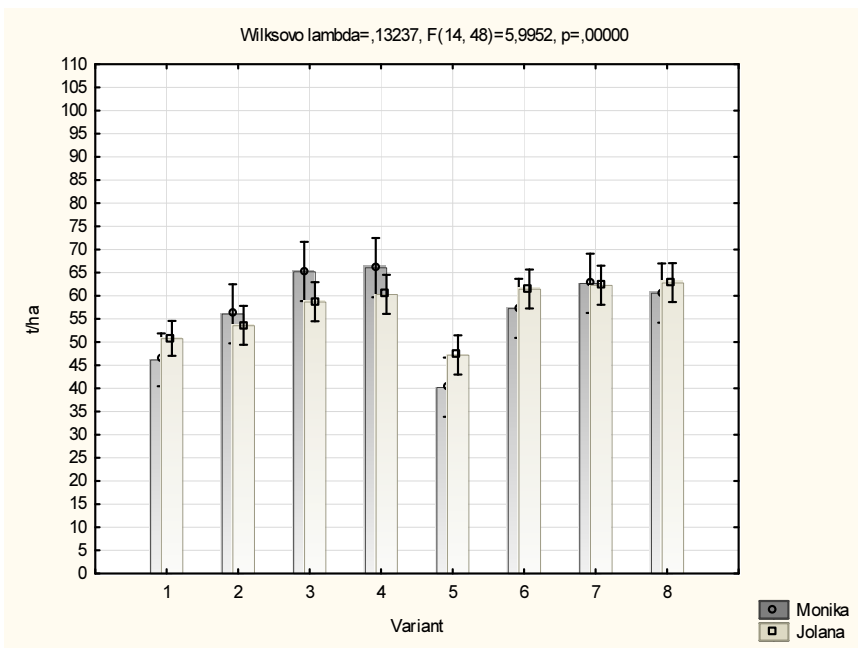


Figure 2. The effect of variants on potato yield in 2017

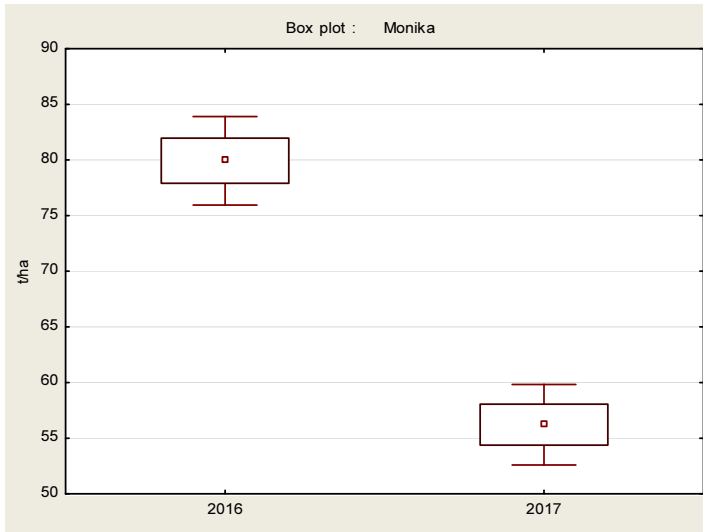


Figure 3. The effect of variants on potato yield of Monika cultivar in 2016 - 2017

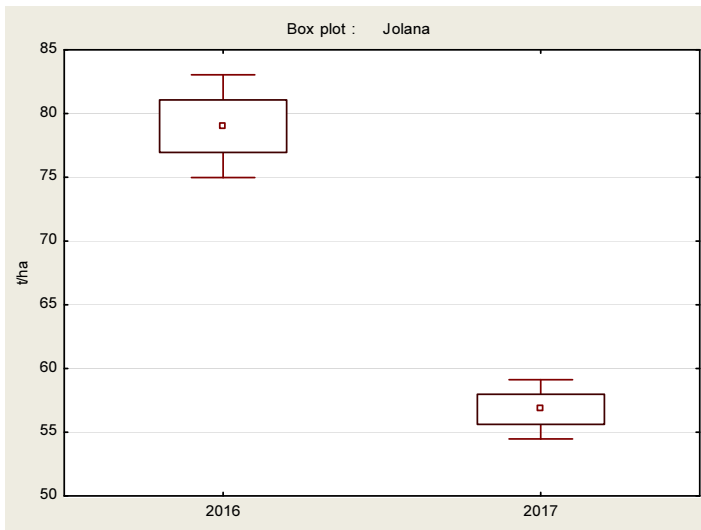


Figure 4. The effect of variants on potato yield of Jolana cultivar in 2016 - 2017

Volumetric soil moisture was measured twice during growing season (July and August), in two soil depths (100 and 200 mm). Results are given in Table 4.

Table 4. Volumetric soil moisture (%) of studied variants

Var.	2016 year				2017 year			
	July		August		July		August	
	Soil depth, mm							
	100	200	100	200	100	200	100	200
1	18.51	20.98	24.83	19.88	16.51	22.86	21.36	22.22
2	21.29	21.78	19.83	21.75	19.11	20.66	22.42	25.56
3	22.82	25.66	21.61	24.91	20.13	21.25	26.02	29.01
4	29.44	30.09	23.85	28.17	29.54	32.53	25.41	28.76

The results of volumetric soil moisture measurements show course of soil moisture and correspond to drip irrigation rates. Higher moisture was recorded for deeper soil profile near potato plant root system. In the variant 1 it is apparent that soil moisture was close to critical values of wilting point. It explains a highly significant effect of irrigation on potato yield in variants, where irrigation increased volumetric soil moisture so that water was not limiting factor for yield formation.

In addition to study of the effect of variants on potato yield it was necessary to design and verify a device, which would bury pipes under the soil surface on the ridge top, for semi-pilot and future operational conditions (Fig. 5).

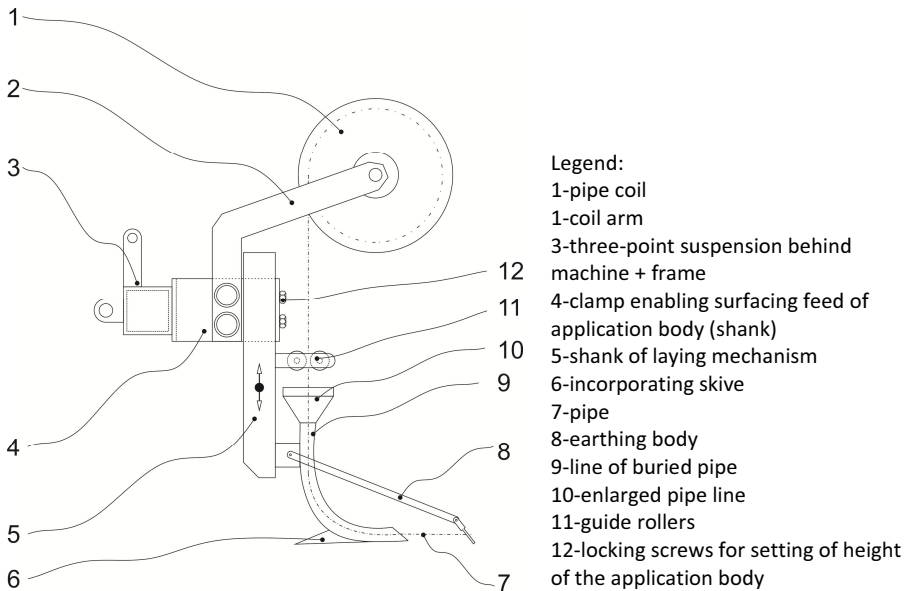


Figure 5. A device for burying irrigation pipes in wide-row crops (e.g. potatoes)

Device description

The device buries pipes (1, 7) under the soil surface for potato drip irrigation. It is intend for connection behind machine using three-point suspension (3) and/or using a clamp (4) to frame. The device is fitted with an arm (2) for carry of the coil (1), a height-adjustable shank

(5) for setting of burial depth for pipe. The pipe put into soil could be earthen with a skive (6,8) of fitting shape. At first, pipe must be fit on the row beginning. Versatility of the device enables connection with planting/sowing machine. The device is planned as multifunctional one and could be also used for extraction of pipes from the soil directly prior to harvest.

CONCLUSIONS

- The positive effect of drip irrigation was confirmed, i.e., yield of two potato cultivars was significantly increased in both studied years
- Any difference was not determined between full application rate and split N rate
- Drip irrigation increased volumetric soil moisture to optimal level for potato plant growth
- A device was constructed for burying irrigation pipes under the soil surface on the ridge top, which could also serve for extraction of pipes prior to harvest after potato haulm desiccation

ACKNOWLEDGEMENT

The contribution was compiled under financial support of the Ministry of Agriculture of the Czech Republic in the project NAZV QJ1610020

REFERENCES

- Ghiyal, V., Bhatia, A.K., Batra, V. K., Dhawan, A. K., Chauhan, S. K., Walia, S. S., Mahdi, S. S. (2017). Nutrient uptake and tuber yield influenced by nitrogen levels and fertigation frequency in potato (*Solanum tuberosum*). *Indian Journal of Ecology* 44: 269-274
- Harris, P. (1992). *The Potato Crop: The Scientific Basis for Improvement*. Second Edition. Chapman and Hall, London.
- Levy, D., Coleman, W. K. (2014). Plant-water relations and irrigation management of potato. In: *The potato: botany, production and uses* (Navarre, R., Pavek, M. J., eds). Boston, CABI, 103-114
- Lu, Y., Liu, Y. X. (2017). Effects of different water and fertilizer management on soil enzyme activities and yield of potato. *Journal of Henan Agricultural Sci* 46: 57-60
- Lynch, D. R., Foroud, N., Kozub, G. C., Farries, B. C. (1995). The effect of moisture stress at three growth stages on the yield components of yield and processing quality of eight potato cultivars. *Am. Potato J.* 72: 375–386.
- Rolbiecki, S., Rolbiecki, R., Kuśmierk-Tomaszewska, R., Dudek, S., Żarski, J., Rzekanowski, C. (2015). Requirements and effects of drip irrigation of mid-early potato on a very light soil in moderate climate. *Fresenius Environmental Bulletin* 24: 3895-3902
- Shock, C.C., Wang F., Flock, R., Eldredge E., Pereira, A., and Klauzer, J. (2013). *Drip Irrigation Guide for Potatoes*. <https://ir.library.oregonstate.edu/downloads/kk91fk865>
- Tal, A. (2016). Rethinking the sustainability of Israel's irrigation practices in the Drylands. *Water Research*. 90: 387-394.
- Wohleb, C. H. Knowles, N. R. Pavek, M. J. (2014). Plant growth and development. In: *The potato: botany, production and uses* (Navarre, R., Pavek, M. J., eds), Boston, CABI, 64-82
- Zhou, Z.J., Andersen, M. N., Plauborg, F., Edlefsen, O. (2015). Response of potato to drip and gun irrigation systems. *CIGR Journal* 17(Special Issue): 1-9



SPINACH PRODUCTION CONDITIONS IN THE DIFFERENT TYPES OF GREENHOUSE CONSTRUCTIONS

Aleksandra DIMITRIJEVIĆ*, Brankica ŠUNDEK, Nikola MATOVIĆ,
Zoran MILEUSNIĆ, Rajko MIODRAGOVIĆ

University of Belgrade, Faculty of Agriculture, Belgrade-Serbia

*E-mail of corresponding author: saskad@agrif.bg.ac.rs

SUMMARY

Spinach is very common in the human nutrition due to its high nutritive value. It is commonly grown in the greenhouses. In region of Serbia, spinach is commonly grown in the tunnel structure greenhouses, covered with single or double PE folia without additional heating. The aim of the research was to see if different greenhouse construction types influence the microclimatic parameters in the spinach production and to see if choosing the certain greenhouse construction type can improve an overall production conditions resulting in higher spinach yield, lower energy consumption and higher energy productivity. Spinach production was tracked in the three different types of greenhouses. The round-shaped greenhouse has its base diameter of 7 m while tunnel type greenhouse was 5.5 m wide and 24 m long. Single span greenhouse was 10 m wide and 50 m long. All greenhouses were covered with PE UV IR 180 μm folia. Results show that production conditions are dependent on type of greenhouse construction. During the winter spinach production solar radiation energy losses in the tunnel structure were 29.38% while the round-shaped greenhouse was losing 19.51% of the solar radiation energy. Losses in the single-span greenhouse were 12% in the morning hours and 43% during the day.

During the day air temperatures in the greenhouses were higher. In the round-shaped and tunnel structure greenhouse this temperature difference lower than 1 $^{\circ}\text{C}$ and are not considered important for the plants. In the case of single-span greenhouse inside-outside differences were 2.52 $^{\circ}\text{C}$ up to 16.26 $^{\circ}\text{C}$.

Key words: round-shaped greenhouse, tunnel greenhouse, single-span greenhouse, spinach, production conditions.

INTRODUCTION

Spinach is very common in the human nutrition due to its high nutritive value, high level of vitamins, folic acid, potassium and antioxidants (Ernst et al., 2012). It is commonly grown in the greenhouses having the yield of 5 to 25 t ha⁻¹, depending on the production technology. According to the farmers in Serbia, growing of spinach is highly profitable. Its price does not vary much during the year. The market is huge and current production in Serbia cannot satisfy the market needs.

Spinach can be grown in the different types of semi-protected and protected production systems. Optimal growing temperature is 14-18 °C (FAO, 2004). Temperatures higher than 20 °C can have a negative effect on the plant growth. It can stand the temperatures up to -10 °C. There are no specific demands concerning the air relative humidity. Due to its cold tolerance greenhouse it is normally grown in the temperate zones, in winter, under the poor light conditions (Glenn et al., 1984). Radiation is, generally, the most important factor that controls the growth of spinach.

One of the simplest methods of spinach production is direct covering (Gimenez et al., 2002) Crop quality in this production technology is enhanced, leaves are thinner, tender and of higher marketable value. All these are achieved at a low cost.

The next step in the semi-protected and protected spinach cropping is usage of tunnel structures and single span greenhouses. Tunnel structures are temporary, relatively inexpensive structures that are heated by solar radiation. Combination of tunnel structures with the direct covering is often used (Ernst, et al. 2012) since it has a significant positive effect on day and night temperatures, when compared to the uncovered production in the tunnel structure itself. In the tunnel, spinach yield can reach 11 t/ha and when the tunnel is combined with the direct covering yield reaches 16 t/ha. Combination of tunnel structure and low tunnel can lead to the yield of 20 t/ha. All these in conditions of not heated high tunnel structure in spring production.

Research in the area of greenhouse construction and its influence on the energy consumption and energy efficiency in the tomato production, showed that the farmers need to use greenhouses with the higher production surfaces and higher specific volume in order to have optimal production conditions and better overall efficiency (Hatirli et al., 2006, Dimitrijevic et al., 2010). Research on the lettuce winter production (Djevic and Dimitrijevic, 2009; Dimitrijevic et al., 2011) showed that production surface does not have a significant influence on the overall production energy efficiency and highly sophisticated multi-span greenhouse are not economically viable in the lettuce winter production. Thus, lettuce is most often grown in the high tunnels and simple single span greenhouses.

Current economical situation in Serbia and, especially, in its rural regions urged a need of having a greenhouse construction and production technology that would be energy, ecology and economy beneficial for the producers on the small scale farms. The idea of the round-shaped greenhouse construction is not new (Hanan, 1998) but it was forgotten due to the previous mentioned reasons of having larger production surfaces. Researchers show that this type of greenhouse is energy efficient providing optimal production condition in sense of good light and temperature distribution which is very important in the winter period of year (Dimitrijevic et al., 2016).

The aim of this paper is to analyze spinach production conditions in the new round shape construction greenhouse and in the tunnel and single span greenhouse constructions in order to see if the type of construction can influence the solar energy transmittance to the greenhouse and the inside / outside temperature differences.

MATERIAL AND METHOD

Spinach production was analyzed in season 2015/16. Three different types of greenhouse constructions were used. The round-shaped greenhouse (R) has its base diameter of 7 m while tunnel type greenhouse (T) has its base of 5.5 x 24 m. Single span greenhouse (S) was 50 m long, 10 m wide and 2.4 m high. All of the greenhouses were covered with PE UV IR 180 μm folia. Spinach was seeded in the rows with the inter-row distance was 20 cm. The used seed was Sacata variety.

For production conditions in greenhouse laboratory equipment from the Department for Agricultural Engineering, Faculty of Agriculture Belgrade was used. It consists of data loggers for measuring temperature and relative humidity as well as of the set of pyranometers. Air temperature was measured in the greenhouse and outside of greenhouse. For that purposes WatchDog Data Logger Model 110 Temp 8K, $\pm 0,6^\circ \text{C}$ was used. Temperatures were measured on the 2 m height in the three different points along the greenhouses. Measuring interval was 10 minutes. Air relative humidity was also measured outside and in the greenhouses. WatchDog Data Logger Model 150 Temp/RH, $t = \pm 0,6^\circ \text{C}$ and $\text{RH} = \pm 3\%$ was used. Measuring interval was also 10 minutes. For measuring the solar radiation energy WatchDog Data Logger Model 450 – Temp, Relative Humidity was used together with the two solarimeters that have measuring range 1–1250 W m^{-2} and precision of $\pm 5\%$. Solar energy was also measured on the 2 m height and every 10 minutes.

RESULTS AND DISCUSSION

Temperature and solar radiation measurements show that they are varying depending on the greenhouse construction.

Results show that the solar radiation variations during the day are smaller in the round-shaped greenhouse if compared with the tunnel structure (Figs. 1, 2 and 3).

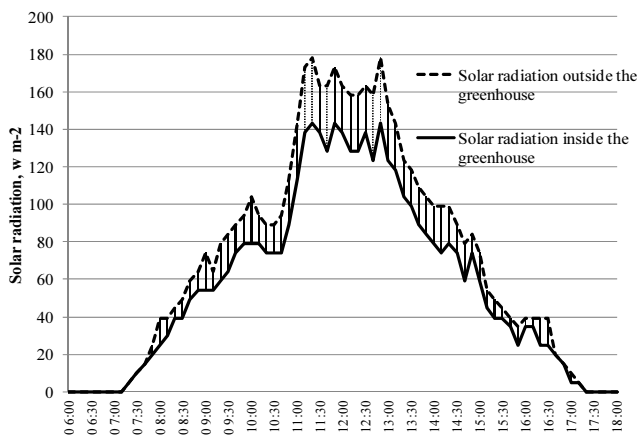


Figure 1. Solar radiation inside and outside the round type greenhouse in spinach production

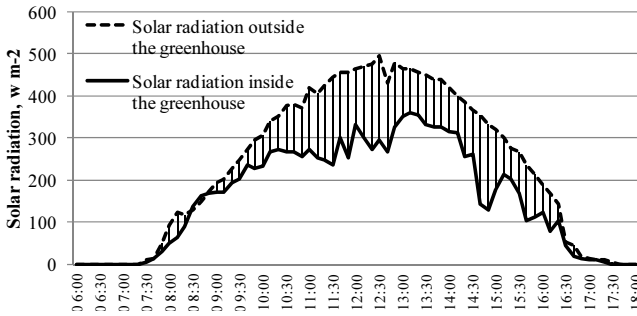


Figure 2. Solar radiation inside and outside the tunnel greenhouse in spinach production

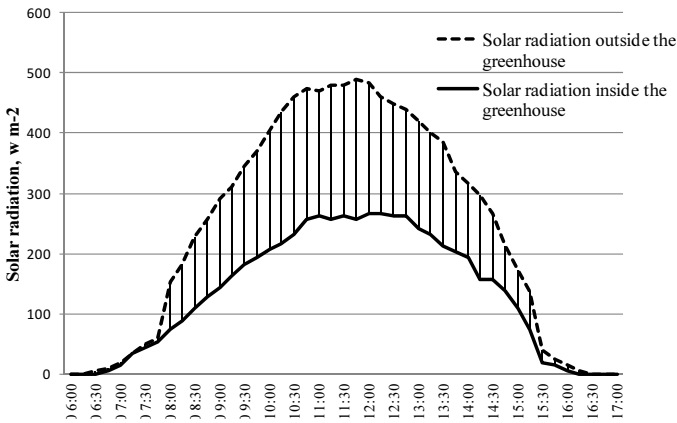


Figure 3. Solar radiation inside and outside single-span greenhouse in spinach production

It can be seen from the figures that round shape greenhouse has the better response to the solar radiation energy changes. Figure 3 shows that the response of the single span greenhouse to the solar radiation energy changes is the slowest if compared to the other two constructions. Newer the last, data obtained (Tab. 1) show that the in the early morning hours the best transmittance properties were observed for the single span greenhouse that had only 13.3% of the energy losses. The highest losses were observed in the case of tunnel structure greenhouse.

As for the midday hours, the best energy transmittance properties were observed in the case of the round shape greenhouse. The highest losses, 42.27% were observed in the case of single span greenhouse. If the average daily values are calculated, the lowest energy losses were observed for the round shape greenhouse (24.44%) and the highest for the tunnel shape greenhouse (28.51%).

Table 1. Solar radiation inside and outside the greenhouses

	Time of the day					
	7h			13h		
	R	T	S	R	T	S
Outside solar radiation, $W m^{-2}$	0.59	27.05	15.41	415.13	252.82	370.75
Inside solar radiation, $W m^{-2}$	0.46	19.89	13.63	303.68	175.60	214.04
Outside / inside difference	0.13	7.16	1.78	111.45	77.22	156.71
Losses, %	22.03	26.47	13.30	26.85	30.54	42.27

Temperature measurements during the winter production season show that there are differences in the production conditions in different greenhouse structures (Figs. 4, 5 and 6). During the winter spinach production temperatures inside round shape and tunnel structure greenhouse were lower compared to the outside temperatures during the night and in the early morning hours. In the single span greenhouse temperatures inside the greenhouse were always higher compared to the temperatures outside.

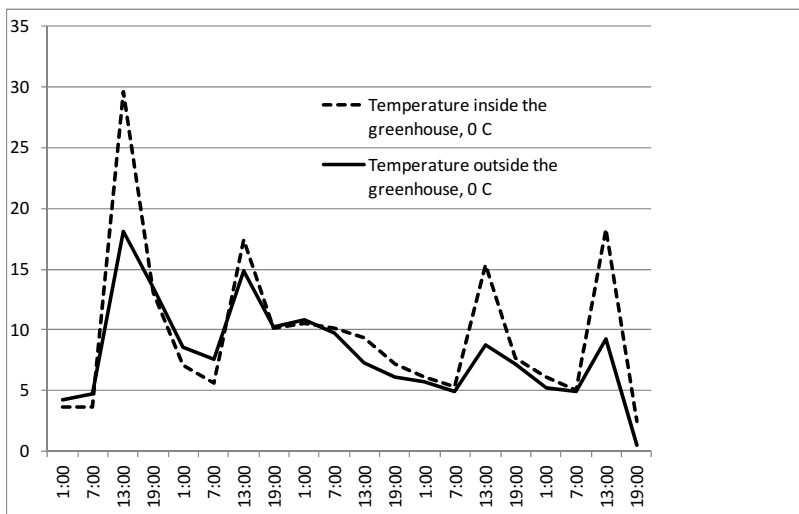


Figure 4. Air temperatures inside and outside the round type greenhouse in spinach production

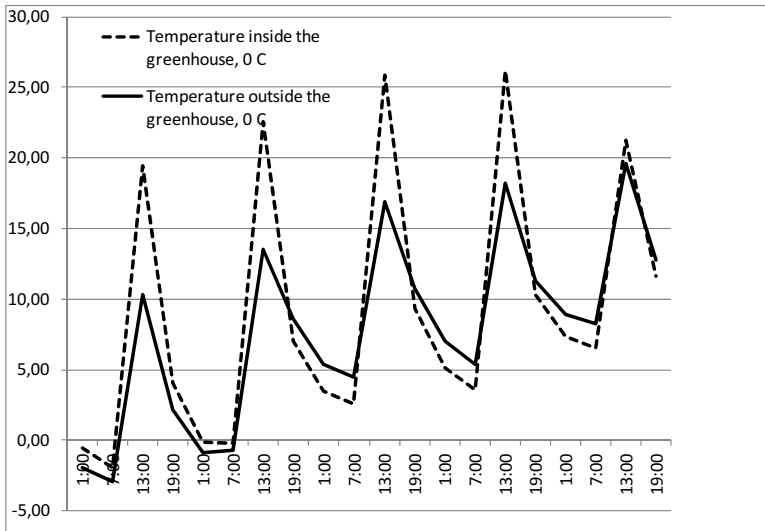


Figure 5. Air temperatures inside and outside tunnel type greenhouse in spinach production

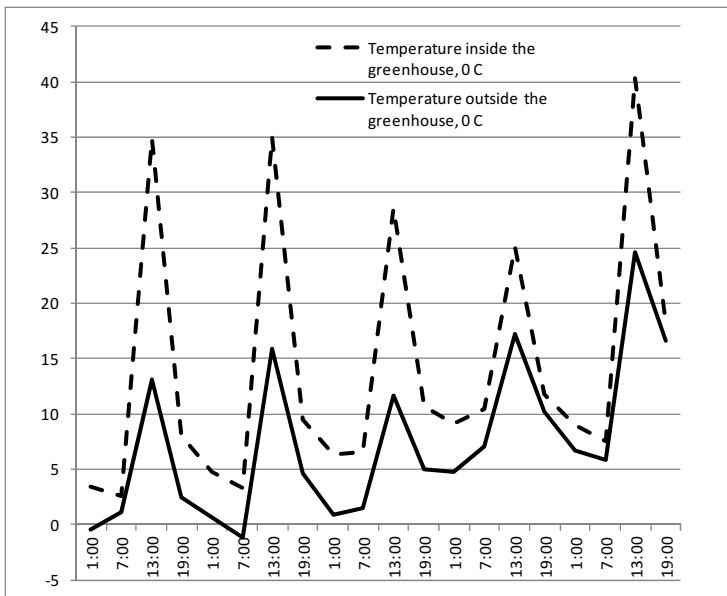


Figure 6. Air temperatures inside and outside single-span greenhouse in spinach production, °C

In the round-shaped construction greenhouse temperature difference between outside and inside air was 0.2 °C while in the tunnel greenhouse this difference was 0.6 °C. During the day air temperatures in the greenhouses were higher. In the round-shaped greenhouse this

temperature difference was 6.5 °C while in the tunnel structure the difference was 7.35 °C. These differences are lower than 1 °C and are not considered to be important for the plants. Statistical analysis shows that temperatures inside the single span greenhouse were significantly higher in the midday and night hours (Tab. 2).

Table 2. Statistical analysis

Parameter	Time											
	7 h			13 h			19 h			1h		
	R	T	S	R	T	S	R	T	S	R	T	S
Absolute difference	0.45	0.77	3.22	6.35	7.35	16.26	0.6	0.66	3.84	0.2	0.63	4.01
Standard error	1.48	0.99	2.12	3.88	1.70	3.50	2.79	1.7	3.11	1.65	0.59	1.7
t statistics	0.31	0.54	1.52	1.64	0.97	4.56**	0.22	0.25	1.23	0.12	0.02	2.26*

* $t_{0.05, 8} = 1.86$; ** $t_{0.01, 8} = 2.89$

Regarding the temperature inside the different types of greenhouse structure, it can be seen that single span greenhouse has the most beneficial production conditions. Temperatures inside the greenhouse are all day higher compared to the outside conditions and in the most critical period, during the night, this inside – outside difference stays significant. The reason for this can be higher specific volume of the single span greenhouse compared to the other two constructions.

CONCLUSIONS

Greenhouse production is one of the most intensive branches in agriculture. It is intensive in sense of high yields, year-around production and high energy consumption. Rural areas are in a very difficult situation in sense of economy and energy. The aim of this paper was to show the possibility of using simple and cost effective greenhouse construction that can ensure energy and economy sustainability of the small-scale family farms in the rural parts of Serbia.

The proposed round-shaped greenhouse construction showed good results regarding the solar energy transmittance inside the greenhouse in the winter production of spinach. Concerning the temperature inside / outside difference, single span can be suggested as most beneficial structure. Problem with the single span greenhouse lies in the poor light conditions and lower transmittance of the solar energy.

Further research will be concentrated on energy analysis of different vegetables production in order to have a better picture of energy, ecology and economy feasibility of this kind of greenhouse construction in the vegetable production on the small-scale family farms.

ACKNOWLEDGEMENT

The authors wish to thank to the Ministry of education, science and technological development, Republic of Serbia for financing the TR 31051 Project.

REFERENCES

- Dimitrijević, A., Blažin, S., Blažin, D., Šundek, B. (2016). Opportunities for the sustainable greenhouse production on small-scale family farms in Serbia In: Kovačev I. (ed) Proc 44th International Symposium on Agricultural Engineering, Vol. 44, Opatija, Croatia, pp 381-386.
- Dimitrijević, A., Đević, M., Bajkin, A., Ponjičan, O., Barać, S. (2011). Energy efficiency of the lettuce greenhouse production. In: Košutić S. (ed) Proc 39th International Symposium on Agricultural Engineering, Vol. 39, Opatija, Croatia, pp 463-472.
- Đević, M. and Dimitrijević, A. (2009). Energy consumption for different greenhouse construction. *Energy*, 34 (9): 1325-1331.
- Đević M. and Dimitrijević A. (2010). Energy efficiency of the open field and greenhouse tomato production. In: Košutić S. (ed) Proc 38th International Symposium on Agricultural Engineering, Vol. 38, Opatija, Croatia, pp 245-253.
- Ernst, T., Drost, D., Black, B. (2012). High tunnel winter spinach production. Utah State University Cooperative Extension.
- FAO (2004). Salata, blitva, spanać (in Serbian). Food and agriculture organization of the United Nations. <http://www.elestra.rs/wp-content/uploads/2013/12/brosura-salata-spanacblitva.pdf>
- Gimenez, C., Otto, R. F., Castilla, N. (2002). Productivity of leaf and root vegetable crops under direct cover. *Scientia Horticulturae*, 94: 1-11.
- Hanan, J.J. (1998). Greenhouses – Advanced Technology for Protected Horticulture, CRC Press, Boca Raton, USA
- Hatirli, S.A., Ozkan, B., Fert, C. (2006). Energy inputs and crop yield relationship in greenhouse tomato production, *Ren Energy*, 31: 427-438.



REAL-TIME MEASUREMENT OF SOLAR ULTRAVIOLET EXPOSURE IN A PLASTIC GREENHOUSE

George IPATE, Gabriel-Alexandru CONSTANTIN*, Gheorghe VOICU,
Gabriel MUSUROI, Mariana-Gabriela MUNTEANU, Elena-Madalina STEFAN

University Politehnica of Bucharest, Faculty of Biotechnical Systems Engineering

*E-mail of corresponding author: constantin.gabriel.alex@gmail.com

SUMMARY

Our study presents a system and methods for accurate real-time measurement of solar ultraviolet (UV) intensity in a plastic greenhouse to provide information to agricultural workers on how to protect themselves from the potentially harmful effects of exposure to ultraviolet radiation. The system was designed based on the Arduino Nano V3 board platform, an optical sensor VEML 6070 and open source software MIT App Inventor to develop the Android application. The tests have shown that the measurements made with the chosen sensor are in line with the daily average UV levels provided to the public, in the form of the UV index, by the National Weather Service Centres.

Keywords: UV levels, Arduino, agricultural workers, greenhouse

INTRODUCTION

Given the increase in solar activity in recent years and the reduction of the ozone layer, the health risks resulting from exposure to ultraviolet radiation in carrying out the current tasks of agricultural workers in general may become greater than any possible benefit that they might have.

Chang et al. (2010) using UV-B exposure measured by the United State Department of Agriculture ground-based network found strong positive correlations between the skin cancer and the UV exposure. Vecchia et al. (2007) in their study shows that the solar UVR to which an individual is exposed depends upon the ambient solar UVR, the fraction of ambient exposure received on different anatomical sites and behaviour and the duration spent outdoors. Diffey (1991) in his research concluded that the observed biological effects in man due to exposure from solar UVR are limited to the skin and to the eyes because of the low penetrating properties of UVR in human tissues. Makgabutlane and Wright (2015) conducted a case study in which levels of solar UVR were measured at a site where an

outdoor worker was working. They concluded that in South Africa, outdoor workers may be potentially exposed to up to 84.11% of the total solar UVR that reaches the ground. The effects of UV radiation on the human body depend on several factors, including: the geographical conditions of the place where a person is; the type of skin of the person (skin phenotypes); the intensity of UV radiation at the Earth's surface (UV index); interaction of UV radiation with various drugs and cosmetics (Belkin et al., 1994).

Considering the above, it is obvious that a constant monitoring of the intensity of UV radiation to which agricultural workers in greenhouses are exposed is necessary. Measurement of the level of UV radiation in different locations of the greenhouse should be done with measuring instruments that will be checked and calibrated at regular intervals.

The main objective of this paper is to develop a system based on the Arduino and Android application to monitor the levels of UV radiation in the greenhouse for preventing the exposure to UV radiation of agricultural workers. The system based on the analysis of existing solutions can collect and submit data in a Google Cloud Platform web application called Fusion Table, which enables agronomic managers to take the most appropriate measures to protect employees' health. Also, the implementation of the concept of precision agriculture at a broad level, thus implies a more advanced research on products that allow them to know exactly what is happening on the farm at any time, as well as investing in innovative technologies.

MATERIALS AND METHODS

Solar radiation includes infrared radiation, light radiation and ultraviolet radiation (Fig.1). Although UV radiation represents only 5% of the solar radiation reaching the Earth's surface, it has a biologically significant role because it has the highest energy in the optical spectrum. Depending on the biological effects they determine, the UV spectrum is divided in 3 spectral bands as follows: UV C 100-280 nm, UV B 280-315 nm and UV A 315-400 nm (Diffey, 1991).

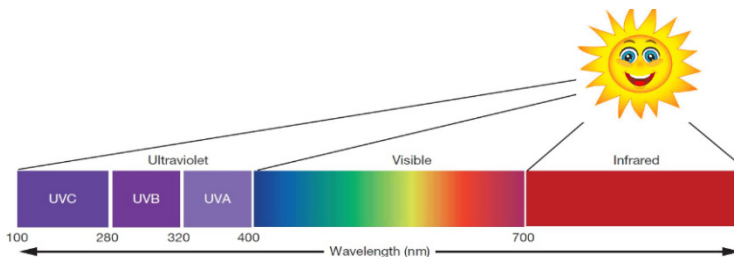


Figure 1. Representation of Light Spectrum

In the real world, the terms intensity and irradiance are sometimes used interchangeably, but from a scientific standpoint irradiance is the UV arriving at a surface based on specified area (Ipate, 2016). UV index is a unit of measure of UV levels relevant to the effects on human skin and it serves to alert people about the potential detrimental effects on health from solar UV exposure. The UV index is defined as erythemally (CIE) weighted irradiance, expressed in the unit's W/m^2 , and calculation is quite complex. McKinlay and Diffey (1987) proposed the following relationship for calculating the UV index:

$$UVI = \frac{1}{25 \frac{mW}{m^2}} \int_{286.5 \text{ nm}}^{400 \text{ nm}} I(\lambda) \cdot w(\lambda) \cdot d(\lambda) \tag{1}$$

where the weighting function for erythema is given as:

$$w(\lambda) = \begin{cases} 1 & 250 < \lambda \leq 298 \\ 10^{0.094 \cdot (298 - \lambda)} & 298 < \lambda \leq 328 \\ 10^{0.015 \cdot (139 - \lambda)} & 328 < \lambda \leq 400 \\ 0 & 400 < \lambda \end{cases} \tag{2}$$

The proposed monitoring system shown in Fig. 2 has, as the main component of the hardware section, the Arduino NanoV3 board, a developer board based on the ATmega328 microcontroller. The small and friendly board can be programmed flexibly to provide specific features regarding requirement function in the intelligent system, such as data handling, data transfer and memory card storage.

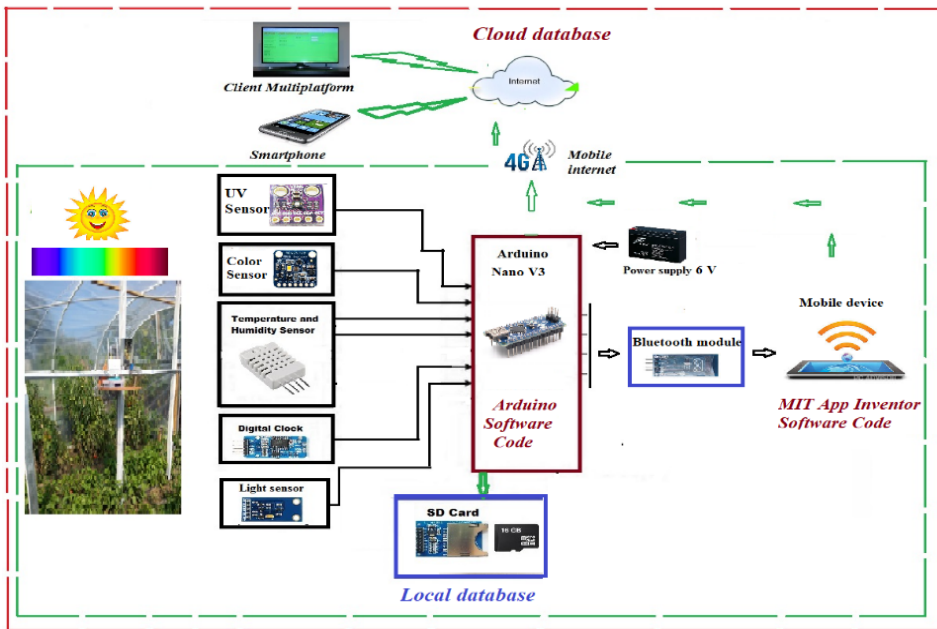


Figure 2. System architecture of UVR monitoring

The UV Light Sensor VEML6070 UV manufactured by Vishay Semiconductors was used to measure UV light intensity. This is an advanced ultraviolet (UVA) light sensor designed with a CMOS process and featuring an I2C protocol interface, who shows linear sensitivity to solar UV light (Scharr, 2015). The VEML6070 incorporates a photodiode, amplifiers, and analog/digital circuits into a single chip as is shown in Fig. 3.

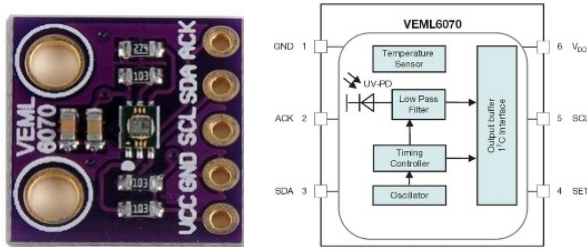


Figure 3. UV Light Sensor VEML6070

The Internet monitoring application of the UV solar radiation intensity includes several computing programs like Arduino and MIT App inventor software. The data acquisition program, written in the Arduino environment, is continually working, reading and storing parameter values in the local database at intervals of 1 minute until eventually stopping this operator software component. Also, the program contains instructions for transmitting data through a Bluetooth device to a phone, tablet, or other peripheral with Android operating system.

The MIT App inventor software is used to develop the Android apps. The data is saved and stored online using the mobile application designed to transmit wireless data to the database via the Internet. The application compares the measured values with the UV effective UV data presented in table 1, calculates the UV index on a scale from 0 to 12 and displays warning messages about the associated risk level.

Table 1. Maximum permissible exposure time for effective irradiance

Ee (uW/cm2)	UVI	UV-INDEX
≥ 8217	≥ 11	Extreme
5977 to 8216	8 to 10	Very High
4483 to 5976	6, 7	High
2241 to 4482	3 to 5	Moderate
0 to 2240	0 to 2	Low

To implement and test this sample code we use a Xiaomi RedmiNote2 phablet (2.1GHz Octa-core CPU, 2GB RAM and 32GB Internal memory) running Android 5.0.

An experimental application provided by Google was used to store, query and view online data tables. Google Fusion Tables is a free service for sharing and visualizing data online. This web application allows data loading, data sharing, and tag data for collaborators, merge data from multiple tables, and create views, such as charts and maps.

The experimental work has been carried in the greenhouse (30x6x3 m) with polyethylene film roof, available in UPB campus, Depart. of Biotechnical Systems to monitor the environmental climate conditions. The thickness of the polyethylene film for the roof is 170 microns (0.17mm), triple layer (3 layers), with UV, EVA, IR, AB additives.

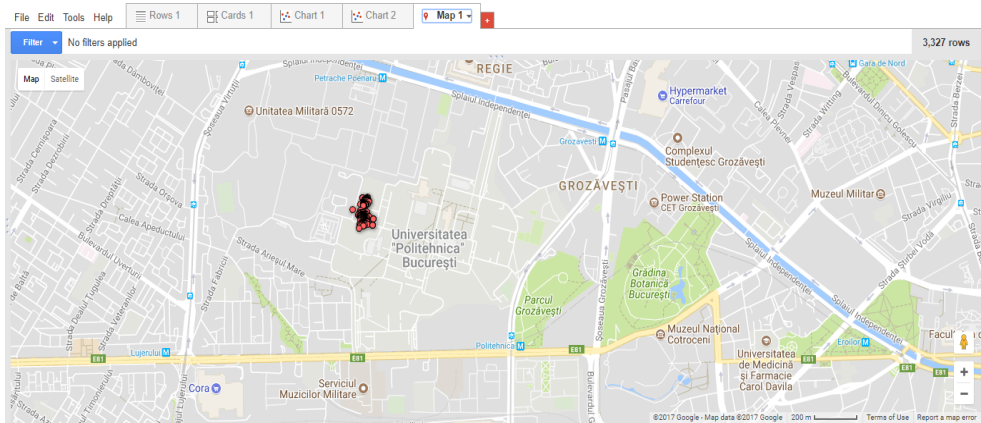


Figure 4. Google map of the measurement location

Measurements of UV solar radiation for the case study were made at a distance of 35 cm from the ground in the conditions in which, in order to ensure a natural ventilation corresponding to the plants, the side walls were rolled. Fusion tables automatically detect location data in a table and display a tab called "Map" as shown in Figure 4. The location of the experimental measurements is determined in the android application using the "LocationSensor" component that can determine the latitude and longitude of the mobile device. For example, GPS coordinates are entered when GPS is turned on in mobile devices settings and a signal is available. If a GPS signal is not available, triangulation methods using cell towers and known wireless networks are used to estimate position.

RESULTS AND DISCUSSION

The virtual monitoring panel can be displayed on any computer connected to internet, indicating the address of the web page: <https://fusiontables.google.com/DataSource?docid=1I4QjFGFiUKZ9UajpkER8ntbNYuFtrIMJQ7BQBwgV#rows:id=1>.

The electrical signals, proportional to the UV solar intensity value, representing the output size of the VEML6070 sensor, are converted to the effective value of the UV solar radiation intensity, and then recorded in the microcontroller memory. It also performs the transmission of recorded values to a mobile device with Android operating system through the Bluetooth wireless communication interface. The main screen of the Android app shown in Fig. 5 displays a sensor values transmitted via the Arduino board and Bluetooth device, location and UV risk level message computed of ultraviolet radiation exposure. For data comparison in Figure 6 shows a screen capture with the average daily value of the UV index provided by a global weather centre.

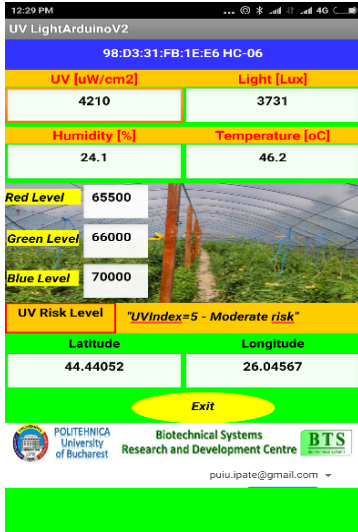


Figure 5. Main screen of Android app

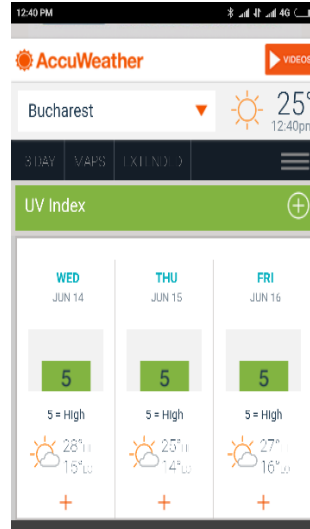


Figure 6. UV index reported by the AccuWeather meteorologist

Further on are some examples of results provided by the component programs of the monitoring system. Figure 7 shows the values of intensity UV solar radiation, recorded in four different days, in the 12 - 15-hour range and displayed with a 1-minute step. It is noted that on 04.07.2016, when the sky was predominantly sunny, the average UV radiation intensity is $4297.17 \mu\text{W} / \text{cm}^2$, compared to only $2085.25 \mu\text{W} / \text{cm}^2$, the value corresponding to 15.06.2017 when the sky has been often cloudy. It should be specified that for technical applications, average values calculated for the daytime are of importance much higher than the average values calculated over the 24h interval. Also, a comparison based on data from 4 days is insufficient to quantify uncertainties of data related to instrument drift or site-specific differences. To quantify long-term behaviour, we need to compare data over 1-yr periods (Bernhard et. al., 2005).

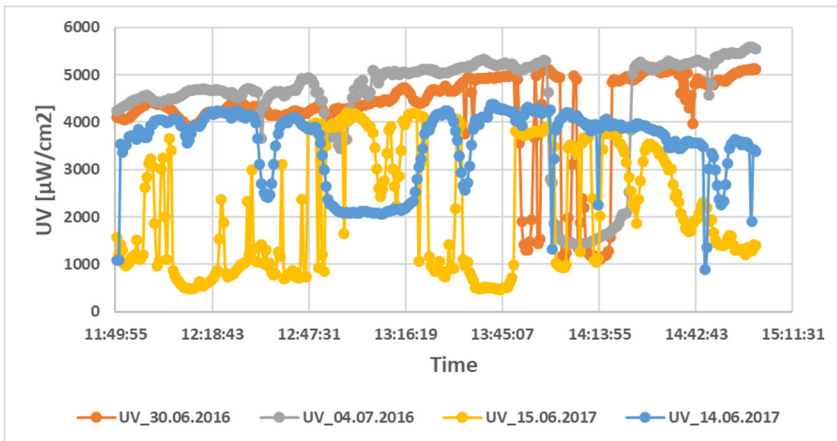


Figure 7. Hourly UV irradiance evolution during the study period

Figure 8 depicts the solar ultraviolet radiation measured as an ultraviolet index (UVI), made based on a monitoring program conducted during June 2016 - July 2017. A calculation was done to determine the percentage of the measured solar UV that the UVI meters measured during the study period. It was found that 35.04% of the values belong to level 5, the moderate risk class and 20.07% to level 6, the high-risk class.

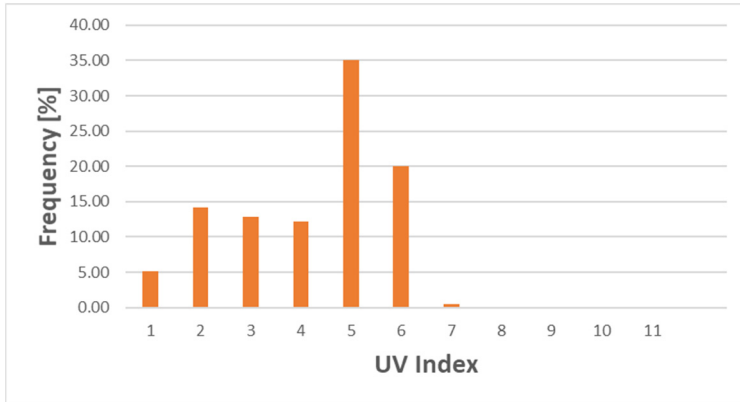


Figure 8. Histogram of ultraviolet index (UVI) on all four days

It can also be seen in Figure 9 that the days 1-3 was sunny and day 4 had variable cloud cover. The maximum solar UVR value on day 2 exceeded 6 UVI levels, whereas the maximum value on day 1 did not.

There is no doubt that excessive UV radiation exposure is harmful — especially to those whose sun exposure patterns are unsuited to their skin type and pigmentation (Lucas et. al, 2006).

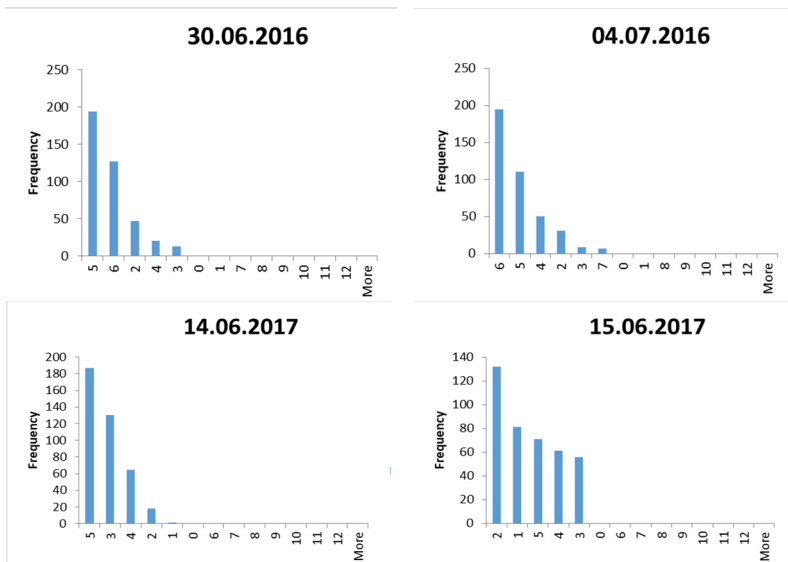


Figure 9. Solar ultraviolet radiation measured as an ultraviolet index (UVI)

In summary, data from accurately characterized and calibrated, instruments can provide reasonably measurement in real time of relevant UV radiation levels. Furthermore, system proposed are easier to deploy and maintain due to their straightforward design, and offer data at higher sampling rates. This makes them useful for quality control of radiometric measurements (Bernhard, 2005).

CONCLUSIONS

The results of this UV solar radiation monitoring study allow for particularly interesting interpretations to be used to determine the risk potential of greenhouse workers' exposure to UV radiation. Such preliminary results have already been obtained, but for the completion of this study, a much longer period of monitoring of the intensity of solar radiation is needed.

By using a smart sensor, the designed instrument can monitor and measure UV index level in any environment, both indoors as well as greenhouses and in open spaces, and in this way we can protect and ensure the health of agricultural workers.

New graphical interfaces make real-time monitoring much more attractive, through better data collection, easier display, or the ability to instantly alert users to text messaging and e-mail on issues that may arise.

ACKNOWLEDGEMENTS

The work has been funded by the Institutional Development Fund of the Ministry of National Education through the Financial Agreement CNFIS-FDI 2017-0172.

REFERENCES

- Belkin, M., Cesarini, J-P, Diffey, B., Hietanen, M., Kojima, M., Mariutti, G. (1994). Protection Against Exposure to Ultraviolet Radiation. INTERSUN report of World Health Organization.
- Bernhard, G., Booth, C.R., Ehranjian, J.C. (2005). Real-time ultraviolet and column ozone from multichannel ultraviolet radiometers deployed in the National Science Foundation's ultraviolet monitoring network, *Optical Engineering* Vol. 44, No. 4, 041011, pp. 1-12.
- Chang ,N.B., Feng, R., Gao ,Z., Gao, W. (2010). Skin cancer incidence is highly associated with ultraviolet-B radiation history. *International Journal of Hygiene and Environmental Health*, Vol. 213, pp. 359–368.
- Diffey, B.L. (1991). Solar ultraviolet radiation effects on biological systems - Review. *Phys. Med. Biol.*, Vol. 36. No 3, pp. 299-328.
- Ipate, G, Voicu, Gh., Ilie, F, Bogoescu, M., Vintila, M., Marin, E. (2016). Natural Ambient Light Monitoring in Greenhouses with Polyethylene Film Roof. *Proceedings of ISB-INMA THE 2016 International Symposium, 27-29 October, Bucharest*, pp.717-722.
- Lucas, R.M., Repacholi, M.H., McMichaela, A.J. (2006). Is the current public health message on UV exposure correct? , *Bulletin of the World Health Organization*, June, Vol. 84, No.6, pp. 485-491.
- Makgabutlane, M. and Wright, C.Y. (2015). Real-time measurement of outdoor worker's exposure to solar ultraviolet radiation in Pretoria, South Africa. *South African Journal of Science*, Vol. 111, No 5/6, Art. #2014-0133, 7 pages.
- McKinlay, A.F. and Diffey, B.L. (1987) in *Human exposure to Ultraviolet Radiation: Risks and Regulations*, ed. W. F. Passchier and B. F. M. Bosnjakovic, Elsevier, pp. 83-87.
- Scharr, R. (2015). Designing the VEMML6070 UV Light Sensor into Applications, *Optical Sensor - Application note*, www.vishay.com.
- Vecchia, P., Hietanen, M., Stuck, B.E., Deventer, E., Niu, S. (2007). Protecting Workers from Ultraviolet Radiation, *Publications of the International Commission on Non-Ionizing Radiation Protection* enjoy.



THE EFFECT OF ROOTS AREA COOLING ON TOMATOES YIELD IN SOLAR

Dragoş MANEA*, Costin MIRCEA, Eugen MARIN, Petru CÂRDEI,
Gabriel GHEORGHE, Florin POP

National Institute of Research - Development for Machines and Installations designed to
Agriculture and Food Industry - INMA, 6 Ion Ionescu de la Brad, 013813, Bucharest, Romania

*E-mail of corresponding author: manea_dragos_05@yahoo.com

ABSTRACT

The principle underlying the temperature optimizing system in the plants roots area is that the temperature gradient between the soil surface and a certain depth is maintaining approximately constant throughout the year. In other words, the temperature of the soil at a certain depth is higher than the temperature of the soil surface during the cold season and lower than that in the hot season. Within the context of current climate change, this temperature difference became significant, reaching and even exceeding 10°C. Due to the cooling effect of the root area during the summer is maintained, soil moisture and evaporation rate is reduced. This paper presents the results of the research carried out by INMA Bucharest as a result of the realization and experimentation of a roots cooling system, which was located inside a solar. The roots cooling system consisted of a network of closed-loop copper pipes, through which water is circulated with a circulation pump. The pipe network is arranged on two levels, the first level is 2 m deep and the other one in the root zone at a depth of 0.2 m. The water filling of the installation is done once and then only necessary to fill in case of possible loss. The effect of cooling the root crop area on hot summer days was studied on a tomato crop, set up on an experimental plot and compared in terms of evolution over time and yield obtained with a control plot placed in the immediate vicinity. Conclusions from experimental research have highlighted the fact that cooling of the root area during the warm season reduces the thermal stress to which plants are subjected and significant crop yields can be obtained.

Keywords: thermal stress , roots cooling, tomatoes

INTRODUCTION

Cultivation of crops in greenhouse and solar is increasing from high altitude and temperate regions to the warmer regions of tropics and subtropics. Greenhouse protects

crops from external bad weather. High temperature and humidity during summer months cause adverse effect on crop production in the context of current climate change (Pek and Hayles, 2004). Consumer interest worldwide in the quality of vegetable products has increased in recent years. Product quality is a complex issue. Many research studies have documented methods for achieving a high-quality vegetable product. Greenhouse production for fresh vegetables offers advantages compared to the open field production with regard to quality assurance principally, because the products are not exposed directly to the rapid changes of climate conditions. On the other hand, vegetable cultivation in a greenhouse under artificially created conditions also affects the quality of the product. This is reflected in a different taste and flavour compared with field vegetables (Gruda, 2005). There is a necessity to develop cheap and effective technology suitable to local climatic conditions to boost up the greenhouse industry. Considerable focus should be oriented towards understanding the physical processes and documenting microclimatic variations in different established designs of greenhouse is necessary to come up with real conclusions (Kumar et al., 2009).

Beyhan et al. (2013) have been developed a new root zone temperature control system based on thermal energy storage in phase change materials (PCM) for soilless agriculture greenhouses. The aim was to obtain optimum growing temperatures around the roots of plants. A maximum temperature difference achieved by the PCM mixture around the roots of peppers was 2.4 °C higher than that near the control plants.

In the experiments conducted by Max et al. (2009) a tomato (*Solanum lycopersicum L.*) crop was grown in four greenhouses during the dry season 2005/06. Sidewalls and roof vents of two greenhouses were covered with nets and these greenhouses were mechanically ventilated when air temperature exceeded 30.8 °C (NET). The other two greenhouses were covered with polyethylene film and equipped with a fan and pad cooling system (EVAP). Overall mean air temperature was significantly reduced by 2.6 and 3.2 °C (day) and 1.2 and 2.3 °C (night) in EVAP as compared to NET and outside air, respectively. The proportion of marketable yield was significantly higher in NET (4.5 kg plant⁻¹) than in EVAP (3.8 kg plant⁻¹), owing largely to an increased incidence of fruit cracking in EVAP.

In this paper, the effect of cooling the root crop area on hot summer days was studied on a tomato crop, set up on an experimental plot and compared in terms of evolution over time and yield obtained with a control plot placed in the immediate vicinity.

MATERIALS AND METHODS

The experiments were carried out at the National Institute of Research - Development for Machines and Installations designed to Agriculture and Food Industry - INMA Bucharest (44°29'58.9"N, 26°04'14.3"E, altitude 100-115 m). Climatic conditions in this area are characterized by warm summers (average temperature 22-23 °C), big differences from day to night and 595 mm total annual precipitation.

The experiments for this study were conducted between 9 May and 22 August 2017 inside a solar with vertical gothic walls. Solar dimensions were 30 m length and 10 m width, height was 5.3 m to the ridge and 2.95 m to the gutter. The entire surface of the solar is covered with air-cushion double polyethylene foil with the following properties: UV resistant, 600% elongation, anti-dust outer layer, 0.15 mm thick, 90% transparency and anti-condensation inner layer. The solar is equipped with an air pump with pressure switch, a sliding door on the front and manual side openings with simple handles by rolling the foil on both sides for

naturally ventilation. The ventilation openings (side walls) remained open day and night throughout the experiment.

The experimental area inside the solar was divided in two equal plots of 45 m² - 15 m length and 3 m width (Figure 1). On the right side plot a roots cooling system was installed, consisted of a network of blind copper pipes mounted in a closed loop, through which water is recirculated. The pipe network is arranged on two levels, the lower level at a depth of 2 m and the upper level in the root area at 0.2 m. Water filling of the system was made only once, from the water tank. The water recirculation was carried out by the circulation pump P, model UPS 15-50 CIL 130. Studies conducted by other researchers (Santamouris et al., 1994) illustrated that pipe length, pipe diameter and fluid velocity inside the pipes influenced the performance of the system considerably, but in this paper we have not addressed this issue.

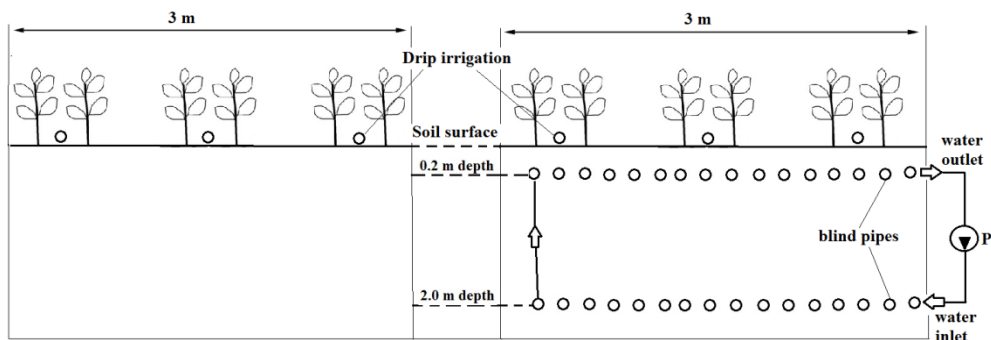


Figure 1. Outline of the experimental area:

left side - the control plot with drip irrigation; right side - drip irrigation and roots cooling system

Irrigation was applied via drip tape (Turbulent Twin Wall, 0.20 m emitter spacing, 0.25 mm thickness, 0.7 l h⁻¹). The early tomato hybrid seedlings 'Prekos' F1 were planted on 24x45 cm spacing. 'Prekos' is the main tomato hybrid cultivated in Romania due to its many qualities. On each plot 200 seedlings, in 6 rows were planted.

The soil temperature was monitored using the Pt100 heat-resistance sensors located in the ground on the two levels mentioned above, in the immediate vicinity of the pipe network. The solar air temperature was monitored by a sensor for measuring the relative humidity and the temperature type 0-10 Vcc. The information taken from the temperature sensors is transmitted to a programmable logic controller model AL2-12MR-D.

RESULTS AND DISCUSSION

Tomato seedlings planting was done on 9 May 2017. The crop development from planting until right before the first harvest can be seen in Figure 2, where can be observed a higher uniformity, rapid growth and bigger plants in the cooled root area rows versus control.

The evolution in time of the soil temperature in the two levels (0.2 m - root zone and 2 m depth) and air temperature has been monitored over entire period (from 9 May till 22 August), but in Figure 3 there is presented only a sequence of these recordings, between 16 and 20 June. The reason we chose this sequence is that it is representative and eloquent to prove the roots cooling system's ability to keep the temperature within an optimal range. In other words, if the air temperature inside the solar increases greatly (47 °C on 16 June), as

happens during very hot days, the roots cooling system keeps the temperature at an optimum level. This fact can be seen in Figure 3. While the air temperature reaches high values (ex. 45 °C on 19 June; 43 °C on 20 June), the temperature evolution at 2 m depth is between 20.5 °C and 24.6 °C.

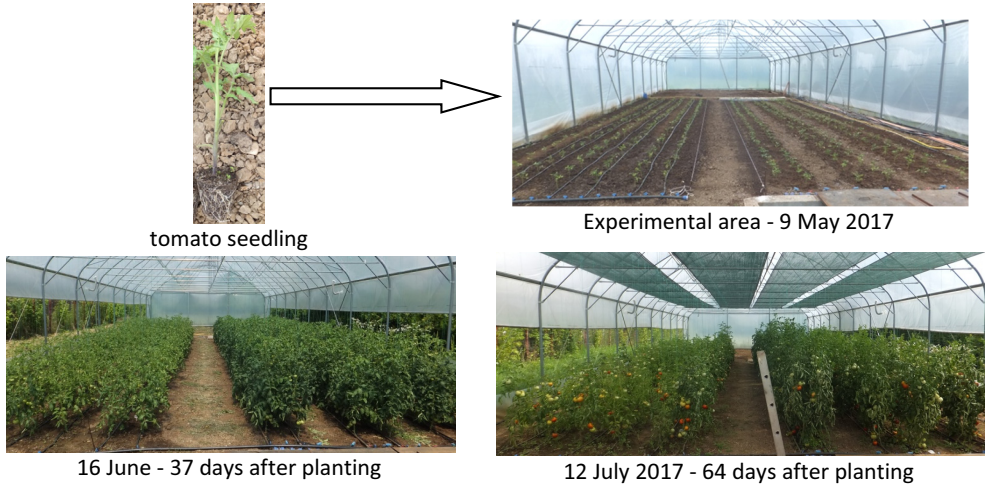


Figure 2. Tomato crop evolution: comparison - cooled root plot (right) versus control (left)

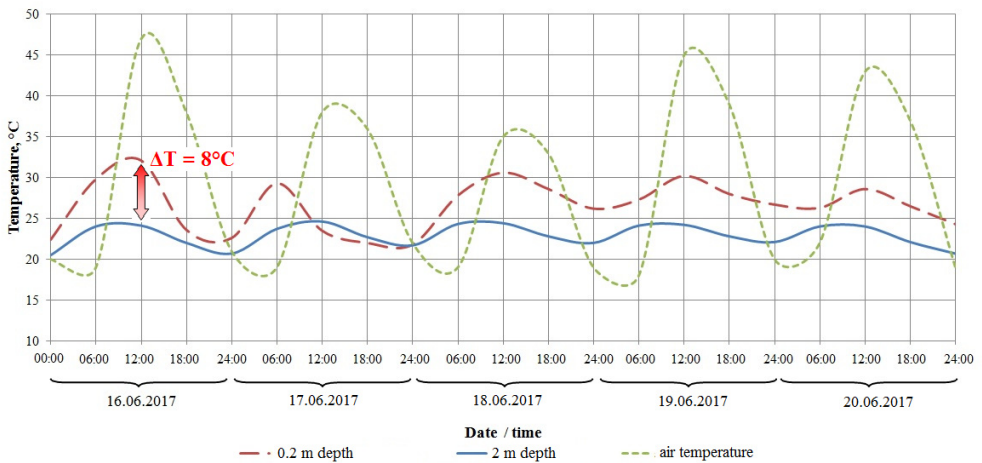


Figure 3. Comparative chart of the evolution in time of the soil temperature at 2 m and 0.2 m depth and air temperature inside the solar, during five hot summer days

Other researchers (Ghosal et al., 2004) developed a thermal model to investigate the potential of using the stored thermal energy of the ground for greenhouse cooling with help of an earth to air heat exchange (EAHES). The temperatures of the greenhouse air, with the experimental parameters of EAHES were 5–6 °C lower in the summer than greenhouse without EAHES.

At the same time, it was noted a soil temperature stabilization around 26 °C during the hottest day in the root area. There is a significant difference between the temperature in the two levels. The maximum temperature difference between the upper level and the lower level over the monitored period was 8°C. Thanks to the cooling effect of the root zone, during very hot days, soil moisture was maintained and the evaporation rate was reduced. Moreover, selection of appropriate technology for cooling depends on the choice of the crops to be grown, maintenance, ease of operation and economic viability (Sethi and Sharma, 2007). Also, large root zone temperature fluctuations negatively affected plant growth, fruit yield, and quality (Gonzalez-Fuentes et al., 2016).

Plots were harvested on 67, 83, 90, 97 and 104 days after transplanting. Total number of harvests were five, between 15 July and 22 August (Figure 4). Tomato yield on the roots cooling plot was significantly higher than on the control plot both on each harvest and on total quantity (280 kg versus 155 kg). The consequences of diurnal roots zone temperature fluctuations during tomato production appear to be small if the minimum soil temperature is above 22 °C.

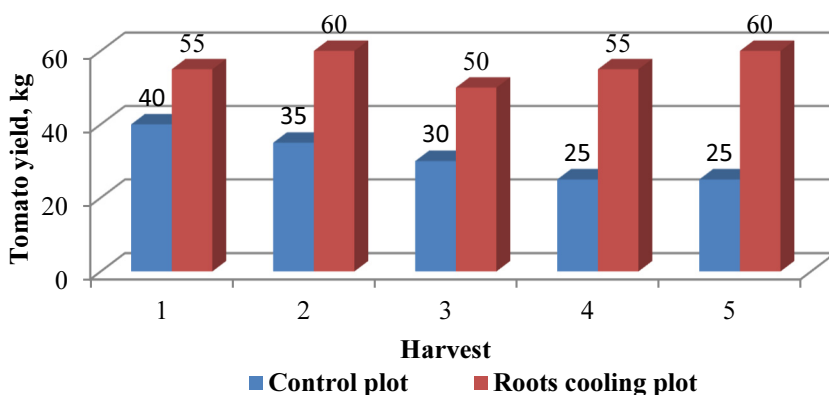


Figure 4. Comparative diagram of the tomato yield on the five harvests

These results are in line with those obtained by Willitsa and Peetb (1998), who analyzed data from six seasons of night cooling experiments conducted at North Carolina State University to determine the effect of night temperature on the yield of tomato. Regression analysis indicated a strong dependence of yield on the night temperature during fruit set when the warm treatment temperature exceeded 21 °C. Total fruit number was 39% higher, and total weights 53% higher, than that observed in the warmer treatment.

CONCLUSIONS

Cooling is considered as the basic necessity for solar and greenhouse crop production, to overcome the problems of high temperatures during summer months. Development of suitable cooling system that provides congenial microclimate for crop growth is a difficult task as the design is closely related to the local environmental conditions.

Cooling of the root area during the warm season reduces the thermal stress to which plants are subjected and significant crop yields can be obtained. In our study, tomato yield on the roots cooling plot was significantly higher than on the control plot.

ACKNOWLEDGEMENTS

This work was funded by the The Ministry of Research and Innovation, within the project PN 16 24 01 01 - *Intelligent system for condensation irrigation in greenhouses and solariums* within the Program NUCLEU 2016 - 2017.

REFERENCES

- Beyhan, B., Paksoy, H., Dasgan, Y. (2013). Root zone temperature control with thermal energy storage in phase change materials for soilless greenhouse applications. *Energy Conversion and Management* 74: 446–453.
- Ghosal, M.K., Tiwari, G.N., Srivastava, N.S.L. (2004). Thermal modelling of a greenhouse with an integrated earth to air heat exchanger: an experimental validation. *Energy and Buildings* 36 (3): 221–227.
- Gonzalez-Fuentes, J.A., Shackela, K., Lietha, J.H., Albornoz, F., Benavides-Mendoza, A., Evans, R.Y. (2016). Diurnal root zone temperature variations affect strawberry water relations, growth, and fruit quality. *Scientia Horticulturae* 203: 169–177.
- Gruda, N. (2005). Impact of Environmental Factors on Product Quality of Greenhouse Vegetables for Fresh Consumption. *Critical Reviews in Plant Sciences* 24 (3): 227–247.
- Kumar, K.S., Tiwari, K.N., Madan, K. Jha. (2009). Design and technology for greenhouse cooling in tropical and subtropical regions: A review. *Energy and Buildings* 41: 1269–1275.
- Max, F.J., Horst, W.J., Mutwiwa, U.N., Tantau, H.J. (2009). Effects of greenhouse cooling method on growth, fruit yield and quality of tomato (*Solanum lycopersicum* L.) in a tropical climate. *Scientia Horticulturae* 122: 179–186.
- Pek, Z. and Hayles, L. (2004). The effect of daily temperature on truss flowering rate of ornamental crops. *Journal of Science of Food and Agriculture* 84 (13): 1671–1674.
- Santamouris, M., Balaras, C.A., Dascalaki, E., Vallindras, M. (1994). Passive solar agricultural greenhouses: a worldwide classification and evaluation of technologies and systems used for heating purposes *Solar Energy* 53 (5): 411–426.
- Sethi, V.P. and Sharma, S.K. (2007). Experimental and economic study of a greenhouse thermal control system using aquifer water *Energy Conversion and Management* 48 (1): 306–319.
- Willitsa, D.H. and Peetb, M.M. (1998). The effect of night temperature on greenhouse grown tomato yields in warm climates. *Agricultural and Forest Meteorology* 92 (3): 191–202.



ENERGETIC AND ECONOMIC CONSIDERATIONS ON THERMAL REGIME EFFECTIVENESS IN A GREENHOUSE

Petre-Florinel NENU¹, Luisa-Izabel DUNGAN^{1*}, Lavinia CERNESCU^{2,3},
Titus SLAVICI^{1,2}

¹Politehnica University of Timisoara, Victoriei no. 2 sq, 300006 Timisoara, Romania

²Ioan Slavici University of Timisoara, Păunescu Podeanu no. 144 st, Timisoara, 300569, Romania

³West University of Timisoara, V. Parvan no. 4 blvd, Timisoara, 300223, Romania

*E-mail of corresponding author: luisa.dungan@upt.ro

SUMMARY

Greenhouses are a sustainable solution for the food production. Ecologic greenhouses optimize the consumption of resources, leading to a minimal impact on the natural and social environment and thus improving the quality of life on short, medium and long term. The paper presents experimental tests performed in a greenhouse, the energetic and economic aspects analysed and the solution found. The greenhouse was provided with central heating system from a stove which transforms agricultural and forestry waste in thermal energy. The thermal energy produced from renewable sources was further stored and heat exchangers were used between the stove and the storage elements. Two constructive solutions were analyzed from both perspective, thermal and economic, over a calendar year. The optimal solution for an efficient heat regime in the greenhouse has been chosen and exposed.

Key words: greenhouse, heat regime, renewable energy sources, economic aspects

INTRODUCTION

Due to the growing global trend of eco-friendly products, our country, having the advantage that soil is less polluted than other EU regions, could be one of the world's first exporting countries of organic certified agricultural products (the areas exploited in the ecological system is about 3.4% of the total agricultural area, Romania being the 20th exporting country in the world).

An adult man must consume about 200 kg of vegetables each year to provide the human body with vitamins, mineral salts, as well as other important ingredients of vegetable products (Alsanius et al., 2017).

Considered at national scale, this aspect highlights the economic significance of vegetable production. This is truth also in case of Romania - a country with tradition in vegetable production.

For food safety, food should be: 1) present in sufficient quantities; 2) physically, economically and socially accessible; 3) nutritious, of a quality that meets the needs and dietary preferences (Alsanius et al., 2017).

The need to consume fresh vegetables and fruits throughout the year has led to the development of new cultivation methods in protected areas in many countries, including Romania. In the last three years the total production of vegetables (the largest share of potatoes, cabbage, tomatoes, carrots, cucumbers, onions, peppers, eggplants, beans) in Romania was around three million tons, from an area of approximately 40000 hectares (of which 317 hectares are occupied by greenhouses and 3000 hectares of solariums), covering only 30-40% of domestic consumption, the rest being imported.

Because it has the advantage of a less polluted soil or advantage it has, a slightly polluted soil, Romania could produce organic vegetables on at least 10-15% of the agricultural area. Statistical data show that currently only about 1% of agricultural land has this destination.

At the same time, through the development of agricultural crops grown in greenhouses and hothouses, vegetable growing has become a determinant factor for the creation and development of specialized economic and industrial production directions and units (for the production of components of protected areas, production of plastic shelters, specific machinery for crop and field crop protection, construction of machines and equipment specific to their processing, storage, etc.). Vegetable cultivation ensures better land use than through many other crops, due to the possibility of large-scale succession, both in open-field and especially protected crops (in greenhouses and hothouses). Vegetables production is an important source of income for cultivators (natural or legal) but also for the country by exporting vegetables (currently Romania exports: tomatoes, cucumbers, peppers, eggplants, onions and different cans).

Other benefits of vegetable production: there is a dynamic balance between income and expenditure (providing monthly income to workers in this area), because vegetables can be produced throughout the year (in protected areas); some of the vegetable debris from some vegetable crops can be used in animal feed (marsh, beets, peas, beans, etc.) and some of the vegetable residues can be used to produce biogas or can be burned in the thermal plant, all combustible materials derived from plant biomass are sustainable (Nenu et al., 2017).

It is also well known that organic farming is a future-proof business with a secure profit, even if the costs are high in the short term, which makes farm gate prices higher than regional prices (Hungary, Poland) (Vlad, 2015).

On a vegetable farm, over a calendar year, electricity costs are high and almost continuous, while those with thermal energy are only seasonal and depending on atmospheric temperature variation. Also, the costs of water supply are important and they are roughly the same throughout the year. However, the highest costs are related to energy and so the solution is to reduce these costs and to automate the production process (automation of processes conducted by human operators).

Greenhouse gases such as heating, cooling, ventilating and enriching with CO₂, estimating energy consumption and other resources when it is applied in greenhouses under different

climatic conditions are important both for the design of greenhouse and for the selection of a greenhouse main crops (Goto et al., 2015).

MATERIALS AND METHODS

Considerations about the location of the greenhouse

The greenhouse must be located under several conditions:

- the land should be flat with south or south-east exposure;
- the soil must have high fertility;
- not be located in the direction of the dominant winds;
- the groundwater level shall be at a depth of 1.5-2.0 m;
- be located so as to lie outside the shadow areas thrown by surrounding objects;
- be close to communication channels for the supply and disposal of production.
- be close to sources of electricity, water and heat.

Based on these conditions, we need to have data for the construction of a greenhouse about:

- a) *The location* where the greenhouse will be built: the farm is located in the western area of the country, near the communication ways;
- b) *Changing weather data* over a long period of time;

Information on soil temperature is required for many constructions in Romania, including the construction of protected areas for growing vegetables and fruits. Meteorological elements such as solar radiation (Figure 1 and Figure 2) and air temperature influence the temperature at the surface of the soil, but also under the surface, affecting the thermal transfer rate between the atmosphere and the soil. Daily sun and seasonal variations influence both the air and soil temperature, with the farm having the advantage of being in the red area where the solar radiation intensity is between 1300 and 1350 kWh m⁻² year⁻¹. The annual average of daily global solar radiation in Romania is 3.34 kWh m⁻², is very good for solar applications (Şerban et al., 2016).

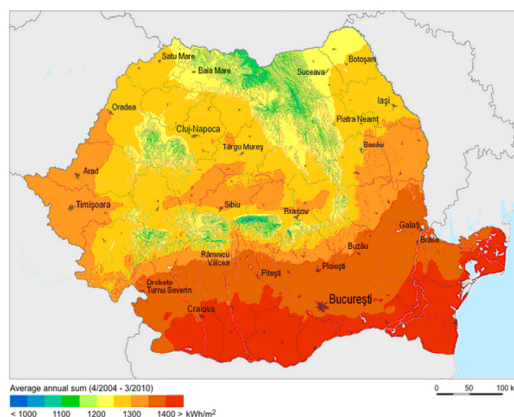


Figure 1. Solar map of Romania [source: Şerban et al., 2016]

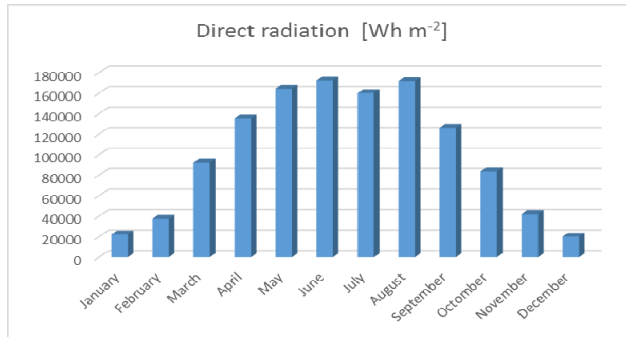


Figure 2. Variation of direct radiation throughout the year in Timisoara city
 [source: <http://solar.physics.uvt.ro>]

Other elements such as wind and rain affect significantly only locally and in the short term. In conclusion, soil temperature varies from one month to the next depending on incident solar radiation, precipitation, seasonal variations in air temperature, local vegetation temperature, soil type and soil depth.

When building a greenhouse, it is necessary to know the seasonal variation of air temperature and soil. The following table shows the temperature variation in Timisoara in the last 10 years, and in Figure 3 the variation of the soil temperature in °C.

Table 1. Minimum temperature in Timisoara

Temperature °C	Year											Month
	2007	2008	2009	2010	2011	2012	2013	2014	2015	2016	2017	
	-6	-12	-15	-14	-15	-12	-12	-7	-15	-14	-16	January
	-5	-10	-13	-10	-11	-23	-6	-7	-8	-4	-7	February
	-1	-4	-5	-6	-7	-6	-5	-2	-4	-2	-2	March
	-3	0	-2	-4	-4	-2	-2	-1	0	1		October
	-6	-6	-4	-3	-7	0	-2	-5	-2	-5		November
	-7	-10	-22	-14	-4	-18	-8	-17	-3	-10		December
Minimum temperature												-22
The temperature in the greenhouse												16
Temperature difference												38

Source: own creation with data from Weather Underground, Giarmata station and Solar Platform of West University of Timisoara

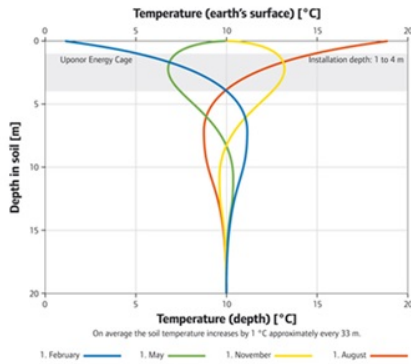


Figure 3. Soil temperature at different depths [source: <http://www.fintherm.com>]

c) *Surface and soil quality:*

As far as the surface and the quality of the soil is concerned, it is on a flat surface, having a forest protection curtain in the direction of the wind and the soil has a high potential (the western plains).

d) *Water source:*

For a commercial operation is essential that the farm has access to large volumes of clean water (Andrews and Pearce, 2011). The farm has its own water source (a pond of approximately 4000 m²), is at the intersection of two irrigation channels (currently not water-fed) but has the advantage of being in a high potential area of geothermal water (Figure 4).

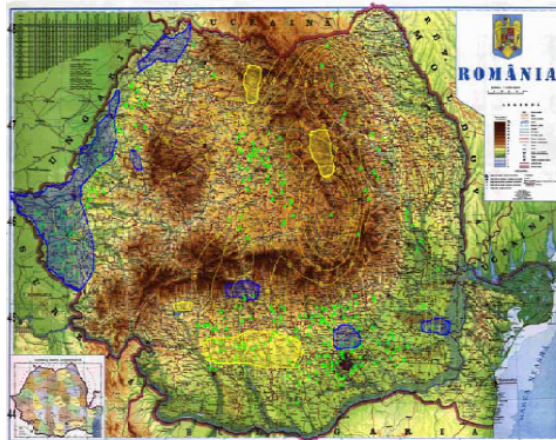


Figure 4. The potential of geothermal energy in Romania [source: IGR 2006]

e) *Source of electric and thermal energy:*

The farm is fed into the national electricity grid, and the thermal energy is produced with a regular wood-fired power plant (low yield) that feeds the farm house and protected areas.

Considerations for greenhouse construction

For the construction of the greenhouse we must keep in mind the following:

- what is to be cultivated: the type of greenhouse differs from the nature of the crop (eg high greenhouses for vineyards or fruit trees, lower greenhouses for onions, potatoes, radishes, etc.);
- the size of the crop: depending on the size of the crop, the surface of the greenhouse will be projected;
- the way of cultivation and harvesting (eg if we want to grow mechanically, the greenhouse must be built with straight side walls);
- the greenhouse equipment (depending on the greenhouse, the price per built square meter increases vertiginously).

The following relationships are recommended to determine the size of the greenhouse:

- length = multiples of 8 m + 4 m (preferred direction: E-W);
- width = multiples of 4 m (preferred direction: N-S).

For the studied farm was chosen the option for a typical greenhouse needed to cultivate vegetables consisting of 3 intervals with a width of 8 m and a length of 28 m.

Cultivation or harvesting will be done mechanically, so the greenhouse is with straight walls (up to 90 cm from the ground, after which the green arches are mounted, giving the possibility of cultivation and close to the side walls, including the higher plants (peppers, cucumbers, tomatoes).

The greenhouse will be equipped with an irrigation system (drip), ventilation system and heating system (e.g. cooling on very hot summer days). Of these, the heating system has special construction features to ensure the minimum required room temperature even at the lowest outside temperatures during the winter months. To have a minimum greenhouse temperature of 16°C, for the minimum temperature of the last 10 years (-22°C as shown in Table 1) we have to ensure a temperature difference of 38°C.

Ensuring the minimum temperature in the greenhouse can be done using the following systems for supplying water to the sidewalls or soil tubes:

- water from a 200 m deep well (18°C) for heating the substrate in winter and cooling it in the summer;
- hot water from solar panels on autumn / spring when the temperature does not drop below zero degrees at night, including in sunny winter days - for side walls;
- hot water from the biomass thermal boiler, additionally on very cold winter days - for the side walls.

Figure 5 shows the two systems (solar panel and thermal boiler).

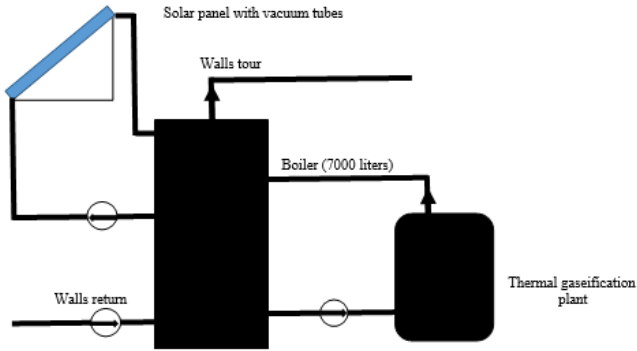


Figure 5. The heating system (for the walls of the greenhouse)

The lateral stone wall (Figure 6) has a thickness of 20 cm (stone) and a total maximum height of 1.5 m (60 cm in the ground and maximum 90 cm above the ground). In the interior of the greenhouse the wall looks like in the figure below, and on the outside it is insulated (polystyrene thickness 10 cm). The inside wall is crossed by a serpentine (starting at the surface of the soil) through which the heat agent circulates at about 25°C (Figure 7).

The advantage of this type of wall:

- in the cold season, the stone is a very good heat accumulator (the stone heats up from the heater circulating through the coils) and gives this heat to the air inside the greenhouse;
- in hot weather (on very hot days) cold water can circulate through the coil and so the wall cools down and the air inside the greenhouse cools through the heat transfer.



Figure 6. Side stone wall

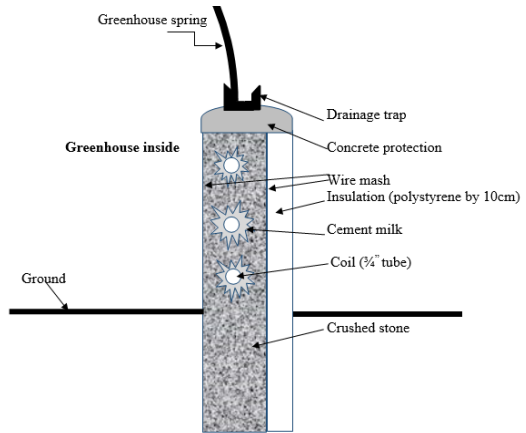


Figure 7. Heating (cooling) through the side wall

Soil heating was achieved by means of thermal accumulators (crushed stone) placed in ditches at a depth of max. 35 cm from the ground, having a height of 30 cm and a width of 30 cm through which pass 3/4 " flexible tubing for underfloor heating, the distance between these accumulators being at least 40 cm (Figure 8). Through these tubes, water will circulate at 18°C from a deep well.

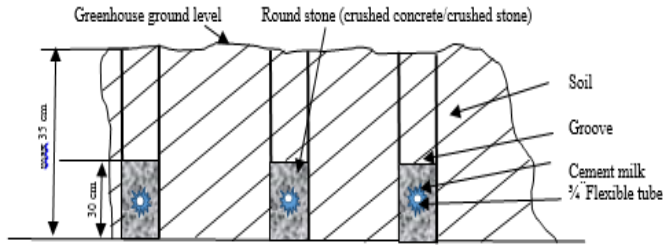


Figure 8. Ground heating

Considerations on the calculation of energy efficiency

The principles for achieving energy saving are:

- maximum use of natural light of the sun (introduction of free energy into the greenhouse, free light for growing and crop production); maximum insulation (prevention of energy losses through greenhouse effect);
- efficient use of energy (eg mechanical dehumidification, diffuse light, optimal CO₂, low temperature heating, high humidity levels);
- replacing fossil fuels with renewable energy sources (e.g. geothermal, biofuels, solar energy, wind) (Hemming et. al., 2015).

By using renewable resources, operating costs are considerably diminishing and yielding profitable effects in terms of being able to support the business.

It is well known that in Romania, energy consumption will be 34.9 Mtoe (million tons of oil equivalent) by 2020 and biomass will cover more than 60% of renewable energy sources (RES), ie 190 -200 PJ / year (Gheorghiescu et al., 2007).

To highlight the energy and economic improvements of the greenhouse, it was turned off from the calculation of thermal losses. For an ordinary greenhouse the losses are those in the Figure 9 (Vasilescu and Nenu, 2013).

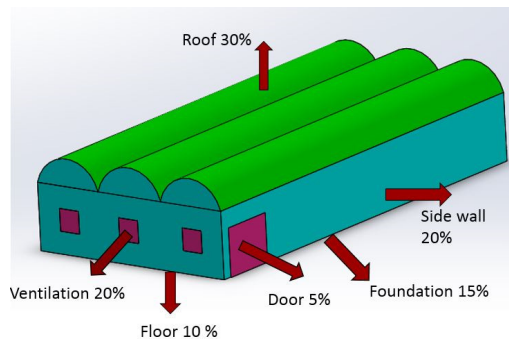


Figure 9. Total losses into the greenhouse

RESULTS AND DISCUSSION

The calculations of thermal losses were made for a night of the cold season for a temperature of -8°C (minimum temperature of the last 10 years, according to Table 1).

Table 2 shows the losses in case we do not have isolated and heated screens, nor the heated substrate, the greenhouse being heated by water-air exchangers, the water heating source being the classic boiler on wood and coal.

Table 2. Losses without considering the heating of the substrate and the walls

	Length [m]	Height [m]	Number	Area [m ²]	Coef	Temperature		Loss energy [Wh ⁻¹]
						Inside [°C]	Outside [°C]	
Roof	28	4.4	3	369.6	3.91	10	-8	26003.13
Slide wall lower	28	0.2	2	11.2	1.46	10	-8	294.68
Slide wall	28	0.9	2	50.4	3.91	10	-8	3545.88
Front wall lower	24	0.2	1	4.8	1.46	10	-8	126.29
Front wall	24	1.5	1	36	3.91	10	-8	2532.77
Front wall backk	24	4.4	1	105.6	0.03	10	-8	49.03
Arce	1	12	3	36	3.91	10	-8	2532.77
Arce lower	1	11.5	3	34.5	0.03	10	-8	16.02
Intermediary screen	28	24	1	672	5.86	10	18	-31519.49
Floor	28	24	1	672	0.24	18	-5	3663.07
								7244.17
Ventilation								1047.71
Various losses								2200.19
TOTAL loss								10492.07

In Table 3, the losses are shown in case we have insulated walls and heated up to 25°C (with hot water from the boiler that comes from the gasification boiler or solar panels) and the crop substrate heated to 18°C (with water from the well).

Table 3. Losses with substrate and wall heating

	Length [m]	Height [m]	Number	Area [m ²]	Coef	Temperature		Loss energy [Wh ⁻¹]
						Inside [°C]	Outside [°C]	
Roof	28	4.4	3	369.6	3.91	10	-8	26003.13
Slide wall lower	28	0.2	2	11.2	1.46	10	18	-130.97
Slide wall	28	0.9	2	50.4	1.46	10	20	-735.84
Front wall lower	24	0.2	1	4.8	1.46	10	18	-56.13
Front wall	24	1.5	1	36	1.46	10	20	-525.60
Front wall backk	24	4.4	1	105.6	0.03	10	-8	49.03
Arce	1	12	3	36	3.91	10	-8	2532.77
Arce lower	1	11.5	3	34.5	0.03	10	-8	16.02
Intermediary screen	28	24	1	672	5.86	10	18	-31519.49
Floor	28	24	1	672	0.24	18	18	0.00
								-4367.07
Ventilation								1047.71
Various losses								2200.19
TOTAL loss								-1119.17

From the calculations presented in Table 3 there is a surplus of thermal agent of 4367 kWh. On a night with temperatures of -8°C, the heat pump should not be turned on, but it is sufficient to use the water from the well and the walls of the greenhouse.

CONCLUSIONS

From the analysis of energy efficiency for the proposed solution for providing thermal energy, it follows that:

- considering the energy price (1 kWh) of 0.6 RON, we will have a benefit of 2200 euros per cold season, not taking into account that the price of the products is higher at this time of the year;
- we can ensure the optimal temperature in the greenhouse and in the hot summer days, just by circulating cold water through the pipes;
- energy savings of about 15 kWh have been achieved, savings of 2000 euros per season (for a minimum temperature of -8°C per night);
- by using geothermal energy, combined with that of a thermal gasification plant (in which all farm forest and farm waste can be burned) and taking into account the reduction of energy losses, the heating costs decrease by 75%. Prior to adopting the solution presented for heating, firewood and charcoal were used. Adding the cost of electricity and labor, the costs reached about 11000 euros/cold season.

With this solution we have as cost: workmanship (reduced by 25%), electricity (recirculation pumps, well pump and fans), so we will have about 2400 euros/season heating costs;

- the pollution in the area has been reduced due to the use of biomass instead of heating coal.

REFERENCES

- Alsanius, B.W., Dorais, M. and Meijer, R. (2017). Vision of COST BioGreenhouse. *Acta Hort.* (ISHS) 1164:1-8. On line: http://www.actahort.org/books/1164/1164_1.htm.
- Andrews, R., Pearce, J.M. (2011). Environmental and economic assessment of a greenhouse waste heat exchange. *Journal of Cleaner Production* 19, pp 1446-1454. On line: <https://doi.org/10.1016/j.jclepro.2011.04.016>.
- Gheorghiescu, P., Teodoreanu, D., Turcu, I., Blujdea, V. (2007). Action plan for use of renewable energy in Romania), Terra Millennium III Foundation, September 2007, Bucharest.
- Goto, E., Ishigami, Y., Okushima, L. (2015). Development of a greenhouse simulation model to estimate energy and resources necessary for environmental controls under various climate conditions. In *International Symposium on New Technologies and Management for Greenhouses - GreenSys2015*.
- Hemming, S., Balendonck, J., Dielman, J.A., Gelder, A. de, Kempkes, F.L.K., Swinkels, G.L.A.M., de Visser, P.H.B, de Zwart, H.F. (2015). Innovations in greenhouse systems - energy conservation by system design, sensors and decision support systems. In *International Symposium on New Technologies and Management for Greenhouses- GreenSys 2015, ISHS Acta Horticulturae 1170*.

- National Research and Development Institute for Energy (2016). Study on the assessment of the current energy potential of renewable energy sources in Romania (solar, wind, biomass, micro hydro, geothermal), identifying the best locations for investment in the development of renewable electricity generation. On line:
http://www.minind.ro/domenii_sectoare/energie/studii/potential_energetic.pdf.
- Nenu, P.F., Maris, S.A., Forgacs, L., Maris, S. (2017). Use of biomass in coal steam boilers. In 45th International Symposium Actual Tasks on Agricultural Engineering, Opatija, Croatia.
- Șerban, A., Bărbuță-Mișu, N., Ciucescu, N., Paraschiv, S., Paraschiv S. (2016). Economic and Environmental Analysis of Investing in Solar Water Heating Systems. *Sustainability*, 8(12), 1286; doi:10.3390/su8121286.
- Vasilescu, M. and Nenu, P. (2013). Consideration on energy efficiency of greenhouses for vegetable production. *Agir Journal*, Supplement 1, pp 162-166.
- Vlad, V.I. (2015). Romania's development strategy in the next 20 years. The Romanian Academy's Publishing House, Vol 1, 2015, ISBN: 978-973-27-2556-6.
- Weather Underground, Giarmata station. Retrieved on 20 October 2017, at link <https://www.wunderground.com/weather/ro/giarmata>.
- West University of Timisoara (2017), Solar Platform Timisoara. Retrieved on 20 October 2017, at link <http://solar.physics.uvt.ro/srms/index.php?target=pasor&lang=en>.



PHOSPHORUS FERTILIZATION AS A COMPONENT OF GROWING TECHNOLOGY OF BARLEY

Tomáš LOŠÁK^{1*}, Jaroslav HLUŠEK¹, Ivana LAMPARTOVÁ¹,
Lubica POSPÍŠILOVÁ¹, Pavel ČERMÁK², Gabriela MÜHLBACHOVÁ²,
Ladislav VARGA³, Július ÁRVAY³, Boris LAZAREVIĆ⁴

¹Mendel University in Brno, Zemědělská 1, 613 00 Brno, Czech Republic

²Crop Research Institute in Prague, Drnovská 507/73, 161 06 Prague 6, Czech Republic

³Slovak University of Agriculture in Nitra, Tr. A. Hlinku 2, 949 76 Nitra, Slovak Republic

⁴University of Zagreb, Svetošimunska cesta 25, 10000 Zagreb, Croatia

*E-mail of corresponding author: losak@mendelu.cz

SUMMARY

Phosphorus (P) belongs among macronutrients and its interaction with other nutrients significantly contributes to optimum crop yields and nutrients utilisation efficiency. As part of the research project a pot experiment was established with spring barley, variety KWS Irina. The experiment was conducted in the vegetation hall of the Botanical Garden of Mendel University in Brno, Czech Republic. The soil (cambisol) had a good supply of phosphorus – 113 mg kg⁻¹ (Mehlich 3) and slightly acid soil reaction. The rates of phosphorus in the form of triple superphosphate (45% P₂O₅) were increased from 0.3 – 0.6 – 1.2 g per pot (5 kg of soil). Nitrogen was applied in the form of CAN (27% N) at a rate of 1 g N per pot in all the treatments incl. the control. The content of post-harvest soil phosphorus increased significantly with the applied rate (173 – 221 – 295 mg kg⁻¹). Dry matter yields of the aboveground biomass were the lowest in the control treatment not fertilised with P (40.3 g per pot) and increased significantly with the P rate applied (45.1 – 45.4 – 43.7 g per pot) without any significant differences among all fertilized rates. The results showed that the application of water-soluble phosphorus forms in soils can significantly increase the P content in soils with a good phosphorus supply moving to higher categories of supply. Therefore, it is very important that fertilisation of crops be based on the soil supply of P.

Key words: phosphorus, fertilization, barley, soil, biomass

INTRODUCTION

Modern agricultural production is based on high input of phosphorus (P) fertilizers which are produced from phosphate rock and it is expected in near future (in the next 50 – 200 years) that the natural sources will be depleted (Jasinski, 2011). European Union is almost completely dependent on the import of raw phosphates (in year 2010 import was 1.4 million tons) (<http://ec.europa.eu/science-environment-policy>). In the Czech Republic the significant decrease in the use of mineral P fertilizers began after the political-social changes in 1989. If in the 1980s 29-33 kg P ha⁻¹ year⁻¹ was applied annually, between 1991-2013 the P supply decreased to 6 kg P ha⁻¹ year⁻¹! Together with the decrease of mineral fertilizers, also phosphorus input into soils from organic fertilizers decreased because of the reduced numbers of livestock (Čermák et al., 2014). Therefore, in the period 1990 to 2005, soil available P content decreased on average from 107 to 92 mg kg⁻¹ (Vaněk et al., 2007). In terms of P-supply the percentage of arable land in the Czech Republic could be categorised as: low - 27.04%, satisfactory - 28.56%, good - 21.35%, high - 16.55%, and very high - 6.47%. Thus, more than 75% of arable land in the Czech Republic is categorised as low, satisfactory, and/or good, and therefore requires P fertilization. A similar situation is also in orchards, vineyards and hop fields (Smatanová and Sušil, 2015).

On the other hand, due to its interactions with other soil nutrients up to 80% of P can be immobilised in the soil after fertilization (Holford, 1997), and therefore farmers often apply four times higher P dosage compared to those that are recommended for the crop production (Goldstein, 1992). However, phosphorus can also be a harmful polluting agent of surface waters (Schröder et al., 2011). Thus, an adequate rate of P-fertilizer (including knowledge about the soil P-content) is a very important environmental aspect.

Phosphorus moves to plant roots primarily by diffusion, and young seedlings of most annual crops are very sensitive to P deficits (Burns, 1987). Phosphorus deficiency is the main limiting factor in cereal production in many regions of the world (Sharpley et al., 1994, Holford, 1997). The uptake of phosphorus converted per 1 ton of barley (*Hordeum vulgare* L.) grain yield from the field is 3.3 kg P ha⁻¹ (Klír et al., 2008). Thus, P deficiencies reduce the yields of barley (Rowe and Johnson, 1995, Hoppo et al., 1999).

Overwhelming evidence indicates that in terms of annual crops, P fertilizers should be largely applied prior to planting, and predicting of P fertilization for each crop should be based on the pre-season soil testing. Soil testing provides farmers with the highest quantity of practically applicable information (Raij, 1994; 1998). Regardless of their present drawbacks chemical methods of agricultural soil testing are the most frequently used tools of diagnostics of the nutrient status of soil and the need for fertilisation derived from it. The main advantage of soil tests is the possibility of preventing potential disorders of the nutrient status of the crop before its own cultivation in a given field (Matula, 2009).

The aim of present study was to examine spring barley biomass accumulation and mineral nutrition under different P fertilization treatments.

MATERIAL AND METHODS

The pot experiment was established (including sowing) on 1st April 2015 in the outdoor vegetation hall of the Botanical Garden and Arboretum of Mendel University in Brno. Mitscherlich vegetation pots were filled with 5 kg of medium heavy soil (on an oven dry basis at 105 °C) characterised as cambisol; Tab. 1 gives the agrochemical properties of the soil used in the experiment.

Table 1. Agrochemical characteristics of the soil prior to trial establishment (Mehlich III) – Regulation of Czech Republic No. 275/1998

pH/CaCl ₂	mg kg ⁻¹			
	P	K	Ca	Mg
6.42	113	148	2,616	235
slightly acid	good	satisfactory	good	good

The experiment was set up as complete randomized block design with 4 P fertilization treatments (Tab. 2).

Table 2. Treatments of the experiment

Treatment No.	Description	Rate of P (g pot ⁻¹)	Rate of N (g pot ⁻¹)
1	P0	0	1
2	P1	0.3	1
3	P2	0.6	1
4	P3	1.2	1

Phosphorus was applied in the form of triple superphosphate (45% P₂O₅) and nitrogen in the form of CAN – calcium ammonium nitrate (27% N) at a rate of 1 g N per pot in all the treatments including the control. The pots were watered with demineralized water to a level of 60% of the maximal capillary capacity and were kept free of weeds. The aboveground biomass of spring barley (variety KWS Irina) was harvested at the stage of milk-wax maturity (10 plants pot⁻¹) on 25 June 2015. Soil analysis prior to the experiment and after the harvest were carried out using Mehlich 3 method (0.015 M NH₄F + 0.2 M CH₃COOH + 0.25 M NH₄NO₃ + 0.013 M HNO₃) (Mehlich, 1984). Plant samples were ground and digested in the microwave Milestone 1200 MLS system in concentrated HNO₃ and H₂O₂. Concentrations of P, K, Ca and Mg in soil extracts were determined using ICP-OES iCAP 7400 Duo, Thermo Fisher Scientific (Newington, USA).

The results were processed statistically using one-way ANOVA and means were compared according to Scheffe (P = 95%).

RESULTS AND DISCUSSION

The content of post-harvest soil phosphorus

The post-harvest phosphorus content in soil in our experiment is shown in Table 3. The soil phosphorus content significantly increased with an increasing rate of P-fertilizer to 173 (P1) – 221 (P2) – 295 (P3) mg kg⁻¹ as compared to 130 mg kg⁻¹ in the unfertilised control (P0). Inorganic phosphorus enters the soil solution by mineralization or fertilizer additions (Sanchez, 2007). Mineralization of organic phosphorus means that after harvest it increases in the unfertilised treatment to 130 mg kg⁻¹ (treatment 1, Table 3) as against its content at the beginning of the experiment, i.e. 113 mg kg⁻¹ (Table 1). It was reported several times that systematic phosphorus fertilization increases the plant extractable soil phosphorus content (Lásztity and Csathó, 1995, Blake et al., 2000, Izsáki, 2009, Ma et al., 2009). The accumulation rate was found to be dependent on the soil type, cropping system, climatic conditions, as

well as on the phosphorus rate. Lošák et al. (2016) stated that in the P-fertilised treatments (using the same methods) the post-harvest increase in the soil phosphorus content in the same barley varieties was similar in the chernozem (96 – 141 – 210 mg kg⁻¹) and in haplic luvisol (128 – 179 – 277 mg kg⁻¹). Phosphorus fertilisers are essential for optimum production, especially when soil test levels are low (McKenzie et al., 1998). In European field experiments (three sites with different soils in the humid oceanic and humid continental climatic regions), where the annual P fertilizer dose ranged between 23 and 35 kg ha⁻¹, the soil phosphorus content did not increase significantly (Blake et al., 2000). On a chernozem soil (Hungary: temperate climate) a 100 kg ha⁻¹ increase of the P balance raised the Al-P content of the ploughed layer by 3.1-4.4 mg kg⁻¹ year⁻¹, when different P fertilizer levels were compared (Izsáki, 2009). At different sites in China on different soil types with a fertilization rate of 65.5 kg P ha⁻¹ year⁻¹ the accumulation rates of P _{Olsen} content ranged between 0.95 and 1.24 mg kg⁻¹ year⁻¹ (Ma et al., 2009).

Table 3. The content of post-harvest soil phosphorus

Treatment No.	Description	Rate of P (g pot ⁻¹)	Soil P content (mg kg ⁻¹)	Supply category
1	P0	0	130 a	high
2	P1	0.3	173 b	high
3	P2	0.6	221 c	very high
4	P3	1.2	295 d	very high

Different letters (a, b, c, d) indicate significant differences between treatments.

Dry matter yields of the aboveground biomass

The yields of aboveground biomass (g DM pot⁻¹) are shown in Table 4. The lowest yield was found in the P-unfertilised treatment (40.3 g DM pot⁻¹) a significant increase in yields was obtained when the rate of applied phosphorus increased to P2 (45.1 - 45.4 - 43.7 g DM pot⁻¹) with no significant differences among the P treatments. No significant differences in yields among the P treatments can be explained by the high (treatment 2) or very high (treatments 3 and 4) supply of soil phosphorus after its application. With the highest P rate in the soil - 295 mg kg⁻¹ (treatment 4) we can see an evident (although insignificant) yield depression compared to other fertilised treatments (Table 4). Lošák et al. (2016) reached similar conclusions stating that dry matter yields of the barley (variety KWS Irina) aboveground biomass grown on chernozem were the lowest in the control treatment not fertilised with P (38.97 g per pot) and increased significantly with the P rate applied (46.02-47.28 g per pot), although there were no significant differences among the fertilised treatments. On haplic luvisol phosphorus fertilisation was not seen at all, demonstrating that the weight of the biomass in all the treatments was balanced: 48.12-49.63 g per pot (Lošák et al., 2016). McKenzie et al. (1998) described that phosphate fertilizer significantly increased barley silage yields at 25 of the 32 site-year locations. Varieties responded differently to applied P. Some varieties responded to P fertilization regardless of the soil test level. Applied P generally increased yields by about 25%, but occasionally the response was much higher.

Table 4. Dry matter yields of the aboveground biomass (g DM pot⁻¹)

Treatment No.	Description	Rate of P (g pot ⁻¹)	Yields (g DM pot ⁻¹)
1	P0	0	40.3 a
2	P1	0.3	45.1 b
3	P2	0.6	45.4 b
4	P3	1.2	43.7 b

Different letters (a, b) indicate significant differences between treatments

Nyborg et al. (1999) conducted field experiments at 60 sites to determine the yield response of barley to phosphorus fertilizer. On the unfertilized plots, barley yields increased with increasing concentration of extractable P in the soil. Nitrogen (Gregory et al., 1984, Léon, 1992, Le Gouis et al., 1999) and phosphorus (Gregory et al., 1984, Rodriguez and Goudriaan, 1995) deficiencies diminish biomass accumulation, but they seem to follow a different timing. P deficiencies usually diminish barley biomass accumulation early in the growth period and the differences between stressed and non-stressed crops tend to be maintained in absolute terms and reduced in relative terms (Gregory et al., 1984). On the other hand, N deficiency also diminished biomass accumulation early in the growth period, but differences between stressed and non-stressed crops tend to increase in absolute terms during crop growth (Gregory et al., 1984, Léon, 1992, Le Gouis et al., 1999). In container experiments with phosphorus (rate corresponding to 19 kg P ha⁻¹ – P1 and 57 kg P ha⁻¹ – P2) Prystupa et al. (2004) described the increase in the aboveground dry matter content of barley at heading: 602 (N0P0) - 878 (N0P1) - 978 (N0P2) g DM m⁻². If the nitrogen was applied additionally, the yield of the aboveground biomass of barley increased only with a lower P-rate: 896 (N0P0) - 1622 (N0P1) - 1390 (N0P2) g DM m⁻².

CONCLUSIONS

The results showed that the application of water-soluble phosphorus forms in soils can significantly increase the P content in soils with a good phosphorus supply moving to higher categories of supply. An adequate amount of available phosphorus in soils increases the efficiency of nutrient utilization which is reflected in a higher yield of biomass. Therefore, it is very important that fertilisation of crops be based on the soil supply of P and according to this supply to correct the fertiliser rate and in this way to prevent both inconvenient extremes – P deficiency or its surplus.

ACKNOWLEDGEMENT

This study is a part of the project of NAZV No. QJ 1530171 called "Extension of applicability and actualization of categories for determination of the content of available macroelements and microelements in a soil for ensuring of the sustainability of fertility and productive capability of agricultural soils" which is financed by the Ministry of Agriculture of the Czech Republic.

We express our thanks to the staff of the Botanical Garden and Arboretum of Mendel University in Brno for their helpfulness and assistance with the experiment.

REFERENCES

- Blake, L., Mercik, S., Körschens, M., Moskal, S., Poulton, P. R., Goulding, K. W. T., Weigel, A., Powlson, D. S. (2000). Phosphorus content in soil, uptake by plants and balance in three European long-term field experiments. *Nutr Cycl Agroecosys* 56: 263-275.
- Burns I. G. (1987). Effect of interruptions in N, P or K supply on the growth and development of lettuce. *J Plant Nutr* 10: 1571-1578.
- Čermák, P., Lošák, T., Hlušek, J. (2014). Fertilization level and available nutrients content in arable land of the Czech Republic. In: Kizilkaya R., Gülser C, (eds) Abstract Book: 9th International Soil Science Congress on The Soul of Soil and Civilization, Side, Turkey, pp 697.
- Dalal, R.C. (1977). Soil organic phosphorus. *Adv Agron* 29: 85-117.
- Fixen, P.E. (2005). Decision support systems in integrated crop nutrient management. *Proceedings 569, The International Fertilizer Society, York.*
- Goldstein A. H. (1992). Phosphate starvation inducible enzymes and proteins in higher plants. *Soc Exper Biol Seminar Series* 49: 25-44.
- Gregory, P.J., Shepherd, K. D., Cooper, P. J. (1984). Effects of fertilizer on root growth and water use in northern Syria. *J Agric Sci* 103: 429-438.
- Haygarth, P.M., Hepworth, L., Jarvis, S.C. (1998). Forms of phosphorus transfer in hydrological pathway from soil under grazed grassland. *Eur J Soil Sci* 49: 65-72.
- Helal, H. M. and Dressler, A. (1989). Mobilization and turnover of soil phosphorus in the rhizosphere. *Z Pflanzener Bodenk* 152: 175-180.
- Helal, H.M. and Sauerbeck, D. (1984). Influence of plant roots on C and P metabolism in soil. *Plant Soil* 76: 175-182.
- Holford, I.C.R. (1997). Soil phosphorus: its measurements, and its uptake by plants. *Aust J Soil Res* 35: 227-240.
- Hoppo, S.D., Elliot, D.E., Reuter, D.J. (1999). Plant tests for diagnosing phosphorus deficiency in barley (*Hordeum vulgare* L.). *Aust J Exp Agric* 39: 857-872.
- Isherwood, K.F. (2003). Fertiliser Consumption and Production: Long Term World Prospects. *Proceeding 507, The International Fertiliser Society, York.*
- Izsáki Z. (2009). Phosphorus turnover of chernozem meadow soil in a long-term mineral fertilisation field experiment. *Cereal Res Commun* 37: 49-52.
- Jasinski S. M. (2011). Phosphate rock. *U.S. Geological Survey Minerals Yearbook – 2010, Reston, Virginia.*
- Jones, C. A., Cole, C. V., Sharpley, A. N., Williams, J. R. (1984). A simplified soil and plant phosphorus model. I. Documentation. *Soil Sci Soc Am J* 48: 800-805.
- Klír, J., Kunzová, E., Čermák, P. (2008). The frame methodics of plant nutrition and fertilization. *Crop Research Institute, Methodology, Praha 6 – Ruzyně.*
- Lásztity, B., Csathó, P. (1995). Studies on the effect of NPK fertilization in long-term experiments on pseudomycelial chernozem soil in the Mezőföld region. *Agroch Soil Sci* 44: 47-62.
- Le Gouis, J., Delebarre, O., Beghin, D., Heumez, E., Pluchard, P. (1999). Nitrogen uptake and utilisation efficiency of two-row and six-row winter barley cultivars grown at two N levels. *Eur J Agron* 10: 73-79.
- Léon J. (1992). Crop growth rate and durativ of spring barley cultivars as affected by varied N supply and seedling rates. *J Agron Crop Sci* 169: 1-8.
- Lošák, T., Hlušek, J., Lampartová, I., Elbl, J., Mühlbachová, G., Čermák, P., Antonkiewicz, J. (2016). Changes in the content of soil phosphorus after its application into chernozem and haplic luvisol and the effect on yields of barley biomass. *Acta Univ Agric et Silv Mendel Bru* 64: 1603-1608.
- Ma, Y., Li, Y., Li, X., Tang, X., Liang, Y., Shaomin, H.S., Wang, B., Liu, H., Yang, X. (2009). Phosphorus accumulation and depletion in soils in wheat-maize cropping systems: Modeling and validation. *Field Crops Res* 110: 207-212.

- Matula, J. (2009). A relationship between multi-nutrient soil tests (Mehlich 3, ammonium acetate, and water extraction) and bioavailability of nutrients from soils for barley. *Plant Soil Environ* 55: 173-180.
- McDowell, R. W., Condrón, L. M., Stewart, I. (2008). An examination of potential extraction methods to assess plant-available organic phosphorus in soil. *Biol Fertl Soils* 44: 707-715.
- McKenzie, R. H., Middleton, A., Solberg, E., DeMulder, J., Najda, H. (1998). Nitrogen and phosphorus optimize barley silage production. *Better Crops* 82: 22-23.
- Mehlich, A. (1984). Mehlich 3 soil test extractant: a modification of the Mehlich 2 extractant. *Commun Soil Sci Plant Anal* 15: 1409-1416.
- Nyborg, M., Malhi, S. S., Murney, G., Penney, D. C., Lavery, D. H. (1999). Economics of phosphorus fertilization of barley as influenced by concentration of extractable phosphorus in soil. *Commun Soil Sci Plant Anal* 30: 1789-1795.
- Phoenix, G. K., Booth, R. E., Leake, J. R., Read, D. J., Grime, J. P., Lee, J. A. (2004). Stimulated pollutant nitrogen deposition increases P demand and enhances root-surface phosphatase activities of three plant functional types in a calcareous grassland. *New Phytol* 161: 279-289.
- Prystupa, P., Savin, R., Slafer, G. A. (2004). Grain number and its relationship with dry matter, N and P in the spikes at fading in response to N x P fertilization in barley. *Field Crops Res* 90: 245-254.
- Raij, van B. (1994). New diagnostic techniques, universal soil extractants, *Commun Soil Sci Plant Anal* 25: 799-816.
- Raij, van B. (1998). Bioavailable tests: alternatives to standard soil extractions, *Commun Soil Sci Plant Anal* 29: 1553-1570.
- Reid, W.V., Scholas, R. (2005). *Millennium Ecosystems and Human Well-being: Synthesis*. Island Press, Washington D.C.
- Roberts, T. L. and Stewart, V.M. (2002). Inorganic phosphorus and potassium productions and reserves. *Better Crops* 86: 1-7.
- Rodriguez, D. and Goudriaan, J. (1995). Effects of phosphorus and drought stress on dry matter and phosphorus allocation in wheat. *J Plant Nutr* 19: 2501-2517.
- Rowe, B. A. and Johnson, D.E. (1995). Residual benefits of limestone and superphosphate on barley yields and soil-water deficits on a krasnozem in north-western Tasmania. *Aus J Exp Agric* 35: 611-617.
- Sanchez, Ch. A. (2007). Phosphorus. In: *Handbook of Plant Nutrition* (A V Barker, D J Pilbeam eds), Taylor and Francis, Boca Raton, 51-90
- Schröder, J.J., Smit, A.L., Cordell, D., Rosemarin, A. (2011). Improved phosphorus use efficiency in agriculture: A key requirement for its sustainable use. *Chemosphere* 84: 822-831
- Sharpley, A.N., Daniel, T.C., Sims, J.T., Pote, D.H. (1996). Determining environmentally sound soil phosphorus levels. *J Soil Water Con* 51: 160-166.
- Sharpley, A.N., Kleinman, P., McDowell, R. (2001). Innovative management of agricultural phosphorus to protect soil and water resources. *Commun Soil Sci Plant Anal* 32: 1071-1100.
- Sharpley, A.N., McDowell, R.W., Kleinman, P.J.A. (2004). Amounts, forms and solubility of phosphorus in soils receiving manure. *Soil Sci Soc Am J* 68: 2048-2057.
- Sharpley, A. N., Sims, J. T., Pierzynski, G. M. (1994). Innovative soil phosphorus availability indices: assessing inorganic phosphorus. In: *Soil Testing: Prospects for Improving Nutrient Recommendations* (J L Havlin, J S Jacobsen, eds.), SSSA Special Publication 40. SSSA/ASA, Madison, 115-142.
- Sharpley, A. N., Smith, S. J., Jones, O. R., Berg, W. A., Coleman, G. A. (1992). Transport of bioavailable phosphorus in agricultural runoff. *J Environ Qual* 21: 30-35.
- Smatanová, M. and Sušil, A. (2015). Results of agrochemical testing of agricultural soils in period 2009-2014. Central Institute for Supervising and Testing in Agriculture, Brno.
- Tilman, D., Cassman, K. G., Matson, A., Naylor, R., Polasky, S. (2002). Agricultural sustainability and intensive production practices. *Nature* 418: 671-676.

- Usherwood, N.R. and Segars, W.I. (2001). Nitrogen interactions with phosphorus and potassium for optimum crop yield, nitrogen use effectiveness, and environmental stewardship. *Sci World J* 1: 57-60.
- Vaněk, V., Čermák, P., Kolář, L., Černý, J. (2007). The consumption of phosphorus fertilizers and development of available phosphorus content in soils of the Czech Republic. In: Vaněk V et al. (eds) Proc of international conference Reasonable use of fertilizers, ČZU, Prague, Czech Republic, pp. 52-59.



TESTING LETTUCE, CULTIVAR 'LJUBLJANSKA LEDENKA', FOR 'BABY LEAF' PRODUCTION

**Damijan KELC, Peter VINDIŠ, Peter BERK, Jurij RAKUN, Denis STAJNKO,
Miran LAKOTA**

University in Maribor, Faculty of Agriculture and Life Sciences, Pivola 10, 2311 Hoče, Slovenija
E-mail of corresponding author: damijan.kelc@um.si

SUMMARY

In the experimental plastic greenhouses at the university agricultural center in Pivola on The Faculty of Agriculture and Life Sciences Maribor we tested lettuce cultivar 'ljubljska ledenka' for a 'baby leaf' production. 'Baby leaf' is often used as an attractive gourmet salad mix. Leaves are fast growing and it can be picked up at almost any growing stage. Treatments included sowing in a plateau of polystyrene with 160 holes with 1 or 2 seeds per hole. Half of the experiment was fertilized with water-soluble fertilizer Rosasol 20:20:20, on the other half we used only water. Two different types of Klasmann substrates, tray substrate and bio potgrund were used. We weighed (g) the yield in one hole on the 21st and 28th day after sowing. Crops in the non-fertilized variant (especially in the case of two seeds per hole) are, as was expected, too low, and the quality of the plants does not reach the market quality. On the 21st day after sowing the higher yield was detected at a tray substrate. The role between substrates is turned on the 28th day. For the fertilized variant it is necessary to make a calculation if the additional yield in two seeds per hole covers the costs of the seeds. Competition between plants will be greater for a light and nutrients on a limited growing area. High density of the plants causes the greater possibility of fungal diseases. In this paper will be presented one prototype machine for cutting lettuce leaves, which was made from a band saw. Another variant is to make a saw that moves on a mobile table in a greenhouse and simultaneously cuts young salad leaves. In this case, it is not necessary to move plateau with planted salad from the tables to the cutting machine.

Key words: Lettuce, cultivar, 'ljubljska ledenka', 'baby leaf', cutting machine

INTRODUCTION

Petropoulos (2016) reported there has been a growing trend towards cultivating leafy vegetables in hydroponic systems. Floating system is an alternative

hydroponic system suitable for the production of baby vegetable products, ready-to eat salads and minimally processed leafy vegetables. However, the implementation of this system for the production of fully grown leafy vegetables is not sufficiently studied. Due to the higher and higher demand of vegetables, various production techniques are tested. Production is moving into greenhouses where new knowledge and technological capabilities are being tested. Outdoor farming throughout the year is limited due to adverse weather conditions. The most common growing technique in greenhouses is hydroponics. Plants grow without the presence of earth. Roots can float in water, above them are polystyrene plate with plants. All nutrients are dissolved in the water and ventilation should be well organized. Often an inert rock wool medium is also used, offering space for the roots. Here is used a droplet irrigation with fertigation. There exists also an aeroponics where the roots grow in air with high air humidity.

By 1519, when the first Spanish conquerors landed in Hernan Cortes in Mexico, the Aztecs controlled the empire in which five to six million people lived. This meant that the exploitation of land for agricultural purposes had to be strengthened. This is evident from the use of the 'chimpas' system, the so-called 'floating gardens' found on the shallow lakes of the Mexican valley. This is one of the first known hydroponics systems in the world. The system was established even before the rise of the Aztecs, which later became a systematic way of building it. The ability to exploit the landscape for their benefit shows human resourcefulness, sophistication and a highly developed society (Ancient Origins, 2014).

In 1940, the first commercial instructions and descriptions for hydroponic planting were published by Dr. W. F. Gericke from California. In English and American military bases, millions of tonnes of vegetables have been produced on the islands of the Pacific and the Atlantic through hydroponics. In 1948 the English agricultural engineers presented hydroponics to the poor Bengals (Kogoj Osvald and Osvald, 2005).

Lettuce (*Lactuca sativa* L.) is a one-year-old vegetable, the pleasant taste gives it organic acids. It contains many vitamins and minerals. From 1 kg of 'baby leaf' salad, 20 portions of containers of 0.5 l and 30 portions of containers of 0.3 l can be made. The young leaves of 'baby leaf' salads are the best, when they are as fresh as possible. Storage for several days is possible but some valuable vitamins are lost. We also need to wash the salad quickly and never irrigate for a long time because of the loss of nutrients and vitamins. Salad and other vegetables have been used as a sedative for centuries. Successfully cleans and regulates blood pH (reduces acidity). It is highly recommended for heart and kidney patients. It also promotes digestion and stimulates the course as it contains bitter substances and citric acid. It also calms cough, asthma, pain, nerves, cramps, etc. Salad substances also treat the harmful effects of radioactive radiation, which is why it is especially good for everyone treated with radiation. In cosmetics it cleanses the skin, and for burns it is used for linings (Kogoj Osvald and Osvald, 1994).

Salad reacts negatively to high temperatures. The daily temperature should be 8-12 °C, and the night temperature is from 6-10 °C. Good illumination is very important, otherwise the vegetation time is prolonged. It is also very useful to add carbon dioxide (CO₂) per week. When used properly, we can increase the crop by 25%. With salad yield (1-4 kg m⁻²), 8 g N, 1.5 g P, 13 g K₂O and 1 g Mg are used (Đubrovka et al., 2006).

The salad production for young cut 'baby leaf' leaves is mostly located in Slovenia in closed, temperature secured rooms on mobile tables or on the ground. Glass greenhouses and plastichouses are suitable. Sliding tables are 2 meters in width and length is determined with the width of the greenhouse. Only the space intended for crossing the greenhouse should be deducted from this width. The most common table length is 9-10 m. Thus, the

usual size of the flood table is 2 m x 10 m. We have about 20 tables on one greenhouse. If the young salad is grown on the ground, the work is still much more demanding, and in this case it is advisable to use machinery and machines adapted to sowing, cutting and picking salad, which represents a big financial contribution. If we grow a salad in sowing plates dimension 520 mm x 323 mm, we get 1 square meter of six styrofoam plates. On a table of 20 m², lay 120 plates (Figure 1). In Slovenia, movable tables are mainly static and cannot be moved and run across rails to another place where they would be driven across the cutting machine and cut all the table at the same time. Since this type of technology represents a great deal of time and a lot of manual work, many other procedures have arisen. It is possible to avoid moving tables and place the plateau with salad on metal supports (Figure 2). Here then comes watering and fertilization from above, the easiest way is to use a flooding ramp that saves a lot of manual work and time. We can also program the watering so that only control is needed if the job was done. There is still a lot of manual work, since all the plateau should be folded manually and later picked up.



Figure 1. 'Baby leaf' Lettuce suitable for cutting in a polystyrene plateau, 160 holes.

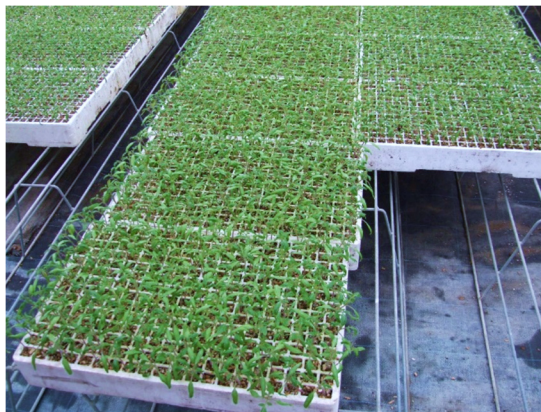


Figure 2. 'Baby leaf' Lettuce plateaus stacked on metal pedestals

Good use of space is achieved through the construction of water pools, where styrofoam floats on the water. Then we just pick them out of the pool and move through the cutting machine. This avoids the cost of investing in moving tables or platforms pedestals. Production pools can be prepared easily and inexpensively. We make an excavation of the terrain and prepare a foil for swimming pools, which is well attached, so that we reach a depth of about 40-50 cm. A larger plateau is used for sowing, with long narrow cracks where the seed is sown (Figure 3). Once the plateau is cut down for the first time, we can return them to the pools and let the salad be cut again. Some people cut it down for the third time, depending on the calculations and the quality obtained.

There are quite a number of companies involved in the production of cutting machines, such as Roopack machines, Hortech, Standen, etc. It is also necessary to connect the technology of salad production and salad harvesting to work quickly and with the lowest possible costs. To start production, it is necessary to test the growing conditions, harvest and marketing. The investment, which is indicated by the market and production, can then be proceed. This is very important because of the expensive investment in machine technology.

If we do not have a greenhouse equipped with moving tables, we can start production on the ground. Such production technology has been increasing in recent years. Here we also have the possibility of machine harvesting of the crop (Figure 4). After testing the technology of production and marketing, it will be easier to make a new investment program.

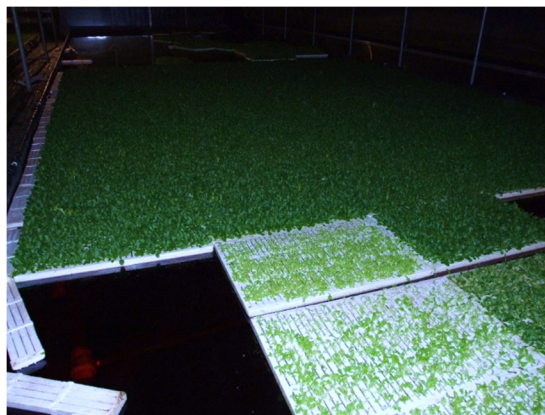


Figure 3. 'Baby leaf' in large plates with long narrow notches on a floating pools.



Figure 4. 'Baby leaf' cutting machine (Simon, Baby leaf harvester, France).

MATERIALS AND METHODS

We chose an autochthonous Slovenian variety, Ljubljanska ledenka. It originates from Ljubljana and its surroundings. It is a crunchy salad with greenish yellow leaves without a red leaf edge. The leaves are slightly bubbling, the leaf edge is corrugated and serrated. They are excellent flavor and very crispy.

Treatment included sowing in a plateau of polystyrene with 160 holes per 1 or 2 seeds per hole. After sowing, the plateau was left in the caliper at a temperature of 25 °C, and relative humidity of 95% until the next day. The seeds wait about 18-21 hours in the caliper, which is enough for quenching. For more than one day is not recommended, as they would quickly 'overgrow'. Half of the plateau was fertilized with water-soluble fertilizers Rosasol 20:20:20, the other half of the plateau was only watered. We used two different types of Klasmann substrate, namely tray substrate and Bio potgrund. The yield of the weight (g) of one hole was weighed on the 21st and 28th day after sowing. With one seed we sown 4 plates in a tray substrate and 4 plates in a bio potgrund substrate. With two seeds, we also sown 4 plates in a tray substrate and 4 plates in a bio potgrund substrate. Then we split the plateau into half. One half was just watered, the other half was fertilized with Rosasol 20:20:20, at a concentration of 2 grams per liter of water.

Table 1. The dates of the sowing and weighing of Lettuce 'baby leaf'

Dates	Date
1. Lettuce sowing	21. March. 2017
2. First weighing	11. April. 2017
3. Second weighing	18. April. 2017

Table 1 shows the salad sowing dates. The first weighing took place 21 days after sowing and the second 28 days after sowing of lettuce.



Figure 5. Movable cutting machine for Lettuce 'baby leaf'.

RESULTS AND DISCUSSION

The experiment shows that 'baby leaf' leaves are not developed enough 21 days after sowing for sale, as their weight (g) is too small compared to day 28 after sowing. Crops in the non-fertilized variant (especially in the case of two seeds per hole) are expected to be too low, and the quality of the plants does not reach the market quality. The harvest at Tray substrate is in day 21 higher than at Bio Potgrund, but the role is turned on the 28th day, when we find higher yields at Bio Potgrund substrate (Figure 6, 7). It would be clever to do some kind of experiment between different types of substrates, as we see that the crop depends on the substrate in which the seeds are sown. In the case of a fertilized variant, a calculation should be made if the (additional) crop in the case of two seeds per hole covers the costs of the seed. We estimate that it does not, especially considering the excessive competition between light and nutrients on an already limited growing area. There is also greater possibilities for the appearance of fungal diseases and mold due to the high density of plants. We see additional possibilities for increasing the yield, as only 2 g per liter of water have been fertilized so far, we could increase to 3 g per liter. This would increase the yield with small financial inputs. At the same time, double sowing is avoided, which means an additional cost of seeds and additional sowing work. On the 21st day of the experiment, we notice that the effect of the two seeds is small. In the Tray substrate with one seed we obtain the same yield if we used fertilizer.

Table 2. Harvest (g) of lettuce leaves on the 21st and 28th day after sowing

Treatment	Days after sowing	Leaf production per hole (g)	Theoretical yield (g) on the plateau (at 91 % of seed germination)
2 seed TRAY fertilized (2STF)	21	1.33	187
1 seed BIO fertilized (1SBF)	21	0.60	86
1 seed TRAY fertilized (1STF)	21	0.91	130
1 seed TRAY (1ST)	21	0.82	115
1 seed BIO (1SB)	21	0.69	101
2 seed TRAY (2ST)	21	0.91	130
2 seed TRAY fertilized (2STF)	28	3.11	430
1 seed BIO fertilized (1SBF)	28	2.52	365
1 seed TRAY fertilized (1STF)	28	2.15	298
1 seed TRAY(1ST)	28	1.62	228
1 seed BIO (1SB)	28	2.1	286
2 seed TRAY (2ST)	28	1.81	264

Table 2 shows that the total yield of 'baby leaf' salad on one plate with 160 holes in the bio fertilized substrate is 365 g. That means that we have about 2,200 g of crop per 1 m², and on a table of 20 m² this amounts to 43 kg of young 'baby leaf' salads every 28 days. Petropoulos (2016) reported that increasing the N application rate resulted in an increase of fresh weight of the aerial parts of lettuce. Total yield ranged between 12.0 to 41.9 kg m⁻² of fresh 'baby leaf' leaves. A similar harvest was also recorded in our experiment, 26.8 kg salads per m² per year increasing the nitrogen rate resulted in higher number of leaves, as well as in a significant increase in the rate of photosynthesis. Richardson and Redgrave (1992), reported that not only temperature but also nitrogen fertilizer rate may affect head weight and total yield of lettuce grown in a glasshouse. Kotsiras et al. (2016) find out significantly lower total yields than at the present study. This was 4.0 to 9.0 kg m⁻² of fresh weight. Difference could be attributed to the different lettuce types (Lollo Rosso and Batavia) and plant densities (20- 30 plants m²), comparing to further study. There was also a clear indication that harvest practice significantly affected storage life (SL), relative fresh weight (RFW) and visual appearance rating (VAR) of all lettuce types.

Now, it depends on us at what price we will be able to sell it on the market. Some sell it at a price of 8 - 10 € kg⁻¹, which is a very good price. This would mean that a single table of 20 m² would earn 350 euros every 28 days. If there is one greenhouse of 20 tables, this would amount to almost 7,000 euro every month. This is quite a lot for one year and could have provide an income of 80,000 euros per year, which is a very good income for one family. And it also means a very big opportunity for future investments. Such a salad is becoming more and more popular, and it still has a lot of possibilities to gain more popularity.

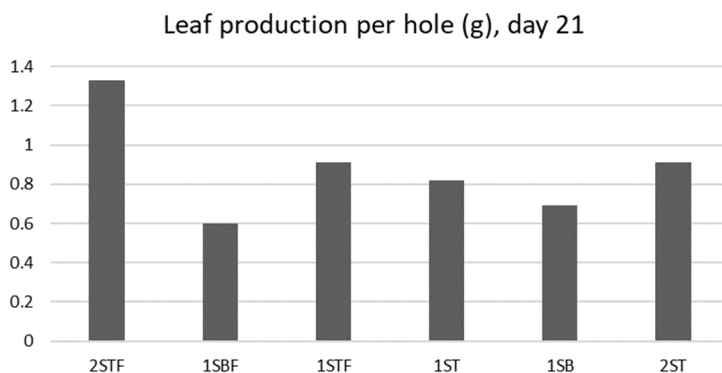


Figure 6. 'Baby leaf' production per hole (g) on the 21st day after sowing (legend in table 2)

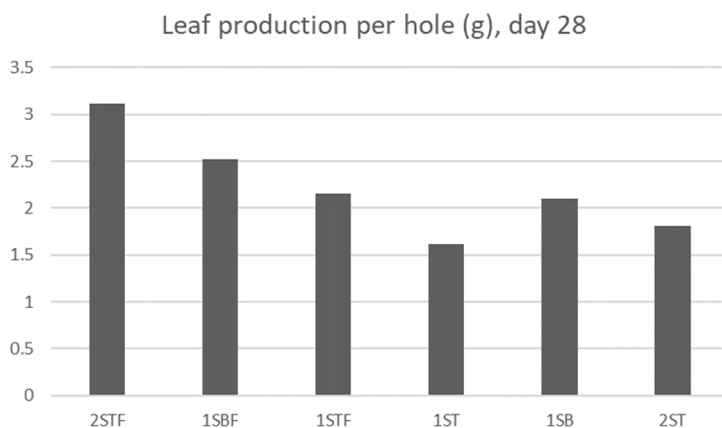


Figure 7. 'Baby leaf' production per hole (g) on the 28th day after sowing (legend in table 2)

CONCLUSIONS

In the research greenhouses of the University Agricultural Center at the Faculty of Agriculture and Life Sciences Maribor, we have tested the lettuce Ljubljanska ledenka, which is becoming increasingly popular due to taste and fragility. We planted 1 and 2 seeds in a 160-hole plate with polystyrene. Half of the plates were fertilized with Rosasol 20:20:20. We used two Klasmann substrates, a tray substrate and a bio potgrund. The yield per hole (g) was weighed on the 21st and 28th day after sowing. The crop is too small and does not achieve market quality as a not fertilized crops. The 21st day after sowing, the largest yield was observed in the tray substrate, and on the 28th day the largest yield was observed at the potgrund substrate. It is therefore sensible to test other substrates as their role in the final result is important. We considered the production to be profitable and meaningful, since it is possible to achieve positive business with a reasonable price. We also propose fertilization at

each watering in the amount of 3 g of fertilizer per liter of water. We estimated that an additional crop with two seeds does not cover the cost of additional seed. We also presented some different types of the machines for cutting young leaves. One prototype was made on the principle of a band saw.

REFERENCES

- Ancient Origins (2014). Chinampas, The Floating Gardens of Mexico. Retrieved on 22. September 2017 at: <http://www.ancient-origins.net/ancient-places-americas/chinampas-floating-gardens-mexico-001537>
- Durovka, M., Lazić, B., Bajkin, A., Potkonjak, A., Marković, V., Ilin, Ž., Todorović, V. (2006). Proizvodnja povrća i cveća u zaštićenom prostoru. Poljoprivredni fakultet, Novi Sad, Poljoprivredni fakultet, Banja Luka, 501 pages.
- Kogoj Osvald, M. and Osvald, J. (1994). Pridelovanje zelenjave na vrtu (1994). Ljubljana. Kmečki glas.
- Kogoj Osvald, M. and Osvald, J. (2005). Hidroponsko gojenje vrtnin (2005). Ljubljana. Univerza v Ljubljani, Biotehniška fakulteta, Oddelek za agronomijo.
- Kotsiras, A., Vlachodimitropoulou, A., Gerakaris, A., Bakas, N., Darras, A.I. (2016). Innovative harvest practices of Butterhead, Lollo rosso and Batavia green lettuce (*Lactuca sativa* L.) types grown in floating hydroponic system to maintain the quality and improve storability. *Scientia Horticulturae* 210:1-9.
- Petropoulos, S.A., Chatzieustratiou, E., Constantopoulou, E., Kapotis, G. (2016). Yield and Quality of Lettuce and Rocket Grown in Floating Culture System. *Notulae Botanicae Horti Agrobotanici Cluj-Napoca*, 44(2):603-612.
- Richardson, S.J. and Hardgrave, M. (1992). Effect of temperature, carbon dioxide enrichment, nitrogen form and rate of nitrogen fertiliser on the yield and nitrate content of two varieties of glasshouse lettuce. *Journal of the Science of Food and Agriculture* 59(3):345-349.
- Standen Engineering (2017). Simon baby leaf harvesters. Retrieved on 27. September 2017 at: <http://www.machines-simon.com/en/our-machines/vegetable-harvester/salad-vegetables/corn-salad-harvester/>



ASSESSMENT OF BUILDING SOLUTION EFFECTIVENESS ON A WINERY THERMAL BEHAVIOUR

Alberto BARBARESI*, Daniele TORREGGIANI, Viviana MAIOLI,
Patrizia TASSINARI

Department of Agricultural Sciences, University of Bologna, Italy

*E-mail of corresponding author: alberto.barbaresi@unibo.it

ABSTRACT

The paper investigates the effects of a pool of building elements on the thermal behavior of a case study winery. Based on the 22 variations considered for the 5 sets of building elements (walls, roof, orientation, glazing, shading), 576 different models have been created, each one analysed by means of 4 energy simulations, according to the combinations of 2 different thermostat settings (temperature ranges suitable for wine ageing and for human activities) and 2 simulation years. The results have been evaluated analyzing the energy needs of each model, showing the high influence of walls and roof on the building energy need. The results have also shown how the influence of each building variant depends also on the temperature range under study. This research can help design and construction professionals to identify the most efficient solutions in relation to the target temperature range.

Keywords: case-study winery, conditioned building, energy efficiency, energy simulations

INTRODUCTION

Building heating and cooling represent the 40% of total European energy consumption. For this reason, in the last decades, government laws and technological developments have been oriented to reduce the building energy needs for temperature control. Even though this problem mainly involves residential and office constructions, the reduction of energy consumption is a delicate matter in farm building design as well, especially in food processing buildings, where indoor temperature can affect food quality or even food safety.

Specifically for wine production in the Mediterranean area, to achieve a good final product, wine farms should keep the wine at specific environmental conditions during storage and wine-ageing. Both temperatures and temperature swings, in fact, play a crucial

role for the quality of wine. Even though the scientific literature does not agree about ideal conditions for wine storage, 15°C is considered a suitable temperature to preserve the wine (Marescalchi, 1965). Wine-ageing involves several chemical reactions that develop at different time rates: in this phase temperatures lower than 20°C help to maintain a balance between reaction products (Boulton et al., 1998). On the contrary low temperatures can play a positive role in the potassium bitartrate removal, but on the other hand can block or prolong the development of wine, thus calling for wine to be stored for longer periods, delaying its sale and requesting more room in the winery. Moreover, temperature variations in the storage room entail changes of pressure inside the wine bottles, rising the risk of cork movements or, in the case of small-headspace fermenters, wine overflows: for this reason the yearly temperature variation should not be higher than 6°C (Vogt, 1971). Under this light, 15°C \pm 3°C can be considered a proper thermal range for wine ageing and storage. Recent studies (Barbaresi et al., 2017b) have highlighted that a typical Italian aboveground and unconditioned building can guarantee the above-said temperature range only for short periods throughout the year, even if provided with specific building solutions for temperature control.

Therefore, maintaining specific temperature ranges in wine storage and aging rooms can be achieved only by means of thermal control systems. However, this solution usually requests a remarkable energy demand, in particular in areas like the Mediterranean region, with an increase in production costs and environmental impacts. An energy demand reduction can be obtained studying specific energy-efficiency-oriented building solutions. It is well known that several building solutions can positively affect the building thermal behavior, but most studies have been made for residential or office buildings (Wang et al., 2009; Boyano et al., 2013), that are characterized by temperature comfort ranges significantly different from food processing ones.

This work aims to evaluate the impact of a pool of building solutions on a case-study winery thermal behavior. Specifically, it assesses and ranks the influence of architectural pools and related single variations. The simulations will take into account two temperature ranges (suitable for wine "comfort" and human comfort).

MATERIALS AND METHOD

The study is structured as follows: a case study building representative of Italian wineries has been chosen; the case-study building has been modeled, calibrated and validated in a previous work for energy simulations (Barbaresi et al., 2017a); 576 different versions of the case-study building have been created, combining 22 variations of 5 building design elements (external walls, roof, windows, solar shading, building orientation), and two different meteorological years and two temperature ranges have been chosen for the energy simulations. Therefore, a total number of 2,304 energy simulations have been run. For each simulation, we have assessed the hourly energy needs of the winery.

Case study

A case study winery (see Fig. 1a) has been chosen, based on its representativeness of central Italy wineries (Torreggiani et al., 2011) in terms of dimensions, building construction, wine production and storage capacity. Moreover, a 5-year survey campaign has provided data about weather conditions, ground temperatures and indoor temperature and humidity, allowing to create, validate and calibrate an energy model of the case-study building (Barbaresi et al., 2017a).

The winery is a one-room aboveground building; its main dimensions are described in the Fig. 1b.



Figure 1a. Case-study winery

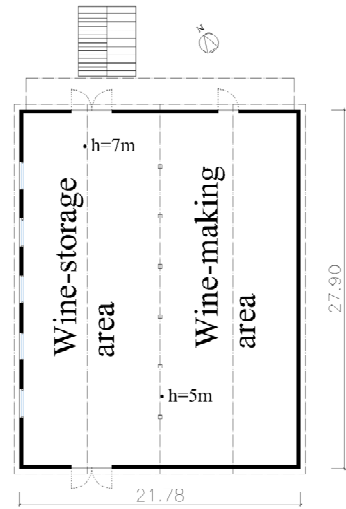


Figure 1b. Winery main dimensions

Building elements and variations

According to Torreggiani et al. (2017), among all building elements, wall and roof constructions, windows, orientation and shading surfaces have been taken into account to evaluate their influence on the thermal behavior of the building.

About walls and roof, we aim to investigate the effectiveness of two characteristics of the envelope constructions: thermal transmittance and time shift. The steady-state thermal transmittance (U) is “the rate of heat transferred through a reference surface in a material from one side to the other side” measured in $Wm^{-2} K^{-1}$. Time shift φ it is “the temporal difference between the time in which the maximum temperature is recorded on the external surface of the building element and the time in which it is recorded in the internal surface”. It is measured in hours [h] (Ente Italiano di Normazione, 2008).

Table 1. Walls and roof characteristics

WALLS			ROOF		
Code	Th. transmittance U [$Wm^{-2}K^{-1}$]	Time shift [h]	Code	Th. transmittance U [$Wm^{-2}K^{-1}$]	Time shift [h]
w01	2.60	3.91	r01	2.01	4.70
w02	1.26	9.69 *	r02	1.66	6.83 *
w03	0.29	12.34	r03	0.25	14.98
w04	0.31	5.19	r04	0.29	7.75
w05	2.42	10.72	r05	0.92	12.08
w06	0.19	22.77	r06	0.19	18.38

To investigate those two characteristics, 6 combinations have been identified, according to material availability on the local market. Tab. 1 shows the selected combinations.

Another building element that remarkably affects the indoor building temperature is glazing, since it usually is the weakest link of the building envelope for two reasons: its U factor is 2-20 times higher than wall and roof constructions one, and it allows the infiltration of outdoor air.

In this work two glazing configurations have been considered: a low performance solution (code: gLP), characterized by simple glazed window and high air infiltration, and a high performance solution (code: gHP), characterized by a double glaze window and an efficient infiltration rate, both set up on the Italian laws for conditioned buildings. Further details are described in Tab. 2.

Table 2. Glazing and orientation characteristics

GLAZING		
Code	Th. transmittance Ug [Wm ⁻² K ⁻¹]	Infiltration [air changes per hour]
gLP	6.00	0.5 *
gHP	2.20	0.3
ORIENTATION		
Code	Orientation	
o032	32° *	
o122	122°	
o212	212°	
o302	302°	

The scientific literature demonstrates the incidence of building orientation on the thermal behavior, therefore this work investigates building orientation as one of the building elements. The energy model can exhibit 4 different orientations starting from the current one (main axis 32°N oriented), and other three 90-degree-rotations as explained in Tab. 2.

The last building element investigated in this work is solar shading. Even though the case study has no solar shading system, this paper aims to assess the contribution of solar shading surfaces on the building thermal behavior. As shown in Fig. 2, solar shading surface is designed as a green wall, located at a distance of 3 meters from the building wall (thus allowing the passage of vehicles for farm winery operations). The sun-shading surface protects the storage area wall in all building variations, regardless of the simulated building orientation.

Table 3. Shading and year characteristics

SHADING		SIMULATION YEAR		
Code	Shading	Code	Average T [°C]	Characteristic
sON	Sun shading included	y07	13.9	Jan-May warmer
sOF	Sun shading non included	* y13	14.1	Aug-Dec warmer

The building thermal behavior, and therefore its energy consumption, obviously depends on outdoor weather conditions. For energy simulations, weather files – representing a typical meteorological year for several worldwide locations – are available on specialized websites. The closest weather file location is located 32 km far from the case study building, and the monitored location shows completely different characteristics. For this reason, specific files have been created using weather data collected on the case-study site through a multi-year survey campaign. Among those years, 2007 and 2013 have been chosen since they both show a yearly average temperature similar to that of the case-study site, and since those two years show different seasonal temperature trends, as explained in the Tab. 3. In Tabs 1 to 3 the star marks the actual case-study condition.

Energy modelling

The energy simulations have been performed using EnergyPlus 8.1 (U.S. Department of Energy, 2013), software largely used in the scientific community for dynamic energy simulations (Mazarrón et al., 2013; Raftery et al., 2011). At first, a model of the current winery has been created and validated by Barbaresi et al. (2017). The same model, hereinafter called “base model”, has been modified according to all building element variations: 6 walls, 6 roofs, 2 glazing, 4 orientations, 2 shading surface scenarios, and 2 thermostat configurations (according to temperature ranges), thus creating new models. Each model has undergone 2 simulations, one per each year. A total number of 2,304 simulations have been run.

4 thermal zones have been identified in the model, as shown in Fig. 2: in particular, this paper focuses on the wine storage area, as explained in Sec. 2.1. The wine hosted in this zone has been modeled using the EnergyPlus InteriorPartition Objects. Each object corresponds to a bottle with the following thermal characteristics: $U= 0.536 \text{ Wm}^{-1}\text{K}^{-1}$, $\delta= 990 \text{ kgm}^{-3}$, $C= 4500 \text{ Jkg}^{-1} \text{ K}^{-1}$ (Boulton et al., 1998).

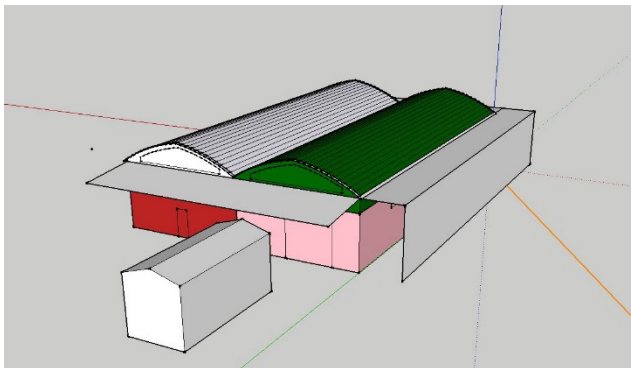


Figure 2. Energy model: the storage area is colored in pink

Temperature ranges

As mentioned in Sec. 1, the temperature range $15\pm 3^\circ\text{C}$ can be considered a suitable range to keep and age the wine. In order to investigate how the results depend on the chosen range, another temperature range, suitable for human activity ($22\pm 2^\circ\text{C}$), has been considered. Since most studies about building conditioning concern residential and office constructions, the results related to this range can be considered as a useful benchmark

(given the purposes of this research, no variation in temperature settings over the seasons, day/night and working/non-working hours has been considered).

Indicator

To calculate the building energy needs, each model has been provided with a thermostat that sets the indoor temperature ranges to be kept by a potential HVAC system. The simulations have been repeated twice, one for each comfort range. Through the simulations, we have obtained the hourly heat to be provided or removed in order to keep indoor temperatures within the chosen ranges. It is important to remark that these values do not represent a real system energy consumption since no system has been inserted in the simulation; it actually represents the building energy request (for heating and cooling) at the basis of HVAC system sizing.

In this work, the hourly heat has been summed in an indicator that comes from the following equations:

$$E_+ = \sum_i^n h_i \quad E_- = \sum_i^n c_i \quad E_t = \sum_i^n (h_i + c_i) = E_+ + E_-$$

E_+ is the total heat that has to be provided to maintain the indoor temperature within the chosen range, E_- is the total energy to be removed, h_i and c_i are the hourly heats respectively to add to and remove from the building. E_t is the total energy need in one year to maintain the comfort range, n is number of hours (8,760) in one year. As energy, it is calculated in kWh.

Variable and variation ranking

A statistical analysis has been performed, in order to assess the influence of each set of building elements (Wall, Roof, Glazing, Orientation and Shading) and the influence of each variation ($w01, w02, \dots, r01, \dots, o032$, etc.). First of all, the distribution of the energy needs of all the simulations has been analyzed calculating their quartiles. The same procedure has been repeated within groups of simulations sharing the same variation (such as $w01, w02$ etc.). The set of building elements have been ranked based on their potential influence on the building energy performance, evaluated by means of the standard deviation of the medians of the energy need distributions calculated for the models of each variation, and referring to the median of all the simulations. The higher the standard deviation, the higher the influence of the set on the energy need. Moreover, the interquartile Q3-Q1 has been used to rank the single variations. A low value of Q3-Q1 means that all the simulations containing that specific variation exhibit energy needs close to an average value, this meaning that the other variations cannot significantly modify the thermal behavior of the building. The above-said procedure applies for both temperature ranges.

RESULTS AND DISCUSSION

This paper has investigated the effects of a pool of building element sets on the thermal behavior of a case-study winery. The results have been evaluated analyzing the energy needs of each model. In particular, this paper aims to assess the influence of each set of building elements and the influence of their single variations on the building energy needs.

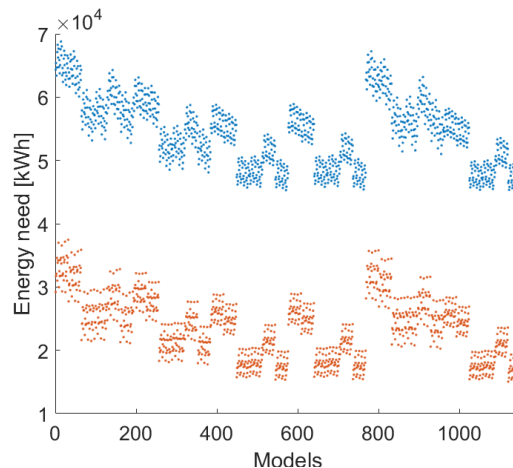
The Tab. 4 shows the thermal system working hours of all 2304 simulations. Specifically, for each thermal range, the maximum, minimum, average hours and standard deviation are exhibited. Moreover, the hourly average consumption is shown.

Table 4. Thermal system working hours

Thermal Range	Max [h]	Min [h]	Average [h]	Standard Deviation [h]	Average consumption [kWh·h ⁻¹]
12-18°C	7,116	6,377	6,723.5	154.47	3.52
20-24°C	7,356	6,562	6,883.2	146.16	7.91

The results in the Tab. 4 show the thermal system works for almost the 75% of the time in one year in order to keep the chosen temperature range in the storage room; no significant differences can be seen between the two thermal ranges. On the contrary the hourly average consumption of 20-24°C thermal range is more than double than the consumption of 12-18°C thermal range, entailing a remarkable difference in the system power sizing.

Fig. 3 shows the results of all simulations for both temperature ranges. The x -axis shows the models, the y -axis the energy needs. As expected, the graph shows the energy needs required by the temperature range 12-18°C is remarkably lower than the temperature range 20-24°C, since the first range is closer to the yearly outdoor average temperature. In both scenarios, the difference between the highest and the lowest energy need is about 25,000 kWh, this showing that a good design can reduce the energy need by 63% for the 12-18°C range and 36% for the 20-24°C range.

**Figure 3. Energy needs: simulations with 12-18°C range are in red, 20-24°C in blue**

Observing the trends, it is possible to identify several “clouds” that are created by specific building element variations. As explained in Sec. 2.6, the energy need distributions related to each single building variation are shown in the boxplots in Figs. 4 and 5.

In both the graphs, the x -axis reports the building variations, the y -axis the energy needs. For each variation, the boxplot shows the median (red line), and the limit of the first (Q1) and third (Q3) quartile (blue rectangle). It is evident that the graphs show very similar trends, this meaning that the building elements and their variations give a similar contribution to the building thermal behavior.

The variations of Walls and Roof exhibit distributions characterized by high differences between the values of their medians and the median of all simulation results (first boxplot), short whiskers, and low interquartile values, this meaning that a single wall or roof variation remarkably affects the building energy needs. In order to compare the influence of building sets and variations, the procedure described in the Sec. 2.6 has been applied and results have been reported in Tabs. 4 and 5.

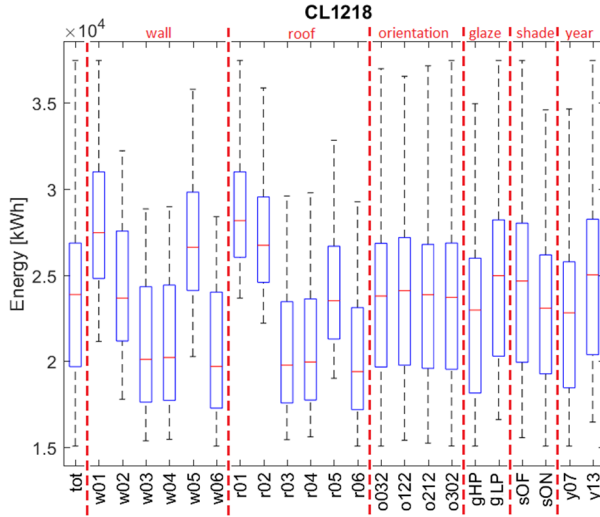


Figure 4. Boxplots for each building variation for the 12-18°C temperature range

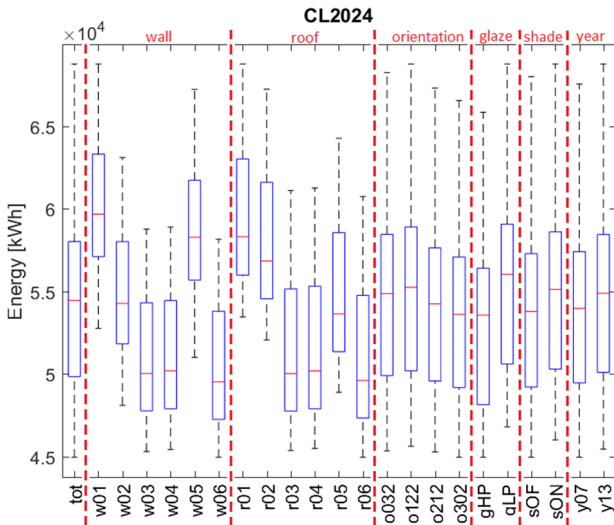


Figure 5. Boxplots for each building variation for the 20-24°C temperature range

Tab. 5 shows the standard deviations of the medians of variations belonging to the same building element set, calculated referring to the median of all simulations (first boxplot). For both temperature ranges, Walls and Roof exhibit the higher values: for the range 12-18°C Roof has more influence, for 20-24°C Walls affect more the thermal behavior.

Table 5. Building set ranking

T range 12-18°C		T range 20-24°C	
Arch. set	St.dev [kWh]	Arch. set	St.dev [kWh]
Roof	3,629.919	Walls	4,167.137
Walls	3,305.428	Roof	3,711.668
Year	1,103.185	Glazing	1,283.052
Glazing	1,005.112	Shading	671.299
Shading	793.268	Orientation	623.169
Orientation	146.141	Year	458.024

Table 6. Building variations ranking

T range 12-18°C		T range 20-24°C	
Arch. var	Q3-Q1 [kWh]	Arch. var	Q3-Q1 [kWh]
r02	4,962.229	w05	6,038.791
r01	4,965.906	w02	6,193.693
r05	5,397.382	w01	6,210.727
w05	5,715.413	w03	6,548.066
r04	5,879.876	w06	6,550.047
r03	5,888.124	w04	6,551.778
r06	5,931.621	r01	7,043.153
w01	6,198.049	r02	7,053.802
w02	6,388.459	r05	7,212.305
w04	6,703.529	r03	7,400.380
w03	6,706.031	r04	7,423.813
w06	6,742.029	r06	7,423.921
sOF	6,911.069	o302	7,906.428
tot	7,188.293	y07	7,958.652
o032	7,191.971	o212	8,067.574
o212	7,202.724	sON	8,086.688
y07	7,316.746	tot	8,178.937
o302	7,336.570	gHP	8,275.327
o122	7,414.996	sOF	8,320.198
gHP	7,833.698	y13	8,351.244
y13	7,875.501	gLP	8,462.494
gLP	7,920.850	o032	8,547.911
sON	8,084.669	o122	8,717.620

Glazing, Shading and Orientation follow the same rank for both temperature ranges. On the contrary, the influence of Year is remarkable for the first range (3rd), and almost negligible for the second range. This can be explained considering that the first temperature range accepts values very close the yearly outdoor average, and therefore it can be more sensitive to outdoor temperature trend variations.

Tab. 6 confirms and specifies what shown in the previous Tabs. The most influencing variations are elements belonging to Walls in the first range and to Roof in the second one. In particular, *w05* appears to have a high influence in both temperature ranges, and analyzing the boxplot of Figs. 4 and 5 it is clear that *w05* has a negative influence, meaning that using a wall with high transmittance and high time shift – as *w05* – requires high energy needs for which other building solutions cannot fully compensate. Therefore, *w05* should be avoided in any energy efficient building. Tab. 4 and Figs. 4 and 5 also show that solutions like *r04* (for the first temperature range) and *w03* (for the second temperature range) have a high influence on the building thermal behavior, giving a positive contribution to energy efficiency. On the contrary, the use of variations such as *gLp*, *o122* or others, does not influence significantly the thermal behavior.

CONCLUSIONS

In this work, a pool of sets of building solutions and their variations have been analyzed, showing that walls and roof have the highest influence on the building thermal behavior if compared to the other sets of building solutions. Nevertheless, the results have shown that the influence of each variation depends also on the target temperature range.

All these elements can influence the building energy need for thermal control, and thus can influence the winery running costs necessary to maintain temperature within specific ranges. The results of this work can thus help the design and construction professionals to define the best and worst solutions in new constructions, as well as to identify the most efficient interventions in building retrofit interventions. The proposed method can be extended to other agricultural and food processing and storage buildings, and can be tested for other temperature ranges.

REFERENCES

- Barbarese, A., Dallacasa, F., Torreggiani, D., Tassinari, P. (2017). Retrofit Interventions in Non-Conditioned Rooms: Calibration of an Assessment Method on a Farm Winery. *Journal of Building Performance Simulation* 10 (January): 91–104. doi:10.1080/19401493.2016.1141994.
- Barbarese, A., Torreggiani, D., Tinti, F., Tassinari, P. (2017). Analysis of the Thermal Loads Required by a Small-Medium Sized Winery in the Mediterranean Area. *Journal of Agricultural Engineering In press*: 9–20. doi:10.4081/jae.2017.670.
- Boulton, R.B., Vernon, L. Singleton, Bisson, L.F., Kunkee, R.E. (1998). *Principles and Practices of Winemaking*. Springer, New York.
- Boyano, A., Hernandez, P., Wolf, O. (2013). Energy Demands and Potential Savings in European Office Buildings: Case Studies Based on EnergyPlus Simulations. *Energy and Buildings* 65 (October): 19–28. doi:10.1016/j.enbuild.2013.05.039.
- Ente Italiano di Normazione. (2008). UNI EN ISO 13786 Thermal Performance of Building Components. *Dynamic Thermal Characteristics. Calculation Methods*.
- Marescalchi, C. (1965). *Manuale Dell Enologo (Winemaking Manual)*. Casale Monferrato: Fratelli Marescalchi.

- Mazarrón, F., López-Ocón, E., Garcimartín, M., Cañas Guerrero, I. (2013). Assessment of Basement Constructions in the Winery Industry. *Tunnelling and Underground Space Technology* 35 (April): 200–206. doi:10.1016/j.tust.2012.07.007.
- Raftery, P., Keane, M., O'Donnell, J. (2011). Calibrating Whole Building Energy Models: An Evidence-Based Methodology. *Energy and Buildings* 43 (9): 2356–64. doi:10.1016/j.enbuild.2011.05.020.
- Torreggiani, D., Barbaresi, A., Dallacasa, F., Tassinari, P. (2017). Effects of Different Architectural Solutions on the Thermal Behaviour in an Unconditioned Rural Building. The Case of an Italian Winery. *Journal of Agricultural Engineering*. In Press.
- Torreggiani, D., Benni, S., Corzani, V., Tassinari, P., Galassi, S. (2011). A Meta-Design Approach to Agroindustrial Buildings: A Case Study for Typical Italian Wine Productions. *Land Use Policy* 28 (1): 11–18. doi:10.1016/j.landusepol.2010.04.001.
- U.S. Department of Energy. (2013). *Energy Plus 8.0*.
- Vogt, E. (1971). *Fabricacion de Vinos (Winemaking)*. Editorial Acribia, Zaragoza.
- Wang, L., Gwilliam, J., Jones, P. (2009). Case Study of Zero Energy House Design in UK. *Energy and Buildings* 41 (11): 1215–22. doi:10.1016/j.enbuild.2009.07.001.



SAKUPLJANJE I ZBRINJAVANJE OTPADNIH MAZIVIH ULJA U REPUBLICI HRVATSKOJ S OSVRTOM NA STANJE U POLJOPRIVREDI

Josip TOMIĆ, Krešimir ČOPEC*, Dubravko FILIPOVIĆ, Stjepan PLIESTIĆ,
Neven VOĆA

Sveučilište u Zagrebu Agronomski fakultet, Svetošimunska 25, 10000 Zagreb, Hrvatska

*E-mail dopisnog autora: copec@agr.hr

SAŽETAK

U Republici Hrvatskoj je u razdoblju od 2007. do 2015. godine prosječni postotak sakupljenih količina otpadnih mazivih ulja iznosio 49.33% od očekivanih količina što je znatno manje u usporedbi s razvijenim europskim zemljama. Uz to je posljednjih godina primijećeno značajno smanjenje postotka sakupljenog otpadnog mazivog ulja što ukazuje da treba poraditi na poboljšanju sustava gospodarenja otpadnim mazivim uljima u Republici Hrvatskoj i unaprijediti kontrolu sakupljanja i predaje ovlaštenim sakupljačima. Gotovo sve sakupljene količine otpadnih ulja se termički oporabe, iako bi prednost trebalo dati materijalnoj oporabi. Sakupljanje i način zbrinjavanja otpadnih mazivih ulja iz poljoprivrede direktno ovisi o načinu održavanja poljoprivredne mehanizacije. U poljoprivrednim poduzećima i na većim gospodarstvima zbrinjavanje otpadnih ulja se u pravilu provodi na propisani način, ali na manjim obiteljskim gospodarstvima se u većini slučajeva otpadna maziva ulja ne zbrinjavaju na propisan način. Glavni razlozi su nemar i nedovoljna educiranost poljoprivrednika o štetnosti otpadnih ulja za okoliš.

Ključne riječi: otpadna maziva ulja, sakupljanje ulja, oporaba ulja, poljoprivredna mehanizacija

UVOD

Tijekom korištenja mazivih ulja dolazi do promjene njihovih svojstava i nakon određenog vremena eksploatacije više ne zadovoljavaju propisane zahtjeve podmazivanja te ih je potrebno zamijeniti (Bridjanian i Sattarin, 2006; Dabić i sur., 2007). Nastala otpadna maziva

ulja često karakteriziraju toksičnost i kancerogenost. Nositelji takvih osobina su različiti zagađivači i degradacijski produkti koji nastaju tijekom uporabe ulja. Stupanj toksičnosti i potencijal kancerogenosti ovise o koncentraciji i karakteru zagađivača, odnosno degradacijskih produkata. Koncentracije zagađivača i degradacijskih produkata ovise o duljini uporabe ulja, uvjetima rada i karakteristikama tehničkih sustava u kojima se koriste (Stojilković i Pavlović, 2009). Otpadna maziva ulja zbog svojih svojstava predstavljaju opasnost po ljudsko zdravlje i okoliš i svrstavaju se u opasan otpad. U Republici Hrvatskoj je 2006. godine donesen Pravilnik o gospodarenju otpadnim uljima kojim se propisuje način gospodarenja otpadnim uljima, obveznici plaćanja naknada, vrste i iznosi naknada koje plaćaju obveznici plaćanja naknada za otpadna ulja, način i rokovi obračunavanja i plaćanja naknada, iznos naknada koje se plaćaju ovlaštenim osobama za sakupljanje otpadnih ulja te druga pitanja u svezi gospodarenja otpadnim uljima (NN, 124/06). Prema tom Pravilniku otpadno mazivo ulje je svako mineralno i sintetičko mazivo, industrijsko, izolacijsko (ulje koje se rabi u elektroenergetskim sustavima) i/ili termičko ulje (ulje koje se rabi u sustavima za grijanje ili hlađenje) koje više nije za uporabu kojoj je prvotno bilo namijenjeno, posebice rabljena motorna ulja, strojna ulja, ulja iz mjenjačkih kutija, mineralna i sintetička maziva ulja, ulja za prijenos topline, ulja za turbine i hidraulička ulja osim ulja koja se primješavaju benzinima kod dvotaktnih motora s unutrašnjim izgaranjem.

Prema stupnju onečišćenja, otpadna maziva ulja se razvrstavaju u četiri kategorije:

- I. kategorija – otpadna ulja mineralnog porijekla sa sadržajem halogena ispod 0,2% i ukupnim polikloriranim bifenilima (PCB) i polikloriranim terfenilima (PCT) ispod 20 mg/kg. Ova se ulja mogu obraditi i ponovo koristiti za proizvodnju svježih ulja.
- II. kategorija – otpadna ulja mineralnog, sintetičkog i biljnog porijekla sa sadržajem halogena iznad 0,2% i ispod 0,5% i ukupnim PCB i PCT iznad 20 mg/kg i ispod 30 mg/kg. Ova se ulja mogu koristiti kao gorivo u energetskim i proizvodnim postrojenjima instalirane snage uređaja veće ili jednake 3 MW ili u pećima za proizvodnju klinkera u tvornicama cementa.
- III. kategorija – otpadna ulja nepoznatog porijekla i sva druga otpadna ulja sa sadržajem halogena iznad 0,5 %, ukupnim PCB i PCT iznad 30 mg/kg i plamištem ispod 550 °C. Ova se ulja moraju spaljivati u pećima za spaljivanje opasnog otpada minimalne djelotvornosti 99,99 %.
- IV. kategorija – poliglikoli/oliglikoli, otpadna ulja na bazi poliglikola/oliglikola koja se radi nemiješanja s ostalim uljima I. i II. kategorije i posebnih zahtjeva u postupku odstranjivanja moraju skupljati i oporabiti i/ili zbrinuti.

Zabranjeno je miješanje otpadnih ulja različitih kategorija, miješanje s drugim otpadom kao i miješanje s opasnim otpadom koji sadrži PCB/PCT. Dozvoljeno je miješanje samo otpadnih ulja I. i II. kategorije koja se predaju ovlaštenom sakupljaču za otpremu na termičku obradu. Gospodarenje otpadnim uljima mora se provoditi na način kojim se ne dovodi u opasnost ljudsko zdravlje i okoliš. Prema Pravilniku o gospodarenju otpadnim uljima (NN, 124/06), prilikom gospodarenja otpadnim uljima zabranjeno je: ispuštanje otpadnih ulja u površinske vode, podzemne vode, priobalne vode i drenažne sustave; odlaganje i/ili ispuštanje otpadnih ulja koje šteti tlu te svako nekontrolirano ispuštanje ostataka od obrade otpadnih ulja; uporaba i/ili zbrinjavanje otpadnih ulja koji uzrokuju onečišćenje zraka iznad razine propisane važećim propisima i utječu na zdravlje ljudi i biljni i životinjski svijet; sakupljanje otpadnih ulja u spremnike koji nisu propisano opremljeni za prihvat otpadnih ulja.

SAKUPLJANJE OTPADNIH MAZIVIH ULJA U REPUBLICI HRVATSKOJ

Gospodarenje otpadnim uljima je skup mjera koje obuhvaćaju prikupljanje otpadnih ulja radi materijalne oporabe ili korištenja u energetske svrhe ili nekog drugog načina konačnog zbrinjavanja kada ih nije moguće uporabiti. Sustav gospodarenja otpadnim mazivim uljima u Republici Hrvatskoj obuhvaća sljedeće procese i sudionike:

- Proizvođači svježih mazivih ulja,
- Posjednici otpadnih mazivih ulja,
- Skladištenje na mjestu proizvodnje otpadnih mazivih ulja,
- Sakupljači i prijevoznici otpadnih mazivih ulja,
- Obrada odnosno uporaba otpadnih mazivih ulja,
- Prikupljanje i obrada podataka o otpadnim mazivim uljima
- Ministarstvo zaštite okoliša i energetike
- Hrvatska agencija za okoliš i prirodu
- Fond za zaštitu okoliša i energetske učinkovitost

Proizvođači svježih mazivih ulja su pravne ili fizičke osobe koje proizvode ili uvoze i stavljaju na tržište u Republici Hrvatskoj svježih maziva ulja pri čemu plaćaju naknadu za zbrinjavanje ulja Fondu za zaštitu okoliša i energetske učinkovitost. Proizvođači ulja dužni su u suradnji s Fondom redovno obavještavati prodavatelje ulja o načinu i mjestima skupljanja otpadnih ulja na način da se izbjegne nastajanje rizika i opasnosti po okoliš i zdravlje ljudi. Prodavatelji koji prodaju svježe mazivo ulje dužni su osigurati kupcu obavijest o mjestu na kojem može predati svoje otpadno ulje bez naplate naknade.

Posjednici otpadnih mazivih ulja su pravne ili fizičke osobe koje posjeduju otpadna ulja i pri čijem obavljanju djelatnosti stalno ili povremeno nastaju otpadna ulja. Posjednici otpadnih ulja dužni su osigurati sakupljanje i privremeno skladištenje otpadnih ulja nastalih njihovom djelatnošću u spremnike za sakupljanje otpadnog mazivog ulja koji moraju biti nepropusni i zatvoreni i uz propisanu oznaku ključnog broja otpadnog ulja moraju nositi i oznaku kategorije otpadnog ulja. Posjednici otpadnih ulja i svi koji gospodare otpadnim uljima dužni su voditi Očevidnik nastanka i tijeka otpadnih ulja (ONTOU) koji se vodi na propisanom obrascu. Uz Očevidnik posjednici otpadnih ulja dužni su za svaku godinu voditi evidenciju o ukupnim količinama kupljenog svježeg ulja, količinama proizvedenog otpadnog ulja, količinama predanim ovlaštenim osobama za gospodarenje otpadnim uljima i ostalim podacima prema posebnim propisima. Posjednici otpadnih ulja dužni su predati otpadna ulja ovlaštenom sakupljaču otpadnih ulja uz popunjeni prateći list koji je sakupljač dužan ovjeriti prilikom preuzimanja otpadnih ulja. Ovlašteni sakupljač otpadnih ulja dužan je preuzeti od posjednika otpadna ulja bez naknade, a za svoje usluge koje uključuju sakupljanje, privremeno skladištenje i prijevoz dobiva naknadu koju mu isplaćuje Fond za zaštitu okoliša i energetske učinkovitost. Ovlašteni sakupljač otpadnih ulja dužan je voditi evidenciju o količini i vrsti sakupljenih otpadnih ulja, te o količini i vrsti otpadnog ulja kojeg je predao ovlaštenoj osobi za uporabu i/ili zbrinjavanje otpadnih ulja. Ovlaštena tvrtka za uporabu otpadnog mazivog ulja dužna je od ovlaštenih sakupljača zaprimiti ulje i bez naknade ga daljnjim postupcima obraditi odnosno zbrinuti. Osobe ovlaštene za sakupljanje i uporabu i/ili zbrinjavanje otpadnih ulja dužne su Hrvatskoj agenciji za okoliš i prirodu i inspekciji zaštite okoliša Ministarstva zaštite okoliša i energetike svaka tri mjeseca dostaviti izvješće na propisanom obrascu s podacima o: sakupljenim vrstama i količinama otpadnih ulja koje su predane ovlaštenoj osobi za uporabu i/ili zbrinjavanje otpadnih ulja i vrsti i

količini oporabljeno i/ili zbrinuto otpadno ulja i vrsti i količini izvezenog otpadnog ulja iz Republike Hrvatske (NN, 124/06; Muharemi, 2012).

U Tablici 1. su prikazane ukupne količine svježih mazivih ulja stavljenih na tržište u Republici Hrvatskoj u razdoblju od 2007. do 2015. godine. U tom razdoblju najveća količina svježih mazivih ulja stavljena je na tržište Republike Hrvatske 2008. godine. Slijedeće dvije godine dolazi do značajnog pada potrošnje mazivih ulja, a nakon toga potrošnja stagnira sve do 2015. godine. Uzroci pada potrošnje maziva su loša gospodarska situacija, recesija, zaustavljanje ili prestanak funkcioniranja industrije sa zastarjelom tehnologijom većinom u državnom vlasništvu, te korištenje strojeva i vozila nove generacije i tehnologije (Mandaković i Novina, 2015). Tek 2015. godine dolazi do značajnog porasta količine stavljenih svježih mazivih ulja na tržište Republike Hrvatske od 43.86% u odnosu na prethodnu godinu, odnosno 48.77% u odnosu na prosječnu količinu svježih mazivih ulja stavljenih na tržište Republike Hrvatske godišnje u razdoblju od 2010. do 2014. godine.

Tablica 1. Ukupne količine svježih mazivih ulja stavljenih na tržište u Republici Hrvatskoj u razdoblju od 2007. do 2015. godine
Table 1. Total quantities of fresh lubricant oils placed on the Croatian market during period 2007.-2015.

Godina/Year	2007.	2008.	2009.	2010.	2011.	2012.	2013.	2014.	2015.
Proizvedeno ulja (t) Produced oils (t)	12501	12413	10417	7031	9205	6723	5535	6789	16852
Uvezeno ulja (t) Imported oils (t)	23794	28518	24212	22939	25095	22253	21214	21889	22079
Izvezeno ulja (t) Exported oils (t)	4816	5355	10567	9482	9633	7757	5723	5887	6144
Stavljeno ulja na tržište (t) Placed on the market oils (t)	31478	35576	24062	20488	24667	21219	21026	22791	32786

Izvori: AZO (2014), HAOP (2016a), HAOP (2016b)

Bez obzira na to što su stupanjem na snagu Pravilnika o gospodarenju otpadnim uljima (NN, 124/06) ukinuti faktori skupljanja iz Pravilnika o vrstama otpada (NN, 27/1996), činjenica je da se ne može skupiti svo ulje koje se stavi u promet. Razlog su gubici zbog isparivosti, manipulacije, prijevoza, načina primjene, havarija u primjeni, gubitaka na filtrima i sl., tako da se za maziva ulja koristi prosječni faktor povrata 0.5 (Čizmić i sur., 2004; Sofilić i sur., 2014). U Tablici 2. su prikazane očekivane, sakupljene i oporabljene količine otpadnih mazivih ulja u Republici Hrvatskoj u razdoblju od 2007. do 2015. godine. Iz tablice je vidljivo da sakupljene količine otpadnog mazivog ulja nisu ovisile o količinama svježih mazivih ulja stavljenih na tržište, čak je u godinama u kojima su stavljene na tržište najveće količine svježih mazivih ulja (2007, 2008 i 2015) bio znatno manji postotak sakupljenih otpadnih ulja od očekivanih količina (32.88-39.73%). S druge strane najveći postotak od očekivane količine otpadnih mazivih ulja (64.82%) sakupljen je 2010. godine. Razlog tome najvjerojatnije je taj što je te godine najmanja količina ulja stavljena na tržište pa je samim tim i postotak sakupljenih količina u odnosu na količine stavljene na tržište bio veći. Hrvatsko društvo za goriva i maziva je 2008. godine u Zagrebu organiziralo seminar o gospodarenju otpadnim uljima na kojem je zaključeno da bi godišnji trend poboljšanja učinkovitosti skupljanja ulja trebao biti oko 10% kako bi se do 2012. godine ostvario zadani cilj od 90% sakupljenih

količina otpadnih mazivih ulja od očekivane količine (Podgorčić, 2008). Nažalost, to se nije ni približno ostvarilo, čak je uslijedio značajan pad postotka sakupljenog otpadnog mazivog ulja što je kulminiralo 2015. kada su u postocima sakupljene najmanje količine otpadnog mazivog ulja u cijelom razdoblju od 2007. do 2015. godine. Prosječni postotak sakupljenog otpadnog ulja u tom razdoblju iznosio je 49.33% očekivane količine. Taj postotak je vrlo mali u odnosu na razvijene europske zemlje gdje se on kreće oko 80%. Za primjer se može uzeti Republika Irska koja je po količinama otpadnog mazivog ulja dosta slična Republici Hrvatskoj gdje se prikupi 86% od očekivanih količina otpadnih mazivih ulja (Audibert, 2006). Budući da se više od polovice proizvedenog otpadnog mazivog ulja ne prikupi pretpostavlja se da taj dio ulja završi u okolišu odnosno da se njime zagađi voda i tlo ili se nepropisnim spaljivanjem u malim privatnim pećima zagađuje atmosfera štetnim plinovima izgaranja. Prema podacima Fonda za zaštitu okoliša i energetske učinkovitost za 2014. i 2015. godinu, najznačajnije količine otpadnih mazivih ulja sakupljene su u Gradu Zagrebu i Zagrebačkoj županiji 23%, te u Splitsko-dalmatinskoj županiji 14%, a zatim slijede Primorsko-goranska županija 9%, Osječko-baranjska županija 8% i Zadarska županija 7%. Najmanje količine otpadnih mazivih ulja sakupljene su u Ličko-senjskoj, Virovitičko-podravskoj i Požeško-slavonskoj županiji (HAOP, 2016a; HAOP, 2016b).

Tablica 2. Očekivane, sakupljene i oporabljene količine otpadnih mazivih ulja u Republici Hrvatskoj u razdoblju od 2007. do 2015. godine
Table 2. Expected, collected and recovered quantities of waste lubricant oils in Republic of Croatia during period 2007.-2015.

Godina/Year	2007.	2008.	2009.	2010.	2011.	2012.	2013.	2014.	2015.
Očekivano otpadnih ulja (t) Expected waste oils (t)	15739	17788	12031	10244	12334	10610	10513	11396	16393
Sakupljeno otpadnih ulja (t) Collected waste oils (t)	6115	7068	6784	6640	6391	5835	5678	5753	5390
Sakupljeno otpadnih ulja (%) Collected waste oils (%)	38.85	39.73	56.39	64.82	51.82	55.00	54.01	50.48	32.88
Oporabljeno otpadnih ulja (t) Recovered waste oils (t)	6364	7131	6842	6535	5906	5125	4829	5244	6830
Oporabljeno otpadnih ulja (%) Recovered waste oils (%)	104.07	100.89	100.85	98.42	92.41	87.83	85.05	91.15	126.72

Izvori: AZO (2014), HAOP (2016a), HAOP (2016b)

ZBRINJAVANJE I OPORABA OTPADNIH MAZIVIH ULJA U REPUBLICI HRVATSKOJ

Otpadna maziva ulja treba zbrinuti tako da se što više iskoristi njihova ekonomska vrijednost kao korisne sekundarne sirovine, ali da se pri tome vodi računa o zaštiti okoliša i zdravlja ljudi (Podgorčić, 2008). Prema Pravilniku o gospodarenju otpadnim uljima kojim se propisuje način gospodarenja otpadnim uljima u Republici Hrvatskoj, prihvatljivi načini zbrinjavanja otpadnih mazivih ulja su oni kojima se vrši njihova oporaba (NN, 124/06). Prema istom Pravilniku predviđena su dva načina oporabe: materijalna oporaba i termička oporaba.

Pod materijalnom oporabom otpadnih mazivih ulja podrazumijeva se svaki postupak oporabe kojim se dobiva novi proizvod ili se procesom pročišćavanja (rafiniranjem) omogućuje njihova ponovna uporaba. Materijalnu oporabu otpadnih mazivih ulja u svrhu dobivanja komercijalno upotrebljivih proizvoda moguće je danas ostvariti različitim postupcima. Koji postupak materijalne oporabe otpadnih mazivih ulja će se koristiti ovisi o stupnju kontaminacije i degradacije ulja. Najjednostavniji i najjeftiniji je postupak pročišćavanja, ali se njime mogu uporabiti samo ona otpadna maziva ulja koja nisu jako kontaminirana i kemijski degradirana. Postupak rerafinacije zahtijeva relativno složenu tehnologiju da bi se dobila kvalitetna bazna ulja. Rerafinacija se posebno stimulira kod otpadnih motornih ulja, jer su ona dominantna po količini sakupljenih otpadnih ulja i takvog nivoa degradacije da se drugi postupak ne može koristiti u cilju ponovnog dobivanja maziva (Rac i Vencl, 2012; Shri Kannan i sur., 2014; Kulkarni, 2017). Mogu se koristiti i drugi postupci materijalne oporabe kao što su različiti postupci kemijske obrade, postupci aktiviranja kiselinom, postupci fizikalne obrade destilacijom i isparavanjem, ekstrakcija raznim otapalima i drugi postupci (Aremu i sur., 2015).

Prema Pravilniku o gospodarenju otpadnim uljima u Republici Hrvatskoj (NN, 124/06), materijalna oporaba otpadnih ulja ima prednost pred ostalim načinima oporabe. U slučaju da se otpadna ulja ne oporabljaju materijalnom oporabom već se oporabljaju termičkom obradom, mora se osigurati da se termička obrada obavlja prema propisima koji uređuju područje zaštite okoliša u energetske i proizvodnim postrojenjima instalirane snage uređaja veće ili jednake 3 MW. Termička oporaba mazivih ulja je proces oporabe u kojem se otpadno ulje koristi kao energent odnosno gorivo i može se provesti na dva načina. Prvi je da se otpadno ulje koristi samo kao gorivo, a drugi je da ga se miješa s nekim drugim gorivom u pećima za izgaranje. Glavni nedostatak termičke oporabe otpadnog mazivog ulja je taj što je potrebno smanjiti emisiju štetnih tvari u dimnim plinovima nastalih njegovim izgaranjem. Također, prije početka postupka oporabe potrebno je iz otpadnog mazivog ulja ukloniti gotovo sve čestice metala jer u protivnome dolazi do pojačanog trošenja dijelova sustava za dobavu goriva. Termička oporaba otpadnih ulja primjenjuje se ponajviše u cementarama, ciglanama i postrojenjima za proizvodnju asfalta.

Iz Tablice 2. je vidljivo da se gotovo sve sakupljene količine otpadnih mazivih ulja u Republici Hrvatskoj oporabe. U razdoblju od 2007. do 2015. godine od sakupljenih količina otpadnih mazivih ulja prosječno je oporabljeno 98.60%. U nekim godinama je postotak oporabe bio veći od 100%, a razlog su oporabljene uskladištene količine iz prethodnih godina. U Republici Hrvatskoj proces materijalne oporabe ulja vrši samo jedna tvrtka koja vrši oporabu manjih količina otpadnih mazivih ulja koje se kreću u prosjeku oko 50 tona godišnje što iznosi manje od 1% od ukupne količine oporabljenog otpadnog mazivog ulja. Svi ostali uporabitelji vrše termičku oporabu ulja tako da otpadna maziva koriste kao gorivo u pećima u procesu proizvodnje cementa ili cigle. Iz navedenih podataka može se zaključiti

da se gotovo sva otpadna maziva ulja sakupljena u Republici Hrvatskoj termički oporabljaju kod domaćih oporabljivača, kojima ne bi bio problem oporabiti i veće količine otpadnog mazivog ulja kad bi ih se uspjelo sakupiti.

OSVRT NA STANJE U POLJOPRIVREDI REPUBLIKE HRVATSKE

Stanje sa sakupljanjem otpadnih mazivih ulja u poljoprivredi Republike Hrvatske je dvojako. U većini poljoprivrednih poduzeća je stanje zadovoljavajuće jer ona u većini slučajeva pravilno zbrinjavaju otpadna maziva ulja iskorištena za podmazivanje traktora, kombajna i druge poljoprivredne mehanizacije. Veća poduzeća u pravilu imaju vlastitu službu održavanja poljoprivredne mehanizacije koja sakupljena otpadna maziva ulja skladišti u odgovarajuće spremnike do predaje ovlaštenom sakupljaču. Pri tome u pravilu vode evidenciju o ukupnim količinama kupljenog svježeg ulja, količinama proizvedenog otpadnog ulja i količinama predanim ovlaštenom sakupljaču otpadnih ulja (Jakobović, 2016). Manja poljoprivredna poduzeća održavanje poljoprivredne mehanizacije u većini slučajeva povjeravaju ovlaštenim servisima koji također u pravilu na propisani način sakupljaju i skladište otpadna maziva ulja te ih predaju ovlaštenom sakupljaču i pri tome vode odgovarajuću evidenciju.

Sasvim drugačije stanje je na manjim obiteljskim gospodarstvima na kojima se u većini slučajeva otpadna maziva ulja ne zbrinjavaju na propisan način. Takvi slučajevi se u pravilu događaju na obiteljskim gospodarstvima na kojima vlasnici sami mijenjaju ulje ili to povjeravaju neovlaštenim osobama koja ispuštena ulja ostavljaju na raspolaganje vlasnicima poljoprivredne mehanizacije. Najčešći način na koji se poljoprivrednici rješavaju otpadnog ulja je spaljivanje u improviziranim pećima bez ikakvih pročišćivala ispušnih plinova čime se vrši velika emisija štetnih, a često i otrovnih tvari i spojeva u atmosferu. S obzirom da se po zakonu otpadno mazivo ulje ne smije spaljivati niti suspaljivati u pećima slabijim od 3 MW, ovakav način oporabe otpadnog ulja je neprihvatljiv. Pri tome proizvođači otpadnog mazivog ulja zbog neznanja poistovjećuju otpadno ulje s loživim uljem pa ga iz tog razloga spaljuju, no posljedice za atmosferu su opasne zbog sadržaja teških metala i drugih opasnih spojeva. Ipak treba napomenuti da ima i pozitivnih primjera da obiteljska gospodarstva koja sama mijenjaju ulje pravilno uskladište otpadna ulja i jednom godišnje predaju ovlaštenom sakupljaču ili izmjenu ulja vrše kod lokalnog serviseru koji to ulje uskladišti do predaje ovlaštenom sakupljaču (Tomić, 2016).

Kiš i sur. (2007) su proveli anketu o načinu zbrinjavanja rabljenog ulja iz motora i transmisije poljoprivrednih traktora i drugih samokretnih strojeva na obiteljskim poljoprivrednim gospodarstvima u Osječko-baranjskoj i Vukovarsko-srijemskoj županiji. Anketa je dala poražavajuće rezultate jer se pokazalo da od 50 anketiranih obiteljskih gospodarstava u Osječko-baranjskoj županiji niti jedno ne zbrinjava rabljeno motorno ulje na propisani način, dok od 35 anketiranih obiteljskih gospodarstava u Vukovarsko-srijemskoj županiji samo jedno predaje rabljeno motorno ulje ovlaštenom sakupljaču otpadnih mazivih ulja. U Osječko-baranjskoj županiji većim dijelom rabljeno motorno ulje koristi se za zaštitu poljoprivrednih strojeva, za bojanje drvene ograde, kao samostalno gorivo za peći ili kao komponenta mješavine s piljevinom. U Vukovarsko-srijemskoj županiji najvećim dijelom, odnosno 40% od ukupnog broja ispitanika, rabljeno motorno ulje koristi za tehničku zaštitu poljoprivredne mehanizacije, iako uporaba istog za tehničku zaštitu nije dopuštena (Jurić i sur., 2001.). Ostali direktnim radnjama utječu na onečišćenje okoliša, tla i podzemnih voda sljedećim postupcima: izlivanjem otpadnog ulja u kanalizaciju, izlivanjem u melioracijske kanale, miješanjem s komunalnim otpadom iz kućanstava, skladištenjem u plastičnim posudama u kojima su kupili novo ulje te bacanjem u komunalni otpad. Pri tome se na

nijednom gospodarstvu nije vodila propisana evidencija o količinama kupljenog svježeg ulja i količinama proizvedenog otpadnog ulja. Slična situacija je i s rabljenim uljima iz transmisije. U obje županije većina ispitanika rabljeno ulje iz transmisije koristi za tehničku zaštitu poljoprivredne mehanizacije, a ostali direktno onečišćuju okoliš korištenjem ulja kao goriva u pećima, izlivanjem u kanalizaciju, izlivanjem u melioracijske kanale, bacanjem u otpad, ispuštanjem u polju i spaljivanjem na otvorenom prostoru. Glavni razlozi nepravilnog zbrinjavanja otpadnih mazivih ulja iz poljoprivrede na obiteljskim gospodarstvima su nemar i nedovoljna educiranost poljoprivrednika o štetnosti otpadnih ulja za okoliš. Ostali razlozi tome bi mogli biti premali broj ovlaštenih sakupljača otpadnih ulja ili njihova loša organiziranost u pogledu sakupljanja ulja i informiranja poljoprivrednika o pravilnom načinu zbrinjavanja otpadnog ulja (Tomić, 2016). Ne treba očekivati da će se stanje u pogledu zbrinjavanja rabljenog ulja u skoroj budućnosti popraviti i doći samo od sebe. Stoga treba provoditi redovite kontrole na obiteljskim poljoprivrednim gospodarstvima te educirati poljoprivredne proizvođače (Kiš i sur. 2007).

ZAKLJUČCI

Zbrinjavanje otpadnih mazivih ulja u Republici Hrvatskoj je na nezadovoljavajućoj razini, prvenstveno što se tiče dijela sakupljanja. Oporaba sakupljenih otpadnih ulja je zadovoljavajuća jer se iz objavljenih podataka može zaključiti da se gotovo sve sakupljene količine na kraju i oporabe, ali pri tome treba naglasiti da se gotove sve količine termički oporabe iako bi materijalna oporaba trebala imati prednost pred ostalim načinima oporabe. Što se tiče unaprjeđenja sustava sakupljanja otpadnih ulja, jedno od rješenja bi moglo biti u tome da se dio naknade namijenjene zbrinjavanju ulja koja se u cijelosti isplaćuje sakupljačima otpadnog ulja isplaćuje i proizvođačima otpadnog ulja po predanoj litri ulja kao poticaj za pravilno zbrinjavanje ulja. Trebalo bi poraditi i na povećanju broja ovlaštenih sakupljača u Republici Hrvatskoj koji se iz nekog razloga iz godine u godinu smanjuje kako bi se povećala pokrivenost pojedinih područja i omogućilo proizvođačima otpadnih ulja odlaganje na mjestima što bližima njihovom gospodarskom dvorištu. Sakupljanje i način zbrinjavanja otpadnih mazivih ulja iz poljoprivrede direktno ovisi o načinu održavanja poljoprivredne mehanizacije. U poljoprivrednim poduzećima koja imaju vlastitu službu održavanja i na većim gospodarstvima koja održavanje povjeravaju ovlaštenim servisima razina zbrinjavanja otpadnih ulja je zadovoljavajuća što se ne može reći za manja obiteljska gospodarstva na kojima vlasnici sami mijenjaju ulje ili to povjeravaju neovlaštenim osobama. U takvim slučajevima često se otpadna maziva ulja zbrinjavaju na sasvim neprihvatljive načine kojima se dovodi u opasnost ljudsko zdravlje i okoliš. Glavni razlozi tome su nemar i nedovoljna educiranost poljoprivrednika o štetnosti otpadnih ulja za okoliš te bi trebalo poraditi na educiranju poljoprivrednika.

LITERATURA

- Aremu, M.O., Araromi, D.O., Dauda, O., Gbolahan, O.O. (2015). Regeneration of used lubricating engine oil by solvent extraction process. *International Journal of Energy and Environmental Research*, 3, 1-12.
- Audibert F. (2006). *Waste Engine Oils Rerefining and Energy Recovery*. Elsevier Science & Technology Books, Amsterdam.
- AZO (2014). *Izvještaj o otpadnim uljima za 2012. i 2013 godinu*. Agencija za zaštitu okoliša, Zagreb.

- Bridjianian, H., Sattarin, M. (2006). Modern recovery methods in used oil re-refining. *Petroleum & Coal*, 48, 40-43.
- Dabić, P., Krolo, P., Lucić, S. (2007). Promjena pojedinih svojstava rabljenih motornih ulja. *Zbornik radova 12. Savjetovanja o materijalima, tehnologijama, trenju i trošenju*, Vela Luka, 46-51.
- Čizmić, V., Pancocha, D., Anić, T., Barišić, A. (2004). Zbrinjavanje rabljenih ulja. *Goriva i maziva*, 43, 279-297.
- HAOP (2016a). Pregled podataka za posebne kategorije otpada za razdoblje do 2014. godine. Hrvatska agencija za okoliš i prirodu, Zagreb.
- HAOP (2016b). Pregled podataka za posebne kategorije otpada za razdoblje od 2008 do 2015. godine. Hrvatska agencija za okoliš i prirodu, Zagreb.
- Jakobović, J. (2016). Gospodarenje otpadom u tvrtki za održavanje poljoprivrednih strojeva. *Završni rad. Sveučilište J.J. Strossmayera u Osijeku Poljoprivredni fakultet, Osijek*.
- Jurić, T., Emert, R., Šumanovac, L., Horvat, D. (2001). Provođenje mjera održavanja na obiteljskim gospodarstvima. *Zbornik radova "Aktualni zadaci mehanizacije poljoprivrede"*, Opatija, 43-49.
- Kiš, D., Plaščak, I., Voća, N., Arežina, M. (2007). Motorno ulje – opasan otpad? *Poljoprivreda*, 13, 53-58.
- Kulkarni, S.J. (2017). Re-refining of used oil - an insight. *International Journal of Petroleum and Petrochemical Engineering*, 3, 37-40.
- Mandaković, R i Novina, B. (2015). Trendovi potrošnje, zahtjevi za kvalitetom kao i paradoksi na vrlo malom tržištu maziva kao što su Hrvatska i susjedne zemlje. *Goriva i maziva*, 54, 187-200.
- Muharemi, S. (2012). Iskustva u tri godine sustava gospodarenja otpadnim mazivim uljima. *Goriva i maziva*, 51, 216-226.
- NN (1996). Pravilnik o vrstama otpada. *Narodne novine*, 27/1996, Zagreb.
- NN (2006). Pravilnik o gospodarenju otpadnim uljima. *Narodne novine*, 124/06, Zagreb.
- NN (2013). Zakon o održivom gospodarenju otpadom. *Narodne novine*, 94/13, Zagreb.
- Podgorčić, D. (2008). Otpadna ulja su korisna, ali opasna sekundarna sirovina. *Goriva i maziva*, 47, 191-192.
- Rac, A., Vencl, A. (2012). Ecological and technical aspects of the waste oils influence on environment. *The Annals of University "Dunarea de Jos" Galati, Fascicle VIII Tribology*, 18, 5-11.
- Shri Kannan, C., Mohan Kumar, K.S., Sakeer Hussain, M., Deepa Priya, N., Saravanan, K. (2014). Studies on reuse of re-refined used automotive lubricating oil. *Research Journal of Engineering Sciences*, 3, 8-14.
- Sofilić, T., Šomek-Gvoždak, V., Brnardić, I. (2014). Croatian experience in waste oil management. *Ecologia Balkanica*, 6, 109-119.
- Stojilković, M., Pavlović, M. (2009). Utjecaj maziva na okoliš. *Goriva i maziva*, 48, 75-81.
- Tomić, J. (2016). Karakteristike suvremenih ulja za traktore i načini zbrinjavanja rabljenog ulja u Republici Hrvatskoj. *Diplomski rad. Sveučilište u Zagrebu Agronomski fakultet, Zagreb*.

COLLECTION AND DISPOSAL OF WASTE LUBRICANT OILS IN THE REPUBLIC OF CROATIA WITH A VIEW TO STATE IN AGRICULTURE

SUMMARY

In the period from 2007. to 2015. the average percentage of collected waste lubricant oils in the Republic of Croatia was 49.33% of the expected quantities, which is a significantly lower percentage compared to the situation in developed European countries. In addition, in recent years was observed a significant decrease in the percentage of collected waste lubricating oil, which indicates that the improvement of the waste lubricating oil management system in the Republic of Croatia needs to be improved and the control of collecting and delivering to authorized collectors should be improved. Almost all the collected quantities of waste oils are thermally recovered, though the advantage should be given to material recovery. Collecting and disposing of waste lubricant oils from agriculture is directly dependent on the way of agricultural mechanization maintaining. In agricultural companies and in larger economies, waste oil disposal is generally carried out in the prescribed manner, but in smaller family farms, in most cases, waste lubricants are not properly disposed. The main reasons are negligence and inadequate educated farmers about the harm of waste oils on environment.

Key words: waste lubricant oils, oils collection, oil recovery, agricultural machinery



NEW CURRICULA AND TEACHING PROGRAMMES ON SUSTAINABLE AGRICULTURE: THE "SAGRI" PROJECT

Pietro PICUNO*, Dina STATUTO

University of Basilicata - SAFE School, via dell'Ateneo Lucano 10, 85100 Potenza, Italy

*E-mail of corresponding author: pietro.picuno@unibas.it

SUMMARY

In the European Union almost 50% of the territory is covered by farmland, which means that agriculture plays a key role in land management, having also a huge responsibility in the preservation of natural resources. In order to practice a sustainable agriculture, farmers and other agricultural operators must adopt correct and environmentally-friendly practices, using appropriate technology and complying with relevant regulations. Recent developments in science and technology are however still unfortunately unutilized in many situations even since - as a recent survey conducted for the European Commission revealed - only 17% of farmers has finished a basic or full training specifically focused on agriculture-related disciplines. In the present paper, the main results achieved so far by the European Project: "*Skills Alliance for Sustainable Agriculture - SAGRI*" are presented. SAGRI is a project financed by the Erasmus+ Programme of the European Commission aimed to give a decisive answer to the request of better trained farmers, agricultural workers and extension staff, thanks to structuring specific courses aimed to increase their knowledge, competence and skills in the field of agro-environmental technology for sustainable agriculture. Through the institution of suitable concerted and standardized study curricula and relevant teaching programmes, the SAGRI Project is aimed to increase the technological level for agricultural operators, then promoting their employment as well.

Keywords: sustainable agriculture; new technologies; farmer skills; study curricula

INTRODUCTION

In the European Union almost 50% of the territory is covered by farmland (both arable and permanent grassland), which means that agriculture plays a key role in land management, having a huge responsibility in the preservation of natural resources as well. In

order to practice a sustainable agriculture, farmers responsible for the management of farmland and other agricultural operators must adopt correct and environmental-friendly practices, using appropriate technology and complying with relevant EU regulations. Recent developments in science and technology, that could be an added value for farmers' crop and land management, are still unutilized in many situations, since farmers have not been introduced to them or have not been trained to use them. "Sustainable agriculture" means an integrated system of plant and animal production practices aimed to:

- Satisfy human food and fiber needs;
- Enhance environmental quality and the natural resource base for agricultural activities;
- Make an efficient use of non-renewable and on-farm resources;
- Sustain the economic viability of farm operations;
- Enhance the quality of life for farmers and society as a whole.

Recent developments in science and technology - that could be an added value for farmers' crop and land management - are however still unfortunately unutilized in many situations, since farmers have not been introduced to them or have not been trained to use them. A critical issue in the 21st century for increasing the sustainability of agricultural production is therefore constituted by the changes and adaptations required in agricultural education aimed to more effectively contribute to improve sustainable agricultural production and rural development. Poor training of agricultural extension staff has been identified as a crucial part of the problem of the relative ineffectiveness of much of extension in the field. This applies not only to extension staff, but to agricultural operators in general. Nevertheless, training of human resources in agriculture is often not a priority in the EU countries' development plans. A recent survey conducted for the European Commission revealed indeed that the majority of the farmers in Europe have received only secondary education (57%) while 15% had only primary education, 16% post-secondary (non-tertiary) education and 12% had tertiary education. Only 17% of farmers finished a basic or full training focused on agriculture-related disciplines.

In the present paper, the main results achieved so far by the European Project: "*Skills Alliance for Sustainable Agriculture - SAGRI*" (Sagri, 2016) are presented. SAGRI is a project financed by the Erasmus+ - *Sector Skills Alliances* - Programme of the European Commission aimed to give, through a trans-national multi-actors approach, a decisive answer to the request of better trained farmers, agricultural workers and extension staff, thanks to structuring specific courses aimed to increase their knowledge, competence and skills in the field of agro-environmental technology for sustainable agriculture. Through the institution of suitable concerted and standardized study curricula and relevant teaching programmes specialized into the most recent developments of science and technology, the SAGRI Project is aimed to increase the technological level for agricultural operators. The official certification of the SAGRI courses will make agricultural operators even more employable, thanks to an enhanced mobility across EU countries, since their own competences will be recognized under the framework of the SAGRI system.

MATERIALS AND METHODS

The contents and relevant Learning Outcomes of the SAGRI courses result from a cross-linking approach connecting the expectations coming from the primary sector – through the farmers associations which are participating into this Project – on the basis of the awareness of farmers, agricultural workers and extension staff in terms of green and

digital/technological skills, once they are intersected with the most recent developments in science and technology - detected and focused by the Universities belonging to the SAGRI Partnership Consortium. They concern:

- Green skills. Skilled agricultural workers increasingly need to have a holistic awareness of sustainability, *i.e.*: understanding climate changing, the need for carbon emission reduction, renewable energy, biomass valorisation and biofuels, water resources and ecosystems management, integrated pest management, to be updated with new regulations and legislation.
- Digital or technological skills. Skilled agricultural workers will need to be able to understand and apply new technologies related to: primary production for both food and non-food uses, soil science, crop and livestock genetics, agri-chemicals, precision technology and general purpose technologies such as remote sensors, satellites and robotics.

Framework conditions under which the SAGRI courses are conceived consider that:

- Technology itself is not sufficient and a well-trained team is also required. Investing solely in technology will not ensure successful implementation of ICT applications; it is necessary to invest in a team that can effectively perform tasks, investing in capacity development of end users who can ensure the sustainability of the project.
- Complex ICT or complex platforms are not necessarily essential: technologies already being used by farmers are anyway taken into consideration.
- Contextual factors: local factors such as the lack of adequate resources must be taken into account beforehand (*e.g.* electricity, gender issues, limited network coverage and low bandwidth, local languages, *etc.*). Implementation approaches need to identify the specific needs of the intended users by working in collaboration with them. There is not one single solution that fits all projects: context, policies, marketing efforts and incentives are all essential factors to ensure participation from community members.
- Data integrity and security must be ensured throughout the project and when using ICT applications. Experts agreed that leveraging location data and other metadata with individual records helps maintain integrity.
- Agricultural worker or farmer would have a minimum education level of high school and a basic knowledge and experience in agriculture at a practical level.

Of course, not all agricultural workers or farmers have sufficient knowledge to understand all the new developments in agriculture applied research, since some of them require a minimum education level. Therefore, prior to identifying the skills, the agricultural worker profile to whom they are destined was defined.

Seven major areas were therefore identified in significant technological developments that can help farmers for a more sustainable agriculture:

1. Precision technology.
2. Remote sensing to assess land capability.
3. Integrated pest management in plant protection.
4. Agricultural reuse of organic residuals.
5. Drip irrigation and water-conserving technologies.
6. Renewable energy and its application as green agricultural energy source.
7. Bioenergy and energy crops.

These skills are the basis for the developing of new innovative curricula integrating the latest advancements of the “agri-tech” sector, and training courses for agricultural workers according to the EQF/ECVET framework.

RESULTS AND DISCUSSION

Transversal skills

Although the analysis was mainly focused about the job-specific skills for agricultural workers, there are some generic and transversal skills that agricultural workers need to have in order to adapt to changing production processes, and to other sector-specific changes and challenges (Cedefop, 2016). Agricultural workers are the women and men who labour in the crop fields, orchards, glasshouses, livestock units, and primary processing facilities to produce the world's food and fibres. They are employed on small- and medium-sized farms, as well as large industrialized farms and plantations. In an integrated farming approach, a correct management and a balanced approach of every farm decision is needed and some specific points cover essential elements of a whole farm management approach:

- Organisation & planning: Planning and evaluation of practices is essential to ensure environmentally responsible production and continuous improvement.
- Human & Social Capital: Standards of employment practice, health and safety at work, and occupational training need to embrace EU standards of employment practice as minimum standard. Using local markets will help to maintain both local business and livelihoods and can also improve efficiency. Besides, open and active involvement of the farmer in local community's life can help generate transparency and trust. This can also include hosting farm visits or holding open days for the public.
- Energy Efficiency: Awareness of sustainable development and the responsible management of natural resources are central. More careful and selective use of inputs, conservation tillage practices, reducing fossil fuel needs where possible and striving for optimum instead of maximum yields are just some strategies to increase the input-output-ratio and hence energy efficiency.
- Water Use & Protection: Use of water resources should be balanced and programmes which determine crop needs should be used. Protecting natural ground and surface water bodies is a key for maintaining and enhancing the environment, wildlife and biodiversity.
- Climate Change & Air Quality: By working in the open, using fossil fuels, keeping livestock, storing and spreading manure and by other agricultural practices, the emission of greenhouse gases and other air pollutants is unavoidable. Farmers' decisions may help to keep carbon stocks in soils by allocating land to annual or perennial crops, to grassland, woods or buffer zones (such as hedges, grass strips, *etc.*). Some practices on reduced tillage or cover crops or incorporation of crop residues to soil may even increase the carbon sequestration to a certain extent and also help to improve air quality.
- Soil Management: Soil is fundamental to agricultural systems and a rich soil ecosystem contributes to crop and livestock performance: “The quality of life below ground determines productivity above”. Good soil husbandry ensures the long-term fertility of soil aids yield and profitability and reduces the risk of soil damage such as erosion, compaction and associated environmental concerns.
- Crop Nutrition: Knowledge of the soil nutrient status is a decisive tool for ensuring that only the necessary and recommended amount is applied. The decision making process

involves crop demands, the supply that is in the soil and available nutrients from farm manure and crop residues. A balanced approach to fertilisation should be adopted, practices should be adapted to local situations, thereby reducing risks of environmental pollution by fertilisation.

- Animal Husbandry, Health & Welfare: Health and welfare of farm animals are linked with performance. Farmers employ and demonstrate techniques directed towards meeting the needs of the livestock and maintaining the animals in good health, comfort and low stress, allowing for natural behaviour to the greatest possible extent.
- Landscape & Nature Conservation: Protecting and enhancing wildlife and biodiversity of the landscape is of great importance within the concept of Integrated Farming. Management practices should consider biodiversity effects such as the threat to larches during mechanical weeding. The structural diversity of land and landscape features will create floral and faunal abundance and diversity.
- Waste Management & Pollution control: Wastes, including farm manure, must be seen as a valuable resource in terms of saving money and reducing pollution. Farming effluents should be managed to optimise recycling and re-use, thereby minimising effects on the environment. Recycling of external materials such as sewage sludge should only be considered if there will be no hazard to soil and environment due to critical ingredients such as heavy metals *etc.*

Specific skills

Precision agriculture

Precision Agriculture (PA) may improve agricultural yield and reduce potential environmental risks. The main benefits are (Iris, 2014):

- Monitor the soil and plant physicochemical parameters: by placing sensors (electrical conductivity, nitrates, temperature, evapotranspiration, radiation, leaf and soil moisture, *etc.*) the optimal conditions for plant growth can be achieved.
- Obtain data in real time: the application of sensing devices in the fields will allow a continuous monitoring of the chosen parameters and will offer real time data ensuring an updated status of the field and plant parameters at all time.
- Automate field management: by incorporating a Decision Support System (DSS) in Precision Agriculture environment, the best conditions for the specific soil and plant species will be automatically optimised based on the data obtained by the sensors. The DSS will suggest the best moment for watering (or whether there is need or not), the need to irrigate to wash the salt content due to an excess in the radicular area, the need to fertilise, *etc.*
- Save time and costs: by introducing a PA system in the daily operation of an agricultural exploitation, time is saved due to the on-line measurement methods. Data from the sensors are automatically transmitted to a central server and this can be consulted using a Smartphone or Laptop. Or even, e-mail or SMS alerts can be programmed to notify the field owner when there is a need to irrigate, fertilise or address any issue in their properties. Moreover, costs in terms of water, pesticides and others could be optimised and easily reduced.
- Improve the farmers' image: by using PA technology, not only the yield and profits will be increased but also the perception of the general public and Public Administration

(through Smart Agriculture and environmental care) towards agricultural activity will be enhanced.

In this way, Precision Agriculture seems to bring many benefits to farmers and land owners who decide to use technology to manage their fields.

Applications of remote sensing to assess land capability

The applications of remote sensing to assess land capability in agriculture are designed to provide the farmer with timely information about crop progress. Here follow just some of the benefits that can be gained from the use of remote sensing:

- Early identification of crop health and stress.
- Ability to use this information to do remediation work on the problem.
- Improve crop yield.
- Crop yield predictions.
- Reduce costs.
- Reduce environmental impact.
- Crop management to maximise returns through the season.
- Crop management to maximise returns during harvest time.

Remote sensing data, used appropriately and at the right times of the season, has the ability to provide benefits to crop health and hence improve production (Regional Institute Online Publishing, 2016).

Integrated Pest Management in plant protection

Integrated Pest Management (IPM) in plant protection focuses on the long term application of ecologically-friendly biological methods such as natural predators, resistant plant strains, sterile male technique, *etc.* IPM aims to slowly reduce the use of pesticides via biological control methods. The main benefits of IPM are (Greentumble, 2016):

- Slower development of resistance to pesticides: pests can develop a resistance to pesticides over time. When the applications of the chemicals are used repeatedly, the pests can develop a resistance to the pesticides via natural selection, where the pests that survive the application of the chemicals will pass on their genes to their offspring.
- Maintaining a balanced ecosystem: the use of pesticides may eradicate the pest population. However, there is a risk that non-target organisms are also affected, which can result in species loss. IPM can eradicate pests while maintaining the balance of the ecosystem.
- Better cost *vs.* value margin: The reduced usage of pesticides is more cost effective in the long term, as IPM controls pests when there are surges, as opposed to the regularly timed application of pesticides.

Agricultural reuse of organic residuals

The agricultural reuse of organic residuals may provide agronomic and environmental benefits that were either not previously well understood and/or that are critical to addressing emerging environmental issues associated with climate change. Environmental benefits are possible from manure application if suitable manure management strategies are applied, as well as timing and placement follow best management practices. When compared to more conventional fertilizer, manure properly applied to land has the potential to provide environmental benefits including:

- Increased soil carbon and reduced atmospheric carbon levels.
- Reduced soil erosion and runoff.

- Reduced nitrate leaching.
- Reduced energy demands for natural gas-intensive nitrogen (N) fertilizers.

Several long-term manure application studies have illustrated its ability to slow or reverse declining soil organic levels of cropland. The ability of manure to maintain or build soil organic matter levels has a direct impact on enhancing the amount of carbon sequestration in cropped soils. Manure organic matter contributes to improved soil structure, resulting in improved water infiltration and greater water-holding capacity leading to decreased crop water stress, soil erosion, and increased nutrient retention (Extension, 2016).

In the recent years the attention has been focused also on the energy from biomass, while the exploitation of agro-industrial residues, although being materials with a limited energy potential, will fit into the goals of the general energy efficient conservation and sustainable protection of the natural resources, as well as within the implementation of the concept of bio-economy (Statuto et al., 2013). Agricultural co-products, by-products and waste (Statuto & Picuno, 2017), other than being considered as an important energy source, are indeed important factors for restoring the level of organic matter in the soil (fig. 1).

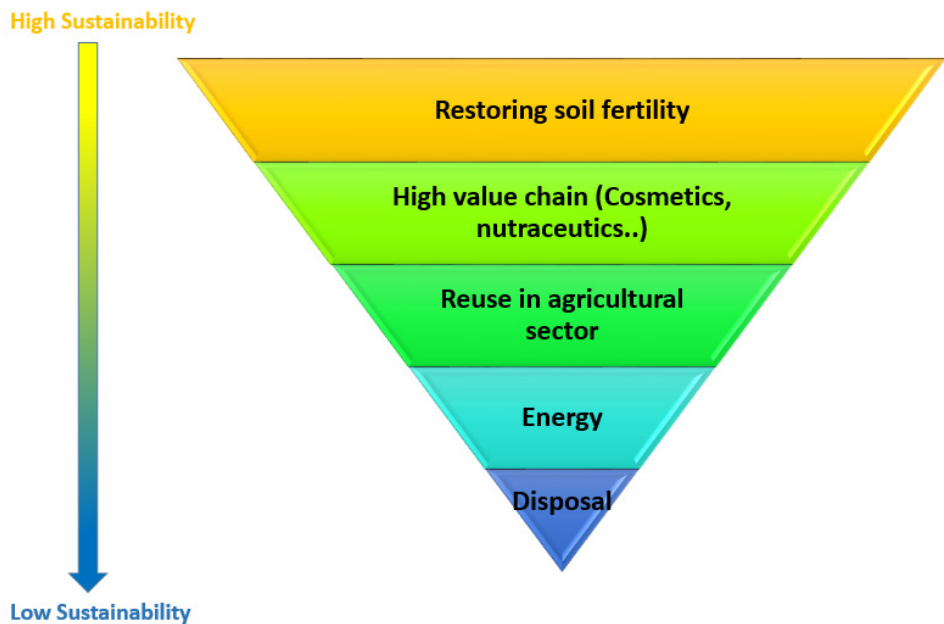


Figure 1. Agricultural by-product, co-product and waste management hierarchy.

Drip irrigation and water-conserving technologies

Drip irrigation is a type of micro-irrigation that has the potential to save water and nutrients by allowing water to drip slowly to the roots of plants, either from above the soil surface or buried below the surface. The goal is to place water directly into the root zone and minimize evaporation.

The advantages of drip irrigation and water-conserving technologies are (Agriinfo, 2015):

- Maximum use of available water.

- No water being available to weeds.
- Maximum crop yield.
- High efficiency in the use of fertilizers.
- Less weed growth and restricts population of potential hosts.
- Low labour and relatively low operation cost.
- No soil erosion.
- Improved infiltration in soil of low intake.
- Ready adjustment to sophisticated automatic control.
- No runoff of fertilizers into ground water.
- Less evaporation losses of water as compared to surface irrigation.
- Improvement of seed germination.
- Decrease of tillage operations.

Renewable energy and its application as green agricultural energy source

Renewable Energy of all sizes has become a familiar sight around the world for a wide variety of reasons, including economic, environmental, and social benefits. Main advantages coming from renewable energy and its application as green agricultural energy source are (Harvest Energy Solutions, 2016):

- Clean water: Turbines and solar panels produce no particulate emissions that contribute to mercury contamination in lakes and streams. Renewable energy also conserves water resources. For example, producing the same amount of electricity can take about 600 times more water with nuclear power, and about 500 times more water with coal.
- Clean air: Other sources of electricity produce harmful emissions, which contribute to global climate change and acid rain. Wind and solar energy is pollution free.
- Mining & transportation: Harvesting the wind and sun preserves resources since there is no need for destructive mining or fuel transportation to a processing facility.
- Land preservation: Wind farms are spaced over a large geographic area, but their actual "footprint" covers only a small portion of the land resulting in a minimum impact on crop production or livestock grazing. Large buildings cannot be built near the turbine, thus wind farms preserve open space.

The diffusion in the use of biomass as a new energy source may determine changes in its characteristics of naturalness, biodiversity and visual quality of the rural landscape (Statuto et al., 2017). The modern concept of landscape may be not indeed only limited to the visual perception that humans receive from the land, since this effect is the results of the interaction among several different ecosystems, that means living natural chains connected to the morphological, geo-pedological, hydrological, meteorological, *etc.* characteristics of a certain area. As well as the word "landscape" itself expresses the role of shaping the lands by natural forces, an "*Energyscape*" may be considered as the effect derived from the role played by energy sources as a force shaping the visible features of the Earth's surface in delimited areas (Statuto & Picuno, 2016). Therefore, similarly as for cultural landscapes, an energyscape is fashioned from a natural landscape by an energy exploitation (Statuto et al., 2016). Energy is the agent, natural area is the medium, the energyscape is the result (fig. 2).



Figure 2. The “Energyscapes”

Bioenergy and energy crops

Energy crops are unique because they don't just produce renewable energy – they also provide other environmental and economic benefits (Clean Energy Council, 2016), since they may lead to both new feed and energy from harvesting, in the framework of a circular economy. Other than creating renewable energy, bioenergy and energy crops also provide:

- Rural & regional benefits.
- Distributed baseload power.
- Competitive cost proven renewable energy generation.

Energy crops provide therefore great economic and social opportunities for rural and regional communities. Farmers, truck drivers, contractors, suppliers, as well as local restaurants and shops are all provided with an economic boost. This provides a source of permanent fulltime employment unique from the seasonal workforce in many rural and regional areas. Energy crops also encourage the development of new and innovative farming techniques and can provide economic returns on land and crop residue with no other identifiable market or environmental value. As these communities deal with the impacts of climate change, energy crops provide rural and regional areas with a more self-reliant labour force less vulnerable to the impacts of drought and flood.

CONCLUSIONS

Traditionally, pen and paper have been used to collect data in the field and for monitoring and evaluation of projects in rural areas. However, this approach is time consuming and susceptible to human error that may affect productivity and accuracy. Information and communication technologies are now being used widely with remarkable positive results to perform these tasks in agricultural development projects. In a recent global discussion organised by the World Bank to point out the benefits of the new tools and methods with respect to the traditional ones, experts from various fields and organisations around the world shared their experiences and discussed the ways in which they were using ICT – mobile phones, tablets, applications, software, *etc.* – to collect data in the field, and to perform Monitoring and Evaluation (M&E) in development projects, while also working closely with rural communities and taking their feedback. The discussion has been summarised in a policy brief and outlines the benefits of using ICT for data collection.

The advancements in the agricultural technologies sector, and in particular new technologies for the above mentioned skills, is going to be transferred to agricultural workers in the frame of the SAGRI Project. Particular focus will be put on environmental technologies that are of direct interest for the participant end-users, but also for European farmers in

general. The SAGRI Project is focused on novel practices and methods for applying advancements in environmental technologies to an agricultural and environmentally challenged society and to facilitate the farmers everyday activities. The information will be applied in order to facilitate the transfer of the most critical points of it to the agricultural workers. The acquisition of these skills is an important step to achieve a more technologically advanced and social, economic and environmentally sustainable agriculture. At the present, it is evident the role of the farmer, who knows not only the traditional cultivation to produce different crops, but that has to take into account the new techniques and technologies able to contribute to a sustainable agriculture.

ACKNOWLEDGEMENTS

The Project “Skills Alliance for Sustainable Agriculture – SAGRI” was financed by the European Union Programme Erasmus+ - Key Action 2: Sectors skills alliances (Contract no. OI 174011).

REFERENCES

- Agriinfo (2015). Advantages and Disadvantages of Drip Irrigation. Available from: <http://www.agriinfo.in/default.aspx?page=topic&superid=8&topicid=2243>.
- Cedefop (2016). Analytical Highlights. Skilled agricultural, forestry and fishery workers: skills opportunities and challenges. Available from: http://skillspanorama.cedefop.europa.eu/en/analytical_highlighths/skilled-agricultural-forestry-and-fishery-workers-skills-opportunities.
- Clean Energy Council (2016). Bioenergy. Available from: <https://www.cleanenergycouncil.org.au/technologies/bioenergy.html>.
- Extension (2016). Environmental Benefits of Manure Application. Available from: <http://articles.extension.org/pages/14879/environmental-benefits-of-manure-application>.
- Greentumble (2016). Advantages and Disadvantages of Integrated Pest Management. Available from: <http://greentumble.com/advantages-and-disadvantages-of-integrated-pest-management/>.
- Harvest Energy Solutions (2016). The Benefits of Renewable Energy. Available from: <http://harvestenergysolutions.com/benefits-renewable-energy/>.
- Iris – Advanced Engineering (2014). 5 benefits of Precision Agriculture to increase your field productivity. Available from: <http://www.iris-eng.com/5-benefits-of-precision-agriculture-to-increase-your-field-productivity/>.
- Regional Institute Online publishing (2016). Using remotely sensed data and GIS to improve farm planning and productivity. Available from: <http://www.regional.org.au/au/gia/08/259woodrow.htm>.
- Sagri (2016). Skills Alliance for Sustainable Agriculture. Available from: <http://www.sagriproject.eu>.
- Statuto, D., Tortora, A., Picuno, P. (2013). A GIS approach for the quantification of forest and agricultural biomass in the Basilicata region. *Journal of Agricultural Engineering*, XLIV(s1):e125: 627-631.
- Statuto, D., Picuno, P. (2016). Analysis of renewable energy and agro-food by-products in a rural landscape: the Energyscapes. In: *Proceedings of the 4th CIGR International Conference of Agricultural Engineering (CIGR-AgEng 2016)*, Aarhus (Denmark), 26-29 June 2016.
- Statuto, D., Cillis, G., Picuno, P. (2016). Analysis of the effect of agricultural land use change on rural environment and landscape through historical cartography and GIS tools. *Journal of Agricultural Engineering*, XLVII:468, pp. 28-39.

- Statuto, D., Picuno, P. (2017). Planning the energy valorization of agricultural co-products, by-products and waste in a landscape context. Proceedings of the 11th International AIAA Conference on: "Biosystems Engineering addressing the human challenges of the 21st century", Bari (Italy), 5-8 July 2017. pp. 206 – 210.
- Statuto, D., Cillis, G., Picuno, P. (2017). Using Historical Maps within a GIS to Analyze Two Centuries of Rural Landscape Changes in Southern Italy. *Land*, 6 (65), 1-15.



EXPERIMENTAL DEVELOPMENT OF CLAY BRICKS REINFORCED WITH AGRICULTURAL BY-PRODUCTS

Dina STATUTO*, Martina BOCHICCHIO, Carmela SICA, Pietro PICUNO

University of Basilicata - SAFE School, via dell'Ateneo Lucano 10, 85100 Potenza, Italy.

*E-mail of corresponding author: dina.statuto@unibas.it

SUMMARY

The valorisation of agricultural co-products, by-products and wastes may play a significant role in the framework of the concept of bio-economy, which is referred to the transition from a linear to a circular economy, based on the exploitation of by-products and transformation of residues from waste to new resources. After contributing to the restoration of the level of organic matter in the soil, these biomasses could be indeed valorised in different ways, *e.g.*, as added-value components in other industrial sectors (nutraceutical, cosmetic, *etc.*), as alternative fuel in energy plants, or in the construction sector, in which they could be incorporated in some building elements with the aim to increase their technical performance.

In order to verify the possibility of employing two among the most diffused agricultural by-products (*i.e.*, wheat straw and sheep wool), some experimental bricks realized with clay mixed with these vegetal and animal fibres were prepared. These bricks (so-called "*adobe*") were tested in their mechanical properties, in order to highlight the differences between the two types of bricks and to evaluate the possibility to use them as building elements in bio-architecture. The results of the mechanical tests showed that the compression strength of the adobe bricks prepared with sheep wool was significantly higher than those incorporating wheat straw, while these latter have exhibited a shrinkage lower than adobe bricks realized without any additive fibre.

Key words: agricultural wastes, wheat straw, sheep wool, adobe bricks, bio-architecture

INTRODUCTION

The diffusion of green technologies is gaining wider spaces thanks to their contribution to the reduction of carbon emissions into the atmosphere generated by traditional fossil material (petroleum, gas, or coal), in the general context of an enhanced environmental protection. The increasing attention to environmental topics has pushed the political and scientific world to develop new strategies able to reduce the environmental impact and to promote a sustainable development through the exploitation of agricultural by-products, co-products and wastes, in order to reduce the waste generation and the use of non-renewable resources. In this framework, the concept of bio-economy - considered as a circular economy that presupposes the re-use of by-products arising from production processes - is suitable in order to obtain new products through ideally processes called "zero-waste" and to create new by-product markets. The use of by-products and residues from agriculture, forestry and agro-industry should anyway be always evaluated and planned with care, so as to avoid an excessive removal of organic matter from the agricultural soil, reducing its fertility on the long term, with negative effects on agricultural and/or natural ecosystems.

In the agro-industrial sector - such as wineries, olive oil mills, cheese factories, *etc.* - a large quantity of secondary products could be available, and they can be used to generate "clean" energy such as biogas and bio-methane. Arising from particular organic waste, some high-value products - such as dietary supplements, cosmetics or pharmaceuticals of great interest for experimentation in green and sustainable chemistry - can so be obtained. Organic waste can also be reused in the aquaculture sector, in particular for sustainable production of fish feed. The scientific community has found good results in the formulation of alternate feed from organic by-products as well (Ayadi et al., 2012).

Moreover, agricultural co-products, by-products and waste may play a significant role in bio-architecture, since they could be valorised also in the construction sector, when incorporated in clay bricks with the aim to increase their technical performance, so contributing to improve traditional building components through the addition of natural elements. Sustainability can only be possible when construction uses renewable materials or materials recycled from construction wastes (Serrano et al., 2016). Mostly within the Mediterranean area, spontaneous architecture still constitutes indeed a visible witness about the role that the rural constructions have historically played in connection with the surrounding environment, joining the agricultural production needed for human nutrition with the control and care of extra-urban land (Picuno, 2012). In some Southern Italian regions - *e.g.* Apulia and Basilicata - extraordinary examples of earthen rural building realized with clay bricks (Fig. 1) are widespread all over the rural landscape (Statuto and Picuno, 2017, Statuto et al., 2017).



Figure 1. Earthen vernacular rural building in Basilicata Region.

The increasing demand for processes with reduced environmental impacts and lower energy consumption also involves the building sector in which "sustainable" buildings are increasingly required (Picuno, 2017; Statuto and Picuno, 2016). The most recent trend is to use natural and/or recycled materials as substitutes for traditional material used in constructions, in order to combine a good energy performance while reducing the environmental impact and protecting human health as well (Sica et al., 2015). Currently re-evaluated by bio-architecture is the "earth material" that, together with wood and stone, is one of the most common building materials in the world, thanks to its ecological and recyclable properties. The use of earth material has very interesting consequences on the current perception of the rural landscape - the colour of the building being similar to its surroundings - as well on the agricultural environment, since this material doesn't represent a waste because it would be, at the end of its useful life, incorporated in the same context (Picuno, 2016).

Today about 30% and 50% of the world's population lives in earth structures, especially in some regions of Africa, Asia and Latin America, while in Europe they are still a niche product of the construction industry (Parisi et al., 2015).

One of the most interesting element of earthen construction is the use of sun-dried earth bricks – made of raw clay soil mixed with barley or wheat straw (so-called "adobe") – as a walling material (Picuno, 2016). The main applied raw materials are coarse sand, argillaceous earth and lime. The natural earth mixtures are often corrected by the addition of fibres, to control cracking while adobes are drying in the sun. Especially in rural building, the use of earth material, in particular clay, is diffused thanks to its good mechanical properties and to the low presence of high-cost crude grains, that are mixed with vegetable fibres and water for the realization of adobe bricks used as walling material (Liberatore et al., 2006).

Adobe is a construction material that presents several attractive characteristics. It is low-cost, locally available, recyclable, adapted to a large variety of soils, presents good thermal and acoustic properties, and it is associated to simple constructive methods that require reduced energy consumption (Millogo et al., 2014; Silveira et al., 2012). To improve the mechanical strength, impermeability and the durability of locally produced adobe, in general, small amounts of hydrated lime or natural fibres are added to the soil matrix.

With the aim to examine the mechanical properties of adobe bricks realized with natural material locally available in the Mediterranean area, in the present paper the results of mechanical tests on adobe bricks prepared with different natural fibres, are presented.

MATERIAL AND METHODS

The experimental tests were performed in the Laboratory for Testing Materials of the SAFE School of the University of Basilicata (Potenza – Italy). Two different types of blocks of clay, manually mixed with sheep wool in one case, and with wheat straw in a second case, were tested to define their mechanical properties.

Sheep's wool has been widely used in the construction field as an insulating material (Corcadden et al., 2014; Zach et al., 2014), thanks to the well-known thermal and acoustic insulation properties of this by-product arising from sheep breeding, whereas no studies have been carried out on the possible use of sheep wool inside the matrix of building elements. The choice of wool was suggested by the widespread sheep breeds in the rural areas examined, which are characterized by a low-quality wool by-product, having short fibres, which are not suitable for the textile industry and a low average selling price (around 0.6 € kg⁻¹ - year 2017). This price is not even enough to pay the costs necessary for the care and well-being of animals; just as a reference, in the same year 2017 the price to shear a sheep is about 1.60 € kg⁻¹ of wool.

Concerning wheat straw, the possibilities of its use as an additive for reinforcing clay bricks have been analysed during some previous studies (Picuno, 2016), in which the mechanical behaviour of some bricks made using straw as reinforcing material has been investigated, expressing the relevant results in terms of their mechanical properties.

In the present research, adobe bricks of cubic shape (150 mm edge) were prepared with local materials, in particular the clay and the wool were found in the municipality of Acerenza, located in the north-east part of Basilicata Region, and three typologies of specimens were prepared:

- Clay bricks (only clay) (typology: “C”);
- Clay bricks mixed with 3% by weight of sheep wool (typology: “W”);
- Clay bricks mixed with 3% by weight of wheat straw (typology: “S”).

Prior to the dough, the clay was sifted to obtain particles not exceeding 4.75 mm (Fig. 2) while the straw and wool fibres were weighed before the preparation of the dough (Fig. 3a and 3b).



Figure 2. Clay material during the sifting process.

For each typology (C, W, S), n. 2 specimens were manually made (Fig. 4a and 4b); therefore, they were placed to dry under the sun in a hot and ventilated place for nine weeks during summer. After the drying period, the dimensions of the blocks were measured in order to calculate the percentage of shrinkage for the three different analysed typologies.



Figure 3a. weighing of straw.



Figure 3b. weighing of sheep wool.

The compression tests (Fig. 5) were performed by using a computerized universal testing machine Galdabini PMA-10 type (Galdabini S.p.A., Italy), by placing the adobe bricks between the rigid steel plates of the testing machine and testing them in terms of unconfined

compression strength through displacement-controlled axial tests. A uniform load was applied without shocks, continuously increasing until failure, with the moving head of the testing machine travelling at a rate of 1 mm min^{-1} . The breaking load was considered as the maximum load reached during the test.



Figure 4a. dough prepared with clay and straw.



Figure 4b. dough prepared with clay and wool.



Figure 5. Compression test on an adobe bricks.

RESULTS AND DISCUSSION

In Table 1 the results of compression tests on the three different types of adobe bricks are reported in terms of average value for each one of the different typologies which were analysed. The results showed that the compression strength of the adobe bricks prepared with sheep wool was significantly higher than those incorporating wheat straw, while these

latter have exhibited a shrinkage lower than adobe bricks realized without any additive fibres. Probably, the greatest resistance to breaking the clay bricks with wool is due own to the structure of the fibres: the scales that cover the filaments make it rough and, at the same time, the interstices among scales increase the surface of contact with clay, making the adobe more compact and durable.

Table 1. Average compressive strength of the adobe bricks experimentally tested.

Adobe brick typology	Maximum compressive strength σ_{max} (N mm ⁻²)	Shrinkage (%)
C	2.05	7.3
W	4.32	6.7
S	1.86	2

The results showed that the compression strength of the adobe bricks prepared with sheep wool (W) has been significantly higher than those incorporating wheat straw (S), while these latter have exhibited a shrinkage lower than adobe bricks realized without any additive fiber (C).

Figure 6 reports a diagram stroke/load for one of the tested adobe bricks prepared with clay and sheep wool. From the analysis of this figure, it can be noticed that the behaviour of this material during the compression test appears as quasi-elastic in the first phase, followed by the definitive failure of the cubic specimen.

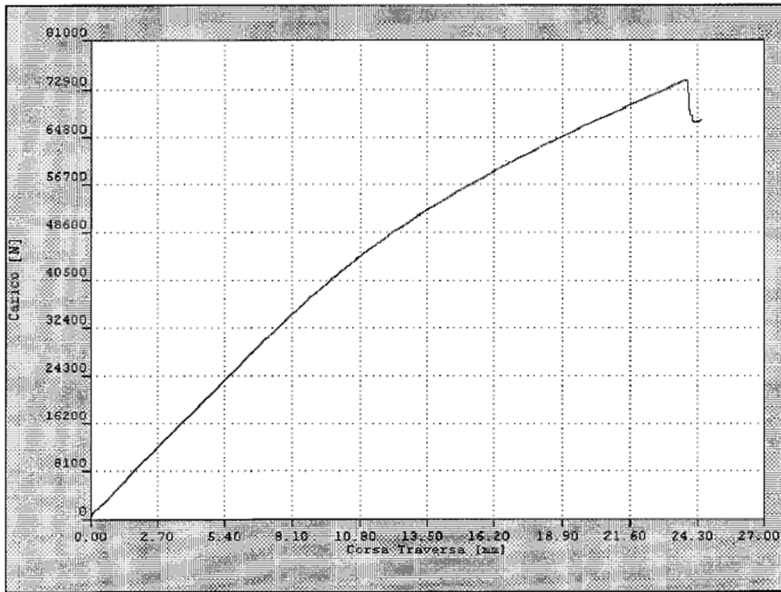


Figure 6. Stroke/load diagram for the compression test on a cubic-shape adobe brick.

The average compressive strength values of the three types of bricks resulted higher than the minimum value of 1 N mm⁻² required for building materials (Vega et al., 2011). The

average values of compression strength of the fibrous reinforced blocks appear to be quite interesting, particularly in the case of adobe bricks reinforced with sheep wool, which have proved to have an interesting mechanical strength, better than those reinforced with straw. From the results obtained through the present experimental tests it can be concluded that further analysis should be performed, aimed to the definition of optimal mixture of soil with natural fibres.

The result obtained from blocks prepared with clay only (C) have shown a slightly better compression resistance than those mixed with straw (S). This aspect appeared quite surprising, since it is expected that the presence of fibres would have played a significant role in the compressive strength of the soil (Sharma et al., 2015), giving a general increase of the mechanical properties of the composite material. This result in our experiment could be probably due to the good mechanical properties of the clay that was used.

Table 2 shows the mean compression strength values of clay blocks realized with straw during similar researches already performed on some blocks of the same type produced in the Materials Testing Laboratory of the University of Basilicata under previous Master/Doctoral thesis (Lista, 2015; Bochicchio, 2017). In the first case the natural materials came from a different area (Municipality of Senise - southeast part of Basilicata Region).

Table 2. Comparison of average compression strength values (N mm^{-2}) of bricks made with clay and straw in previous studies (Lista, 2015) and the new ones (Bochicchio, 2017).

Analyzed bricks	Maximum compressive strength σ_{max} (N mm^{-2})	Shrinkage (%)
Clay bricks with straw (Lista,2015)	0.92	5
Clay bricks with straw (Bochicchio,2017)	1.86	2

As it is possible to notice from table 2, the average compressive strength in case of bricks realized in the year 2017 is about the double of that one of bricks made in 2015. This result seems again probably connected to the better mechanical characteristics of the clay itself. To collect more data to improve the knowledge of mechanical behaviour of adobe, future studies are needed to understand the interaction between fibres and clay (Silveira et al., 2013).

CONCLUSIONS

The recovery and reuse of by-products arising from the agricultural sector is a good solution to preserve non-renewable raw materials and mitigate the emissions into the atmosphere. Through the use of "green" processes and reuse of by-products, co-products and wastes it is possible to reduce the amount of waste and to solve some problems concerning the disposal. This practice of reuse is applicable to several productive sectors, including the bio-building sector, with the aim to achieve low-impact structures on the environment, to preserve human health and to reach good energy performance. The reuse of agricultural by-products in bio-architecture could be applied especially in the rural building sector. The role of rural building is indeed fundamental for enabling practices aimed to reduce resources consumption, combat environmental degradation and create better living environments,

preserving at the same time architectural and historical assets. Since a suitable restoration and functional requalification of the farm building obtained through the use of traditional construction material may contribute to the sustainability of the rural environment, the use of adobe bricks would be a very interesting option, since it is an environmentally-friendly construction material that presents several attractive characteristics, being low cost, locally available, recyclable, adapted to a large variety of soils, presenting good thermal and acoustic properties, and it is associated to simple constructive methods that require reduced energy consumption.

The experimental tests presented in the present paper confirm the general results available in the scientific literature about adobe material, with some possible improvements of its mechanical characteristics. The addition of natural fibres, in particular in the case of sheep wool, has been revealed as an interesting option, able to improve the compression strength of the adobe bricks; other mechanical parameters would probably benefit from this reinforcement as well. Furthermore, considering that non-sold wool must be disposed of as a special waste, with heavy economic and management burdens for the farmer, its valorisation would lead both to the reduction of woollen volumes - characterized by a low quality, so not suitable for the textile industry - and the reduction of environmental damage, due to the illicit disposal by some farmers and to the wrong management of waste water resulting from their washing.

Future analysis appears thence necessary, mainly focused on the role that natural fibres could perform when mixed into the earthen mixture of adobe bricks, that could be better explored through the study at microscopic level of the adhesion of the fibres to the clay matrix and the consequent effects on the general mechanical properties of the reinforced earth construction.

ACKNOWLEDGEMENT

Many thanks to Mr. Cosimo Marano – technical staff at the SAFE School of the University of Basilicata – for his kind support in the performance of the experimental tests.

REFERENCES

- Ayadi, F.Y., Rosentrater, K.A., Muthukumarappan, K. (2012). Alternative Protein Sources for Aquaculture Feeds. *Journal of Aquaculture Feed Science and Nutrition* 4 (1): 1- 26, 2012.
- Bochicchio, M. (2017). Valorizzazione di sottoprodotti derivanti dal settore primario attraverso lo sviluppo sperimentale di elementi costruttivi per tecniche di architettura sostenibile (*Valorisation of agricultural by-products through the experimental development of building elements for sustainable architectural techniques* – in Italian). M. Sc. Thesis, University of Basilicata.
- Corscadden, K.W., Biggs, J.N., Stiles, D.K. (2014). Sheep’s wool insulation: A sustainable alternative use for renewable resource? *Resources, Conservation and Recycling* 86 (2014) 9- 15.
- Liberatore, D., Spera, G., Mucciarelli, M., Gallipoli, M.R., Santarsiero, D., Tancredi, C., (2006). Typological and Experimental Investigation on the Adobe Buildings of Aliano (Basilicata, Italy). *Structural Analysis of Historical Constructions*, New Delhi 2006.
- Lista, A. (2015). Ricerca e sviluppo di materiali costruttivi tradizionali per tecniche di bioarchitettura finalizzata alla valorizzazione del territorio rurale (*Research and experimental development of traditional building materials for bioarchitecture techniques aimed to enhance the rural land* – in Italian). Ph. D. Thesis, University of Basilicata.
- Millogo, Y., Morel, J.C., Aubert, J.E., Ghavami, K. (2014). Experimental analysis of Pressed Adobe Blocks reinforced with Hibiscus cannabinus fibers. *Constr. Build. Mater.* 52, 71–78.

- Parisi, F., Asprone, D., Fenu, L., Prota, A. (2015). Experimental characterization of Italian composite adobe bricks reinforced with straw fibers. *Composite structures* 122: 300-307.
- Picuno, P. (2012). Vernacular farm buildings in landscape planning: a typological analysis in a southern Italian region. *Journal of Agricultural Engineering*, XLIII:e20: 130-137.
- Picuno, P. (2016). Use of traditional material in farm buildings for a sustainable rural environment. *International Journal of Sustainable Built Environment*. 5 (2): 451-460. DOI: <http://dx.doi.org/10.1016/j.ijbsbe.2016.05.005>
- Picuno, P. (2017). Biosystems engineering techniques for habitat restoration in protected areas. Proceedings of the 45th Symposium on: "Actual Tasks on Agricultural Engineering – ATAE 2017, Opatija (Croatia), 21-24 February 2017. UDC 551.58:631.23, pp. 557-566.
- Serrano, S., Barraneche, C., Cabeza, L.F. (2016). Use of by-products as additives in adobe bricks: Mechanical properties characterization. *Construction and Building Materials*, 108:105-111.
- Sharma, V., Vinayak, H.K., Marwaha, B.M. (2015). Enhancing sustainability of rural adobe houses of hills by addition of vernacular fiber reinforcement. *Int. J. Sustainable Built Environ.* 4, 348–358.
- Sica, C., Lista, A., Picuno, P. (2015). Mechanical characterization of adobe bricks: ancient constructive elements for an eco-friendly building renovation. Proceedings of the 43rd Symposium on: "Actual Tasks on Agricultural Engineering – ATAE 2015, Opatija (Croatia), 24-27 February 2015. UDC 631.2:691, pp. 819-827.
- Silveira, D., Varum, H., Costa, A. (2013). Influence of the testing procedures in the mechanical characterization of adobe bricks. *Construction and Building materials* 40: 719-728.
- Silveira, D., Varum, H., Costa, A., Martins, T., Pereira, H., Almeida, J. (2012). Mechanical properties of adobe bricks in ancient constructions. *Construction and Building materials* 28: 36-44.
- Statuto, D., Picuno, P. (2016). Analysis of renewable energy and agro-food by-products in a rural landscape: The Energyscapes. In: Proceedings of the 4th CIGR International Conference of Agricultural Engineering (CIGR-AgEng 2016), Aarhus (Denmark), 26-29 June 2016.
- Statuto, D.; Cillis, G., Picuno, P. (2017). Using Historical Maps within a GIS to Analyze Two Centuries of Rural Landscape Changes in Southern Italy. *Land* 2017, 6(3), 65; doi:10.3390/land6030065.
- Statuto, D.; Picuno, P. (2017). Valorisation of vernacular farm buildings for the sustainable development of rural tourism in mountain areas of the Adriatic-Ionian macro-region. *J. Agric. Eng.*, 48, 21–26.
- Vega, P., Juan, A., Guerra, M. I. (2011). Mechanical characterisation of traditional adobes from the north of Spain. *Construction and Building Materials*, Elsevier, 25:3020.
- Zach, J., Hrudova, J., Brozovsky, J. (2014). Study of hydrothermal behavior of thermal insulating materials based on natural fibers. *World Academy of Science, Engineering and Technology. International Journal of Civil, Environmental, Structural, Construction and Architectural Engineering* Vol:8, No:9, 2014.



ODNOS PROIZVOĐAČKIH CIJENA ODABRANIH POLJOPRIVREDNIH PROIZVODA U REPUBLICI HRVATSKOJ I REFERENTNIH CIJENA U EUROPSKOJ UNIJI

Ivo GRGIĆ^{1*}, Jernej PRIŠENK², Vladimir LEVAK³, Tea KOVAČ⁴,
Magdalena ZRAKIĆ¹

¹ Sveučilište u Zagrebu, Agronomski fakultet, Svetošimunska cesta 25, 10000 Zagreb, Hrvatska

² Fakulteta za kmetijstvo in biosistemske vede, Pivola 10, 2311 Hoče, Slovenija

³ Poljoprivredna zadruga JALŽABET, Suhodolska 21, 42 203 Jalžabet, Hrvatska

⁴ Guldsmedsvägen 5, 121 32 Enskededalen, Stockholm, Švedska

*E-mail dopisnog autora: igrgic@agr.hr

SAŽETAK

Hrvatska glavninu vanjskotrgovinske razmjene ostvaruje s državama Europske unije a od 2013. godine svojim članstvom postala je i formalni dio toga jedinstvenog tržišta. To je za domaću proizvodnju i tržište poljoprivredno – prehrambenih proizvoda donijelo određene promjene od kojih su najveći otvorenost domaćeg tržišta konkurenciji te olakšan pristup velikom europskom tržištu za hrvatske proizvode. Cilj rada je utvrditi promjene hrvatskih proizvođačkih cijena pšenice, kukuruza, šećerne repe, uljane repice i kravljeg mlijeka u odnosu na referentne cijene Europske unije u razdoblju od 2005. do 2015. godine. Istraživanje je pokazalo da nacionalne cijene odabranih poljoprivrednih proizvoda uglavnom prate trend referentnih cijena EU. Do 2020. godine predviđeno je povećanje domaćih cijena pšenice, kukuruza i kravljeg mlijeka ali smanjenje cijena šećerne repe i uljane repice. Navedene promjene će u značajnoj mjeri biti posljedica utjecaja referentnih cijena EU izuzev kod šećerne repe.

Ključne riječi: Europska unija, proizvođačke cijene, poljoprivredni proizvodi

UVOD

Europska unija (EU) je, uz Sjedinjene Američke Države (SAD) i Kinu, jedna od vodećih svjetskih trgovinskih sila. Jedinstveno EU tržište pretpostavlja slobodan protok roba, usluga, kapitala i ljudi te su nacionalne ekonomije ostale bez do tada svih oblika zaštite. Republika Hrvatska (RH) je od 1. srpnja 2013. godine punopravna članica EU te je time i formalno

postala dio jedinstvenog tržišta EU. Sve europske uredbe postale su izravno primjenjive i u domaćem zakonodavstvu. Uklonjene su carinske i druge prepreke između Hrvatske i drugih zemalja članica, omogućen je slobodni protok roba i usluga te slobodan pristup tržištu svih članica EU pa tako i tržištu tzv. trećih država s kojima pojedina članica ima sklopljene trgovinske sporazume (Turčić, 2015).

Glavninu vanjskotrgovinske razmjene Hrvatska ostvaruje s državama EU. Hrvatskoj je kao i svakoj novoj članici za domaću proizvodnju i domaće tržište poljoprivredno – prehrambenih proizvoda, članstvo u Uniji značilo veliku promjenu. Proizvođači imaju mogućnost lakšeg poslovanja na tržištu uz manje troškove i niže cijene zbog ujednačenog sustava standardizacije i izbjegavanja dvostrukog testiranja, dok je potrošačima osigurana bolja sigurnost proizvoda uz veći izbor cijena i kvalitete.

U EU se obrađuje 135 milijuna ha poljoprivrednog zemljišta. Oko 80% tih površina nalazi se na teritoriju pet država: Španjolske, Francuske, Ujedinjenog Kraljevstva, Njemačke i Italije. Sukladno tomu i proizvodnja je koncentrirana u ograničenom broju država - u samo šest država članica (Francuskoj, Italiji, Njemačkoj, Španjolskoj, Ujedinjenom Kraljevstvu i Nizozemskoj) se proizvodi 80% vrijednosti proizvodnje. Po vrijednosnoj strukturi proizvodnje u razvijenim poljoprivredama EU na prvom je mjestu stočarska proizvodnja (40%), zatim proizvodnja voća i povrća (16%) te proizvodi od žita (9%) (Jukić, 2016).

RH u Uniji ne zauzima značajnije mjesto niti po poljoprivrednim resursima niti po samoj proizvodnji. Zbog toga je i njen utjecaj na ponudu, potražnju i cijenu pojedinog proizvoda EU tržišta mali. Za domaću proizvodnju veliku važnost predstavljaju ratarske kulture posebice kukuruz, pšenica, kod industrijskog bilja su šećerna repa i uljana repica, a kod stočarske proizvodnje to je kravlje mlijeko.

Tržne cijene ovih proizvoda pod znatnim su utjecajem cijena Unije odnosno cijena tržišta najvećih država proizvođača pojedinih poljoprivrednih proizvoda.

Cilj rada je utvrditi međuodnos hrvatskih proizvođačkih cijena odabranih poljoprivrednih proizvoda i referentnih cijena EU.

MATERIJAL I METODE

Izrada referentne cijene nužna je s obzirom da cijene u najznačajnijim državama proizvođačima pojedinih proizvoda na tržištu EU nisu iste jer je tržište poljoprivrednih proizvoda iznimno složeno (Kovač, 2017).

U radu se koristi referentna cijena, točnije prosjek proizvođačkih cijena triju količinski najvećih proizvođača određenog proizvoda u EU. Referentna proizvođačka cijena za pšenicu je prosjek proizvođačkih cijena Francuske, Njemačke i Velike Britanije, za kukuruz Francuske, Mađarske i Rumunjske, za šećernu repu i uljanu repicu Francuske, Njemačke i Poljske te za kravlje mlijeko prosjek cijene Njemačke, Francuske i Velike Britanije. „Prosječne proizvođačke cijene jesu cijene u koje su uključeni porezi (osim PDV-a), a isključene su subvencije i ostali novčani poticaji“ (https://www.dzs.hr/Hrv_Eng/publication/2016/01-01-04_01_2016.htm). Za utvrđivanje postojanja veze između referentnih i hrvatskih cijena korištena je korelacija, a za jakost veze Pearsonov koeficijent (Petz i sur., 2012).

Za potrebe projekcije pojave korišten je linearni, kvadratni i kubni trend (Franić i sur., 2005). Za domaće cijene vrelo podataka su publikacije Državnog zavoda za statistiku Republike Hrvatske (DZS) (<https://www.dzs.hr/>), a za europske Eurostat (<http://ec.europa.eu/eurostat>), sve za razdoblje od 2005. do 2015. godine. Domaće cijene u

kunama preračunate su u euro prema prosječnom tečaju (DZS Statistički ljetopis, različita godišta).

Za ovaj rad postavljene su dvije hipoteze:

Hipoteza 1: Prisutna je pozitivna korelacija nacionalnih cijena i referentnih cijena proizvoda u EU.

Hipoteza 2: Jakost statističkih veza je različita kod pojedinih analiziranih proizvoda.

REZULTATI I DISKUSIJA

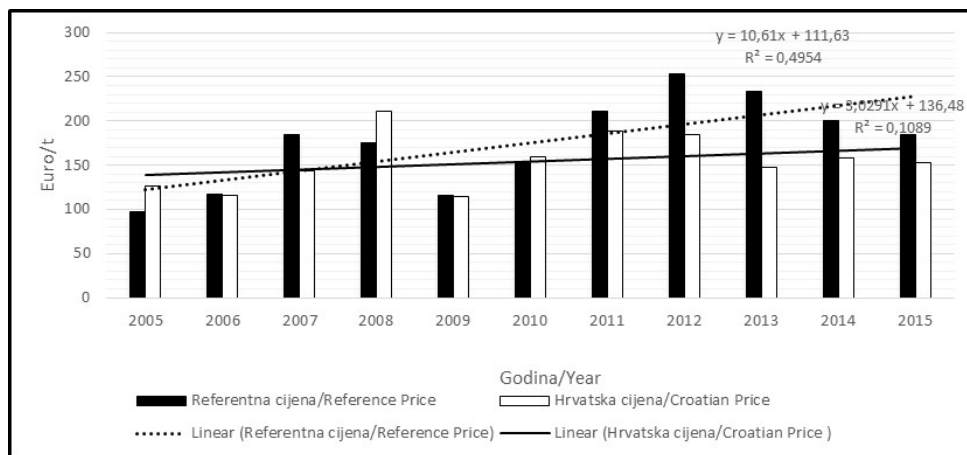
Pšenica

Površine i proizvodnja pšenice u Hrvatskoj i u državama EU tijekom analiziranog razdoblja bile su pod utjecajem klimatskih promjena te su stoga zabilježene godišnje oscilacije.

Francuska je tijekom analiziranog razdoblja proizvodila oko 38 milijuna tona godišnje, Njemačka 24 milijuna tona te Velika Britanija oko 15 milijuna tona odnosno prosjek ove tri države je bio oko 77 milijuna tona godišnje. U isto vrijeme u Hrvatskoj se proizvelo oko 800 tisuća tona ili 1,0% ukupne proizvodnje ove tri države. U svim državama prisutne su značajne godišnje oscilacije proizvodnje koje su utjecale i na tržišne cijene pšenice.

U Hrvatskoj je najviša proizvođačka cijena pšenice bila 2008. godine (210 EUR/t dok je najviša referentna proizvođačka cijena bila 2012. godine (253 EUR/t).

Izuzev 2005., 2008. i 2010. godine, referentne cijene su bile značajno iznad cijene pšenice u Hrvatskoj što je pogodovalo domaćim izvoznicima. Godine 2009. hrvatska i referentna cijena bile su gotovo iste, ali i najniže u analiziranom razdoblju. Ovo je bio rezultat povećanja površine i priroda što je rezultiralo ukupno većom proizvodnjom. (Grafikon 1).



Grafikon 1. Cijena pšenice u Hrvatskoj i referentna cijena EU

Graph 1. Wheat prices in Croatia and EU reference price

Izvor: Izračun autora prema Eurostat i DZS-a, različite godine
Source: Author's calculation to Eurostat and CBS, different years

Nakon 2007. godine referentna cijena pšenice brže raste od cijene pšenice u Hrvatskoj, a koeficijent korelacije od 0,65 pokazuje relativno jak utjecaj referentne na hrvatsku cijenu pšenice. Do 2020. godine se predviđa nastavak porasta cijena pri čemu bi se povećavala i razlika između referentne i cijene pšenice u Hrvatskoj što bi pogodovalo domaćim proizvođačima, ali ne i prerađivačima.

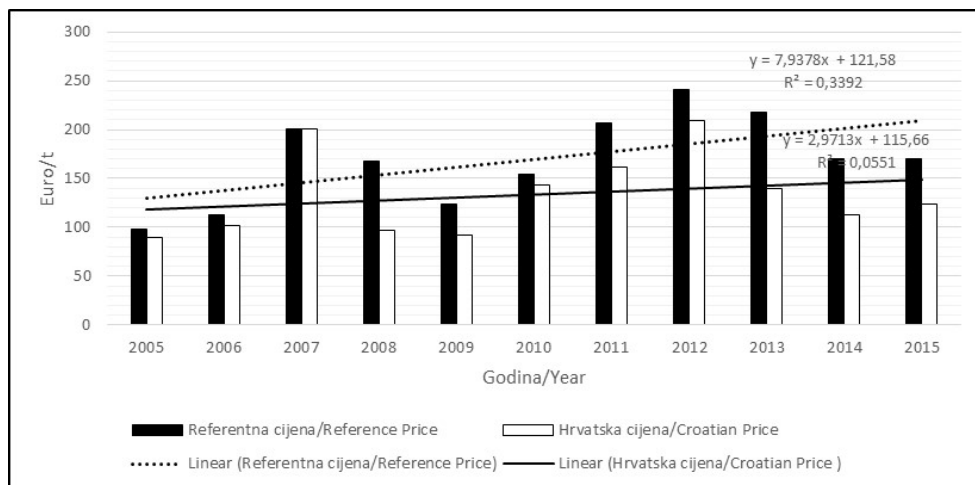
Kukuruz

Francuska je i najveći proizvođač kukuruza u EU i prosječno se godišnje proizvede oko 15 milijuna tona. Na drugom mjestu je Rumunjska (8,9 milijuna tona) te je treća Mađarska s oko 7,5 milijuna tona godišnje.

Kukuruz je dominantno žito u Hrvatskoj i površinom zauzima više od 50% površina pod žitaricama, a u vrijednosnoj strukturi žitarica sudjeluje s oko 62%.

Godišnja proizvodnja kukuruza (prosječno godišnje oko 1,9 milijuna tona) je pod velikim utjecajem prosječnih priroda, a površine kolebaju ovisno od tržišnih očekivanja. U Hrvatskoj površine pokazuju tendenciju smanjenja uz blago povećanje priroda.

Cijena kukuruza korelira s razinom razvijenosti stočarskog sektora i to posebice svinjogojske i peradarske proizvodnje. Smanjenja ovih proizvodnji utječu na cijenu kukuruza iz razloga što višak kukuruza uzrokuje nižu cijenu na tržištu i obrnuto (Grgić, 2000). U Hrvatskoj je zbog velikih suša i visokih temperatura u 2012. godini proizvodnja kukuruza bila vrlo niska, ali je cijena bila najviša i iznosila je 208,85 EUR/t (Grafikon 2).



Grafikon 2. Cijena kukuruza u Hrvatskoj i referentna cijena EU
Graph 2. Maize prices in Croatia and EU reference price

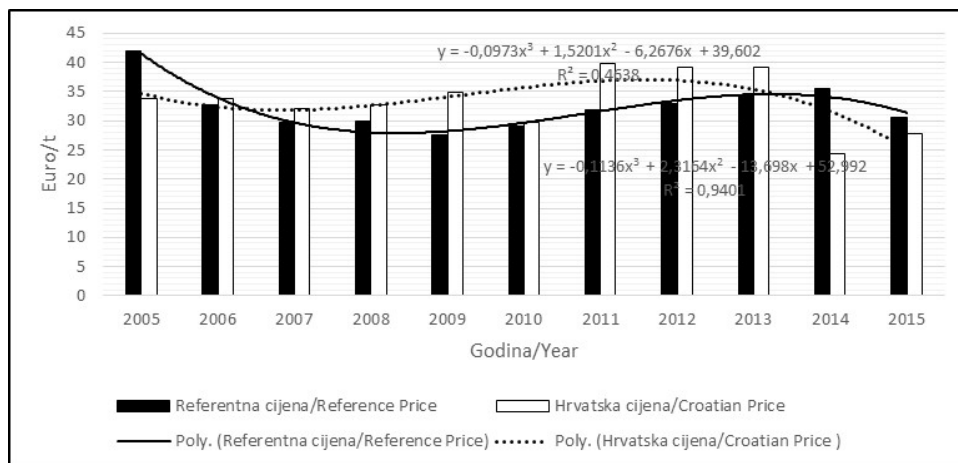
Izvor: Isti kao za Grafikon 1/ Source: Same as for Graph 1

Izračunata je snažna korelacija između cijene kukuruza u Hrvatskoj i referentne cijene u EU koja iznosi 0,82 i pokazuje jaku, pozitivnu vezu između referentne i cijena u Hrvatskoj. Do 2020. godine očekuje se daljnji rast cijena kukuruza na što će značajan utjecaj imati i rast potražnje na svjetskom tržištu uvjetovan potrošnjom izvan poljoprivrede (proizvodnja biogoriva, alkohol i sl.).

Šećerna repa

Europski najveći proizvođač šećerne repe je Francuska s oko 33,5 milijuna tona korijena godišnje, zatim Njemačka (oko 25 milijuna tona) te Poljska s 11,2 milijuna tona. Proizvodnja u Hrvatskoj je oko 1,2 milijuna tona ili 1,8% proizvodnje ove tri države.

Cijene šećerne repe relativno su stabilne kroz analizirano razdoblje i bile su u prosjeku oko 30 EUR/t. Najviša referentna cijena bila je 2005. godine kada je iznosila 42 EUR/t. U razdoblju do 2013. godine Hrvatska je imala povoljniji trend cijena šećerne repe u odnosu na referentnu što se mijenja nakon ulaska Hrvatske u EU. Referentna cijena u EU 2015. godine iznosila 30,66 EUR/t, a u Hrvatskoj 27,76 EUR/t (Grafikon 3).



Grafikon 3. Cijena šećerne repe u Hrvatskoj i referentna cijena EU

Graph 3. Sugar beet prices in Croatia and EU reference price

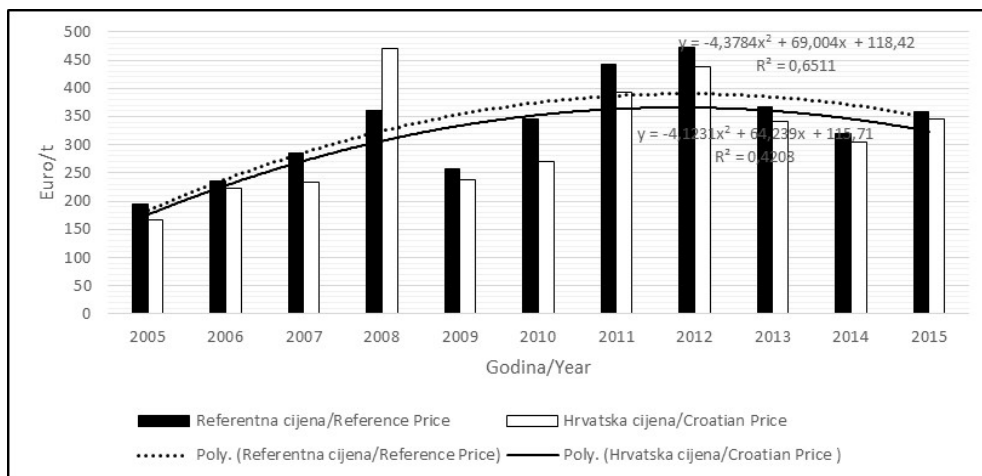
Izvor: Isti kao za Grafikon 1/ Source: Same as for Graph 1

Izračunati koeficijent korelacije između cijena šećerne repe u Hrvatskoj i referentnih cijena u EU iznosi 0,03 što pokazuje pozitivan ali neznatan međusobni utjecaj. Predviđa se da će u razdoblju koje je pred nama taj utjecaj biti znatno veći. Do 2020. godine predviđa se blago smanjenje cijena šećerne repe.

Uljana repica

Uljane repice se najviše proizvodi u Njemačkoj (oko 5,3 milijuna tona godišnje), zatim u Francuskoj (5,0 milijuna tona) te Poljskoj (2,2 milijuna tona). Republika Hrvatska s proizvodnjom od 48 tisuća tona predstavlja samo 0,4% proizvodnje ove tri države.

Cijena uljane repice bila je najniža 2005. godine, a 2008. u Hrvatskoj se cijena naglo povećala na 470,31 EUR/t i ta je cijena najviša zabilježena u odnosu na ostale godine razdoblja. Najviša referentna cijena bila je 240,43 EUR/t 2012. godine što pokazuje i trend, a nakon toga dolazi do smanjenja kako referentne tako i domaće cijene uljane repice. Do 2012. godine u Hrvatskoj je zabilježeno prosječno godišnje povećanje cijena od 14,761 euro te nešto više referentne (16,463 eura po toni).



Grafikon 4. Cijena uljane repice u Hrvatskoj i referentna cijena EU
Graph 4. The price of rapeseed in Croatia and the EU reference price

Izvor: Isti kao za Grafikon 1/ Source: Same as for Graph 1

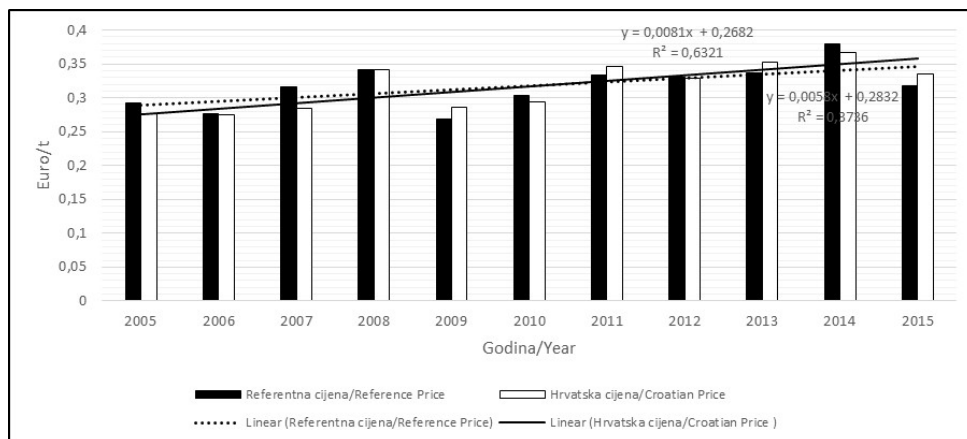
Između cijena uljane repice u Hrvatskoj i referentnih cijena u EU postoji jaka međusobna veza (Pearsonov koeficijent je 0,87). Do 2020. godine očekuje se nastavak smanjenja cijena započet 2013. godine.

Kravlje mlijeko

Njemačka je najveći proizvođač kravljeg mlijeka (oko 30 milijuna tona godišnje), zatim Francuska (24 milijuna tona) te Velika Britanija (14 milijuna tona). Hrvatska s proizvodnjom od oko 759 tisuća tona čini 1,1% proizvodnje ovih država.

Hrvatska nema problem s viškom mlijeka niti je imala s prekoračenjem kvota, no nema dovoljnu proizvodnju kako bi pokrila vlastite potrebe. Ukidanjem kvota 2015. godine sve je veća količina mlijeka na tržištu Europe i cijene su niže te je upitna konkurentnost hrvatskih proizvođača (Šakić Bobić, 2015). Negativni učinci povećanja proizvodnje kravljeg mlijeka i ponude mliječnih proizvoda u EU trenutno su prisutni na tržištu (povećanjem ponude - pala je otkupna cijena mlijeka i mliječnih proizvoda u EU što je uzrokovalo odustajanje proizvođača od proizvodnje te posljedično povećanje cijene npr. maslaca). Kako su projekcije ekonometrijskim modelom pokazale (Zrakić i sur., 2015) nakon ukidanja kvota u Europskoj uniji, trend smanjenja domaće proizvodnje se nastavio a izloženost slobodnom europskom tržištu znatno utječe na konkurentnost domaće proizvodnje. U Hrvatskoj se tako cijena maslaca povećala za oko 30% (u EU oko 21%).

U 2008. godini cijena kravljeg mlijeka bila je jednaka u Hrvatskoj i EU i iznosila je 0,341 EUR/l, međutim već sljedeće godine cijene su pale. Nakon 2009. cijene su počele rasti i 2014. bile su najviše u odnosu na 2005. godinu. U Hrvatskoj je cijena iznosila 0,367 EUR/l dok je referentna cijena iznosila nešto više - 0,379 EUR/l (Grafikon 5).



Grafikon 5: Cijena kravljeg mlijeka u Hrvatskoj i referentna cijena EU

Graph 5: Price of cow's milk in Croatia and EU reference price

Izvor: Isti kao za Grafikon 1/Source: Same as for Graph 1

U Grafikonu 5 iz jednadžbi linearnog trenda vidljivo je da je prosječno godišnje povećanje cijena kravljeg mlijeka bilo vrlo malo: za 0,0081 eura u RH i za 0,0058 u EU te su cijene u prosjeku bile više kroz razdoblje (0,2682 u RH odnosno 0,2832 u EU). Dobivena je vrlo snažna korelacija od 0,89 što govori da cijene kravljeg mlijeka u Hrvatskoj prate kretanje cijena u EU, odnosno snižavanje referentne cijene praćeno je snižavanjem cijena u Hrvatskoj što nam ukazuje na veliku izloženost domaćeg tržišta promjenama na europskom. Do 2020. godine očekuje se blagi porast cijena.

ZAKLJUČAK

Tržište poljoprivrednih proizvoda osjetljivo je zbog raznih faktora koji utječu na proizvodnju i to od sve češćih i jačih klimatskih promjena do potražnje za određenim proizvodom. Poljoprivredna proizvodnja pa tako i cijene iznimno su godišnje kolebljivi te su vrlo teške i nezahvalne za prognoze.

Hrvatsko tržište poljoprivrednih proizvoda ima relativno mali udio (količinski i vrijednosni) u robnim tržištima Europske unije. Zbog potpune liberalizacije tržišta između država članica EU, ekonomski učinci "velikih" tržišta prelijevaju se na relativno mala tržišta kao što je i hrvatsko te uvelike utječu na cijene poljoprivrednih proizvoda.

Referentne cijene Unije za pšenicu, kukuruz, šećernu repu, uljanu repicu i kravlje mlijeko utječu na hrvatske cijene ovih istih proizvoda za istraživano razdoblje (od 2005. do 2015. godine). Jakost veze između referente i hrvatske cijene izražena Pearsonovim koeficijentom je pozitivna i najveća je kod mlijeka (0,89), zatim kod uljane repice (0,87), kukuruza (0,82), pšenice (0,65) te najmanje kod uljane repice (0,03).

Do 2020. godine očekuje se daljnji rast referente i domaće cijene pšenice, kukuruza i mlijeka, ali i smanjenje cijena šećerne repe i uljane repice ali s različitim intenzitetom.

Napomena

Rad je izvod iz završnog rada studentice Tee Kovač, bacc. ing. agr., studentice preddiplomskog studija Agrarna ekonomika na Agronomskom fakultetu u Zagrebu

LITERATURA

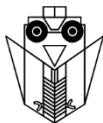
- Eurostat statistics explained: Agricultural production – crops
http://ec.europa.eu/eurostat/statistics-explained/index.php/Agricultural_production_-_crops
(23. travnja .2017.).
- Eurostat statistics explained: Milk and milk products statistics http://ec.europa.eu/eurostat/statistics-explained/index.php/Milk_and_milk_product_statistics (24. travnja 2017.).
- Grgić, I. (2000). Promjenjivost proizvođačkih cijena glavnih poljoprivrednih proizvoda u Hrvatskoj. Disertacija. Sveučilište u Zagrebu, Agronomski fakultet. Zagreb.
- Jukić, J. (2016). Uloga poljoprivrede Republike Hrvatske u europskom kontekstu, diplomski rad, Sveučilište Josipa Jurja Strossmayera u Osijeku Poljoprivredni fakultet, Osijek.
- Kovač, T. (2017). Međuodnos hrvatskih proizvođačkih cijena odabranih poljoprivrednih proizvoda i referentnih cijena EU-usporedna analiza, završni rad, Sveučilište u Zagrebu Agronomski fakultet, Zagreb.
- Petz, B., Kolesarić, V., Ivanec, D. (2012). Petzova statistika: Osnove statistike za nematematičare. Naklada slap. Zagreb. 281- 349.
- Šakić Bobić, B. (2015). Gdje smo mi na europskoj mljekarskoj sceni. Mljekarski list 10: 46-47.
- Turčić Z. (2015). Hrvatsko gospodarstvo u vanjskotrgovinskoj razmjeni, Poslovna izvrsnost Zagreb 1/2015, Zagreb 167-189.
www.dzs.com
www.eurostat.com
- Zrakić, M., Salputra, G., Levak, V. (2015). Potential impact of EU Common Agriculture Policy on Croatian dairy sector - modelling results. Mljekarstvo 65(3): 192-202.

PRODUCTION PRICES OF SELECTED AGRICULTURAL PRODUCTS IN THE REPUBLIC OF CROATIA AND REFERENCE PRICES OF EUROPEAN UNION

SUMMARY

Croatia has a major share of foreign trade with the European Union, and since 2013 it has become a formal part of this single common market. These changes have made some changes for domestic production and the agri-food products market, most suitable for domestic competition and has enabled access of Croatian products to major European markets. The aim of the paper is to determine the changes in Croatian producer prices of wheat, maize, sugar beet, rape and cow's milk compared to the reference prices of the European Union from 2005 to 2015. Research has shown that national prices of selected agricultural products followed the trend of the reference price EU in general. By 2020, domestic prices of wheat, maize and cow's milk will increase, but sugar beet prices will be reduced. The mentioned changes will be significantly affected by the impact of EU reference prices, except for sugar beet.

Key words: European Union, producer prices, agricultural products



VANJSKOTRGOVINSKA RAZMJENA REPUBLIKE HRVATSKE S EKONOMSKIM GRUPACIJAMA ZA ODABRANE POLJOPRIVREDNO-PREHRAMBENE PROIZVODE U VREMENU 2010. - 2017. GODINE

Ivo GRGIĆ^{1*}, Lari HADELAN¹, Josip GUGIĆ², Paula JURJEVIĆ³,
Magdalena ZRAKIĆ¹

¹ Sveučilište u Zagrebu, Agronomski fakultet, Svetošimunska cesta 25, 10000 Zagreb, Hrvatska

² Veleučilište Marko Marulić, Knin, Hrvatska

³ Remetinečka cesta 77, 10000 Zagreb, Hrvatska

*E-mail dopisnog autora: igrgic@agr.hr

SAŽETAK

Vanjskotrgovinska razmjena poljoprivredno-prehrambenih proizvoda ovisi o domaćoj proizvodnji, razvijenosti prehrambene industrije, stvarnoj i potencijalnoj domaćoj potražnji, promjenama na domaćem i svjetskom tržištu i sl. Hrvatska je pristupanjem u međunarodne organizacije kao što su WTO, CEFTA, EFTA te na kraju i EU, liberalizirala tržište poljoprivredno-prehrambenih proizvoda. U radu se istražuje vanjskotrgovinska razmjena s državama članicama EFTA-e, CEFTA-e i OPEC-a u razdoblju od 2010. do 2017. godine ukupno te za pojedine proizvode i to goveđe i svinjsko meso, pšenica, ječam, zob, kukuruz, raž, riža, prirodni med, jaja peradi, mlijeko, šećer te čokolada. Iako tijekom analiziranog razdoblja postoje kolebanja, u prosjeku Hrvatska u razmjeni s CEFTA-om ostvaruje suficit dok s OPEC-om i EFTA-om ostvaruje deficit. U ukupnom izvozu vrijednost triju robnih sektora koji se odnose na poljoprivredno-prehrambene proizvode (hrana i žive životinje, pića i duhan te životinjska i biljna ulja i masti) činili su oko 25% u ukupnom izvozu u CEFTA-u, odnosno 3 i 10% u EFTA-u i OPEC te 20% ukupnog izvoza iz CEFTA-e odnosno 4 i 20% ukupnog izvoza u EFTA-u i OPEC. Najveći suficit u razmjeni s CEFTA-om je kod pšenice te manje kod kukuruza.

Ključne riječi: vanjskotrgovinska razmjena, poljoprivredno-prehrambeni proizvodi, EFTA, CEFTA, OPEC

UVOD

Vanjskotrgovinska razmjena poljoprivredno-prehrambenih proizvoda Hrvatske je negativna uz značajna godišnja kolebanja tijekom analiziranog razdoblja (Grgić i sur. 2011).

Vanjskotrgovinska politika Republike Hrvatske u najvećoj mjeri određena je njezinim članstvom u Svjetskoj trgovinskoj organizaciji (WTO) i EU. Za „malu“ državu kao što je Hrvatska bilo je od velike važnosti da se uključi u globalne procese gospodarskog povezivanja. Proces liberalizacije odnosno otvaranja tržišta poljoprivrednih proizvoda donio je značajne promjene u domaćoj ponudi i vanjskotrgovinskoj razmjeni, a sve je to započelo pristupanjem Hrvatske WTO-u. Hrvatska je članicom WTO-a postala 30. studenog 2000. godine i to kao 140. članica. Njeno članstvo je predstavljalo temelje integriranja hrvatskog gospodarstva u europsko i globalno tržište sa svrhom povećanja efikasnosti i konkurentnosti te povećanja izvoza (Turčić, 2015). Nakon ulaska u WTO, Hrvatska se pridružuje europskim i regionalnim gospodarskim integracijama poput CEFTA-e (Srednje-europski ugovor o slobodnoj trgovini) i EFTA-e (Europsko udruženje za slobodnu trgovinu).

Hrvatska je prije pristupa CEFTA-i (2002. godine) ispunila potrebne preduvjete kao što su članstvo u WTO-u, potpisan Sporazum o pridruženom članstvu s EU te pristanak svih članica CEFTA-e u obliku zaključenih pregovora bilateralnim ugovorima o slobodnoj trgovini. Pristupom CEFTA-i Hrvatska je značajno liberalizirala trgovinu poljoprivredno-prehrambenim proizvodima s drugim članicama kao npr. s Bosnom i Hercegovinom, dok su se snižene carinske stope primjenjivale u izvozu sa Srbijom koja je ujedno i drugi najvažniji hrvatski vanjskotrgovinski partner (Ćudina i Sušić, 2013).

Iste, 2002. godine, Hrvatska je potpisala Ugovor o slobodnoj trgovini s EFTA-om nakon čega su u potpunosti ukinute carine na uvoz industrijske robe porijeklom iz Hrvatske te istodobno za najveći dio industrijskih proizvoda pri uvozu u Hrvatsku.

Hrvatska je 1. srpnja 2013. godine postala punopravnom članicom EU. Prestali su se primjenjivati dotadašnji sporazumi o slobodnoj trgovini uključujući i Srednjoeuropski ugovor o slobodnoj trgovini što znači da je i ujedno prestala biti članica CEFTA-e. Osim što su se prestali primjenjivati navedeni sporazumi, prestali su važiti carinski propisi i drugi zakoni koji su bili određeni tim sporazumima. Izlaskom Hrvatske iz spomenutih integracija, nisu prekinuti važni trgovinski odnosi, dok Hrvatska i dalje većinu razmjene svojih poljoprivredno-prehrambenih proizvoda ostvaruje s EU (Koloper, 2016).

Tržišta na kojima će biti fokus rada su trgovinske grupacije država EFTA-e (Island, Lihtenštajn, Norveška i Švicarska), CEFTA-e (Albanija, Bosna i Hercegovina, Crna Gora, Kosovo, Makedonija, Moldavija i Srbija) i OPEC-a (Alžir, Angola, Ekvador, Iran, Irak, Kuvajt, Libija, Nigerija, Katar, Saudijska Arabija, Ujedinjeni Arapski Emirati i Venezuela).

Iako Hrvatska većinu svoje vanjske trgovine i robne razmjene obavlja s državama EU, CEFTA je još od vremena punog članstva važan trgovinski partner. Članice CEFTA-e većinom su države s kojima je Hrvatska imala i kroz povijest jake trgovinske odnose, kako zbog povijesnih razloga tako i blizine samih tržišta tako ali i zbog preferencija potrošača koje su vrlo slične na domaćem tržištu i tržištu članica. Većinu ukupne vanjske trgovine s CEFTA-om Hrvatska obavlja s Bosnom i Hercegovinom (oko 50% izvoza i uvoza) i Srbijom (oko 25% izvoza i 40% uvoza). Naša glavna izvozna tržišta jesu Italija, Slovenija, Bosna i Hercegovina, Mađarska, Srbija i Njemačka, dok su glavna uvozna tržišta Njemačka, Italija, Mađarska, Slovenija, Nizozemska i Poljska. Ulaskom Hrvatske u EU poljoprivreda i ribarstvo te prehrambeno-prerađivačka industrija bilježe rast plasmana proizvoda na EU tržište od 64%, odnosno 62%, dok s druge strane bilježe i veliku izloženost konkurentskim proizvodima iz drugih zemalja članica (Agrobiz, 2016).

MATERIJAL I METODE

Rezultati rada temelje se na podacima Državnog zavoda za statistiku (DZS) – Robna razmjena s inozemstvom. U radu će se analizirati vrijednost izvoza i uvoza odabranih poljoprivredno-prehrambenih proizvoda u izabrane ekonomske integracije, ukupni izvoz i uvoz te na kraju izračunati pokrivenost uvoza izvozom.

Promatrani proizvodi trgovinske razmjene s državama članicama EFTA-e, CEFTA-e i OPEC-a su: goveđe i svinjsko meso, pšenica, ječam, zob, kukuruz, raž, riža, prirodni med, jaja peradi, mlijeko, šećer te čokolada. Podatci se odnose na razdoblje od 2010. do 2017. godine prema danim carinskim tarifama (CT) do 2013. godine odnosno kombinirane nomenklature (KN) od 2014. godine. Carinska tarifa je sustavni pregled svih predmeta koji podliježu carinjenju i carinskim stopama. Kombinirana nomenklatura je slična sistematizacija, koja uz carinsku tarifu uključuje i statističke trgovinske nomenklature EU. Izračunata je i pokrivenost uvoza izvozom sveukupno za pojedine integracije te za žitarice, meso, mlijeko, jaja peradi, prirodni med, šećer i čokoladu u razmjeni sa CEFTA-om. CEFTA je izabrana zbog važnosti u vanjskotrgovinskom prometu poljoprivredno-prehrambenim proizvodima i zbog toga što su za odabrane proizvode dostupni podaci i za uvoz i za izvoz.

REZULTATI I DISKUSIJA

CEFTA je ekonomska grupacija zemalja s kojom je Hrvatska ostvaruje suficit u međusobnoj razmjeni roba (Grafikon 1), a do formalnog pristupa u EU i sama je bila članica. Hrvatska je u članice CEFTA-e u analiziranom razdoblju najviše izvozila u 2014. godini (2,1 milijarde eura), a najmanje 2010. godine (1,7 milijuna eura). Uvoz je uz manja kolebanja bio od 811,8 milijuna eura u 2010. do 1,167 milijardi eura u 2016. godini. Za prvih šest mjeseci u 2017. godini zabilježen je također suficit s čime se nastavlja pozitivan trend pri čemu je vrijednost izvoza 1,133 milijarde a uvoza 652 milijuna eura. U ukupnom izvozu vrijednost triju robnih sektora (hrana i žive životinje, pića i duhan te životinjska i biljna ulja i masti) činili su oko 25% u ukupnom izvozu u CEFTA-u i 20% ukupnog izvoza iz CEFTA-e (Jurjević, 2017).



Grafikon 1. Ukupna razmjena Hrvatske i CEFTA-e u razdoblju od 2010. do 2016. godine
Graph 1. Total exchange of Croatia and CEFTA from 2010 to 2016

Izvor: izračun prema podacima Statistički ljetopis Republike Hrvatske, DZS
 Source: calculation according to the Statistical Yearbook of the Republic of Croatia, CBS

Tablica 1. Vanjskotrgovinska razmjena Hrvatske i CEFTA-e odabranim proizvodima od 2010. do 2017. godine, milijuna eura
Table 1. Foreign trade of Croatia and CEFTA with selected products from 2010 to 2017, EUR million

		2010	2011	2012	2013	2014	2015	2016	I.-VI. 2017.
Žitarice*	X	25,158	31,623	48,505	23,050	27,008	37,873	19,093	8,416
Cereals*	M	1,029	4,373	7,627	11,367	10,396	6,545	5,229	3,304
Meso**	X	9,755	5,210	0,126	6,914	6,731	6,087	9,448	3,108
Meat**	M	0,439	0,973	0,399	-	0,019	-	-	-
Mlijeko	X	12,105	15,767	14,594	8,376	4,698	5,187	6,215	3,555
Milk	M	12,299	15,495	15,177	11,066	3,945	0,280	0,720	2,166
Jaja peradi	X	0,014	0,036	0,422	-	0,116	0,149	0,096	-
Poultry eggs	M	2,366	1,633	2,405	1,322	-	0,168	0,013	-
Prirodni med	X	0,948	0,771	0,719	0,600	0,446	0,558	0,491	0,371
Honey	M	0,039	0,189	0,279	0,266	0,185	0,118	-	0,045
Šećer	X	5,096	3,539	3,729	2,477	0,782	0,692	14,577	0,287
Sugar	M	0,708	0,079	0,493	5,977	5,169	2,206	7,653	2,077
Čokolada	X	30,402	29,053	26,159	29,311	43,206	58,077	60,780	27,389
Chocolate	M	6,610	5,857	5,026	5,162	4,821	4,776	4,659	1,982
% u ukupnom	X	5,0	8,9	4,3	12,9	4,5	6,0	3,5	12,8
% in total	M	2,8	5,0	2,8	4,7	3,5	7,3	3,0	10,2

*pšenica, zob, raž, ječam, kukuruz, riža; ** goveđe i svinjsko meso; X – izvoz, M – uvoz Izvor: isti kao za Grafikon 1/* wheat, oats, rye, barley, maize, rice; ** beef and pork meat; X - Export, M – Import Source: same as for Graph 1

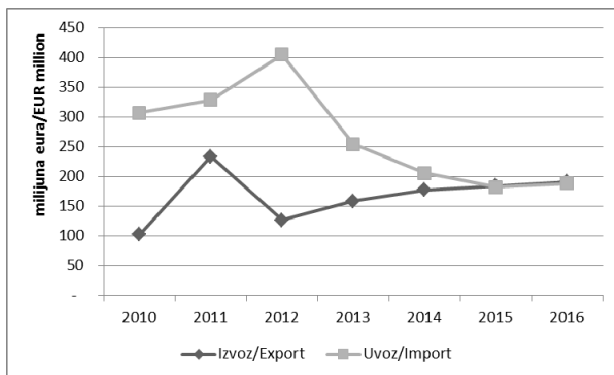
Tijekom analiziranog razdoblja Hrvatska je s državama CEFTA-e imala pozitivnu vanjskotrgovinsku bilancu što se nastavilo i u prvih šest mjeseci 2017. godine. Izuzetak je vanjskotrgovinska razmjena šećera kod kojeg smo imali pozitivnu bilancu do 2013. godine. Nakon toga zabilježena je trogodišnja negativna bilanca (do 2015.), da bismo 2016. opet imali suficit vanjskotrgovinske razmjene šećerom. U prvih 6 mjeseci vanjska trgovina šećerom je ponovo negativna. Kod grupe žitarica, pšenica i kukuruz su najzastupljenije kulture u razmjeni s državama CEFTA-e. Kod izvoza žitarica pšenica je zastupljena u prosjeku sa 70%, a kukuruz sa oko 25%. U prometu sa pšenicom ostvarena je pozitivna bilanca svake godine promatranog razdoblja, dok kod kukuruza bilježimo blagi deficit od oko 2 milijuna eura u 2013. i 2014. godini. Kod izvoza goveđeg i svinjskog mesa, i jedna i druga vrsta mesa je vrijednosno podjednako zatupljena (49% goveđe meso, 51% svinjsko meso). U razdoblju od 2010. do 2016. godine vrijednost promatranih proizvoda u ukupnom izvozu u članice CEFTA-e je u prosjeku 6,4%, a u uvozu čine u prosjeku 4,1% ukupne vrijednosti uvoza iz CEFTA-e.

EFTA

EFTA (*European Free Trade Association*/Europska slobodna trgovinska zona) je utemeljena 1960. godine i danas je čine Švicarska, Lihtenštajn, Island i Norveška. Te četiri članice sudjeluju u jedinstvenom tržištu Europske unije Sporazumom o europskom gospodarskom prostoru (Šafarić, 2016). Hrvatska je ekonomskoj integraciji pristupila 2002. godine.

Od 2010. do 2016. godine Hrvatska ostvaruje veći uvoz nego izvoz dok je u 2015. i 2016. godini bila povoljnija situacija – razlika (neto izvoz) je bila oko 2,2 odnosno 3,2 milijuna eura.

Hrvatska je najviše uvozila 2012. godine (405 milijuna eura), dok je najviše izvozila 2011. godine (233 milijuna eura) (Grafikon 2). U ukupnom izvozu vrijednost triju robnih sektora (hrana i žive životinje, pića i duhan te životinjska i biljna ulja i masti) činili su oko 3% u ukupnom izvozu u EFTA-u i 4% ukupnog izvoza iz EFTA-e (Jurjević, 2017).



Grafikon 2. Ukupna razmjena Hrvatske i EFTA-e u razdoblju od 2007.do 2015. godine

Graph 2. Total exchange of Croatia and EFTA from 2010 to 2016

Izvor: isti kao za Grafikon 1/ Source: same as for Graph 1

Tablica 2. Vanjskotrgovinska razmjena Hrvatske i EFTA-e odabranim proizvodima od 2010. do 2017. godine, milijuna eura

Table 2. Foreign trade of Croatia and EFTA with selected products from 2010 to 2017, EUR million

		2010	2011	2012	2013	2014	2015	2016	I.-VI. 2017.
Žitarice*	X	0,613	0,093	0,000	0,000	-	-	-	-
Cereals*	M	-	0,049	0,050	0,123	0,000	0,001	0,005	0,001
Meso**	X	-	-	-	0,000	-	0,001	0,010	0,003
Meat**	M	0,015	0,104	2,097	0,434	-	-	-	-
Mlijeko	X	-	-	-	-	-	-	-	-
Milk	M	-	-	-	-	-	-	-	-
Jaja peradi	X	-	-	-	-	-	-	-	-
Poultry eggs	M	-	-	-	-	-	-	-	-
Prirodni med	X	0,028	0,308	0,193	0,049	0,009	0,084	0,069	0,016
Honey	M	0,002	0,002	0,002	-	-	-	-	-
Šećer	X	-	-	-	-	-	-	0,000	0,000
Sugar	M	-	0,000	-	-	-	-	-	-
Čokolada	X	0,146	0,134	0,165	0,146	0,167	0,201	0,387	0,153
Chocolate	M	0,875	0,767	0,963	0,385	0,308	0,340	0,305	0,134
% u ukupnom	X	0,77	0,23	0,28	0,12	0,10	0,16	0,24	0,18
% in total	M	0,29	0,28	0,77	0,37	0,15	0,19	0,16	0,15

*pšenica, zob, raž, ječam, kukuruz, riža; ** goveđe i svinjsko meso; X – izvoz, M - uvoz
Izvor: isti kao za Grafikon 1/* wheat, oats, rye, barley, maize, rice; ** beef and pork meat; X -
Export, M – Import Source: same as for Graph 1

Hrvatska relativno malo izvozi u EFTA-u. U promatranom razdoblju najviše se izvezio kukuruz i to 2010. godine (oko 2,4 milijuna kg ili 506 tisuća eura) nakon čega se izvoz kukuruza smanjivao te se nakon 2013. godine više ne izvozi. Iste tendencije bilježi i izvoz ječma i pšenice, U izvozu promatranih proizvoda kontinuitet imaju dva proizvoda: prirodni med (prosjeak razdoblja 68.000 eura) i čokolada (prosjeak razdoblja 123.000 eura). Čokolada je jedini proizvod čiji se izvoz iz godine u godinu povećava, pa se tako najviše izvezila 2016. godine (387.000 eura).

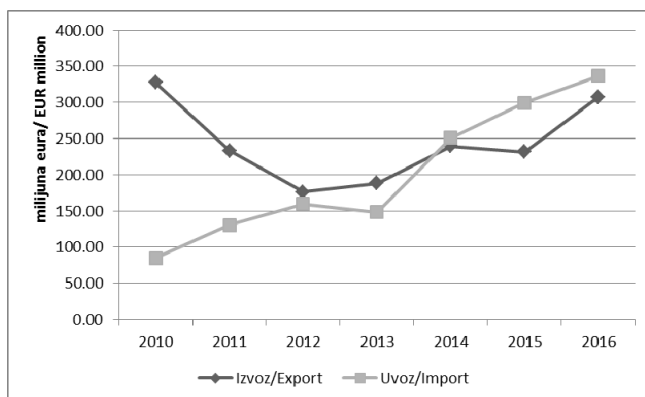
Hrvatska uvozi svinjsko meso, kukuruz, čokoladu, šećer i prirodni med. Od navedenih proizvoda najviše uvozimo svinjsko meso (najviše 2012. godine - 1.059 tona ili 2 milijuna eura), dok je uvoz čokolade malo kolebljiv i godišnje je na razini od oko 500 tisuća eura. Uvoz prirodnog meda i mlijeka do 2012. je mali, a nakon toga se ne uvoze

Udio sume vrijednosti promatranih proizvoda u ukupnoj vanjskoj trgovini s EFTA-om je u prosjeku ispod 1%, što imputira činjenicu da iz te ekonomske grupacije uvozimo poljoprivredno-prehrambene proizvode višeg stupnja i većinu dobara i usluga iz drugih proizvodnih sektora.

OPEC

OPEC (*Organization of the Petroleum Exporting Countries*) je međunarodna organizacija koja je osnovana 1960. godine u Bagdadu u danas broji 13 članica: Irak, Iran, Kuvajt, Saudijska Arabija, Venezuela, Alžir, Angola, Ekvador, Gabon, Libija, Nigerija, Katar te Ujedinjeni Arapski Emirati.

Hrvatska s OPEC-om ima značajne godišnje oscilacije vanjskotrgovinske razmjene pri čemu se suficit zamjenjuje deficitom. Najveći izvoz Hrvatske u OPEC je bio 2010. godine (oko 330 milijuna eura). Od 2011. godine vrijednost se smanjuje do 2012. godine kada ostvarujemo najmanji izvoz razdoblja (oko 190 milijuna eura). Nakon toga izvoz raste do 307 milijuna eura u 2016. godini. Iako kod uvoza imamo veća kolebanja nego kod izvoza, tijekom cijelog analiziranog razdoblja on ima pozitivan trend. Najveći uvoz je bio 2016. godine (336 milijuna eura), a najmanji 2010. godine (94 milijuna eura). Do 2013. godine Hrvatska je s grupacijom OPEC imala pozitivnu vanjskotrgovinsku bilancu. U ukupnom izvozu vrijednost triju robnih sektora (hrana i žive životinje, pića i duhan te životinjska i biljna ulja i masti) činili su oko 10% u ukupnom izvozu u OPEC i 20% ukupnog izvoza iz OPEC-a (Jurjević, 2017).



Grafikon 3. Ukupna razmjena Hrvatske i OPEC-a u razdoblju od 2010. do 2016. godine

Graph 3. Total exchange of Croatia and OPEC from 2010 to 2016

Izvor: isti kao za Grafikon 1/ Source: same as for Graph 1

Tablica 3. Vanjskotrgovinska razmjena Hrvatske i OPEC-a odabranim proizvodima od 2010. do 2017. godine, milijuna eura
Table 3. Foreign trade of Croatia and OPEC with selected products from 2010 to 2017, EUR million

		2010	2011	2012	2013	2014	2015	2016	I.-VI. 2017.
Žitarice*	X	5,494	-	8,262	1,088	0,128	5,753	0,009	-
Cereals*	M	0,001	-	0,039	-	0,086	0,082	-	-
Meso**	X	-	-	0,039	-	0,086	0,082	-	-
Meat**	M	-	-	-	-	-	-	-	-
Mlijeko	X	-	-	-	-	-	0,028	-	-
Milk	M	-	-	-	-	-	-	-	-
Jaja peradi	X	-	-	-	-	-	-	-	-
Poultry eggs	M	-	-	-	-	-	-	-	-
Prirodni med	X	-	-	-	0,000	0,000	0,000	0,000	0,000
Honey	M	-	-	-	-	-	-	-	-
Šećer	X	0,252	-	-	-	-	-	-	1,822
Sugar	M	0,262	-	0,162	-	-	-	-	-
Čokolada	X	-	-	-	0,128	0,024	0,105	0,240	0,087
Chocolate	M	0,000	0,000	0,000	-	0,000	-	-	-
% u ukupnom	X	1,8	0,0	21,7	0,6	0,1	2,6	0,1	1,8
% in total	M	0,3	0,0	0,0	0,0	0,0	0,0	0,0	0,0

*pšenica, zob, raž, ječam, kukuruz, riža; ** goveđe i svinjsko meso; X – izvoz, M - uvoz;

Izvor: isti kao za Grafikon 1/* wheat, oats, rye, barley, maize, rice; ** beef and pork meat;

X - Export, M – Import Source: same as for Graph 1

Hrvatska u OPEC izvozi relativno male količine, a količinski i vrijednosno najznačajniji proizvodi su pšenica, kukuruz i šećer. Od navedena tri proizvoda najviše se izvezlo kukuruz i to 2015. godine u iznosu od 31,5 tisuća tona, dok se šećer izvezlo samo 2010. godine (500 tona) te 2017. godine (3,7 tisuća tona odnosno 1,8 milijuna eura). Niti jedan od promatranih proizvoda nema zabilježen kontinuirani godišnji izvoz tako se kukuruz izvozi 2010., 2012, 2015. i 2016. godine, a pšenica 2010., 2012. i 2013. godine.

I vrijednosno je kukuruz najvažniji izvozni proizvod te se najviše izvezlo 2015. godine u iznosu od 5,5 milijuna eura. Na drugom mjestu je pšenica koje se najviše izvezlo 2010. godine (4,1 milijuna eura), dok je vrijednost izvezenog šećera prosječno 1,04 milijuna eura. Od ostalih odabranih proizvoda, bilježe se manje izvezene količine svinjskog mesa (godine 2012./14./15.), ječma (2012./14./15.), prirodnog meda (2013.-2017.), čokolade (2013.-2017.) i mlijeka (2015.).

Hrvatska je iz OPEC-a uvozila šećer, rižu i čokoladu, a u toj strukturi količinski najznačajniji proizvod je šećer (od 2010-2017. uvezeno je 861,5 tona). Najviše ga se uvezlo u 2010. godini (oko 560 tona).

Sličan redoslijed je i kod vrijednosti uvoza.

Pokrivenost uvoza izvozom

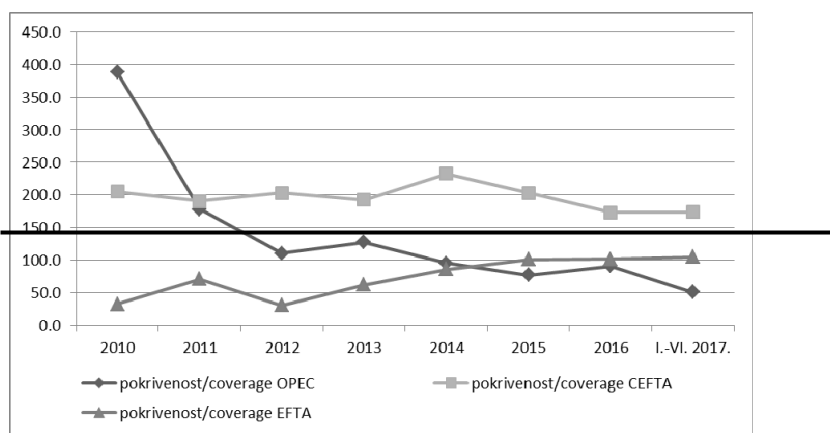
Pokrivenost uvoza izvozom (r) je indikator koji služi kao kvantitativni pokazatelj vanjskotrgovinske razmjene te njegova formula glasi (Grgić i sur., 2011):

$$r'_{ij} = \frac{X'_{ij}}{M'_{ij}} * 100$$

gdje je:

r'_{ij} - Pokrivenost uvoza izvozom u godini t ; X'_{ij} - Izvoz sektora i odsjeka j u godini t ; M'_{ij} - Uvoz sektora i odsjeka j u godini t

Ako je vrijednost indikatora pokrivenosti 100 to znači da pojedina zemlja ostvaruje vanjskotrgovinski deficit, a ako je vrijednost indikatora iznad 100 onda se ostvaruje vanjskotrgovinski suficit te se pokrivenost najčešće iskazuje u postotku (Grgić i sur., 2011).



Grafikon 4. Pokrivenost ukupnog uvoza ukupnim izvozom prema ekonomskim integracijama (vrijednosno), %

Graph 4. Coverage of total imports by total exports by economic integration (value), %

Izvor: isti kao za Grafikon 1/ Source: same as for Graph 1

Hrvatska u vanjskotrgovinskoj razmjeni s EFTA-om ostvaruje deficit do 2014. nakon čega ima mali suficit. Sa CEFTA-om ima suficit tijekom cijelog razdoblja, a s OPEC-om do 2013. ima suficit nakon čega deficit.

Najveći suficit u ukupnoj razmjeni Hrvatska ostvaruje s OPEC-om 2010. godine kada pokrivenost iznosi čak 388%, dok 2017. godine ostvaruje deficit kada je pokrivenost 51,2%. U vanjskotrgovinskoj razmjeni s CEFTA-om, Hrvatska u razdoblju od 2007. do 2015. godine ostvaruje suficit a najveći je suficit bio ostvaren 2014. godine kada je pokrivenost iznosila 233%. Hrvatska s EFTA-om u ukupnoj razmjeni ostvaruje uglavnom deficit do 2015. godine. Te godine se javlja blagi suficit od 101,2% i taj trend se nastavlja u 2016. (101,7%) i 2017. (105,0%) godini.

Hrvatska sa članicama CEFTA-e ostvaruje najznačajnije količine i vrijednosti razmjene. U tablici 4 prikazana je pokrivenost uvoza izvozom za odabrane proizvode.

Tablica 4. Pokrivenost uvoza izvozom kod odabranih poljoprivredno-prehrambenih proizvoda iz vanjskotrgovinske razmjene Hrvatske i CEFTA-e, %
Table 4. Coverage of import by exports of selected agricultural and food products from foreign trade of Croatia and CEFTA, %

	2010	2011	2012	2013	2014	2015	2016	I.-VI. 2017.
Žitarice*/ Cereals*	2444,90	723,14	635,96	202,78	259,79	578,66	365,14	254,72
Meso**/Meat**	2222,10	535,46	31,58	n/a	35426,32	n/a	n/a	n/a
Mlijeko/Milk	98,42	101,76	96,16	75,69	119,09	1852,50	863,19	164,13
Jaja peradi/ Poultry eggs	0,59	2,20	17,55	n/a	n/a	88,69	738,46	n/a
Prirodni med/Honey	2430,77	407,94	257,71	225,56	241,08	472,88	n/a	824,44
Šećer/Sugar	719,77	4479,75	756,39	41,44	15,13	31,37	190,47	13,82
Čokolada/ Chocolate	459,94	496,04	520,47	567,82	896,20	1216,02	1304,57	1381,89

*pšenica, zob, raž, ječam, kukuruz, riža; ** goveđe i svinjsko meso; n/a = postoji samo izvoz ili uvoz/* wheat, oats, rye, barley, maize, rice; ** beef and pork meat; n / a = only export or import;
 Izvor: isti kao za Grafikon 1/Source: same as for Graph 1

Dobiveni izračuni pokrivenosti pokazuju da Hrvatska kod većine promatranih proizvoda u razdoblju 2010.-2017. godine izvozi više nego što uvozi. Pokrivenost uvoza izvozom manja od 100% javlja se samo u pojedinim godinama kod jaja peradi, šećera, mesa i mlijeka.

ZAKLJUČAK

Vanjskotrgovinska razmjena poljoprivredno-prehrambenih proizvoda izravno je ovisna o domaćoj proizvodnji, razvijenosti prehrambene industrije, stvarnoj i potencijalnoj domaćoj potražnji te promjenama na domaćem i svjetskom tržištu. Hrvatska je pristupanjem u trgovinske/ekonomske organizacije kao što su WTO, CEFTA, EFTA i EU, liberalizirala i otvorila tržište poljoprivredno-prehrambenih proizvoda.

Hrvatska s CEFTA-om ostvaruje suficit dok s preostale dvije grupacije ostvaruje i deficit i suficit, ovisno o godini. Od proizvoda najveći i stalni suficit u razmjeni s CEFTA-om ostvaruje sa žitaricama (pšenica i kukuruz). Kod vanjskotrgovinske razmjene s EFTA-om i OPEC-om zabilježen je deficit kod pšenice, kukuruza, svinjskog i goveđeg mesa. Ulazak Hrvatske u EU donio je sa sobom mnogo dobrih i loših promjena. Hrvatska je dobila nove partnere i ulazak na veće tržište, ali i izlazak iz CEFTA-e što za sobom donosi ukinuće bescarinskog režima prema toj grupaciji. Od 2013. godine izvoz poljoprivredno-prehrambenih proizvoda u CEFTA-u je varirao dok je uvoz bio smanjen, ali se u preostale grupacije izvoz i uvoz smanjio. Ulaskom Hrvatske u EU poljoprivreda i ribarstvo te prehrambeno-prerađivačka industrija bilježe rast plasmana proizvoda na EU tržište, tako da vanjski promet poljoprivredno-prehrambenim proizvodima s ekonomskim grupacijama jest važan dio vanjskotrgovinske razmjene Hrvatske ali nije ključan.

Napomena

Rad je izvod iz završnog rada studentice Paule Jurjević, bacc. ing. agr., studentice preddiplomskog studija Agrarna ekonomika na Agronomskom fakultetu u Zagrebu.

LITERATURA

- Agrobiz (2017). HGK: Nakon ulaska u EU najbolje rezultate bilježe poljoprivreda i prehrambena industrija, <http://www.agrobiz.hr/agrovijesti/hgk-nakon-ulaska-u-eu-najbolje-rezultate-biljeze-poljoprivreda-i-prehrambena-industrija-2578> (24.10.2017.).
- Carinska tarifa: <http://www.moj-bankar.hr/Kazalo/C/Carinska-tarifa> (03. 04. 2017.).
- Ćudina, A. i Sušić, G. (2013). Utjecaj pristupanja Hrvatske Europskoj uniji na trgovinske i gospodarske odnose sa zemljama CEFTA-e, *Ekonomski pregled*, br. 64, str. 376-396.
- Grgić I., Zrakić M., Županac G. (2011). Hrvatska vanjskotrgovinska razmjena poljoprivredno-prehrambenih proizvoda, *Agronomski glasnik* 73, br. 4-5, str. 263-276.
- Jurjević, P. (2017). Vanjskotrgovinska razmjena poljoprivredno-prehrambenih proizvoda u Hrvatskoj od 2007. do 2016. godine s državama izvan EU, završni rad, Sveučilište u Zagrebu Agronomski fakultet, Zagreb.
- Koloper, A. (2016). Utjecaj ulaska Hrvatske u Europsku uniju na vanjskotrgovinsku razmjenu, Diplomski rad, Ekonomski fakultet Sveučilišta u Zagrebu, Zagreb.
- Kombinirana nomenklatura: <https://carina.gov.hr/propisi-i-sporazumi/carinska-tarifa-vrijednost-i-podrijetlo/carinska-tarifa/zakonodavstvo-4240/kombinirana-nomenklatura/2934> (23.10.2017.).
- Organization of the Petroleum Exporting Countries, dostupno na: http://www.opec.org/opec_web/en/index.htm (24. travnja 2017.)
- Statistički ljetopis Republike Hrvatske (2007.–2016. godine), dostupno na: <http://www.dzs.hr/> (01. travnja 2017.).
- Šafarić, H. (2016). Regionalne ekonomske organizacije i udruženja, Diplomski rad, Sveučilište Sjever Sveučilišnog centra Varaždin, Varaždin
- Turčić, Z. (2015). Hrvatsko gospodarstvo u vanjskotrgovinskoj razmjeni, *Poslovna izvrsnost* Zagreb, br. 1.

FOREIGN TRADE OF THE REPUBLIC OF CROATIA WITH ECONOMIC GROUPS IN SELECTED AGRICULTURAL AND FOOD PRODUCTS FROM 2010 TO 2017

SUMMARY

Foreign trade of agricultural and food products depends on domestic production, development of the food industry, real and potential domestic demand, changes in the domestic and world market, etc. Croatia has liberalized the market for agri-food products by joining international organizations such as the WTO, CEFTA, EFTA and EU. This study examines the foreign trade with the countries of EFTA, CEFTA and OPEC in the period from 2010 to 2017 in total and for individual products and to beef and pork, wheat, barley, oats, corn, rye, rice, natural honey, poultry eggs, milk, sugar and chocolate. Although fluctuations exist during the analyzed period, on average, Croatia exchanges with CEFTA surplus while achieving deficit with OPEC and EFTA. In total exports, the value of the three commodity sectors related to agricultural and food products (food and live animals, beverages and tobacco, and animal and vegetable oils and fats) accounted for about 25% of total exports in CEFTA, respectively 3 and 10% with EFTA and OPEC and 20% of total exports from CEFTA, ie 4 and 20% of total exports to the EFTA and OPEC. The biggest surplus in trade with CEFTA is for wheat and less for maize.

Key words: foreign trade, agricultural and food products, EFTA, CEFTA, OPEC



ANALIZA REGISTRIRANIH TRAKTORA U SLOVENIJI U 2016. GODINI

Tomaz POJE

Kmetijski inštitut Slovenije, Oddelek za kmetijsko tehniko in energetiko,
Hacquetova ulica 17, SI – 1000 Ljubljana, Slovenija
E-mail dopisnog autora: tomaz.poje@kis.si

SAŽETAK

U Sloveniji je u 2016. godini registrirano 1.103 novih traktora, čija kupovina nije bila subvencionirana. Fizičke osobe su vlasnici 72,7 % novih traktora, a 27,3 % vlasnika su pravne osobe. Među fizičkim osobama ima 92,3 % muških vlasnika. Najviše vlasnika je dobne starosti između 50 i 60 godina. Prosječna snaga novih traktora iznosila je 61,5 kW. New Holland vodeći je po prodaji sa 14,5 %. Na kraju 2016. godine bilo je registrirano ukupno 108.914 traktora. Prosječna snaga motora traktora proizvedenih godine 1952. bila je 19,6 kW, dok je u 2016. prosječna snaga novih traktora bila 61,5 kW.

Ključne riječi: snaga motora, registrirani traktori, vlasnici traktora, Slovenija

UVOD

Prema podacima Statističkog ureda Republike Slovenije (SURS, 2017) bilo je u Sloveniji prvog lipnja 2016. 69.902 poljoprivrednih gospodarstava. Poljoprivredna gospodarstva imaju 418.684 uvjetnih grla stoke (UG), što je za 3 % više nego u godini 2013. Od 2013. godine broj poljoprivrednih gospodarstava smanjen je za 3,4 %. Svako gospodarstvo obrađuje u prosjeku 6,9 hektara poljoprivrednog zemljišta (0,3 ha više nego u 2013. godini) i uzgajaju 7,5 uvjetnih grla.

Prema Popisu poljoprivrede iz 2010. (SURS, 2012) u Sloveniji je bilo 101.756 traktora, dok za 2013. godinu SURS navodi 106.696 traktora. Uz ove dvoosovinske traktore u 2013. godini SURS navodi i 21.292 jednoosovinskih traktora. Prema podacima SURS-a prosječna starost registriranih traktora je više od 21 godinu. Ukupno 83.291 traktora registriranih u 2014. godini, bili su stariji od 12 godina. Poje (2006, 2010, 2012, 2015) proučava traktorski park u Sloveniji glede broja traktora, njihove snage, starosti itd.

Traktor je omogućio razvoj poljoprivrede i to kao vučna i pogonska jedinica za različite priključke za rad u poljoprivredi. Proizvodnja traktora predstavlja industriju koja je u svijetu u 2014. godini prodala 2,13 milijuna traktora, a godinu dana prije 2,20 milijuna traktora (Tractor Market Report, 2015). Najveće tržište traktora u 2014. godini predstavlja Kina i

Indija, gdje je registrirano oko 50 % proizvedenih traktora, u prosjeku su manje snage (zbog toga i jeftiniji) nego traktori prodani u poljoprivredno razvijenim zemljama, gdje je struktura posjeda znatno veća (SAD, Brazil, Rusija, Zapadna Europa). Na europskom tržištu, na kojem se proda 8 % svjetske proizvodnje traktora, ostvaruje se 20 – 25 % svjetskog prometa traktorima (što iznosi oko 8,2 milijarde eura). Tržište traktora u SAD i azijsko tržište traktora u posljednjih nekoliko godina raste, dok prodaja u Europskoj uniji "stagnira". U EU najveće tržište u 2014. godini predstavlja Njemačka sa 34.611 prodanih traktora. U Francuskoj, koja je do tada bila najveći kupac traktora, u 2014. godini prodaja traktora smanjila se za 20 %. Te godine prodali su 33.127 traktora (prethodne godine 42.656). Italija u 2014. godini bilježi pad kupovine traktora i to svega 18.178 traktora što je najmanje nakon drugog svjetskog rata.

Cilj ovog rada je analiza razvojnih trendova traktorskog parka u Sloveniji na temelju podataka o registriranim traktorima.

MATERIJALI I METODE

Slovenija ima dvije važne baze podataka o traktorima. Prva je pri Statističkom uredu Republike Slovenije (SURS), koji svakih 10 godina provodi Popis poljoprivrede, koji također uključuje poljoprivrednu tehniku odnosno traktore. Druga je baza podataka resornih ministarstava o registriranim vozilima (traktorima). Ova baza podataka je od 2014. godine na novom portalu NIO, koje je web mjesto namijenjeno objavljivanju otvorenih podataka javnog sektora u Sloveniji. Ovaj portal sadrži i informacije o novo registriranim vozilima u Sloveniji. Za ove podatke brine Ministarstvo infrastrukture i prostornog uređenja i Ministarstvo unutarnjih poslova, gdje su bili ti podaci do 2013. godine.

U ovom se radu analiziraju novi, registrirani traktori u Sloveniji u 2016. godini, odnosno razvojni trendovi traktorskog parka u Sloveniji. Za obradu podataka korištene su odgovarajuće statističke analize (deskriptivna statistika).

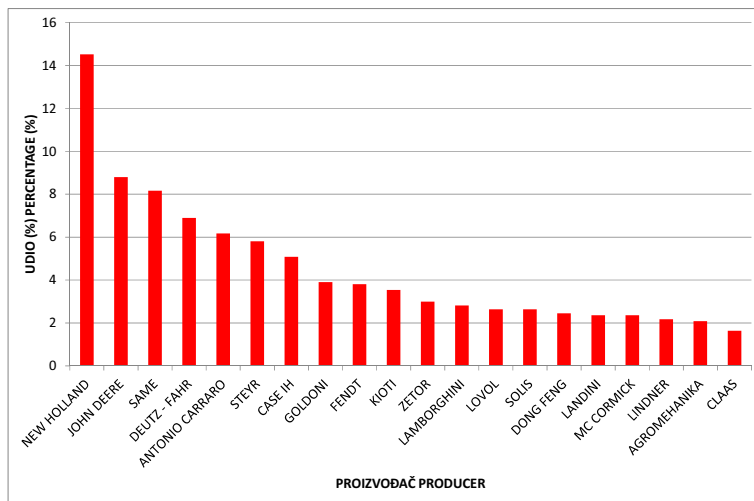
REZULTATI I RASPRAVA

U Sloveniji je u 2016. registrirano 1.103 novih traktora, što je u biti jednako kao u godini ranije. Prosječna snaga novih traktora iznosila je 61,5 kW. Ako nove traktore razvrstamo u kategorije prema snazi, tada je najviše prodanih traktora u kategoriji snage od 60 do 80 kW, odnosno više od 33 % svih traktora. Slijedi kategorija traktora snage između 40 i 60 kW sa 29,9 %. Kategorije traktora od 20 do 40 kW i iznad 80 kW imaju 19,3 % odnosno 15,7 % udjela. Najniža kategorija snage traktora (do 20 kW) predstavlja vrlo mali udio ili nešto manje od 2 % prodanih traktora.

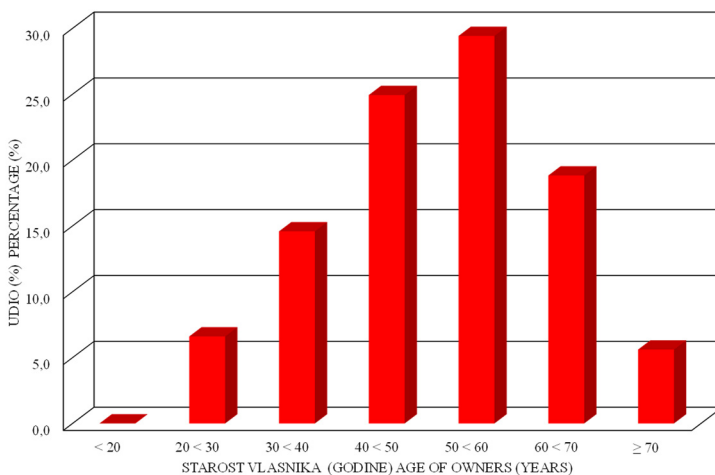
Analiza novih traktora u 2016. godini pokazuje da je New Holland prvi po prodaji traktora sa 14,52 %. New Holland je u Sloveniji već dugi niz godina vodeći po prodaji traktora. U 2016. drugi po prodaji je John Deere, a treći Same. U grafikonu 1 je prikazano prvih 20 proizvođača po zastupljenosti. Sve ukupno je u Sloveniji u 2016. godine prodano traktora od 38 različitih proizvođača. Na kraju ljestvice prema prodaji su Tym, BCS, Armtrac, Zoomlion.

Analiza vlasnika novih traktora pokazuje da je 72,7 % vlasnika fizička osoba i 27,3 % pravnih osoba. Među fizičkim osobama je 92,3 % muškaraca i 7,7 % žena. Broj pravnih osoba među kupcima traktora je značajan. Iz podataka za povrat trošarine za gorivo koje se koristi u poljoprivredi evidentirano je da u Sloveniji ima oko 90 pravnih osoba (tvrtki) koje se bave poljoprivredom. Trend u Sloveniji je da poljoprivrednici formiraju vlastita poduzeća zbog niza olakšica ili zahtjeva u poslovanju (razne subvencije, porezne olakšice itd.).

U 2016. godini je, kao i godinu ranije, najviše kupaca - vlasnika novih traktora (29,4 % udjela) u dobnoj skupini između 50 i 60 godina (grafikon 2). Slijedi skupina vlasnika dobi između 40 i 50 godina s udjelom od 24,9 %. Nema vlasnika novih traktora mlađih od 20 godina. 5,6 % kupaca je starijih od 70 godina, najstariji ima čak 83 godine.



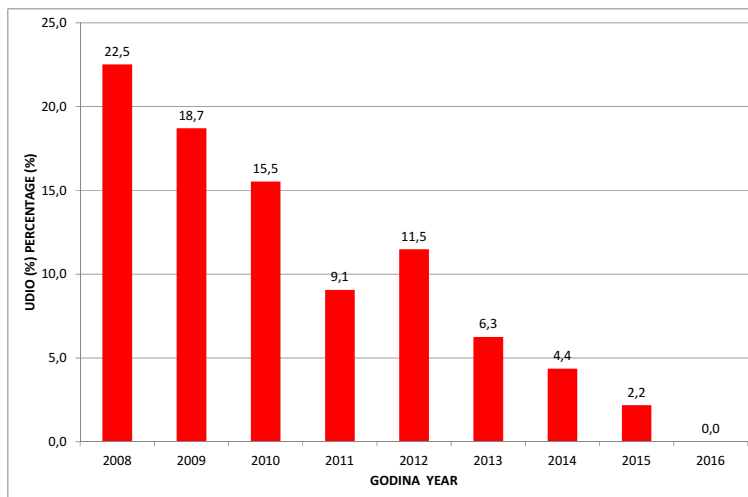
Grafikon 1. Udio novih traktora prema proizvođaču u godini 2016
Graph 1. Percentage of new tractors in the year 2016 with regard to producer



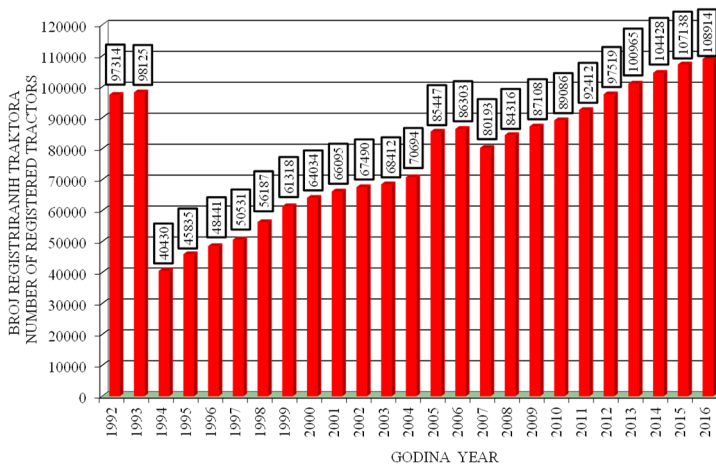
Grafikon 2. Udio vlasnika novih traktora u godini 2014. glede na dobne starosti
Graph 2.: Percentage of owners of new tractors with regard to their age

Ministarstvo poljoprivrede je u okviru PRP 2007.-2013. (Mjere za razvoj poljoprivrede) sufinanciralo kupnju novih traktora. Iznos subvencije je 30 do 60 % od priznatih vrijednosti ulaganja u novi traktor. Između 2008. i 2016. godine bilo je kupljeno 13.711 novih traktora.

Od toga je 1.593 novih traktora bilo sufinanciranih (subvencioniranih) u visini 25.661.389 EUR. Udio sufinanciranih traktora za pojedine godine je prikazan u grafikonu 3. Vidljivo je kako je sufinanciranje iz godine 2008. kad je bilo 22 % traktora palo u 2016. na nula traktora. U tom razdoblju u prosjeku je sufinancirano 11,6 % svih novih traktora. U 2017. godini očekuje se opet porast subvencioniranih traktora.



Grafikon 3. Udio sufinanciranih investicija u nove traktore
Graph 3. Percentage of subsidized buying of new tractors



Grafikon 4. Broj registriranih traktora u Sloveniji po godinama
Graph 4. Number of registered tractors in Slovenia with regard to the year

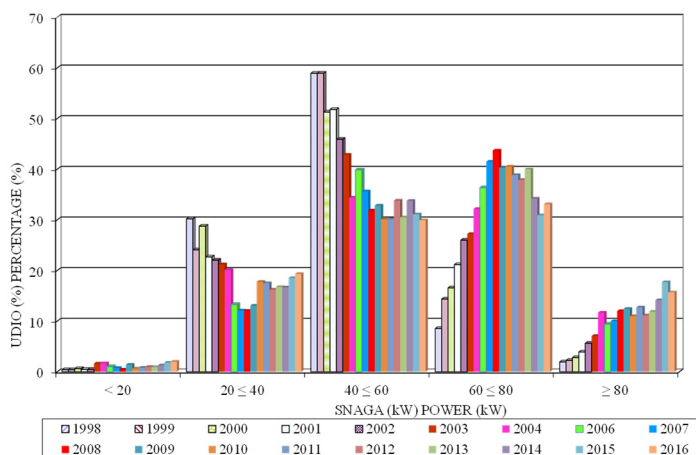
Grafikon 4 prikazuje broj registriranih traktora u Sloveniji za razdoblje od 1992. do 2016. godine. U 1993. je bilo 98.125 registriranih traktora, dok se u sljedećoj godini broj

registriranih traktora smanjio na 40.430 traktora zbog prelaska na nove slovenske tablice i tada mnogi vlasnici više nisu registrirali traktore. Nakon te godine, broj registriranih traktora polako raste. Veliki porast registriranih traktora zabilježen je u 2005. godini, kada je u Sloveniji bila mogućnost da se stari traktor može registrirati bez podataka o vlasništvu. Na kraju 2016. godine bilo je registriranih 108.914 traktora.

Iz podataka registriranih traktora dobivena je prosječna snaga traktora registriranih u pojedinoj godini. Iz tablice 1 vidljivo je kako se povećavala prosječna snaga u razdoblju od 10 godina. Za traktore proizvedene i registrirane u 1952. godini dobivena je prosječna snaga 19,6 kW. U 2016. godini prosječna snaga novih traktora u Sloveniji bila je nešto više od 61 kW.

Tablica 1. Prosječna snaga motora registriranih traktora u Sloveniji u razdoblju od 1952. do 2016.
Table 1. Average power of registered tractors between years 1952 and 2016

Godina - Year	1952.	1962.	1972.	1982.	1992.	2002.	2012.	2016.
Prosječna snaga (kW)	19,6	21,7	24,9	34,4	40,2	53,5	60,2	61,5
Average power (kW)								



Grafikon 5. Novi traktori registrirani u Sloveniji u periodu od 1998. do 2016. godine prema različitim kategorijama snage
Graph 5. New tractors registered in Slovenia between year 1998 and 2016 with regard to the category of power

U grafikonu 5 prikazani su novi registrirani traktori prema kategoriji snage od 1998. godine. Grafikon pokazuje do 2008. godine porast kategorija traktora sa snagom motora između 60 i 80 kW te iznad 80 kW. Nakon te godine udio tih traktora se stabilizirao. Udio novih traktora kategorije snage između 20 i 40 kW te između 40 kW i 60 kW na početku proučavanog razdoblja se smanjivao. Posljednjih 7 godina udio traktora u te dvije kategorije se stabilizirao. U apsolutnom iznosu, kategorija traktora između 40 i 60 kW i dalje ima veliki broj traktora (preko 30 %). Postotak novih traktora u Sloveniji sa snagom motora ispod 20 kW je mali i relativno konstantan. Općenito možemo reći, da poljoprivrednici ne kupuju traktore prevelikih snaga, jer okrupnjavanje (povećanje površine) poljoprivrednog posjeda u Sloveniji sporo raste - prosječna veličina je 6,9 ha.

ZAKLJUČCI

Slovenija ima veliki broj registriranih traktora prema broju svih stanovnika. Većina tih traktora u prosjeku je starija od 20 godina. Sa tim traktorima koji su tehnički zastarjeli još uvijek se može izvoditi poljoprivredne radove. Ali je iz stanovišta očuvanja okoliša, komfornijeg rada, veće produktivnosti i veće sigurnosti bitno da se traktorski park modernizira. U 2016. godini registrirano je 1.103 novih traktora ali nijedan nije bio subvencioniran iz strane države. U posljednjih nekoliko godina prosječna snaga novih traktora u Sloveniji iznosi oko 61 kW, što pokazuje stabilizaciju nabave presnažnih traktora.

LITERATURA

- Agricultural census 2010, Slovenija, 2010 – final data. 29. marec 2012 (2012). Prva objava Statistični urad Republike Slovenije – SURS http://www.stat.si/novica_prikazi.aspx?id=4594 (pristupljeno 6.11.2017)
- Farm Structure Survey, Slovenia, 2016. (2017). Statistični urad Republike Slovenije - SURS, E-objava 29.6.2017, <http://www.stat.si/StatWeb/News/Index/6742> (pristupljeno 6.11.2017)
- Poje, T., Jejčič, V., Cunder, T. (2006). Technical level of tractors on farms in Slovenia. *Acta agriculturae Slovenica*, let. 87, št. 2, str. 343-354.
- Poje, T. (2010). State of tractor pool in Slovenia. Zbornik radova 38. Međunarodnog simpozija iz područja mehanizacije poljoprivrede Aktualni zadaci mehanizacije poljoprivrede, Opatija, 22. - 26. veljače 2010, Sveučilište u Zagrebu, Agronomski fakultet, Zavod za mehanizaciju poljoprivrede, Zagreb, str. 67-74
- Poje, T. (2012). The development trends of the fleet of tractors in Slovenia. Zbornik radova 40. Međunarodnog simpozija iz područja mehanizacije poljoprivrede Aktualni zadaci mehanizacije poljoprivrede, Opatija, 21. - 24. veljače 2012, Sveučilište u Zagrebu, Agronomski fakultet, Zavod za mehanizaciju poljoprivrede, Zagreb, str. 23-29
- Poje, T. (2015). Situation in the field of agricultural tractors in Slovenia. Zbornik radova 43. Međunarodni simpozij iz područja mehanizacije poljoprivrede Aktualni zadaci mehanizacije poljoprivrede, Opatija, 24. - 27. veljače 2015. Zagreb: Sveučilište u Zagrebu, Agronomski fakultet, Zavod za mehanizaciju poljoprivrede, 2015, str. 101-110
- Tractor Market Report Calendar year 2014. Global Alliance for Agriculture Equipment Manufacturing Associations – Agrievolution economic Committee, <http://www.agrievolution.com/PDF/2014-Agrievolution-Tractor-Market-Report.pdf> (pristupljeno 6.11.2017)

ANALYSE OF REGISTERED TRACTORS IN SLOVENIA IN THE YEAR 2016

ABSTRACT

In Slovenia, 1,103 new tractors were registered in 2016, but not co-financed. 72.7% of the new owners were individuals and 27.3% legal entities. Among individuals were 92.3% male owners and most owners were aged between 50 and 60 years. Average power of new tractors is 61.5 kW. The leading seller is New Holland, with 14.5% share. At the end of 2016 the number of all registered tractors was 108,914 and in comparison with the year 1952, the average power of tractors was much higher (1952: 19.6 kW, 2016: 61.5 kW).

Keywords: power of tractors, registered tractors, owners of tractors, Slovenia



ANALIZA PROMETNIH NESREĆA S TRAKTORIMA U SLOVENIJI

Tomaz POJE

Kmetijski inštitut Slovenije, Oddelek za kmetijsko tehniko in energetiko,
Hacquetova ulica 17, SI – 1000 Ljubljana, Slovenija
E-mail dopisnog autora: tomaz.poje@kis.si

SAŽETAK

U radu su analizirani su podaci Ministarstva za unutrašnje poslove Republike Slovenije o prometnim nesrećama sa traktorima u razdoblju od 2012. do 2016. godine u Republici Sloveniji. U tom razdoblju sa traktorima bilo je 788 prometnih nesreća; poginulo je 11 traktorista, teško je bilo ozlijeđenih 22, a 91 lakše ozlijeđenih. Bez ozljeda su prošle 664 prometne nesreće sa traktorima. Traktoristi, koji su uglavnom muškarci, bili su uzročnici nesreće sa više od 60 %. Najviše (20,4 %) je traktorista starosti između 41 i 50 godina. Najviše nesreća se događa u periodu od travnja do listopada, između 11 i 12 sati te između 17 i 18 sati. Većina prometnih nesreća događa se u naseljima, a više od četvrtine svih nesreća je bočni sudar.

Ključne riječi: traktor, prometna nesreća, ozljede, Slovenija

UVOD

Prema popisu poljoprivrede iz 2010. godine u Sloveniji ima 101.756 traktora. Statistički ured Republike Slovenije za 2013. godinu navodi broj od 106.696 traktora. Krajem 2016. godine bilo je registrirano 108.914 traktora. Prosječna snaga motora traktora registriranih 1952. godine bila je 19,6 kW, dok je u 2016. godini prosječna snaga novih traktora bila 61,5 kW. Stručnjaci u Sloveniji ocjenjuju da ima još 20 do 30 tisuća traktora, koji nisu registrirani i nemaju kabinu niti sigurnosni luk. Traktori spadaju u vozila i učestvuju u prometu. U prometu, a još više izvan prometnica dolazi do nesreća sa traktorima.

Dolenšek i sur. (2010) navode, da je od 1981. do 2009. godine (28 godina) u udesima sa traktorima u Republici Sloveniji tragično nastradalo ukupno 874 osoba. Utvrđen je trend opadanja broja udesa i smrtno stradalih, naročito u prometu, a manje kod korištenja traktora izvan javnih prometnica. Prvi veći pad broja udesa i smrtno stradalih osoba, bio je poslije obaveznog uvođenja kabine za sve traktore od 1986. godine, ispod 40 stradalih osoba godišnje. Dolenšek i Bernik (2017) navode broj poginulih u nesrećama u poljoprivredi i šumarstvu u Sloveniji između godine 2006. i 2015. godine. Kod toga navodi i broj smrtnih

nesreća sa traktorima u prometu. U prosjeku je 2,4 smrtnih slučajeva sa traktorom. Ustanovljuju i porast poginulih u šumarstvu jer sve više neobučeni ljudi radi u šumarstvu, gdje je godišnji prosjek 13,5 smrtnih slučajeva. Bernik i Jerončič (2011) kod analize broja poginulih u nesrećama sa poljoprivrednim i šumarskim traktorima ustanovljuju da reljef pojedine države i stupanj gospodarskog razvoja u velikoj mjeri ne utječu na broj smrtno stradalih. Na osnovi analiza smrtnih slučajeva u Austriji, Sloveniji i Srbiji najveći utjecaj na broj smrtnih slučajeva imaju zakonski propisi za traktore i vozače – traktoriste. Bernik i Dolenšek (2006) navode da u prosjeku ima 34 smrtnih slučajeva kao posljedica nesreća s traktorom, kako na javnim prometnicama kao i izvan njih. Najbitniji uzroci nesreća su tehnička neispravnost starih traktora i nepravilno rukovanje vozača-traktorista. Oljača i sur. (2010) ustanovljuju, da je u periodu od 1999. do 2009. godine, u javnom saobraćaju Srbije, tragično je nastradalo u prosjeku godišnje 62 traktorista. Utvrđen je broj od 144 teško povrijeđenih (trajna invalidnost) vozača traktora, godišnje. Prema njemu je evidentno, da nedostaje osnovna, i posebno dodatna stručna obuka rukovatelja strojevima, i stručno-tehnički tečajevi za sigurno i pravilno korištenje traktora. Dimitrovski i sur. (2010) navodi, da se u periodu istraživanja od 2004. do 2008. godine na javnim prometnicama u Republici Makedoniji dogodilo ukupno 495 nesreća u kojima su učestvovali traktori, ili prosječno 99 nesreća godišnje. Prema kategoriji prometnice u naseljenim mjestima dogodilo se 79 ili u prosjeku po 15,8 prometnih nesreća godišnje, na lokalnim putovima. Također prema kategoriji prometnice, na lokalnim putovima izvan naseljenih mjesta dogodilo se najviše nesreća, 180 ili u prosjeku po 36 godišnje. U nesrećama na javnim putovima u kojima su učestvovali traktori nastradalo je ukupno 820 osoba, od kojih 242 osoba u nesrećama u naseljenim mjestima i 578 osoba u nesrećama izvan naseljenih mjesta. U nesrećama sa traktorima na javnim putovima izvan naseljenih mjesta nastrada dva puta više, a smrtno strada tri puta više osoba.

CEMA - europsko udruženje proizvođača poljoprivredne tehnike u 2015. godini naglašava, da je kod prometnih nesreća sa traktorima najveći problem stara mehanizacija (Road accident..., 2015). Izvještavaju, da se kod sedam EU članica 56 % od svih nesreća sa traktorima dogodilo sa traktorima koji su stariji od 12 godina. U 2017. godini CEMA objavljuje švicarsku ekspertizu (Revealed: 5 major..., 2017) o prometnim nesrećama gdje su uključeni traktori i druga poljoprivredna mehanizacija. Među pet najznačajnijih uzroka za 80 % prometnih nesreća sa poljoprivrednim strojevima spadaju prevrtanje stroja (24 %), ponašanje drugih sudionika na cestama (20 %), vidljivost operatera - traktorista (15 %), održavanje strojeva (13 %) i ponašanje vozača – traktorista (11 %). CEMA potiče i na širu EU implementaciju standarda EN 16831 o formatu za izvještavanje o nesrećama sa traktorima i drugom poljoprivrednom mehanizacijom.

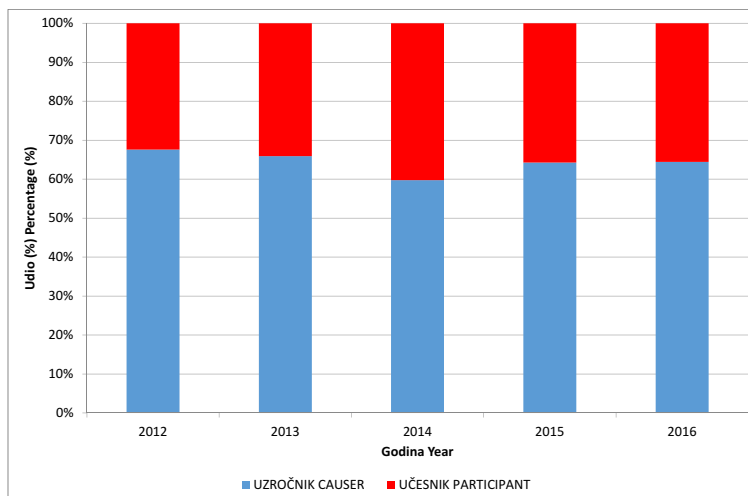
Cilj ovog rada je analizirati prometne nesreće sa traktorima u Sloveniji u razdoblju od 2012. do 2016. godine.

MATERIJALI I METODE

Za analizu nesreća sa traktorima na cestama u Sloveniji upotrijebili smo bazu podataka Ministarstva za unutrašnje poslove Republike Slovenije odnosno Policije. U toj podatkovnoj bazi nalaze se podaci za svaki udes, koji se dogodi u Sloveniji na cestama i kod toga se uvodi izvještaj policije. Iz ove podatkovne baze upotrijebili smo podatke o nesrećama sa traktorima za 5 godina – od 2012. do 2016. godine. Podaci iz baze statistički su obrađeni deskriptivnom statističkom metodom.

REZULTATI I RASPRAVA

U podatkovnoj bazi slovenske Policije nalaze se podaci za svaki udes, koji se dogodi u Sloveniji na cestama i kod toga se uvodi u izvještaj policije. Iz ove podatkovne baze upotrijebili smo podatke o nesrećama sa traktorima za 5 godina – od 2012. do 2016. godine. Iz tih podataka vidljivo je, da je u nesrećama u prometu na cestama sa traktorima uključeno od 145 traktorista u godini 2013. pa do 170 traktorista u godini 2017. U godini 2014. bilo je 159 nezgoda sa traktorima, u 2015. 151 i u 2016. godini 163 nesreća gdje je bio uključen traktor (traktorist). Sve ukupno je bilo između 2012 i 2016 godine 788 prometnih nesreća sa traktorima. U grafu 1 prikazan je udio uzročnika nezgoda i učesnika nesreća. Vidljivo je, da su traktoristi u proučavanom razdoblju većim dijelom uzročnici nesreća.

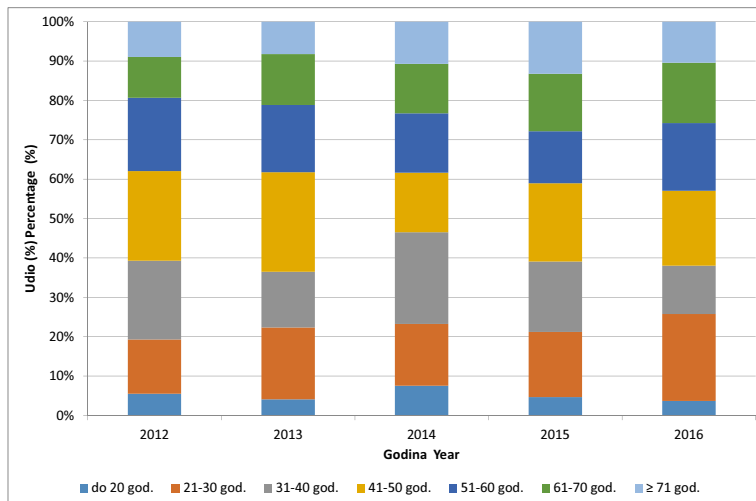


Graf 1. Udio uzročnika i učesnika u nesrećama na cesti, gdje je bio uključen traktor (traktorist)
Graph 1. Percentage of causer and participant in road accident with tractor (tractor driver)

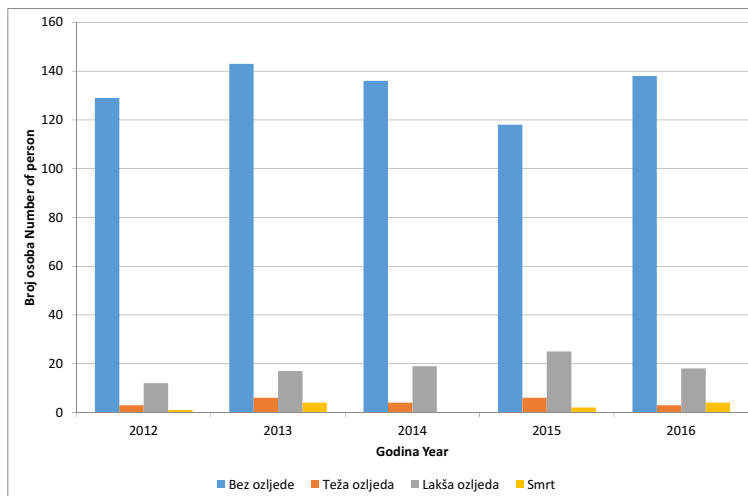
U nesrećama prevladavaju muškarci, žena ima samo mali udio. I to od 2 do 4 ženske osobe godišnje, što iznosi od 1,2 do 2,6 %.

Analizirali smo i starost sudionika u nezgodama. Iz grafa 2 razvidno je, da ima tri godine (2012., 2013., i 2015.) najviše učesnika iz grupa starosti od 41 do 50 godina. U 2014. godini najviše traktorista uključenih u prometni udes bilo je iz grupe starosti 31 do 40 godina, a u 2016. godini bilo je najviše sudionika iz grupe starosti 21 do 30 godina.

Analizirali smo i vrstu ozljeda koje su se dogodile vozaču traktora kod prometnog udesa. Prevladavaju prometni udesi, gdje nije došlo do ozljede traktorista. Ovaj udio prema godini istraživanja iznosi od 78,1 do 89 %. Slijede lakše ozlijede i teže ozlijede. Na žalost, ima i smrtnih slučajeva. U 2012. godini imali smo jedan smrtni slučaj, u 2013. godini 4 smrtna slučaja. U 2014. godini nije bilo smrtnih slučajeva sa traktorima kod prometnih nesreća. Ali opet u 2015. godini 2 smrtna slučaja, i u 2016. godini čak 4 smrtna slučaja.

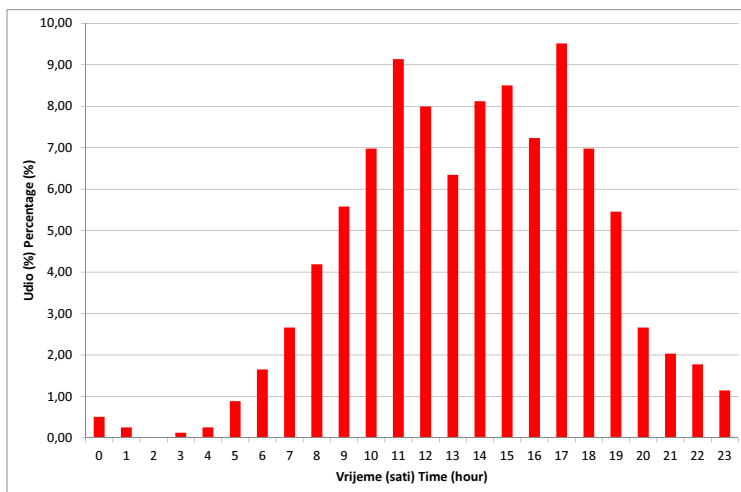


Graf 2. Udio traktorista uključenih u nesreće sa traktorima na cestama u godinama 2012. do 2016. prema starosti
Graph 2. Percentage of the tractor drivers included in road accident with regard to their age for the years 2012 to 2016



Graf 3. Broj osoba prema vrsti ozljede po pojedinim godinama
Graph 3. Number of person with regard to kind of injures and years

Ako se pogleda mjesec događaja prometne nesreće sa traktorima onda se može kazati, da se najviše nesreća dogodi od mjeseca travnja pa do listopada. To su i mjeseci kada je poljoprivredna aktivnost sa traktorima najveća. U grafu 4 prikazano je vrijeme (sat) događaja nesreće za sve godine proučavanja zajedno. Ističu se dva lokalna maksimuma i to jedan prijepodne od 11 do 12 sati, a drugi maksimum je poslijepodne, između 17 i 18 sati.

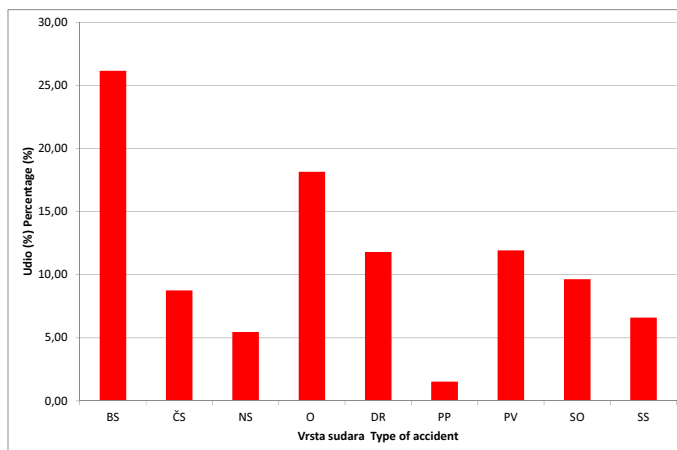


Graf 4. Vrijeme – sat prometne nesreće sa traktorima za sve godine između 2012. i 2016.
Graph 4. Hour of road accident with tractor for the year between 2012 and 2016

Tablica 1. Udio prometnih nesreća sa traktorima prema mjesecu i godini događaja
Table 1. Percentage of road accident with tractors with regard to month and year of accident

Mjesec Month	Udio prometnih nesreća (%) Percentage of road accident (%)				
	Godina - Year				
	2012	2013	2014	2015	2016
Siječanj - January	6,2	7,6	3,8	6,0	2,5
Veljača - February	6,9	7,6	5,0	2,0	2,5
Ožujak - March	7,6	4,7	9,4	4,6	6,1
Travanj - April	5,5	11,8	7,5	13,9	9,2
Svibanj - May	11,0	6,5	13,8	7,3	12,3
Lipanj - June	11,7	17,6	10,7	10,6	13,5
Srpanj - July	13,1	7,6	8,2	10,6	16,0
Kolovoz - August	8,3	5,3	8,2	12,6	9,8
Rujan - September	10,3	12,4	9,4	11,3	10,4
Listopad - October	12,4	11,2	11,9	8,6	8,0
Studeni - November	6,2	4,1	8,2	6,6	3,1
Prosinac - December	0,7	3,5	3,8	6,0	6,7

Većina nesreća dogodila se u naseljima. Udio takvih nezgoda u naseljima najmanji je u godini 2014. i iznosi 64,1 %. Najveći udio nesreća u naseljima je bio 2012. godine, kada je iznosio 75,1 %.



Graf 5. Udio nesreća prema vrsti sudara. Legenda: BS – bočni sudar, ČS – čeonni sudar, NS – naletni sudar, O – okrnucé, DR – drugo, PP – gaženje pješaka, PV – prevrnuće vozila, SO – udar u objekt, SS – udar u zaustavljeno (parkirano) vozilo.

Graph 5. Percentage of accident with regard to type od accident: Legend: BS – side accident, ČS – front accident, NS – clash accident, O – graze accident, DR – other, PP – run over of pedestrian, PV – overthrowing of vehicle, SO – collide in object, SS – collide in standing vehicle (parked vehicle).

Prema vrsti prometne nesreće ima 206 primjera odnosno 26,1 % kada je to bio bočni sudar. Slijede okrnucá sa 143 primjera ili 18,1 %. Najmanje je bilo gaženja pješaka, 12 slučajeva odnosno 1,52 %.

ZAKLJUČAK

Analizom podataka slovenske Policije ustanovili smo, da je između 2012. i 2016. godine bilo 788 prometnih nesreća sa traktorima. Kod toga je smrtno stradalo 11 traktorista. U Sloveniji više smrtnih slučajeva ima kod rada sa traktorima izvan ceste, dakle na polju, vinogradu, šumi itd. Veći dio prometnih nesreća sa traktorima nije imalo zdravstvene posljedice za traktorista, bez ozljede završilo je 664 nesreća. Bilo je međutim i 22 teže te 91 lakše ozlijeđenih traktorista. Traktoristi su bili uzročnici prometnih nesreća u više od 60 % slučajeva. Prije svega, traktoristi su muška populacija a četvrtina od njih je starosti između 41 i 50 godina. Veći dio prometnih nesreća sa traktorima događa se u naseljima i to od travnja do listopada i između 11 i 12, odnosno između 17 i 18 sati. Prema tipu nesreće najveći udio je bočnih sudara.

Iako cijelo društvo u Sloveniji želi postići „Viziju ništa“: Ništa smrtnih slučajeva kod prometnih nesreća, ništa teže ozlijeđenih kod prometnih nesreća, realnost je drugačija. Na lošu sliku utječu i traktoristi, koji su uzrokovali ili doživjeli prometnu nesreću. Obuka traktorista pa i drugih vozača mora biti još više usmjerena na specifična svojstva traktora kao sprog vozila.

LITERATURA

- Bernik, R. and Dolenšek, M. (2006). Analysis of technical legislation and tractors market influence on tractor accidents in the last 15 years. *Acta agriculturae Slovenica*, 87(2), pp. 365-380.
- Bernik, R. and Jerončič, R. (2011). The comparison of number of deaths in accidents with the agriculture and forestry tractors among European countries. *Acta agriculturae Slovenica*, 97(3), pp. 213-222.
- Dimitrovski, Z., Oljača, M.V., Gligorević, K., Ružičić, L. (2010). Accidents with tractors on public roads in F.R.Macedonia. *Agricultural Engineering, Faculty of Agriculture, University of Belgrade*, 35(1), pp. 89-97. <http://www.agrif.bg.ac.rs/files/publications/55/Poljoprivredna-tehnika-01-2010.pdf> Accessed: 15.11.2017
- Dolenšek, M., Jerončič, R., Bernik, R., Oljača, M.V. (2010). Tractors accidents in Slovenia in last three decades. *Agricultural Engineering, Faculty of Agriculture, University of Belgrade*, 35(1), pp. 83-88. <http://www.agrif.bg.ac.rs/files/publications/55/Poljoprivredna-tehnika-01-2010.pdf> Accessed: 15.11.2017
- Dolenšek, M. and Bernik, R. (2017). Problems of accidents with agricultural and forestry machinery. In: Čeh B., et al. (eds) *Zbornik simpozija Novi izzivi v agronomiji 2017, Laško, 2017* Slovensko agronomsko društvo, pp. 225-230.
- Oljača, M.V., Kovačević, D., Radojević, R., Gligorević, K., Pajić, M., Dimitrovski, Z. (2010). Accidents with tractor drivers in public traffic of the Republic of Serbia. *Agricultural Engineering, Faculty of Agriculture, University of Belgrade*, 35(1), pp. 75-82. <http://www.agrif.bg.ac.rs/files/publications/55/Poljoprivredna-tehnika-01-2010.pdf>. Accessed: 15.11.2017
- Road accidents with tractors: Main problem is older machinery. <http://cema-agri.org/sites/default/files/publications/Press%20Release%20CEMA-EU%20Tractors%20Accident%20Database%2017%2007%202015.pdf> Accessed: 15.11.2017
- Revealed: 5 major factors causing more than 80% of on-road. accidents with farm machines. (2017). <http://cema-agri.org/sites/default/files/publications/CEMA%20Press%20Release%20Analysis%20accident%20data%20ag%20machinery%20Switzerland%20FINAL%2012%2006%202017.pdf> Accessed: 15.11.2017

ANALYSIS OF TRAFFIC ACCIDENTS WITH TRACTORS IN SLOVENIA

ABSTRACT

According to the Police data, in period 2012 to 2016, 788 tractor traffic accidents were recorded in the Republic of Slovenia. In 11 accidents tractor drivers have died, in 22 cases tractor drivers were heavily, in 91 minor injured, in 664 road accidents were no injuries. Tractor driver, which were mainly man with age between 41 and 50 years (20.4%), cause more than 60% accidents. Most of the accidents happened between April and October, between 11 and 12 am and 5 to 6 pm. Most traffic accidents occur in settlements, and more than a quarter of all accidents are side collisions.

Key words: tractor, traffic accident, injuries, Slovenia

Snaga održavanja

ULJA I MAZIVA ZA POLJOPRIVREDU



INAMAMAZIVA



<http://atae.agr.hr/>